SOVIET PHYSICS

JETP

VOLUME 5 NUMBER 4

A Translation

of the

Journal of Experimental and Theoretical Physics

of the

Academy of Sciences of the USSR

Volume 32

NOVEMBER, 1957

Published by the

AMERICAN INSTITUTE OF PHYSICS
INCORPORATED

SOVIET PHYSICS
JETP

A translation of the Journal of Experimental and Theoretical Physics of the USSR.

A publication of the

AMERICAN INSTITUTE OF PHYSICS

SOVIET PHYSICS is a monthly journal published by the American Institute of Physics for the purpose of making available in English reports of current Soviet research in physics as contained in the Journal of Experimental and Theoretical Physics of the Academy of Sciences of the USSR. The page size of SOVIET PHYSICS will be 7⅞" x 10½", the same as other Institute journals.

Transliteration of the names of Russian authors follows the system employed by the Library of Congress.

This translating and publishing project was undertaken by the Institute in the conviction that dissemination of the results of researches everywhere in the world is invaluable to the advancement of science. The National Science Foundation of the United States encouraged the project initially and is supporting it in large part by a grant.

The American Institute of Physics and its translators propose to translate faithfully all the material in the Journal of EXPERIMENTAL AND THEORETICAL PHYSICS OF THE USSR appearing after January 1, 1955. The views expressed in the translated material, therefore, are intended to be those expressed by the original authors, and not those of the translators nor of the American Institute of Physics.

Two volumes are published annually, each of six issues. Each volume contains the translation of one volume of the Journal of EXPERIMENTAL AND THEORETICAL PHYSICS OF THE USSR. New volumes begin in February and August.

Subscription Prices:

Per year (12 issues)
United States and Canada $60.00
Elsewhere 64.00

Back Numbers
Single copies ..... $ 6.00

Subscriptions should be addressed to the American Institu of Physics, 335 East 45th Street, New York 17, New York.

SOVIET PHYSICS

JETP

A translation of the Journal of Experimental and Theoretical Physics of the USSR.

SOVIET PHYSICS–JETP Vol. 5, No. 4, pp 527-778 November, 1957

Bremsstrahlung and Pair Production at High Energies in Condensed Media

A. B. MIGDAL

(Submitted to JETP editor January 17, 1957)
J. Exptl. Theoret. Phys. (U.S.S.R.) 32, 633-646 (April 1957)

The effect of multiple scattering on bremsstrahlung and pair production is considered. The probability of these processes decreases appreciably at energies $\sim 10^{13}$e. The computation is carried out with the aid of the density matrix. Equations are derived for the probability of pair production and bremsstrahlung per unit path for electrons and quanta of arbitrary energy.

1. INTRODUCTION

IN BREMSSTRAHLUNG and pair production at high energies the participating particles travel in the same direction and the characteristic length associated with these processes will be considerable. Thus, the characteristic length associated with the emission of a quantum of wavelength $\lambda\!\!\!^{-}$ by bremsstrahlung is given by $l \sim \lambda\!\!\!^{-} / (1 - v/c)$ where v is the velocity of the electron. Landau and Pomeranchuk[1,2] have shown that the multiple scattering occurring in a length of that order will considerably reduce the probability of these processes. The cross-sections for pair production and bremsstrahlung have been given in Ref. 2 for the case of extremely high energies ($E \gg 10^{13}\, e$).

In an earlier paper[3] the author calculated the intensity of soft quanta emitted by an electron of arbitrary energy by determining the radiation emitted classically by an electron moving along a given trajectory and then averaging over all possible trajectories. This was accomplished by means of a distribution function averaged over the different arrangements of the atoms of the scattering medium and obeying the usual transport equation.

The present paper is devoted to the derivation of expressions for the probability of bremsstrahlung [Eq. (67)] and of pair production [Eq.(69)] per unit path length in a condensed medium without restrictions on the electron and photon energies. A connection is first established between the transition probabilities and the density matrix. Certain expressions for the density matrix averaged over the coordinates of the scattering atoms, which were derived in earlier papers[4,5], are then employed.

At low energies Eqs. (67) and (69) become the Bethe-Heitler expressions[6], and at very high energies they confirm the estimate of Ref. 2. For photon energies much smaller than the electron energy, (67) becomes identical with the expressions of Ref. 3.

Finally, for very soft quanta for which the dielectric constant is appreciably different from 1 Eq. (62) of the present paper gives in the limiting cases the results obtained by Ter-Mikaelian[7].

Eqs. (67) and (69) can be used as starting points for the formulation of a shower theory in condensed media for energies greater than 10^{13}e.

2. CONNECTION BETWEEN TRANSITION PROBABILITIES AND THE DENSITY MATRIX

To solve our problem we must average the probability of bremsstrahlung and pair production over all possible arrangements of the atoms of the scattering medium. We shall express the number of radiating transitions per unit time in terms of the density matrix, and then utilize the expressions of Ref. 4 in averaging the density matrix.

Denoting the eigenfunctions of the electron in the scattering medium by ψ_s and the initial wave function by ψ_0 we have to first order in the interaction between electron and the radiation field

$$i\dot{C}_s^{(1)} = \sum_{s'} (\psi_s | e^{iHt} A e^{ikt} e^{-iHt} | \psi_{s'}) C_{s'}^0$$

$$= (\psi_s | e^{iHt} A e^{ikt} e^{-iHt} | \psi_0), \; A = \varepsilon_\nu \alpha e^{-i\mathbf{kr}} e \sqrt{2\pi / k},$$

Here A is the photon emission operator, ϵ_ν the polarization vector, k the wave vector, and H is the Hamiltonian for the electron, including the potential from all scattering centers:

$$H = H_0 + \sum_m V(\mathbf{r} - \mathbf{r}_m); \quad H\psi_s = E_s \psi_s.$$

We use units such that $m = \hbar = c = 1$. The ψ-functions of the electrons and quanta are normalized per unit volume.

For the number of radiating transitions per unit time we obtain

$$Q_s = \frac{d}{dt} |C_s|^2 = 2 \operatorname{Re} \dot{C}_s^* C_s$$

$$= 2\operatorname{Re} \int_0^t (\psi_0 | e^{iHt_1} A^+ e^{-iHt_1} | \psi_s) (\psi_s | e^{iHt} A e^{-iHt} | \psi_0)$$

$$\times e^{ik(t-t_1)} \, dt_1. \qquad (1)$$

We now shall sum over the final electron states. First we consider the case of bremsstrahlung. We introduce the operator of the sign of the energy

$$K = (H + |E(\mathbf{p})|) / 2 |E(\mathbf{p})|,$$

where $\mathbf{p}$ is the momentum operator for the electron. With

$$\sum_s \psi_s^*(x) \psi_s(x') = \delta(x - x'),$$

we obtain

$$Q = \sum_{E_s > 0} Q_s = 2 \operatorname{Re} \int_0^t (\psi_0 | e^{iHt_1} A^+ K e^{iH(t-t_1)} A e^{-iHt} | \psi_0)$$

$$\times e^{ik(t-t_1)} \, dt_1. \qquad (2)$$

In (2) the operator K at large energies can be replaced with negligible error by

$$K_0 = (H_0 + |E_p^0|) / 2 |E_p^0|$$

which is the equivalent operator for a free electron. Then the coordinates of the scattering centers enter in (2) only through the factor $e^{\pm iHt}$.

The averaging over the coordinates of the scatterers can be performed independently in the factors $e^{\pm iHt_1}$ and $e^{\pm iH(t-t_1)}$. Indeed, the coordinates in the former term correspond to collisions occurring during the time interval $0 - t_1$ while the latter term contains the coordinates of scatterers participating in collisions during the later time interval $t_1 - t$.

If after the time t_1 there are many collisions, then after averaging over the first collisions the factors of the form $e^{\pm iHt_1}$ will become practically independent of the collisions which took place close to t_1.

We now shall write the integrand of (2) as a matrix element of a product of operators in the representation of the wave functions.

$$\varphi_p^\lambda = u_p^\lambda e^{i\rho r}$$

of the free electron. Putting $\psi_0 = \varphi_{p_0}^{\lambda_0}$ (p_0 - initial momentum of the electron) and denoting average by $\langle\,\rangle$ we obtain from (2)

$$\langle Q \rangle = 2 \operatorname{Re} \int_0^t d\tau e^{ik\tau} J,$$

$$J = \langle (\psi_0 | e^{iHt_1} A^+ K_0 e^{iH\tau} A e^{-iH\tau} e^{-iHt_1} | \psi_0) \rangle \qquad (3)$$

$$= \sum_{\substack{p_1 p_2 \\ \lambda_1 \lambda_2}} \langle (e^{iHt_1})_{p_0 p_1}^{\lambda_0 \lambda_1} (A^+ K_0 e^{iH\tau} A e^{-iH\tau})_{p_1 p_2}^{\lambda_1 \lambda_2} (e^{-iHt_1})_{p_2 p_0}^{\lambda_2 \lambda_0} \rangle;$$

here $\tau = t - t_1$. Because of the statistical independence of the factors $e^{\pm iHt_1}$ and $e^{\pm iHt}$ we have

$$J = \sum_{\substack{p_1 p_2 \\ \lambda_1 \lambda_2}} \langle (e^{-iHt_1})_{p_2 p_0}^{\lambda_2 \lambda_0} (e^{iHt_1})_{p_0 p_1}^{\lambda_0 \lambda_1} \rangle \langle (A^+ K_0 e^{iH\tau} A e^{-iH\tau})_{p_1 p_2}^{\lambda_1 \lambda_2} \rangle.$$

At high energy the momentum changes of the electron are essentially small, and the spin does not change in the scattering process, i.e.

$$(e^{\pm iHt})_{pp'}^{\lambda\lambda'} = \delta_{\lambda\lambda'} (e^{\pm iHt})_{pp'}^{\lambda\lambda'}$$

with an error on the order $|\mathbf{p}' - \mathbf{p}| / p$. In this approximation

$$J = \sum_{p_1 p_2} \langle (e^{-iHt_1})_{p_2 p_0}^{\lambda_0 \lambda_0} (e^{iHt_1})_{p_0 p_1}^{\lambda_0 \lambda_0} \rangle \langle (A^+ K_0 e^{iH\tau} A e^{-iH\tau})_{p_1 p_2}^{\lambda_1 \lambda_2} \rangle. \qquad (4)$$

The first factor in (4) satisfies as a function of p_2, p_1 and t_1 the same equation as the averaged density matrix

$$\langle \rho^{\lambda_0\lambda_0}_{p_2p_1} \rangle = \langle (e^{-iHt_1}\rho_0 e^{iHt_1})^{\lambda_0\lambda_0}_{p_2p_1} \rangle.$$

It follows from this (see Ref. 4 and 5) that the difference $p_2 - p_1$ does not change in the scattering (this is is due to the homogeneity of the scattering medium). Since the first factor in (4) for $t_1 = 0$ is $\delta_{p,p_0}\delta_{p_2p_0}$ one can write it in the form

$$\langle (e^{-iHt_1})^{\lambda_0\lambda_0}_{p_2p_0} (e^{iHt_1})^{\lambda_0\lambda_0}_{p_0p_1} \rangle = f_0^{\lambda_0\lambda_0}(p_1, t_1)\,\delta_{p_2p_1}. \quad (5)$$

We shall now write the second factor of (4) as a sum of products of operators in the momentum representation. Using (5) and the expression for the operator A we obtain

$$\langle (A^+ K_0 e^{iH\tau} A e^{-iH\tau})^{\lambda_0\lambda_0}_{p_1p_1} \rangle$$
$$= \frac{2\pi e^2}{k} \Big\langle \sum_{\substack{P_0\,\lambda_1 \\ E^{\lambda_1}>0}} (\alpha\varepsilon_\nu)^{\lambda_0\lambda_1}_{p_1,\,p_1-k}\,(e^{iH\tau})^{\lambda_1\lambda_1}_{p_1-k,\,p-k/2}\,(\alpha\varepsilon_\nu)$$
$$\times\, {}^{\lambda_1\lambda_0}_{p-k/2,\,p+k/2}\,(e^{-iH\tau})^{\lambda_0\lambda_0}_{p_1+k/2,\,p_1} \Big\rangle.$$

Here

$$(\alpha\varepsilon_\nu)^{\mu_1\mu_2}_{g_1g_2} = (u^{\mu_1}_{g_1}\alpha\varepsilon_\nu u^{\mu_2}_{g_2}),$$

where u^μ_g are spin functions.

We introduce

$$\langle (e^{-iH\tau})^{\lambda_0\lambda_0}_{p+k/2,\,p_1} (e^{iH\tau})^{\lambda_1\lambda_1}_{p_1-k,\,p-k/2} \rangle = f_k^{\lambda_0\lambda_1}(p, \tau). \quad (6)$$

Both the coefficients in the equations for $f_k^{\lambda_0\lambda_1}(p, \tau)$ and $f^{\lambda_0\lambda_1}(p_1 t_1)$ and their boundary conditions [see below, Eq. (10) and (12)] do not depend on the spin orientation. At a fixed sign of the energy, one can therefore omit these indices in the summation with respect to λ_0 and λ_1.

Inserting (5) and (6) into (4), summing over the photon polarization, and averaging over the spin of the initial state we obtain

$$J_1 = \frac{1}{2} \sum_{\substack{\lambda_0,\,\nu \\ E^{\lambda_0}>0}} J$$
$$= \frac{\pi e^2}{k} \int \mathcal{L}(p_1, p)\, f_0(p_1, t_1)\, f_k(p, \tau)\, \frac{d\,p_1}{(2\pi)^3}\, \frac{d\,p}{(2\pi)^3}; \quad (7)$$

$$\mathcal{L}(p_1, p) = \sum_{\substack{\lambda_0\lambda_1\nu \\ E^{\lambda_0},\,E^{\lambda_1}>0}} (\alpha\varepsilon_\nu)^{\lambda_0\lambda_1}_{p_1,\,p-k} (\alpha\varepsilon_\nu)^{\lambda_1\lambda_0}_{p-k/2,\,p+k/2}. \quad (8)$$

We note that

$$\rho^{\lambda_0\lambda_1}_{p+k/2,\,p-k/2} = (e^{-iH\tau})^{\lambda_0\lambda_0}_{p+k/2,\,p_1} (e^{iH\tau})^{\lambda_1\lambda_1}_{p_1-k,\,p-k/2}$$
$$= (e^{-iH\tau}\rho_0 e^{iH\tau})^{\lambda_0\lambda_1}_{p+k/2,\,p-k/2}$$

satisfies the equation

$$\partial\rho/\partial\tau = -i\,[H, \rho].$$

Furthermore

$$\mathrm{Sp}\,\rho = \sum_{g_1\mu_1} \rho^{\mu_1\mu_1}_{g_1g_1} = \sum_{p\lambda_1} (e^{iH\tau})^{\lambda_0\lambda_1}_{p_1,\,p} (e^{-iH\tau})^{\lambda_1\lambda_0}_{p,\,p_1} = 1,$$

i.e. ρ is an element of the density matrix in the momentum representation. We shall call $f_k(p, \tau)$ the averaged density matrix.

Thus the problem of averaging the number of transitions per unit time has been reduced to finding the averaged density matrix and doing the summation (8) and the integration (7).

3. EQUATIONS FOR THE AVERAGED DENSITY MATRIX

As shown in Ref. 4 the averaged density matrix satisfies the equation

$$\partial f_k^{\lambda_0\lambda_1}(p, \tau)/\partial\tau + i\,(E^{\lambda_0}_{p+k/2} - E^{\lambda_1}_{p-k/2})\, f_k^{\lambda_0\lambda_1}(p, \tau)$$
$$= n\pi \int \frac{d\,p'}{(2\pi)^3} |V_{p'-p}|^2 \{\delta(E^{\lambda_0}_{p'+k/2} - E^{\lambda_0}_{p+k/2}) \quad (9)$$
$$+ \delta(E^{\lambda_1}_{p'-k/2} - E^{\lambda_1}_{p'-k/2})\}\,[f_k^{\lambda_0\lambda_1}(p', \tau) - f_k^{\lambda_0\lambda_1}(p, \tau)]$$

with the initial conditions following from the definition of $f_k(p, \tau)$:

$$f_k^{\lambda_0\lambda_1}(p, \tau)|_{\tau=0} = \delta_{p,\,p_1-k/2}. \quad (10)$$

These equations differ from the classical transport equations in these points. First, $k\,\delta E/\delta\rho$ has been replaced by the difference $E^{\lambda_0}_{p+k/2} - E^{\lambda_1}_{p-k/2}$. Further, the term describing the collisions has been replaced by one half the sum of a term for the momentum $p + k/2$ and energy $E^{\lambda_0}_{p+k/2}$ and a term for $p - k/2$ and energy $E^{\lambda_0}_{p-k/2}$. For $k \ll p$ and $\lambda_0 = \lambda_1$, Eq. (9) goes over into the classical equation for the k th Fourier component of the distribution function.

The equation for $f_0(p_1, t_1)$ is

$$\frac{\partial f_0^{\lambda_0\lambda_0}(p_1, t_1)}{\partial t_1} = 2\pi n \int \frac{d\,p'}{(2\pi)^3} |V_{p'-p_1}|^2\, \delta(E^{\lambda_0}_{p_1} - E^{\lambda_0}_{p'})$$
$$\times [f_0^{\lambda_0\lambda_0}(p', t_1) - f_0^{\lambda_0\lambda_0}(p_1, t_1) \quad (11)$$

with an initial condition

$$f_0^{\lambda_0\lambda_0}(\mathbf{p}_1, t_1)|_{t_1=0} = \delta_{\mathbf{p}_1, \mathbf{p}_0}. \quad (12)$$

From (11) and (12) we have

$$\int (2\pi)^{-3} f_0^{\lambda_0\lambda_0}(\mathbf{p}_1, t_1)\, d\mathbf{p}_1 = 1. \quad (13)$$

From (11) and (12) follows that $f_0^{\lambda_0\lambda_0}$ is different from zero only for $p_1 = p_0$. One can therefore introduce a function $v_0(\theta, t_1)$ where θ is the vector associated with the angle between $\mathbf{p}_0$ and $\mathbf{p}_1$:

$$f_0^{\lambda_0\lambda_0}(\mathbf{p}_1, t_1)(2\pi)^{-3} d\mathbf{p}_1 = \delta(p_1 - p_0)\, v_0(\theta, t_1)\, dp_1\, d\theta,$$
$$v_0(\theta, 0) = \delta(\theta). \quad (14)$$

From (13) we obtain

$$\int v_0(\theta, t_1)\, d\theta = 1. \quad (14')$$

It is easy to see that $f_{\mathbf{k}}(\mathbf{p}, \tau)$ differs from zero only for p close to $g = p_0 - k/2$. For $\tau = 0$ this follows from (10):

$$p^2 = p_0^2 + \frac{k^2}{4} - p_0 k + p_0 k\,(1 - \cos\widehat{\mathbf{p}_1 \mathbf{k}}) = g^2\left(1 - \frac{p_0 k}{g}\,\eta_1^2\right),$$

Here η_1 is the acute angle between $\mathbf{p}_1$ and $\mathbf{k}$.

We introduce the vectors for the angles between $\mathbf{p}$ and $\mathbf{k}$, and $\mathbf{p}'$ and $\mathbf{k}$.

$$\boldsymbol{\eta} = \mathbf{p}_\perp / g; \quad \boldsymbol{\eta}' = \mathbf{p}'_\perp / g; \quad g = p_0 - k/2. \quad (15)$$

Here $\mathbf{p}_\perp$ and $\mathbf{p}'_\perp$ denote the projections of $\mathbf{p}$ and $\mathbf{p}'$ respectively on a plane normal to $\mathbf{k}$. The δ-functions on the right hand side of (9) can be rewritten as

$$\delta(E_{\mathbf{p}'\pm\mathbf{k}/2} - E_{\mathbf{p}\pm\mathbf{k}/2}) \approx \delta\left(p' - p \pm \frac{gk\,(\eta'^2 - \eta^2)}{2\,(g \pm k/2)}\right) \approx \delta(p' - p).$$

Hence the absolute value of $\mathbf{p}$ is approximately conserved in a collision.

The values of p for which the function $f_{\mathbf{k}}(\mathbf{p}, \tau)$ appreciably differs from zero are given by $(p - g)/g \sim \eta^2$ An estimate of the magnitude of η^2 will be given below.

Taking into account the approximate constancy of p, the function $v(\eta, \tau)$ will be given by

$$f_{\mathbf{k}}(\mathbf{p}, \tau)(2\pi)^{-3} d\mathbf{p} = \delta(p - g)\, v(\boldsymbol{\eta}, \tau)\, dp\, d\boldsymbol{\eta}. \quad (16)$$

From (10) we have

$$v(\boldsymbol{\eta}, \tau)|_{\tau=0} = \delta(\boldsymbol{\eta} - \boldsymbol{\eta}_0);$$
$$\boldsymbol{\eta}_0 = (\mathbf{p}_1 - \mathbf{k}/2)_\perp / g = \frac{\mathbf{p}_{1\perp}}{g}, \quad (17)$$

where η_0 is the vector of the angle between $\mathbf{p}_\perp - \mathbf{k}/2$ and $\mathbf{k}$. The vector η_0 is connected with the previously introduced vector $\boldsymbol{\theta}$ by the relation

$$\boldsymbol{\theta} = \mathbf{p}_1/p_0 - \mathbf{p}_0/p_0 = \mathbf{p}_1/p_0 - \mathbf{n} + \mathbf{n} - \mathbf{p}_0/p_0$$
$$= \mathbf{p}_{1\perp}/p_0 + \boldsymbol{\vartheta} = g\boldsymbol{\eta}_0/p_0 + \boldsymbol{\vartheta}. \quad (18)$$

Here $\boldsymbol{\vartheta} = \mathbf{n} - \mathbf{p}_0/p_0$ denotes the vector of the angle between $\mathbf{n} = \mathbf{k}/k$ and the initial direction of the electron. From (15) we obtain

$$\mathbf{p} = (\mathbf{pn})\,\mathbf{n} + \mathbf{p}_\perp \approx g\mathbf{n} + g\boldsymbol{\eta}; \quad \mathbf{p} + \mathbf{k}/2 \approx p_0\mathbf{n} + g\boldsymbol{\eta};$$
$$\mathbf{p} - \mathbf{k}/2 \approx (p_0 - k)\,\mathbf{n} + g\boldsymbol{\eta}. \quad (19)$$

The energy difference entering as an argument in (9) can be written as

$$E^{\lambda_0}_{\mathbf{p}+\mathbf{k}/2} - E^{\lambda_1}_{\mathbf{p}-\mathbf{k}/2}$$
$$= \sqrt{1 + (p_0\mathbf{n} + g\boldsymbol{\eta})^2} - \sqrt{1 + [(p_0 - k)\,\mathbf{n} + g\boldsymbol{\eta}]^2}$$
$$= k\,[1 - 1/2p_0\,(p_0 - k) - g^2\eta^2/2p_0\,(p_0 - k)]. \quad (20)$$

Utilizing (18) in integrating (9) with respect to p we find

$$\frac{\partial v(\boldsymbol{\eta}, \tau)}{\partial \tau} + i\left(a - b\,\frac{\eta^2}{2}\right) v(\boldsymbol{\eta}, \tau)$$
$$= \frac{ng^2}{(2\pi)^2} \int |V_{g(\boldsymbol{\eta}' - \boldsymbol{\eta})}|^2 \{v(\boldsymbol{\eta}', \tau) - v(\boldsymbol{\eta}, \tau)\}\, d\boldsymbol{\eta}', \quad (21)$$

$$a = k\left(1 - \frac{1}{2p_0\,(p_0 - k)}\right); \quad b = \frac{g^2 k}{p_0\,(p_0 - k)}; \quad \boldsymbol{\eta}' = \frac{\mathbf{p}'_\perp}{g}.$$

For $V_{\mathbf{q}}$ we choose the expression

$$V_{\mathbf{q}} = 4\pi Z e^2/(q^2 + \varkappa^2), \quad \varkappa \sim 1/a, \quad (22)$$

where a is the Thomas-Fermi radius $a \sim 137\,Z^{-1/3}$.

Inserting (22) into (21) gives

$$\frac{\partial v}{\partial \tau} + i\left(a - b\,\frac{\eta^2}{2}\right) v$$
$$= \frac{4nZ^2e^4}{g^2} \int \frac{d\boldsymbol{\eta}'}{[(\boldsymbol{\eta}' - \boldsymbol{\eta})^2 + \theta_\perp^2]^2} [v(\boldsymbol{\eta}', \tau) - v(\boldsymbol{\eta}, \tau)],$$
$$\theta_\perp = \varkappa/g. \quad (23)$$

By expanding $v(\eta', \tau)$ into a power series in $\boldsymbol{\eta}' - \boldsymbol{\eta}$ we obtain from (23) the Fokker-Planck differential equation

$$\frac{\partial v}{\partial \tau} + i\left(a - b\,\frac{\eta^2}{2}\right) v = q\Delta_\eta v,$$
$$q = \frac{2\pi n Z^2 e^4}{g^2} \ln\frac{\theta_2}{\theta_1} = \frac{B}{g^2}. \quad (24)$$

We will determine the quantity θ_2 from the conditions of validity of the Fokker-Planck equation. The first term of the expansion is

$$\int_{\theta_1}^{\theta_2} \frac{\theta d\theta}{\theta^4}\,\theta^2\,\frac{1}{4}\,\Delta_\eta\, v \approx \frac{1}{4}\ln\frac{\theta_2}{\theta_1}\Delta_\eta v.$$

The next term of the expansion is of the order

$$\int_{\theta_1}^{\theta_2} \frac{\theta d\theta}{\theta^4}\,\theta^4\,\frac{\partial^4 v}{\partial\eta^4} \sim \theta_1^2\frac{1}{\eta^2}\Delta_\eta v.$$

We furthermore need

$$\int_0^\infty v e^{-ik\tau}\,d\tau = \int_0^\infty v'\,d\tau, \qquad v' = e^{-ik\tau}v;$$

v' satisfies an equation which one obtains when replacing in (24) the quantity a by the quantity $a' = a - k$.

The essential values of η^2 are given by the relations

$$(a' - b\eta_1^2/2)\,v \sim b\eta_1^2 v \sim q\Delta_\eta v;\ \eta_1^2 \sim \sqrt{q/b}. \quad (25)$$

This estimate will be confirmed below. The condition for the possibility of the series expansion of v therefore has the form

$$\theta_2^2\sqrt{\frac{b}{q}} \sim \ln\frac{\theta_2}{\theta_1};\ \theta_2 \sim \left(\frac{q}{b}\right)^{1/4} L^{1/2};\quad L = \ln\frac{\theta_2}{\theta_1}. \quad (26)$$

At sufficiently large energies θ_2 becomes equal to the diffraction angle of the nucleus, which is $1/gR$. Then the upper limit of integration of (23) over $|\eta' - \eta|$ is given by $1/gR$ and the value of L becomes identical with the well-known expression from the theory of multiple scattering[6]. Putting $R \approx 0.5\, r_0 Z^{1/3}$, we obtain for $\theta_2 > 1/gR$.

$$L = \ln(137^2/0{,}5\, Z^{2/3}) = 2\ln(190\, Z^{-1/3}). \quad (27)$$

4. SUMMATION OVER ELECTRON SPIN AND PHOTON POLARIZATION

The summation over λ_0 and λ_1 cannot be performed in the usual manner since the momenta are different for the different spin functions.

It is however possible to reduce the sum (8) to an evaluation of the trace of two-by-two matrices. The spin functions can be written in the form

$$u_g^\mu = \left\{\begin{matrix} v_\mu \\ \dfrac{\sigma g}{E_g+1}v_\mu \end{matrix}\right\} N_g; \qquad v_1 = \left\{\begin{matrix}1\\0\end{matrix}\right\},\ v_2 = \left\{\begin{matrix}0\\1\end{matrix}\right\};$$

$$N_g^2 = \frac{1}{1 + g^2(E_g+1)^{-2}} \approx \frac{1}{2}. \quad (28)$$

Here $\sigma_{1,2,3}$ are the Pauli spin matrices, and the z axis is parallel to $\mathbf{n}$. Substitution in (8) yields

$$\mathscr{L}(\mathbf{p}_1\mathbf{p}) = \frac{1}{4}\sum_{i=1,2}\mathrm{Sp}\left\{\left[\frac{\sigma_i\sigma(\mathbf{p}_1-\mathbf{k})}{E_{\mathbf{p}_1-\mathbf{k}}+1} + \frac{\sigma\mathbf{p}_1\sigma_i}{E_{p_1}+1}\right] \times \left[\frac{\sigma_i\sigma(\mathbf{p}+\mathbf{k}/2)}{E_{\mathbf{p}+\mathbf{k}/2}+1} + \frac{\sigma(\mathbf{p}-\mathbf{k}/2)\sigma_i}{E_{\mathbf{p}-\mathbf{k}/2}+1}\right]\right\}. \quad (29)$$

We introduce the abbreviations

$$\mathbf{A} = \frac{\mathbf{p}_1}{E_{\mathbf{p}_1}+1};\quad \mathbf{B} = \frac{\mathbf{p}_1-\mathbf{k}}{E_{\mathbf{p}_1-\mathbf{k}}+1};\quad \mathbf{C} = \frac{\mathbf{p}+\mathbf{k}/2}{E_{\mathbf{p}+\mathbf{k}/2}+1};$$

$$\mathbf{D} = \frac{\mathbf{p}-\mathbf{k}/2}{E_{\mathbf{p}-\mathbf{k}/2}+1}. \quad (30)$$

We then have from (29)

$$\mathscr{L}(\mathbf{p}_1,\ \mathbf{p}) = \frac{1}{4}\sum_{i=1,2}\mathrm{Sp}\,(\sigma_i\mathbf{B}\sigma + \mathbf{A}\sigma\sigma_i)(\sigma_i\sigma\mathbf{C} + \mathbf{D}\sigma\sigma_i)$$
$$= \mathbf{BD} + \mathbf{AC} - (\mathbf{Bn})(\mathbf{Cn}) - (\mathbf{An})(\mathbf{Dn}). \quad (31)$$

Each of the scalar products of (31) has a value close to unity. However, as will become clear later, the complete expression is of order $\sim\eta^2$. We therefore rewrite (31) as a sum of small terms so that it will be possible to keep only the main terms of expansions in powers of $1/p$.

We express each of the vectors A, B, C, D as a sum of two terms, one is parallel and the other perpendicular to $\mathbf{n}$: $\mathbf{A} = \mathbf{A}_1 + \mathbf{A}_2$; $\mathbf{A}_1 \| \mathbf{n}$, $\mathbf{A}_2 \perp \mathbf{n}$ and similarly for B, C, and D. Then (31) becomes

$$\mathscr{L} = (\mathbf{D}_1 - \mathbf{C}_1)(\mathbf{B}_1 - \mathbf{A}_1) + \mathbf{B}_2\mathbf{D}_2 + \mathbf{A}_2\mathbf{C}_2. \quad (32)$$

In (32) each term is of order $\sim p^{-2}$ or η^{+2}.

From (17), (19), and (30) we obtain up to terms of required accuracy

$$A_1 = C_1 = 1 - 1/p_0;\ B_1 = D_1 = 1 - 1/(p_0 - k),$$
$$\mathbf{A}_2 = g\boldsymbol{\eta}_0/p_0;\quad \mathbf{B}_2 = g\boldsymbol{\eta}_0/(p_0-k);\quad \mathbf{C}_2 = g\boldsymbol{\eta}/p_0;$$
$$\mathbf{D}_2 = g\boldsymbol{\eta}/(p_0-k). \quad (33)$$

Inserting these expressions into (32) we finally obtain

$$\mathscr{L} = K_1 + K_2 \boldsymbol{\eta}\boldsymbol{\eta}_0,$$
$$K_1 = \frac{k^2}{p_0^2 (p_0 - k)^2}; \quad K_2 = \frac{g^2 [p_0^2 + (p_0 - k)^2]}{p_0^2 (p_0 - k)^2}. \tag{34}$$

5. PROBABILITY OF BREMSSTRAHLUNG

Let $W_r(p_0 k)dk$ denote the probability of emission of a photon of energy between k and $k + dk$ per unit path. Since the initial ψ-function of the electron was normalized to unit volume (or to unit flux for $c = 1$) we have from (3) and (7)

$$W_r = \frac{1}{2} \sum_{\substack{\lambda_0 \nu \\ E^{\lambda_0} > 0}} \int <Q> d\vartheta \frac{k^2}{(2\pi)^3}$$
$$= \frac{k^2}{(2\pi)^3} 2 \operatorname{Re} \int_0^t d\tau e^{ik\tau} \int J_1 d\vartheta. \tag{35}$$

Inserting into (7) the expressions for v_0, v, and $\mathscr{L}$, as given by (14), (16), and (33) respectively, we find

$$\int J_1 d\vartheta = \frac{\pi e^2}{k} \int v_0(\theta, t_1)\, v(\boldsymbol{\eta}, \tau) [K_1 + K_2 \boldsymbol{\eta}\boldsymbol{\eta}_0]\, d\theta\, d\boldsymbol{\eta}\, d\vartheta.$$

We now express θ in terms of $\boldsymbol{\eta}_0$ and ϑ according to (18) and so obtain

$$\int J_1 d\vartheta = \frac{\pi e^2}{k} \int v_0 \left(\frac{g}{p_0} \boldsymbol{\eta}_0 + \vartheta,\ t_1 \right)$$
$$\times v(\boldsymbol{\eta},\ \tau)\ (K_1 + K_2 \boldsymbol{\eta}\boldsymbol{\eta}_0)\ \frac{g^2}{p_0^2}\ d\boldsymbol{\eta}_0\, d\boldsymbol{\eta}\, d\vartheta.$$

Utilizing the normalization condition (14′) for v_0 we have

$$W_r = \frac{e^2 g^2 k}{(2\pi)^2 p_0^2}$$
$$\times \operatorname{Re} \int_0^t d\tau e^{ik\tau} \int (K_1 + K_2 \boldsymbol{\eta}\boldsymbol{\eta}_0)\, v(\boldsymbol{\eta}, \tau)\, d\boldsymbol{\eta}\, d\boldsymbol{\eta}_0. \tag{36}$$

We denote by τ_0 the values of τ that are significant in the integral (36). From (24) and (25) we obtain the estimate

$$\eta^4 \sim q/b,\ \tau_0 \sim 1/b\eta_l^2 \sim (bq)^{-1/2},\ \eta_l^2 \sim q\tau_0. \tag{37}$$

If the time τ the electron spends in the medium is much larger than τ_0 the upper limit of the integral over τ in (35) can be replaced by infinity and then W will not depend on τ. We shall treat below the case $\tau \gg \tau_0$ or $1 \gg l \gg l_k$, where here l is the thickness of the scattering medium, and $l_k = c\tau_0$.

From (37) one obtains for a condensed medium ($n \approx 3 \times 10^{23}$)

$$l_k \sim (p_0/\sqrt{k}\, Z)\, 10^{-6}\ \text{см}. \tag{38}$$

For $Z = 10$, $E_0 = 10^{18}$ eV $\left(p_0 = \frac{10^{18}}{5 \cdot 10^5} = 2 \cdot 10^{12}\right)$, $k = p_0/2$, this gives $l_k \sim 0.2$ cm.

For $t \gg \tau_0$ one easily obtains the angular distribution of the photons. The width of the angular distribution is given by the function $v_0(\theta, t_1)$ and has the order $\bar{\theta}^2 \sim q t_1$. Furthermore, $\eta_0^2 \sim \eta^2 \sim q\tau$ and therefore one can replace the function $v_0(g^2 \boldsymbol{\eta}_0/p_0^2 + \vartheta,\ t_1)$ by $v_0(\vartheta,\ t)$ and the photon angular distribution is given by

$$W_r'(p_0,\ k,\ \vartheta)\, d\vartheta = v_0(\vartheta, t)\, W_r(p_0, k)\, d\vartheta, \tag{39}$$

i.e., the angular distribution of the photons is the same as the angular distribution of multiply scattered electrons of energy p_0.

We now define

$$\int v(\boldsymbol{\eta},\ \tau;\ \boldsymbol{\eta}_0)\, d\boldsymbol{\eta}_0 = h_1(\boldsymbol{\eta},\ \tau);$$
$$\int v(\boldsymbol{\eta},\ \tau;\ \boldsymbol{\eta}_0)\, \boldsymbol{\eta}_0 d\boldsymbol{\eta}_0 = \mathbf{R}(\boldsymbol{\eta},\ \tau).$$

Since the coefficients of Eq. (24) do not depend on $\boldsymbol{\eta}_0$, the equations for h_1 and $\mathbf{R}$ are identical to (24). The boundary conditions are $h_1(\boldsymbol{\eta},\ 0) = 1$; $\mathbf{R}(\boldsymbol{\eta},\ 0) = \boldsymbol{\eta}$ which can be obtained immediately from (17).

The coefficients of Eq. (24) depend only on $\boldsymbol{\eta}^2$. One can therefore write the solutions in the form

$$h_1(\boldsymbol{\eta},\ \tau) = h(z,\ \tau);$$
$$\mathbf{R}(\boldsymbol{\eta},\ \tau) = \boldsymbol{\eta} g(z,\ \tau), \quad z = \eta^2/2.$$

Here h and g satisfy the equations

$$\frac{\partial h}{\partial \tau} + i(a - bz)\, h = 2zq \left(\frac{\partial^2 h}{\partial z^2} + \frac{1}{z} \frac{\partial h}{\partial z} \right),$$
$$\frac{\partial g}{\partial \tau} + i(a - bz)\, g = 2zq \left(\frac{\partial^2 g}{\partial z^2} + \frac{2}{z} \frac{\partial g}{\partial z} \right). \tag{40}$$

We introduce the functions

$$\varphi_1(z) = \int_0^\infty e^{ik\tau} h(z,\ \tau)\, d\tau; \quad \varphi_2(z) = z \int_0^\infty e^{ik\tau} g(z,\ \tau)\, d\tau. \tag{41}$$

Then (36) becomes

$$W_r = \frac{e^2 k g^2}{2\pi p_0^2} \operatorname{Re} \left\{ K_1 \int_0^\infty \varphi_1 dz + 2K_2 \int_0^\infty \varphi_2 dz \right\}. \tag{42}$$

The equations for φ_1 and φ_2 are obtained by integrating (40) with respect to τ taking into account the initial conditions for h and g:

$$z\varphi_1'' + \varphi_1' + i(\alpha + \beta z)\varphi_1 = -1/2q; \quad (43)$$

$$z\varphi_2'' + i(\alpha + \beta z)\varphi_2 = -z/2q; \quad (44)$$

$$\alpha = \frac{k-a}{2g} = \frac{k}{4p_0(p_0-k)q} > 0, \qquad \beta = \frac{kg^2}{2p_0(p_0-k)q} > 0. \quad (45)$$

Eq. (43) and (44) can be solved by means of the Laplace transformation. Putting

$$u(\lambda) = \int_0^\infty \varphi_1(z)\, e^{-\lambda z}\, dz,$$

we have from (43)

$$u' + \frac{\lambda - i\alpha}{\lambda^2 + i\beta}\, u = \frac{1}{2q\lambda(\lambda^2 + i\beta)}. \quad (46)$$

This gives

$$u(\lambda) = \frac{1}{2q(\lambda_1^2 - \lambda^2)^{1/2}} \left(\frac{\lambda_1 + \lambda}{\lambda_1 - \lambda}\right)^{\mu} \int_\lambda^{\lambda_1} \frac{d\xi}{\xi(\lambda_1^2 - \xi^2)^{1/2}} \left(\frac{\lambda_1 - \xi}{\lambda_1 + \xi}\right)^{\mu},$$

$$\lambda_1 = \sqrt{\beta}\, e^{-i\pi/4}, \quad \mu = (\alpha/2\sqrt{\beta})\, e^{-i\pi/4}. \quad (47)$$

The arbitrary constant ξ_1 is determined by the condition of boundedness of $\varphi_1(z)$ for $z \to \infty$. For this to hold it is necessary that the function $u(\lambda)$ has no singularities on the right half-plane, which gives $\xi_1 = \lambda_1$.

In (42) we need the expression

$$\operatorname{Re} \int_0^\infty \varphi(z)dz = \operatorname*{Re}_{\lambda \to 0} u(\lambda).$$

The function $u(\lambda)$ has a logarithmic singularity at $\lambda = 0$. The above limit therefore depends on the way λ approaches zero. It follows from

$$\operatorname{Re} u(\lambda) = \int_0^\infty e^{-\lambda^0 z} (\operatorname{Re}\varphi_1 \cos \lambda' z - \operatorname{Im}\varphi_1 \sin \lambda' z)\, dz; \qquad \lambda = \lambda^0 + i\lambda'$$

that in order for

$$\int_0^\infty \operatorname{Re}\varphi_1(z)\, dz = \operatorname{Re} u(0)$$

to hold λ has to approach zero along the real axis.

We now separate in the integral (47) the part which is singular at $\xi = 0$. We thus obtain

$$\operatorname*{Re}_{\substack{\lambda \to 0 \\ \arg\lambda = 0}} u(\lambda) = \operatorname*{Re}_{\substack{\lambda \to 0, \\ \arg\lambda = 0}} \frac{1}{2q} \frac{1}{\lambda_1} \left\{ \int_\lambda^{\lambda_1} \frac{d\xi}{\xi} \left[\frac{1}{(\lambda_1^2 - \xi^2)^{1/2}} \left(\frac{\lambda_1 - \xi}{\lambda_1 + \xi}\right)^{\mu} - \frac{1}{\lambda_1} \right] + \frac{1}{\lambda_1} \ln \frac{\lambda_1}{\lambda} \right\}.$$

Since

$$\operatorname*{Re}_{\substack{\lambda \to 0 \\ \arg\lambda = 0}} \frac{1}{\lambda_1^2} \ln \frac{\lambda_1}{\lambda} = \frac{\pi}{4\beta},$$

this equals

$$\operatorname*{Re}_{\substack{\lambda \to 0 \\ \arg\lambda = 0}} u(\lambda) = \frac{\pi}{8\beta q} - \frac{1}{2\beta q} \operatorname{Im} \int_0^1 \frac{dx}{x} \left\{ \frac{1}{(1-x^2)^{1/2}} \left(\frac{1-x}{1+x}\right)^{\mu} - 1 \right\}.$$

Putting $x = \tanh(t/2)$ and separating the imaginary part we find

$$\int_0^\infty \operatorname{Re}\varphi_1 dz = \frac{1}{12q\alpha^2}\, G(s);$$

$$G(s) = 48\, s^2 \left(\frac{\pi}{4} - \frac{1}{2} \int_0^\infty e^{-st} \frac{\sin st}{\sinh st}\, dt \right); \quad (48)$$

$$s = \frac{\alpha}{2\sqrt{2\beta}} = \frac{1}{8g} \sqrt{\frac{k}{p_0(p_0-k)q}}.$$

To solve (44) we introduce

$$f = \varphi_2 - \frac{i}{2q\beta}, \quad zf'' + i(\alpha + \beta z) f = \frac{\alpha}{2q\beta}. \quad (44')$$

We further introduce

$$v(\lambda) = \int e^{-\lambda z} f dz, \quad v' + \frac{2\lambda - i\alpha}{\lambda^2 + i\beta}\, v = \frac{f(0) - \alpha/2q\beta\lambda}{\lambda^2 + i\beta}. \quad (49)$$

Since $\varphi_2(0) = 0$, we have $f(0) = -i/2q\beta$. The solution of (49) is

$$v(\lambda) = -\frac{i}{2q\beta} \frac{1}{\lambda_1^2 - \lambda^2} \times \left(\frac{\lambda_1 + \lambda}{\lambda_1 - \lambda}\right)^{\mu} \int_\lambda^{\lambda_1} \left(1 - \frac{i\alpha}{\xi}\right) \left(\frac{\lambda_1 - \xi}{\lambda_1 + \xi}\right)^{\mu} d\xi.$$

The calculation of $\operatorname{Re} v(0)$ is completely analogous to the above calculation of $\operatorname{Re} u(0)$.

Introducing once more the substitution $\xi/\lambda_1 = x$

and separating the divergent part of the integral we obtain

$$\operatorname*{Re}_{\substack{\lambda\to 0\\ \arg\lambda=0}} v(\lambda) = \frac{1}{2q\beta^2} \operatorname*{Re}_{\substack{\lambda\to 0\\ \arg\lambda=0}} \left\{\lambda_1 \int_0^1 \left(\frac{1-x}{1+x}\right)^{\mu} dx \right.$$

$$\left. - i\alpha \int_0^1 \frac{dx}{x}\left[\left(\frac{1-x}{1+x}\right)^{\mu} - 1\right] - i\alpha \ln\frac{\lambda_1}{\lambda}\right\}.$$

Introducing $x = \tanh(t/2)$ and separating the real part we find

$$\operatorname*{Re}_{\substack{\lambda\to 0\\ \arg\lambda=0}} v(\lambda) = \frac{1}{2q\beta^2}\left\{-\frac{\pi\alpha}{4} + \alpha\int_0^{\infty} e^{-st}\frac{\sin st}{\sinh t}\,dt \right.$$

$$\left. + \frac{1}{2}\sqrt{\frac{\beta}{2}}\int_0^{\infty} e^{-st}\,\frac{\cos st + \sin st}{\sinh\frac{t}{2}}\,dt\right\}.$$

Thus we obtain

$$\int_0^{\infty} \operatorname{Re}\varphi_2 dz = \int_0^{\infty} \operatorname{Re} f dz = \frac{1}{6\alpha\beta q}\Phi(s), \qquad (50)$$

$$\Phi(s) = 3s\int_0^{\infty} e^{-sx}\,\frac{\cos sx + \sin sx}{\cosh^2(x/2)}\,dx$$

$$+ 24s^2\int_0^{\infty} e^{-sx}\frac{\sin sx}{\sinh x}\,dx - 6\pi s^2 \qquad (51)$$

$$= 12s^2\int_0^{\infty}\coth\frac{x}{2}\,e^{-sx}\sin sx\,dx - 6\pi s^2.$$

The function $\Phi(s)$ was introduced in Ref. 3. The functions $\Phi(s)$ and $G(s)$ can be expressed in terms of the logarithmic derivative of the Γ-function*

$$\Phi(s) = 12s^2\{-\operatorname{Im}[\Psi(s-is) + \Psi(s+1-is)] - \pi/2\}$$

$$= 6s - 6\pi s^2 + 24s^3\sum_{k=1}^{\infty}\frac{2}{(s+k)^2+s^2}, \qquad (52)$$

$$G(s) = 48s^2[\pi/4 + \operatorname{Im}\Psi(s+1/2-is)]$$

$$= 12\pi s^2 - 48s^3\sum_{k=0}^{\infty}\frac{1}{(k+s+1/2)^2+s^2}.$$

These formulae are useful for tabulating the functions.

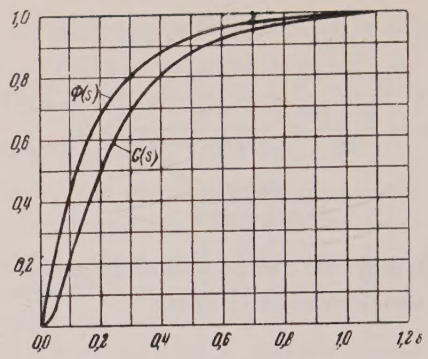

Some values of the functions Φ and G are given in the table, and the functions are plotted in the graph.

s	$\Phi(s)$	$G(s)$
0	0	0
0,05	0,258	0,094
0,1	0,446	0,206
0,2	0,686	0,475
0,3	0,805	0,695
0,4	0,880	0,800
0,5	0,93	0,875
0,6	0,95	0,917
0,7	0,965	0,945
0,8	0,975	0,963
0,9	0,985	0,975
1,0	0,990	0,985
1,5	0,998	0,994
2	0,999	0,998

The asymptotic behavior of Φ and G is: for $s \to 0$

$$\Phi \to 6s;\quad G \to 12\pi s^2;$$

and for $s \to \infty$

$$\Phi \to 1 - 0{,}012/s^4;\quad G \to 1 - 0{,}029/s^4. \qquad (53)$$

For $s \lesssim 1$ we have

$$\eta_0^2 \sim \eta^2 \sim \frac{\operatorname{Re}\int\varphi_2 dz}{\operatorname{Re}\int\varphi_1 dz} \sim \frac{\alpha}{\beta s} \sim \frac{1}{\sqrt{\beta}} = \sqrt{\frac{2q}{b}},$$

This confirms the previously given estimate of the significant values of η^2.

Inserting (48) and (50) into (42) we obtain

$$W_r = \frac{ekg^2}{2\pi p_0^2}\left\{K_1\frac{G}{12q\alpha^2} + 2K_2\frac{\Phi}{6\alpha\beta q}\right\},$$

or, utilizing (24), (34), and (45) this becomes

$$W_r = \frac{2e^2}{3\pi p_0^2 k_{\perp}} B\{k^2 G(s) + 2[p_0^2 + (p_0 - k)^2]\Phi(s)\};$$

$$B = 2\pi Z^2 e^4 n \ln\frac{\theta_2}{\theta_1}. \qquad (54)$$

* Expression (52) has been derived by S. A. Kheifets.

The estimate (26) for θ_2 can be rewritten in the more convenient form

$$\theta_2 \sim (q/b)^{1/4} L^{1/2} = (2\beta)^{-1/4} L^{1/2} \sim L^{1/2}/gs^{1/2}. \quad (55)$$

For $s \lesssim 1$

$$W_r = (2e^2/3\pi p_0^2 k)\, B\,\{k^2 + 2\,[p_0^2 + (p_0 - k)^2]\}. \quad (56)$$

This expression differs from known formulae (*e.g*, Ref. 6) only by a factor of the order of magnitude unity inside the logarithm. The inaccuracy connected with the appearance of this factor is associated with the inaccuracy introduced by the use of the Fokker-Planck method. More accurate formulae can be obtained by solving the integral equation (23). This however, is a rather difficult task.

Since for $s = 1$ both Φ and G have values close to 1, one can obtain a simple formula. For the logarithm one has

$$L = \ln(\theta_2/\theta_1) = \ln(190/Z^{1/3}s^{1/2}). \quad (57)$$

Then W_r is determined for $s \leq 1$; for $s = 1$ the expression becomes the Bethe-Heitler formula.

For $s \ll 1$ we obtain from (53) and (55)

$$W_r = \frac{8e^2}{\pi p_0^2 k} Bs\,[p_0^2 + (p_0 - k)^2] = \frac{e^2}{\pi p_0^2} \sqrt{\frac{B}{k p_0 (p_0 - k)}}\,[p_0^2 + (p_0 - k)^2]\,. \quad (58)$$

In this case the probability is proportional to the square root of the density.

For $k \ll p_0$, (55) yields (see Ref. 3)

$$W_r = (8e^2/3\pi k)\, B\Phi(s)\,. \quad (59)$$

For extremely soft quanta one has to take into account the fact that the dielectric constant differs from unity. The dielectric constant ϵ enters the expressions via the normalization of the operator A; further in the integral over τ in (3) one has to replace $e^{ik\tau}$ by $e^{i\omega\tau}$ where $\omega = k/\sqrt{\epsilon}$. Considering frequencies $\omega \gg \omega_0 = \sqrt{4\pi n Z e^2}$ we have

$$\varepsilon \approx 1 - \omega_0^2/\omega^2;\ \omega = k/\sqrt{\varepsilon} \approx k\,(1 + \omega_0^2/2\omega^2). \quad (60)$$

The change of normalization of A due to ϵ results in the multiplication of W_r by a factor which has a numerical value close to unity; it can therefore be discarded. Thus one takes into account the influence of the dielectric constant by replacing in (45) the quantity α by α'.

$$\alpha' = \frac{\omega - a}{2q} \approx \alpha + \frac{\omega - k}{2q} \approx \alpha\left(1 + p_0^2 \frac{\omega_0^2}{\omega^2}\right). \quad (61)$$

Using (54) we obtain for small k the more general formula

$$W_r = (8e^2/3\pi k)\, B'\Phi(s\gamma)/\gamma;\ \gamma = 1 + p_0^2\omega_0^2/\omega^2, \quad (62)$$

where B' differs from B in that in the logarithm s is replaced by $s\gamma$. For $s\gamma > 1$; $\gamma \gg 1$ we have

$$W_r = (4/3\pi)\, Ze^4 Lk/p_0^2 \quad (63)$$

in accordance with the result obtained by Ter-Mikaelian[7] for this limiting case. Thus, the difficulties associated with the infrared catastrophe do not appear for the case of radiation inside a medium.

We now will give an expression for the radiation length. For that purpose we define a function $\xi(s)$ which describes the change of L with energy:

$$\xi(s) = 1 + \frac{\ln(1/s)}{2\ln(190\,Z^{-1/3})};\quad \xi(s) = 1;\quad 1 \geqslant s \geqslant s_1 \qquad s > 1$$
$$\xi(s) = 2;\quad s_1^{1/2} = Z^{1/3}/190;\quad s < s_1. \quad (64)$$

Here s_1 is the value of s for which $L = 2\ln(190\,Z^{-1/3})$.

From (55), (57), and (64) we have

$$B = 2\pi n e^4 Z^2 \xi(s) \ln\frac{190}{Z^{1/3}} = \frac{\pi}{2t_0'}\frac{137}{}\xi(s)\,,$$
$$1/t_0' = (4ne^4Z^2/137)\ln(190/Z^{1/3})\, t_0' = t_0 mc/\hbar\,, \quad (65)$$

Here t_0 is the radiation length in cm.

From (48) we have for s

$$s = 1{,}4\cdot 10^3\,[kt_0/p_0(p_0 - k)\,\xi(s)]^{1/2}. \quad (66)$$

The probability for radiation in a path length equal equal to one radiation length is

$$W_r t_0' = (\xi(s)/3\,kp_0^2)\,\{k^2 G(s) + 2\,[p_0^2 + (p_0 - k)^2]\,\Phi(s)\}. \quad (67)$$

In lead ($t_0 \approx 0.5$ cm) for $k = p_0/2$ and at $s = 1$ we have $p_0 = 2 \times 10^6 t_0 = 5 \times 10^{11}$ ev; at $s = 0.2$, which corresponds to a deviation of (62) from the Bethe-Heitler formula by 30%, we have $p_0 \approx 1.2 \times 10^{13}$ ev; $s = s_1$ corresponds to an energy $p_0 \approx 10^{15}$ ev.

6. PROBABILITY OF PAIR PRODUCTION

We denote by $W_p(k, p_0)$ the probability of pair

production per unit path length for an electron energy between p_0 and $p_0 + dp_0$; W_p is summed over all possible positron states.

The probability of the inverse reaction to pair production, $\tilde{W}_r$, can be found in a similar manner as W_r; one just has to sum (8) over the negative energy states, and one has to invert the sign of E^{λ_1} in (9). The final formulae can be obtained from the ones written down by replacing $p_0 - k$ by $k - p_0$. So, for example, the quantity $g = (p_0 + p_0 - k)/2$ becomes $\tilde{g} = (p_0 - p_0 + k)/2$.

Thus for the probability $\tilde{W}_r$, which differs from W_p only by a statistical weight factor, one obtains from (55)

$$W_p = \frac{p_0^2}{k^2}\tilde{W}_r = \frac{2e^2}{3\pi k} B\left\{G(\tilde{s}) + 2\left[\frac{p_0^2}{k^2} + \left(1 - \frac{p_0}{k}\right)^2\right]\Phi(\tilde{s})\right\}, \quad (68)$$

$$\tilde{s} = \frac{1}{8}\sqrt{\frac{k}{p_0(k-p_0)B}} = 1{,}4\cdot 10^3\sqrt{\frac{kt_0}{p_0(k-p_0)\xi(\tilde{s})}}.$$

Here $\tilde{s}$ differs from s only by the replacement of $p_0 - k$ by $k - p_0$. The probability for pair creation in a path length equal to one radiation length is

$$W_p t_0' = \frac{\xi(\tilde{s})}{3k}\left\{G(\tilde{s}) + 2\left[\frac{p_0^2}{k^2} + \left(1 - \frac{p_0}{k}\right)^2\right]\Phi(\tilde{s})\right\}. \quad (69)$$

For $\tilde{s} = 1$ this expression becomes the well-known formula for pair creation[6]. For $\tilde{s} \ll 1$ we have

$$W_p t_0' = \frac{4\xi(\tilde{s})}{k}\left\{\frac{p_0^2}{k^2} + \left(1 - \frac{p_0}{k^2}\right)^2\right\}\tilde{s}. \quad (70)$$

The equations (67) and (69) represent the solution to the problem of bremsstrahlung and pair creation at high energies.

The author is grateful to V. M. Galitski for his critical discussion of the results and to S. A. Kheifets for numerical computations.

[1] L. D. Landau and I. Ia. Pomeranchuk, Dokl. Akad. Nauk SSSR **92**, 535 (1953)

[2] L. D. Landau and I. Ia. Pomeranchuk, Dokl. Akad. Nauk SSSR **92**, 735 (1953)

[3] A. B. Migdal, Dokl. Akad. Nauk SSSR **96**, 49 (1954)

[4] A. B. Migdal, Dokl. Akad. Nauk SSSR **105**, 77 (1955)

[5] A. B. Migdal and N. M. Polievktov-Nikoladze, Dokl. Akad. Nauk SSSR **105**, 233 (1955)

[6] B. Rossi and K. Greisen, *Interaction of Cosmic Rays with Matter* (Russ. Transl.) I.I.L, Moscow (1948)

[7] M. L. Ter-Mikaelian, Dokl. Akad. Nauk SSSR **94**, 1033 (1954)

Translated by M. Danos
157

Effect of the Diffuseness of the Nuclear Boundary on Neutron Scattering

V. N. GRIBOV

(Submitted to JETP editor February 14, 1956)
J. Exptl. Theoret. Phys. (U.S.S.R.) 32, 647-652 (April, 1957)

It is shown that the scattering amplitude for a potential with a diffuse boundary whose width is small compared with the wavelength of the incident particle can be expressed in terms of the phase shifts for scattering by a rectangular potential of a smaller radius and three numerical parameters which determine the shape of the potential. The parameters have been computed for potential (1) and the scattering amplitude has been determined. The problem of passage through a barrier whose width is small compared with the wavelength of the incident particle is also considered.

IN THE OPTICAL MODEL of neutron scattering at low energies (up to 3 Mev) a rectangular-well potential has been assumed[1]. In actuality the potential clearly becomes zero in a smooth fashion. The thickness of the diffuse boundary should be of the order of the range of the nuclear forces. In the considered range of energies the wavelength of the incident neutron is large compared with the surface thickness; its wavelength inside the nucleus is of the same order as the surface thickness. Under these circumstances the diffuse boundary can have an appreciable effect on the magnitude of the total cross section and on its dependence on the atomic weight. We shall use in the present work the smallness of the surface thickness compared with the wavelength of incident neutron. It will turn out that under these circumstances it is possible to neglect near the boundary the total and the "centrifugal" energies in the Schrödinger equation. This simplifies the problem considerably and permits the scattering amplitude of a neutron of arbitrary momentum to be expressed in terms of three numerical parameters which are determined solely by the shape of the potential in the boundary region. Furthermore, since the Schrödinger equation in the region of the boundary is then the same as for an s-wave, it is possible to give exact solutions for a number of potentials, as for example

$$V(r) = -K_0^2 [1 + e^{\alpha(r-R_0)}]^{-1} \qquad (1)$$

In this paper these numerical parameters will be calculated for a potential of the form (1).

It is possible to treat in a completely analogous manner the passage of a particle through a barrier whose thickness is small compared to the wavelength of the incoming particle. Section 3 of this paper is devoted to that problem.

1. INFLUENCE OF THE DIFFUSENESS OF THE NUCLEAR BOUNDARY ON NEUTRON SCATTERING

We shall write the Schrödinger equation for the wave-function, multiplied by r, for a neutron of given momentum in the form

$$d^2u_l(r)/dr^2 + [k^2 - V_0(r) - V_1(r) - l(l+1)/r^2]\, u_l(r) = 0. \qquad (2)$$

Here the complex potential $V(r)$ (multiplied by $2m/\hbar^2$) has been split into two parts:

$$V_0(r) = 0 \quad \text{for} \quad r > R_1,$$
$$V_1(r) = 0 \quad \text{for} \quad r < R_1, \quad r > R_2. \qquad (3)$$

We now consider (2) under the condition

$$(k\Delta R)^2 \ll 1, \quad l \sim kR \quad (\Delta R = R_2 - R_1), \qquad (4)$$

which expresses the smallness of the boundary thickness compared with the wavelength of the incoming neutron. We now show that for $R_1 < r < R_2$ it is possible to neglect in (2) the terms k^2 and $l(l+1)/r^2$. The precision of this approximation corresponds to keeping all terms of order up to and including $k\Delta R$. We write (2) in the form

$$U_l(r) = j_l(kr) - \frac{h_l(kr)}{k}\int_0^r j_l(kr')\, V_1(r')\, u_l(r')\, dr' - \frac{j_l(kr)}{k}\int_r^\infty h_l(kr')\, V_1(r')\, u_l(r')\, dr'. \qquad (5)$$

for $r > R_1$

$$j_l(x) = \frac{1}{2i}[h_l(x)\, e^{2i\delta_l} - h_l^*(x)],$$
$$h_l(x) = \sqrt{\frac{\pi x}{2}}\, H^{(1)}_{l+1/2}(x), \qquad (6)$$

where δ_l is the complex scattering amplitude for the potential $V_0(r)$.

Because of (4) one can expand the functions j_l and h_l in the region $R_1 < r < R_2$ in powers of $k(r - R_1)$ and keep only the first two terms. Utilizing the identity

$$j_l' h_l - j_l h_l' = 1,$$

we obtain for (5)

$$u_l(r) = F_l^{(1)} + (r - R_1)\, F_l^{(2)} + \int_0^r (r - r')\, V_1(r')\, u_l(r')\, dr', \tag{7}$$

$$F_l^{(1)} = j_l - \frac{1}{k} j_l h_l [\xi_l + k\Phi_l \eta_l]; \quad F_l^{(2)} = k\chi_l F_l^{(1)}, \tag{8}$$

$$j_l = j_l(kR_1), \quad h_l = h_l(kR_1), \quad \Phi_l = h_l'/h_l; \quad \chi_l = j_l'/j_l,$$

$$\xi_l = \int V_1(r)\, u_l(r)\, dr; \quad \eta_l = \int (r - R_1)\, V_1(r)\, u_l(r)\, dr. \tag{9}$$

Because of the matching conditions $j_l(kR_1)$ is of the order k/k' (k' is the wave vector in the region $r < R_1$), an anomalously small quantity. At the same time j'_l is of order unity. Therefore in the expansion of the products $j_l(kr)h_l(kr')$ and $j_l(kr')h_l(kr)$ terms of order $j_l' h_l'\,(k\Delta R)^2$ have been kept.

Differentiating (7) twice with respect to r one can convince oneself that with the employed precision

$$d^2u_l/dr^2 = V_1(r)\, u_l(r). \tag{10}$$

It then follows that for $R_1 < r < R_2$

$$u_l(r) = A\varphi_1(r) + B\varphi_2(r), \tag{11}$$

where $\varphi_1(r)$ and $\varphi_2(r)$ are two linearly independent solutions of (10), satisfying the boundary conditions

$$\varphi_1(R_1) = 1, \ \varphi_1'(R_1) = 0; \ \varphi_2(R_1) = 0, \ \varphi_2'(R_1) = 1. \tag{12}$$

Assuming $\varphi_1(r)$ and $\varphi_2(r)$ to be known one could obtain the scattering amplitude by matching (11) to the solutions in the regions $r < R_1$ and $r > R_2$. In the usual matching procedure one needs $u_l'(r)$. However the function $u_l(r)$ has been obtained only with a precision to $k\Delta R$, and in the process of differentiation the precision decreases by one order. We therefore use the following procedure. It follows from (7) that

$$A = F_l^{(1)}, \quad B = F_l^{(2)}. \tag{13}$$

It turns out therefore that $u_l(r)$ is expressed in the region $R_1 < r < R_2$ the standard functions and by the quantities ξ_l and η_l which enter into $F_l^{(1)}$ and $F_l^{(2)}$. On the other hand, because of (9) ξ_l and η_l are given by $u_l(r)$ in the region $R_1 < r < R_2$. Equations for ξ_l and η_l are therefore obtained by inserting (11) into (9); taking (13) and (8) into account one has

$$\xi_l = (\alpha_1 + \alpha_2 k\chi_l)\left\{ j_l - \frac{1}{k} j_l h_l [\xi_l + k\Phi_l \eta_l] \right\}, \tag{14}$$

$$\eta_l = (\beta_1 + \beta_2 k\chi_l)\left\{ j_l' - \frac{1}{k} j_l' h_l [\xi_l + k\Phi_l \eta_l] \right\},$$

$$\alpha_{1,2} = \int V_1(r)\, \varphi_{1,2}(r)\, dr;$$
$$\beta_{1,2} = \int (r - R_1)\, V_1(r)\, \varphi_{1,2}(r)\, dr. \tag{15}$$

The scattering amplitude $(\beta_l - 1)/2ik$ can be given in terms of ξ_l and η_l by

$$\beta_l = e^{2i\delta_l} - \frac{2i}{k} \int j_l(kr)\, V_1(r)\, u_l(r)\, dr. \tag{16}$$

Expanding $j_l(kr)$ in powers of $k(r - R_1)$ we obtain

$$\beta_l = e^{2i\delta_l} - \frac{2i}{k} j_l \xi_l - 2i j_l' \eta_l. \tag{17}$$

Inserting (14) in (17) yields

$$\beta_l = \frac{h_l^*}{h_l} \frac{k\chi_l(1 + \alpha_2) + \alpha_1 - k\Phi_l^* [1 - \beta_1 - \beta_2 k\chi_l]}{k\chi_l(1 + \alpha_2) + \alpha_1 - k\Phi_l [1 - \beta_1 - \beta_2 k\chi_l]}. \tag{18}$$

This result can be written in the form

$$\beta_l = \frac{h_l^*}{h_l} \frac{(k\chi_l)_{\text{эф}} - k\Phi_l^*}{(k\chi_l)_{\text{эф}} - k\Phi_l}, \tag{19}$$

$$(k\chi_l)_{\text{эф}} = \frac{k\chi_l(1 + \alpha_2) + \alpha_1}{1 - \beta_1 - \beta_2 k\chi_l}.$$

Using the fact that $\varphi_1'\varphi_2 - \varphi_2'\varphi_1$ is a constant it is easy to show that the parameters $\alpha_{1,2}$ and $\beta_{1,2}$

satisfy the relationship

$$\alpha_1\beta_2 - \alpha_2\beta_1 + \alpha_2 - \beta_1 = 0. \tag{20}$$

The scattering amplitude is thus given by the scattering phase shifts due to $V_0(r)$ [see (8) and (6)] and three parameters which do not depend on k or l.

2. SCATTERING FROM A POTENTIAL OF THE FORM (1)*

Choosing R_1 and R_2 such that $e^{\alpha(R_1 - R_0)}$ and $e^{\alpha(R_0 - R_2)}$ are negligible, $V_0(r)$ can be considered to be a square well, and therefore

$$\begin{aligned} k\chi_l &= K' f_l(K'R_1), \\ f_l(x) &= [\sqrt{x}\, J_{l+1/2}(x)]' / \sqrt{x}\, J_{l+1/2}(x), \\ K' &= \sqrt{K_0^2 + k^2}. \end{aligned} \tag{21}$$

We now have to obtain $\alpha_{1,2}$ and $\beta_{1,2}$. From (15), (10) and (12) we find

$$\begin{aligned} \alpha_1 &= \varphi_1'(R_2); \quad \alpha_2 = \varphi_2'(R_2) - 1, \\ \beta_1 &= \varphi_1'(R_2)\,\Delta R - \varphi_1(R_2) + 1; \\ \beta_2 &= \varphi_2'(R_2)\,\Delta R - \varphi_2(R_2). \end{aligned} \tag{22}$$

With the considered potential $V(r)$ one can solve Eq. (10) exactly[2]. In the actual cases the imaginary part of the potential is small[1]. One can therefore neglect the absorption in the diffuse boundary. This means that one can consider the quantities $K_0\Delta R$ and K_0/α to be real. We shall assume this from now on.

Neglecting terms of the order $e^{\alpha(R_1 - R_0)}$ one obtains easily

$$\begin{aligned} \varphi_1(r) &= \frac{1}{2}\left\{e^{iK_0(r-R_1)}\, F\left(i\frac{K_0}{\alpha},\ i\frac{K_0}{\alpha},\ 1 + 2i\frac{K_0}{\alpha},\ -e^{\alpha(r-R_0)}\right) + \text{c.c.}\right\}, \\ \varphi_2(r) &= \frac{1}{2i}\left\{e^{iK_0(r-R_1)}\, F\left(i\frac{K_0}{\alpha},\ i\frac{K_0}{\alpha},\ 1 + 2i\frac{K_0}{\alpha},\ -e^{\alpha(r-R_1)}\right) - \text{c.c.}\right\} \end{aligned} \tag{23}$$

Here $F(\alpha, \beta, \gamma; z)$ is the hypergeometric series. Neglecting terms of the order $e^{\alpha(R_0 - R_2)}$ and utilizing the formulae

$$\begin{aligned} F(\alpha, \beta, \gamma; z) &= \frac{\Gamma(\gamma)\Gamma(\beta-\alpha)}{\Gamma(\beta)\Gamma(\gamma-\alpha)} F\left(\alpha, \alpha+1-\gamma, \alpha+1-\beta; \frac{1}{z}\right)(-z)^{-\alpha} \\ &+ \frac{\Gamma(\gamma)\Gamma(\alpha-\beta)}{\Gamma(\alpha)\Gamma(\gamma-\beta)} F\left(\beta, \beta+1-\gamma, \beta+1-\alpha; \frac{1}{z}\right)(-z)^{-\beta}, \\ F(i\gamma, i\gamma, 1+2i\gamma; z) &\sim \frac{\Gamma(1+2i\gamma)}{\Gamma(i\gamma)\Gamma(1+i\gamma)}(-z)^{-i\gamma}\ln(-z) \\ &+ \frac{\Gamma(1+2i\gamma)}{\Gamma(i\gamma)\Gamma(1+i\gamma)}[2\psi(1) - \psi(i\gamma) - \psi(1+i\gamma)](-z)^{-i\gamma} \quad \text{at} \quad z\to\infty, \\ \psi(x) &= \Gamma'(x)/\Gamma(x), \end{aligned}$$

we obtain from (23) for $r \approx R_2$

$$\begin{aligned} \varphi_1(r) = \sqrt{\frac{\tanh\pi\gamma}{\pi\gamma}}\Big\{&-[\gamma\Delta_1 + K_0(r-R_0)]\sin[K_0(R_0-R_1)+\Delta] \\ &+ \frac{\gamma\pi}{\tanh\gamma\pi}\cos[K_0(R_0-R_1)+\Delta]\Big\}, \end{aligned} \tag{24}$$

* The author is grateful to L. D. Landau for pointing out the importance of investigating potentials of this form.

$$\varphi_2(r) = \frac{1}{K_0}\sqrt{\frac{\tanh \pi\gamma}{\pi\gamma}}\left\{[\gamma\Delta_1 + K_0(r-R_0)]\cos[K_0(R_0-R_1)+\Delta] - \frac{\gamma\pi}{\tanh\gamma\pi}\sin[K_0(R_0-R_1)+\Delta]\right\}, \tag{25}$$

$$\Delta = \arg\frac{\Gamma(1+2i\gamma)}{\Gamma^2(1+i\gamma)}; \quad \Delta_1 = 2\psi(1) - 2\mathrm{Re}\,\psi(1+i\gamma),\ \gamma = K_0/\alpha.$$

The solution to the problem is obtained by inserting (24) into (22) and using (19). Before writing the final formulae we note that we have to neglect k^2 compared to K_0^2 since in the actual case $K_0\Delta R \sim 1$; in other words, we take $K_0 \approx K'$ since we have already neglected terms of the order $(k\Delta R)^2$ compared to unity.

The following expressions occur when substituting (24), (22) and (21) into (19):

$$f_l(K'R_1)\cos[K'(R_0-R_1)+\Delta] - \sin[K'(R_0-R_1)+\Delta],$$

$$f_l(K'R_1)\sin[K'(R_0-R_1)+\Delta] + \cos[K'(R_0-R_1)+\Delta].$$

We consider the first of these expressions. It is proportional to

$$[\sqrt{K'R_1}J_{l+1/2}(K'R_1)]'\cos[K'R_0+\Delta-K'R_1] - \sqrt{K'R_1}J_{l+1/2}(K'R_1)\sin[K'R_0+\Delta-K'R_1].$$

The function $\sqrt{x}J_{l+1/2}(x)$ has the form

$$C_l(x)\sin\left(x-\frac{l\pi}{2}\right) + \tilde{C}_l(x)\cos\left(x-\frac{l\pi}{2}\right),$$

where $C_l(x)$ and $\tilde{C}_l$ are of the order 1 for $x > l$. In the present case $x = K'R_1 \gg kR_1 \sim l$. Further,

$$[\sqrt{x}J_{l+1/2}(x)]' = C_l(x)\cos(x-l\pi/2) - \tilde{C}_l(x)\sin(x-l\pi/2) + C_l'(x)\sin(x-l\pi/2) + \tilde{C}_l'(x)\cos(x-l\pi/2).$$

Here

$$C_l'(x) \sim \tilde{C}_l'(x) \sim l^2/x^2 \sim l^2(kR)^{-2}(k/K')^2 \sim k^2/K'^2 \ll 1,$$

and they therefore can be neglected. Our expression therefore equals

$$[\sqrt{K'R_0+\Delta}J_{l+1/2}(K'R_0+\Delta)]' / \sqrt{K'R_1}J_{l+1/2}(K'R_1).$$

The second of the two expressions can be similarly evaluated. In this manner we obtain

$$\frac{1}{(k\chi_l)_{\partial\Phi}} = -\frac{\Delta_1}{\alpha} + R_0 - R_1 + \frac{\gamma\pi}{\tanh\gamma\pi}\frac{1}{f_l(K'R_0+\Delta)}. \tag{26}$$

Taking into account

$$k^2\Delta R/K' \sim (k\Delta R)^2/K'\Delta R \sim (k\Delta R)^2 \ll 1,$$

we obtain by inserting (26) into (19)

$$\beta_l = \frac{h_l^*(x_1)}{h_l(x_1)}\left[\frac{\tanh\pi\gamma}{\pi\gamma}K'f_l(x) - k\Phi_l^*(x_1)\right] \Big/ \left[\frac{\tanh\pi\gamma}{\pi\gamma}K'f_l(x) - k\Phi_l(x_1)\right], \tag{27}$$

$$x = K'R_0 + \Delta, \quad x_1 = kR_0 - k\Delta/\alpha.$$

It has been shown in Ref. 1 that the optical model not only gives the scattering amplitude but also gives the ratio of the average value of the widths of the levels of the compound nucleus to the average level spacing. For our diffuse boundary potential this ratio is

$$\frac{\Gamma}{D} = \frac{2}{\pi} \operatorname{Im} \left\{ k \Big/ \left[\frac{\tanh \pi\gamma}{\pi\gamma} \cot (K'R_0 + \Delta) - ik \right] \right\}. \quad (28)$$

We note that if one assumes that γ does not depend on A and is of order 1, then $\tanh \pi\gamma/\pi\gamma \sim 1/3$ and Γ/D as a function of A has higher and steeper resonances than in the case of a rectangular well potential.

3. TRANSMISSION COEFFICIENT FOR THE PENETRATION OF POTENTIAL BARRIERS AT LOW ENERGIES.

The above problem of the influence of the diffuseness of the nuclear boundary on neutron scattering is formally very closely related to the passage of particles through potential barriers whose thickness is considerably smaller than the wavelength of the incoming particle. We arrive at this problem by putting $V_0(r) = 0$, $l = 0$, and by dropping the boundary condition $u_l(0) = 0$. This has the effect that one has to replace $j_l(kr)$ and $h_l(kr)$ in (5) by e^{-ikr} and $(i/2)e^{ikr}$ respectively if the particle approaches from the direction of positive r.

To obtain the transmission coefficients we consider (5) with the above substitutions. For $r < R_1$ we obtain

$$u(r) = e^{-ikr} \left[1 + \frac{1}{2ik} \int e^{ikr} V_1(r)\, dr \right]. \quad (29)$$

By definition, the transmission coefficient is given by

$$D = \left| 1 + \frac{1}{2ik} \int e^{ikr} V_1(r)\, dr \right|^2. \quad (30)$$

Expanding e^{ikr} in powers of $k(r - R_1)$ we have

$$D = \left| 1 + \frac{e^{ikR_1}}{2ik} \xi + \frac{e^{ikR_1}}{2i} \eta \right|^2 \quad (31)$$

where ξ and η are quantities analogous to the quantities ξ_l and η_l.

We now obtain ξ and η up to the same precision and in a similar manner like in Section 1. Inserting these into (31) we have

$$D = k^2/(k^2a^2 + b^2), \quad a = 1 + \alpha_2 - \beta_1, \quad b = \alpha_1/2.$$

The parameters $\alpha_{1,2}$ and $\beta_{1,2}$ are obtained according to (15).

The author wishes to express his deep gratitude to K. A. Ter-Martirosian for helpful suggestions in the course of this work.

---

[1] Feshbach, Porter and Weisskopf, Phys. Rev. 96, 448 (1954)

[2] L. Landau and E. Lifshitz, *Quantum Mechanics*, OGIZ, Moscow (1948)

Translated by M. Danos
158

Hydrodynamics of Solutions of Two Superfluid Liquids

I. M. KHALATNIKOV
Institute for Physical Problems, Academy of Sciences, USSR

(Submitted to JETP editor February 15, 1956)
(J. Exptl. Theoret. Phys. (U.S.S.R.) 32, 653-657 (April, 1957)

The hydrodynamical equations are obtained for solutions of two superfluid liquids on the basis of the conservation laws. In this case, three independent motions are possible in the liquid: a normal one with velocity v_n and two superfluid (potential) ones with velocities v_s' and v_s''. Three different types of sound vibrations can be propagated in such solutions.

WE CONSIDER here two superfluid liquids, for example, liquid He^4 and liquid He^6. In such a case, three possible motions are possible (in principle) in the liquid: the normal motion with velocity $\mathbf{v}_n$, and two superfluid motions with velocities $\mathbf{v}_s'$ and $\mathbf{v}_s''$. We shall show how the equations of this three-velocity hydrodynamics can be obtained from the conservation laws and from the principle of the potential character of the superfluid motion. In the derivation of these equations, we shall consider the liquid in a frame of reference in which the normal (non-superfluid) portion of the liquid is at rest. In this system, the total energy of the liquid can be written in the form

$$E = \rho \mathbf{v}_n^2/2 + (\mathbf{p}' + \mathbf{p}'')\,\mathbf{v}_n + \varepsilon. \tag{1}$$

Here we have adopted the following notation: ρ is the density of the liquid, $\mathbf{p}'$ and $\mathbf{p}''$ the respective momenta of the two superfluid motions, and ε the internal energy of the liquid. The latter is a function both of the thermodynamic variables density ρ_1, ρ_2 and entropy S, and of the relative velocities $\mathbf{v}_s' - \mathbf{v}_n$ and $\mathbf{v}_s'' - \mathbf{v}_n$ and is defined by a thermodynamic identity.

The form of the thermodynamic identity is established in the following way. We recall the expression for the total energy E which we used in the derivation of the hydrodynamical equations for He II[1]:

$$E = \rho \mathbf{v}_s^2/2 + \mathbf{p}'\mathbf{v}_s + \varepsilon'. \tag{2}$$

Here $\mathbf{p}'$ is the momentum of the relative motion in the reference system, which moves with velocity $\mathbf{v}_s$; it is expressed in terms of the total momentum of the liquid j:

$$\mathbf{p}' = \mathbf{j} - \rho \mathbf{v}_s. \tag{3}$$

The energy is defined by the thermodynamic identity

$$d\varepsilon' = \mu' d\rho + TdS + (\mathbf{v}_n - \mathbf{v}_s,\ d\mathbf{p}'). \tag{4}$$

If we replace the momentum $\mathbf{p}'$ by the momentum p in the reference system which moves with velocity $\mathbf{v}_n$:

$$\mathbf{p} = \mathbf{j} - \rho \mathbf{v}_n = \mathbf{p}' + \rho(\mathbf{v}_s - \mathbf{v}_n), \tag{5}$$

the expression for the energy E reduces to the form

$$E = \rho \mathbf{v}_n^2/2 + \mathbf{p}\mathbf{v}_n + \varepsilon, \tag{6}$$

where the internal energy ε is already defined by a different identity than Eq. (4). namely,

$$d\varepsilon = \mu d\rho + TdS + \mathbf{p}d(\mathbf{v}_s - \mathbf{v}_n) \tag{7}$$

with the chemical potential μ connected with μ' by the relation

$$\mu = \mu' + (\mathbf{v}_n - \mathbf{v}_s)^2/2.$$

Thus, when we transform to the reference system associated with the normal motion, we must regard the internal energy ε as a function of the density, entropy and relative velocity. In this case, Eq. (7) is also a definition of the momentum of the relative motion p.

In the case of three-velocity hydrodynamics, the thermodynamic identity is written, in analogy with Eq. (7), as

$$\begin{aligned} d\varepsilon = {} & \mu_1 d\rho_1 + \mu_2 d\rho_2 + TdS \\ & + \mathbf{p}'d(\mathbf{v}_s' - \mathbf{v}_n) + \mathbf{p}''d(\mathbf{v}_s'' - \mathbf{v}_n), \end{aligned} \tag{8}$$

μ_1 and μ_2 are the chemical potentials of the components of the solution. The densities ρ_1 and ρ_2 are expressed in terms of the concentration c of the solution

$$\rho_1 = \rho c, \quad \rho_2 = \rho(1 - c). \tag{9}$$

We now write down the conservation laws for the energy E, the momentum of the liquid $\mathbf{j} = \mathbf{p}' + \mathbf{p}'' + \mathbf{v}_n$, the mass, and the entropy. For the energy we have:

$$E + \operatorname{div} \mathbf{Q} = 0, \tag{10}$$

Q is the vector flow of energy; its form is unknown

to us at present. The time derivative of the momentum j must be equal to the divergence of some tensor:

$$\dot{j}_i + \partial \Pi_{ik} / \partial x_k = 0. \tag{11}$$

The form of the symmetric tensor of the momentum flux Π_{ik} can be established as was done in the derivation of the hydrodynamical equations of a superfluid [1]. We represent the tensor Π_{ik} in terms of its value π_{ik} in a reference system moving with velocity $\mathbf{v}_n$:

$$\begin{aligned}\Pi_{ik} = &\rho v_{ni} v_{nk} + (p_i' + p_i'') v_{nk} \\ &+ (p_k' + p_k'') v_{ni} + \pi_{ik}.\end{aligned} \tag{12}$$

We shall give the explicit form of the tensor π_{ik} below.

The mass conservation laws are written as equations of continuity:

$$\begin{aligned}\dot{\rho}_1 + \operatorname{div}(\mathbf{p}' + \rho_1 \mathbf{v}_n + \mathbf{g}') = 0, \\ \dot{\rho}_2 + \operatorname{div}(\mathbf{p}'' + \rho_2 \mathbf{v}_n + \mathbf{g}'') = 0,\end{aligned} \tag{13}$$

these contain the unknown vectors $\mathbf{g}'$ and $\mathbf{g}''$. Inasmuch as the equation of continuity holds for all liquids,

$$\dot{\rho} + \operatorname{div} \mathbf{j} = 0, \tag{14}$$

the following relation exists between $\mathbf{g}'$ and $\mathbf{g}''$:

$$\mathbf{g}' + \mathbf{g}'' = 0. \tag{15}$$

We write the entropy equation of continuity in the form

$$\dot{S} + \operatorname{div}(S\mathbf{v}_n + \mathbf{f}) = 0 \tag{16}$$

with the unknown vector $\mathbf{f}$ in the energy flux.

We represent the equations for superfluid motion in such a fashion that the conditions $\operatorname{curl} \mathbf{v}_s' = 0$ and $\mathbf{v}_s'' = 0$ are satisfied:

$$\begin{aligned}\dot{\mathbf{v}}_s' + \nabla\left(\varphi_1 - \frac{\mathbf{v}_n^2}{2} + \mathbf{v}_n \mathbf{v}_s'\right) = 0, \\ \dot{\mathbf{v}}_s'' + \nabla\left(\varphi_2 - \frac{\mathbf{v}_n^2}{2} + \mathbf{v}_n \mathbf{v}_s''\right) = 0.\end{aligned} \tag{17}$$

Here φ_1 and φ_2 are unknown functions at present.

Our problem now is this: using the conservation laws, to find the form of the unknown functions. For this purpose, we compute the time derivative of E and, with the aid of the hydrodynamical equations (13), (16) and (17), eliminate all terms that represent total divergences. In accord with Eq. (1), we have:

$$\begin{aligned}\dot{E} = {}&{}^1/_2 \dot{\rho}' \mathbf{v}_n^2 + \rho \dot{\mathbf{v}}_n \mathbf{v}_n + (\dot{\mathbf{p}}' + \dot{\mathbf{p}}'') \mathbf{v}_n + (\mathbf{p}' + \mathbf{p}'') \dot{\mathbf{v}}_n + \mu_1 \dot{\rho}_1 + \mu_2 \dot{\rho}_2 \\ &+ T\dot{S} + (\mathbf{p}', \dot{\mathbf{v}}_s' - \dot{\mathbf{v}}_n) + (\mathbf{p}'', \dot{\mathbf{v}}_s'' - \dot{\mathbf{v}}_n) = \\ = {}&- {}^1/_2 \dot{\rho} \mathbf{v}_n^2 + \mathbf{j} \dot{\mathbf{v}}_n + \mathbf{p}' \dot{\mathbf{v}}_s' + \mathbf{p}'' \dot{\mathbf{v}}_s'' + \mu_1 \dot{\rho}_1 + \mu_2 \dot{\rho}_2 + T\dot{S}.\end{aligned}$$

We further represent all the time derivatives here with the help of Eqs. (13)–(17):

$$\begin{aligned}\dot{E} = &- (\mu_1 - \mathbf{v}_n^2/2) \operatorname{div}(\mathbf{p}' + \rho_1 \mathbf{v}_n + \mathbf{g}') - (\mu_2 - \mathbf{v}_n^2/2) \operatorname{div}(\mathbf{p}'' + \rho_2 \mathbf{v}_n + \mathbf{g}'') \\ &- \mathbf{p}' \nabla(\varphi_1 - \mathbf{v}_n^2/2 + \mathbf{v}_n \mathbf{v}_s') - \mathbf{p}'' \nabla(\varphi_2 - \mathbf{v}_n^2/2 + \mathbf{v}_n \mathbf{v}_s'') - v_{ni} \partial \Pi_{ik} / \partial x_k \\ &- T \operatorname{div}(S\mathbf{v}_n + \mathbf{f}).\end{aligned}$$

Eliminating all total divergences, we ultimately get

$$\begin{aligned}\dot{E} = - \operatorname{div} \Big\{ &(\mathbf{p}' + \rho_1 \mathbf{v}_n + \mathbf{g}') \left(\mu_1 - \frac{\mathbf{v}_n^2}{2}\right) + (\mathbf{p}'' + \rho_2 \mathbf{v}_n + \mathbf{g}'') \left(\mu_2 - \frac{\mathbf{v}_n^2}{2}\right) \\ &+ T(S\mathbf{v}_n + \mathbf{f}) \Big\} + \Big\{ - \rho \mathbf{v}_n \nabla \frac{\mathbf{v}_n^2}{2} + \mathbf{v}_n (\rho_1 \nabla \mu_1 + \rho_2 \nabla \mu_2 + S \nabla T) \\ &- v_{ni} \frac{\partial \Pi_{ik}}{\partial x_k} - \mathbf{p}' \nabla(\mathbf{v}_n \mathbf{v}_s') - \mathbf{p}'' \nabla(\mathbf{v}_n \mathbf{v}_s'') \Big\} + \{ \mathbf{p}' \nabla(\mu_1 - \varphi_1) \\ &+ \mathbf{p}'' \nabla(\mu_2 - \varphi_2) + \mathbf{g}' \nabla \mu_1 + \mathbf{g}'' \nabla \mu_2 + \mathbf{f} \nabla T \}.\end{aligned} \tag{18}$$

We now take up the transformation of the second brace in Eq. (18). In this case it is appropiate to represent the tensor π_{ik} in the following fashion ($\mathfrak{N}_{ik}$ is an unknown tensor):

$$\pi_{ik} = (-\varepsilon + \mu_1 \rho_1 + \mu_2 \rho_2 + TS)\,\delta_{ik} + \mathfrak{M}_{ik}. \quad (19)$$

After substitution of Π_{ik} in the form (12) with this π_{ik} the second brace reduces to

$$-\operatorname{div}\{(\mathbf{j}\,\mathbf{v}_n)\,\mathbf{v}_n + \mathbf{p}'(\mathbf{v}_n\mathbf{v}_s') + \mathbf{p}''(\mathbf{v}_n\mathbf{v}_s'')\}$$
$$- v_{ni}\frac{\partial}{\partial x_k}\{\mathfrak{M}_{ik} - p_k'(v_{si}' - v_{ni}) - p_k''(v_{si}'' - v_{ni})\}.$$

Making use of this result, we get

$$\dot{E} = -\operatorname{div}\{(\mathbf{p}' + \rho_1\mathbf{v}_n + \mathbf{g}')(\mu_1 - \mathbf{v}_n^2/2) + (\mathbf{p}'' + \rho_2\mathbf{v}_n + \mathbf{g}'')(\mu_2 - \mathbf{v}_n^2/2)$$
$$+ \mathbf{v}_n(\mathbf{j}\mathbf{v}_n) + \mathbf{p}'(\mathbf{v}_n\mathbf{v}_s') + \mathbf{p}''(\mathbf{v}_n\mathbf{v}_s'')\} + \{\mathbf{p}'\nabla(\mu_1 - \varphi_1) + \mathbf{p}''\nabla(\mu_2 - \varphi_2) \quad (20)$$
$$+ \mathbf{g}'\nabla(\mu_1 - \mu_2) + \mathbf{f}\nabla T + v_{ni}\frac{\partial}{\partial x_k}[p_k'(v_{si}' - v_{ni}) + p_k''(v_{si}'' - v_{ni}) - \mathfrak{M}_{ik}]\Big\}.$$

In the absence of dissipation, the quantities φ_1, φ_2, $\mathbf{f}$, $\mathbf{g}'$ and $\mathfrak{M}_{ik}$ can depend only on the thermodynamic variables and the velocities, and cannot depend on their time and space derivatives. Examining isolated cases, such as: temperature equal to zero, small concentration of one of the components, *etc.*, we can establish the form of the unknown functions uniquely. To simplify the problem, we draw upon some physical considerations. Thus, in a superfluid, all the entropy is contained in the thermal excitations which partake only of the normal motion. Therefore, the entropy flow is equal to the product $S\mathbf{v}_n$, and the vector $\mathbf{f}$ (which we introduced into the entropy flow) must be set equal to zero. So far as the tensor $\mathfrak{M}_{ik}$ is concerned, we also know its form to a certain degree. Actually, if we introduce the liquid densities connected with the normal (ρ_n) and the two superfluid motions (ρ_s' and ρ_s''), then we can write the tensor Π_{ik} in the form

$$\Pi_{ik} = \rho_n v_{ni} v_{nk} + \rho_s' v_{si}' v_{sk}' + \rho_s'' v_{si}'' v_{sk}'' + p\delta_{ik} \quad (21)$$

(p = pressure).

The sum $\rho_n + \rho_s' + \rho_s''$ is equal to the total density of the liquid. The momenta of the relative motion are then equal to

$$\mathbf{p}' = \rho_s'(\mathbf{v}_s' - \mathbf{v}_n), \quad \mathbf{p}'' = \rho_s''(\mathbf{v}_s'' - \mathbf{v}_n). \quad (22)$$

Taking (22) and (23) into account, we find that the tensor $\mathfrak{M}_{ik}$ is equal to*

$$\mathfrak{M}_{ik} = p_k'(v_{si}' - v_{ni}) + p_k''(v_{si}'' - v_{ni}). \quad (23)$$

It now remains for us only to consider the combination of the remaining terms in (20), which do not have the form of a divergence:

$$\mathbf{p}'\nabla(\varphi_1 - \mu_1) + \mathbf{p}''\nabla(\varphi_2 - \mu_2) + \mathbf{g}'\nabla(\mu_1 - \mu_2).$$

For this purpose, we make use of the limiting case in which the concentration of one of the components is close to zero. Then, as is well known (see Ref. 2) this component will partake entirely of the normal motion, *i.e.*, one of the momenta of the superfluid motion ($\mathbf{p}'$) will be strictly equal to zero, except in the case in which and $\mathbf{g}' = -\mathbf{g}'' = 0$ (see Ref. 2). Inasmuch as the vector $\mathbf{g}'$ is equal to zero in this case for all values of the densities of the components, then, by means of simple calculations, we can conclude that this condition is always satisfied. In similar fashion, we find

$$\mu_1 = \varphi_1, \quad \mu_2 = \varphi_2, \quad \mathbf{g}' = 0. \quad (24)$$

Taking (21), (23) and (24) into account, we write down the final form of the hydrodynamical equations for the solution of two superfluid liquids. The equations of continuity:

$$\dot{\rho}_1 + \operatorname{div}(\mathbf{p}' + \rho_1\mathbf{v}_n) = 0,$$
$$\dot{\rho}_2 + \operatorname{div}(\mathbf{p}'' + \rho_2\mathbf{v}_n) = 0. \quad (25)$$

One of these can be substituted in the equation of continuity for the entire liquid:

$$\dot{\rho} + \operatorname{div}\mathbf{j} = 0, \quad \mathbf{j} = \rho\mathbf{v}_n + \mathbf{p}' + \mathbf{p}''. \quad (26)$$

The equation of continuity for the entropy:

$$\dot{S} + \operatorname{div} S\mathbf{v}_n = 0. \quad (27)$$

The equations of superfluid motion:

$$\dot{\mathbf{v}}_s' + \nabla\left(\mu_1 - \frac{\mathbf{v}_n^2}{2} + \mathbf{v}_n\mathbf{v}_s'\right) = 0,$$
$$\dot{\mathbf{v}}_s'' + \nabla\left(\mu_2 - \frac{\mathbf{v}_n^2}{2} + \mathbf{v}_n\mathbf{v}_s''\right) = 0. \quad (28)$$

Equation of motion of the liquid as a whole:

$$j_i + \partial\Pi_{ik}/\partial x_k = 0, \quad (29)$$

where the momentum flux tensor is equal to

$$\Pi_{ik} = \rho v_{ni} v_{nk} + (p_k' v_{si}' + v_{nk} p_i') + (p_k'' v_{si}'' + v_{nk} p_i'') + p\delta_{ik}, \quad (30)$$

*It is easy to see that the tensor $\mathfrak{M}_{ik}$ is symmetric, because of (22).

and the pressure is equal to

$$p = -\varepsilon + TS + \mu_1 \rho_1 + \mu_2 \rho_2. \tag{31}$$

Taking the thermodynamical identity (7) into consideration, we then obtain

$$\begin{aligned} dp &= \rho_1 d\mu_1 + \rho_2 d\mu_2 \\ &+ SdT - \mathbf{p}' d(\mathbf{v}_s' - \mathbf{v}_n) - \mathbf{p}'' d(\mathbf{v}_s'' - \mathbf{v}_n). \end{aligned} \tag{32}$$

Finally, the law of conservation of energy takes the form

$$\begin{aligned} &\dot{E} + \operatorname{div} \mathbf{Q} = 0, \\ &\mathbf{Q} = (\mathbf{p}' + \rho_1 \mathbf{v}_n)\left(\mu_1 - \frac{\mathbf{v}_n^2}{2}\right) \\ &+ (\mathbf{p}'' + \rho_2 \mathbf{v}_n)\left(\mu_2 - \frac{\mathbf{v}_n^2}{2}\right) + \mathbf{v}_n (\mathbf{j}\mathbf{v}_n) \\ &+ \mathbf{p}' (\mathbf{v}_n \mathbf{v}_s') + \mathbf{p}'' (\mathbf{v}_n \mathbf{v}_s''). \end{aligned} \tag{33}$$

For low velocities, we find the dependence of the chemical potentials on the relative velocities from Eq. (32):

$$\begin{aligned} \mu_1 &= \mu_{10} + \frac{\rho_s'}{2\rho} (\mathbf{v}_s' - \mathbf{v}_n)^2, \\ \mu_2 &= \mu_{20} + \frac{\rho_s''}{2\rho} (\mathbf{v}_s'' - \mathbf{v}_n)^2. \end{aligned} \tag{34}$$

Here μ_{10} and μ_{20} are the velocity-independent parts of the chemical potentials.

The presence of three motions in solutions of superconducting liquids can lead to a series of singular phenomena. Thus, for example, in such solutions propagation of sound vibrations of three types is possible, with different velocities. In addition to ordinary sound waves, propagation of two types of waves is possible, in which vibrations of temperature and solution concentration occur.

In conclusion, we note that we know of only two superconducting liquids: liquid He^4 and liquid He^6. Unfortunately, the isotope of He^6 is short-lived (half life = 0.8 sec), and this circumstance naturally makes difficult the possibility of experiments with solutions of these liquids.

I consider it my duty to express my deep gratitude to Academician L. D. Landau for valuable discussions.

[1] I. M. Khaltnikov, J. Exptl. Theoret. Phys. (U.S.S.R.) **23**, 169 (1952).

[2] L. Landau, and I. Pomeranchuk, Dokl. Akad. Nauk SSSR **59**, 669 (1948).

Translated by R. T. Beyer
159

Some Problems Related to the Statistical Theory of Multiple Production of Particles

V. M. MAKSIMENKO AND I. L. ROZENTAL'
The P. N. Lebedev Physical Institute of the Academy of Sciences USSR

(Submitted to the JETP editor February 16, 1956)
J. Exptl. Theoret. Phys. (U.S.S.R.) **32**, 657-666 (April, 1957)

The exact values of the statistical weights of a system consisting of N particles of arbitrary masses are computed by taking into account the laws of conservation of energy and momentum. The solution is expressed as a series expansion in terms of the ratio $\nu_i = \frac{M_i}{E_0}$ (M is the mass of the particle and E_0 is the total energy of the system). Since the obtained series converges slowly, another expansion in the form of a power series of the total kinetic energy of the system to the total mass of the heavy particles has been obtained for values of ν_i which are close to unity.

THE TRANSITION PROBABILITY of a system from one quantum state into another is determined by the product of the modulus of the matrix element squared and the statistical weight of the final state. Based on the fact that for a sufficiently large number of particles the latter factor is characterized by a sharp maximum, Fermi[1] expressed the idea that the basic outlines of the processes that lead to the formation of multiple particles are determined by statistical factors. A similar view concerning multiple processes can be extended somewhat by taking into account the effect of change of the matrix element. The latter effect, however, should be computed rather approximately, while the second, statistical factor, must be computed with maximum possible accuracy*.

It is known that the statistical term consists of three factors. The first factor $(V/8\pi^3\hbar^3)^{N-1}$ (N is the number of particles) is determined by the volume V in the coordinate space; the second term is determined by the laws of conservation of momentum and isotopic spin and is computed by means of standard rules of quantum mechanics; the third factor constitutes the density of states $dQ_N(E_0)/dE_0 = W_N(E_0)$ in momentum space ($Q_N(E_0)$ is the volume of the system in momentum space, determined by the laws of conservation of energy and momentum). The present work deals with the problem of computing the accurate value of $W_N(E_0)$. Only certain special values were known until now: 1) for non relativistic particles, with only approximate allowance for the law of conservation of momentum[1]; 2) an accurate expression for $W_N(E_0)$ for $N = 2$;[3] 3) an accurate expression for two extreme cases: all particles are either non relativistic or highly relativistic[4,5]; 4) an accurate expression for the case when the mass of one particle is arbitrary and the masses of the remaining two or three particles are zero[6].

Computation of the expression $W_N(E_0)$ is important not only to the statistical theory described in the above discussion but also to any future consistent theory, inasmuch as the quantity W_N enters into the general expression for the transition probability.

1. We shall base the computation of the statistical weight for the mixed case (m slow and n relativistic particles) on the general formula:

$$W_N(E_0) = \int_{-\infty}^{+\infty}\int\cdots\int \delta\left(E_0 - \sum_{i=1}^{N}\sqrt{p_i^2 + M_i^2}\right)\delta\left(\sum_{i=1}^{N} p_{xi}\right) \times \delta\left(\sum_{i=1}^{N} p_{yi}\right)\delta\left(\sum_{i=1}^{N} p_{zi}\right)\prod_{i=1}^{N} d^3p_i, \quad (1)$$

where δ stands for the δ-function. The velocity of light is $c = 1$

Assuming a kinetic energy $T_i = p_i^2/2M_i$ for slow particles and $M_i = 0$ for fast particles, and using the integral presentation of the function, we obtain*:

*Actually, the influence of the interaction between nucleons and π mesons was approximated quite successfully by Belen'kii and Nikishov[2] by introducing the method of isobars.

*We assume for the present $M_1 = M_2 = \ldots M_m$. The generalization for different masses is carried out without difficulty (see Eq. 13 below).

$$W_{m,n}(E_0) =$$

$$= (2\pi)^{-4} \int_{-\infty}^{+\infty} \exp[iT_0\tau_1]\, d\tau_1 \int\int\int_{-\infty}^{+\infty} d\tau_2\, d\tau_3\, d\tau_4 \tag{2}$$

$$\times \left\{ \int_{-\infty}^{+\infty} \exp\left[-i\left(\frac{p^2\tau_1}{2M} + p_x\tau_2 + p_y\tau_3 + p_z\tau_4 \right) \right] d^3p \right\}^m$$

$$\times \left\{ \int_{-\infty}^{+\infty} \exp[i(p\tau_1 + p_x\tau_2 + p_y\tau_3 + p_z\tau_4)]\, d^3p \right\}^n,$$

where $T_0 = E_0 - mM$ is the kinetic energy of the system. Making use of the results obtained in Ref. 5, we write (2) as

$$W_{m,n}(E_0) = -2\frac{(2\pi M)^{3m/2}}{(2\pi)^3}\left[-\frac{i(1-i)}{2^{1/2}} \right]^m [8i\pi]^n$$

$$\times \int_{-\infty}^{+\infty} \tau_1^{n-3m/2} \exp[iT_0\tau_1]\, d\tau_1 \int_0^{\infty} \frac{\tau^2 \exp[imM\tau^2/2\tau_1]}{(\tau^2-\tau_1^2)^{2n}}\, d\tau.$$

$$\alpha = \tau_1/2M, \quad \tau = \sqrt{\tau_2^2+\tau_3^2+\tau_4^2}. \tag{3}$$

Let us evaluate the integral:

$$I = \int_0^{\infty} \frac{\tau^2 \exp[i\tau^2\eta]}{(\tau^2-\tau_1^2)^{2n}}\, d\tau = \frac{1}{i}\frac{dY}{d\eta},$$

$$\eta = \frac{mM}{2\tau_1}; \quad Y = \int_0^{\infty} \frac{\exp[i\tau^2\eta]}{(\tau^2-\tau_1^2)^{2n}}\, d\tau. \tag{4}$$

Let us further construct a differential operator from Y such that in the final analysis it is determined by the simple integral

$$\int_0^{\infty} \exp[i\tau^2\eta]\, d\tau = (\pi/2)^{1/2}(1+i)/2\eta^{1/2}.$$

Making use of the relationship

$$\frac{d^m Y}{d\eta^m} = i^m \int_0^{\infty} \frac{\tau^{2m} \exp[i\tau^2\eta]}{(\tau^2-\tau_1^2)^{2n}}\, d\tau,$$

we obtain

$$\sum_{k=0}^{2n} C_{2n}^k \left(\frac{\tau_1^2}{i} \right)^k \frac{d^{(2n-k)}Y}{d\eta^{(2n-k)}} = (-1)^n \left(\frac{\pi}{2} \right)^{1/2} \frac{1+i}{2\eta^{1/2}}. \tag{5}$$

The characteristic equation corresponding to (5) is

$$\sum_{k=0}^{2n} C_{2n}^k \left(\frac{\tau_1^2}{i} \right)^k \rho^{2n-k} = (\rho - i\tau_1^2)^{2n} = 0. \tag{6}$$

Therefore, $\rho = i\tau_1^2$ is the root of a characteristic equation of order $2n$; the general solution of the homogeneous equation corresponding to (5) is

$$Y_0 = P(\eta)\exp\{i\tau_1^2\eta\}, \tag{7}$$

where $P(\eta)$ is a polynomial of degree $2n-1$. We write the solution of the non-homogeneous equation in the form

$$Y = D(\eta)\exp\{i\tau_1^2\eta\}.$$

For the function $D(\eta)$ we have the following equation:

$$d^{2n}D(\eta)/d\eta^{2n} = (-1)^n 2^{-3/2}\pi^{1/2}(1+i)\,\eta^{-1/2}\exp[-i\tau_1^2\eta]. \tag{8}$$

From this

$$D(\eta) = (-1)^n \left(\frac{\pi}{2} \right)^{1/2} \frac{1+i}{2} \underbrace{\int\int\cdots\int}_{2n} \frac{\exp[-i\tau_1^2\eta]}{\eta^{1/2}}\, d\eta$$

$$+ D_1\eta^{2n-1} + D_2\eta^{2n-2} + \ldots + D_{2n}, \tag{9}$$

where $D_1, D_2 \ldots D_{2n}$ are constants.

Analysis of the asymptotic behavior of the function Y shows readily that $Y(\eta) \to 0$ when $\eta \to \infty$. Therefore, $D_1 = D_2 = \ldots = D_{2n} = 0$.

Let us expand the integral (9) in powers of $\eta^{-1/2}$. After simple but tedious transformations we obtain:

$$D(\eta) = (-1)^n \left(\frac{\pi}{2} \right)^{1/2} \frac{\exp[-i\tau_1^2\eta]}{2(-1/2)!}$$

$$\times \sum_{k=0}^{\infty} C_{k+2n-1}^k \frac{(k-1/2)!}{\eta^{k+1/2}(i\tau_1^2)^{k+2n}} \tag{10}$$

and finally

$$Y = -\left(\frac{\pi}{2} \right)^{1/2} \frac{1+i}{2i(-1/2)!}$$

$$\sum_{k=0}^{\infty} C_{k+2n-1}^k \frac{(k+1/2)!\, i^{-k}}{(mM/2)^{k+3/2}\tau_1^{4n+k-3/2}}. \tag{11}$$

Inserting into (3) and computing the residue at $\tau_1 = 0$ we get:

$$W_{m,n}(E_0) =$$

$$= 2^{3n}\pi^n (2\pi)^{3(m-1)/2} M^{3m/2} (mM)^{-3/2} T_0^{3n+3(m-1)/2-1}$$

$$\times \sum_{k=0}^{\infty} C_{k+2n-1}^k \frac{(-1)^k (2k+1)!!}{(k+3n+(3m/2)-5/2)!} \left(\frac{T_0}{mM} \right)^k. \tag{12}$$

The series obtained can be readily generalized to include particles of different masses:

$$W_{m,n}(E_0) = 2^{3n}\pi^n (2\pi)^{3(m-1)/2} \left(\prod_{i=1}^{m} M_i\right)^{3/2} \left(\sum_{i=1}^{m} M_i\right)^{-3/2} T_0^{3n+3(m-1)/2-1}$$
$$\times \sum_{k=0}^{\infty} C_{k+2n-1}^{k} \frac{(-1)^k (2k+1)!!}{(k+3n+(3m/2)-5/2)!} \left(T_0 \Big/ \sum_{i=1}^{m} M_i\right)^k ; \qquad (13)$$
$$T_0 = E_0 - \sum_{i=1}^{m} M_i.$$

It should be noted that the first term of expansion (12) was obtained by Fermi [1]. However, it follows from the nature of the series (12) that it is not well converging (especially at $T_0 \sim mM/2$), and therefore the first term represents the entire series only very roughly.

2. In this section we shall give an accurate expression for the statistical weight in the general case. We shall rely on the expression obtained by Lepore and Stuart[4] (in the final state there are formed N particles of arbitrary mass):

$$W_N(E_0) = \frac{(2\pi^2)^N}{(2\pi)^3} \left(\prod_{i=1}^{N} M_i^2\right) \int_{-\infty}^{+\infty} d\tau_1 \tau_1^N e^{i\tau_1 E_0}$$
$$\times \frac{\tau^2 d\tau}{(\tau_1^2-\tau^2)^N} \prod_{j=1}^{N} \{H_2^{(2)}[M_j(\tau_1^2-\tau^2)^{1/2}]\}, \qquad (14)$$

where integration is to be understood in the sense of Cauchy *i.e.*, the integration path is taken to be a straight line parallel to the real axis and approaching it from below*; $H_2^{(2)}$ is the Hankel function.

Let us introduce new variables:

$$\tau_1 = \frac{y+z}{E_0}\ ;\ \tau = \frac{y-z}{2}\ ;\ \nu_j = \frac{M_j}{E_0}\ ;$$

then

$$W_N(E_0) =$$
$$\frac{\pi^{2N-3}}{2^{N+2}} E_0^{3N-4} \left(\prod_{i=1}^{N} \nu_i^2\right) \sum_{k=0}^{N} \sum_{l=0}^{2} (-1)^l C_N^k C_2^l \qquad (15)$$
$$\times \int_{-\infty}^{+\infty}\int_{-\infty}^{+\infty} y^{k+l-N} z^{2-k-l} e^{i(y+z)} \prod_{j=1}^{N} \{H_2^{(2)}[2\nu_j (zy)^{1/2}]\}.$$

Since the Hankel function approaches zero as the argument approaches infinity, it is permissible, according to the Jordan lemma, to close the integration path from above by an arc of infinitely large radius with a cut at point $i\infty$.

We next make use of the series form of the Hankel function:

$$H_2^{(2)}[2\nu_j (yz)^{1/2}] = J_2[2\nu_j (yz)^{1/2}]$$
$$-(2i/\pi) J_2[2\nu_j (yz)^{1/2}] \ln[\nu_j (yz)^{1/2}]$$
$$+ \frac{i}{\pi}\left[1 + \frac{1}{\nu_j^2 yz}\right] - \frac{i}{\pi} \sum_{t=0}^{\infty} \frac{(-1)^t [\nu_j (yz)^{1/2}]^{2t+2}}{t!\,(2+t)!}$$
$$\left[2C - \sum_{r=1}^{t+r} \frac{1}{r} - \sum_{r=1}^{t} \frac{1}{r}\right], \qquad (16)$$

where J_2 is the Bessel function and $C = 0.577$ is Euler's constant. Inasmuch as $\nu_j < 1$, it is appropriate to use these quantities as small parameters in which integral (16) is expanded. By comparing series (16) with (15) we expect the expansion of (15) to be of the following form:

$$W_N(E_0) = \left(\frac{\pi}{2}\right)^{N-1} E_0^{3N-4} \times$$
$$\left\{\sum_{k=0}^{\infty} W_{kN}^{(0)} + \sum_{k=0}^{\infty} W_{kN}^{(1)} + \sum_{k=0}^{\infty} W_{kN}^{(2)} + \ldots + \sum_{k=0}^{N} W_{kN}^{(N)}\right\} \qquad (17)$$

where the terms $W_{kN}^{(l)}$ are proportional to $\nu^{2k} \ln^l \nu$.

---

*A relatively simple derivation of Eq. (14), different from that presented in Ref. 4, can be obtained. Write equation (1) in the form:

$$W_N(E_0) = (2\pi)^{-4} \int_{-\infty}^{+\infty} e^{-iE_0\tau_1} \iiint_{-\infty}^{+\infty} d\tau_2 d\tau_3 d\tau_4$$
$$\times \prod_{j=1}^{N} \left\{\iiint_{-\infty}^{+\infty} \exp[i(\tau_1 \sqrt{p_j^2 + M_j^2} + (\tau \mathbf{p}_j))]\, dp_{jx} dp_{jy} dp_{jz}\right\}.$$

Using the singular functions $\Delta^{(1)}$, Δ introduced by Dirac[7], it can be shown that

$$\iiint_{-\infty}^{+\infty} \exp[\tau_1 \sqrt{p_j^2 + M_j^2} + (\tau \mathbf{p}_j))]\, dp_{jx} dp_{jy} dp_{jz}$$
$$= \frac{(2\pi)^3 d}{i\, d\tau_1} [\Delta^{(1)}(M_j, \tau_1^2 - \tau^2) + i\Delta(M_j, \tau_1^2 - \tau^2)].$$

Using further the presentation of $\Delta^{(1)}$, Δ in terms of Hankel functions (see, for example, Ref. 8) we obtain (14).

To determine $W_{kN}^{(j)}$ it is necessary to select from the expansion (16), multiplied by N, the terms which contribute to $W_{kN}^{(j)}$, substitute into (15), as was done in Ref. 5 for the computation of $W_{0N}^{(0)}$, and determine find the indicated coefficients by computing the residues at $y = z = 0$. To determine certain coefficients it is necessary to evaluate integrals of the type

$$I_1(k, l) = \int y^{-k} e^{iy} \ln^l y \, dy. \tag{18}$$

The transformed integration contour starts from $i\infty - \delta$ ($\delta \to +0$), follows the imaginary axis, encircles zero from below and returns to point $i\infty + \delta$. It is easy to note, that

$$I_1(k, l) = \frac{d^l}{dk^l} \int e^{iy - k \ln y} dy = (-1)^k 2\pi \frac{d^l}{dk^l} \frac{i^k}{\Gamma(k)}, \tag{19}$$

where Γ is the gamma function.

For further computations it is convenient to represent (19) by means of the well-known logarithmic derivatives of the Γ-function, which are in turn expressed through the Rieman ζ function (see, for example, Ref. 9). Thus,

$$(d/dk)/\Gamma(k) = -\psi(k)/\Gamma(k). \tag{20}$$

Making use of the expression

$$\psi(k) = -C + \sum_{r=1}^{k-1} \frac{1}{r}, \tag{21}$$

it is easy to reduce this problem also to an evaluation of residues. In particular, at $l = 1$

$$I(k, 1) = 2\pi \cdot \frac{d}{dk} \frac{i^k}{\Gamma(k)} = 2\pi i^k \left\{ \frac{\Gamma'(k)}{\Gamma^2(k)} - \frac{\pi i}{2} \frac{1}{\Gamma(k)} \right\}. \tag{22}$$

If $k = 1, 2, 3 \ldots$,

$$\frac{\Gamma'(k)}{\Gamma^2(k)} = \frac{1}{\Gamma(k)} \frac{\Gamma'(k)}{\Gamma(k)} = \frac{1}{\Gamma(k)} \left\{ -C + \sum_{r=1}^{k-1} \frac{1}{r} \right\}. \tag{23}$$

If $k = 0, -1, -2, -3 \ldots$,

$$\Gamma'(k)/\Gamma^2(k) = (-1)^{k+1} \Gamma(1-k); \quad 1/\Gamma(k) = 0. \tag{24}$$

In this manner, the problem is, in principle, completely solved.

Naturally, the series (17) is convenient for the computation of $W_N(E_0)$, if the kinetic energy $T_0 < \Sigma M_i$. Otherwise it is necessary to use too many terms of series (17) which, of course, complicates the computation. Therefore, if $T_0 < \Sigma M_i$, it is necessary to use expression (12)*.

We shall give next the values of the first several terms of series (17). For convenience we introduce the following symbols for the quantities found in the expressions for the first terms of series (17):

$$D_N^{(A)} = (-1)^A \sum_{r=0}^{N} C_N^r (N - 2r + 1)/[2N - r - (A+1)]! \, [N + r - (A+2)]! =$$
$$= (-1)^A [4N - 2(A+2)]! \, [2N - (A+1)]/[3N - 2(A+2)]! \{[2N - (A+1)]!\}^2;$$

$$F_N^{(A)} = (-1)^A \sum_{r=0}^{N} C_N^r \left\{ \frac{\alpha[2N - r - A]}{[N + r - (A+3)]!} - \frac{\alpha[2N - r - (A+1)]}{[N + r - (A+2)]!} + \right.$$
$$\left. + \frac{\alpha[N + r - (A+2)]}{[2N - r - (A+1)]!} - \frac{\alpha[N + r - (A+1)]}{[2N - r - (A+2)]!} \right\} = D_N^{(A)} \{2[4N - 2(A+2)]! \times$$
$$\times \alpha[4N - 3 - 2A] - 2[3N - 2(A+2)]! \, \alpha[3N - 2A - 3] - [2N - (A+1)]! \times$$
$$\times \alpha[2N - A] - [2N - (A+2)]! \, \alpha[2N - A - 1]\};$$

*If $T_0 \ll mM$, it is permissible to use only the first term of series (11) or (12) or to make use of their generalized representation, in the case when terms proportional to μ^2 are computed for relativistic particles:

$$W_{m,n}(E_0) = 2^{3n} \pi^n (2\pi)^{3(m-1)/2} M^{3m/2} (mM)^{-3/2} T_0^{3n + 3(m-1)/2 - 1}$$
$$\times \left\{ \sum_{k=0}^{\infty} C_{k+2n-1}^k \frac{(-1)^k (2k+1)!!}{(k + 3n + 3m/2 - 5/2)!} \left(\frac{T_0}{mM} \right)^k + \frac{n}{4} \left(\frac{\mu}{T_0} \right)^2 \sum C_{k+2n-2}^k \frac{(-1)^k (2k+1)!! \, (T_0/mM)^k}{(k + 3n + 3m/2 - 9/2)!} \right\}.$$

where A is a positive integer;

$$\alpha(z) = \begin{cases} (-1)^{z+1}|z|! & z = 0, -1, -2, \ldots \\ 0 & z = 1 \\ \dfrac{1}{(z-1)!}\displaystyle\sum_{r=1}^{z-1}\frac{1}{r} & z = 2, 3, 4, \ldots \end{cases}$$

A. *All particles have the same mass:*

$$\begin{gathered} W_{0N}^{(0)} = D_N^{(0)},\ W_{1N}^{(0)} = N\nu^2 D_N^{(1)},\ W_{2N}^{(1)} = N\nu^4 \ln\frac{1}{\nu} D_N^{(2)}, \\ W_{2N}^{(0)} = \nu^4\left\{\left[\frac{3}{4}N + \frac{N(N-1)}{2}\right]D_N^{(2)} + \frac{N}{2}F_N^{(2)}\right\}, \\ W_{3N}^{(1)} = \nu^6 \ln\frac{1}{\nu}\left[N(N-1) - \frac{N}{3}\right]D_N^{(3)}, \\ W_{3N}^{(0)} = \nu^6\left\{\left[\frac{N(N-1)(N-2)}{6} + \frac{3}{4}N(N-1) - \frac{17}{36}N\right]D_N^{(3)}\right. \\ \left. + \left[\frac{N(N-1)}{2} - \frac{N}{6}\right]F_N^{(3)}\right\}, \\ W_{4N}^{(2)} = \nu^8 \ln^2\frac{1}{\nu}\ \frac{N(N-1)}{2} D_N^{(4)}, \\ W_{0N}^{(1)} = W_{1N}^{(1)} = W_{0N}^{(2)} = \ldots = W_{3N}^{(2)} = 0. \end{gathered} \tag{25}$$

B. The derived expressions can be readily generalized for the case when all *particles have different masses.**

$$\begin{gathered} W_{1N}^{(0)} = \left(\sum_{i=1}^{N}\nu_i^2\right)D_N^{(1)},\ W_{2N}^{(0)} = \left(\frac{3}{4}\sum_{i=1}^{N}\nu_i^4 + \frac{1}{4}\sum_{\substack{i=1\\ i\neq j}}^{N}\sum_{j=1}^{N}\nu_j^2\nu_j^2\right)D_N^{(2)} + \frac{1}{2}\left(\sum_{i=1}^{N}\nu_i^4\right)F_N^{(2)}, \\ W_{2N}^{(1)} = \left(\sum_{i=1}^{N}\nu_i^4 \ln\frac{1}{\nu_i}\right)D_N^{(2)},\ W_{3N}^{(1)} = \left(\frac{1}{2}\sum_{i,j=1}^{N}{}'\nu_i^4\nu_j^2 \ln\frac{1}{\nu_i} - \frac{1}{3}\sum_{i=1}^{N}\nu_i^6 \ln\frac{1}{\nu_i}\right)D_N^{(3)}, \\ W_{3N}^{(0)} = \left(\frac{1}{36}\sum_{i,j,k=1}^{N}\nu_i^2\nu_j^2\nu_k^2 + \frac{3}{8}\sum_{i,j=1}^{N}{}'\nu_i^4\nu_j^2 - \frac{17}{36}\sum_{i=1}^{N}{}'\nu_i^6\right)D_N^{(3)} \\ + \left(\frac{1}{4}\sum_{i,j=1}^{N}{}'\nu_i^4\nu_j^2 - \frac{1}{6}\sum_{i=1}^{N}\nu_i^6\right)F_N^{(3)}, \\ W_{4N}^{(2)} = \left(\frac{1}{2}\sum_{i,j=1}^{N}{}'\nu_i^4\nu_j^4 \ln\frac{1}{\nu_i}\cdot\ln\frac{1}{\nu_i}\right)D_N^{(4)}; \end{gathered} \tag{26}$$

where the primed summation sign indicates that the term $(i = j = k)$ is omitted.

3. The equations derived can be used to compare the predictions of the statistical theory with experimental data on multiple production of particles. Leaving the detailed comparison for a later paper, we are presenting now only a brief discussion of the nature of the obtained results.

The expressions obtained were compared with certain special values of $W_N(E_0)$ computed by other

*The value of $W_{0N}^{(0)}$ does not depend on ν and is the same in all cases: the equations of the last line also apply in either case.

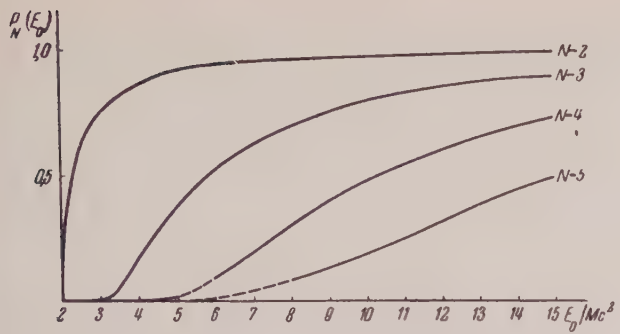

FIG. 1. $P_N(E_0)$ for the case of N particles of equal mass M. (E_0 is the total energy of all the particles, center of mass system).

methods, namely: $W_2(E_0)^3$ and $W_3(E_0)$, $W_4(E_0)$ for the condition $M_1 \neq 0$ and $M_2 = M_3 = M_4 = 0$[6]. Identical corresponding coefficients were obtained in all cases.

In conclusion we present results of certain numerical computations. Since $W_N(E_0)$ is a rapidly increasing function of E_0, it is convenient to introduce the dimensionless quantity

$$P_N(E_0) = W_N(E_0) / W_N^{\text{rel}}(E_0),$$

where $W_N^{\text{rel}}(E_0) = (\pi/2)^{N-1} D_N^{(0)} E_0^{3N-4}$ is the extremal relativistic expression for $W_N(E_0)$; obtained earlier[4,5]. Fig. 1 shows $P_N(E_0)$ for the case of N

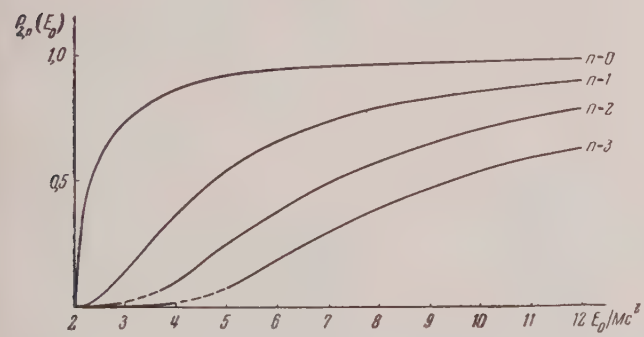

FIG. 2. $P_{2,n}(E_0)$ for the case of two nucleons and n π-mesons. (M denotes the nucleon mass, E_0 the total energy of all particles, center of mass system)

particles of equal mass M; Fig. 2 shows $P_{2,n}(E_0)$ for the case of two nucleons and n π-mesons. The first section of each curve is plotted from Eq. (12), the remaining portion is drawn according to Eq. (17), using 8 to 12 terms; the dotted lines show the sections of the curves which were interpolated between the two equations.

A simple analysis of these curves shows that in a very important case when the condition $E_0 \sim \sum_{i=1}^{N} M_i$, is satisfied, the use of the extremal expressions may lead to completely incorrect results.

The authors express their appreciation to I. G. Aramanovich, E. I. Feinberg and D. S. Tchernavskii for their participation in the discussions of various problems involved in this work. The authors also note with thanks the useful discussions with the late Prof. S. Z. Belen'kii'.

Note added in proof. It was determined, after sending this paper to press, that series (13) can be summed and written in closed form. Unable to present here the derived expressions in general form we will give only the most interesting case of two nucleons and n π-mesons ($M = 1$):

$$W_{2,n}(E_0) = \frac{2^{3n+3}\pi^{n-1}}{(2n-1)!}\left\{\arctan\sqrt{E_0-2}\times\sum_{k=1}^{3n} p_{3n-k}(E_0-2)^{3n-k} - \sqrt{E_0-2}\cdot\sum_{l=0}^{3n-2} q_l(E_0-2)^l\right\},$$

where $p_{3n-k} = \dfrac{(-1)^{k-1}(2k-1)!\,(2n-3/2-k)!}{[(k-1)!]^2\,(3n-k)!\,2^{2k}\sqrt{\pi}}$;

$$q_l = \sum_{i=0}^{l} (-1)^i \frac{p_{l-i}}{2i+1}.$$

[1] E. Fermi, Progr. Theor. Phys. **5**, 570 (1950).

[2] S. Z. Belen'kii and A. I. Mikishov, J. Exptl. Theoret. Phys. (U.S.S.R.) **28**, 744 (1955).

[3] M. I. Podgoretskii and I. L. Rosental', J. Exptl. Theoret. Phys. (U.S.S.R.) **27**, 129 (1954).

[4] J. V. Lepore and R. N. Stuart, Phys. Rev. **94**, 1724 (1954).

[5] I. L. Rozental', J. Exptl. Theoret. Phys. (U.S.S.R.) **27**, 1 (1955).

[6] R. Milburn, Rev. Mod. Phys. **27**, 1 (1955).

[7] P. Dirac, Proc. Camb. Phil. Soc. **30**, 150 (1934).

[8] A. I. Akhiezer and V. B. Berestetski, *Quantum Electrodynamics*, GITTL (1953)

[9] E. G. Whittaker and G. H. Watson, Modern Analysis II, GTTI, (1934).

Translated by J. L. Herson
160

Investigation of the Energy and Angle Distribution of Neutral Pions Produced by 470-and 660-Mev Protons in Carbon

IU. D. BAIUKOV, M. S. KOZODAEV AND A. A. TIAPKIN
Joint Institute for Nuclear Research

(Submitted to JETP editor October 28, 1956)
J. Exptl. Theoret. Phys. (U.S.S.R.) **32**, 667-677 (April, 1957)

Results of measurements of the energy spectra of γ-rays from the decay of neutral pions produced by 660–Mev protons in carbon are reported. The angle and energy distributions of the neutral pions obtained from an analysis of the spectra of γ-rays produced by 660–and 470–Mev protons in carbon are also given.

INTRODUCTION

BECAUSE neutral pions have a very short lifetime (5×10^{-15} sec) studies of the production processes and the interaction of these particles with nuclei are carried out by studying the hard γ-radiation which is produced in the decay of these mesons. From a measurement of the angle distribution of the γ-rays it is possible to determine the angle distribution of the neutral pions. Moreover, an investigation of the energy spectra of the γ-rays yields information both as to the energy as well as the angle distributions of the neutral pions which are produced.

The results of a study of the energy spectrum of γ-rays from the decay of neutral pions produced in Be and C targets by 470-Mev protons have been reported in Refs. 1 and 2. From an analysis of the spectra which were obtained the conclusion was reached that the neutral mesons are produced with energies close to the maximum possible energy and with an angle distribution which is approximately proportional to $\cos^2\theta$. Ref. 3 reported the results of a measurement of the spectra of γ-rays observed in the decay of neutral pions produced in a carbon target by 340-Mev protons. The authors of this work also concluded that the angle distribution of the neutral pions produced in complex nuclei is anisotropic.

In the present work* we report measurements of the energy spectra of γ-rays from the decay of neutral pions produced by 660-Mev protons in carbon nuclei and present an analysis of the spectra of the γ-rays. The data which were obtained are analyzed in conjunction with the results of similar measurements carried out earlier with 470-Mev protons.[1,2]

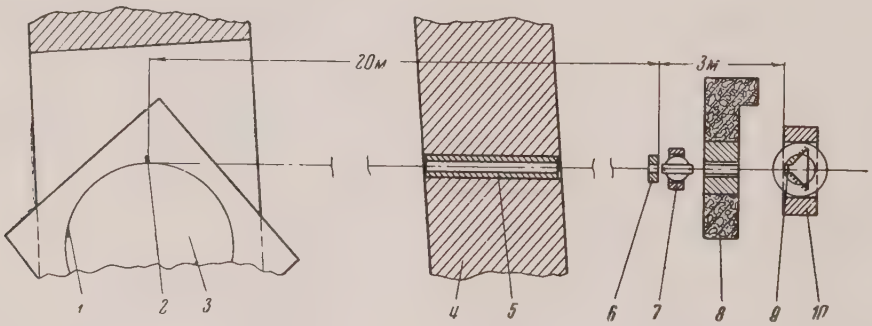

FIG. 1. Diagram of the experiment. 1) Proton trajectory, 2) target, 3) synchrocyclotron chamber, 4) concrete wall, 5) collimator, 6) diaphragm, 7) separation magnet, 8) supplementary shield, 9) converter of the spectometer, 10) spectrometer.

EXPERIMENTAL ARRANGEMENT

Fig. 1 shows the experimental arrangement. The carbon target, located inside the vacuum chamber of the accelerator, is bombarded by protons with a mean energy of 660 Mev. The γ-rays produced in the target pass through an aperture in a 4-meter concrete wall and are collimated by a diaphragm in

*The results of the present work have been presented at the CERN Symposium at Geneva in 1956.

a lead block. Charged particles are separated from the collimated beam of γ-rays by a magnetic field produced by a special electromagnet; the beam then strikes the converter of a 12-channel magnetic pair γ-spectrometer. The spectrometer is located 23 meters away from the target along a line tangent to the circular proton orbit.

The magnitude of the proton flux through the target is determined from the temperature difference at the ends of a copper rod which serves to support the target. The thermal conductivity of the rod is chosen so that the target temperature rises by several tens of degrees; hence, the heat loss by radiation is insignificant. In determining the proton flux, in addition to the target heating due to ionization loss, account is taken of heating due to star production.

PAIR γ-SPECTROMETER

The magnetic field in the spectrometer is produced by an electromagnet with a pole-piece diameter of 85 cm. The gap between the pole pieces is 6 cm. In studying γ-ray pole tips with an opening angle of 180° are used (Fig. 2a) are used to study γ-ray spectra in the energy range from 20 to 200 Mev because this arrangement yields semi-circular focusing of electrons and positrons is obtained and since wider and thicker converters can be used, it is possible to increase significantly the spectrometer efficiency. Pole tips with an opening angle of 90° (Fig. 26) are used to measure spectra in the energy region from 100 to 450 Mev, and also γ-ray spectra at energies up to 600 Mev but in the latter case the unit containing the counters is placed at a greater distance from the converter.

Along the edges of the pole tips are placed two units with proportional counters which record electrons and positrons. Each unit contains a bank of six groups of coordinate counters and two banks of supplementary selection counters (Fig. 2). Each coordinate group, in turn, consists of three or four counters the center conductors of which are connected to the input of a single amplifier. The proportional counters used in the spectrometer are filled with pure methylal $[CH_2(OCH_3)_2]$. The cathodes of the counters are fabricated from thin-wall stainless steel tubing 10 mm in diameter.

After amplification and shaping, the pulses from each group of coordinate counters and from each bank of selection counters are fed to a coincidence circuit which produces a control pulse. The resolving time of the coincidence circuit is 5×10^{-7} sec. In addition to this coincidence circuit, the electronic system of the spectrometer contains a six-fold coincidence circuit which can be reduced to a five-fold coincidence circuit by disconnecting one of the banks of coordinate counters or selection counters. From the ratio of the counts in the main six-fold coincidence circuit to the counts in the five-fold coincidence circuit it is possible to determine the efficiency of the bank of counters which is disconnected.

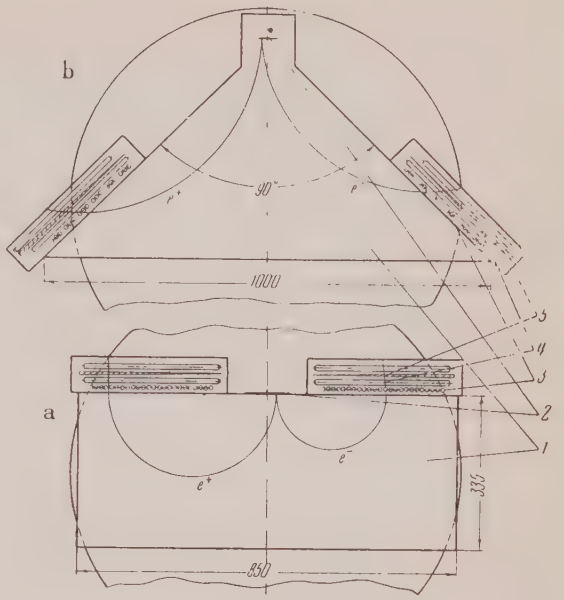

FIG. 2. Pole pieces and arrangement of the counters in the pair γ-spectrometer. 1) pole pieces, 2) converters, 3) coordinate counters, 4) selection counters, 5) filters.

The amplified pulses from the coordinate counters cause operation of the corresponding six-contact relay when the control signal is present. On closure of the contacts of the different pairs the relay operates one of eleven electro-mechanical registers, thus recording a γ-quantum of the appropriate energy. The number of γ-quanta detected by each group of coordinate counters is also determined by the corresponding electro-mechanical registers. The readings of these twelve counters are used for calculating the relative efficiency of the different coordinate counters and for the subsequent calculation of the relative average efficiency for detecting γ-rays in various energy ranges.

The resolving power of the spectrometer for each energy range, which is defined as the ratio of the average energy to the effective width of the energy interval, depends both on the geometry of the instrument as well as the thickness of the converter.

In our experiment rather thick copper converters were used (0.1, 0.3 and 0.5 mm respectively for measurements in the γ-ray energy regions 20–60, 50–200, and 200–600 Mev). The resolving power of the spectrometer for the sixth channel, determined mainly by the geometry of the device, is 13 with an opening angle $2\varphi = 180°$ and 25 in the second case ($2\varphi = 90°$).

Another important characteristic of the spectrometer is its efficiency, which is defined as the probability of detecting γ-rays which are incident on the converter. The efficiency of the spectrometer for a given energy range is given by the following expression:

$$\Phi = \kappa t_c \psi(\epsilon_\gamma, \Delta\epsilon_\gamma, \epsilon_e)\, \xi(\epsilon_\gamma, t_c)\, f_r.$$

Here, κ is the number of pair combinations of counters which record γ-rays of a given energy interval; $t_c\psi(\epsilon_\gamma, \Delta\epsilon_\gamma, \epsilon_e)$ is the probability for the production in the converter of thickness t_c of an electron-positron pair with energy sufficient for detection by the spectrometer counters; $\epsilon(\epsilon_\gamma, t_c)$ is a factor which takes into account the reduction in spectrometer efficiency due to scattering of electrons and positrons in the converter and f_r is the efficiency of the counters in the spectrometer measured by disconnecting various series of counters successively.

RESULTS OF THE MEASUREMENTS

The energy spectra of γ-rays from the decay of neutral pions produced by 660-Mev protons in carbon have been measured at angles of 0° and 180° with respect to the bombarding proton beam. In the spectrum measurements at 0° approximately 6×10^4 electron-positron pairs were recorded. The spectrum at 180° has been plotted on the basis of a measurement of the energies of 4×10^4 pairs. In each separate run, at a fixed intensity of magnetic field, measurements were made of a section of the γ-ray spectrum at eleven different energy intervals. The intensity of the magnetic field in the individual measurements was chosen in such a way that each section of the spectrum was measured in two runs by different energy channels of the spectrometer. This procedure made it possible to normalize the separate measurements in overlapping sections of the spectrum. The normalizing factors determined in this fashion were found to be in agreement, within the error limits, with the ratios of spectrometer efficiencies calculated for the corresponding magnetic-field intensity.

Fig. 3 shows the results of a measurement of the

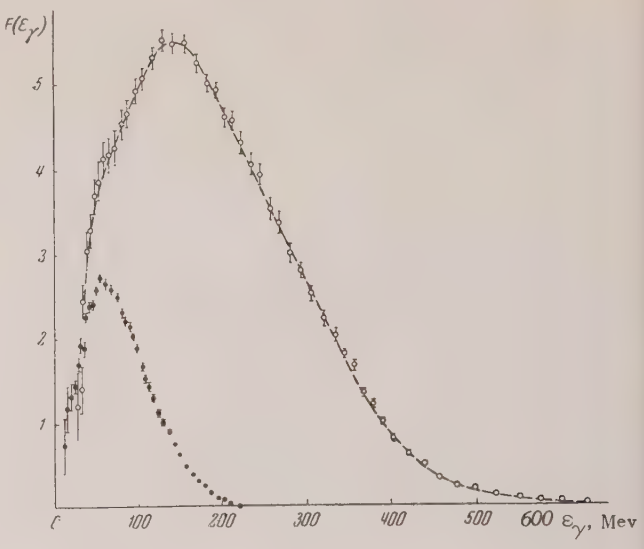

FIG. 3. Energy spectrum of γ-rays from the decay of neutral pions produced by 660-Mev protons in carbon. ○) angle of observation 0°; ●) angle of observation 180°.

γ-spectra at angles of 0° and 180°, obtained by averaging the results of individual measurements, taken with weighting factors proportional to their statistical accuracy.

In the laboratory coordinate system the differential cross-section for the production of γ-quanta in carbon by 660 Mev protons at an angle of 180° is

$$d\sigma_C^\gamma / d\omega\,(180°) = (1{,}5 \pm 0{,}2) \cdot 10^{-27}\ \text{cm}^2/\text{sterad},$$

which is in agreement with the data of Ref. 4. The ratio of the total flux of γ-rays at 0° and 180° is 5.1 ± 0.3.

ANALYSIS OF THE γ-RAY ENERGY SPECTRA

1. *Dependence of the energy spectrum of γ-rays from carbon on the angle and energy distributions of the neutral pions.* The energy spectrum of the γ-rays $F(\epsilon_\gamma)$ at angles of 0° and 180° in the center of mass system (CMS) of the colliding nucleons is related to the function $\psi(\epsilon_\pi, \theta)$, which determines the energy and angle distributions of the neutral pions, by the following expression:

$$F(\varepsilon_\gamma) = \int_{\varepsilon_\pi^*}^{\infty} \frac{\psi(\varepsilon_\pi, \theta)}{\sqrt{\varepsilon_\pi^2 - \varepsilon_0^2}}\, d\varepsilon_\pi. \qquad (1)$$

Here the lower integration limit $\epsilon_\pi^* = \epsilon_\gamma + (\epsilon_0^2 / 4\epsilon_r)$ is the rest energy of the neutral pion and $\theta = \arccos\{[\epsilon_\pi - (\epsilon_0^2 / 2\epsilon_\gamma)] / \sqrt{\epsilon_\pi^2 - \epsilon_0^2}\}$ is the

angle between the direction of motion of the neutral pion and the detected γ-quantum.

In the production of neutral pions in complex nuclei, because of internal motion of the nucleons, there is no single CMS for the colliding neutrons. However, it is possible to make use of an effective CMS, which is found in the impulse approximation from a calculation of the energy dependence of the meson-production cross section. Since the momentum of the proton which bombards the nucleus is considerably greater than the momenta of the nucleons inside the nucleus, we may use the expression given in Eq. (1) for analyzing the spectra of γ-rays converted to an averaged coordinate system. Furthermore, in analyzing the spectra we will take account of the angle and energy distributions independently, that is, we assume

$$\psi(\varepsilon_\pi, \theta) = f(\varepsilon_\pi)\varphi(\theta),$$

where $f(\epsilon_\pi)$ and $\varphi(\theta)$ are the energy spectrum and angle distribution of the neutral pions.

From Eq. (1) it is apparent that for an isotropic neutral-pion distribution, regardless of the energy distribution, the γ-ray spectrum plotted on a graph with a logarithmic scale along the abscissa axis should be symmetric with respect to the energy $\frac{1}{2}\epsilon_0$. The presence of anisotropic effects in the pion angle distribution disturbs the logarithmic symmetry of the spectrum. Thus, with an angle distribution proportional to $\cos^2\theta$ the maximum of the spectrum is displaced toward higher energies.

If the function $\psi(\epsilon_\pi, \theta)$ in Eq. (1) can be given in the form of a product of the functions $f(\epsilon_\pi)$ and $\varphi(\theta)$ (the energy and angle distributions of the neutral pions in the CMS of the colliding nucleons respectively), we obtain upon differentiation of Eq. (1) with respect to ϵ_γ the following expression for the pion energy distribution:

$$f(\varepsilon_\pi^*) = -\frac{\varepsilon_\gamma}{\varphi(\theta)}\frac{dF(\varepsilon_\gamma)}{d\varepsilon_\gamma} - \frac{\varepsilon_\gamma}{\varphi(\theta)}\int_{\varepsilon_\pi^*}^{\infty}\frac{f(\varepsilon_\pi)}{\sqrt{\varepsilon_\pi^2-\varepsilon_0^2}}\frac{d\varphi}{d\theta'}\frac{d\theta'}{d\varepsilon_\gamma}d\varepsilon_\pi. \quad (2)$$

For an isotropic angle distribution $\varphi(\theta) = \text{const}$. the second term in Eq. (2) vanishes. In this case the neutral pion spectrum is determined from the simple relation

$$f(\varepsilon_\pi^*) = -\varepsilon_\gamma dF(\varepsilon_\gamma)/d\varepsilon_\gamma.$$

The meson energy distribution $f(\epsilon_\pi^*)$ can be found independently by using the section of the energy spectrum $F(\epsilon_\gamma)$ located in the γ-ray energy region $\epsilon_\gamma \geq \frac{1}{2}\epsilon_0$ as well as the section in which $\epsilon_\gamma \leq \frac{1}{2}\epsilon_0$. In the general case, to determine the energy spectrum of the neutral pions it is necessary to know the angle distribution $\varphi(\theta)$. However, examination of Eq. (2) indicates that if the function $f(\epsilon_\pi^*)$ is determined from the hard part of the spectrum $F(\epsilon_\gamma)$, the second term in the right-hand part yields only a small correction to the first term even for an angle distribution which is given by the expression $\varphi(\theta) = \cos^2\theta$. This is due to the fact that the hard part of the spectrum is determined basically by the energy spectrum of neutral pions which move in the direction of the spectrometer and is only slightly dependent on the angle distribution if it is given by an expression of the form $\varphi(\theta) = a + b\cos^2\theta$ (for $a > 0$ and $b > 0$). In the case of the angle distribution indicated above, the ratio between the constants a and b is important for the spectrum $F(\epsilon_\gamma)$ only in the energy region $\epsilon_\gamma < 150$ Mev in the CMS of the nucleons.

The energy spectrum of the neutral pions $f(\epsilon_\pi)$ is found in first approximation by solving the integral equation (2) in the hard region of the spectrum $F(\epsilon_\gamma)$ by a method of successive extrapolation from high values of ϵ_π to smaller values, using the approximate expression for $\varphi(\theta)$ in the angle distribution. Using the neutral meson spectrum found in this way it is possible to find a more exact expression for the angle distribution function $\varphi(\theta)$ by comparing, in the lower energy region, the experimental γ-ray spectrum with the spectra calculated for various values of the constants a and b. In turn, using the more accurate angle distribution it is possible to find a more accurate spectrum $f(\epsilon_\pi)$. However, this determination of the angle distribution of neutral pions is possible only if the energy spectrum of the neutral pions in the CMS is weakly dependent on the meson emission angle.

2. *Comparison of the energy spectra for γ-rays from the decay of neutral pions produced by 470 and 660 Mev protons.* The γ-ray spectra obtained by bombarding a carbon target with 660-Mev protons (Fig. 3) differs considerably from the spectrum measured at a proton energy of 470 Mev (Figs. 4, 5 and Ref. 2). As the proton energy is changed from 470 to 669 Mev the upper limit of the spectrum increases in correspondence with the increased maximum collision energy

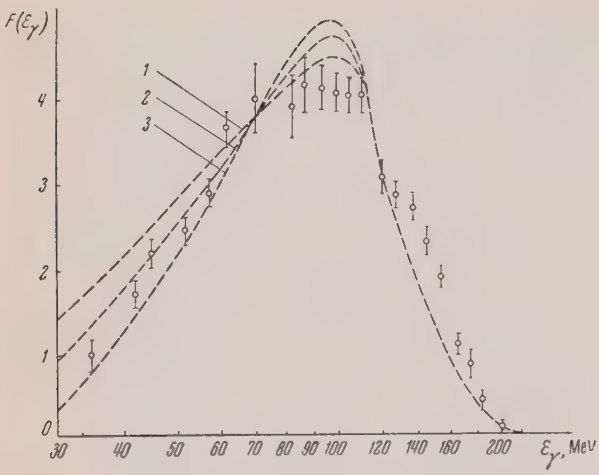

FIG. 4. Energy spectrum of γ-rays from the decay of neutral pions produced by 470-Mev protons in beryllium. Angle of observation 180°. O) measured spectrum. The dashes indicate the spectra computed under different assumptions as to the value of the constant a in the angle distribution $\varphi(\theta) = a + \cos^2\theta$: 1) $a = 0.3$; 2) $a = 0.15$; 3) $a = 0$.

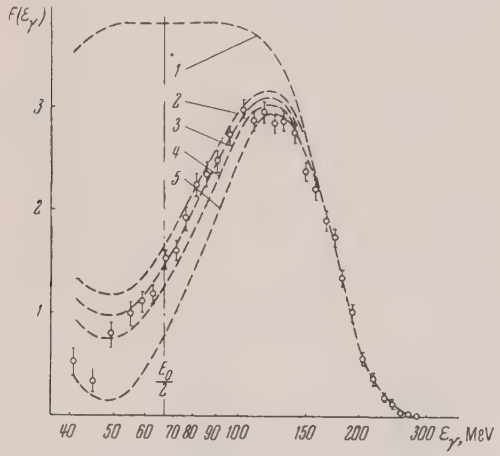

FIG. 5. Energy spectrum of γ-rays from the decay of neutral pions produced by 470-Mev protons in carbon in the CMS. Angle of observation 0°. O) measured spectrum. The dashes indicate the spectra computed under various assumptions as to the magnitude of the constant a in the angle distribution $\varphi(\theta) = a + \cos^2\theta$: 1) isotropic; 2) $a = 0.4$; 3) $a = 0.3$; 4) $a = 0.2$; 5) $a = 0$.

of the proton and the nucleon in the nucleus. At the same time the mean energy of the γ-rays does not increase but, indeed, is found to be smaller: this energy is 190 Mev at $E_p = 470$ Mev and 170 Mev at $E_p = 660$ Mev for spectra measured at an angle of 0° with respect to the proton flux. This fact means that there is a change in the character of the energy and angle distributions of the neutral pions which are produced.

The form of the γ-ray spectra measured at a proton energy of 470 Mev indicates that the neutral-pion angle distribution contains a term proportional to $\cos^2\theta$. The γ-ray spectrum measured at an angle of 0° at $E_p = 660$ Mev has greater logarithmic symmetry (Figs. 5 and 6). This would seem to indicate that the angle distribution for neutral pions produced by 660-Mev protons is more isotropic.

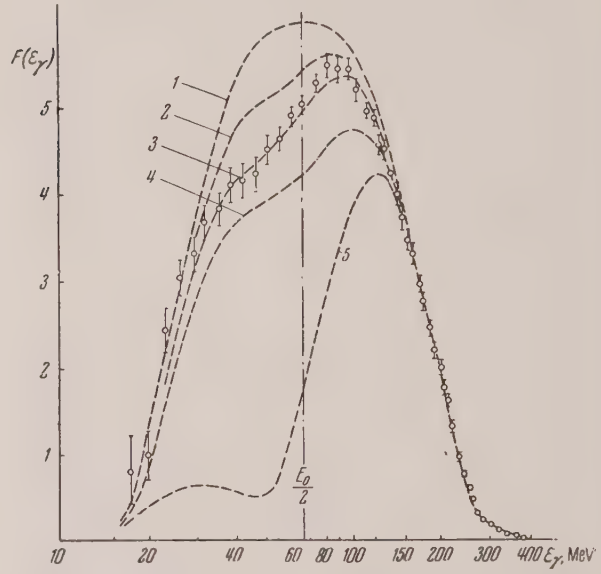

FIG. 6. Energy spectrum of γ-rays from the decay of neutral pions produced by 660-Mev protons in carbon in the CMS. Angle of observation 0°. The dashes indicate the spectra computed under various assumptions as to the magnitude of the constant b in the angle distribution $\varphi(\theta) = 1 + b\cos^2\theta$: 1) $b = 0$; 2) $b = 0.2$; 3) $b = 0.4$; 4) $b = 0.6$; 5) $\varphi(\theta) \sim \cos^2\theta$.

A comparison of the γ-ray spectra also indicates that there is an essential change in the nature of the energy spectra of the neutral pions as the proton energy is increased from 470 to 660 Mev. At proton energies of 470 Mev the neutral pions are produced with energies close to the maximum possible energy which the meson can acquire in the reaction. This conclusion is drawn on the basis of a comparison of the measured γ-ray spectra with the spectra calculated in the impulse approximation from the dependence of the pion production cross section on the collision energy of the nucleons under the assumption that the meson acquires the maximum possible energy. A comparison of the spectra calculated with various assumptions as to the magnitude of the constant a in the angle distribution $\varphi(\theta) = a + \cos^2\theta$ with the spectrum for γ-rays measured at 180° with respect to the proton flux (Be target) is given in Fig. 4. From a

comparison of the calculated spectra and the experimental spectrum it is possible to make an estimate of the constant a in the angle distribution of the neutral pions which are produced:

$$a = 0{,}15 \pm 0{,}15.$$

A comparison of the γ-ray spectra calculated under the assumptions given above with the experimentally-determined spectra at proton energies of 660 Mev indicates a considerable difference. Regardless of the magnitude of the constant a in the pion angle distribution the calculated γ-ray spectra are found to be considerably harder than the spectrum measured at an angle of 0°. If follows from this fact that at proton energies of 660 Mev the neutral pions are produced mainly with energies considerably below the maximum possible energy. This conclusion has also been reached on the basis of an analysis of the γ-ray spectrum measured at 180°[5] and the mean energies of γ-quanta at angles of 0° and 180° as measured by an absorption method.[4]

3. *Energy spectra of neutral pions produced by 470 and 660 Mev protons.* Fig. 7 shows the pion energy distributions in the effective CMS for meson production in carbon by 470 Mev protons. These distributions have been calculated from the hard portion of the spectrum measured at 0° assuming an isotropic pion angle distribution and a distribution proportional to $\cos^2\theta$. In this same figure the dashed curve indicates the pion spectrum calculated in the impulse approximation under the assumption that the mesons which are produced always acquire the maximum possible energy. The calculation was carried out under the assumption that the momentum distribution of nucleons in the nucleus is given by a Gaussian function with a mean-square momentum of 120 Mev/c. Comparison of the pion spectrum (Curve 1) with the spectrum calculated as indicated above (dashed curve) shows that when the carbon target is bombarded by 470-Mev protons the mesons are produced with energies close to the maximum possible energy. The difference between these curves is actually smaller if account is taken of the proton energy loss due to passage through the carbon nucleus. The hard part of the spectrum $F(\epsilon_\gamma)$ contains γ-quanta due to the decay of neutral ions which enter the spectrometer. Considering the strong absorption of neutral pions in nuclear matter[4,2] it may be assumed that the γ-quanta recorded by the spectrometer (hard part of

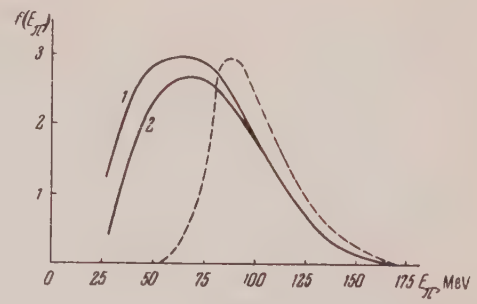

FIG. 7. Energy spectrum of neutral pions produced by 470-Mev protons in carbon in the CMS. The solid curves are the spectra computed for the hard part of the measured spectrum under the following assumptions: 1) isotropic distribution, 2),distribution proportional to $\cos^2\theta$.

the spectrum) appear as a result of the decay of neutral pions which are formed at the surface of the nucleus facing the observer. In measurements of the γ-ray spectra at an angle of 0° the surface of the nucleus facing the observer is bombarded by protons which have first passed through the nucleus. In this case the proton flux becomes energetically less homogeneous and the average particle energy is reduced. This effect has not been taken into account in calculating the spectrum shown by the dashed curve. A considerably smaller difference is observed between the spectra measured at 180° and the spectrum calculated in the impulse approximation (cf. Fig. 4). However,in this case the energy spectrum of the γ-quanta may be distorted in the hard portion because of scattering of neutral pions in the same nucleus in which they are produced.

Fig. 8 shows the pion energy spectrum in the CMS for proton energies of 660 Mev. The spectrum was

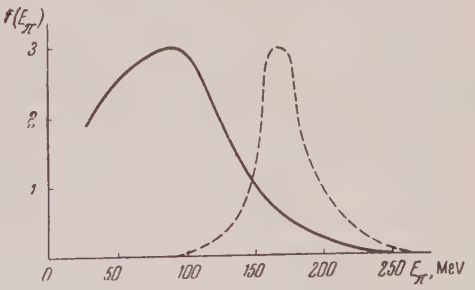

FIG. 8. Energy spectrum of neutral pions produced by 660-Mev protons in carbon in the CMS. The dashed curve is the spectrum calculated in the impulse approximation.

calculated under the assumption of an isotropic pion distribution in the hard part ($\epsilon_\gamma > \frac{1}{2}\epsilon_0$) of the γ-ray spectrum measured at an angle of 0° represented by the smooth curve (cf. Fig. 3). The dashed curve denoted the pion spectrum computed in the impulse

approximation; the calculation was carried out under the assumption that the produced mesons acquire the maximum possible energy.

4. *Angle distributions for neutral pions produced by 470 and 660 Mev protons.* In the energy region $\epsilon_\gamma \leq \frac{1}{2}\epsilon_0$ the shape of the γ-ray spectrum depends strongly on the pion angle distribution. This fact can be utilized to obtain a more accurate determination of the angle distribution by a comparison of the measured γ-ray spectrum with the spectra calculated in accordance with different assumptions to the angle distribution. The calculation of the spectra is carried out using the neutral-pion energy distribution found earlier from the hard part of the measured γ-ray spectrum.

From a comparison of the computed and measured γ-ray spectra at proton energies of 470 Mev and an angle of observation of 0° (cf. Fig. 5) it is apparent that the best agreement is found for the angle distribution $\varphi(\theta) = 0.3 + \cos^2\theta$. Taking into account the uncertainty in the measured spectrum, it may be assumed in agreement with the data of Ref. 6. that the constant $a = 0.3 \pm 0.1$. The less accurate determination of this constant presented above, using the γ-ray spectrum measured at 180°, yields $a = 0.15 \pm 0.5$. The values of the constant are in agreement within the error limits. A comparison of the computed γ-ray spectra with that measured at an angle of 0° for a proton energy of 660 Mev (Fig. 6) indicates that satisfactory agreement obtains for an angle distribution $\varphi(\theta) = 1 + 0.4\cos^2\theta$. Taking account of the errors in the measurement of the γ-ray spectrum it may be assumed that the constant $b = 0.4 \pm 0.2$.

The angle distributions $\varphi(\theta)$ which have been obtained can, in turn, be used to calculate a more exact spectrum of the neutral pions. However, this correction to the neutral pion spectra is considerably smaller than the uncertainty in the spectra which arise as a result of the simplifying assumptions which have are used in the analysis and the errors in the measurements of the γ-ray spectra which are being analyzed.

It has already been noted above that the use of this method of analysis of γ-ray spectra can give only approximate information on the angle and energy distributions of neutral pions produced in complex nuclei. It should be pointed out that in addition to the approximations which have been indicated earlier, which are valid for this analysis, there is still one more source of uncertainty in the determination of the angle distributions and the spectra of the neutral pions. The additional errors in the analysis are due to changes in the meson energy and angle distributions due to the particular opacity of the nucleus to the bombarding protons and also due to the interaction of mesons with nucleus in which they are produced. It has been shown in Ref. 4 that even for light nuclei (Li and C) these effects can cause a considerable change in the γ-ray angle distribution. This finding is also corroborated by the change in the ratio of the γ-ray flux observed in the present work at angles of 0° and 180°. As has already been remarked, this ratio, measured in carbon with the γ-spectrometer, was found to be 5.1 ± 0.3. Measurements with a scintillation-counter telescope and a Cerenkov counter show this ratio to be 5.5 ± 0.1.[7] However, for a pion angle distribution which is symmetric in the CMS with respect to the motion of the colliding nucleons, this ratio should be 9.6 in the case in which meson production occurs in nucleons at rest, and 8–9 in the case of meson production in nucleons moving inside the nucleus. In the determination of the pion angle distribution form the γ-ray spectrum measured at an angle of 0° with respect to the motion of the protons which bombard the target, the indicated effects lead to a value which is too high for the constant a as found by the method described above.

DISCUSSION OF THE RESULTS

From an investigation of the energy spectra and the angle distributions for neutral pions produced in the bombardment of complex nuclei by protons it is possible to draw certain conclusions as to the nature of the pion production process in nucleon collisions.

The energy and angle distributions for neutral pions found from the γ-ray spectrum measured at a proton energy of 470 Mev indicate that in this case the neutral mesons produced in the nucleon collision acquire a large part of the free collision energy and also a large angular momentum, and, consequently are produced for the most part in P-states. This same pattern has been observed at lower proton energies as indicated on the basis of the γ-ray spectra measured in Ref. 3. At proton energies of 470 Mev the neutral pions are produced mainly in $(p-n)$ collisions since the cross-section $\sigma_{pp}^{\pi^0}$ is approximately four times smaller then $\sigma_{pn}^{\pi^0}$.[6] Hence the conclusion which has been indicated pertains to the production

of neutral pions in the collision of protons with neutrons in the nucleus. Using this same ratio for the cross-sections $\sigma_{pn}^{\pi^0}/\sigma_{pp}^{\pi^0} = 4$ the neutral pions produced in p–p collisions can have an important effect on the magnitude of the constant a in the angle distribution for mesons produced in complex nuclei if the angle distribution for the reaction $p + p \to \pi^0 + p + p$ is almost isotropic. However, according to the data of Ref. 7, the angle distribution for neutral pions in the latter reaction for a proton energy $E_p = 470$ Mev within the limits of the experimental error, does not differ from the meson angle distribution $\varphi(\theta) = (0.3 \pm 0.1) + \cos^2\theta$ in production in complex nuclei. Hence, it may be assumed that the angle distribution for neutral pions produced in collisions of protons with neutrons in the nucleus does not differ considerably from the obtained distribution $\varphi(\theta) = 0.3 + \cos^2\theta$.

Investigations of the reaction $n + p \to \pi^0 + d$ at a neutron energy $E_n = 400$ Mev carried out by Hildebrand[8] and Schulter[9] show that the meson angle distribution in this case is given by a function of the form $\varphi(\theta) = a + \cos^2\theta$ with the constant $a = 0.21 \pm 0.6$ [sic!] according to the data of the first reference and $a = 0.28 \pm \frac{0.26}{0.14}$ according to the data of the second reference. The fact that the neutral-pion angle distribution, for pions produced in collisions of protons with neutrons in the nucleus, does not differ, within the experimental errors, from the angle distribution in the reaction $n + p \to \pi^0 + d$ may indicate that in the production of mesons in complex nuclei in p–n collisions there is a strong interaction between the final nucleons in the S-state.

This conclusion follows more directly from the fact that the neutral pions which are produced acquire a large part of the free energy of the reaction. A similar pattern has also been observed in reactions which involve the production of charged pions.[10]

In Ref. 4 mention was also made of the change in the nature of the pion production process found with an increase of proton energy from (340–470) to 670 Mev. An examination of the angle and energy distributions obtained in this work leads to the same conclusion. While the spectrum for neutral pions produced in complex nuclei at a proton energy of 470 Mev is not greatly different from the spectrum computed a maximum possible energy, at a proton energy of 660 Mev there is a considerable difference between the observed spectrum and the spectrum computed according to this same assumption. At a proton energy of 660 Mev in the great majority of cases the pions are produced with energies considerably below the maximum possible energy. It follows from this situation that in the production of neutral pions by 660 Mev protons the nucleons in the final state possess a large kinetic energy and, consequently, a high momentum. However, this is possible only if the nucleons are emitted at large angles with respect to each other, consequently, in the final state of the reaction the nucleons interact in states with high angular momentum (in the P-, D-, ... states).

As the proton energy is increased from 470 to 660 Mev the pion angle distribution changes considerably. At a proton energy of 470 Mèv the ratio of the number of pions, distributed isotropically in the CMS of the colliding nucleons to those distributed according to a $\cos^2\theta$ law is approximately 1 : 1; at a proton energy of 660 Mev this ratio becomes 8 : 1.

In conclusion the authors wish to express their gratitude to A. N. Sinaev for assistance in operating the apparatus and to L. A. Kuliukin for help in carrying out the calculations.

[1] Kozodaev, Tiapkin, Markov and Baiukov, Report of the Institute for Nuclear Problems, Acad. of Sciences USSR (1952).

[2] Kozodaev, Tiapkin, Baiukov, Markov and Prokoshkin, Izv. Akad. Nauk SSSR, Ser. Fiz 19, 589 (1955).

[3] W. E. Crandall and B. J. Moyer, Phys. Rev. 92, 749 (1953).

[4] Tiapkin, Kozodaev and Prokoshkin, Dokl. Akad. Nauk SSSR 100, 689 (1955).

[5] Baiukov, Kozodaev and Tiapkin, Report of the Institute for Nuclear Problems, Acad of Sciences USSR (1954).

[6] Iu. D. Prokoshkin and A. A. Tiapkin, J. Exptl. Theoret. Phys. (U.S.S.R.) this issue, p. 618.

[7] Iu. D. Prokoshkin and A. A. Tiapkin, J. Exptl. Theoret. Phys. (U.S.S.R.) 33, (in press).

[8] R. H. Hildebrand, Phys. Rev. 89, 1090 (1953).

[9] R. A. Schulter, Phys. Rev. 96, 734 (1954).

[10] K. M. Watson and K. A. Brueckner, Phys. Rev. 83, 1 (1951).

Translated by H. Lashinsky
161

Production of Neutral Pions by Neutrons on Deuterons and Complex Nuclei*

V. P. DZHELEPOV, K. O. OGANESIAN AND V. B. FLIAGIN
Joint Institute for Nuclear Research

(Submitted to JETP editor November 19, 1956)
J. Exptl. Theoret. Phys. (U.S.S.R.) 32, 678-681 (April, 1957)

The γ-ray yield from the decay of neutral pions produced by 590-Mev neutrons in deuterium has been measured at an angle of 90° in the laboratory system. The total cross-sections for the production of neutral pions in (nd) and (nn) collisions, determined on the basis of these measurements, were found to be $\sigma_{nd}^{\pi^0} = (7.4 \pm 2.0) \times 10^{-27}$ cm^2, $\sigma_{nn}^{\pi^0} = (1.7 \pm 0.5) \times 10^{-27}$ cm^2.

The relative yield of γ-rays from the decay of neutral pions produced in various elements was also measured at this angle. The γ-ray yield can be described approximately by the function $A^{2/3}$.

1. INTRODUCTION

PROCESSES in which neutral mesons are produced in the interaction of high-energy neutrons with nucleons and complex nuclei have been investigated less thoroughly than similar processes induced by protons. This situation arises as a result of the difficulties encountered in neutron experiments. On one hand one finds relatively weak neutron flux intensities; on the other there is the small cross-section for the production of neutral pions at neutron energies on the order of 400 Mev, which are typical of the large majority of existing synchrocyclotrons.

The fact that a neutron beam with an energy of approximately 600 Mev was available at the synchrocyclotron of the Laboratory for Nuclear Problems made it possible to start a systematic investigation of the production of neutral pions by neutrons on nucleons and complex nuclei. We have already reported the results of measurements of the cross-section $\sigma_{np}^{\pi^0}$ for the production of neutral pions in $(n-p)$ collisions.[1] When the present work was finished, we had obtained more complete data on the neutron spectrum which was used in our experiments and also completed the measurements of the differential cross-sections for elastic $(n-p)$ scattering which was used in Ref. 1 to determine the absolute magnitude of the cross-section $\sigma_{np}^{\pi^0}$. The new data have made it possible to obtain a more accurate cross-section $\sigma_{np}^{\pi^0}$ at an effective proton energy of 590 Mev and yield the value

$\sigma_{np}^{\pi^0} = (5.7 \pm 1.5) \times 10^{-27}$ cm^2.

In the present work we present the results of measurements of the total cross-sections for the production of neutral pions in collisions with neutrons and deuterons as well as data on the γ-ray yields in the decay of neutral pions produced by neutrons in nuclei of various elements. The most interesting of these experiments is the investigation of the production of neutral pions in neutron-neutron collisions since this reaction has not been observed until recently.

2. PRODUCTION OF NEUTRAL PIONS IN DEUTERIUM

Difference experiments with D_2O and H_2O targets were performed to study the production of neutral pions in deuterium. The containers for the heavy water and the ordinary water were plexiglass cylinders 40 mm in diameter, 40 mm long, with a wall thickness of 0.5 mm. As in Ref. 1, the γ-rays from the decay of neutral pions were detected with a telescope oriented at an angle of 90° with respect to the neutron beam, and consisting of scintillation counters and a Cerenkov detector. The magnitude of the total cross-section for the production of neutral pions, determined from the γ-ray yield at an angle of 90° in the laboratory system, is relatively weakly dependent on the angle distribution of the neutral pions in the center of mass system (CMS) of the colliding nucleons (provided only the odd powers of cos θ are relatively weak in the angle distribution, where θ is the pion angle in the CMS). Hence, in determining the cross-section $\sigma_{nd}^{\pi^0}$ for the production of neutral pions on the deuteron, and also in determining the

*The results of this work have been reported at the Moscow and Geneva conferences on high-energy particle physics in 1956.

difference $\sigma^{\pi^0}_{n(d-p)}$ in the cross-sections for the deuteron and hydrogen, we have started from this assumption; furthermore, we have neglected the difference in angle distribution for neutral pions produced in the bound nucleons in the deuteron as compared with the distribution of pions produced by collisions of free nucleons.

In view of the fact that the effect due to the neutron bound in the deuteron is small as compared with effects due to D_2O and H_2O a long observation time was required to obtain the necessary statistical accuracy.

The results of the measurements were used to determine the ratio

$$(\sigma^{\pi^0}_{nd} - \sigma^{\pi^0}_{np}) / \sigma^{\pi^0}_{np} = 0.30 \pm 0.04$$

This relation makes it possible to determine from the known cross-section $\sigma^{\pi^0}_{np}$ the difference in the cross-sections for the production of neutral pions in (nd) and (np) collisions

$$\sigma^{\pi^0}_{n(d-p)} = (1.7 \pm 0.5) \cdot 10^{-27}\ cm^2,$$

and also to determine the cross-section for the production of neutral pions in (nd) collisions

$$\sigma^{\pi^0}_{nd} = (7.4 \pm 2.0) \cdot 10^{-27}\ cm^2.$$

The difference $\sigma^{\pi^0}_{n(d-p)}$, if one neglects the binding of the nucleons in the deuteron, is the quantity of interest—the cross-section for the production of neutral pions in neutron-neutron collisions $\sigma^{\pi^0}_{nn}$.

The effective energy corresponding to the cross-section which is found is determined from the neutron spectrum and the excitation function for the processes being investigated. However, as has been shown by calculation, for a given neutron spectrum this quantity is relatively insensitive to the excitation function. Thus, for example, if one replaces the excitation function $K^{3.5}$ by K^5 (where K is the maximum momentum of the neutral pions in the CMS of the colliding nucleons), the effective energy increases only by 3–5 Mev. According to Ref. 2 the excitation function for the reaction $p + n \to \pi^0 + (p + n)$ is similar to the first function while the excitation function for the reaction $p + p \to \pi^0 + p + p$ is similar to the second. This fact makes it possible to take the effective neutron energy as approximately 590 Mev, as in Ref. 1, for the measured cross sections for the production of neutral pions on deuterons as well as complex nuclei.

As is well known, in the experiments carried out by Pontecorvo and Selivanov[3] with deuterons at energies of 400 Mev, no systematic difference in the intensity of γ-rays from targets of D_2O and H_2O was observed; the authors give only an estimate of the upper limit for the cross-section for the production of neutral pions in neutron-neutron collisions: $\sigma^{\pi^0}_{nn} < 10^{-28}$ cm^2. A comparison of the data obtained by the present authors with these results indicates that there is an extremely rapid increase in the probability of production of neutral pions in $(n-n)$ collisions, similar to that which occurs in $(p-p)$ collisions. In both cases this situation can be explained by the fact that transition to higher energies means that final nucleon states characterized by high orbital moments ($l > 0$) become important; hence the production of neutral pions in $(p-p)$ and $(n-n)$ collisions tends to be inhibited by considerations connected with conservation of total momentum and parity in the emission of a pseudoscalar neutral pion in a P-state and nucleons in an S-state.

The value of $\sigma^{\pi^0}_{nn}$ found in the present work coincides, within the error limits, with the cross section for the production of neutral pions in $(p-p)$ collisions, which is (1.8 ± 0.4) cm^2 at an energy of 590 Mev according to measurements of Prokoshkin and Tiapkin;[2] these data are not in contradiction with charge symmetry for nuclear forces. On the hand, the ratio of the cross-sections $\sigma^{\pi^0}_{n(d-p)} / \sigma^{\pi^0}_{np}$ measured by us with considerably greater accuracy than the absolute value of the corresponding cross-sections, was found to be smaller than the ratio $\sigma^{\pi^0}_{pp} / \sigma^{\pi^0}_{p(d-p)} = 0.41 \pm 0.08$ measured at a proton energy of 580 Mev. This fact apparently indicates that in assuming the equality $\sigma^{\pi^0}_{pp} = \sigma^{\pi^0}_{nn}$ the cross-section for the production of neutral pions on a deuteron is smaller than the sum of the cross-sections for the production of neutral mesons on a free proton and neuteron.

3. PRODUCTION OF NEUTRAL PIONS BY NEUTRONS IN COMPLEX NUCLEI

Using a similar method (also at 90°), measurements were made of the relative yield of γ-rays from the decay of neutral pions produced in collisions of neutrons with an effective energy of approximately 590 Mev with Be, C, Al, Cu, Sn, Pb and U nuclei. Measurements with heavy water and ordinary water made it possible to also determine the γ-ray yield in deuterium nuclei and oxygen nuclei. The amount of material in the targets was chosen to give approximately the same γ-ray yield. The ab-

sorption of γ-rays in the samples themselves was determined from the well-known experimental data on the total cross-section for the absorption of γ-rays in various materials.[4] The results of the measurements are given in the table and the figure. The abcisa axis represents, on a logarithmic scale, the atomic weight of the material. Along the ordinate

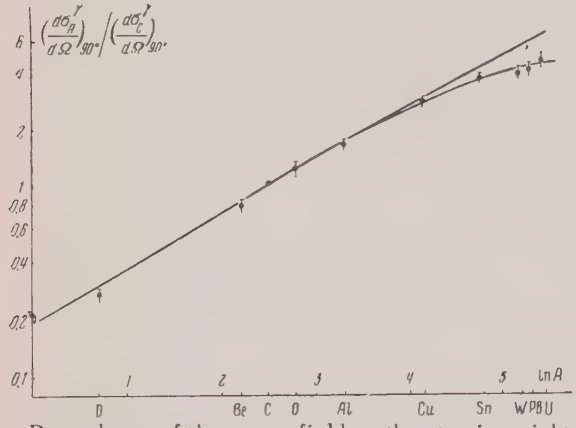

Dependence of the γ-ray field on the atomic weight of the material. The straight line corresponds to the relation $[(A-Z)\,\sigma_{nn}^{\pi^0} + Z\sigma_{np}^{\pi^0}]\,A^{1/3}$

axis is plotted the ratio of the γ-ray yield for a given material to the γ-ray yield from carbon. For purposes of comparison, the figure shows the function

$$[(A-Z)\,\sigma_{nn}^{\pi^0} + Z\sigma_{np}^{\pi^0}]\,A^{-1/3} \approx A^{2/3} \qquad (1)$$

(in relative units) which gives the production of neutral pions as a function of the atomic weight of the material under the assumption that the mesons are effectively produced only by surface nucleons of the nucleus.*

As can be seen, the experimental dependence on the atomic weight obtained for the γ-ray yield is in agreement with that calculated from Eq. (1), for elements from carbon to copper. For the light nuclei, H, D, and Be, the dependence of the γ-yield obtained as a function of atomic weight also differs only slightly from the relation given in (1). For the heavier elements Sn, W, Pb and U, the γ-ray yield increases less rapidly.

The experimental dependence of the γ-ray yield on the atomic weight indicates that the neutral pions are produced effectively mainly by surface nucleons in the nucleus. Assuming that the mesons are produced only at the surface of the nucleus and also that the γ-rays from the decay of neutral pions move in the same direction as the neutral pions and that the neutron flux falls off exponentially in passing through the thickness of the nucleus, we have made an estimate of the relative yield of γ-rays from various elements at an angle of 90° in the laboratory system. In this case the departure from the $A^{2/3}$ law can be satisfactorily explained by the relatively lower transparency of heavy nuclei to high-energy neutrons as compared with light nuclei. A similar picture of the interaction, as presented by the authors of Ref. 5, is in qualitative agreement with their experiments, in which the dependence of the γ-ray yield on atomic weight at angles of 0° and 180° was determined for the same nuclei under bombardment by 660-Mev protons. However, we have not been able to obtain complete quantitative agreement of all results using the assumptions that have been made.

Element	A	$\sigma_A^\gamma/\sigma_C^\gamma$	$[(A-Z)\sigma_{nn}^{\pi^0} + Z\sigma_{np}^{\pi^0}]\,A^{-1/3}$
H	1	0.21 ± 0.015	—
D	2	0.27 ± 0.02	—
Be	9	0.78 ± 0.04	0.77
C	12	1	1
O	16	1.2 ± 0.1	1.21
Al	27	1.61 ± 0.08	1.70
Cu	63.5	2.80 ± 0.14	2.93
Sn	119	3.8 ± 0.2	4.30
W	184	4.0 ± 0.3	5.60
Pb	207	4.2 ± 0.3	6.05
U	238	4.8 ± 0.4	6.75

[1] Dzhelepov, G. Oganesian and Fliagin, J. Exptl. Theoret. Phys. (U.S.S.R.) **29**, 886 (1955).

[2] Iu. D. Prokoshkin and A. A. Tiapkin, J. Exptl. Theoret. Phys. (U.S.S.R.) this issue, p. 618.

[3] B. M. Pontecorvo and G. I. Selivanov, Dokl. Akad. Nauk SSSR **102**, 253 (1955).

*In calculating this function we have used the values of $\sigma_{nn}^{\pi^0}$ and $\sigma_{np}^{\pi^0}$ found by us.

[4] DeWire, Ashkin and Beach, Phys. Rev. 83, 505 (1951).
[5] Tiapkin, Kozodaev and Prokoshkin, Dokl. Akad. Nauk SSSR 100, 689 (1955).

Translated by H. Lashinsky
162

SOVIET PHYSICS JETP VOLUME 5, NUMBER 4 NOVEMBER, 1957

Internal Conversion Electron Spectrum of Radiothorium II

A. I. ZHERNOVOI, E. M. KRISIUK, G. D. LATYSHEV,
A. S. REMENNYI, A. G. SERGEEV AND V. I. FADEEV
Leningrad Institute of Railroad Engineering

(Submitted to JETP editor September 24, 1956)
J. Exptl. Theoret. Phys. (U.S.S.R.) 32, 682-689 (April, 1957)

The internal conversion electron spectrum of a sample of RaTh has been investigated in the $H\rho$ range from 500 to 1380 gauss-cm. The energies and relative intensities of the conversion lines have been determined. It is shown that spectrometers can be calibrated with an accuracy of 5×10^{-4} through the use of Auger electrons.

1. CALIBRATION OF THE SPECTROMETER

AN INVESTIGATION OF A CONVERSION spectrum has been carried out using a magnetic spectrometer with improved focusing[1] with an instrument line width of 0.25%. The aperture angle of the spectrometer in the horizontal plane is 40° and the height of the diaphragms 16 mm. The source and counter slits measure 0.3×16 mm. The magnetic field is measured by the proton-resonance method.[2] The electrons are detected in two self-quenching Geiger counters, connected in coincidence; the count at the first counter is also recorded.

The calibration of the instrument was carried out with the most accurate presently available values of $H\rho$ for the conversion lines for radiothorium. These values are given in the second column of Table 1.

The values of $H\rho$ for the A, B, F, I and J-lines were taken from the work of Siegbahn and Edvardson.[3] These values have an uncertainty of approximately 7×10^{-5}. The value of $H\rho$ for the L-line was taken from the work of Lindstrom[4] which has an uncertainty of approximately 1.2×10^{-4}. The values of $H\rho$ for the Aa and Ab-lines were calculated by using the values of $H\rho$ for the A-line given by Siegbahn. In this calculation we have used the fact that the A, Aa and Ab lines are produced by the conversion of the same 39.85-kev γ-quanta in the T1 atom in the L_I, L_{II} and L_{III}-subshells respectively. In these calculations, as in all similar calculations in this work, we have used the binding energies given by Hill[5] and the tables given by Gerholm for the conversion of $H\rho$ to energy.[6] The Hill tables are apparently the most accurate; by the author's estimate the accuracy is of order of ±10 ev for the absolute values of the binding energy and of the order ±1 ev for the differences in binding energy.

The value of $H\rho$ for the E-line was calculated starting from the fact that this line is obtained in the conversion of 115.14-kev γ-quanta in the L_I-subshell of the bismuth atom. The energy of these quanta was determined using the fact that the A-line is complex and consists of two lines, one of which is obtained in the conversion of 39.85-kev γ-quanta in the L_I-subshell of the T1 atom and the other in the conversion in the K-shell of those γ-quanta which yield the E-line. The spacing between these lines is 110 ev.[7]

Column 3 of Table 1 lists the nuclear-resonance frequencies f corresponding to the maxima of the lines, while column 4 gives the value of k, which is the ratio of $H\rho$ to the frequency f. From Table 1 and Fig. 1 it is obvious that $H\rho$ is not linear with f for $H\rho < 2600$ gauss-cm. The departure from linearity for the A-line is approximately 0.2%. This departure from linearity may be explained qualitatively by the change in the magnetic-field configuration in the low-field region. Because measurements of the magnetic field by the nuclear resonance method require the placement of the pick-up coil in

TABLE I. Conversion lines used in calibrating the instrument.

Line	$H\rho$	E, MeV	kc/sec	$k = H\rho/f$
A	534.21	24.510	284.248	1.87938
Aa	541.40	25.159	287.975	1.87980
Ab	563.50	27.201	299.748	1.87992
B	652.40	36.153	346.955	1.88036
E	1109.71	98.756	589.765	1.88162
F	1388.44	148.08	737.494	1.88266
I	1753.91	222.22	931.254	1.88338
J	1811.11	234.60	961.586	1.88346
L	2607.17	422.84	1383.04	1.88510

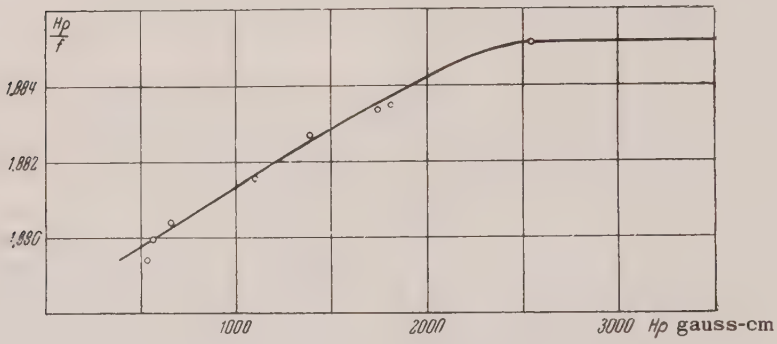

FIG. 1. Calibration curve for the ketron at low energies.

a homogeneous region of the field, we measured the field not directly at the electron trajectories, but in the region of maximum homogeneity. Hence, a change in the magnetic field configuration will lead to nonlinear effects in the instrument.

It should be noted that the value of k for the A-line departs from the smooth curve more than for the other points; this situation may be due to the complex structure of the A-line. Hence, in plotting the curve this point was not included. As has been shown earlier,[8] for $H\rho > 2600$ gauss-cm, the instrument is linear within the limits of accuracy of the experiment.

The nonlinearity of the instrument reduces strongly the accuracy in the determination of the energies of the lines in our instrument. Whereas in the region $H\rho > 2600$ gauss-cm, in which the instrument is linear, the accuracy of the relative measurements of $H\rho$, according to our estimates,[8] reaches 10^{-4}, the uncertainty in $H\rho$ for strong lines is approximately 3×10^{-4} in the nonlinear region.

2. AUGER ELECTRONS FROM Bi^{212} (ThC)

The calibration of the instrument can be checked by a measurement of the energies of Auger electrons.

We have used the following series of Auger electrons: $KL_p\,L_q$, KL_pM_q, KL_pN_q and KL_pO_q. The series KL_pM_q, KL_pN_q, KL_pO_q contain a large number of components which are located close to one another. Fig. 2 shows the composite curve for these series. We did not attempt to resolve these lines graphically but only determined the total intensity of the group with respect to the I-line. This ratio was found to be 0.0782. The arrows denote the positions of the maxima of the individual lines, calculated under the assumption that the absence of electrons in the L-shell reduces the shielding of the nucleus by an amount corresponding to an increment in the charge of the nucleus of $\Delta Z = 1$. It is apparent from Fig. 2 that this assumption, within the limits of the accuracy, does not contradict the experimental result. The series KM_pM_q, KM_pN_q etc. were not observed because of their low intensity.

The KL_pL_q Auger electron series consists of six rather closely spaced lines. In our work and in Refs. 9 and 10 these have been partially resolved (Fig. 3). Table 2 shows the positions and intensities of the Auger electrons of this series. Our data are compared with the results of Ellis[11] and Mladjenovic and Slätis,[10] who investigated Auger

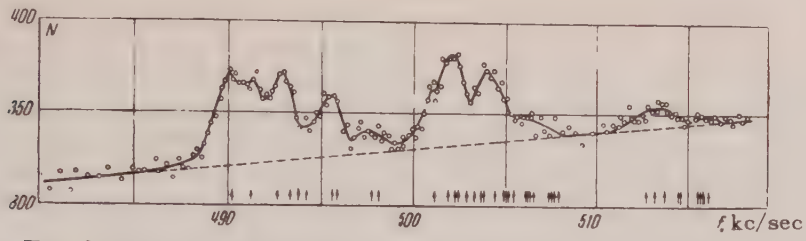

FIG. 2. Auger electrons from Bi^{212} (ThC) of the series KL_pM_q, KL_pN_q and KL_pO_q. The arrows indicate the positions of the maxima of the individual lines computed under the assumption that $\Delta Z = 1$.

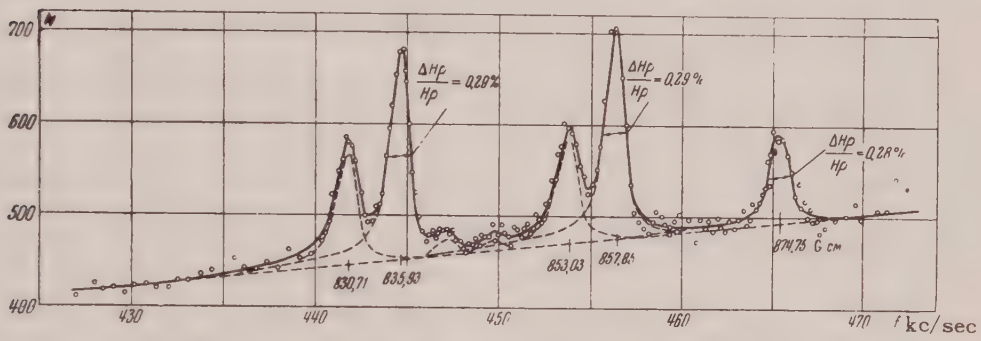

FIG. 3. Auger electrons from B^{212} (ThC) KL_pL_q series.

TABLE II. Spectrum for Auger electrons; KL_pL_q series.

Transition	Present data				Ref. 10		Ref. 11	
	$H\rho$	E	I	I_1	I	$H\rho$	I	$H\rho$
$KL_I\ L_I$	830.71	57.458	1.00	0.0247	1.0	830.77	1	826.6
$KL_I\ L_{II}$	835.93	58.147	1.72	0.0425	1.8	836.17	1.8	832.3
$KL_{II}\ L_{II}$	840.75	58.783	0.17	0.0043	<0.2	—	0.2	—
$KL_I\ L_{III}$	853.03	60.423	0.91	0.0224	1.1	853.00	1.3	849.5
$KL_{II}\ L_{III}$	857.85	61.070	1.64	0.0404	1.6	858.01	2.3	854.5
$KL_{III}L_{III}$	874.75	63.367	0.69	0.0170	0.8	875.04	1.3	871.5

electrons of this series for the same Z. It is apparent from the table that our date are in good agreement with the results of Mladjenovic and Slätis. The average discrepance in the magnitude of $H\rho$ in our work and in Ref. 10 is approximately 2×10^{-4} while the error in both papers is approximately 3×10^{-4}. The relative line intensities are also found to be in good agreement with the data of Mladjenovic and Slätis if it is assumed that the errors in both papers are on the order of 10%. The quantity I_1 given in the table is the intensity with respect to the I line.

The energy of Auger electrons can be calculated from the formula:

$$E_{KL_pL_q} = E_K^Z - E_{L_p}^Z - E_{L_q}^{Z+\Delta Z},$$

where E_K^Z and $E_{L_p}^Z$ are the binding energies for K and L-electrons respectively in the normal atom while $E_{L_s}^{Z+\Delta Z}$ is the binding energy of the L_q-electrons in the atom with the L_p-electron absent. The binding energy of the L_q-electron is increased because of the reduction in the shielding of the nuclear charge due to the absence of the L_p-electron. Quantitatively the reduction in the shielding can be written in terms of an effective increase in the charge as in Refs. 9 and 10:

$$\Delta Z = (E_{L_q}^{Z+\Delta Z} - E_{L_q}^{Z})/(E_{L_q}^{Z+1} - E_{L_q}^{Z}).$$

A theoretical calculation of the quantity ΔZ is extremely complicated and has not been carried out at the present time. The best experimental determination is that given in Refs. 9 and 10. Table 3 lists the calculated values of ΔZ and also the results of Mladjenovic and Slätis[10] for $Z = 83$ and those of Bergström and Hill[9] for $Z = 80$. These quantities are found to be in agreement within the error limits.

In the first approximation it follows from our results, as has already been noted,[9,10] that the binding energy of the L_q-electron is independent of which of the L-subshells has a missing electron. Hence, as in Refs. 9 and 10, we have determined ΔZ from the average value of $E_{L_q}^{Z+\Delta Z}$ (averaging three values of $L_{L_q}^{Z+\Delta Z}$ corresponding to the absence of L_I, L_{II} and L_{III} electrons). However, if one takes into account the departure from the average for the case of a missing L_I electron and for a missing L_{III} electron, it turns out that both our data as well as those of Mladjenovic and Slätis should show a difference between the binding energy of the L_q-electrons when there is an electron missing in the L_I subshell and the energy when an electron is missing in the L_{III} subshell; on the average this difference is approximately 20 ev. This corresponds to a quantity of the order of 4×10^{-4} of the electron energy, whereas the error in both investigations is approximately 3×10^{-4}. The binding energy of the L_q-electrons for a missing L_{III}-electron is greater than in the case of a missing L_I electron. The results of Bergström and Hill[9] have not been taken into account in this connection since the relative error in their work is approximately 10^{-3}. As regards the case in which an L_{II} electron is ejected, the results of the present work and those of Ref. 10, indicate only that the binding energy of the L_q-electron when an electron is absent in the L_{II} shell lies between the values which apply for electrons missing in the L_I and L_{III} subshells.

The results of the measurements of the spectrum for Auger electron indicate that our data are in good agreement with the results of Mladjenovic and Slätis and those of Bergström and Hill; this fact verifies the calibration of the spectrometer and also indicates, that at the present time, the energy of Auger electrons is known with an accuracy of approximately 5×10^{-4} or better and can be used for calibrating spectrometers in the soft region.

3. INTERNAL CONVERSION ELECTRONS

The spectrum of internal conversion electrons from radiothorium has been investigated earlier by Ellis,[12,13] Surugue,[14,15] and Arnoult.[16] In all these papers photographic detection of the electrons was employed. The shortcoming of this method lies in the large error in the determination of the relative line intensities. This error is due chiefly to the necessity of introducing corrections for the spectral sensitivity of photographic plates and the nonlinear dependence of the blackening density on radiation intensity. In work performed by Flammersfield[17] electron detection was carried out with a Geiger counter; however, the resolving power in this work was rather low (approximately 1 percent) and since it was not possible to resolve many of the lines, total intensities were given in many cases.

We have found it worthwhile to repeat the measurements of the spectrum of internal conversion electrons from radiothorium with an instrument half-width of 0.25%. With this half-width, the majority of lines in the soft region are resolved an the instrument has good transmission factor, thus making it

TABLE III.

Transition	$E_{KL_pL_q}$	$E_{L_q}^{83+\Delta Z}$	$E_{L_q}^{83+\Delta Z}$	$E_{L_q}^{83}$	$E_{L_q}^{84}$	ΔZ		
						Present work	Ref. 9	Ref. 10
$KL_I\ L_I$	57.458	16.677						
$KL_{II}\ L_I$	58.147	16.665	16.674	16.386	16.93	0.53	0.51	0.54
$KL_{III}L_I$	60.423	16.681						
$KL_I\ L_{II}$	58.147	15.988						
$KL_{II}\ L_{II}$	58.783	16.029	16.012	15.709	16.23	0.58	0.52	0.55
$KL_{III}L_{II}$	61.070	16.034						
$KL_I\ L_{III}$	60.423	13.712						
$KL_{II}\ L_{III}$	61.07	13.742	13.730	13 417	13.81	0.80	0.76	0.76
$KL_{II}L_{III}$	63.36	13.737						

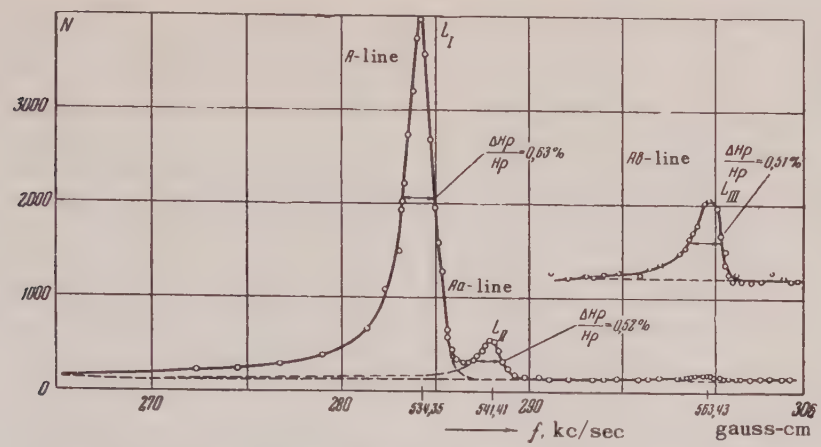

FIG. 4. *A*, *Aa* and *Ab* lines. The *Ab* lines is given separately with a magnification of 16.

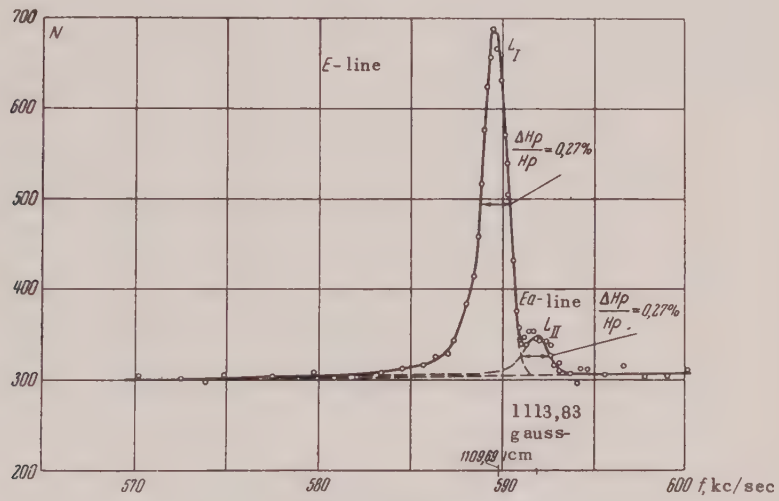

FIG. 5. *E* and *Ea* lines.

possible to detect rather weak lines.

High stability in the counter efficiency is required in making an accurate determination of line intensities. We have taken a number of measures to obtain good stability. The voltage for the counter was obtained from a rectifier with high stability (VS-16). The change in the supply voltage in the course of a day (after a three-hour warm-up period) was less than 1 volt. The voltage at the counters monitored with a kilovoltmeter, connected in parallel with a galvanometer having a scale which made it possible to measure counter voltage to 1 volt. The source was introduced into the instrument without disturbing the vacuum; hence it was not necessary to pump out the mixture from the counter on changing sources. This feature also improved the counter stability. The counter plateau did not shift by more than 3–5 volts in six hours of operation. These variations were checked periodically and appropriate adjustments made in the counter voltage.

The relative intensities were determined with respect to the *l*-line of ThB. Three series of measurements were performed. Several conversion lines are shown in Figs. 4–5. The relative half-width depends on the $H\rho$ of the line up to $H\rho = 1000$ gauss-cm. This effect may be due to scattering of electrons in the source and to a change in the magnetic field configuration.

The average values of $H\rho$ and the line intensities are shown in Table 4 (the lines for the Auger electrons are not included in the table). For comparison purposes, the same table shows the results of Ellis, Surugue, Arnoult, and Flammersfeld. It is apparent from the table that there is a marked difference in the relative intensities as compared with the work in which the photographic method for detecting elec-

TABLE IV. Spectrum of internal conversion electrons from radiothorium. $H\rho$=500 – 1380 gauss-cm.

Present work									Ellis		Surugue		Arnoult		Flammersfeld
Ellis designation	f, kc/sec	$H\rho$	E_γ, keV	Transition	Z	Level	E_γ, keV	I	$H\rho$	I	$H\rho$	I	$H\rho$	I	I
A	284.25	534.21	24.510	CC''	81	L_I	39.854	4.31	536.50	—	534	0.27	534	0.55	
A_1	—	—	—	BC	83	K	115.14	—	538.95	—	536	0.009	538	0.023	4.07
Aa	288.00	541.40	25.159	CC''	81	L_{II}	39.854	0.395	542	—	541	0.027	541	0.055	
Ab	299.70	563.50	27.201	CC''	81	L_{III}	39.854	0.0343	564.53	—	563	0.005	563	0.009	—
B	346.97	652.40	36.153	CC''	81	M_I	39.854	0.997	652.57	—	652	0.18	652	0.37	0.69
Ba	—	—	—	CC''	81	M_{II}	—	—	655.45	—	655	0.005	655	0.009	
Bb	360.86	678.62	39.012	CC''	81	N	39.854	0.244	678.33	—	678	0.05	678	0.09	
Bb_1	—	—	—	—	—	—	—	—	—	—	680	—	—	—	0.171
Bc	364.26	685.05	39.728	CC''	81	O	39.854	0.0542	685.00	—	684	0.009	686	0.018	
$C2$	449.52	845.46	59.411	CC''	81	K	144.94	0.0029	841.5	0.013	845	0.009	841	0.015	—
Dg	547.79	1030.63	86.150	BC	83	K	176.671	0.0184	1027.1	0.017	1030	0.027	1021	0.073	—
Dh	—	—	—	—	—	—	—	—	—	—	1096	0.005	1060	0.009	—
E	589.74	1109.71	98.756	BC	83	L_I	115.142	0.1004	1106.6	0.099	1110	0.15	1101	0.12	0.123
Ea	591.93	1113.83	99.430	BC	83	L_{II}	115.139	0.0123	1110.4	0.009	1114	0.009	1105	0.009	
$Ea1$	—	—	—	—	—	—	—	—	—	—	1170	—	1144	0.009	
Eb	629.00	1183.72	111.139	BC	83	M	115.139	0.0224	1180.5	0.032	1183	0.027	1177	0.027	0.037
Eb_1	638.46	1201.55	114.204	BC	83	N	115.142	0.0070	1199.1	0.009	1202	0.009	1195	0.009	
	640.86	1206.08	114.986	BC	83	O	115.143	0.0027	—	—	—	—	—	—	—
$Et2$	—	—	—	—	—	—	—	—	1226.2	0.002	1226	—	1235	0.009	—
Ec	666.23	1253.92	123.380	$C''D$	82	K	211.38	0.0125	1251.1	0.013	1253	0.018	1247	0.018	—
Ec_1	—	—	—	—	—	—	—	—	1273.8	—	1295	—	1281	0.009	—
Ec_2	—	—	—	—	—	—	—	—	—	—	1323	—	—	—	—
E_d	730	1374	145.4	$C''D$	82	K	233.4	0.009	1370.8	0.009	1372	0.009	1364	0.009	—

trons was used. The differences between our data and the result of Flammersfeld are smaller. A number of lines which were detected in the photographic work were not seen in the present work since the sensitivity of the photographic method is higher.

The relative intensities of the conversion lines have been computed from the reading of the first counter. Since the cutoff energy of the film in the first counter was 4 kev, no corrections for absorption were introduced. According to Ref. 18, this effect is less than one percent for electron energies four or five times greater than the cutoff energy.

The accuracy in the relative intensity measurements for the conversion lines is 3–5 percent for the strong lines and 20–30 percent for the weak lines.

[1] Latyshev, Sergeev, Krisiuk, Ostretsov, Egorov and and Shirshov, Izv. Akad. Nauk SSSR, Ser. Fiz. 20, 354 (1956).

[2] Sergeev, Latyshev and Leonov, Izv. Akad. Nauk SSSR, Ser. Fiz. 20, 369 (1956).

[3] K. Siegbahn and K. Edvardson, Nuc. 1, 1937 (1956).

[4] G. Lindstrom, Phys. Rev. 87, 678 (1952).

[5] R. D. Hill in *Beta and Gamma-Ray Spectroscopy* (Interscience Pub., Amsterdam, 1955), p. 914.

[6] T. Gerholm, bid., p. 926

[7] Krisiuk, Latyshev and Sergeev, Izv. Akad. Nauk SSSR, Ser. Fiz. 20, 367 (1956).

[8] Krisiuk, Vitman, Vorob'ev, Latyshev and Sergeev, Izv. Akad. Nauk SSSR, Ser. Fiz. 20, 877 (1956).

[9] I. Bergstrom and R. D. Hill, Arkiv f Fysik 8, 21, (1954).

[10] M. Mladjenovic and H. Slatis, Arkiv f Fysik 9, 41 (1955).

[11] C. Ellis, Proc. Roy. Soc. A 139, 336 (1933).

[12] C. Ellis, Proc. Roy. Soc. A 138, 318 (1932).

[13] C. Ellis, Proc. Roy. Soc. A 143, 350 (1934).

[14] J. Surugue, Ann. phys. 8, 484 (1937).

[15] J. Surugue, J. phys. et radium 9, 438 (1938).

[16] R. Arnoult, Ann. phys. 12, 241 (1939).

[17] A. Flammersfeld, Z Physik 114, 227 (1939).

[18] R. O. Lane and D. J. Zaffarano, Phys. Rev. 94, 960 (1954).

Translated by H. Lashinsky
163

SOVIET PHYSICS JETP VOLUME 5, NUMBER 3 NOVEMBER, 1957

Generation of Slow π-Mesons by Cosmic Ray Particles

D. K. KAIPOV AND ZH. S. TAKIBAEV
Physico-Technical Institute of the Academy of Sciences of the USSR

(Submitted to JETP editor July 20, 1956)
J. Exptl. Theoret. Phys. (U.S.S.R.) 32, 690-696 (April, 1957)

Results of experiments on the transition effect of π-mesons are presented and discussed. The results presented allow one to conclude that low energy mesons are abundant in the spectrum of the generated mesons and that the plural mechanism of meson creation is correct. Most of the generating particles are probably cosmic ray neutrons.

1. SOURCES OF THE π-MESONS OBSERVED IN PHOTOGRAPHIC PLATES EXPOSED TO COSMIC RAYS

IN EXPERIMENTS, reported in Refs. 1-3, investigating the transition curve of π-mesons and the intensity of their generation as a function of the atomic weight of the target, no account was taken of the current of slow π-mesons from extraneous dense materials situated near the photographic plate or of the presence of π-mesons in the air. Both of these factors can influence the form of the transition curve.

Before embarking on an investigation of the transition effect of π-mesons and the intensity of their generation as a function of the atomic weight of the target, it is necessary to study the current of π-mesons coming from the air and from nearby extraneous dense absorbers. We set up special experiments for this purpose on a mountain top (altitude 4000 m). A pair of photographic plates were exposed during the course of two months on a mast 10 m high, with

another pair in direct contact with the surface of the earth. After chemical treatment (developing and fixing), these photographic plates were scanned with a microscope at high magnification. Identification of the stopped π-mesons was made by means of π-μ decays and σ-stars.

The reduced results of this experiment are given in Table 1. It is clear from the table that the number of π-mesons observed in the photographic plates exposed at the surface of the earth is significantly greater (by 5–6 times) than in those on the mast. It follows from this that in studying the generation of slow π-mesons by cosmic rays all the photoemulsions used in the experiment should be placed as far as possible from extraneous dense absorbers.

TABLE I.

Number of the experiment	Position of the photographic plates	Number of π-mesons observed in 6 cm^2	Number of π-mesons after exclusion of background
1	On the mast	8	5
	On the ground	30	27
2	On the mast	3	—
	On the ground	8	—

What fraction of the π-mesons recorded in a photographic emulsion are π-mesons formed in the air? An experimental study of this question by the method of photographic emulsions is extremely difficult, since these emulsions are always enveloped in wrapping material when they are exposed. Hence the question as to which part of the recorded mesons comes from the air and which part is formed in the wrapping material represents a definite experimental difficulty. By means of an elementary calculation, however, we can obtain the necessary information on the current of π-mesons coming from the air.

The number of π-mesons with energy less than E_0 originating in the atmosphere within a depth of x g/cm^2 from the boundary of the atmosphere is equal to

$$S_{\pi} = \int_0^{E_0} n(E) \left[\int_0^{x} \frac{S_0}{\lambda_0} e^{-t/l} e^{-(x-t)/\lambda} (t/x)^{\gamma} dt \right] dE, \quad (1)$$

where $n(E)$ is the differential energy spectrum of the generated π-mesons, $S_0 e^{-t/l}$ is the number of nucleons with energies greater than E_c at depth t, E_c is the threshold energy for the formation of mesons; $\exp\{-(x-t)/\lambda\}$ is the probability that a meson originating at depth t will reach depth x without undergoing a nuclear interaction; $(t/x)^2$ is the probability that a meson formed at depth t with momentum p_{π} will reach depth x without undergoing disintegration. Here.

$$\gamma = z_0 m_{\pi}/\tau_{\pi} p_{\pi} = z_0 m_{\pi} c^2/\tau_{\pi} c \, (E^2 + 2 m_{\pi} c^2 E)^{1/2},$$

where $z = 6.4 \times 10^5$ cm in the stratosphere, λ_0 and λ are the respective ranges of the nucleon and meson for nuclear interaction. For air and also for the wrapping material and the glass backing of the photographic plates, we take $\lambda_0 = \lambda = 60$ g/cm^2 and $l = 2\lambda$. For a condensed medium of the type of carbon, formula (1) takes the form

$$S_{0\pi} = \int_0^{E_0} n(E) \left[\int_0^{x} \frac{S_0}{\lambda_0} e^{-t/l} e^{-(x-t)/\lambda} dt \right] dE. \quad (2)$$

Calculation shows that the π-mesons originating in the air and slowed down and stopped in the photographic emulsion amount to less than 1% of such mesons formed in the wrapping material and the glass backing of the photographic plate. Hence the basic sources of the π-mesons observed in photographic emulsions exposed to cosmic rays are the dense absorbers situated in direct proximity to the detector.

2. CHANGE IN THE NUMBER OF π-MESONS UPON PENETRATION FROM AIR INTO LEAD

Refs. 1–3 are devoted to the study of the penetration effect of π-mesons at mountain altitudes. However, it is not possible to make an unambiguous conclusion from these references as to the change in the number of slow π-mesons as a function of the thickness of the absorber. Moreover, the results of Refs. 1–4 and 5 do not agree among themselves, and there are no data on the penetration effect for π-mesons in the stratosphere given in the literature, unless we count the brief communication of Blau et al.[6], in which no experimental results are reported. The results given in Ref. 7 also seem quite doubtful.

We have carried out experiments studying the penetration effect of π-mesons. Electron sensitive photographic plates of type NIKFI were exposed in the stratosphere at an altitude of 25–27 km and at a mountain elevation (2.5 km). In one of the stratosphere experiments (Fig. 1a) some of the photo-

graphic plates were placed inside a hollow lead hemisphere with walls 2 cm thick and in an aperture made in the center of a solid hemisphere of lead of radius 8 cm, while the rest, kept far away from dense absorbers, were exposed without lead shielding and with thin shields. A schematic of the arrangement of the photographic plates in the other stratosphere experiment is given in Fig. 1b. Lead absorbers in the form of slabs of dimensions $9\times5\times2$ cm and $9\times5\times3$ cm and thin absorbers of thickness 3–4 g/cm^2 were used in this experiment.

In the mountain experiment the photographic plates were placed inside cylindrical absorbers made of lead (with walls of thickness 0.2, 2 and 6 cm) and

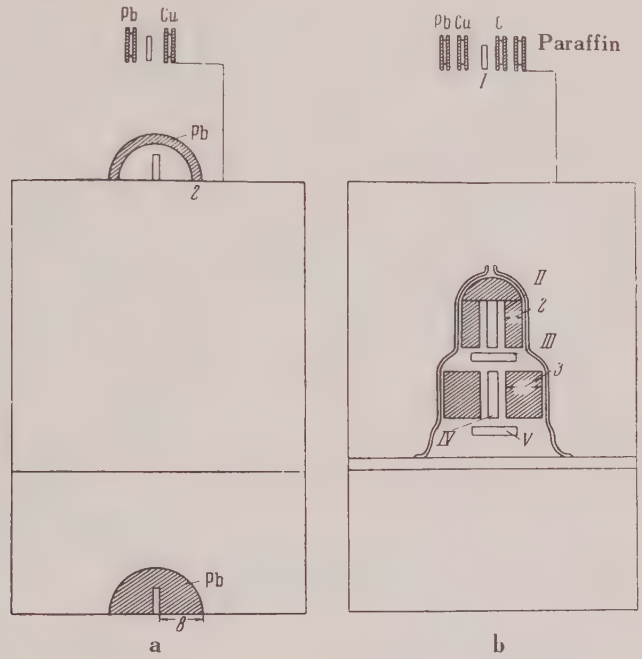

FIG. 1. Schematic of the stratosphere experiments.

aluminum (with walls of thickness 0.8 cm), and afterwards were exposed at a distance of 7 m from the earth. To reduce shrinkage, the photographic plates were placed inside a flat-sided glass vessel of thickness 1.5–2 mm, filled with nitrogen. In the stratosphere experiments the photographic plates were exposed without an absorber and with thin shields at a distance of 2.5 and 5 m above the container.

The reduced results of the two stratosphere experiments and one of the experiments at a mountain elevation are given in Table 2. This table also includes ρ-mesons. It should be noted that not all of the ρ-mesons are μ-mesons. A certain part of the negative π-mesons ($\sim$27%) does not give observable stars[8], and they are counted as ρ-mesons. Moreover, a certain part of the μ-mesons is connected with the decay of π^+-mesons generated in the absorber (local origin). Taking account of these factors leads to the estimate of the number of μ-mesons which is given in the last column of Table 2. This estimate corresponds approximately to an estimate of the number of μ-mesons by $\mu \to e$ decay.

It is clear from Table 2 that 1) the number of slow π-mesons increases strongly with increasing thickness of the lead absorber, while the number of μ-mesons is almost independent of the change in the thickness of the lead; 2) a very strong increase in the number of π-mesons occurs when the photographic emulsion is surrounded by a layer of lead of small thickness, while a further increase in thickness does not lead to a strong increase in the number of π-mesons; 3) no notable dependence of the penetration of π-mesons on height above sea level is observed.

It follows from these results that π-mesons are generated directly in the absorber surrounding the photographic emulsion, with low-energy mesons (having a range in lead less than 4 g/cm^2) being the most abundant among those generated. The fact that the form of the penetration curves for slow mesons in the stratosphere and at a mountain elevation are the same is probably due to the fact that

TABLE II.

No. of the experiment	Altitude above sea level, km	Thickness of the lead shielding	Area examined, cm²	Number of mesons identified		
				π	σ	p
1	27	Air	22	7 ± 2.6	55	54
		1.7	22	25 ± 5	61	57
		23	22	40 ± 6.3	53	46
		90	22	57 ± 8.3	56	42
2	26	Air	20	6 ± 2.4	—	—
		3.4	20	26 ± 5.0	—	—
		23	20	28 ± 5.3	—	—
		III *	20	22 ± 4.7	—	—
		34	20	32 ± 5.6	—	—
		V *	20	30 ± 5.5	—	—
3	2.5	Air	17	2	102	102
		2.27	17	16	72	69
		23	17	22	98	94
		60	17	30	85	79

*III and IV indicate the positions of the photographic plates relative to the lead absorbers (see Fig. 1).

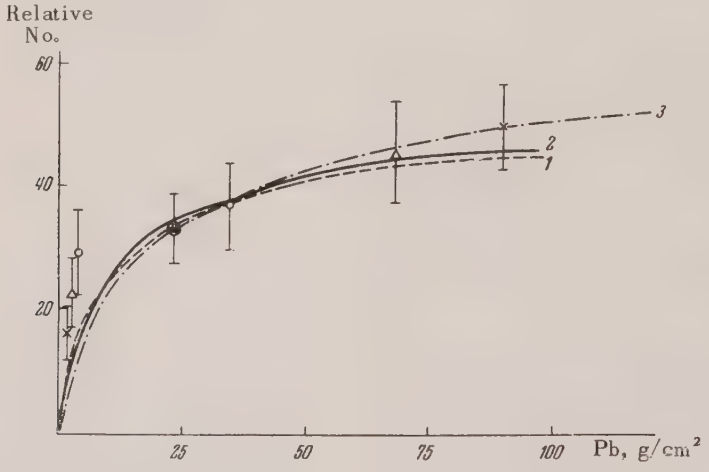

FIG. 2. Number of π-mesons generated: ×, experiment No. 1, ○, experiment No. 2, △, mountain experiment.

they arise basically as secondary particles. The number of generated mesons is shown in Fig. 2 as a function of the thickness of the lead absorber.

We can obtain an idea of the form of the energy spectrum of the generated π-mesons from the penetration curve. The energy spectrum of the π-mesons formed in the nuclei of the emulsion has been investigated by Camerini et al.[9] and Yagoda[10]. According to the results of Ref. 9, the energy spectrum of the π-mesons in the energy region 200–1100 Mev may be represented by the expression $P(E)dE \sim E^{-1.4}dE$ (E is the total energy), and in the region of small energies by the expression[10] $P(E_k)dE_k \sim E_k^{0.6}dE_k$ (E_k is the kinetic energy). On the assumption of a spectrum of the form:

$$P(E)dE = AE^{-\gamma}dE \quad \text{for } E \geqslant 40 \text{ Mev} \qquad (3)$$

$$P(E)dE = BE^{0.6}dE \quad \text{for } E \leqslant 40 \text{ Mev} \qquad (4)$$

the expected penetration curves were calculated for values of γ of 1.5, 1.3 and 1 (the corresponding curves in Fig. 2 are indicated by the numbers 1, 2 and 3). It is clear from a comparison that in the region of small thickness the experimental points systematically go beyond the limits of the calculated curves. We are inclined to think that in the region of small energies the energy spectrum of the π-mesons is different from the spectrum (4) which we assumed. It should be pointed out, however, that the dependence of the angular distribution and the scattering of π-mesons on their energy may essentially

influence the number of stopped π-mesons. Taking account of these factors in the calculation of the transition curve does not seem possible to us at the present time. But there seems no doubt that mesons of small energy, with ranges in lead of less than 4 g/cm^2, are abundantly represented among the mesons generated by cosmic rays.

3. DEPENDENCE OF THE CROSS SECTION FOR GENERATION OF π-MESONS ON THE ATOMIC WEIGHT OF THE MATERIAL OF THE TARGET

It is shown in Ref. 11 that the stratosphere data on the dependence of the cross section for formation of slow mesons on the atomic weight of the absorber can be explained by the essential role of the number of nucleons (in which number δ-nucleons are to be counted) which take part in the collisions.

It should be pointed out that taking account of the difference in stopping power of carbon, copper, and lead does not change the general conclusion just made, since according to the data on the penetration effect the number of stopped π-mesons is almost the same for lead thicknesses of 3–4 and 23 g/cm^2 (see Table 2). The results of our stratosphere experiments on the cross section for the formation of π-mesons in various nuclei confirm the results obtained by Abraham and Coldsack [12].

Thus, the conclusions made in Ref. 11 relative to the formation of slow π-mesons in heavy and light nuclei by cosmic rays in the stratosphere must be considered correct.

In this connection it is interesting to study the formation of slow π-mesons in various nuclei at mountain altitudes. The formation of π-mesons in various elements at a mountain altitude was studied in Ref. 13. According to the results of this reference, the cross section for the generation of π-mesons falls with increasing atomic weight of the target material. This fact cannot be accepted without a supplementary confirmation, since according to the results of Gregory and Tinlot [14], at an altitude of 3240 m the greater part ($\sim$90%) of the protons which produce nuclear interactions have energies less than 1 Bev, while only $\sim$10% of the nuclear interactions may be ascribed to protons with energies greater than 1 Bev. It must be presumed that the neutrons in the cosmic radiation at mountain altitudes possess approximately these same energies. It is clear from this that the average energy of the nucleons of cosmic rays at mountain altitudes cannot be much greater than the energy of the protons used in Refs. 15 and 16.

As is well known, the results given in Refs. 15 and 16 lead unambiguously to the conclusion that the cross section for the generation of π-mesons at a proton energy of approximately 400 Mev is proportional to the geometrical cross section of the nucleus. Hence it was expedient to set up a special experiment at a mountain altitude for an investigation of the formation of π-mesons in light and heavy nuclei. The experiment was set up at an altitude of 2500 m and the duration of the exposure was two months. Thin absorbers of lead and aluminum were used as generators, and photographic emulsions of type NIKFI of 400μ thickness were used as detectors. The absorbers were in the form of cylinders. The generator thicknesses were chosen to make the ionization ranges of the mesons in these substances equal. The use of thin absorbers, with thickness approximately equivalent with respect to ionization range, obviated the necessity of introducing corrections connected with nuclear and electromagnetic absorptions. Taking account of such corrections is difficult at present, since the energy spectrum of the low energy π-mesons generated in various substances at the given altitude has as yet been little studied. In order to guarantee the cleanness of the experiment, all the photographic emulsions used were removed a distance of 7 m from the surface of the earth. The average decay range of π-mesons with energies less than 50 Mev is about 6 m. Hence when the detector is taken a distance of 7 m from the surface of the earth, the contribution which π-mesons formed in the surface layer make to the number of recorded events is strongly dreceased.

The reduced results of the mountain experiment are given in Table 3. It is clear from the table that the number of π-mesons, relative to 1 g/cm^2 of material, decreases somewhat more weakly with increasing atomic weight than would be expected from the $A^{2/3}$ law. The relative cross section for generation σ_{Al}/σ_{Pb}, calculated from the data of Table 3, is equal to 0.16 ± 0.04. The corresponding relative cross section to be expected on the basis of the $A^{2/3}$ law is 0.25. It is clear from this that the cross section for the generation of mesons by cosmic ray particles at mountain altitudes increases with increasing A somewhat more rapidly than the geometrical cross section of the nucleus. If we attribute definite significance to this fact, then it shows that cosmic ray particles at mountain altitudes are capable of generating mesons not only by

TABLE III

Absorber	Absorber thickness, g/cm²	Number of π-mesons per cm³ day, g/cm²	Number of π mesons per cm³ day g/cm²
Air	—	0.040 ± 0.03	—
Al	2.2	0.33 ± 0.026	0.132 ± 0.02
Pb	4.45	0.52 ± 0.03	0.108 ± 0.01

collision with surface nucleons, but also as a result of collisions with volume nucleons of a nucleus. The results of our mountain experiments are in agreement with the results of work carried out in a cloud chamber[17].

Using the results of Gregory and Tinlot[14], we can calculate the effective relative cross section for the generation of mesons, assuming that 90% of the cosmic ray nucleons at mountain altitudes generate mesons with cross section proportional to $A^{2/3} 2^a$, where $a = A^{1/3}/1.5$. Then the expected relative cross section calculated on the basis of these assumptions is given by $\sigma_{Al}/\sigma_{Pb} \approx 0.13$, which agrees with the experimentally observed magnitude of the relative cross section.

4. ON THE NATURE OF COSMIC RAY PARTICLES THAT GENERATE SLOW π-MESONS

In order to determine the nature of the meson-generating particles, we studied the altitude dependence of the meson production. For this purpose photographic plates were exposed at various altitudes under 2 cm of lead. Out of all the stratosphere flights made to determine the altitude dependence of the production of π-mesons, only those flights were used in which the drift time exceeded by 4 or more times the time of ascent and descent of the apparatus. Only in these cases can we ascribe the observed intensity to a definite height. The data from two stratosphere experiments and one mountain experiment have been reduced. The results concerning the altitude dependence of the number of π-mesons is the following:

Altitude above sea level, km	2.5	23.5	27
Number of π-mesons in 1 cm² in 1 min $\times 10^{-5}$	1.96 ± 0.42	625 ± 96	625 ± 81

The absorption ranges for meson-generating particles have also been determined for two altitude intervals: 23.5–2.5 km and 27–2.5 km; they are equal respectively to $(127 \pm 11/7)$ g/cm² and $(130 \pm 11/7)$ g/cm². It should be noted that the absorption range of the meson-generating particles assumes a value intermediate between that for the range of particles generating penetrating showers (118 g/cm²) and that for the range of particles which give rise to ordinary stars (140 g/cm²). Although the statistical error does not allow us to make a choice as to which of these processes plays the main role, it seems quite probable that we should consider slow mesons to be generated both in showers and in ordinary stars.

In conclusion we give the results of an investigation of the ratio of positive and negative π-mesons, which may yield information on the nature of the generating particles (Table 4). Table 4 yields the following results:

1. An increase in the ratio π^+/π^- both in the stratosphere and at mountain altitude is observed with increasing energy interval of the π-mesons,

TABLE IV.

Absorber thickness g/cm²	Altitude above sea level 26–27 km						Altitude above sea level 3–4 km		
	Pb target			C target			Pb target		
	π^+	π^-	π^+/π^-	π^+	π^-	π^+/π^-	π^+	π^-	π^+/π^-
3—5	29	48	0.60	—	—	—	6	18	0.33
23	13	22	0.82	—	—	—	18	39	0.46
20	—	—	—	16	34	0.50	—	—	—
26	—	—	—	26	30	0.87	—	—	—
70—80	37	37	1	—	—	—	13	21	0.62
114 (18)	—	—	—	—	—	—	30	41	0.73

which is (roughly) determined by the thickness of the absorber.

2. The negative "charge asymmetry" is significant for low energy π-mesons.

3. The ratio π^+/π^- changes only slightly in going from a heavy element (Pb) to a light element (C).

4. The magnitude of the ratio π^+/π^- increases in going from a mountain altitude to the stratosphere. All these regularities are easy to explain, if we take account of the fact that an overwhelming part of the slow π-mesons is generated by neutrons. The participation of protons in the formation of π-mesons increases with increasing energy of the π-mesons.

[1] J. Harding and D. Perkins, Nature **164**, 285 (1949).
[2] J. Harding, Phil. Mag. **42**, 651 (1951).
[3] U. Camerini et al., Phil. Mag. **42**, 1241 (1951).
[4] V. Kamalian, Doklady Akad. Nauk SSSR **95**, 1169 (1954).
[5] A. Vaisenberg, Doklady Akad. Nauk SSSR **91**, 483 (1953).
[6] M. Blau, J. Nafe and H. Bramson, Phys. Rev. **78**, 320 (1950).
[7] M. Schein and J. Lord, Phys. Rev. **76**, 170 (1949).
[8] F. Adelman and S. Jones, Phys. Rev. **75**, 1468 (1949).
[9] U. Camerini et al., Phil. Mag. **41**, 413 (1950).
[10] H. Yagoda, Phys. Rev. **85**, 891 (1952).
[11] D. Kaipov and Zh. Takibaev, J. Exper. Theoret. Phys. (U.S.S.R.) **30**, 471 (1956), Soviet Phys. JETP **3**, 385 (1956).
[12] M. Abraham and S. Coldsack, Bull. Am. Phys. Soc. **30**, 15 (1955).
[13] Dallaporta, Merlin, Pierucci and Rostagni, Nuovo Cimento **9**, 202 (1952).
[14] B. Gregory and J. Tinlot, Phys. Rev. **81**, 667 (1951).
[15] R. Sagane and W. Dudziak Phys. Rev. **92**, 212 (1951).
[16] Block, Passman and Havens, Phys. Rev. **88**, 1239 (1952).
[17] B. Rossi, *High-Energy Particles*, (Prentice-Hall, Inc., New York, 1952).
[18] Brown, Cameri ni, Fowler, Muirhead, Powell and Ritson, Nautre **163**, 82 (1949).

Translated by M. J. Gibbons
164

SOVIET PHYSICS JETP VOLUME 5, NUMBER 3 NOVEMBER, 1957

Construction of the Thermodynamic Potential of Rochelle Salt from the Results of the Optical Investigation of Domains

V. L. INDENBOM AND M. A. CHERNYSHEVA
Institute of Crystallography of the Academy of Science, USSR

(Submitted to JETP editor November 22, 1956)
J. Exptl. Theoret. Phys. (U.S.S.R.) **32**, 697-701 (April, 1957)

From the experimental temperature dependence of the monoclinic parameter η and the specific heat c_p, the thermodynamic potential of Rochelle salt can be constructed with accuracy to terms of the order of η^4. The advantages of the optical method of determination of the monoclinic parameter are analyzed in comparison with the electrical and mechanical methods. Results of calculation of the thermodynamic potential surface from the temperature dependence of the angle of spontaneous rotation of the optical indicatrix are given. The possibilities of a rigorous construction (without interpolation) of this surface from data of the optical investigation of domains are pointed out.

AS GINSBURG HAS SHOWN[1], the theory of piezoelectric phenomena can be developed on the basis of the general theory of phase transitions of the second kind[2]. In the general theory it is demonstrated that in the vicinity of the Curie point $T=\Theta$, the expansion of the thermodynamic potential in a power series of the parameter η which characterizes the degree of asymmetry of the system has the form

$$\Phi = \Phi_0 + A\eta^2 + C\eta^4 + \cdots \qquad (1)$$

Ordinarily it is assumed that in expansion (1) we can confine ourselves to only the terms written

down, for which $A = a(T-\Theta)$, and C = const. (hereinafter the pressure is assumed constant). The following expressions are then obtained for the temperature dependence of the asymmetry parameter and of the heat capacity.

$$\text{For } T>\Theta:\ \eta=0,\ c_p=c_{p_0};$$
$$\text{For } T<\Theta:\ \eta^2=-A/2C,\ c_p=c_{p_0}+Ta^2/2C. \tag{2}$$

Here $c_{p_0}=-T\partial^2\Phi_0/\partial T^2$. The jump in the specific heat at the Curie point is evidently $\Delta c_p=\Theta a^2/2C$.

In the theory of ferroelectricity, the polarization P is chosen as the asymmetry parameter and the effect of an external electric field E is taken into account by adding the term $-PE$ to the thermodynamic potential [Eq. (1)]. In the case of Rochelle salt there is only one ferroelectric axis, parallel to the x axis. Therefore the additional term has the form $-PE_x$.

Considering a characteristic property of Rochelle salt, namely, its having two Curie points, Ginsburg[1] showed that the function $A(T)$ in this case must be described by a cup-shaped curve whose points of intersection with the abscissa coincide with the Curie points. Only in the neighborhood of these points can we assume $A = a(T-\Theta)$ and have confidence in the correctness of expressions of the type of Eqs. (2).

The question arises whether it is permissible to piece together the form of the function $A(T)$ and in general the complete contour of the thermodynamic potential over the entire ferroelectric interval from the experimental data. First of all, let us forego the simplifying assumptions made in the derivation of Eqs. (2) and assume simply $\Phi = \Phi(T, \eta^2)$. The dependence of the asymmetry parameter on temperature is found from the conditions $\partial\Phi/\partial\eta = 0$, and $\partial^2\Phi/\partial\eta^2 > 0$, whence there follow two solutions: $\eta = 0$ for $(\partial\Phi/\partial\eta^2)_{\eta=0} > 0$ (outside the piezoelectric interval) and $\eta = \eta_0$, where $\eta_0(T)$ satisfies the equation $(\partial\Phi/\partial\eta^2)_{\eta=0} = 0, (\partial^2\Phi/\partial(\eta^2)^2)_{\eta=0} > 0$ (in the piezoelectric interval). Differentiating Φ twice with respect to temperature along the the equilibrium curve $\eta = \eta(T)$, we obtain the expression for the specific heat

$$c_p = -T\left[\frac{\partial^2}{\partial T^2} - \left(\frac{d\eta^2}{dT}\right)^2 \frac{\partial^2}{\partial(\eta^2)^2}\right]\Phi. \tag{3}$$

If η and c_p were known as functions of temperature it would be possible to set up the position of the equilibrium curve of the phases in (Φ, η, T) space. Unfortunately, reliable data even on the magnitude of the jumps of the specific heat at both Curie points[3] are not available. Meanwhile, these data already would allow one to determine the character of the temperature dependence of the coefficient C in the expansion Eq. (1). Actually, from Eq. (3) it follows that at the Curie point ($T = \Theta$, $\eta = 0$)

$$\Delta c_p = \Theta\left(\frac{d\eta^2}{dT}\right)^2 \frac{\partial^2\Phi}{\partial(\eta^2)^2} = 2\Theta\left(\frac{d\eta^2}{dT}\right)^2 C(\Theta). \tag{4}$$

In the case C = const., the value of the jump at one Curie point can be predicted from the known jump of the specific heat at the other Curie point.

We set aside for the time being the question of the rigorous construction of the surface $\Phi = \Phi(T, \eta)$ and note that this surface can be found from the two known functions $\eta = \eta(T)$ and $c_p = c_p(T)$, naturally, only by way of interpolation.

Thus if we confine ourselves to terms of the order η^4 in the expansion Eq. (1) (which, as Ginsburg noted[1] is apparently fully admissible) for Rochelle salt these two functions permit us to find the coefficients $A(T)$ and $C(T)$. For C = const. in the Curie interval

$$A(T) = -2C\eta^2(T) = -\frac{\Delta c_p}{\Theta}\left(\frac{d\eta^2}{dT}\right)^{-2}_{T=\Theta}\eta^2(T). \tag{5}$$

There remains to find the temperature dependence of the asymmetry parameter. The monoclinic angle, the spontaneous polarization, or the spontaneous deformation can serve as this parameter—the monoclinic parameter—for the given case of Rochelle salt. It turns out, however, that X-ray determination of the monoclinic angle[4] gives only semi-quantitative results and studies of the macroscopic polarization[5, 6] or of the macroscopic deformation[7] on specimens which consist of domains of opposite signs do not permit one to strictly distinguish the changes in characteristics of the individual domains, which interest us, and the effects brought about by the motion of domain (twin) boundaries.

Use of the optical method[8, 3] which permits one to obtain an individual characteristic of the domains, appears more reliable. Here it is convenient to take as the asymmetry parameter the angle of rotation of the optical indicatrix about the x axis, proportional to the spontaneous deformation of the domain. This angle is simply determined from the angle 2α between the positions of extinction in neighboring domains[3].

The results of a preliminary study of the temperature dependence of the asymmetry parameter chosen in this manner (the monoclinic parameter) are brought to light in the dissertation of one of the authors[3]: the results of a more careful investigation were reported at the recent conference (June of this year) on ferroelectricity.

The measurement of the angle between the positions of extinction in the components of a twin (of adjacent antiparallel domains) was carried out by means of a bi-quartz plate. In connection with the observed dispersion of the extinction positions, the measurements were carried out with a 540 mμ filter (transmission bandwidth 10 mμ).

The results of the measurements carried out on one of the specimens are presented in Fig. 1. Each

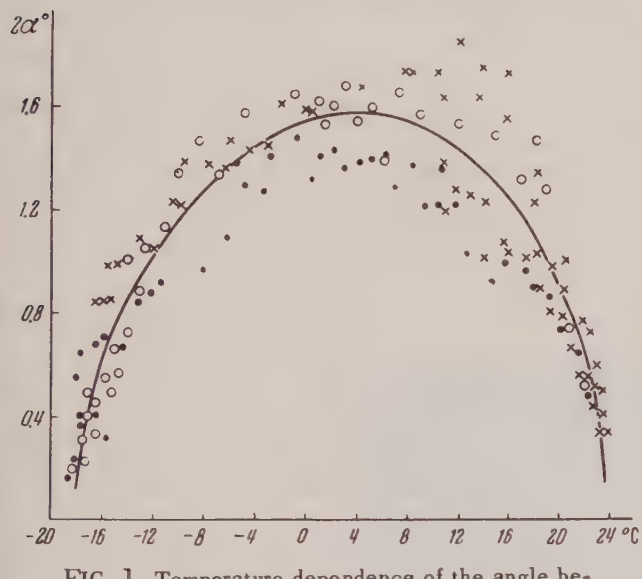

FIG. 1. Temperature dependence of the angle between the positions of extinction in adjacent domains in a Rochelle salt crystal.

point corresponds to the arithmetic mean of not less than five readings. The monoclinic parameter of Rochelle salt crystals in the interval between the Curie points varies continuously and reaches a maximum value at a temperature which lies midway between the Curie points (about 3°C). In accordance with Eqs. (2) the curve displays in the vicinity of the Curie points characteristic parabolic portions, which are linear if one plots the curve $\eta^2 = \eta^2(T)$. The latter curve also characterizes the temperature dependence of the coefficient A.

We calculated the coefficient C from the jump in specific heat (5 cals/mol)[9,5] at the upper Curie point to be approximately 5.10^7 cal/mol (the monoclinic parameter expressed in radians, $\eta = \alpha^\circ\pi/180$). Since the maximum value of the monoclinic parameter is $\eta_{max} = 1.4 \times 10^{-2}$, the maximum change of the value of the thermodynamic potential brought about by a deviation of the system from the symmetrical state amounts to $\Delta\Phi = -C\eta^4_{max} = -2$ cal/mol.

The surface of the thermodynamic potential calculated according to Eq. (1) is characterized in Fig. 2 by a contour plan corresponding to constant values of the thermodynamic potential (relative to Φ_0). Curves outside the ferroelectric interval are obtained by extrapolation. The general form of the three dimensional model of the surface $\Phi = \Phi(T, \eta)$ constructed from this data is shown in Fig. 3. In the ferroelectric region the "gorge" goes over to a "valley" with two depressions of depth 2 cal/mol.

Conversion from one monoclinic parameter to another (for example, to the polarization P_x or to the deformation ϵ_{yz}) corresponds simply to a change in one of the scales of the model. The slope of the curves obtained in cross-sections for $T = \text{const}$. gives the value of the generalized force pertaining to this parameter (for example, the electric field intensity E_x or the tangential stress τ_{yz}), while the curvature of these curves gives the corresponding moduli (for example, the dielectric constant of the crystal or the shear modulus).

The effect of a mechanical-stress field or of an external electric field is taken into account by adding to the thermodynamic potential terms of the type $-P_xE_x$ and $-\epsilon_{yz}\tau_{yz}$ which is equivalent to a rotation of the base of the model about the temperature axis. This causes the equilibrium positions on the potential wells to shift until the slope exceeds a certain critical value and one of the equilibrium positions becomes unstable. At this instant one of the domain systems in the specimen must completely disappear.

The above points to the possibility of a rigorous construction of the thermodynamic potential surface (without interpolation) directly from the optical characteristics of the domains measured on loaded crystals. By such means, evidently, it is possible to obtain experimental points on any portion of the surface with the exception of the region of unstable equilibrium adjoining the temperature axis, in which in general the system of domains under study fades out.

In conclusion the authors express deep thanks to V. I. Ginsburg for his interest in the work and for his valuable comments during its discussion.

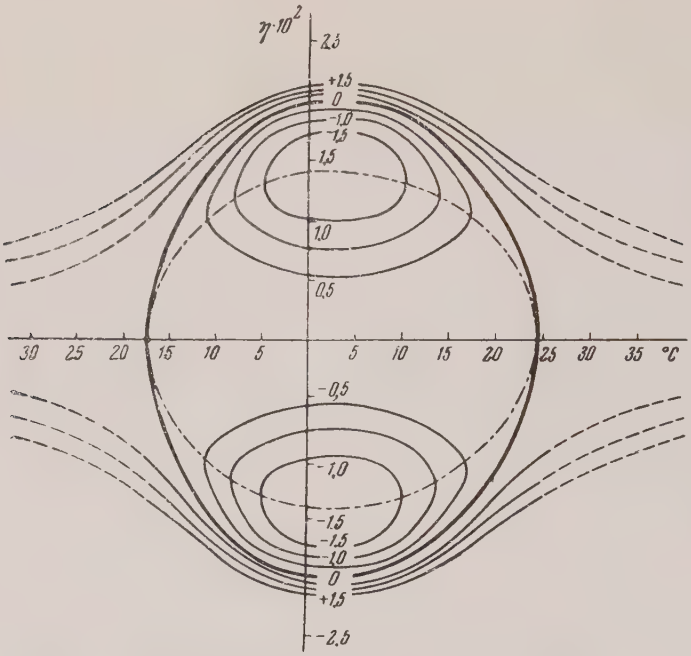

FIG. 2. Chart of the thermodynamic potential surface. The numbers on the contours are in cal/mol. The zero contours are set off by broad lines. The portions of the contours outside the ferroelectric region are obtained by extrapolation and are marked by dashes. The dot-dash curve gives the experimental temperature dependence of the monoclinic parameter.

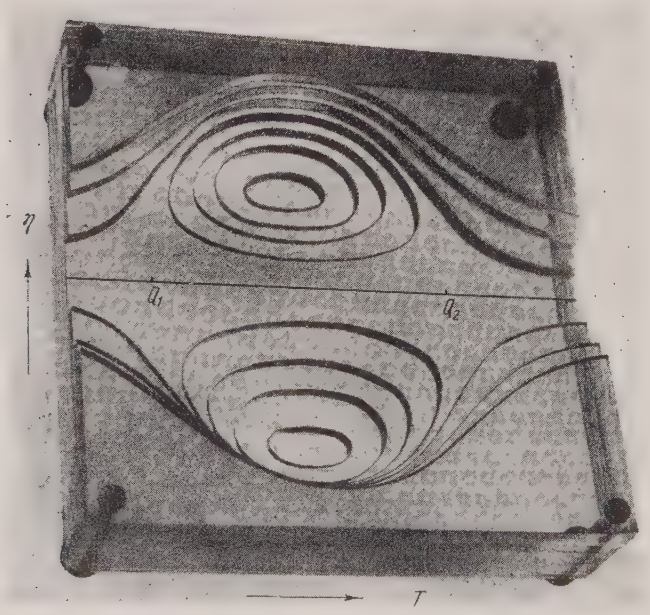

FIG. 3. Three dimensional model of the thermodynamic potential. The scale is 0.5 cal/mol per step. The zero contour consists of the straight line parallel to the temperature axis, and of an oval curve which envelops the potential wells intersecting at the Curie points (denoted by Q_1 and Q_2 in the figure).

[1] V. L. Ginsburg, Usp. Fiz. Nauk. SSSR 38, 490 (1949)
[2] L. D. Landau and E. M. Lifshitz, *Statistical Physics*, M-L (1951) p. 428; trans. by D. Shoenberg, Oxford Clarendon (1938).
[3] M. A. Chernysheva, Moscow, Institute of Crystallography, Acad. of Science, U.S.S.R. (1955).
[4] A. R. Ubbelohde and I. Woodward, Proc. Roy. Soc. 185A, 448 (1946).
[5] H. Mueller, Ann. N. Y. Acad. Sci. 40, 321 (1940.
[6] J. Hablutzel, Helv. Phys. Acta 12, 489 (1939).
[7] W. M. Mason, *Piezoelectric Crystals and their Application in Ultrasonics* (Russ. Transl.) IIL, (1952)
[8] M. V. Klassen-Nekliudova, M. A. Chernysheva and A. A. Sternberg, Dokl. Akad. Nauk SSSR 63, 527 (1948).
[9] P. P. Kobeko and I. Iu. Nelidov, J. Exptl. Theoret. Phys. (U.S.S.R.) 1, 228 (1931).

Translated by R. L. Eisner
165

SOVIET PHYSICS JETP VOLUME 5, NUMBER 4 NOVEMBER, 1957

The Effect of Fast Neutron Irradiation on the Recombination of Electrons and Holes in Germanium Crystals

V. S. VAVILOV, A. V. SPITSYN, L. S. SMIRNOV AND M. V. CHUKICHEV
P. N. Lebedev Physical Institute of the Academy of Science, USSR

(Submitted to JETP editor November 24, 1956)
J. Exptl. Theoret. Phys. (U.S.S.R.) 32, 702-705 (April, 1957)

It is found that irradiation of germanium crystals with fast neutrons leads to an increase of the rate of volume recombination. The probability of recombination trapping of charge carriers by defects which appear as a result of irradiation is estimated. The strong effect of neutron irradiation on the lifetime of carriers can be used to record and measure integral fluxes of fast neutrons.

1. STRUCTURAL DEFECTS OCCUR in crystals under the influence of fast neutrons. The disturbance of the periodic structure changes the mechanical, electrical, and optical properties of the crystals. The changes of the electrical conductivity of germanium and of silicon subjected to the action of fast neutrons have been studied by many investigators, in particular Lark-Horowitz[1] and Fan [2], and have been utilized in a dosimeter proposed by Cassen[3].

Structural defects in crystals of semiconductors serve as recombination trapping centers for electrons and holes. The effective capture cross-section for holes by defects formed in the bombardment of germanium by electrons with energy above 0.5 Mev was estimated in our work[4] and came to $0.7 \cdot 10^{-16}$ cm², *i.e.*, close to the capture cross-section of thermoacceptors, according to the data of Kalishnikov and Ostroborodova[5].

The purpose of the present work is to estimate the effect of germanium-crystal neutron-produced lattice defects on the recombination of electrons and holes.

The number of germanium nuclei displaced owing to scattering of fast neutrons by the lattice sites as a result can be calculated on the basis of data on the transverse cross-sections for the interaction of fast neutrons with Ge nuclei[6]. According to Ref. 6, the transverse cross-sections for the scattering of germanium nuclei by fast neutrons with energy E_n in the range 0.4 – 3.5 Mev are respectively

E_n, Mev	0.4	1.0	1.5	2	3.5	14
T, barns	5.5	5.0	3.5	3.3	3.5	2*

As a consequence of the fact that the energy transferred to a germanium nucleus by fast neutron can amount to a significant figure ($0.054\, E_n$), secondary and higher atomic displacements can occur. Ref. 7, gives a method of calculating the total number $\bar{N}_d$ of Ge atoms displaced as a result of primary energy transfer. Allowing for the possibility that an

*The atlas of transverse cross-sections contains no data on σ_t for $E_n = 14$ Mev. The value 2×10^{-27} cm² is obtained by extrapolation. The accuracy of the estimate is not lower than ± 50%.

incident atom takes up the position of a displaced atom[2], $\bar{N}_d$ is expressed as

$$\bar{N}_d = [E_m/(E_m - E_d)] \times [0.766 + 0.352 \ln (E_m/4E_d)],$$

where E_m is the maximum energy which a fast neutron transfers to a nucleus; $E_m = E_n\, 4mM/(m+M)^2$, where m is the mass of the neutron and M is the mass of the germanium neucleus; E_d is the minimum energy which must be transferred to a Ge atom in order to displace it from a lattice site. According to data obtained in experiments on bombarding germanium with fast electrons, the energy E_d is 22.5 ev[8], where only defects which are stable at room temperature are taken into account. In the following it is assumed that the effect of self recovery of defects during the time of irradiation can be disregarded.

For neutrons with energies E_n from 0.01 to 14 Mev, $\bar{N}_d$ in a germanium crystal comes to

E_n, Mev	0.01	0.05	0.1	0.5	1	5	10	14
N_d	1.46	1.97	2.22	2.78	3.03	3.59	3.83	3.95

The range of the germanium atoms in the crystal is small. On account of this, groups of vacant lattice sites and interstitial atoms situated close to one another arise during neutron bombardment along with the usual isolated Frenkel defects.[9]

2. We carried out experiments on fast neutron bombardment of single crystals of n-type germanium with specific resistances of 24 and 35 Ω cm. and initial bulk lifetimes at room temperature equal to 650 ±50 and 1400 ±200 microseconds. Crystals were obtained in our laboratory by a drawing technique. Both crystals were irradiated simultaneously. They were placed at equal distances (2.0 ±0.4 cm.) from the tritium target which served as the source of neutrons.

The temperature of the crystals during the time of the experiment did not exceed room temperature by more than 10°C. In one of the specimens studied, the lifetime of the charge carriers was measured immediately before and after irradiation. A bridge method[10,11] was used for the measurement. The lifetime τ_0 of the carriers before the beginning of irradiation was 1400 ± 200 μ sec; after irradiation it fell to 420 ± 10 μ sec.

In the second specimen a p–n junction was obtained by fusing on some indium. The measured quantity, from which it was possible to judge the change in recombination rate, was in this case the short-circuit current between the p and n regions, flowing upon illumination of the opposite face by a light flux of constant intensity (see Fig. 1). The results of the measurements are given in the table.

Dark current, which could have been due to ionization in the germanium on account of the γ background and of the rearrangement of the electron shells of the displaced atoms, was not observed

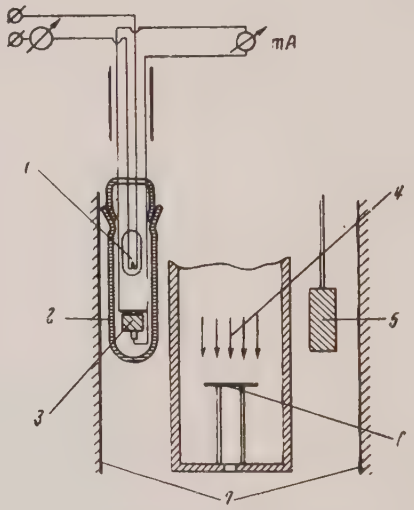

FIG. 1. 1—lamp, 2—glass ampoule, 3—germanium photocell, 4—deuteron beam,, 5—germanium crystal, 6—tritium target, 7—lead.

Number of neutrons per cm^2, $n_n \times 10^{11}$	Number of defects per cm^3.	Short circuit current I_{sc} ma.
0	0	0.87
0.45	$0.15 \cdot 10^{10}$	0.80
0.95	$0.34 \cdot 10^{10}$	0.735
1.41	$0.50 \cdot 10^{10}$	0.708
1.95	$0.69 \cdot 10^{10}$	0.649
2.40	$0.85 \cdot 10^{10}$	0.615
3.23	$1.15 \cdot 10^{10}$	0.578
3.80	$1.35 \cdot 10^{11}$	0.540
4.37	$1.55 \cdot 10^{10}$	0.510
5.0	$1.78 \cdot 10^{10}$	0.481

with apparatus having a sensitivity of 10^{-7} amp. The mean intensity of the 14-Mev neutron flux amounted to $\sim 1.10^7$.neutrons/sec. per square cm. of surface of the specimen. Experiments were carried out with a set-up used neutron spectrometry [12]. The additional flux of the neutrons scattered and slowed down by the lead surrounding the tritium target was taken into account in the calculation of the total number of defects formed in the crystals.

Owing to the fact that with the comparatively small integral neutron fluxes used in our experiments, the concentration of carriers could be considered constant, the initial lifetime τ_0, the lifetime after irradiation τ, and the concentration of formed defects n are connected by a simple relation [4]:

$$(1/\tau)-(1/\tau_0) \doteq n_d v_p \theta.$$

Considering that the defects formed trap carriers separately, i.e. act on the recombination independently of one another, then taking the thermal speed of the holes as $v_p = 1.1 \times 10^7$ cm/sec, we obtain the value of the cross-section for recombination trapping θ.

$$\theta = (1 \pm 0.5) \times 10^{-15} \text{ cm}^2.$$

For an estimate of the change of the recombination rate from the drop of the short circuit current, the following considerations were used. Let us examine the scheme shown in Fig. 2, the crystal with the fused-on p–n junction having a thickness d. The

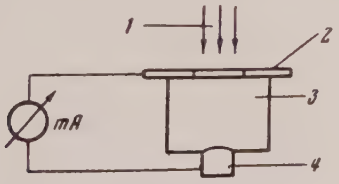

FIG. 2. 1—light, 2—nickel collar, 3—n-type germanium, 4—indium.

generation of surplus carriers by the light proceeds in a layer close to the surface, thin in comparison with d. Let the total number of holes generated by the light in unit time be G. The short circuit current I_{sc} can be expressed as $I_{sc} = q\alpha G$, where q is the electron charge, and α the effective quantum yield or collection coefficient of the carriers [14]. In the one-dimensional case [15], under the condition that the reciprocal value of the linear absorption coefficient of light $1/k \gg 1/L$; $1/k \gg s/D_p$, where L is the diffusion length of the holes, s is the rate of surface recombination, and P_p is the diffusion coefficient, we have

$$\alpha = \frac{2}{(1-sL/D_p)e^{-d/L}+(1+sL/D_p)e^{d/L}}$$

The formula for α can be reduced to the simple expression $\alpha = Ae^{d/L}$, where A = const., under the following conditions: $d/L \gtrsim 2$, $L \lesssim 5 \times 10^{-2}$cm, and and with surface recombination rates such as are obtained on etching germanium in hydrogen peroxide. For constant G, the ratio of I_{sc} after irradiation to the original value $I^0_{sc} = q\alpha_0 G$,

$$I_{sc}/I^0_{sc} = \alpha/\alpha_0.$$

Calculating α_0 with a reasonable assumption about the value of s established by means of a surface treatment, on the basis of known data on the original diffusion length L_0 in the non-irradiated material, one can determine α, and consequently L and τ, knowing the measured ratio I_{sc} to I^0_{sc}. With the lower limit of possible values for s equal to 150 cm /sec, θ turns out equal to 1.05×10^{-15} cm^2; for s = 600 cm/sec. $\theta = 1.29 \times 10^{-15}$ cm^2.

The dependence of the reciprocal value of the short circuit current on the integral radiation dose is presented in Fig. 3, calculated on the basis of the last formula and experimental values for L_0 and I^0_{sc}.

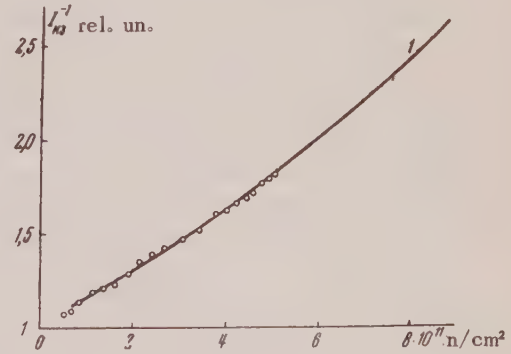

FIG. 3. 1—s = 300 cm/sec; $\theta = 1.1 \times 10^{-15}$ cm^2; ○—experimental points. The ordinate is labeled I^{-1}_{sc} (relative units) and the abscissa in labeled neutrons/cm^2.

The relation between $1/I$ and the integral radiation dose can be utilized for the determination of dosage of fast neutrons starting with neutron fluxes of the order of 5×10^6 neutrons/cm^2 sec. Dosimeteric apparatus, based on the change in lifetime of carriers in germanium crystals can have a sensitiv-

ity of Cassen's dosimeter[3], based on the measurement of electric conductivity of crystals. The sharp difference in recombination trapping cross-sections for the cases of defect formation by fast neutrons and β-particles found in our experiments is explained, apparently, by the high hole-trapping efficiency of an agglomeration of defects.

On the basis of available data one can not also exclude the possibility of local melting of the germanium upon displacement of a germanium nucleus, to which a neutron transfers an energy of several hundred kev, inside the crystal. Rapid cooling of a small region[13] can lead to the appearance of additional defects of the crystal lattice which are not taken into account in the Snyder-Neufeld theory[7] which we used to calculate the number of displaced atoms.

The authors express their sincere thanks to B.M. Vul for valuable comments, and also to F. L. Shapiro for discussion of a series of questions and for affording us the opportunity to work with a fast neutron source.

---

[1] K. Lark-Horovitz, *Semi-Conducting Materials*, London, Butterworths (1951) pp. 47–69.

[2] H. Fan and K. Lark-Horovitz, *Paper delivered at the International Conference on Semi-Conductors and Crystals-Phosphors*, Munich (1956) (in press).

[3] B. Cassen, Proceedings of the Geneva Conference, 14, 218 (1955).

[4] L. S. Smirnov and V. S. Vavilov, J. Tech. Phys. (U.S.S.R.) 27, 427 (1957).

[5] V. V. Ostroborodova and S. G. Kalashnikov, J. Tech. Phys. (U.S.S.R.) 25, 1163 (1955).

[6] D. J. Hughes and J. A. Harvey, *Neutron Cross-Sections*, McGraw Hill, N. Y. (1955).

[7] W. S. Snyder and J. Neufeld, Phys. Rev. 97, 1637 (1955).

[8] Vavilov, Smirnov, Galkin, Patskevich and Spitysyn, J. Tech. Phys. (U.S.S.R.) 26, 1865 (1956).

[9] J. Frenkel, Z. Physik 35, 652 (1926).

[10] A. Many, Proc. Phys. Soc., 67A, 9 (1954). (Collection: Problems in Modern Physics 2, 80 (1955)).

[11] B. D. Kopylovskii and S. V. Bogdanov, Prib. i Tekhn. Eksper. (Instr. and Exptl. Engg.) 1, 66 (1956).

[12] A. A. Bergman et. al. Report presented by the USSR to the Geneva Conference on the Peaceful Uses of Atomic Energy.

[13] F. Dessauer Z. Physik 12, 38 (1923).

[14] V. S. Vavilov and L. S. Smirnov, Radiotekhnika i Electronika 1, 1147 (1956).

[15] Rappaport, Loferski and Linder, RCA Rev. 17, 100 (1956); W. Pfann, and W. van Roosbroeck, J. Appl Phys., 25, 1422 (1954).

Translated by R. L. Eisner
166

Investigation of the Penetrating Component of Electron-Nuclear Showers by the Delayed Coincidence Method in Conjunction with a Hodoscope

G. B. ZHDANOV AND A. A. KHAIDAROV
"Nigrizoloto" Scientific Research Institute of the Ministry of Non-ferrous Metals
(Submitted to JETP editor November 27, 1956)
J. Exptl. Theoret. Phys. (U.S.S.R.) 32, 706-713 (April, 1957)

The distribution in range of slow mesons created by cosmic rays on lead and graphite nuclei at effective energies on the order of 5 Bev and higher has been investigated by a method described in Ref. 1. Some peculiarities of secondary interactions of penetrating particles of electron-nuclear showers at the same energies are also examined.

1. INTRODUCTION

WE HAVE CARRIED OUT, at an altitude of 3860 m above sea level, experiments investigating the energy spectrum of slow π^+-mesons generated in electron-nuclear showers. We used the method of delayed coincidences in conjunction with a hodoscope.

The present article gives the basic results obtained. A study of the generation of comparatively slow mesons during nuclear interactions of cosmic ray particles with matter was carried out for primary particles in an average energy range of ~5 Bev or higher. The experimental method used has been set forth in detail in Ref. 1 and partially in Ref. 2. Schematic diagrams of the apparatus used in the present work are given in Figs. 1 and 2.

Let us carry out the analysis of the experimental data which is involved in the classification of the phenomena registered by the apparatus. Analyzing the hodoscope photographs, we may divide all the showers into several types according to the following characteristics: 1) a double δ-shower, the criterion for which is the presence of operated counters only among the directing group $M1$ and $M2$ and only in immediate proximity to each other; 2) showers with air accompaniment, among which we include events where at least one charged particle has passed through a group of counters located 2-3 m to one side of the main apparatus; 3) showers accompanied by the operation of several counters placed over the main apparatus, but without having a charged particle go to the side group of counters, have been conditionally classified as narrow showers; 4) all the remaining showers have either been included in the group of electron-nuclear showers or else have been put in the category of cases difficult to interpret if the picture observed in the hodoscope could not be explained as a nuclear interaction in the layer of material between counters $M1$ and $M2$. Cases of secondary interaction (produced by a radioactive particle belonging to a registered shower) in the hodoscope may be recognized during visual analysis of the hodoscope photographs. The distribution of the showers according to the different categories with various filters present in the apparatus is given in the table.

The first and second lines of the table give the data relative to sparse ($n \leqslant 3$) and dense ($n \geqslant 4$) electron-nuclear showers, while the third line gives data relative to electron-nuclear showers with secondary interactions a) from charged shower particles, b) from neutral shower particles. The fourth and fifth lines give the number of sparse double δ-showers and dense double δ-showers (the density being estimated from the number of activated counters). The sixth and seventh lines give the number of narrow and extensive air showers, and, finally, the eighth line gives the cases that are difficult to interpret.

An analysis of the results given in the table shows that it is possible to collect a great deal of experimental material by means of the present method.

If they are related to the corresponding nuclear ranges, the numbers of electron-nuclear showers produced in the Pb and C filters per time unit are experimentally equal and amount to ~9 per hour (for dense showers). This shows that these filters are not essentially different in their effectiveness in registering such showers.

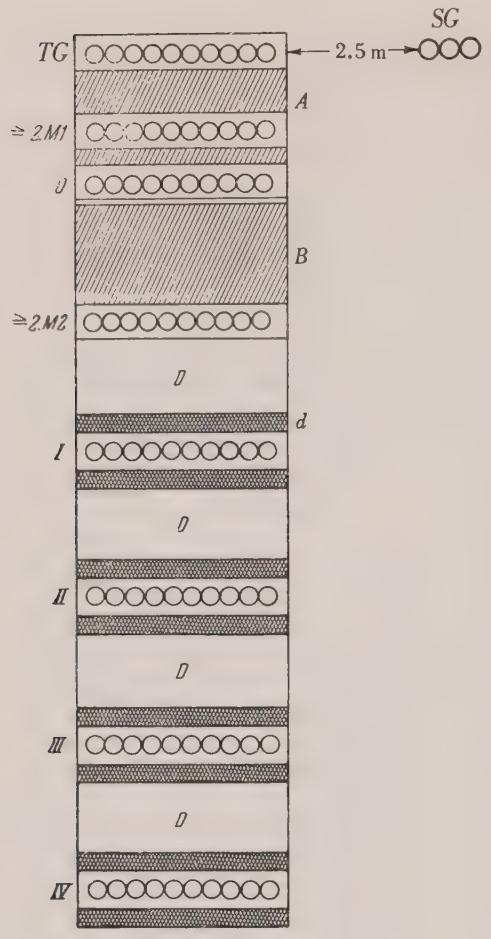

FIG. 1

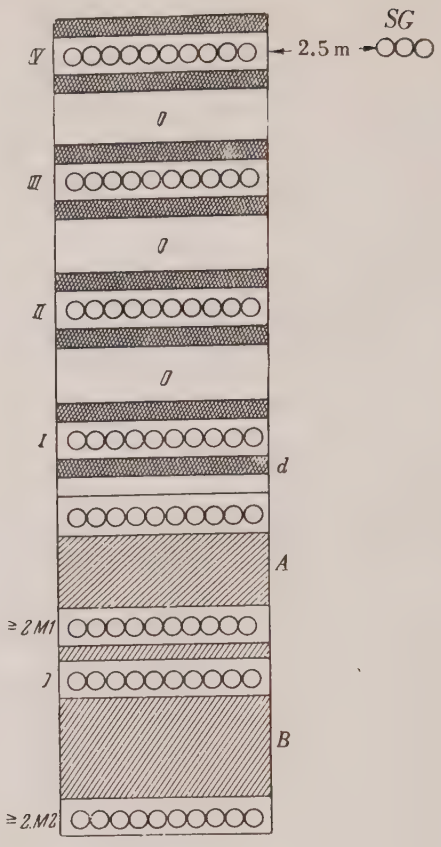

FIG. 2

FIG. 1. Arrangement of counters and filters in the apparatus (basic variant). *TG*—top group of counters; *SG*—side group of counters (for recording wide showers); *M*1—upper directing group; *M*2—lower directing group (all the indicated counters are connected to an ordinary hodoscope of type GK-3, groups *M*1 and *M*2 separate out the cases where $\geqslant 2$ particles pass through); 0—IV are rows of counters connected to the double screen of a hodoscope of type GK-5; *A* is an interchangeable filter (Pb and C) in which the showers under investigation are generated; *B* and *D* are interchangeable filters (Pb or Fe) which determine the ranges of the mesons registered by the counter trays of the type GK-5 hodoscope; the filters *d* are fixed filters (of 2.5 cm thickness) which are sources of the decay electrons. The working dimensions of all the counters are 33 × 300 mm.

FIG. 2. Arrangement of counters and filters in the experiment for the study of the vertical return current. The designations are the same as in Fig. 1.

2. SECONDARY INTERACTIONS IN SHOWERS

The currents of neutral and charged radioactive particles produced in electron-nuclear showers have been compared for the configuration of counters shown in Fig. 1. We determined these currents by means of the number of secondary nuclear interactions in the filters of the hodoscope. In 220 hours of measurements with iron filters of total thickness 160 g/cm² present in the hodoscope, 260 cases of secondary nuclear interactions from nuclear particles were obtained. If we also take into account the presence of neutrons which do not interact in passing through the filters (assuming the interaction cross section to equal the geometric ones) the total flux of fast neutrons becomes $N_0 = (6 \pm 0.65)$ hr^{-1}. Relative to a single electron-nuclear shower, this number amounts to $n_N = (0.2 \pm 0.025)$. Reasoning in an analogous manner about the interactions with charged particles, after the exclusion of δ-showers, we obtain $N_0 = (16.8 \pm 1.2)$ hr^{-1} and $n_C = (0.62 \pm 0.043)$. Here we use n_N and n_C to indicate the average number of neutral and charged radioactive particles, respectively, in a single shower emitted within the limits of a definite angle with respect to the vertical. Assuming that the

Character of the observed phenomenon	A = 6 cm Pb, d = 2.5 cm Fe						A = 16 cm C, d = 2.5 cm Fe						A = 6 cm Pb, d = 2.5 cm Fe						A = 16 cm C, d = 2.5 cm Fe					
	D = 0			D = 8 cm Fe filters			D= 0			D = 8 cm Fe filters			D = 0			D = 8 cm Fe filters			D = 0			D = 8 cm Fe filters		
	ν	s	N	ν	s	N	ν	s	N	ν	s	N	ν	s	N	ν	s	N	ν	s	N	ν	s	N
Group number	1			2			3			4			5			6			7			8		
1. Sparse electron-nuclear showers (number of penetrating particles in the lower row of counters $n \leqq 3$)	17.7	22	369	18	21	340	16	21	334	17	25	409	0.12	28	49	0.16	25	44	0.08	20	20	0.09	22	23
2. Dense electron-nuclear showers (number of penetrating particles $n \geqq 4$)	8.8	11	184	9	11	170	7.9	10	166	8.6	12	207	0.18	42	73	0.26	43	74	0.14	33	33	0.13	30	32
3. Electron-nuclear showers with secondary interactions																								
a) from charged shower particles	2.7	3.3	57	1.84	2.2	35	3.1	4.0	65	1.9	2.7	45	0.012	2.9	5	0.018	2.9	5	0.13	7	7	0.016	3.7	4
b) from neutral shower particles	1.4	1.7	29	1.80	2.1	34	2.6	3.4	55	1.5	2.2	36	0.007	1.7	3	0.021	3.5	6	0.017	4	4	0.02	4.7	5
4. Sparse double δ-showers	24	29	503	25.7	30	488	22.9	30	480	17.5	25	420	0	0	0	0	0	0	0	0	0	0	0	0
5. Dense double δ-showers	6.3	7.7	132	6	7	113	5.0	6.5	106	6.2	8.8	149	0	0	0	0	0	0	0	0	0	0	0	0
6. Narrow air showers	10.3	13	217	10.5	12	191	6.2	8.1	131	5.2	7.5	125	0.06	14	24	0.064	10	18	0.05	12	12	0.044	10	11
7. Extensive air showers	6	7.3	125	6,6	7.8	125	7.7	10	162	7.0	9.1	168	0.015	3.4	6	0.056	9.2	16	0.06	15	15	0.096	22	24
8. Cases difficult to interpret	4.4	5.4	93	6.0	7.1	115	5.6	7.3	118	4.6	6.6	110	0.027	6	3	11	0.035	5.8	10	0.04	9	9	0.032	8	8
General total of all events	1709			1611			1617			1666			174			173			100			107		
Time of measurement (in hours)	21			19			21			24			403			283			237			250		

NOTES. The data of groups 1, 2, 3, and 4 refer to showers without meson decays, while those of groups 5, 6, 7, and 8 refer to showers with meson decays. ν is the event frequency per hour; s is the relative number of events; N is the total number of cases treated.

number of fast protons in electron-nuclear showers is equal to the number of fast neutrons, that is, 0.2, we find the number of π^+-mesons to be ~ 0.4. The basic result of the given measurements is the following: 0.2 of the particles in a shower consist of fast neutrons (with minimum energy on the order of 0.5 Bev), 0.2 of the particles are protons with the same energy, and 0.4 of the particles are π-mesons. Here all the fluxes are with respect to a comparatively small interval of angle with the vertical and, hence, also with respect to the primary particles.

The intensities obtained for the fluxes of secondary radioactive particles of various kinds agree satisfactorily with the absorption ranges for the radioactive component in air and in dense materials. Actually, it is known that the average ranges for the absorption and interaction of the radioactive component in a material λ_a and λ_0, are connected by the simple relationship

$$1/\lambda_a = (1/\lambda_0)(1-n_g),$$

where n_g is the average number of radioactive particles. If we substitute $\lambda_0 = 60$ g/cm^2, $\lambda_a = 2\lambda_0$ for air and $\lambda_a = 3\lambda_0$ for dense materials, it turns out that on the average ~ 0.5 secondary high-energy radioactive particles are generated for each interaction in air, and that all of them must be stable particles, that is, nucleons. For a dense material the number of nucleons turns out to be $\frac{2}{3}$ rather than $\frac{1}{2}$, and unstable radioactive particles, that is, fast mesons, must also be included. Under the actual conditions of our experiments, the energies of the secondary interactions are selected to be much less than those of the primary interactions and, moreover, tertiary interactions are taken into account. All this, when summed up, leads to the conclusion that the total number of secondary radioactive particles in a dense material turns out to be 0.8 instead of the expected $\frac{2}{3}$. In the present instance the definiteness of the results is not great enough to permit their being used except as an order of magnitude.

In order to obtain a comparison of the intensity of the generation of mesons in different materials (C and Pb), the results on the decay of mesons in sparse ($n_s \leqslant 3$) and dense ($n_s > 3$) showers in the different configurations of the experiment were added up (n_s is the number of penetrating particles). During the same time interval 108 and 240 decay events were found in C and Pb, respectively.

These results (taken relative to one hour of measurement) give the following values for the number of mesons decaying in the apparatus: 0.22 ± 0.02 for C and 0.36 ± 0.02 for Pb.

The results obtained show that for generating particles having the same energies ($E_{gen} \sim 5$ Bev) the total number of comparatively slow mesons (with energies up to 800 Mev) generated by them in nuclear acts depends weakly on the atomic number of the nucleus.

3. DETERMINATION OF THE RANGE SPECTRUM OF THE π^+-MESONS

Both variants of the apparatus were used in the measurements (see Figs. 1 and 2). The treatment of the experimental results in determining the spectrum of the meson ranges in the showers was begun with the choice of groups for the meson decays. The place of the decays was determined to an accuracy of the thickness of a single filter. After determining the location of the meson decays on each of the photographs, we were able to unite in a single group all the cases with given range R_i, where $i = 1, 2, 3, \ldots, 8$ is the number of filters located between the points of generation and decay of the meson.

On grouping the direct results of the experiment we obtained the number of decays $N(R_i)$ corresponding to various ranges R_i and for a definite time of measurement. After this, with the aid of special control experiments and statistical methods of treating the hodoscope photographs, we carried out an evaluation of the following effects concerned with the apparatus:

1. Accidental delayed coincidences. The probability of such a "decay" is not greater than one case in 1000 showers for the data used in the calculations.

2. Effect of the occupancy of the counters of the hodoscope rows by prompt shower particles on the registration of mesons (as a result of this effect, mesons decaying at different distances from the place of generation of the shower are registered with different efficiencies).

3. Difference in the "transmission factor" of the different counter rows of the hodoscope. A special control experiment (without filters in the hodoscope) permits the determination of the so-called geometrical factor for each row, that is, the correction factor which takes account both of the difference in the distances of the rows from the point of generation of the shower and of the angular distribution of the shower particles.

Corrections were also applied to the nuclear interactions. These consisted of, first, allowances

for the nuclear absorption of π-mesons in the filters of the apparatus (with effective cross section $\sigma = 0.7\ \sigma_{0\ geom}$) and, second, allowances for the secondary generation of π-mesons in these filters by radioactive particles (the number of which amounts to no less than $^2/_3$ per shower).

After introducing all these corrections and taking account of the effectiveness of the apparatus in registering the stopped mesons, we obtained the range spectrum of the π^+-mesons generated in C and Pb. The weak dependence of the form of the generated spectra on the nature of the nucleus permits the results obtained for lead and graphite to be combined in order to obtain greater statistical accuracy. The averaged range spectra of the mesons is shown in Fig. 3 for the direct and return vertical fluxes. It should be kept in mind that owing to a certain indefiniteness in the corrections for the secondary nuclear interactions, the form of the spectrum for path lengths exceeding the average range of the nuclear interactions also becomes somewhat indefinite.

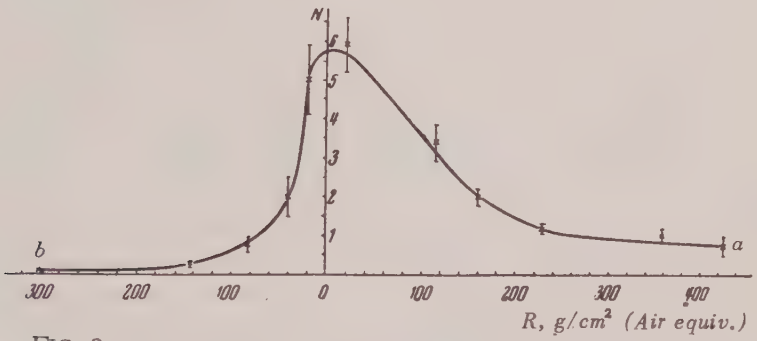

FIG. 3. Average range spectra for the direct and return fluxes of π^+-mesons generated in graphite and lead: a (portion of the curve for $R < 100$)—direct flux, b—return flux

We have compared the spectrum which we have obtained for the ranges of the π^+-mesons in the direct current with the results of other authors[3-5]. A comparison of photographic plate data (for the stratosphere) with the results of our experiments gives (on taking account of secondary interactions) satisfactory agreement, in spite of a considerable difference in the conditions of measurement. Actually, our apparatus recorded showers with higher average energy than in the experiments with photographic plates, owing to the presence of a control system which selected showers for which the number of penetrating particles was not less than two. A comparison with the momentum spectrum obtained at a height of 3200 m by the mass spectrometer method[4] and with the range spectrum obtained by the method of delayed coincidences[5] showed a rather significant deviation from these spectra. This difference is connected primarily with the fact that in the mass spectrometer[5] and in the apparatus used in Ref. 6 the particles studied were generated by nucleons of comparatively small energy, while we chose interactions of higher energy in our apparatus. From the comparison of our results with those referred to, we can conclude that the energy spectrum of slow mesons becomes harder with increasing energy of the generating component. It follows from this that the meson energy spectra studied by different methods depend to a very high degree on the "hardness" of the control system of the apparatus.

The amount of the return current of π^+-mesons in electron-nuclear showers was also determined and found to be $24 \pm 7\%$ of the primary current. This result does not contradict (to within the limits of error of the experiment) the photographic plate data.

4. INTENSITY OF GENERATION OF SLOW MESONS FOR DIFFERENT NUCLEAR INTERACTION ENERGIES

To explain how the form of the meson spectrum depends on the average energy of the generating particles, we determined the number of very slow mesons (with range of 20 g/cm² air equivalent) relative to the number of "fast" mesons (that is, mesons decaying in the remaining rows of the hodoscope) as a function of the energy of the electron-nuclear showers. In this determination, the electron-nuclear showers were grouped by energies according to the number of particles in these showers. The results obtained (after applying the corrections for the ap-

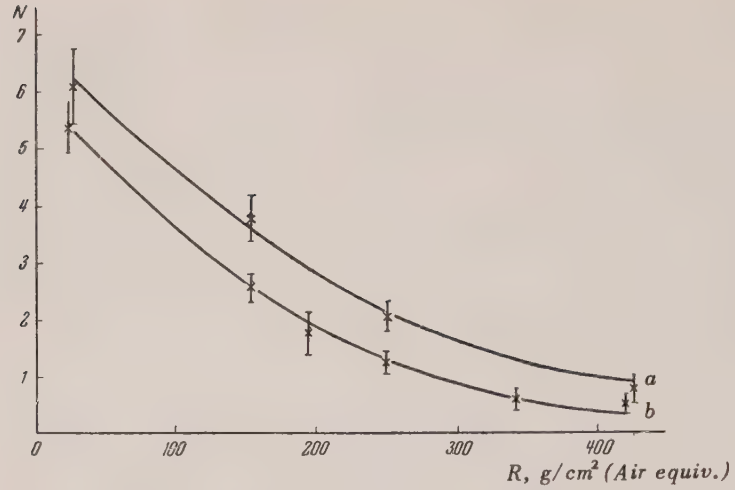

FIG. 4. Meson range distribution curves for showers of different densities: *a*—for dense showers ($n > 3$), *b*—for sparse showers ($n \leqslant 3$). n is the number of counters triggered (in row M2).

paratus) are displayed as curves in Fig. 4. From these curves it may be established that π^+-mesons with ranges of up to 20 g/cm² make up as much as 20% of the total number of π^+-mesons for sparse showers ($n \leqslant 3$) and about 15% for denser showers ($n > 3$), with an accuracy of the order of 20% in both estimates.

To clarify the same question, the relative numbers of slow mesons were compared for the cases where the generation of the mesons was accompanied by the passage of an air shower and the cases where the generation of the mesons occurred in the absence of an air shower. The probability of the appearance of a slow π^+-meson (with range of up to 20 g/cm²) is $(5.8 \pm 1.15) \times 10^{-3}$ in the first case and $(11.6 \pm 0.9) \times 10^{-3}$ in the second. From the experiments of Liubimov *et al.*[6] and Zatsepin *et al.*[7], it follows that the average energy of generating particles accompanied by an air shower is several times greater than the average energy of generating particles not accompanied by such a shower. Analyzing the data given above, we can say that as the energy of the generating particles is increased, the number of slow mesons decreases approximately twice as fast.

This result was double checked. For this purpose while processing the experimental material we selected and set aside data on showers with two or more penetrating particles, the half angle of separation of which was of the order of 15°. In such a case the number of slow mesons relative to a single shower amounted to $(4.4 \pm 1.2) \times 10^{-3}$, while for cases in which the average energies of the generating particles are 3–5 Bev it amounts to $(11.6 \pm 0.9) \times 10^{-3}$. The energy of the generating particles of the shower selected as indicated above is calculated from

$$\cot \theta_{1/2} = \gamma_c = \sqrt{(\gamma_0 + 1)/2}$$

where $\gamma_0 = E_0/Mc^2$, and is of the order of magnitude of 2×10^{10} ev. From the results obtained it is evident that on going over to primary energies of the order 2×10^{10} ev, the number of slow mesons relative to a single shower is smaller by at least a factor of two than the number of such mesons which are observed for particle energies of 3–5 Bev.

From the curves shown in Fig. 4 it is clear that in the interval of ranges up to 100 g/cm² the number of mesons depends weakly on the total number of particles in the shower, while for mesons with larger values of range this dependence is stronger, and the total number of mesons increases considerably with the number of particles. A dependence of such a nature is partially explained by secondary generation of slow mesons by shower particles, and not merely by changes in the energy spectrum of the mesons in the act of primary interaction.

If we consider the simplest model of a nucleon-nucleon collision and take account of the fact that the meson distribution is isotropic in the center of mass system, we find that for an energy of the generating particles of the order of 10 Bev the probability of generation of a slow meson (with range ~ 20 g/cm²) is not greater than 7% (since these mesons emerge at an angle of not less than 150° in the

center of mass system). In the experiment this portion amounts to 15–20%. However, the results at our disposal do not yet allow us to decide to what extent such a discrepancy should be attributed to the doubtfulness of the simplest statistical model and to what extent it should be attributed to intranuclear or extranuclear cascade processes.

CONCLUSIONS

1. In the present work the range spectrum for the return component of $\pi^{\pm}$-mesons generated in lead nuclei has been determined and compared with the range spectrum in the direct current. The return meson flux was found to amount to 24 ± 7% of the direct meson flux.

2. It has been established that the number of π^{+}-mesons with a range of the order of 20 g/cm^2 depends weakly on the energy of the generating particles, decreasing somewhat with increase in this energy.

3. It has been shown that for measured energies of the generating particles (not higher than 5 Bev) the number of slow mesons formed also depends weakly on the atomic number of the nucleus.

[1] G. B. Zhdanov, J. Exper. Theoret. Phys. (U.S.S.R.) 30, 437 (1956), Soviet Physics JETP, 3, 323 (1956).

[2] A. A. Abdullaev, G. B. Zhdanov, L. N. Korablev, A. A. Khaidarov, J. Exper. Theoret. Phys. (U.S.S.R.) 21, 1072 (1951).

[3] U. Camerini *et al.*, Phil. Mag. 42, 1241 (1951).

[4] V. Kamalian and A. Alikhanian, Doklady Akad. Nauk SSSR 97, 425 (1954).

[5] A. A. Abdullaev, Dissertation, Moscow, Physical Institute of the Academy of Sciences, 1954.

[6] Korablev, Liubimov and Nevraev, Doklady Akad. Nauk SSSR 68, 273 (1949).

[7] Anishchenko, Zatsepin, Rosental' and Sarycheva, J. Exptl. Theoret. Phys. (U.S.S.R.) 22, 143 (1952).

Translated by M. J. Gibbons
167

SOVIET PHYSICS JETP VOLUME 5, NUMBER 4 NOVEMBER, 1957

Measurement of High Temperatures in Strong Shock Waves in Gases

I. SH. MODEL'
Institute of Chemical Physics, Academy of Sciences SSSR

(Submitted to JETP editor, November 30, 1956)
J. Exptl. Theoret. Phys. (U.S.S.R.) 32, 714-726 (April, 1957)

A photographic method for the measurement of high temperatures and the absorption coefficient of radiation by the gases in a plane shock wave is described. Results of the measurement of the temperature and absorption coefficient of a plane shock wave in air are presented for wave velocities between 6.4 and 8 km/sec. In strong shock waves in heavy inert gases the experimentally measured temperatures are much lower than the calculated values. It is suggested that this phenomenon is due to screening of the shock wave front by a layer of gas heated by radiation from the shock front.

INTRODUCTION

DURING THE PAST FEW YEARS, methods have been developed to obtain powerful shock waves using explosives. Calculated temperatures up to 70000 °K at pressures of the order of 10^4 kg/cm^2 may be obtained in the wave front by propagating such shock waves is argon ($p_0 = 1$ kg/cm^2, $T_0 = 273$ °K). In spite of the difficulties associated with explosion experiments, the investigation of strong shock waves is of great interest for the study of the properties of gases at such high temperatures and pressures.

At the present time, many perfected techniques and instruments are available in experimental gas dynamics for the investigation of rapidly-occurring processes. However, comparatively little attention has been paid to the development of methods of temperature measurement. Most of the work devoted to the luminosity of gases in a shock wave has been

limited to the investigation of the character of the radiation and to very approximate temperature estimates.

Optical methods based on the temperature dependence of the radiation from a body are most convenient for the measurement of the temperature of a gas under the conditions of a compression shock. It should be noted, first of all, that the luminous spectrum of a gas compressed by a strong shock wave is continuous. Therefore, methods which are widely used for measuring the temperatures of transparent flames (using the radiation of spectral lines) are not suitable for the determination of the temperature of a gas in a strong shock wave. These methods may be applied only with weak shock waves in which the compressed gas layer is still semitransparent in the spectral region in which measurements are being made, and at relatively low temperatures limited by the standard light source. Color and brightness methods are the most widely used for the measurement of the temperature of bodies with continuous radiation spectra. The color method has been used to measure the temperatures of explosion products[1], of adiabatically compressed gases[2] and of technical flames[3]. However, the accuracy of this method, while satisfactory at temperatures on the order of 5000 °K, is insufficient at 10000 °K and above, because the relative distribution of energy in the visible region of the spectrum becomes only slightly sensitive to temperature changes. It was concluded from a comparison of the various known methods of optical pyrometry that the brightness method was the most suitable for the determination of the temperature of the gas in a shock wave, this method providing the greatest accuracy at high temperatures. Since the measurements are carried out over a narrow region of the spectrum, there is no necessity for an accurate determination of the sensitivity of the radiation receiver over a broad region of the spectrum, which is one of the basic difficulties in the comparison of the intensities of radiation of different wavelengths. The method does not require the use of complex spectral apparatus, and may be put into practice with the usual instruments widely used in the study of rapid processes.

PHOTOGRAPHIC METHOD OF HIGH TEMPERATURE MEASUREMENT

The photographic method of high temperature measurement is based on the determination of the ratio of brightnesses in a narrow spectral interval by the corresponding blackening of a photographic film.* compared with a standard with a known brightness temperature. The unknown temperature is found from the equation

$$(e^{C_2/\lambda T} - 1) / (e^{C_2/\lambda T_0} - 1) = \tau a \qquad (1)$$

where T_p is the brightness temperature of the standard, T is the temperature of the body under study, λ is the effective wavelength of the spectral interval used, τ is the ratio of the brightness of the standard to the brightness of the body being investigated a is the absorptivity of the body, $C_2 = 1.438$ cm-deg.

A luminous body whose brightness temperature can be measured in an independent way (temperature tube for calibration of optical pyrometers, the crater of a voltage arc, or any stable source of "black" or "grey" radiation of high brightness) may be used as a standard. For increased accuracy it is advisable to use a source whose temperature is near that being measured. In most of our experiments the sun was chosen as a standard.

The basic instrument for the measurement of the high temperatures arising during the shock compression of gases is the high-speed two-objective photochronograph with a rotating mirror developed by the author in 1948. The optics of the instrument are shown in Fig. 1. The image of the phenomenon being studied is focussed in the plane of slit D by objective O_1 ($f = 75$ cm, 1 : 6.3). The part of the image cut out by the slit is projected by objective O_2 ($f = 7.5$ cm, 1 : 2) on the photographic film P after reflection from rotating mirror M. A red light-filter F which combined with the photographic film form a simple monochromatization system is placed in front of objective O_2. Film blackening is kept withing the limits of the rectilinear part of the characteristic curve of the film by a suitable diaphragm over the first objective. When the mirror rotates, the image of the illuminated slit moves across the film with the velocity $v = 4\pi Rn$, which for a given R is determined by the angular velocity of the mirror n. The maximum velocity with the image moved across the film (sweep velocity) was 2.4 km/sec. Control of the slit width and the sweep velocity varied the exposure time between 10^{-15} and 10^{-7} sec. The process being studied was synchronized

*The photographic pyrometer for the measurement of nonstationary temperatures in the range 1000 – 1400 °K proposed by Male[4] in 1951 was based on the same principle.

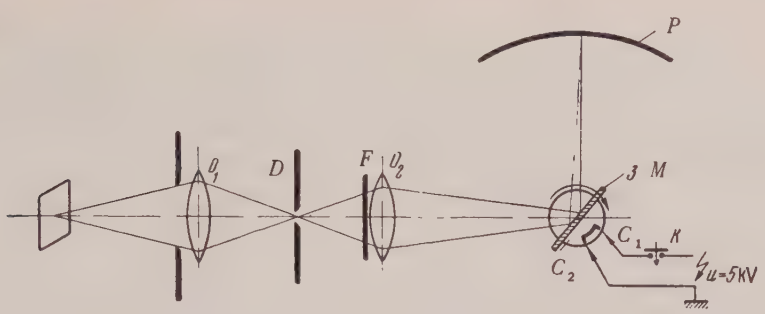

FIG. 1. Optical schematic of the photochronograph with a red filter for recording high temperatures in rapidly occurring processes.

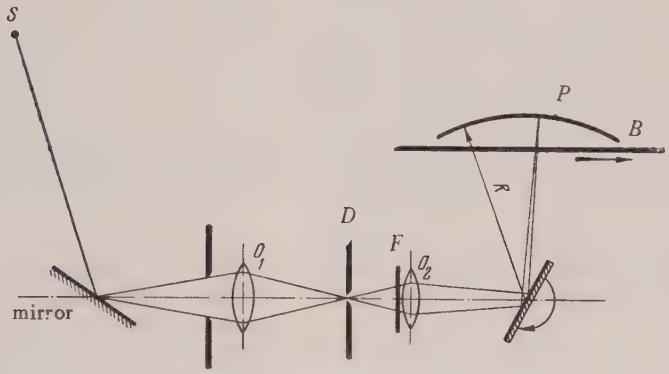

FIG. 2. Schematic of the photochronographic recording of solar film density.

with the mirror position by the rotating spark switch C, rigidly attached to the axis of the mirror, and by the two regulating contacts C_1 and C_2 included in the circuit of the electrodetonator. The circuit is completed by closing push-button K.

Photography of the standard S (the sun) was carried out on the same apparatus, equiped with a special shutter (Fig. 2). Blind B has a rectangular slot 5 mm wide. Initially (extreme left position) the film is covered by the blind. When triggered a spring mechanism moves the blind from left to right with a velocity of 2 m/sec. The angular velocity of the mirror is chosen such that the velocity of the image of the slit over the film is ~ 0.5 km/sec. With this relation between the sweep velocity and the blind velocity, a new part of the film is illuminated during each revolution of the mirror. By obtaining on one film two series of images taken with different exposures H_1 and H_2, we may determine the tangent of the slope angle of the characteristic curve γ, which is necessary for the calculation of brightness ratios from density differences:

$$\gamma = (d_1 - d_2) / \log (H_1/H_2).$$

At the instant of photographing, the brightness temperature of the sun was measured by an optical pyrometer with a vanishing filament and an additional neutral filter.

The films of each series of experiments and the photographs of the sun were developed together. The results were thus protected from the influence of the photographic solutions. The photochronograms were prepared with a Zeiss nonrecording photoelectric microphotometer.

In photography it is usually assumed that the exposure within the limits of the image (neglecting atmospheric absorption) is independent of the distance to the object of the photograph and is determined only by the transmission of the optical system. This assumption is valid if the distance L between the object of the photograph and the instrument is considerably greater than the focal length f of the optical system. When L is comparable with f, it is necessary to take into account the difference in effective transmission which is determined by the ratio

$$k = \left(\frac{L_1 - f}{L_1}\right)^2 \Big/ \left(\frac{L_2 - f}{L_2}\right)^2.$$

In our work in which the shock wave is photographed at a distance of 10–20 m, and the standard (the sun) is practically at infinity, this condition must be taken into account.

It is well known that the photographic effect is a function of two independent variables; the illumination E and the exposure time t. However, the investigations of Kartuzhanskii and Meikliar[5] have shown that for exposure times less than 10^{-5} sec the reciprocity law holds – the blackening of the photographic emulsion is determined by the product of the illumination and the exposure time. This simplifies considerably the use of photographic recording for short-duration processes because deviations from the reciprocity law need not be investigated. To guarantee these conditions in all our experiments, the time during which light acted on the photographic film did not exceed 10^{-5} sec.

The wavelength λ of the part of the spectrum in which measurements of brightness ratios are made enters into Eq. 1, used for the determination of the temperature T. We singled out a narrow region of the spectrum by using the combination of a red glass light filter with a lower transmission limit $\lambda_1 = 0.57\,\mu$ and photographic film with an upper sensitivity limit $\lambda_2 = 0.66\,\mu$. The sensitivity of the photographic film v_λ and the transmissivity of the red filter τ_λ are plotted against wavelength in Fig. 3. The portion of the figure with double crosshatching represents the working spectral interval, extending over $\sim 0.09\,\mu$. In this case the effective wavelength for

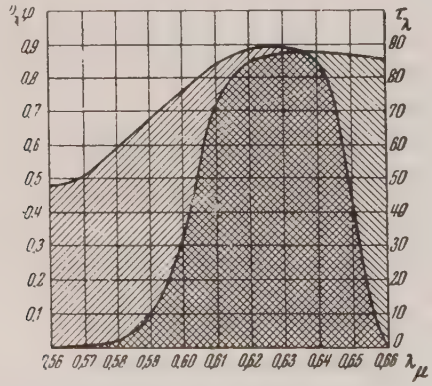

FIG. 3. Sensitivity of the photographic film and transmissivity of the red filter as a function of the wavelength λ; v_λ is the sensitivity of the film in relative units and τ_λ is the percentage transmissivity of the red filter.

the determination of the temperature T from the known temperature T_0 may be calculated from the ratio of the respective light fluxes F and F_0 passing through the red filter and received by the light-sensitive emulsion.

$$\frac{F}{F_0} = \int_0^\infty v_\lambda \tau_\lambda b_{\lambda, T}\, d\lambda \Big/ \int_0^\infty v_\lambda \tau_\lambda b_{\lambda, T_0}\, d\lambda$$
$$\approx \sum_{\lambda_1}^{\lambda_2} v_\lambda \tau_\lambda b_{\lambda, T}\, \Delta\lambda \Big/ \sum_{\lambda_1}^{\lambda_2} v_\lambda \tau_\lambda b_{\lambda, T_0}\, \Delta\lambda,$$

where $b_{\lambda, T}$ and b_{λ, T_0} are the spectral brightnesses at the temperatures T and T_p respectively, calculated by Planck's formula

$$b_{\lambda, T} = C_1 \lambda^{-5} (e^{C_2/\lambda T} - 1)^{-1},$$
$$C_1 = 3{,}71 \cdot 10^{-5} \text{ erg-cm}^2/\text{sec}.$$

Knowing the ratio F/F_0, we find the value of the effective wavelength λ satisfying the equation

$$F/F_0 = (e^{C_2/\lambda T_0} - 1) / (e^{C_2/\lambda T} - 1).$$

In the high temperature region ($T > 8000\,^\circ$K) the effective wavelength λ changes only slightly with changes of the measured temperature, and a single value may be used for calculations. For the filter and photographic film described by Fig. 3, the effective wavelength was $0.625\,\mu$ at measured temperatures on the order of $10000\,^\circ$K and at a standard brightness temperature $T_0 = 5500\,^\circ$K.

APPLICATION OF THE PHOTOGRAPHIC METHOD TO THE MEASUREMENT OF THE AIR TEMPERATURE IN A PLANE SHOCK WAVE

Three series of experiments were carried out, differing from one another by the velocity of the shock wave. The experimental setup is shown in Fig. 4. In one series of experiments a plane shock wave in air was created directly by the explosion products of a cylindrical charge of explosive 120 mm in diameter (Fig. 4a). In the other series (Fig. 4b) the shock wave velocity was decreased by placing an aluminum of organic-glass plate 2 mm thick in front of the charge. The axis of the charge was always situated parallel to the axis of rotation of the photochronograph mirror. A plane fixed mirror was placed in front of the charge at an angle of 45° with respect to its axis. With this arrangement the instrument records simultaneously the variations of wave front brightness and the velocity of propagation of the shock wave. A photochronogram of an experiment of this type is shown in Fig. 5. The sun

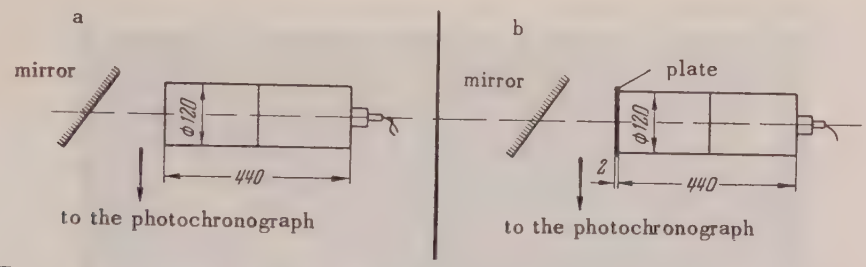

FIG. 4. Experimental setup for the simultaneous measurement of the temperature and propagation velocity of a shock wave in air. a—shock wave in air created directly by explosion products; b—shock wave created by a plate of organic glass or aluminum, accelerated by explosion products.

was photographed on the same apparatus using two different exposure times. The photographic conditions (diaphragm, slit width, sweep velocity) were selected such that the film density lay within the limits of the rectilinear part of the characteristic curve of the film. A fixed mirror whose reflection coefficient was practically equal to the reflection coefficient of the mirror in the actual experiment was used to aim the sun onto the entrance objective. By appropriate choice of the charge dimensions, the shock wave parameters were constant during the 10–12 microseconds following the instant at which the detonation wave left the end of the charge.

The film density in region 1 (Fig. 5) was used to determine the air temperature behind the shock wave front. The absorptivity of the shock wave front was calculated from the increase of the intensity of the luminosity using the method described below. The temperature in the shock wave was also determined from the film density of photographs taken in a direction perpendicular to the axis of the charge (region 2 in Fig. 5). In this case the absorptivity was taken to be unity in accordance with the measurements presented below.*

The results obtained from the photographs in the three series of experiments are presented in Tables 1, 2, and 3. Both values of temperature are given in the tables: T_p calculated from photometric data in region 1, and T_l calculated in region 2. The mean values of the temperatures from all three series of experiments are plotted graphically in Fig. 6. The solid points refer to measurements of T_p made in a direction parallel to the propagation of the shock wave front, and the circles refer to T_l measured laterally. Also shown on the figure is the temperature dependence of the shock wave velocity, calculated by Davies[6]. The dissociation of oxygen and nitrogen molecules and the formation of nitric oxide at high temperatures is taken into account in the calculations. Since at present the dissociation energy of nitrogen remains a subject of discussion, calculations were carried out for two probable values of the dissociation energy. The upper branch of the curve was calculated with an assumed dissociation energy D_{N_2}=9.76 ev, and the lower curve results from the value D_{N_2} = 7.38 ev. The experimental results are in satisfactory agreement with the theoretical calculations. One might suppose that the data obtained, might decide between the two

TABLE I. Air temperature in a plane shock wave. Experimental setup as in Fig 4a (V=8.5 km/sec).

V, km/sec.	T_p °K	T_l °K
7.93	11900	10640
8.12	12050	10870
8.22	9650	9120
8.10	10900	9800
8.18	11430	12050
8.24	9550	9750
8.13	10260	9850
8.03	10600	10320
8.03	10100	9800
7.93	11850	10300
7.95	10420	10200
7.91	11100	10640
7.92	12320	10300
8.10	10260	9650
Arithmetic mean 8.05	10900	10235

*Temperature measurements using the photometric data in region 1 are more reliable. With photography in a direction perpendicular to the propagation of the wave front, the radiation passes through a region of lateral discharge, which may lead to error in the determination of temperature.

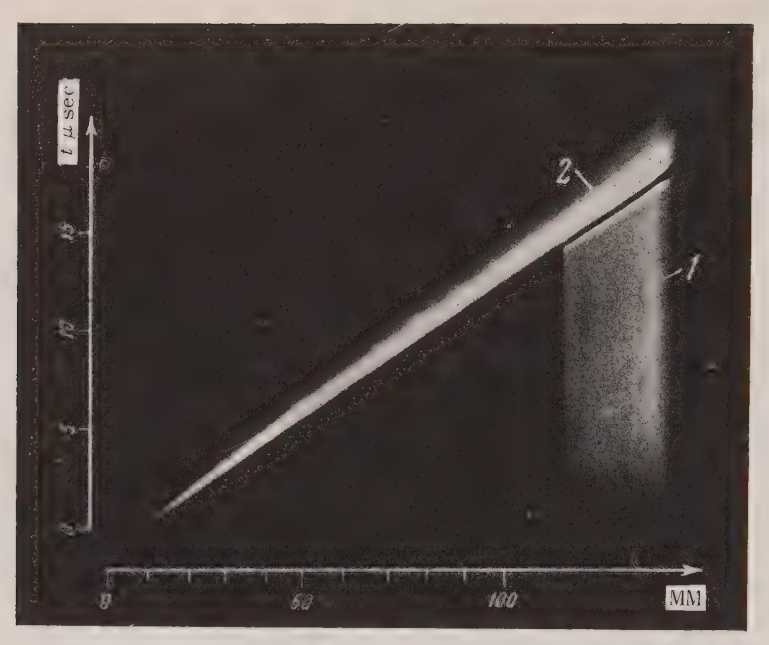

FIG. 5. Photochronogram of the experiment described in Fig. 4.

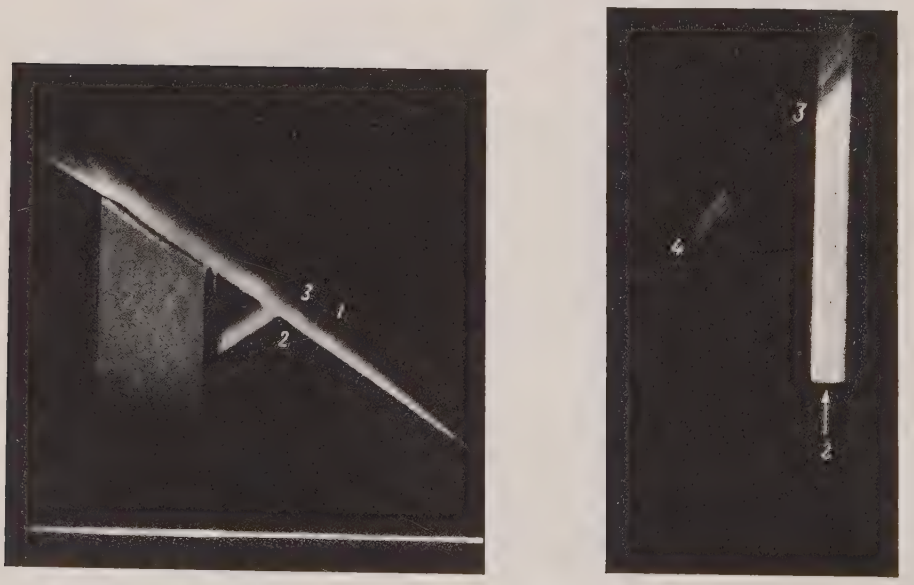

a *б*

FIG. 8. a—Photochronogram of the experiment described by Fig. 7a; b—photochronogram of the experiment described by Fig. 7b.

TABLE II. Air temperatures in a plane shock wave. Experimental setup as in Fig. 4b; plate material—organic glass (V=7.1 km/sec).

V, km/sec	T_p °K*	T_l °K
7.08	9500	8650
7.05	8780	8450
7.12	10100	9000
7.15	8700	8150
Arithmetic mean 7.1	9270	8560

*Values of the absorptivity of air for the calculation of T_p in this series of experiments was determined by interpolation between the absorption coefficients obtained for shock wave velocities of V=6.4 and 8.05 km/sec. A direct determination of the absorption coefficient by the increase of brightness of the shock wave front was not possible because the film density was too slight.

conflicting values of the dissociation energy of the nitrogen molecule. Unfortunately, the measuring accuracy achieved thus far and the insufficient number of experiments does not allow us at present to solve this problem uniquely.*

An analysis of the possible sources of error in the photographic method of measurement of high temperatures indicates that the accuracy of the method is ±6% at 7500 °K, ± 13% at 25000 °K, and ± 16% at 50000 °K. The experimental error depends to a considerable extent on the magnitude of the temperature being measured, the ratio of the measured temperature and the standard temperature, and also on the effective wavelength of the spectral interval being used. Temperature measurements in the short-wave part of the spectrum provide greater accuracy than in the red end. However, the use of the red region of the spectrum has substantial advantages (smaller absorption of radiation in the atmosphere and optical parts, and simplicity of the monochronizing arrangement). The experimental error may be reduced somewhat by a more accurate determination of the standard temperature and of the angular velocity of the mirror of the photochronograph, and by making more precise the effective wavelength and the characteristic curve of the photographic film. According to our estimates, it is possible to decrease the probable error in the temperature measurement by a factor of 1.5–2.

*After the completion of these experiments an article by Christian et al[7] appeared, in which measurements of the mass and wave velocities of shock waves in nitrogen were used to determine the dissociation energy of nitrogen. According to these experiments, the higher value of D_{N_2} = 9.76 ev is correct.

MEASUREMENT OF THE ABSORPTION COEFFICIENT AND THE ABSORPTIVITY

To determine the true temperature of a body according to Eq. (1), it is necessary to know its absorptivity a. In many cases the determination of the absorption coefficient of radiation by gases at high temperatures is also of considerable interest.

TABLE III. Air temperatures in a plane shock wave. Experimental setup as in Fig. 4b; plate material—aluminum (V= 6.4 km/sec).

V km/sec	T_p °K	T_i °K
6.22	7310	8530
6.46	7600	8300
6.51	8180	9670
6.51	7200	7500
6.32	7220	7850
6.40	7350	8480
Arithmetic mean 6.4	7480	8390

Experiments to determine the absorptivity were set up according to the scheme shown in Fig. 7. Here, the front of the plane shock wave created by the explosion of a cylindrical charge of explosive is

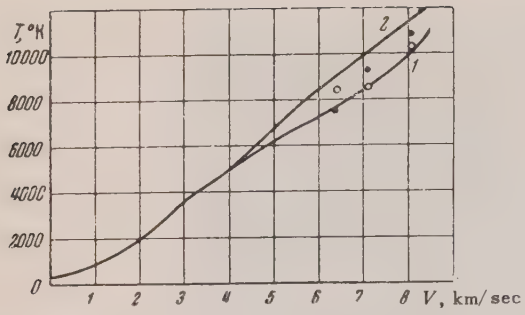

FIG. 6. Theoretical dependence of temperature on the propagation velocity of a plane shock wave in air, and experimentally measured temperatures. Solid circles represent measurements in the direction of propagation of the shock wave front (T_p); open circles represent lateral measurements (T_s). 1 – D_{N_2} = 7.38 ev; 2 – D_{N_2} = 9.76 ev.

illuminated by an auxiliary source of light in the direction of the arrow. In the first experiments (Fig. 7a) the auxiliary source of light was a shock wave in air from the same kind of charge, located behind the shock wave being studied. The principal and the illuminating charges were triggered simultaneously. On the photochronogram of this kind of experiment (Fig. 8a) the density of portions 1 and 2 corresponds to the brightness of a shock wave in air from the principal and auxiliary charges, and portion 3 corresponds to the brightness of the shock wave the auxiliary charge photographed through the shock wave being investigated.

If the absorptivity of the layer of gas under study differs from unity, an increase of brightness

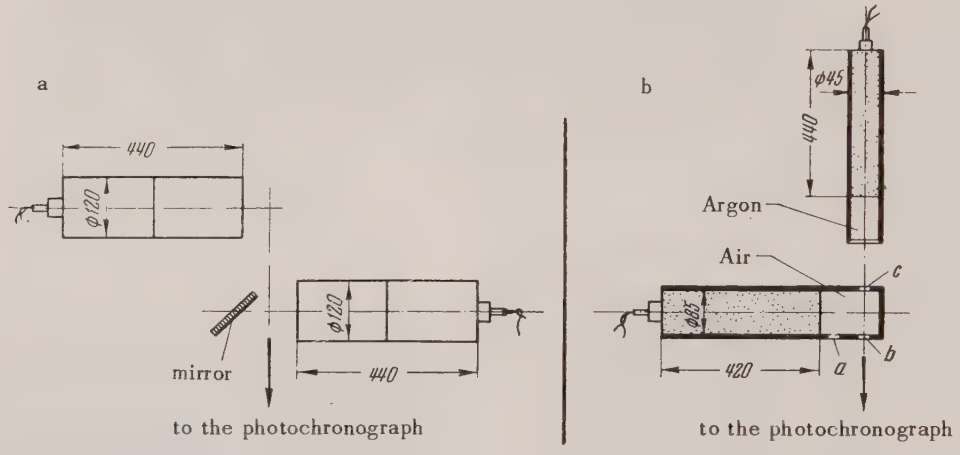

FIG. 7. Experimental setup for the measurement of the opacity of air in a plane shock wave.

would be observed in region 3. In these first experiments it was noted that the absorptivity of the air in a shock wave (V = 6.4 to 8 km/sec) was equal to unity within the limits of photometric error, with the direction of photography perpendicular to the direction of propagation of the wave front.

In order to obtain more precise results, additional experiments were performed in which the luminosity of a shock wave front in argon was used to "illuminate" the shock wave in air (Fig. 7b). A plane wave in air was created by a cylindrical charge of explosive enclosed in a duraluminum container in whose walls three apertures (a, b, c) were made. Apertures b and c are located at the bottom of the container, opposite one another. An additional charge was placed perpendicular to the axis of the principal charge. The additional charge was determinated by a container with a transparent organic glass bottom. This container was filled with argon at atmospheric pressure. The axis of the additional charge coincided with the centers of windows b and c. Both charges were triggered simultaneously. On the photochronogram of this kind of experiment (Fig. 8b) we see first the brighter luminosity of the shock wave front in argon (the sweep direction is indicated by arrow 2), then the luminosity of the shock wave in air through window a (region 4), and finally, the luminosity or argon observed through the shock wave in air (region 3). Since the brightness of the shock wave in argon is greater than the brightness of the wave in air, this variant of the method substantially increases its sensitivity. It is clear from the photographs presented that the layer of air under investigation, compressed by the shock wave, is not transparent. Photometric results which give the same value of film density in regions 3 and 4 confirm this conclusion.

The large value of the absorption coefficient in

the shock wave leads to complete opacity of the gas layer, even when it is very thin. Therefore, the determination of the absorption coefficient by the methods described is quite difficult. It is possible only when the width of the wave front is very small (a fraction of a centimeter). However, this requirement is not realizable in practice because of the extremely rapid discharge during the explosion of charges of small diameter.

The absorption coefficient and the absorptivity of gases under shock compression were determined by us using the following method, based on an examination of the variation of brightness of the shock wave front in the direction which it is propagating (Fig. 9). Let us assume that the parameters characterizing the shock wave (velocity, temperature, etc.) remain constant.* As the shock wave propagates, the thickness of the compressed gas layer continuously. The transmissivity of layer 1, "assembled" by the shock wave during the time t_1-t_0, is given by the relation $g_1=(b_{0,1}-b_1)/b_0$; similarly, for layer 2, $g_2=(b_{0,1,2}-b_2)/b_{0,1}$. Here, B_0 is the brightness of the wave front at the instant t_0, b_1 and b_2 are the brightnesses of layers 1 and 2 respectively, $b_{0,1}$ is the brightness of the wave front at the instant t_1, and $b_{0,1,2}$ is the brightness of the wave front at the instant t_2. If the intervals t_1-t_0 and t_2-t_1 are equal, then $b_1=b_2$, and

$$g_1=g_2=(b_{0,1,2}-b_{0,1})/(b_{0,1}-b_0)=g'. \qquad (2)$$

Thus, the transmissivity g' of a gas layer of thickness l', "assembled" by the shock wave during the time $\Delta t=(t_1-t_0)=(t_2-t_1)$, may be found from three successive measurements of the brightness of the wave front, if the interval between measurements is Δt. For a homogeneous layer of gas the transmissivity if $g'=e^{-\varkappa l'}$, from which the coefficient of absorption $\varkappa$ may be determined if the thickness of the absorbing layer l' is known.

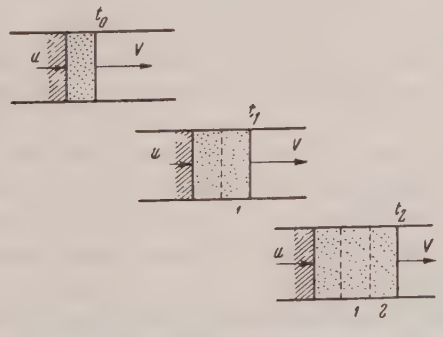

FIG. 9. Propagation of a plane shock wave in a gas.

For a layer of of arbitrary thickness l, the transmissivity $g=g'^{l/l'}=g'^{t/\Delta t}$ (since $l\sim t$). The last formula makes it possible for us to calculate the transmissivity of the gas layer "assembled" by the shock wave during the time t (considered from the instant the shock wave starts to propagate) and consequently, its absorptivity $a=1-g'^{l/l'}=1-g'^{t/\Delta t}$, which is necessary for the determination of the temperature using Eq. 1.

Measurements of the absorptivity and the absorption coefficient in a shock wave by the method suggested above are easily accomplished using the apparatus as used to determine gas temperatures, without any auxiliary sources of light. The method is applicable only to plane shock waves where conditions may be chosen such that the gas-dynamic parameters remain constant.

In Fig. 10, the solid curve shows the increase of intensity of the luminosity of the shock wave front ($V=8.05$ km/sec) observed in the direction in which it is propagating. This curve is the mean result of 13 experiments. Photometry was done at intervals of 0.5 mm of film in the sweep direction. This corresponds to a shock wave front movement of 2.8 mm ($\sim 0.35\,\mu$ sec).

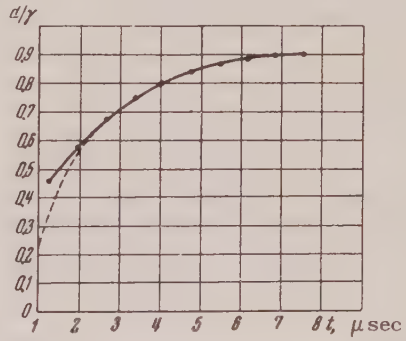

FIG. 10. Increase of the intensity of the luminosity of a plane shock wave front in air at $T=10900°$K; solid line—results of film photometry (mean of 13 experiments); dotted line—calculated curve corresponding to the value $\varkappa=8.7$ cm^{-1}.

The transmissivity of the layer "collected" by the shock wave during $\Delta t=1\,\mu$ sec is determined by Eq. 2:

$$g_{\Delta t}=e^{-\varkappa\Delta t}=\frac{(b_{t+\Delta t}/b_t)-1}{1-(b_{t-\Delta t}/b_t)},$$

*This condition may be guaranteed during the initial stages of propagation of the shock wave by suitable choice of the size of the explosive charge.

where the values of $b_{t+\Delta t}/b_t$ and $b_{t-\Delta t}/b_t$ are calculated from the corresponding density differences

$$\log(b_{t+\Delta t}/b_t) = (d_{t+\Delta t} - d_t)/\gamma,$$

$$\log(b_{t-\Delta t}/b_t) = (d_{t-\Delta t} - d_t)/\gamma.$$

To increase the accuracy, it is necessary to determine $g_{\Delta t}$ at various parts of the curve and to take the mean of these values. The initial portion, which is outside the limits of the region of proportional blackening, must be excluded from consideration.

The calculated variation of intensity based on values of the absorption coefficient obtained in this way is shown by the dotted line in Fig. 10 (the calculated curve was made to fit the experimental curve at one point). Except for the initial portion, the calculated and the experimental curves are in almost complete agreement. Using this method, we determined the absorption coefficient for radiation ($\lambda = 0.625\,\mu$) with shock wave velocities in air $V = 6.4$ km/sec ($T = 7480\,^\circ$K) and $V = 8.05$ km/sec ($T = 10900\,^\circ$K). The initial air pressure in both cases was one atmosphere. Values of the absorption coefficient $\varkappa/\text{cm}^{-1}$ obtained experimentally, and also calculated with the known Kramers formula, taking account of the formation of nitrogen oxides, are presented in Table 4. The shock wave compression ρ/ρ_0 was assumed to be 10. The deviation of our results

TABLE IV. Values of the absorption coefficient of air in a shock wave for $\lambda = 0.625\,\mu$.

V, km/sec	$T\,^\circ$K	$\varkappa\ \text{cm}^{-2}$	
		experimental*	theoretical
8.05	10900	$3.7_{(13)}$	0.6
6.4	7480	$1.66_{(6)}$	0.083

*The subscripts following the experimental values of the absorption coefficient indicate the number of experiments.

from the values calculated by Kramers' formula may by partially explained by the insufficient accuracy of the temperature determination,. Thus, if the absorption coefficient measured at $V = 6.4$ km/sec is referred to the temperature $T = 9200\,^\circ$K (this results from calculations based on $D_{N_2} = 9.76$ ev), the deviation is substantially decreased ($\varkappa_{\text{theor.}} = 0.55$ cm^{-1}). It should also be kept in mind that the application of Kramers' formula to non-hydrogenlike atoms or ions may lead to significant errors[8,9].

TEMPERATURE MEASUREMENTS IN HEAVY INERT GASES IN STRONG SHOCK WAVES

From a theoretical consideration of the processes involved in a shock compression, it follows that the highest temperatures may be obtained by propagating a shock wave in heavy monatomic gases[10]. Using the method described above, experiments were carried out to verify the calculated temperatures of inert gases in shock waves. Shock wave temperatures were measured in argon, krypton, and xenon. For the determination of temperature, the absorptivity of the shock wave front was assumed to be unity.*

The results of calculations of the temperature in a shock wave front as a function of its propagation velocity, taking account of energy loss in ionization and thermal radiation, are presented in Fig. 11. Also shown in the figure are experimentally measured temperatures in the shock wave front. Comparing the experimental points with the calculations, it is clear that all the measured values lie below those calculated. This discrepancy can not be explained by errors in the method used to measure temperature. The experimental error in the temperature interval under consideration did not exceed ±20%, while the experimental value of temperature is lower than the theoretical value by a factor of 3 in krypton and by a factor of 3.5 in xenon. It should be noted that the experimentally observed temperatures, the theoretical calculations nothwithstanding, decrease in the order argon–krypton–xenon.

The most probable explanation of this interesting fact was proposed by Zel'dovich[11]. It is based on the assumption that a layer of gas in contact with the shock wave front is opaque owing to heating by radiation emanating from the wave front. A considerable part of the radiated energy at high temperatures is absorbed in the atmosphere directly in front of the shock wave front. If it is assumed that under these conditions the absorption of radiation

*A sufficient basis for this assumption is the extremely sharp increase in the intensity of the luminosity during the initial period of propagation of the shock wave, attesting to a large value of the absorption coefficient.

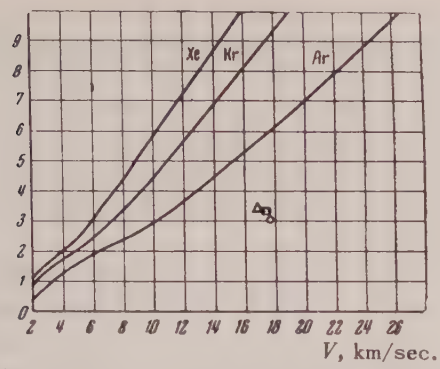

FIG. 11. Temperature of heavy inert gases in the front of a strong shock wave. Experimental values: O—argon, □—krypton, Δ—xenon.

may be explained on the basis of photoexcitation and photoionization of the gas, then at comparatively low temperatures behind the wave front (up to ~ 10000°K), when the heat flux is small and the principal part of the radiation is produced in the region of the visible spectrum, there is practically no absorption. At higher temperatures where the principal part of the total radiation is produced in the region of characteristic absorption of the gases, the absorption of radiation must lead to heating of the gas in front of the shock wave front.

The radiation energy produced in the region of wavelengths from $\lambda = 0$ to $\lambda = \lambda_1$, may be calculated by Planck's formula

$$S = \frac{\int_0^{\lambda_1} C_1 \lambda^{-5} (e^{C_2/\lambda T} - 1)^{-1} d\lambda}{\int_0^{\infty} C_1 \lambda^{-5} (e^{C_2/\lambda T} - 1)^{-1} d\lambda}.$$

The calculated fractions of the total black-body radiation energy, produced in the wavelength region between $\lambda = 0$ and $\lambda = 0.11\,\mu$ (corresponding approximately to the limit of opacity for argon, krypton, and xenon under normal conditions), are presented in Fig. 12.

Let us now estimate the heating of the gas in in front of the shock wave front by radiation emanating from the wave front. As an example we consider a stationary wave in xenon with $V = 17.5$ km/sec in a system of coordinates moving with the wave front. Gas flows into the wave with velocity V, and radiation E leaves the surface of the wave front (Fig. 13). The velocity $V = 17.5$ km/sec in xenon corresponds to a temperature behind the wave front $T = 106000$°K (see Fig. 11) and the flux of radiant energy is $E = \sigma T^4 = 7.15 \times 10^{15}$ erg/sec-cm^2. Hence, the energy absorbed by the gas in front of the

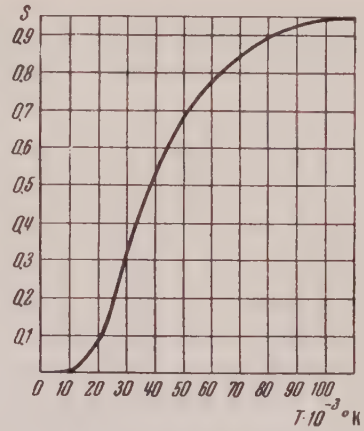

FIG. 12. Ratio of the energy radiated by a black body in the spectral interval $\lambda = 0$ to $\lambda = 0.11\,\mu$ to the total energy radiated, as a function of temperature.

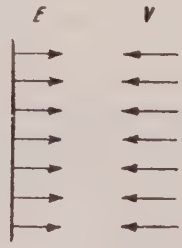

FIG. 13. Schematic for the calculation of the heating of the gas in front of the shock wave front by radiation emanating from the front.

shock wave front is, according to Fig. 12, $E' = ES = 6.72 \times 10^{15}$ erg/sec-cm^2. This energy is distributed among $N = nV = 4.72 \times 10^{25}$ atoms ($n = 2.7 \times 10^{19}$ is the number of atoms per cm^3 of gas at standard conditions). The energy per atom is

$$E'/N = 1.43 \times 10^{-10} \text{ erg}.$$

Let us assume that the mean value of the heat capacity during the rise of gas temperature is $C = \epsilon/T'$, where ϵ is the energy falling on one gas atom, calculated by taking account of ionization and by assuming that the heating occurs at constant volume up to the temperature $T' = E'/Nc$. By the method of successive approximations, we find for the temperature of the incoming flow, $T = 63000$°K. Such heating of the gas by radiation from the shock wave must lead to a rounding out of the temperature jump at the wave front. The temperature distribution in this case will be approximately as shown in Fig. 14. With the increase of the temperature of the gas in front of the shock wave front, the absorption coefficient increases and an optical thickness on the order of several units is realized under these conditions when the thickness of the layer is a

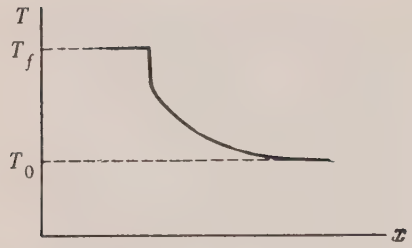

FIG. 14. Temperature distribution in the gas in front of the shock wave front.

fraction of a centimeter. Optical methods of temperature measurement are not applicable in this case because they give only the value of some effective temperature of the opaque gas layer that screens the shock wave front located behind it.

Similar effects of the "saturation" of the brightness temperature have been repeatedly observed by many investigators. In Glaser's experiments[12] on the measurement of the temperatures of condenser spark discharges in argon at high initial pressure, an increase of the specific power from 0.21×10^{15} to 0.42×10^{15} erg/sec-cm^3 led to a marked temperature rise from 20000 to 40000°K. However, a further increase in specific power to 1×10^{15} erg/sec-cm^3 did not increase the measured temperature. A similar "saturation" of the measured temperature was definitely established in experiments by Azarkh, Voinov, and the author on condenser spark discharges in argon with an initial pressure of 20 kg/cm^2. Here, a change of the energy of the discharge circuit from 0.75×10^9 to 1.5×10^9 ergs led to an increase of the measured temperature from 32000 to 37000°K. Increasing the energy of the circuit still further to 2.4×10^9 ergs left the maximum value of the temperature practically unchanged at 37000°K. Vul'fson, Libin, and Charnaia[13] also observed the existence of a limiting brightness during pulsed discharges in inert gases.

The above limitation on the possibilities of optical pyrometry depends on external conditions (density, pressure) as well as on the individual properties of the substance (excitation and ionization potentials), and the limits of applicability of optical methods must be established in each specific case, based on the concrete experimental conditions and accuracy requirements.

CONCLUSIONS

1. The photographic method of measurement of high temperatures in strong shock waves uses a comparison of the density of the photographic image of the shock wave front with the density of the image of a temperature standard, over a narrow interval of wavelengths. The method permits simultaneous measurement of temperature and shock wave velocity. Methods were developed to use the photochronograms for the determination of the coefficient of absorption of radiation in the front of a plane shock wave.

2. The temperatures measured in plane shock waves in air were 7480°K for a shock wave velocity of $V = 6.4$ km/sec, 9270°K for $V = 7.1$ km/sec, and 10900°K for $V = 8.05$ km/sec. The temperature measurements were accurate to within ±10%. The experimental results were in satisfactory agreement with theoretical calculations. The coefficient of absorption of radiation ($\lambda = 0.625\mu$) in the front of a plane shock wave in air was 1.66 cm^{-1} at $T = 7480$°K, and was 3.7 cm^{-1} at $T = 10900$°K.

3. The temperatures definitely established in the front of strong shock waves in heavy inert gases were several times lower than calculated. An analysis of the possible causes of the observed discrepancy indicated that at very high temperatures the heating of the gas located in front of the wave front by radiation from the shock wave strongly influences the measurement results. The gas layer heated by the radiation becomes opaque and screens the "hotter" front of the shock wave. The tempeture of this layer is always lower than the true temperature of the wave front.

In conclusion, the author expresses profound thanks to his principal coworkers Z. M. Azarkh and F. O. Kuznetsov who carried out a large number of laborious experiments and reduced the experimental results. The author also thanks the sponsors of the work, Prof. V. A. Tsukerman, Prof. Ia. B. Zel'dovich, and Prof. D. A. Frank-Kamenetskii, for valuable advice and constant help during the investigation

[1] Alentsev, Beliaev, Sobolev and Stepanov, J. Exptl. Theoret. Phys (U.S.S.R.) 16, 990 (1946).

[2] Riabinin, Sobolev, Markevich and Tamm, J. Exptl. Theoret. Phys. (U.S.S.R.) 23, 564 (1952).

[3] N. N. Sobolev and T. N. Shchetinin, J. Exptl. Theoret. Phys. (U.S.S.R.) 20, 356 (1950).

[4] D. W. Male, Rev. Sci. Instr. 22, 769 (1951).

[5] A. L. Kartuzhanskii and P. V. Meikliar, J. Exptl. Theoret. Phys. (U.S.S.R.) 21, 532 (1951).

[6] D. R. Davies, Proc. Phys. Soc. 61, 105 (1948).

[7] Christian, Duff and Varger, J. Chem. Phys. 23, 2045 (1955).

[8] L. Page, M. N. Roy. Astron. Soc. 99, 385 (1939).
[9] A. Unzol'd, *Physics of Stellar Atmospheres*, IIL, 1948.
[10] Ia. B. Zel'dovich and O. I. Leipunskii, J. Exptl. Theoret. Phys. (U.S.S.R.) 13, 183 (1943).
[11] Ia. B. Zel'dovich, J. Exptl. Theoret. Phys. (U.S.S.R.) 32, 1028 (1957). [sic!]
[12] G. Glaser, ZS. Naturforsch. 6a, 706 (1951).
[13] Vul'fson, Libin and Charnaia, Izv. Akad. Nauk SSSR, Ser. Fiz. 19, 61 (1955).

Translated by D. Lieberman
168

SOVIET PHYSICS JETP VOLUME 5, NUMBER 4 NOVEMBER, 1957

Paramagnetic Absorption at High Frequencies in Gadolinium Salts in Parallel Fields

A. I. KURUSHIN
Molotov State University

(Submitted to JETP editor November 20, 1956)
J. Exptl. Theoret. Phys. (U.S.S.R.) 32, 727 (1957)

Measurements were carried out at room temperature on the dependence of paramagnetic absorption on the intensity of a stationary field parallel to a high frequency ($\nu = 9.377 \times 10^9$ cps) field. The experimental absorption curves are in good agreement with Shaposhnikov's spin absorption theory[1]. This made it possible to determine the internal field constant and the isothermal spin relaxation time for several gadolinium salts, and to determine in absolute units the absorption coefficient of $Gd_2(SO_4)_3.8H_2O$ as a function of the intensity of the stationary field.

PARAMAGNETIC ABSORPTION has been experimentally studied in a number of salts by Gorter and his coworkers[2], Garif'ianov[3], and Sitnikov[4], over the frequency range of 10^6-10^8 cps with the high frequency field parallel to the stationary field. Garif'ianov and Sitnikov made their measurements at room temperature at frequencies of the order of 6×10^8 cps (using electronic circuitry) and with fields from 0 to 6000 oersteds. Their experiments indicated that the experimentally determined absorption as a function of the strength of the stationary field, with fixed frequency of the variable field, is in good agreement with the values obtained from Shaposhnikov's theoretical formula[1] for spin absorption if the isothermal spin relaxation time τ_s, entering into this formula, is considered to be independent of the strength of the stationary field. This made it possible for the authors of Refs. 3 and 4 to use Shaposhnikov's formula for the experimental determination of the internal field constant b/C (b is the magnetic heat capacity constant and C is the Curie constant).

The above-mentioned experiments (Refs. 2-4) were conducted at frequencies considerably lower than the reciprocal of the isothermal spin relaxation time (τ_s^{-1}). For a more complete study of spin absorption at room temperature, the author[5] performed similar experiments at frequencies for which $\tau_s \nu \geqslant 1$. This was accomplished by using centimeter wave techniques. High-frequency power from the generator was sent through a coaxial waveguide into a cylindrical resonator in which an H_{011} wave was excited. From the resonator the power went to an indicator with a germanium detector and a mirror galvanometer. It is well known that the magnetic field of an H_{011} wave is axially symmetrical, and that near the center of the resonator the lines of force are directed along the axis of the cylinder in the form of a cable. The field near the center of the resonator is therefore quite uniform. Our experimental setup differs from others known to us in that we are able to perform absorption measurements in arbitrary units for any angle between the stationary and the high-frequency fields, made possible by a rotating flange in the coaxial guide joining the resonator and the generator. A more detailed description is given in Ref. 5. The powdery paramagnetic substance was thoroughly dried and then

hermetically sealed in a polystyrene flask. The flask was fastened to the bottom of the resonator by a polystyrene rod in such a way that the paramagnetic substance was near the center of the resonator.

It was shown by Cummerow *et al.*[7] that it is possible to determine experimentally the dependence on H of a quantity d, proportional to the imaginary part of the magnetic susceptibility χ''

$$d(H) \equiv a\chi''(H) = \sqrt{\alpha_e/\alpha_m} - 1, \qquad (1)$$

where α_e and α_m are the respective galvanometer readings in the absence and in the presence of magnetic absorption in the sample, and a is a constant which depends on the construction and tuning of the apparatus.

It was established earlier by the author[5] that at frequencies for which $\tau_s\nu \gtrsim 1$, paramagnetic absorption decreases monotonically as the strength of the stationary field is increased, and the form of the experimental curve is described well by Shaposhnikov's theoretical formula[1],

$$\chi''/\chi_0 = (1 - F)^2\tau_s\nu/[1 + (1 - F)^2\tau_s^2\nu^2], \qquad (2)$$

where $F = H^2/(H^2 + b/C)$ and χ_0 is the static magnetic susceptibility of the sample if it is assumed that τ_s is independent of H. Eq. 2 makes it possible to determine the quantities b/C, τ_s and the constant a experimentally, *i.e.*, allows us to determine the relation $\chi'' = \chi''(H)$ in absolute units. This is accomplished by taking any three values of the quantity $d(H)$ at three values of the field, and using Eq. 2 to solve the system of three equations in the unknowns b/C, τ_s and a (assuming that τ_s is independent of H). If, for example, we take the value $d_1(H_1) = d_1$ at $H_1 = 0$, $d_2(H_2) = d_1/2$ (H_2 is the half-width of the curve) and $d_3(H_3) = d_1/3$, we obtain (see Ref. 5):

$$b/C = {}^1/_2\,(H_3^4 - 2H_2^4)/(2H_2^2 - H_3^2). \qquad (3)$$

$$\tau_s = \sqrt{H_2^4 + 2\,(b/C)\,H_2^2 - (b/C)^2}\,/(b/C)\nu, \qquad (4)$$

$$a = (1 + \tau_s^2\nu^2)\,d_1/\chi_0\tau_s, \qquad (5)$$

so that

$$\chi''(H) = \chi_0\tau_s\nu d(H)/(1 + \tau_s^2\nu^2)\,d_1. \qquad (6)$$

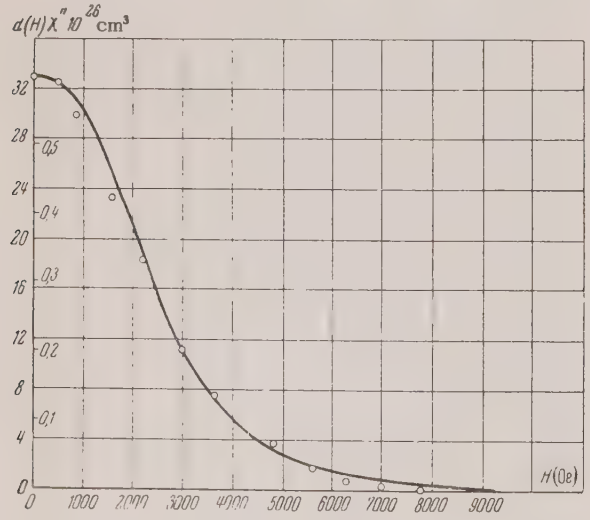

$Cd_2(SO_4)_3\,8H_2O$: O—experimental points for $T = 291°K$ and $\nu = 9.15 \times 10^9$ cps. Solid line—theoretical curve from Eq. 2, for $b/C = 3.4 \times 10^6$ (oer.)^2 and $\tau_s = 0.25 \times 10^{-9}$ sec.

It must be borne in mind that for a sufficiently accurate determination of the values of b/C and τ_s we require very accurate knowledge of the values of H_2 and H_3 (differences of high powers of H occur in Eq. 3). With the usual calibration of the field to within 20-25 oersteds at field strengths in the range of 1000-2000 oersteds (as in our experiments), the values of b/C and τ_s obtained from Eqs. 3 and 4 have a comparatively large error (of the order of 30-40%).

In the present work, the absorption in parallel fields was determined experimentally in arbitrary units for hydrated halide salts of gadolinium at room temperature at the frequency $\nu = 9.377 \times 10^9$ cps. All of the absorption curves for these salts are similar in form to the curve for gadolinium sulphate shown in the figure for the frequency $\nu = 9.15 \times 10^9$ cps (this curve was obtained by us earlier[5]), the only differences being the magnitude of the initial absorption (at $H = 0$) and the width of the curves. The constants b/C and τ_s for these salts were determined by the method described above, and are given in the table. Our values of b/C and τ_s for $Gd_2(SO_4)_3 \cdot 8H_2O$ agree with those of other authors within the limits of experimental error (see Ref. 2). We found no data on b/C and τ_s for the other salts in the literature.

Using Eq. 6, we transformed our experimental curves to absolute units. The specific static susceptibility of $Gd_2(SO_4)_3 \cdot 8H_2O$ at room temperature is $\chi_0 = 73.4 \times 10^{-6}$.[6] Values of b/C and τ_s (see table) were found from the experimental curve using Eqs. 3 and 4. Substituting the values of b/C, τ_s, and χ_0 into Eq. 6, and dividing the left and

Substance	Frequency $\nu = 10^{-9}$	$b/C \times 10^{6}$ (Oer.)$^{-2}$	$\tau_s \times 10^{9}$ sec
$Gd_2(SO_4)_3 \cdot 8H_2O$	9.15	3.4	0.25
GdF_3	9.377	6.0	0.16
$GdCl_3 \cdot 6H_2O$	9.377	3.1	0.13
$GdBr_3 \cdot 6H_2O$	9.377	5.2	0.17
$GdI_3 \cdot 6H_2O$	9.377	1.0	0.9

right hand sides by the number of ions per cubic centimeter, we obtain per ion:

$$\chi''(H) = 0{,}6 \cdot 10^{-26} \frac{d(H)}{d_1} \text{ cm}^3;$$

where $H = 0$, $d(0) = d_1$ и $\chi''(0) = 0{,}6 \cdot 10^{-26}$ cm^3. (7)

Values of $\chi''(H)$ in absolute units, calculated from Eq. 7, are plotted along the right side of the ordinate in the figure. Having determined the experimental setup constant a by experiments in parallel fields using the method described above, we may then use this constant for the construction of absorption curves in absolute units for any angle between the high frequency and the stationary fields.

We also performed measurements of paramagnetic absorption at room temperature with perpendicular fields (paramagnetic resonance), using the substances indicated in the table. With stationary fields up to 8000 oersteds, all of these substances exhibited a single resonance absorption peak with a g-factor in the neighborhood of 2. A particularly strong paramagnetic resonance effect was observed in $GdI_3 \cdot 6H_2O$.

In conclusion, the author expresses thanks to I. G. Shaposhnikov for suggesting the subject and maintaining interest in the work.

[1] I. G. Shaposhnikov, J. Exptl. Theoret. Phys.(U.S.S.R.) 18, 533 (1948).
[2] K. Gorter, "Paramagnetic Relaxation", IIL, 1949.
[3] N. S. Garif'ianov, J. Exptl. Theoret. Phys.(U.S.S.R.) 25, 359 (1953).
[4] K. P. Sitnikov, Dissertation, Kazan University, 1954.
[5] A. I. Kurushin, Izv. Akad. Nauk SSSR, Ser. Fiz. 20, 1232 (1956).
[6] Ia. G. Dorfman and S. E. Frish, "Collection of Physical Constants," ONTI, 1937.
[7] Cummerow, Halliday and Moor, Phys. Rev. 72, 1233 (1947).

Translated by D. Lieberman
169

SOVIET PHYSICS JETP VOLUME 5, NUMBER 4 NOVEMBER, 1957

A Source of Polarized Nuclei for Accelerators

E. K. ZAVOISKII

(Submitted to JETP editor December 14, 1956)
J. Exptl. Theoret. Phys. (U.S.S.R.) 32, 731-735 (April, 1957)

A possible method of obtaining beams of polarized nuclei by making use of the Lamb shift of the metastable level is described.

THE SPIN DEPENDENCE of nuclear forces over a broad range of energies has in the recent past been studied intensively in experiments on the scattering of nucleons by nuclei. It is well known that such experiments require double scattering of the nucleons because contemporary accelerators produce unpolarized beams.

It can be shown by a relatively easy calculation that all types of accelerators (electrostatic accelerators, linear accelerators, cyclotrons, proton synchrotrons and cosmotrons) are able to accelerate polarized particle beams without depolarizing them. An accelerator which can produce polarized particles whose spins form any given angle with the beam direction would enable us to perform many polarization experiments without double scattering.

Certain proposed sources of polarized protons for accelerators[1] make use of atomic hydrogen beams that traverse a strongly inhomogeneous magnetic field after which the polarized atoms are ionized outside of the magnetic field by collisions with electrons. The calculated intensities of such sources do not exceed 1 μa of proton current. Since in the majority of accelerators large particle losses

occur during acceleration (accelerator currents comprise 10^{-3} to 10^{-6} of the ion source current) the resulting currents will be extremely small except in the case of electrostatic accelerators, where particle losses are insignificant. Such sources also require a very high vacuum (10^{-6}-10^{-8} mm Hg) in the ionization region of the atomic beam and are not adapted to pulsed operation.

We shall show that it is possible to construct sources of polarized protons and some other nuclei by making use of the Lamb shift of the $2S_{1/2}$ and $2P_{1/2}$ levels and the metastability of the first of these levels.

It must be mentioned first of all that the Lamb experiment with a beam of atomic hydrogen can produce polarized proton beams if the hydrogen atoms with polarized electron spins in the metastable state are removed adiabatically from the magnetic field and ionized by either light or electrons. This is apparent from the fact that when the polarized atomic beam leaves the magnetic field it consists of 50% pure and 50% mixed states, and after ionization of the metastable atoms outside of the magnetic field a 50% polarized proton beam is obtained. It is thus possible to obtain 100% polarized protons if a rf field is used to keep only the atoms of the pure states in the beam and to ionize these. This method does not require a high vacuum in the region where the metastable atoms are ionized.

Let us consider a more efficient method of polarizing protons. An electron beam passes through a space filled with atomic hydrogen in a homogeneous magnetic field $H = 540$ oersteds subject to the conditions that: 1) the population of the $2S_{1/2}$ levels is considerably greater than that of the P states, and 2) the ionization is due principally to the $2S_{1/2}$ atoms. A resonance field in the gas can result in practically pure $2S_{1/2}$ states thus leading to almost 100% polarization of the protons.

The polarized protons can be extracted from the space by the usual method and directed into the accelerator. It is known that a magnetic field of 540 oersteds mixes one of the $2S_{1/2}$ sublevels with a $2P_{1/2}$ sublevel, as a result of which all the remaining atoms in the metastable state are polarized with respect to their electron spins.

Moreover, at the resonant frequency one of the remaining mixed metastable states makes a transition to the corresponding $2P_{1/2}$ sublevel and then to the $1S_{1/2}$ ground state during the P-state lifetime τ_p. In this way atoms are polarized in a $2S_{1/2}$ state. The polarized $2S_{1/2}$ atoms can be ionized either by light in the range $3700\ \text{Å} \geqslant \lambda \geqslant 1216\ \text{Å}$ or by by electrons in the energy range $13.4\ \text{ev} \geqslant V \geqslant 3.4\ \text{ev}$. We shall denote by n_H the number of hydrogen atoms per cm^3, p the hydrogen pressure, σ_s and σ_p the cross sections for electronic excitation of hydrogen atoms to $2S_{1/2}$ and $2P_{1/2,3/2}$ states respectively, τ_p the $2P_{1/2}$ lifetime, $\tau_s = \xi\tau_p$ the lifetime of the metastable $2S_{1/2}$ state under the given conditions, n_s^* and n_p^* the equilibrium concentrations of hydrogen atoms in $2S_{1/2}$ and $2P_{1/2}$ states, and n_s and n_p the number of atoms per second which enter $2S_{1/2}$ and $2P_{1/2}$ states per unit volume. We thus have

$$n_s^* = {}^1/_4 n_s \xi \tau_p, \quad n_p^* = n_p \eta_l \tau_p, \tag{1}$$

where η is the number of acts of emission and resonance absorption during the transitions of hydrogen atoms from the P to the $1S_{1/2}$ ground state and *vice versa*. η depends on the gas pressure and size and shape of the gas-containing vessel. The factor $^1/_4$ in the first equation of (1) takes into account the fact that the field H and the resonant rf field remove $^3/_4$ of all the metastable atoms from that state.

We obtain from (1)

$$n_s^* / n_p^* = 0{,}25\xi\sigma_s (1 - k)/\eta_l \sigma_p, \tag{2}$$

where k is the fraction of metastable atoms in the pure state eliminated by the rf field. In first approximation we can set $k = 0$. The order of magnitude will be obtained in Eq. (3).

To obtain an estimate of σ_s and σ_p we can use Bethe's calculations in the Born approximation and neglect exchange effects. These calculations give $\sigma_s/\sigma_p \approx 0.1$ and $\sigma_s \approx 10^{-17}$ cm^2 when the energy of the electrons is near the threshold*. The exchange effects can evidently only increase σ_s.

The magnitude of ξ depends essentially on the electric field intensity E in the gas, the velocity of metastable atoms in the magnetic field H, the ion concentration, and the gas density. The dependence of ξ on E is given by the Lamb-Retherford formula.

$$\xi = \hbar^2 (\omega^2 + {}^1/_4 \tau_p^2) V^{-2}, \tag{3}$$

where V is the matrix element of the energy of the perturbing field and $\hbar\omega$ is the splitting of interacting levels. The hyperfine splitting has little effect

* The cross section for $3P$ excitation is one order smaller than σ_s.

on ξ. The dependence of ξ on the velocity v of the atoms in the field H is also given by (3) since the moving atom is acted on by the electric field $\mathbf{E} = \mathbf{v} \times \mathbf{H}/c$.

The dependence of ξ on the ionic concentration is given by (3) if we use for the electric field the familiar expression $E = en_+^{2/3}$, where e is the electron charge and n_+ is the concentration of ions (or electrons) in the gas.

The relation between ξ and the gas pressure p can be represented by

$$\xi = L/\tau_p v, \tag{4}$$

where L is the mean free path of a metastable atom. Eq. (4) is valid only when the linear dimensions of the gas vessel are greater than L.

In (2) η can be estimated in accordance with Holstein's paper[2] from which it follows that η depends on the pressure, the linear dimensions of the hydrogen vessel, and the mean free path of photons at Lyman frequencies. Thus for a cylindrical tube of radius R

$$\eta = (1/1{,}6)\, k_0 R \sqrt{\pi \ln k_0 R}, \tag{5}$$

and for a layer of gas between parallel walls separated by the distance l

$$\eta = (1/1{,}875)\, k_0 l \sqrt{\pi \ln k_0 l}, \tag{6}$$

where $\kappa_0 = an_H/\sqrt{T}$, a is a constant and T is the temperature.

We shall now consider the density W of rf energy required to polarize the metastable hydrogen atoms. The probability $1/\tau_\omega$ of a transition resulting from the absorption of a quantum of frequency ω_0 is, of course,

$$\frac{1}{\tau_\omega} = \frac{2\pi e^2 W}{c\hbar^2} \frac{|(|e, r|)|^2}{(\omega - \omega_0)^2 + (1/2\,\tau_p)^2}, \tag{7}$$

where the required density W must be determined from the condition $\omega = \omega_0$ and

$$\tau_\omega / \xi\tau_p < 1 \tag{8}$$

in order that the hydrogen shall consist mainly of pure metastable atoms.

The value of W determined from (7) and (8) will correspond to the fraction φ of metastable atoms affected by the rf field:

$$\varphi = 1 - \exp(-\xi\tau_p/\tau_\omega). \tag{9}$$

We shall now determine the part played by depolarization of protons as a result of the interaction of the magnetic moments of metastable atoms and protons with hydrogen atoms. In order to estimate the relaxation time t we use the calculations of Gurevich[3], which can give only the order of magnitude for hydrogen:

$$t \approx \hbar^2 a_0 v / 15S(S+1)\mu^4 n_H \tag{10}$$

where a_0 is the atomic radius, μ is the Bohr magneton and S is the atomic spin.

The value of t obtained for the relaxation time of proton magnetic moments must be considerably larger than given by (10) for electron spins, and proton depolarization will be brought about largely by charge transfer to neutral atoms.

A numerical estimate of t according to (10) for electrons shows that depolarization due to magnetic interaction is negligible even at relatively high gas pressures*.

Let us now consider the part played by charge exchange in the depolarization of protons extracted from the gas. We denote by l the linear dimensions of the gas volume from which polarized protons are pumped. Denoting the charge-exchange cross section of the protons by σ_0, they will undergo charge exchange $0.5 ln_H\sigma_0$ times in their path, so that when $0.5\, ln_H\sigma_0 \ll 1$ the depolarization of a proton beam is given by

$$\Delta = {}^1/_4\, ln_H\, \sigma_0, \tag{11}$$

since after the charge exchange the proton spin can with equal probability be parallel or antiparallel to the field H. A similar estimate can be made of the order of magnitude of proton depolarization in the gas through charge exchange with the hydrogen atoms. Denoting the mean proton lifetime in the volume of gas by t_0 we obtain the number $\bar{n}$ of proton charge exchanges:

$$\bar{n} = \sigma_c n_H\, v t_0. \tag{12}$$

The lifetime t_0 evidently depends on the electric field strength in the gas, the spacing of the elec-

* Van Vleck's formula also gives a large value for the relaxation time t.

trodes, and the dimensions of the hydrogen-containing vessel.

Let us consider the ionization of metastable atoms by light of wavelengths 3700 Å $\geqq \lambda \geqq$ 1216 Å, We assume that the gas container is illuminated and the photon flux density is N_{ph} so that the number n^+ of protons formed per second per cm^3, with $n^+ \ll n_s$, will be

$$n^+ = 0{,}25\, n_s^* \int_{\lambda_1}^{\lambda_2} \sigma_{ph}(\lambda) dN_{ph}, \qquad (13)$$

where $\sigma_{ph}(\lambda)$ is the photoionization cross section of a metastable hydrogen atom, $\lambda_1 = 3700$ Å. $\lambda_2 = 1216$ Å. and dN_{ph} is the photon flux density in the wavelength interval $d\lambda$. A similar calculation is made of electronic ionization of metastable atoms for a given electron velocity distribution.

The preceding calculations enable us to choose the optimum conditions for the intensity and polarization of a proton source. Thus, for given geometry, Eqs. (2), (4), and (5) or (6) determine the hydrogen pressure, after which all other parameters of the source are easily obtained. These equations show that the source intensity is limited principally by the diffusion of resonant emission in the hydrogen, which results in a large increase of the P level population.

There are several experimental methods of reducing the effect of resonant Lyman radiation diffusion. For example, the region of the gas where intense excitation of $2S_{1/2}$ and $2P$ levels occurs (in a gas discharge, part of a Wood tube etc.) can be separated from the ionization region of $2S_{1/2}$ atoms by apertured plates which easily pass metastable atoms and greatly reduce the resonant radiation through absorption in the walls of the apertures [Eq. (6)]. The mean free path of the metastable atoms must exceed the thickness of the plate. Atoms in P states cannot pass through the plates because of their very short lifetime. This arrangement produces in the space behind the plate a large concentration of atoms in metastable states with a small admixture of atoms in P states.

The strong diffusion of Lyman radiation can also be employed to polarize protons. Two procedures are possible: 1) An increased concentration of pure $2S_{1/2}$ states as a result of rf-induced or spontaneous transitions from $2P$ states and the ionization of atoms in metastable states, and 2) the use of the low population of $2S_{1/2}$ compared with $2P_{1/2}$ levels, which apparently should occur at relatively large hydrogen pressures when $\eta \gg 1$ and $\xi \ll \eta$. In the latter case P states can be excited by electrons with less than 13.4 ev of energy, but the applied magnetic field must be such that one of the hyperfine sublevels of the $2P_{1/2}$ state will overlap or be close to a $2S_{1/2}$ hyperfine sublevel in order that the population of pure $2P_{1/2}$ states shall greatly exceed that of the mixed states. If under these conditions the hydrogen atoms are ionized only out of P states by Lyman radiation (which is of great density because $(\eta \gg 1)$ or by electrons, the protons will be polarized. The degree of polarization depends on the relative populations of the $2P_{1/2}$ and $2P_{3/2}$ levels and for equal concentrations cannot exceed 9%. The use of radio frequencies which reduce the population of mixed P states through transitions to $2S_{1/2}$ can greatly increase the degree of polarization.

We note in conclusion that protons issuing from the source will move parallel to the axis of quantization (the magnetic field H); but auxiliary magnetic or electric fields can produce any desired angle.

---

[1] Ad'iasevich, Beliaev and Polunin, Abstracts of Reports at the Moscow Conference on the Physics of High-Energy Particles, 1956; R. L. Garwin, Bull. Am. Phys. Soc. Series II, 1, 61 (1956).

[2] T. Holstein, Phys. Rev. **83**, 1159 (1951); **72**, 1212 (1947).

[3] L. Gurevich, J. Exptl. Theoret. Phys. (U.S.S.R.) **6**, 544 (1936).

Translated by I. Emin
170

Mesonic Decay of a Tritium Hyperfragment

A. O. VAISENBERG AND V. A. SMIRNITSKII

(Submitted to JETP editor December 14, 1956)
J. Exptl. Theoret. Phys. (U.S.S.R.) 32, 736-737 (April, 1957)

An analysis is made of the mesonic decay of a hyperfragment according to the scheme ${}^{3}_{\Lambda^0}H^* \rightarrow p + p + n + \pi^- + Q$, where $Q = 35.9 + 0.7$ Mev.

IN THE SYSTEMATIC scanning of a stack of 30 Ilford G 5 pellicles provided by Professor Powell, which had been exposed in Italy at 25 km for 8 hours during the autumn of 1955, we observed the mesonic decay of a tritium hyperfragment with the π^--meson coming to rest in the emulsion. Since there are few known decays of this type which permit a relatively exact measurement of the Λ^0 particle binding energy[1-4] we wish to add this case to the available data.

A slow singly-charged particle *hf* is ejected from the primary $10 + 0_n$ star (see the projection drawing), is stopped in the same pellicle, and produces a secondary three-prong star. The range of *hf* is 360 μ, its mass is greater than a proton mass as estimated either from the gap count and range or from the scattering and range (the second difference $\bar{D}$, as measured on the basis of $\bar{D} = 0.5\,\mu$, is $0.23 \pm 0.10\,\mu$). A single charge is found for *hf* from the gap count, range, and grain density.

The two short-range particles of the secondary star (tracks 1 and 2) have identical ranges $12 \pm 0.6\,\mu$. The charge which results from comparison of the grain densities of tracks 1 and 2 with the grain densities of α particle tracks from Be^8 and ThC′ decay gives $z = 1$. Track 3 belongs to a π^--meson with 15,700 μ range. This π^--meson passed through 8 pellicles and produced a one-prong σ star at the end of its range. The details of the measurements are given in the tables.

The combined momentum of particles 1, 2 and 3 is 91.2 ± 1.2 Mev/c. If it is assumed that an equal and opposite momentum was borne off by a neutron we obtain the following decay scheme:

$$^3H^* \rightarrow p + p + n + \pi^- + Q,$$

where $Q = 35.9 \pm 0.7$ Mev. Hence we obtain for the Λ^0 binding energy in tritium

$$B_{\Lambda^0} = -1.2 \pm 1.2 \text{ Mev.}$$

The most accurate values of B_{Λ^0} for similar ${}^3H^* \rightarrow p + p + n + \pi^-$ decays are 1.4 ± 0.6[1]; 0.4 ± 0.7[2]; 5.4 ± 1[3] and -3.0 ± 0.8[4] Mev.

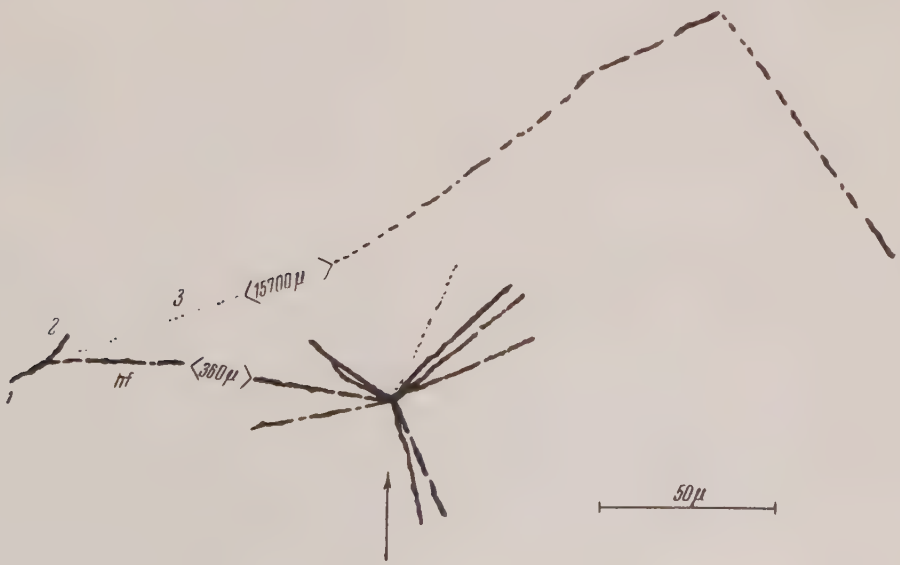

TABLE I. Hyperfragment track

Primary star	Associated phenomena	Range, μ	Dip angle in undeveloped emulsion	Proof of stopping	Z_F	Mass measurement	Energy per nucleon in Mev
$10 + 0_n$	Unobserved	360 ± 5	10°40′	1) Scattering	1	$> M_p$ (α, R)	≈ 4.2 (if H^3)
				2) Grain density	—	$> M_p$ (g, R)	

TABLE II. Secondary star

Track	Range, μ	Total experimental error	Straggling in %	Dip angle θ	Error $\Delta\theta$	Polar angle φ	Error $\Delta\varphi$	Type of particle	Measured mass	Energy in Mev
1	12	$\pm$ 0.6	~ 2.5	−15°20′	±30′	214°30′	± 1°	p	—	0.9
2	12	$\pm$ 0.6	~ 2.5	+27°	±40′	55°	± 1°	p	—	0.9
3	15700	$\pm$ 500	~ 2.4	+17°40′	±6′	18°40′	±10′	π^-	230^{+90}_{-50} in 1 mm of track	29.8 ± 0.6

The decay scheme $^4H^* \to p + d + n + \pi^-$ cannot be entirely excluded. In this case the large negative values -4.7 ± 1.2 and -4.4 ± 1.2 Mev are obtained for B_{Λ^0} depending upon whether track 1 or 2 is the deuteron. The decay $^4H^* \to p + p + n + n + \pi^-$ into 5 particles also cannot be excluded but possesses small probability.

In our reduction of the data we used values of constants taken from Shapiro's survey article[5].

[1] Haskin, Bouwen, Glasser and Schein, Phys. Rev. **102**, 244 (1956).

[2] Fry, Schneps and Swami, Phys. Rev. **101**, 1526 (1956)

[3] H. Yagoda, Phys. Rev. **98**, 153 (1955).

[4] Anderson, Lawler and Negin, Nuovo Cimento **7**, 605 (1955).

[5] A. M. Shapiro, Revs. Modern Phys. **28**, 2 (1956).

Translated by I. Emin
171

On the Fluctuation Resolution Limit of An Optical Modulation Interferometer

S. M. KOZEL
The Moscow Institute of Physics and Technology
(Received by JETP editor December 15, 1956)
J. Exptl. Theoret. Phys. (U.S.S.R.) 32, 738-749 (April 1957)

A theoretical model of a modulation optical interferometer designed to measure the angular dimensions of a source is considered. Expressions have been obtained for the fluctuation limits of sensitivity and precision. Experiments are described which indicate that the theoretical sensitivity and precision limits can be obtained in practice. The influence of atmospheric perturbations in a stellar modulation interferometer is estimated.

1. STATEMENT OF THE PROBLEM

WE DESIGNATE as an optical mudulation interferometer an interferometer arrangement where: (a) one or more of the parameters of the system (for example, the position of one of the mirrors) change periodically with time and thereby give rise to periodic changes in the interference pattern, which depends on some physical quantity to be investigated, and (b) these changes generate through a photoelectric process an electrical signal which is then separated by suitable electrical filter.

The sensitivity (resolving power) of this arrangement is determined by its optical parameters and the smallest detectable electrical signal. It is well known that in an expedient design the second of the factors is determined solely by the fluctuations and not by the technical imperfections of the system (as for example, the amplifier drift). The smallest detectable electrical signal (the fluctuation limit of sensitivity) can be made as small as desired if a filter with a high time constant is used. This means that in principle the sensitivity (resolving power) of a modulation optical interferometer with given optical parameters can be made as high as desired[1].

A similar statement can be made also with respect to the precision with which an optical quantity surpassing the threshold value can be measured with the modulation optical interferometer. With proper design, the measurement error of the instrument is determined by the fluctuation error and can be made as small as desired by increasing the observation time. The modulation optical interferometer can also be used to measure small periodic (or transformed into periodic) changes in the relative motion of two light beams[1,2] (cf. also survey, Ref. 3). The fluctuation limit of sensitivity of these measurements has been calculated theoretically and attained experimentally by Bershtein[4]. Under relatively simple realizable conditions this limit is on the order of 10^{-2} or even 10^{-3} A. It should also be pointed out that in a similar problem Tolansky[5] was able to obtain the maximum possible sensitivity on the order of tens of Angstrom units by means of multiple beam interferometry in conjunction with a visual analysis of the interference pattern.

A number of applications of the modulation optical interferometer and related arrangements is described in the literature (see for example, Refs. 6 and 7). Equally as important as interference measurements where it is required to determine changes in path differences are measurements where it is required to determine changes in the intensity contrast of an interference pattern caused by changing one of the system parameters. Measurements of this type are used to obtain information on the size of a light source (Michelson's stellar interferometer) or of the degree of its monochromaticity. A modulation optical interferometer properly designed can also be used for measurements which will be discussed in this paper.

It is of interest to estimate for a certain model of the modulation optical interferometer the theoretical fluctuation limit of detectable changes in intensity of the interference pattern, and thereby obtain an estimate of the fluctuation limit of resolution and of the fluctuation error in measuring the intensity of the interference pattern. It is also of interest to investigate experimentally the attainability of the theoretical values of the fluctuation limits of sensitivity and precision.

2. THEORETICAL MODEL OF THE MODULATION INTERFEROMETER

We will consider a sufficiently simple theoretical model of a modulation interferometer designed to obtain information on the size of a light source. In the choice of the theoretical model consideration was given to the fact that it was contemplated to use this model as a basis for an experimental setup (as was indeed done). Partly because of this a readily realizable practical arrangement of the Rayleigh type interferometer was chosen.

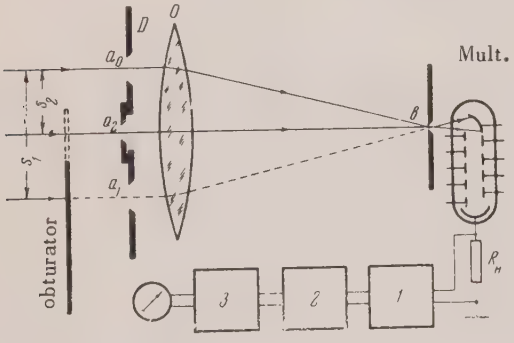

FIG. 1. Theoretical model of the modulation optical interferometer designed to measure the angular spread of a light source.

Consider a distant light source of angular dimension Ψ observed through an (optical) objective. If the objective is covered by a non-transparent screen with two parallel slits, separated from each other by a distance s, a system of interference fringes will be observed in the focal plane of the objective. The intensity distribution of the interference fringes is uniquely given by the separation of the slits, i.e. the base s and the angular dimension of the source. Consider now that in one of the interfering light beams a section is created with a periodically varying optical path length. We will refer to this operation as the modulation of the interference fringes. It can be realized, for example, by an oscillating plano-parallel glass plate covering one of the slits. The modulation of the interference fringes leads to intermittent time variations of the interference pattern. If now a slit which is parallel to the interference fringes and is narrow compared with their width is placed in the focal plane of the objective and the light beam passing this slit directed to the cathode of a photo multiplier, the photo-multiplier current would reproduce as a time function the spatial intensity distribution of the interference pattern.

Let us now assume that the screen covering the objective has three slits a_0, a_1, and a_2 (as shown in Fig. 1), and that a mechanical closing structure (obturator) covers alternately slits a_1 and a_2 with frequency F_0. In this case the length of the base s will be the variable quantity. We will refer to this operation as base-length modulation. We will assume that in the light beam common to both bases modulation of the interference fringes is accomplished as before. At a finite angular dimension of the light source, i.e. $\Psi > 0$, the modulation of the base length s leads to periodical changes in the intensity contrast of the interference fringes and consequently to modulation of the photomultiplier current with a modulation frequency F_0. The depth of this modulation depends on the angular dimension of the source and the geometry of the arrangement. For a point source ($\Psi = 0$) the modulation is absent, since the intensity contrast is equal to unity in either base.

Suitable electronic apparatus permits determination of the site of the light source from the presence of periodic amplitude modulation in the variable component of the photocurrent. The electronic apparatus (see Fig. 1) may, in particular, consist of an amplifier *1* tuned to the frequency with which the interference slits are passing by the slit of the photomultiplier, an amplitude detector *2*, and a narrow-band filter *3* to separate the frequency F_0 of the baselength modulation. In this arrangement the smallest detectable electrical signal of frequency F_0 at the detector output determines the threshold value of the angular dimension of the light source and, consequently, the limit of the resolving power of the setup.

This raises an additional problem. Suppose the angular dimension of the source exceeds the minimum detectable value; with what accuracy can it be measured? The unknown accuracy is obviously determined by the smallest detectable changes in the modulation depth of the electrical signal. The smallest detectable change will be a minimum if a null method is used to measure the electrical signal. This will exclude the effect of slow drifts in the amplification of the instrument (see, for example, Ref. 8). The precision of the measurements is then determined by the same factors as the threshold value of sensitivity—by the amplifier and filter fluctuations and bandwidths.

In our arrangement the null method can be accomplished by varying the width of the slit a_2. The variable portion of the photocurrent which corresponds to base s_2 is proportional to the width of this slit (we will denote the width of any slit with

the same symbol as the slit itself). It is obviously possible to choose such a slit width $a_2 < a_1$ which will compensate for the increase in the variable component of the photocurrent due to shifting from bases s_1 to s_2. The instrument at the filter output will then read zero. This will also eliminate at sufficiently high modulation frequencies F_0 (in practice, 20 – 30 cps) the effect of slow drifts in the amplification of the system. The width of the slit a_2 can be callibrated directly in values of the angular dimension of the source.

A close analysis of Fig. 1 makes apparent one intrinsic shortcoming of the system, which fortunately can be easily removed. The point is, that when $a_1 \neq a_2$ the "dc" component of the photocurrent will also be modulated and with it, consequently, the shot noise of the photo-multiplier. Such modulation of the internal noise is extremely undesirable in modulation systems. In our system this modulation can be eliminated, for example, in the following way. A new slit, a_3, is cut through the screen not far from slit a_2. This slit is covered with a thick plano-parallel glass plate in order that the oscillations of the light waves passing through this slit are incoherent with the oscillations of the waves passing through the other slits. With a proper choice of a_3, the modulation of the "dc" component of the photocurrent is eliminated. The slit a_3 is not shown in Fig. 1.

To conclude the theoretical investigation it is necessary to express the fluctuation limit of sensitivity (the smallest detectible angular dimension of the source) Ψ_{fl} and the fluctuation error $|\Delta\Psi/\Psi|_{fl}$ (of the measurement) in terms of the optical and electrical parameters of our model. It would be of interest to consider this problem from the general statistical point of view which is at present extensively used in problems of radio-signal detection (see, for example, Refs. 9 and 10). However, we will restrict ourselves in this paper to a simpler approach using the signal to noise ratio. We shall assume arbitrarily, as is customary in problems of this kind, that the limiting value of the signal which can be detected is approached when the signal to noise ratio at the output of the system is unity. The smallest detectable angular dimension Ψ_{fl} of the source will thus be determined as the value which results in a signal to noise ratio of one at the output of the system (provided that the system is balanced for $\Psi = 0$). In a similar way we will determine the relative fluctuation error $|\Delta\Psi/\Psi|_{fl}$.

In the analysis of the system it is convenient to introduce instead of the angular dimension Ψ of the light source the normalized dimension ψ, defined as Ψ/Ψ_0, where $\Psi_0 = \lambda/s_1$, and s_1 is the length of the larger base (i.e. the distance between the slits a_0 and a_1). We will, as before, refer to ψ_{fl} as the fluctuation limit of sensitivity and to $|\Delta\psi/\psi|_{fl} = |\Delta\Psi/\Psi|_{fl}$ as the relative fluctuation error of the measurement. In the analysis we shall assume that the source is monochromatic. More detailed calculations show, however, that the obtained results can be adapted also for sources with rather broad spectral bands (practically up to 500 – 700 Å).

3. THE BALANCE CONDITION

If the shot noise of the photomultiplier is neglected the current i of the photocathode is the sum of the dark current i_d and a component proportional to the light flux striking the photo-cathode through slit b (see Fig. 1). Slit b is assumed to be narrow compared with the width of the interference fringes and even more so compared with the dimensions of the Fraunhofer diffraction pattern produced by slits a, and is located near the common center of these images. The light flux striking slit b through each slit a is therefore proportional to the square of the width of the respective slit.

Applying the general theory of interferometry, we obtain for the base s_1, i.e. when the slits a_0 and a_1 are open,

$$i = I\{a_0^2 + a_1^2 + 2a_0a_1V_1U_1\cos\varphi(t)\} + i_d, \quad (1)$$

and for the base s_2, when the slits a_0, a_2 and a_3 are open,

$$i = I\{a_0^2 + a_2^2 + a_3^2 + 2a_0a_2V_2U_2\cos\varphi(t)\} + i_d. \quad (2)$$

Here I is the value of the photocurrent when only one of the slits a is open and its width is unity; V_1 and V_2 are the values of the intensity contrast of the interference pattern for $s = s_1$ and $s = s_2$ respectively, given by

$$V = \sin[\pi\psi(S/S_1)]/\pi\psi(S/S_1); \quad (3)$$

U_1 and U_2 are the values of the function

$$U = \sin[\pi\gamma(S/S_1)]/\pi\gamma(S/S_1), \quad (4)$$

for $s = s_1$ and $s = s_2$ respectively, which describes the leveling off of the variable component of the photocurrent because of the finite width of slit b. The parameter γ is the ratio of the width b to the

width of the interference fringes at base s_1. The function $\varphi(t)$ describes the modulation of the interference fringes.

It is obvious that when

$$a_2^2 + a_3^2 = a_1^2, \tag{5}$$

the modulation of the quasi-constant component of the photocurrent will be absent. If in addition, $a_1 = a_0$, then

$$i = i_0 \{2 + 2m(t) \cos \varphi(t)\} + i_d, \tag{6}$$

where

$$m(t) = \begin{cases} V_1 U_1 \text{ if } s = s_1, \\ \xi V_2 U_2 \text{ if } s = s_2, \end{cases} \tag{7}$$

Here $i_0 = I a_0^2$, and $\xi = a_2/a_0$.

We will assume that $\varphi(t)$ is a linear sawtooth function of time with an amplitude $\varphi_0 = 2\pi n$, where n is a sufficiently large number. In this case we may write approximately

$$\cos \varphi(t) = \cos \omega_0 t, \tag{8}$$

where $\omega_0 = 8\pi n/T$.

The system will obviously be balanced when $m(t)$ is independent of time. Denoting by ξ_0 the value of ξ at balance, we obtain

$$V_1 U_1 = \xi_0 V_2 U_2, \tag{9}$$

or, using equations (3) and (4),

$$\xi_0 = (s_2/s_1)^2 \frac{\sin \pi\gamma}{\sin \pi\gamma (s_2/s_1)} \frac{\sin \pi\psi}{\sin \pi\psi (s_2/s_1)}. \tag{10}$$

4. DETERMINATION OF FLUCTUATION LIMITS OF SENSITIVITY AND PRECISION

We will now consider with what accuracy it is possible to satisfy condition (10) in the presence of shot noise in the photomultiplier. (The shot noise of the photomultiplier is under usual conditions of the experiment several orders of magnitude higher than the noise in other part of the system). We will therefore trace the useful signal and the noise through all sections of the system shown in Fig. 1.

(a). *Photocathode Current.* Taking the shot noise into consideration and taking equation (8) into account, equation (6) becomes

$$i = i_0 \{2 + 2m(t) \cos \omega_0 t\} + i_d + i_n \tag{11}$$

where i_n is the noise component of the photocurrent.

Since the signal component of the current is a function of time, the noise i_n is a nonstationary random process. However it can be shown that in our case the noise at the amplifier output is the same as if the photocurrent were a stationary random process with a mean square spectral density $G_i(f)$ corresponding to the case when $m = 0$. Moreover (see, for example, Ref. 11),

$$G_i(f) = 2e(1 + B)(2i_0 + i_d), \tag{12}$$

where e is the electron charge and B is a constant which, according to Chichik[11], can be assumed to be equal to 1.5.

(b). *Detector Input Voltage.* The regular portion of the photocurrent establishes a voltage at the detector input which, apart from its phase, can be represented by

$$E_c \cos \omega_0 t, \quad E_c = 2 i_0 K_1 m(t). \tag{13}$$

In this equation $K_1(f)$ is the frequency response of of the instrument portion up to the detector. For simplicity we will assume that $K_1(f)$ is a rectangle of width Δf. In writing equation (13) the assumption was made that $\Delta f \gg F_0$.

The spectral density $G_u(f)$ of the noise voltage at the detector input within the band Δf is given by

$$G_u(f) = 2eK_1^2(1 + B)(2i_0 + i_d). \tag{14}$$

Outside of this band $G_u(f) = 0$.

(c). *Detector Output Current.* Assuming specifically that the detector is linear and denoting the slope of its characteristic by S we obtain, using the result obtained by Bunimovich[12]:

$$I_{lf}(t) = (S\sigma/\sqrt{2\pi})[\alpha q(t) + e^{-\alpha q(t)}], \tag{15}$$

$$G_{lf}(F_0) \approx G_{lf}(0) = (S^2\sigma^2/4\pi\Delta f)(\tilde{b}_1 + \tilde{b}_2). \tag{16}$$

In these equations $I_{lf}(t)$ is the regular component of the low frequency detector current; $G_{lf}(F)$ is the spectral density of the low frequency current fluctuations (the condition $\Delta f \gg F_0$ is assumed); $G_{lf}(F_0)$ is practically equal to $G_{lf}(0)$; σ is the norm of the noise voltage at the detector output, given by

$$\sigma = [G_u(f)\Delta f]^{1/2}; \tag{17}$$

$q(t)$ is a shorthand notation for

$$q(t) = E_c(t)/\sigma\sqrt{2;} \tag{18}$$

α is a constant coefficient equal to $2/\sqrt{\pi}$, and $\tilde{b}_1$ and $\tilde{b}_2$ are time averages of the functions

$$b_1(q) = (8/\pi)[1 - 1.5\, e^{-\alpha q(t)} + 0.5\, e^{-3\alpha q(t)}],$$
$$b_2(q) = 1.5\, e^{-\alpha q(t)} - 0.5\, e^{-3\alpha q(t)}. \quad (19)$$

Expanding $I_{lf}(t)$ into a Fourier series and taking into account that $\Delta q(t) \ll 1$, the following approximate expression is readily obtained for the amplitude I_1 of the first harmonic (of frequency F_0):

$$I_1 = 2\pi^{-3/2}\, i_0 K_1 S\alpha (1 - e^{-\alpha q_0})\, [\xi V_2 U_2 - V_1 U_1], \quad (20)$$

where q_0 is the time average of $q(t)$:

$$q(t) = q_0 + \Delta q(t). \quad (21)$$

In the sense of the problem we assumed $\Delta q \ll 1$, since otherwise it would be possible to detect the amplitude modulation without any filter. Considering that $\Delta q(t)$ is small we may also in calculating $G_{lf}(F_0)$ replace $q(t)$ in (19) by its time average q_0. This gives

$$G_{lf}(F_0) = (S^2\sigma^2 / 4\pi\Delta f) \times (2{,}5 - 2{,}3\, e^{-\alpha q_0} + 0{,}8\, e^{-3\alpha q_0}). \quad (22)$$

In the determination of q_0 it is natural to assume that the balance condition (10) is satisfied. Then,

$$q_0 = i_0\, [e(1 + B)(2i_0 + i_d)\, \Delta f]^{-1/2}\, \xi_{00}, \quad (23)$$

where ξ_{00} is a shorthand notation for $V_1 U_1$. It should be noted that by its definition ξ_{00} is equal to ξ_0 for $s_2 = 0$.

(d) *Filter Ouput Voltage.* The amplitude of the sinusoidal voltage of frequency F_0 at the filter output is

$$A = K_2 I_1. \quad (24)$$

The dispersion of the filter output noise is

$$\sigma_f^2 = K_2^2 G_{lf}(F_0)\, \Delta F, \quad (25)$$

where ΔF is the filter bandwidth.

(e) *Fluctuation Error of the Measured Angular Dimension of the Source.* In accordance with the assumption made in Section 2 we will determine the fluctuation error $|\Delta\psi/\psi|_{fl}$ from the condition of equality of signal and noise at the filter output, i.e. from

$$A^2 / 2 = \sigma_f^2. \quad (26)$$

Setting $\xi = \xi_0 + \Delta\xi$ and taking into account equations (20), (22), (24), (25), and (26), we obtain after some simple transformations

$$|\Delta\xi/\xi_0|_{fl} = \frac{\pi}{2} X(\alpha q_0) \left[\frac{\Delta F}{\Delta f}\right]^{1/2}, \quad (27)$$

where

$$X(\alpha q_0) = \frac{(2{,}5 - 2{,}3\, e^{-\alpha q_0} + 0{,}8\, e^{-3\alpha q_0})^{1/2}}{\alpha q_0 (1 - e^{-\alpha q_0})}, \quad (28)$$

$|\Delta\xi/\xi_0|_{fl}$ represents the normalized fluctuation error of the measured quantity ξ_0 for a given angular spread of the source. $|\Delta\psi/\psi|_{fl}$ is readily obtained from this quantity.

From equation (10) it follows that

$$\Delta\xi/\xi_0 = \pi\psi\,[\cot\pi\psi - (S_2/S_1)\cot\pi\psi(S_2/S_1)]\,(\Delta\psi/\psi), \quad (29)$$

from which

$$|\Delta\psi/\psi|_{fl} = \tfrac{1}{2} X(\alpha q_0)\, Y(\psi)\, [\Delta F / \Delta f]^{1/2}, \quad (30)$$

where,

$$Y(\psi) = \frac{1}{\psi[(S_2/S_1)\cot\pi\psi S_2/S_1 - \cot\pi\psi]} \quad (31)$$

It is obvious that equation (30) is correct for values of ψ only which are not too close to either zero or unity.

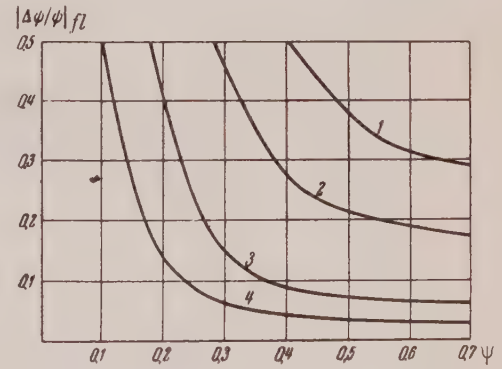

FIG. 2. The fluctuation error $|\Delta\psi/\psi|_{fl}$ as a function of the relative angular dimension ψ of the source with the photocurrent i_0 as a parameter. The values of i_0 are: $1 - 5\times10^{-16}$, curve $2 - 10^{-15}$, curve $3 - 10^{-14}$, and curve $4 - 10^{-13}$ amp.

(f) *Fluctuation Limit of Sensitivity.* To determine ψ_{fl} we will rewrite equation (20). We will first assume that the apparatus is balanced for a point source. Then, $\xi = \xi_0 = U_1/U_2$. Taking U_1 in equation (20) outside the parenthesis and setting it equal to unity, we obtain, approximately

$$I_1 = \frac{2}{\pi\sqrt{\pi}}\, i_0 K_1 S\alpha\, (1 - e^{-\alpha q_0})\, [V_2 - V_1]. \quad (32)$$

In view of the relatively small value of $\pi\psi$ in comparison with unity, we may expand V_1 and V_2 in a power series in terms of $\pi\psi$ and neglect all terms of order higher than 2. This gives,

$$V_2 - V_1 = (1/6)\,\pi^2\psi^2[1-(S_2/S_1)^2]. \quad (33)$$

According to our previous assumption the signal is considered detected when the signal to noise ratio at the filter output is not less than unity. If this condition for signal detection is written down, we obtain after some simple transformations

$$\psi_{fl} = [1-(S_2/S_1)^2]^{-1/2}\,[X(aq_0)]^{1/2}\,[\Delta F/\Delta f]^{1/4}. \quad (34)$$

In Fig. 2 the fluctuation error $|\Delta\psi/\psi|_{fl}$ is shown as a function of ψ for several values of i_0. Fig. 3 shows the fluctuation limit of sensitivity ψ_{fl} as a function of the photocurrent i_0 (lower graph). The following values for the parameters are assumed for the plots: $B = 1.5$, $i_d = 2\times10^{-16}$ amp, $\Delta f = 1$ cps, $s_2/s_1 = 2/3$ and $\gamma = 0.35$. (This value of γ is an optimum from the point of view of signal to noise ratio.)

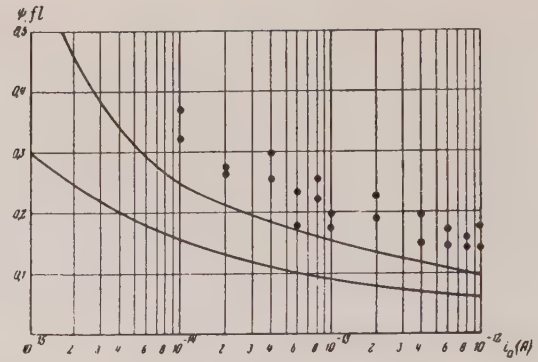

FIG. 3. The fluctuation limit of sensitivity ψ_{fl} as a function of the photocurrent i_0. For the upper curve $i_d = 4\times10^{-15}$ amp, $B = 6.5$; for the lower curve $i_d = 4\times10^{-16}$ amp, $B = 1.5$.

5. THE EXPERIMENT

The described thoretical model was adapted as a basis for developing the experimental setup. A more detailed arrangement of the setup is shown in Fig. 4.

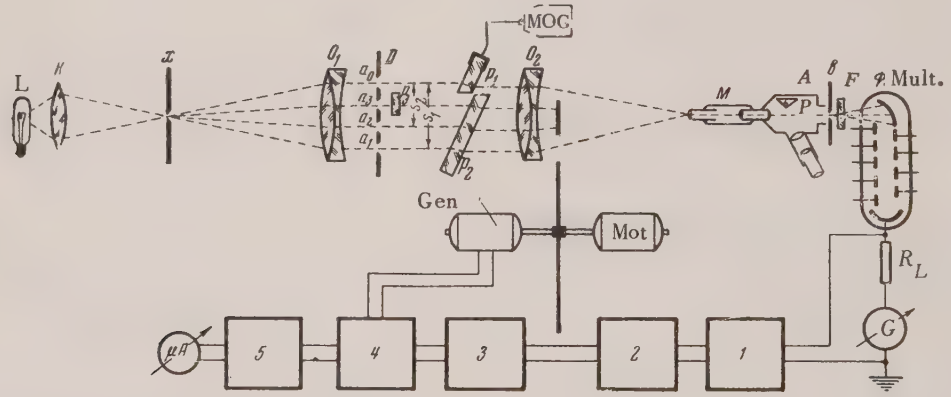

FIG. 4. Schematic diagram of the experimental set-up.

The light source used is a calibrated slit x illuminated with a very strong motion-picture projection lamp. The light beam from the collimator illuminates diaphragm D. Four parallel slits are cut through the diaphragm. The widths two slits, a_2 and a_3, can be varied by means of micrometer screws. The interference fringes are modulated by means of a plane parallel plate p_1 on which angular oscillations are imparted from a mechanical oscillation generator MOG. Plate p_2 is used for compensation of the constant difference of the (optical) path lengths. The modulation of the base length is produced by means of a obturator of frequency $F_0 = 23$ cps. The interference fringes formed in the focal plane of the objective O_2 are projected with large magnification on the slit of the photomultiplier. The width of this slit is only a fraction of the width of the interference fringes and is such to give the optimum condition for γ, i.e. $\gamma = 0.35$.

For visual control of the position of the interference fringes an adaptor A behind the microscope is used. By means of a tilting prism P this enables to observe the interference pattern through a viewing telescope. When the prism is tilted back the light

beam passing through the slit b and a green filter F ($\Delta\lambda \approx 500$ A) strikes the photocathode of a FEU-19-M multiplier. The voltage of the photomultiplier load is applied to the input of amplifier *1*. This amplifier is tuned to the frequency $f_0 = 1100$ cps ,with which the interference fringes are passing (the slit b) and has a bandwidth $\Delta f = 100$ cps. The photomultiplier output voltage is applied to linear detector *2*. A sinusoidal signal of frequency $F_0 = 23$ cps appears at the output of the detector. The balance is accomplished at the output of a narrow-band filter tuned to the frequency F_0, comprising a heterodyne filter which consists of a preliminary filter *3*, a balancing detector *4* and a dc filter *5*. A reference voltage is applied to the balancing detector from a generator, the rotor of which is rigidly coupled with the obturator. The phase of the reference voltage can be varied by rotating the stator of the generator. Its value was chosen to obtain maximum sensitivity for the filter. The bandwidth of the heterodyne filter, determined by the dc filter, was set equal to 1 cps.

We made experimental estimates of sensitivity and precision with which the angular dimension of a source can be measured. The result of these measurements is shown in Fig. 3, where the smallest detectable values of ψ are shown as a function of the photocurrent i_0. A comparison with the lower graph of the same figure, which gives the theoretical values of the fluctuation limit of sensitivity calculated for the parameter values assumed in Section 4, shows a wide discrepancy in the results. This discrepancy can be explained by the fact that the photomultiplier used in the experiment had parameters inferior than assumed in the theoretical calculations. Measuring the spectral density of the shot noise of the photomultiplier used in the experiment at 1100 cps it was found that $i_d = 4\times10^{-15}$ amp and $B = 6.5$. The theoretical dependence of ψ_{fl} on i_0 for the corrected values of i_0 and B is shown in the upper graph of Fig. 3.

The result of experimental estimates of the error in measuring the angular dimension of the source is shown in Fig. 5. Also shown in the same figure are the theoretical curves of the fluctuation error calculated for the parameters of the experimental set-up. The agreement between the experimental and theoretical results can be regarded as satisfactory. The theoretically found fluctuation limits of sensitivity and precision can thus be attained also in practice.

An essential advantage of the modulation interferometer is its noise rejection with respect to shifts of the interference fringes due to changes in path differences of the interfering beams. Such shifts may result, in particular, from mechanical disturbances of the interferometer. Based on theoretical considerations it may be expected that the modulation interferometer is insensitive to random shifts of the interference fringes provided the following conditions are fulfilled: (1) the mean square value of the shifts is less than or equal to the width of the fringes and (2) the correlation time of the shifts is much larger than $\tau = 1/\Delta f$.

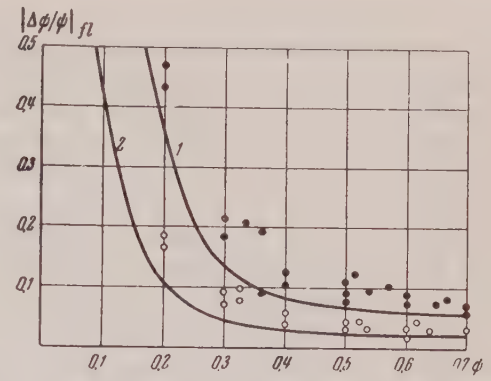

FIG. 5. The fluctuation error $|\Delta\psi/\psi|_{fl}$ as a function of the relative angular dimension ψ of the source. $B = 6.5$; $i_d = 4\times10^{-15}$ amp. Curve *1* and points marked ● are for $i_0 = 4\times10^{-14}$ amp; curve *2* and points marked ○ – for $i_0 = 4\times10^{-13}$ amp.

These theoretical considerations have also been confirmed experimentally. In a number of investigated cases where the presence of mechanical disturbances made the interference pattern completely indistinguishable in visual observations the modulation interferometer was still practically able to utilize completely its theoretical possibilities.

6. SOME REMARKS ON THE POSSIBILITY OF USING THE OPTICAL MODULATION INTERFEROMETER TO MEASURE ANGULAR DIAMETERS OF STARS

It is well known that the idea of using the interference principle for measuring angular diameters of stars was first expressed by Fizeau in 1868. Later this idea was developed further by Michelson, who proposed the so-called stellar interferometer, in which the folded optical paths made it possible in principle to increase indefinitely the dimensions of the base and, consequently, to increase indefinitely the resolving power of the interferometer

(see, for example, Ref. 13). In 1920 Michelson was able to measure the angular diameters of some of the bigger stars. Equipment was used with base lengths of 6 and 18 meters. Michelson considered that a further increase in the base length is prevented by the atmospheric and mechanical disturbances which impose an upper limit on the practically realizable base values and at the same time establish the lower limit of the measurable angular diameters. This consideration is in accordance with the capabilities of visual observations.

Some years ago Bershtein and Gorelik pointed out in their notes[14] that the application of radio-physical methods to analysis of the interference pattern of an optical steller interferometer may substantially widen its potentialities. One of the steps in this direction may be the application of the balanced modulation interferometer described above. Of special importance here is the previously mentioned stability of the modulation interferometer with respect to phase fluctuations of the interference fringes.

It is of interest to estimate the potentialities of the modulation method in its application to the stellar interferometer when atmospheric disturbances are considered. Below we will give a brief report on the results of these estimates.

In our calculations we used a theoretical model of the modulation stellar interferometer which was in principle very close to the model shown in Fig. 1. Since stars can be replaced as uniformly luminous disks we have, instead of equation (3),

$$V = 2J_1(1.22\pi\psi s/s_1)/1.22\pi\psi s/s_1, \qquad (35)$$

where $J_1(X)$ is the Bessel function of first order, and ψ now denotes the quantity $\Psi_{s_1}/1.22\lambda$. In addition, making use of a folded path of the rays it is possible to obtain in the modulation stellar interferometer the same width of the interference fringes for both bases s_1 and s_2. The indicated distinguishing characteristics are not essential. Their effect is that the values of ψ_{fl} and $|\Delta\psi/\psi|_{fl}$ obtained for theoretical model of the stellar interferometer in the absence of atmospheric disturbances differ by no more than 5 to 10 percent from the corresponding results for the investigated model. These can therefore be used also for the stellar interferometer.

The photocathode current i_0 can be calculated from the following approximate equation:

$$i_0 = 3\cdot 10^{-14}\cdot 2.5^{-m}\ \text{A}, \qquad (36)$$

where m is the visual star magnitude. This equation was obtained under the assumption that the investigated model has geometrical dimensions of the same order as the latest version of Michelson's stellar interferometer. The sensitivity of the photocathode was assumed to be 3×10^{-5} amperes per lumen.

The following was found concerning the effect of atmospheric disturbances:

(a) There is no sense in using modulation interferometer unless the average turbulence angle t_0 is much smaller than λ/l, where l is the linear dimension of the interferometer mirror (the notation of Danjon and Kude[15] is used). It should be pointed out that the corresponding condition is apparently even more stringent for the common stellar interferometer.

(b) If the condition $t_0 \ll \lambda/l$ is fulfilled it is always possible, at least in principle, to choose such parameters (for example, the modulation frequency F_0) that the phase fluctuations of the interference fringes, which are caused by the fluctuations in the optical path lengths in the passage of the light through the turbulent medium, have a negligible effect on the results of the measurement.

(c) As to the intensity fluctuations, the calculations show that they increase the spectral density of the noise component of the photocurrent from the value given by Eq. (12) to

$$i_0^2 g(|f-f_0|), \qquad (37)$$

where $g(f)$ is the spectral density of the relative intensity fluctuations. This result is obtained under the assumption that the intensity fluctuations in the various paths of the interferometer are independent of each other.

A number of experiments on the investigation of $g(f)$ is described in the literature (see, for example, Ref. 16 and 17). On the basis of these studies it was possible to estimate $g(|f-f_0|)$ for frequencies close to f_0, i.e., for frequencies in the pass band of the amplifier. For good atmospheric conditions it may be assumed that in the region of the amplifier pass band $g(|f-f_0|)$ is 3×10^{-4} cps.

It is convenient to introduce the ratio of the spectral density of the photocurrent fluctuations brought about by the atmospheric disturbances to the spectral density of the shot noise in the amplifier pass band. Denoting this ratio by C and assuming for B the value 1.5 we obtain

$$C = 2\cdot 10^{14}\, i_0 = 6\cdot 2.5^{-m}. \qquad (38)$$

It can be shown that under the atmospheric conditions discussed above for very bright stars the

fluctuation limit of sensitivity ψ_{fl} and the fluctuation error in measuring the angular quantity $|\Delta\psi/\psi|_{fl}$ are given approximately by

$$\psi_{fl} = (\psi_{fl})^0 (1 + C)^{1/4}, \quad (39)$$

$$|\Delta\psi/\psi|_{fl} = |\Delta\psi/\psi|^0_{fl} (1 + C)^{1/2}. \quad (40)$$

In the above equations the index 0 refers to the ideal case of quiet (undisturbed) atmosphere. The effect of "atmospheric" noise is, as should be expected, stronger for the bright stars than for the weak stars. For $m = 0$, for example, "atmospheric" noise increases the fluctuation error in measuring the angular quantity by 2.65 times, and the smallest detectable angular dimension by 1.63 times. At a very quiet state of the atmosphere the effect of atmospheric disturbances is even smaller.

Comparisons with visual observations show that the use of the modulation optical interferometer to measure the angular dimension of a light source does not under readily realizable experimental conditions result in a large increase of the resolving power. However, the theoretical possibilities of the modulation interferometer may be fully realized under conditions of strong disturbances (noise rejection). This, in part, implies that the modulation stellar interferometer can have much larger bases than are permissible in visual observations.

I would like at this point ot express my thanks to Professor G. S. Gorelik for his constant interest in this work.

[1] G. S. Gorelik, Dokl. Akad. Nauk SSSR 83, 549 (1952).

[2] Brusin, Gorelik, Pikovsky, Dokl. Akad. Nauk 83, 553 (1952).

[3] G. S. Gorelik, Izmeritel'naia Tekhnika 3, 10 (1955).

[4] I. L. Bershtein, Dokl, Akad. Nauk SSSR 94, 655 (1954).

[5] S. Tolansky, Science Progress 37, 1 (1949).

[6] J. Peters and G. Stroke, J. Opt. Soc. Am. 43, 688 (1953).

[7] H. W. Babcock, Astrophys. J. 107, 73 (1948).

[8] W. S. Troitskii, J. Tech. Phys. (U.S.S.R.) 21, 995 (1951).

[9] P. M. Woodward, *Probability and Information Theory with Application to Radar*, London, 1953.

[10] Peterson, Birdsall, and Fox, Trans. I. R. E. PGIT-4, 171 (1954).

[11] N. O. Chechik, Usp. Fiz. Nauk 37, 74 (1949).

[12] V. I. Bunimovich, *Fluctuation Processes in Radio Receiving Installations*, Moscow, 1951.

[13] A. A. Michelson, *Light Waves and their Applications*, (Rus. Trans.). Gostekhizdat 1934.

[14] I. L. Bershtein and G. S. Gorelik, Dokl. Akad. Nauk SSSR 86, 47 (1952).

[15] A. Danzhon, A. Kude, Astr. Zhurnal 17, 1 (1940).

[16] Mikesell, Hong, and Hall, J. Opt. Soc. Am. 41, 689 (1951).

[17] W. M. Protheroe, Contribution from the Perkins Observatory, Series II, 4.

Translated by L. Bergstein
172

π° Meson Production in p-p and p-n Collisions in the 390-660 Mev Energy Region*

IU. D. PROKOSHKIN AND A. A. TIAPKIN
Joint Institute for Nuclear Studies

(Submitted to JETP editor December 24, 1956)
J. Exptl. Theoret. Phys. (U.S.S.R.) 32, 750-766 (April, 1957)

The total cross sections and angular distributions for the reactions of π° production in p-p and p-n collisions have been measured at various energies. The total cross sections at 660 Mev were found to be $\sigma_{pp}^{\pi^\circ} = (3.6 \pm 0.2) \times 10^{-27}$ cm^2 and $\sigma_{pn}^{\pi^\circ} = (7.0 \pm 1.1) \times 10^{-27}$ cm^2. In the energy range 390–660 Mev, the total cross section for the $p + p \to \pi^\circ + p + p$ reaction is proportional to the 5.5 power of the maximum π° meson momentum. The π° meson angular distribution, which is appreciably anisotropic at the proton energy 450 Mev, becomes isotropic as the energy is increased to 660 Mev.

1. INTRODUCTION

BECAUSE THE LIFETIME of the π° is short, information about the total production cross section for π° mesons and their angular distribution can be obtained from a measurement of the absolute flux and angular distributions of secondary particles—γ-rays from the decay of the π° mesons. Previous experiments[1-8] have determined only the differential cross sections for the yield of γ-rays from the decay of π° mesons produced in the reactions:

$$p + p \to \pi^0 + p + p \quad \text{(I)};$$

$$p + n \to \pi^0 + \begin{cases} d & \text{(a)} \\ p + n & \text{(b)} \end{cases} \qquad \text{(II)}$$

Since the angular distributions of the γ-rays were not investigated in these experiments, in order to determine the magnitude of the total cross section it was necessary to make various assumptions as to the nature of the angular distribution of the π° mesons, which materially reduced the reliability of the results obtained.

The investigation of reaction (I) is beset with great experimental difficulties, since the cross section for this reaction is small, due to the fact that the transition in the S state for the protons and p state for the π° mesons is forbidden by conservation laws. Measurements of the differential cross section at 340[1] and 430–480 Mev[4-7] have shown that the total cross section for reaction (I) increases sharply with energy. The rapid increase of the cross section for this reaction continues into the proton energy region 500–660 Mev[8]. The cross section for reaction (II) was measured at two proton energies: 340[2,3] and 660 Mev[8]. The angular distribution of the π° mesons produced in the reaction (II, a) was measured at the neutron energy 400 Mev[9]. The angular distribution of the π° mesons in reactions (I) and (II, b) have not yet been investigated.

The energy distribution of the π° mesons may be obtained from measurements of the energy spectra of the γ-rays produced upon their decay. Appropriate experiments have been conducted only for π° meson production in heavy nuclei[3,4,6]. A study of the γ-ray spectra also permits one to infer the character of the angular distribution of the π° mesons. Thus in Ref. 3 and 6 analysis of the γ-spectra obtained led to inferences concerning the anisotropy of the angular distribution of the mesons in reaction (II) at proton energies of 340 and 470 Mev.

We have measured the yield of γ-rays from the decay of π° mesons produced in reactions (I) and (II) at various angles, in the proton energy range 390–660 Mev. These measurements allowed us to determine the absolute total cross sections, excitation functions and π° angular distributions for the indicated reactions.

2. EXPERIMENTAL METHODS

The setup of the experiments described below is depicted in Figure 1. Neutral pions were produced in a target bombarded by protons of the internal cyclotron beam, with a maximum energy of 680 Mev. The γ-rays from the π° meson decays proceeded through a steel collimator in a four meter concrete wall to a lead diaphragm. A γ-ray telescope was placed at a distance of three meters from the diaphragm.

*The results of this paper were reported at conferences in Moscow (May, 1956) and Geneva (June, 1956).

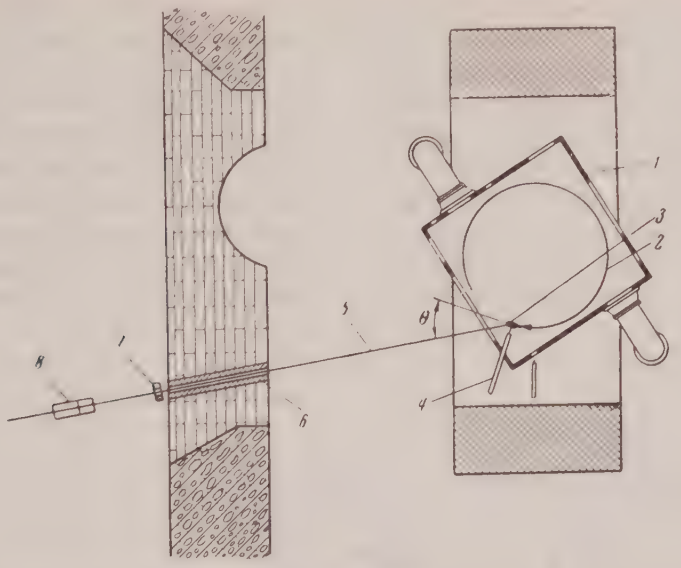

FIG. 1. The experimental setup. 1—vacuum chamber of the synchrocyclotron, 2—circulating beam of protons, 3—internal target, 4—trial rod, 5—γ-ray beam, 6—steel collimator, 7—lead diaphragm, 8—γ-telescope

The selection of the indicated experimental arrangement was dictated by the advantages associated with the use of the high intensity internal proton beam. The proton current through the graphite target reached $(1.6 \pm 0.1) \times 10^{13}$ (protons/sec)/(gm/cm^2). With so high a beam intensity, one can place the telescope at a large distance from the target (≈20 m) and be adequately shielded from stray radiation. At this distance, the magnetic field of the accelerator clears the γ-ray beam thoroughly of charged particles. The high intensity of the internal beam makes possible the use of a calorimetric method for measuring the proton current. With this method, one need not consider the dimensions and density of the targets, and consequently one is rid of the errors associated with the measurement of these quantities.

Since the amplitude of the free radial oscillations of the particles in the cyclotron is large, the internal beam is appreciably non-monoenergetic. The mean energy dispersion of the particles bombarding the target reaches 10 Mev. Therefore, for an accurate determination of the cross section, it is necessary to know the energy spectrum of the internal beam protons. An attempt at the experimental determination of the spectrum was undertaken in Ref. 10. The spectra obtained, at proton energies of 400, 550 and 660 Mev, proved to be identical within the limits of experimental error. They are presented in Fig. 2. The mean square deviation of the energy from its maximum value was found to be 22 Mev. The dotted curve in Fig. 2 represents the normal distribution corresponding to this standard deviation.

γ-Telescope

The γ-rays arising from the decay of π^0 mesons are distributed over a broad energy interval. A detector suitable for the investigation of π^0 meson

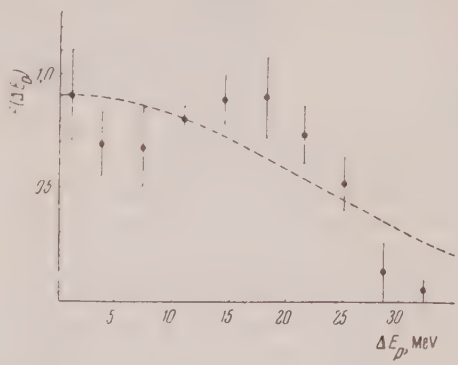

FIG. 2. The energy dispersion of the internal beam protons $F(\Delta E_p)$ (in relative units). ΔE_p is the deviation of the proton energy from the maximum possible.

production processes must efficiently count γ-rays with energies from 10–15 Mev and higher, *i.e.*, it must possess a very low energy threshold. In addition, it must not be sensitive to other forms of radiation—neutrons, protons, etc. A γ-telescope, which, in addition to scintillation counters, contains a Cerenkov counter, satisfies the above requirements. However, such a telescope has not been often applied to absolute γ-ray flux measurements, because the efficiency of the Cerenkov counter is

appreciably less than unity and is difficult to calculate. Thus, in references 7 and 11, the Cerenkov counter was used only for measurements of the relative γ-ray flux; for getting absolute measurements, a telescope containing only scintillation counters was used. A γ-telescope will be described below whose efficiency can be experimentally determined.

The γ-telescope used contained a scintillation counter and a Cerenkov counter, placed in two separate blocks (Fig. 3). By varying the distance between the blocks, it was possible to vary the telescope angle from 3° to 45°. In the first block a tolane crystal, of dimensions $50 \times 50 \times 90$ mm, was placed, with two photomultipliers attached; in the second block were a plexiglass radiator, of dimensions $105 \times 115 \times 40$ mm, and two photomultipliers. A removable lead converter was set in front of the scintillation counter. Electrons and positrons, produced in the converter by high energy γ-rays and continuing through the telescope counters, are regis-

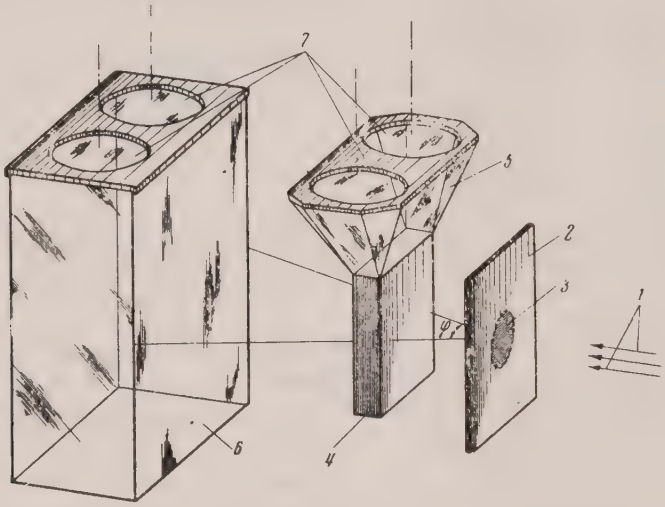

FIG. 3. The layout of the γ-telescope. 1—collimated γ-ray beam, 2—lead converter, 3—area of the converter irradiated by γ-rays, 4—crystal scintillator, 5—light conductor, 6—plexiglass radiator, 7—connection positions of the photomultipliers.

tered by a quadruple coincidence scheme with a resolution time of 2×10^{-8} sec[12].

Since the fringing field of the accelerator satisfactorily clears the beam of charged particles, it was not necessary to place a counter, in anticoincidence with those of the γ-telescope, in front of the converter. The telescope count, without the converter, was 7–12% of that with the converter present.

At small angles with respect to the direction of motion of the bombarding protons, an appreciable quantity of high energy neutrons is contained in the γ-ray beam, which raises the telescope count somewhat. For an estimate of the background associated with the neutrons, a 5 cm thick lead absorber was placed in the beam, with "good geometry", clearing the γ-ray beam almost completely of neutrons. Measurements indicated that the γ-telescope is slightly sensitive to fast neutrons. At 660 Mev the neutron background was 3% of the total count.

Measurement of the Efficiency

The total efficiency of the γ-telescope is given by

$$F_\gamma = (1 - e^{-\mu d})\,\xi f_1 f_2. \qquad (1)$$

where μ is the absorption coefficient in lead of the γ-rays studied, d is the thickness of the lead converter, ξ is a coefficient measuring the decrease in the efficiency due to scattering and absorption of electrons and positrons in the converter and counters, f_1 and f_2 are the efficiencies for the counting of electrons and positrons by the scintillation and Cerenkov counters. The magnitude of μ depends on the spectrum of the γ-rays counted, and therefore was measured for each value of the energy and angle of observation. For these measurements, a lead absorber was inserted into the γ-ray beam, and the telescope counts with and without absorber were compared. In this way the quantity $(1-e^{-\mu d})$ was determined to an accuracy of 2%.

One of the principal difficulties of a measurement of the absolute γ-ray flux is the determination of ξ. Due to the fact that the ratio of the counts "with converter/without converter" was large, and the efficiency of the telescope was high, the thickness of the converter was usually chosen to be close to a radiation length. As a consequence, the energy threshold of the telescope is high and is appreciably less than unity and can be calculated only by the Monte Carlo method. When d is decreased, ξ rapidly approaches unity and can be measured. The determination of ξ was carried out in the following way: the dependence of the telescope count on the thickness of the converter was measured, and a small thickness d_0 was chosen such that the deviation of the experimental points from the curve $(1-e^{-\mu d})$ was not large, *i.e.*, the telescope had a low energy threshold. This dependence is given in Fig. 4 at a proton energy of 660 Mev and for angles of observation of 0°, 30° and 180°. As is seen from Fig. 4, there is a strong dependence on the angle of observation, which is related to differences in the γ-ray spectra. The magnitude of d_0 was chosen to be 0.05 cm. For the determination of ξ, at this value of d, the dependence of the count on the magnitude of the telescope angle was measured (the distance between the telescope counters was increased). Typical curves, obtained at 660 Mev, are given in Fig. 5. In the above described manner $\xi(d_0)$ was determined to an accuracy $\approx 1\%$.

For the measurement of the relative γ-ray flux, we used a lead converter of thickness 0.2 cm. Under these conditions the spectral efficiency of the telescope $K_\gamma = (1-e^{-\mu d})$ is 0.170 ± 0.003 at 0° and 660 Mev; when the angle is increased to 180°, K_γ decreases to 0.134 ± 0.002.

In order to increase the efficiency of the counter, we used a photomultiplier with a large multiplication factor and operating with a non-uniform distribution of the voltage between the dynodes at a total voltage of 3.5 kv. Also, amplifiers with distributed parameters (70 Mc band-pass, amplification factor ~ 7) were introduced between the coincidence scheme and the photomultipliers. It should be remarked that due to the low intensity of the Cerenkov radiation, the efficiency f_2 is appreciably less than unity even in the sloping portion of the counter characteristic.

For the measurement of the efficiency f, we switched from a quadruple coincidence scheme to one of triple coincidence between any three of the four telescope photomultipliers. Under these conditions the sensitivity of the channels remained constant. Since two photomultipliers are adjoined respectively to the plexiglass radiator and to the scintillator, the exclusion of one of them does not

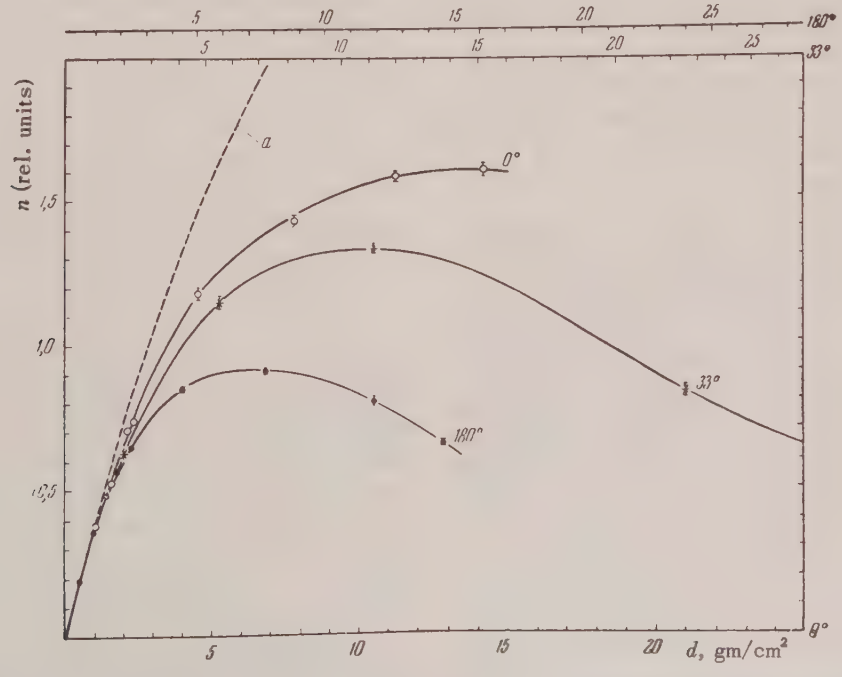

FIG. 4. The variation of the efficiency of the γ-telescope with the thickness of the lead converter d. The scales along the abcissa are chosen such that, for the angles indicated, the magnitudes of μd are the same. The values of μ used in the construction of the scales are given in Table 2. The curve a is that of $(1-e^{-\mu d})$.

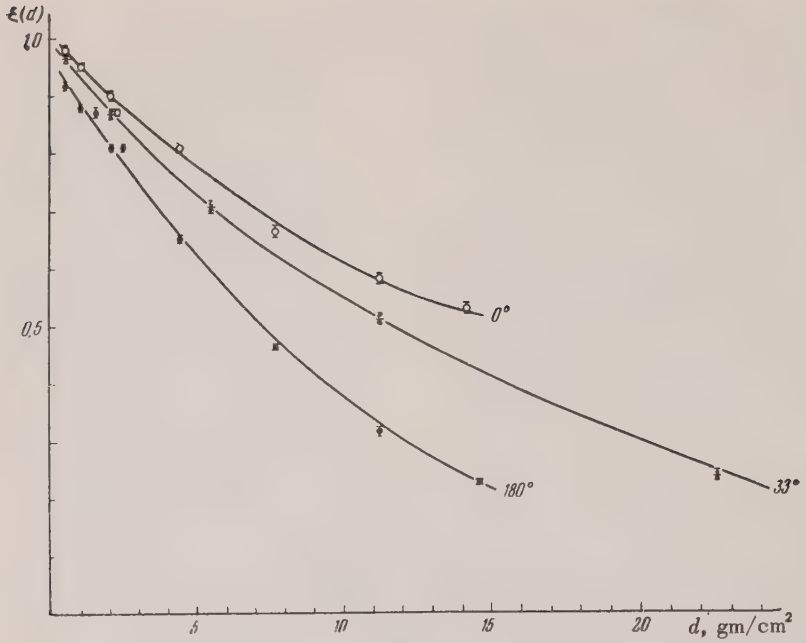

FIG. 5. The coefficient ξ as a function of d at the proton energy 660 Mev, measured at the angles 0°, 33° and 180° in the laboratory system.

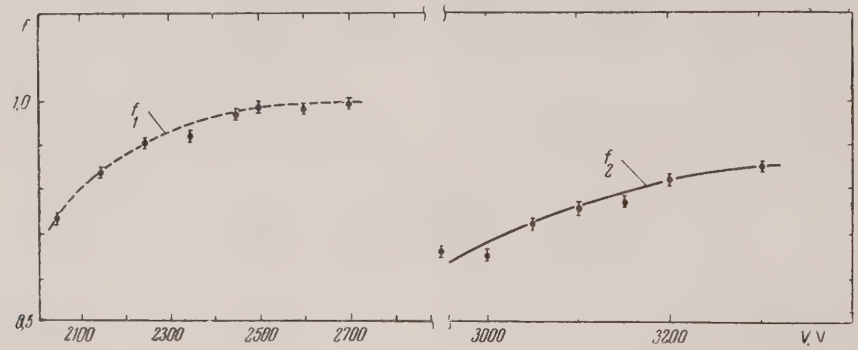

FIG. 6. The efficiency of the telescope counters as a function of the voltage on the photomultipliers.

change the geometry of the telescope. Consequently, by measuring the increase in the γ-ray count when one switches from a quadruple to a triple coincidence scheme, it is possible to determine the ineffectiveness of the excluded photomultiplier and its channel. With a view to checking the data, the method was used for the determination of the efficiency of a scintillation counter, which should not differ much from unity in the region of the plateau of the counter characteristic. We obtained: $f_1 = (99 \pm 1)\%$. The efficiency of the Cerenkov counter was appreciably less: $f_2 \approx 80\%$ (see Fig. 6). At 0° the magnitude of f_2 was somewhat larger than at 180°, which, seemingly, is explained by the difference in the average number of electrons coming out of the converter. By the above described method, the magnitude of $f_1 f_2$ was determined to 2%. The accuracy of the measurement of the total efficiency F_γ was $\approx 3\%$.

Measurement of the Proton Current

The proton current through the target, which was placed inside the accelerator chamber, was measured from the heating of the target by means of a calibrated battery of 40 copper-constantan thermocouples. The sensitivity of the "thermobattery" was measured in a special evacuated assembly to better than 1%, and was $(2.38 \pm 0.02) \times 10^{12}$ Mev/sec mv. The thickness of the heat conductor which held the target, was chosen to be sufficiently large so that the target was not heated more than 50°–70°. As the measurements carried out in the evacuated assembly indicated, the loss by radiation under these conditions is not appreciable.

For an estimate of the radiation loss, the ratio of the γ-ray flux to the heat flux through the target at different intensities of the internal beam was also measured. In the flux interval investigated this quantity was constant, to an accuracy $\approx 1\%$. Prior to this, it had been shown that the counting characteristic of the γ-telescope was linear.

The heat generated by the protons in the target is the sum of the ionization loss ϵ_{st}. The first quantity is well known[13,14]. The quantity ϵ_{st} was calculated on the basis of the spectra of particles—light stars, measured by E. L. Grigor'ev and L. P. Solov'ev. For carbon, at 660 Mev, it was found that $\epsilon_{st}/\epsilon = 0.15 \pm 0.05$. The indicated error represents the maximum error of the calculation.

Since this gives the largest contribution to the error in the absolute cross section, we undertook an experimental determination of the ratio ϵ_{st}/ϵ. By placing an aluminum target, exposed to the protons, at various distances from the center of the accelerator, the energy dependence of the yield of the reaction $Al^{27}(p, 3pn)Na^{24}$ was measured. The products of the reaction were identified from the well known[15] half life of the Na. A comparison of the excitation function for the above reaction in the region 260–660 Mev with those measured in Refs. 16–18 gives, at 660 Mev and after converting to carbon, $\epsilon_{st}/\epsilon = 0.16 \pm 0.06$.

The differential cross section for the production of γ-rays is given by

$$d\sigma_A^{\gamma}/d\Omega = n\varepsilon(1 + \varepsilon_{st}/\varepsilon) A (1 + \delta)/mF_{\gamma}N\Omega. \quad (2)$$

where n is the number of γ-rays counted per unit time by the telescope, m is the heat flux through the target, ϵ is the specific ionization loss (per gm/cm^2), δ is a small correction measuring the absorption of the γ-rays counted in the target and in air, Ω is the solid angle of the counter, A is the atomic weight of the target material, and N is Avogadro's number. The quantities N, A and ϵ are tabulated. The mean square error associated with the measurement of the remaining quantities in Eq. (2), after numerous measurements, comes to 5.2%.

Measurement of the γ-ray Production Cross Section in Hydrogen

By a difference method, the γ-ray production cross section was measured by means of the exposure of polythene $(CH_2)_n$ and graphite targets. The small thermal conductivity of polythene does not permit in this case the use of the calorimetric method. For the determination of the ratio of the cross sections for hydrogen and carbon, a measurement of the activity of the targets was employed. In these experiments the polythene and graphite targets were exposed one after the other and the flux of the γ-rays and the activity of the targets were compared. As in the calorimetric method, the measured ratio did not depend on the shape or density of the target:

$$(d\sigma_H^{\gamma}/d\Omega)/(d\sigma_C^{\gamma}/d\Omega) = [(n'/I') - 1]/p_H'. \quad (3)$$

where n and I' are the ratios of the γ-ray flux and the activities induced in the polythene and graphite targets and p_H' is the relative number of hydrogen nuclei in the polythene. For the polythene used, $p_H' = 2.05$.

The polythene and graphite targets were simultaneously placed in the accelerator chamber and, by means of a coil and current, were alternately introduced into the beam. Synchronously with the interchange of the targets, switching of the counting portions of the telescope is carried out by means of a special commutator, which takes advantage of the fact that distinct γ-ray counts are obtained from the polythene and carbon targets. The targets were switched once every minute. For so frequent an interchange of the targets, the efficiency of the counting devices would only be insignificantly changed, owing to the fact that the experimental error was reduced to 1–2%. When measuring the ratio of the target activities I', an alternate interchange of the targets with a simultaneous commutation of the counting apparatus was also carried out automatically.

The polythene and carbon used did not contain any heavy impurities. It was demonstrated that the γ-activity had a half life of (20.8 ± 0.2) min., which remained constant over a period of several hours. The energy of the γ-rays, measured by the absorption method, was shown to be 0.5 Mev. Thus it was demonstrated that the γ-activity of the targets was associated only with the annihilation of positrons arising from the decay of the C_6^{11} nucleus.

3. EXPERIMENTAL RESULTS

Determination of the Total Cross Sections

The angular distribution of the π^0 mesons produced in the reactions (I, II) can be represented in

the center of mass system (CMS) of the colliding nucleons as a polynomial in powers of the cosine of the angle of emission of the mesons, ϑ. At proton energies ≈ 600 Mev and less, the terms of the polynomial containing high powers of the cosine must be comparatively small, as at these energies the contribution of final states with large momenta is still small. As was shown in Refs. 19 and 20, the γ-ray angular distribution function $F(\vartheta)$ has in this case a characteristic property: the magnitude of the function at the points $\vartheta^* = \arccos(\pm 1/\sqrt{3})$ is practically independent of the relations between the parameters, which determine the contribution of the various powers of the cosine in the angular distribution. It follows from this that the differential cross section for the production of γ-rays obtained at the "isotropic" angle ϑ^* is related to the magnitude of the total π^0 meson production cross section by

$$\sigma^{\pi^0} = 2\pi\, d\sigma^{\gamma}(\vartheta^*)/d\Omega. \qquad (4)$$

Thus from a measurement of the γ-ray yield at the angle ϑ^*, it is possible to determine the total cross section without carrying out an investigation of the angular distribution.

The above simplifying circumstance was employed in the measurement of the absolute total cross sections for the π^0 meson production reactions (I) and (II). The measurement of the cross section was carried out at an angle of $\theta^* = 33°$, which, for protons with an effective energy of 660 Mev, corresponds to an "isotropic" angle of $\vartheta^* = 55°$ in the CMS. In determining the effective energy, the energy dispersion of the protons bombarding the target was teken into account (see Fig. 2). The absolute differential cross section for the production of γ-rays in carbon at 660 Mev was found to be

$$d\sigma_C^{\gamma}/d\Omega = (8{,}1 \pm 0{,}4)\cdot 10^{-27} \text{ cm}^2/\text{sterad} \qquad (5)$$

At this angle the ratio of the differential cross sections for hydrogen and for carbon was also measured

$$(d\sigma_H^{\gamma}/d\Omega)/(d\sigma_C^{\gamma}/d\Omega) = 0{,}162 \pm 0{,}006.$$

Thus the total cross section for reaction (I) was found to be

$$\sigma_{pp}^{\pi^0}(660) = (3{,}6 \pm 0{,}2)\cdot 10^{-27} \text{ cm}^2.$$

Information about reaction (II) is usually obtained by a difference method, D–H. The cross section for the production of π^0 mesons in deuterium was measured by exposing targets of LiD, Li and C. The "deuterium/carbon" ratio was found to be

$$(d\sigma_D^{\gamma}/d\Omega)/(d\sigma_C^{\gamma}/d\Omega) = 0{,}48 \pm 0{,}05.$$

The total cross section was:,

$$\sigma_{pd}^{\pi^0}(660) = (10{,}6 \pm 1{,}3)\cdot 10^{-27} \text{ cm}^2.$$

Neglecting the nucleon binding in the deuterium nucleus, we find

$$\sigma_{pn}^{\pi^0}(660) = (7{,}0 \pm 1{,}1)\cdot 10^{-27} \text{ cm}^2.$$

Excitation Function

By the above methods, the energy dependence of the total cross section for the production of π^0 mesons by protons in hydrogen and deuterium in the proton energy range 390–660 Mev was obtained. The variation of the proton energy in these experiments was obtained by placing the targets at varying distances from the center of the accelerator. Simultaneously, the angle θ was varied from 33° to 36° in order that the angle of emission of the γ-rays remained equal to the "isotropic" angle $\vartheta^* = 55°$ in the CMS. The spectral efficiency of the γ-telescope was experimentally determined for each value of the energy. As was shown in Ref. 6, the γ-ray spectra are only insignificantly changed upon going from light to heavy elements. Because of this, the spectral efficiency K_γ was the same, within the limits of experimental error, for all the elements at fixed values of E_p and θ. The energy dependence of K_γ and the value of the absorption coefficient μ at various energies are presented below, in Table 1. To each value of μ there is juxtaposed an average γ-ray energy $\bar{E}_p$, for the determination of which the γ-ray absorption data obtained from Ref. 21 was used. Since the absorption coefficient is slightly dependent on $\bar{E}_p$, the obtained value must be only somewhat less than the average energy of the spectrum. Thus, for an energy of 660 Mev at an angle of 0°, we found, using the absorption method $\bar{E}_p = 160 \pm 20$ Mev, while the average energy of the spectrum measured in Ref. 22 was 190 Mev.

The obtained energy dependence of the total cross section for the reactions (I) and (II) is presented in Fig. 7. The errors indicated in Fig. 7 are those of the absolute measurements. Except at 660 Mev, they are everywhere little different from

TABLE 1*

E_p, Mev	270	355	445	550	660
$K_\gamma \cdot 10$	—	—	1.53±0.02	1.57±0.03	1.61±0.02
$\mu \cdot 10^2$ (cm²/gm)	9.20±0.25	9.35±0.33	9.20±0.25	9.56±0.10	9.40±0.17
E_γ (Mev)	100±10	105±15	100±10	115±5	110±10

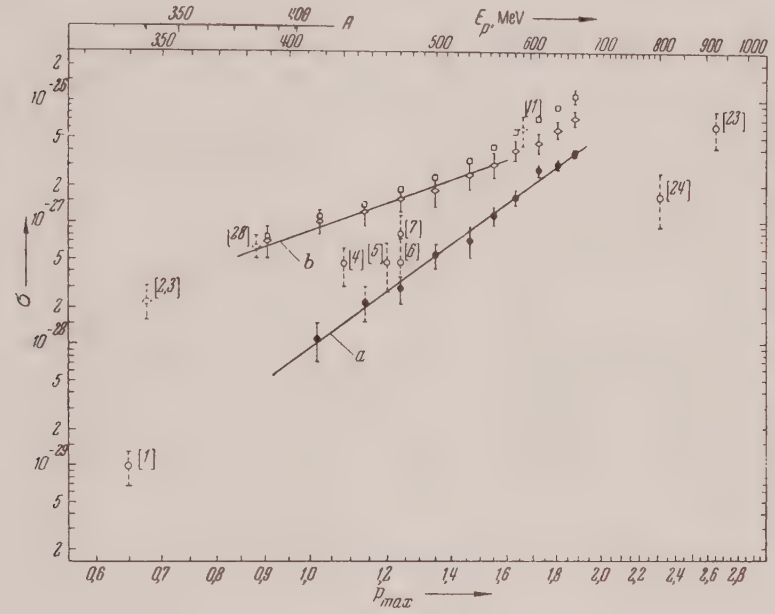

FIG. 7. The total cross sections for reactions (I) and (II). Along the abcissa is the maximum π^0 momentum in units of $m_\pi c$. To the p_{max} scale is compared that of the energy of the protons, for reactions (I) and (II, b), and scale A for reaction (II, a); the curve a is that of $9p_{max}^{5.5} \times 10^{-29}$ cm², $b - 8.2p_{max}^3 \times 10^{-28}$ cm². In this and the following figures, solid lines indicate the results of our work, dashed lines that of others, presented in the references indicated.

the errors in the relative measurements. The values of the cross section $\sigma_{pn}^{\pi^0}$ presented are the differences of the cross sections for deuterium and hydrogen.

The Angular Distribution of the π^0 Mesons

Experiments to investigate the angular distribution of the particles in the final states of the reactions (I) and (II) are of special interest, as they allow one to ascertain the role of various transitions in greater detail than is possible from a study of the excitation functions. Angular measurements usually present complex experimental problems, and in the case of the angular distribution of π^0 mesons one must encounter an additional specific difficulty. It is associated with the fact that knowledge of the angular distribution of π^0 mesons can be obtained only from measurement of the angular (or energy) distribution of the γ-rays from the decay of the π^0 mesons. The angular distribution of the γ-rays and the π^0 mesons are connected by relations, the analysis of which shows that even at very high energies and with an anisotropic distribution of the π^0 mesons, the γ-ray angular distribution differs comparatively little from isotropic. Only at π^0 meson energies > 200 Mev does the angular distribution of the γ-rays approach that of the π^0 mesons. Thus, if the π^0 meson angular distribution is proportional to $\cos^2\vartheta$, then 50% of the γ-ray distribution is anisotropic at a proton energy of 660 Mev, and at 340 Mev already 10% of the total is. Therefore, when conducting experiments to investigate

*The magnitude of K_γ is given in Tables 1 and 2 for a lead converter of thickness 0.2 cm.

the angular distribution of the π^0 mesons, high accuracy is required, which requirement becomes all the more strict the lower the energy of the π^0 mesons.

As was already noted earlier, high powers of the cosine must be weakly represented in the π^0 meson angular distribution; to a first approximation, the angular distribution is of the form $a/3 + b\cos^2\vartheta$. To determine the ratio a/b, it is sufficient to compare the yield of γ-rays at two angles. By way of such angles, we chose θ^* and its complement $\pi - \theta^*$. The switch from θ^* to $\pi - \theta^*$ was accomplished by a change in the direction of rotation of the internal proton beam. Under these circumstances, naturally, the geometry of the experiment remained the same. The investigation of the π^0 angular distribution was carried out in the energy interval 450–660 Mev. When varying the proton energy, the angle ϑ_2 in the CMS, corresponding to the angle $\pi - \theta^*$, changed somewhat from 160° at 660 Mev to 157° at 400 Mev.

Since the efficiency of the γ-telescope depends on the spectrum of the γ-rays, it was measured for each value of the energy and angle of observation. Table 2 lists the values of the spectral efficiency K_γ, the absorption coefficient μ, and the effective energies E_γ obtained at the proton energy 660 Mev. In the next to last row are given, for comparison, the magnitudes of μ calculated from the γ-ray spectra measured in Ref. 22.

TABLE II

ϑ°	0	33	90	147	180
$K_\gamma \cdot 10$	1.70±0.03	1.61±0.03	1.45±0.06	1.32±0.04	1.34±0.02
$\mu \times 10^2$ (cm^2/gm)	10.1±0.1	9.40±0.17	8.84±0.15	8.6±0.3	8.95±0.15
μ [22]	9.9±0.1	—	—	—	8.7±0.1
E_γ, Mev	160±20	110±10	82±10	75±15	85±10

The ratio of the γ-ray yields for reaction (I), measured at 55° and 160° in the CMS and at proton energy 660 Mev, was found to be

$$\eta_{pp}(660) = 0.99 \pm 0.04.$$

From this it follows that the π^0 meson angular distribution is:

$$f_{pp}(660) \sim {}^1/_3 + (0.01 \pm 0.06)\cos^2\vartheta.$$

Similar measurements were also carried out at lower energies (Table 3).

TABLE III

E_p (Mev)	445	500	555	610	660
η_{pp}	0.80±0.09	0.72±0.12	0.76±0.13	0.93±0.12	0.99±0.04
$f_{pp}(\vartheta) \sim$	$\left(0.3^{+0.6}_{-0.3}\right) + \cos^2\vartheta$	$\left(0.2^{+0.5}_{-0.2}\right) + \cos^2\vartheta$	$\left(0.3^{+1.1}_{-0.3}\right) + \cos^2\vartheta$	${}^1/_3 + (0.1 \pm 0.4)\cos^2\vartheta$	${}^1/_3 + (0.01 \pm 0.06)\cos^2\vartheta$

The angular distribution of the π^0 mesons in reaction (II) was measured at 660 Mev with less accuracy than was the case for hydrogen:

$$\eta_{pn}(660) = 0.98 \pm 0.17.$$

It follows from this that

$$f_{pn}(660) \sim {}^1/_3 + (0.0 \pm 0.6)\cos^2\vartheta.$$

Similar measurements at 445 Mev gave

$$\eta_{pn}(445) = 0.90 \pm 0.25.$$

The large experimental error in the last instance does not permit the determination of the coefficient b in a distribution of the type ${}^1/_3 + b\cos^2\vartheta$.

4. DISCUSSION

The p + p → π^0 + p + p *Reaction*

In the energy region 400–660 Mev the total cross section for reaction (I) measured by us goes, on the average, as $\sigma_{pp}^{\pi^0} \sim p_{max}^{5.3 \pm 0.5}$, where p_{max} is the maximum momentum of the π^0 in the CMS in units of the π^0 meson mass $m_\pi c$. As can be shown, it follows from this

that the transition matrix element for reaction (I) in the indicated energy region varies directly as the momentum of the meson. This result differs from that obtained in Ref. 7, where the energy dependence of the differential cross section for reaction (I) at an angle ≈90° in the CMS was measured. If one considers the data in Table 3 concerning the angular distribution of the π^0 mesons, then, from the energy dependence given in Ref. 7, it follows that the excitation function for the total cross section for reaction (I) goes as $\sigma_{pp}^{\pi^0} \sim p_{\max}^4$. This is not in agreement with the dependence obtained by us. Correspondingly, our conclusions as to the nature of the variation of the matrix element with the momentum of π^0 are also different.

In the energy interval 600-660 Mev some slowing down of the rate of increase of the matrix element for reaction (I), which becomes appreciable at higher values of the energy is observed. A comparison of our results with recently published data [23] indicates that in the region of 700-800 Mev the matrix element goes through a maximum.

As is seen from Fig. 7, the magnitude of the cross section for reaction (I), determined by us in the energy region 420-480 Mev, is on the average two times less than that measured earlier[4-7]. From a comparison of our cross sections with that obtained at 340 Mev[1], it follows that in this energy interval $\sigma_{pp}^{\pi^0}$ increases as $p_{\max}^{5.5 \pm 1.5}$, and not as $p_{\max}^8$.[25] This implies that, in reaction (I), along with the Pp transition* (which goes as $\sim p_{\max}^8$), the Ss transition, the intensity of which is weakly dependent on energy ($\sim p_{\max}^2$), plays a very appreciable role. The variation of the cross section (I) with energy in the region 340-400 Mev can be represented as follows:

$$\sigma_{pp}^{\pi^0} = (0{,}025\, p_{\max}^2 + 0{,}12\, p_{\max}^8) \cdot 10^{-27} \text{ cm}^2.$$

The Ss transition can be appreciable only near threshold; with an increase in energy, the relative contribution of this transition quickly decreases, and at energies ≈ 400 Mev the transition in the Pp state is the principal one. The contribution to the reaction from the Ps transition is, apparently, not large. In view of this, the angular distribution of the π^0 mesons, obtained by us at 445 Mev and exhibiting an appreciable anisotropy, is affirmed.

*Here the letters indicate, respectively, the orbital angular momenta of the nucleons (in the nucleon-nucleon system) and of the pion.

The p + n → π^0 + p + n *Reaction*

At proton energies less than 400 Mev, the reaction (II, a) in which a deuteron is created in the final state, is the main contributor. Near threshold it is characterized by a cross section that goes as $\sim p^3_{\max}$.[25] An analysis of the angular[26] and energy[22] distribution of the γ-rays produced in light nuclei by 450-480 Mev protons, indicate that, at these energies, the angular distribution of the π^0 mesons in reaction (II) is appreciably anisotropic. Together with the energy dependence obtained by us

$$\sigma_{pn}^{\pi^0} = (8{,}7 \pm 1{,}5)\, p_{\max}^{3{,}0 \pm 0.5} \cdot 10^{-27} \text{ cm}^2,$$

This attests to the fact that at 450 Mev and lower, the transition with a final S state for the nucleons and p state for the π^0 meson is the principal one for reaction (II).

With an increase of the energy in (II), reaction (II, b), proceeding without the production of a deuteron, begins to predominate (Fig. 8). The presence of three particles in the final state of the last reaction must lead to a stronger dependence of the statistical factor on the momentum of the π^0 meson.

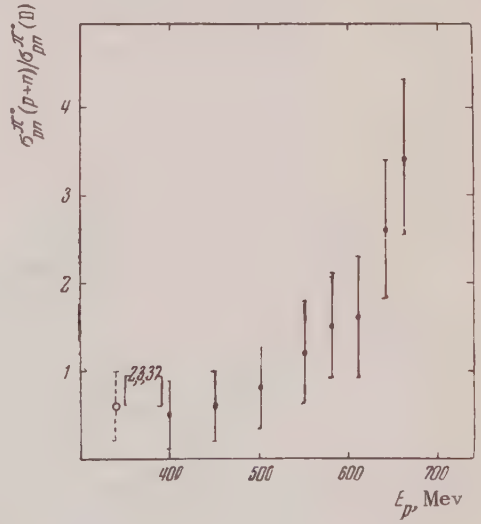

FIG. 8. The ratio of the cross sections for π^0 meson production in reactions (II, b) and (II, a) at various proton energies. The cross section $\sigma_{pn}^{\pi^0}(D)$ is gotten from the equation $2\sigma_{pn}^{\pi^0}(D) = \sigma_{pp}^{\pi^0}(D)$. The data used is that of Ref. 27.

There is, apparently, associated with this a more rapid growth of the cross section $\sigma_{pn}^{\pi^0}$ in the energy region 550-660 Mev than at lower energies. The relatively slow rate of increase of the cross section

$\sigma^{\pi^\circ}_{pn} = \sigma^{\pi^\circ}_{pd} - \sigma^{\pi^\circ}_{pp}$ in the low energy region can also be partially due to the presence of internal motion of the nucleons in the deuteron; with a decrease in the energy, this factor should play an increasingly significant role. At an energy ≈400 Mev the influence of the nucleon binding in the deuteron is, apparently, still not large, since the cross section obtained by us at 385 Mev agrees well with the π° production cross section in *n-p* collisions at 380 Mev recently published by Rosenfeld *et al.*[28]

Production of π° Mesons by Protons of Energy ~600 Mev

A comparison of the magnitudes of the relative cross sections for hydrogen and deuterium measured by us, shows that in the energy region up to 600 Mev the ratio $\sigma^{\pi^\circ}_{pp}/\sigma^{\pi^\circ}_{pn}$ increases rapidly, reaches a magnitude of ½ and remains constant upon further increasing the energy (Fig. 9). As Lapidus[29] has shown, the ratio of the cross sections for the reactions (I) and (II) must equal ½ if, in the final state of these reactions, the meson-nucleon system has an isotopic spin of $T = 3/2$. The data, presented in Fig. 9, shows that, in the 600–660 Mev energy region, the $T = 3/2$ transition is apparently the principal one.

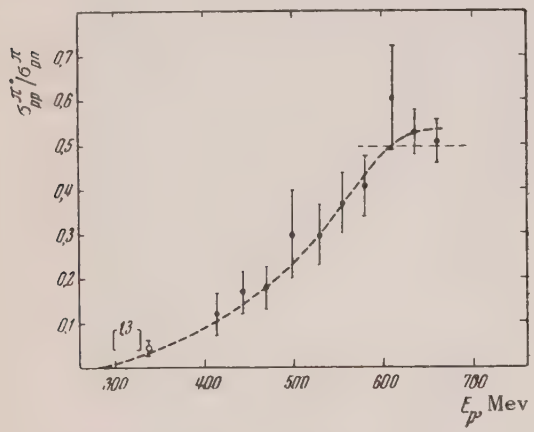

FIG. 9. The ratio of the cross sections for reactions (I) and (II) as a function of energy.

We can also arrive at this conclusion if we consider the energy dependence of the ratio of the cross section $\sigma^{\pi^\circ}_{pp}/\sigma^{\pi^+}_{pn}$ (see Fig. 10). The rate of increase of this ratio is retarded at 600 Mev and thereafter approximately constant and close to ⅕ over a broad energy interval. As was shown in Refs. 29 and 30, such a ratio occurs if $T = 3/2$ for the meson-nucleon system in the final state of the indicated reactions.

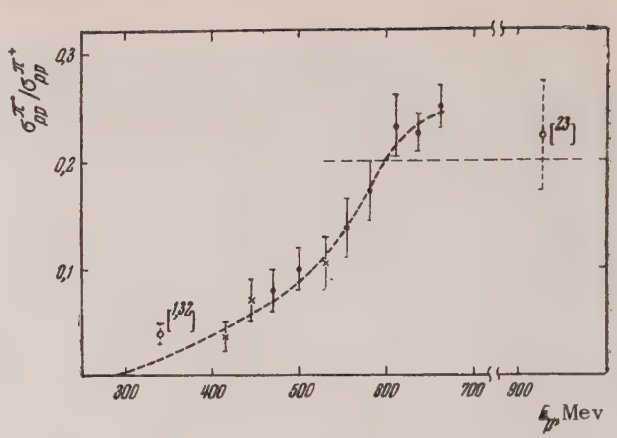

FIG. 10. The ratio of the cross sections for the production of neutral and charged pions in *p-p* collisions at various energies: • indicate values obtained from a comparison of our results with those of Refs. 27 and 31; the data of Refs. 33 and 34 were used for the values marked ×.

The data given in Table 3 indicate that, with increasing energy, the angular distribution of the π° mesons becomes more and more isotropic, and at a proton energy of 660 Mev, the anisotropic portion of the π° distribution does not exceed 7%. For reaction (II) there occurs a similar transition from an anisotropic to an isotropic angular distribution with increasing collision energy. Such a change in the angular distribution is, apparently, associated with the fact that the more the energy is increased, the increasingly larger a role is played by a "resonance" transition in which the mesons interact strongly with one of the nucleons in the final state ($T = 3/2$, $J = 3/2$), and the orbital angular momentum of the second nucleon is equal to zero. The disintegration of such a system, and consequently the emission of the π° mesons, takes place isotropically.

Thus, all the conclusions from the above experimental data favor the assumption of a preeminent role for resonance transitions ($T = 3/2$, $J = 3/2$) in the energy region ≈600 Mev.

At proton energies 340–480 Mev, the pions are created for the most part with energies close to the maximum possible, as a consequence of the fact that the nucleons in the final states interact relatively strongly. In Refs. 8 and 22 it was established that when the proton energy is increased to 660 Mev, there occurs a relative "smearing" of the spectrum of the γ-rays from the decay of the π° mesons. The π° mesons, at this proton energy, carry away on the average only about half of the maximum possible energy.

If, when going from 450 to 660 Mev, the portion of the energy being carried away by the mesons were to remain unchanged, then the average energy

of the γ-rays counted at 33° and at proton energies of 450, 560 and 660 Mev would be, respectively, 100, 120 and 145 Mev. A comparison of these values with the data in Table 1 indicates that the "smearing" of the π^0 spectrum occurs in the proton energy region of 560–660 Mev. It is possible that the indicated change in the nature of the π^0 spectrum is also a consequence of the strong interaction in the meson-nucleon system.

Comparison with the Production Cross Sections for Charged Pions

The total π^0 production cross sections obtained by us allow one to make, within the limits of the charge independence hypothesis, a crude estimate of the production cross section for charged mesons where the latter are unknown. Thus, the inequality

$$^1/_2\,\sigma_{pp}^{\pi^0} \leqslant \sigma_{pn}^{\pi^+} \leqslant \sigma_{pn}^{\pi^0} + {}^1/_2\,\sigma_{pp}^{\pi^0} \qquad (5)$$

permits one to estimate the cross section $\sigma_{pn}^{\pi^+} = \sigma_{pn}^{\pi^-}$ at 660 Mev, experimental data about which is as yet lacking:

$$(1.8 \pm 0.1)\cdot 10^{-27}\ \text{cm}^2 \leqslant \sigma_{pn}^{\pi^-} \leqslant (8.8 \pm 1.1)\cdot 10^{-27}\ \text{cm}^2.$$

The magnitude of the cross section $\sigma_{pn}^{\pi^+}$ can be determined by means of a comparison of our results with the data of Refs. 27 and 31 if one uses the identity $\sigma_{pn}^{\pi^+} = \sigma_{pn}^{\pi^0} + \sigma_{pp}^{\pi^0} - (^1/_2)\sigma_{pp}^{\pi^+}$:

$$\sigma_{pn}^{\pi^+}(660) = (3.5 \pm 1.3)\cdot 10^{-27}\ \text{cm}^2.$$

TABLE IV

E_p (MeV)	400[35]	500	555	580	610	640	660
$\sigma_{pn}^{\pi^+} \times 10^{27}$, cm^2	0.16±0.04	⩽0.6	⩽0.8	0.8±1.1	1.6±1.1	2.1±1.2	3.5±1.3

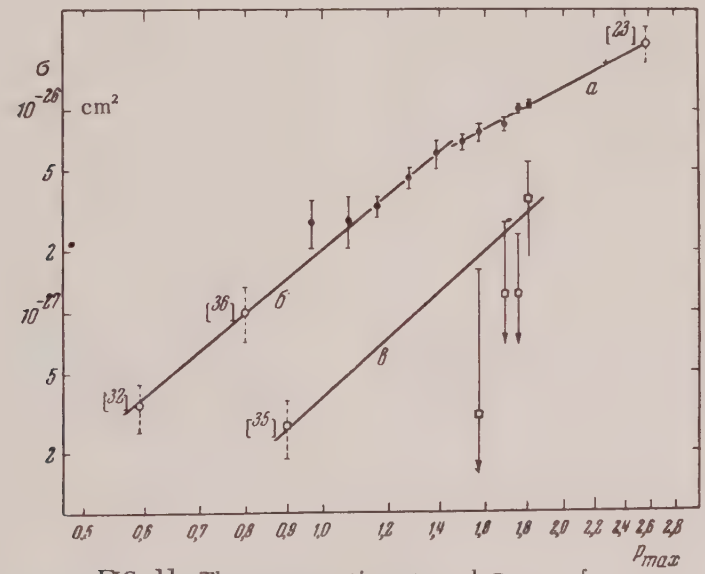

FIG. 11. The cross sections σ_{01} and σ_{10} as a function of the maximum pion momentum. The curve *a* is that of $3p_{max}^2 \times 10^{-27}$ cm^2, *b*–$2p_{max}^{3.2} \times 10^{-27}$ cm^2 and *c*–$3.6p_{max}^{3.5} \times 10^{-28}$ cm^2. In constructing the abcissa scale, the values of the pion masses used were: $m_{\pi^0} = 134.8$ Mev and $m_{\pi^+} = 139.3$ Mev.

Comparison with the data presented in a paper by G. Yodh[35] indicates that this cross section increases rapidly with increasing energy:

If one approximates the energy dependence of the

cross section by a function $\sim p_{max}^{\alpha}$, then in the energy region below 650 Mev, we have $\sigma_{pn}^{\pi^+} = (0.3 \pm 0.1)\, p_{max}^{4\pm1} \times 10^{-27}$ cm².

Partial Cross Sections

Within the bounds of the charge-independence hypothesis all the cross sections for pion production in nucleon collisions can be represented as a linear combination of three partial cross sections σ_{02}, σ_{11} and σ_{10} (the notation of Ref. 25 is used here; the indices denote the magnitudes of the isotopic spins of the nucleons in the initial and final states). Using our data and that of Refs. 27 and 31, it is possible to determine the magnitude of these cross sections at the proton energy 660 Mev:

$$\sigma_{11} = (3{,}6 \pm 0{,}2) \cdot 10^{-27} \text{ cm}^2,$$

$$\sigma_{01} = (3{,}6 \pm 1{,}8) \cdot 10^{-27} \text{ cm}^2,$$

$$\sigma_{10} = (10{,}6 \pm 0{,}6) \cdot 10^{-27} \text{ cm}^2.$$

The cross section $\sigma_{11} = \sigma_{pp}^{\pi^\circ}$ at various energies has been determined above (see Fig. 7).

A comparison of the magnitudes of the cross section σ_{01} at various energies indicates (Fig. 11) that σ_{01} varies as $p_{max}^{3.5\ \pm 1.0}$, which is in good agreement with the conclusions of Rosenfeld[25].

The reaction $T_N = 1 \rightarrow T_N = 0$ is characterized by a slower rate of increase of the cross section with energy (see Fig. 11). In the region up to 580 Mev, the cross section σ_{10} is proportional to the third power of the momentum,

$$\sigma_{10} = (2{,}0 \pm 0{,}4)\, p_{max}^{3{,}2\pm0{,}6} \cdot 10^{-27} \text{ cm}^2$$

in agreement with Ref. 25. At higher values of the energy, the rate of increase of the cross section is retarded and in the 550–1000 Mev region can be written as

$$\sigma_{10} = (3{,}0 \pm 0{,}2)\, p_{max}^{2{,}0\pm0{,}4} \cdot 10^{-27} \text{ cm}^2.$$

From a comparison of the data of Refs. 38 and 39, it follows that in the energy region ≈1000 Mev the cross section σ_{10} goes through a broad maximum and thereafter slowly decreases with increasing proton energy.

In conclusion, we take the opportunity to express profound thanks to M. S. Kozodaev, B. M. Pontecorvo and L. I. Lapidus for the discussion of our results. We are indebted to M. M. Kuliukin for his aid in the construction of the apparatus.

[1] J. Mather and E. Martinelli, Phys. Rev. **92**, 780 (1953).
[2] R. Hales and B. Moyer, Phys. Rev. **89**, 1047 (1953).
[3] W. Crandall and B. Moyer, Phys. Rev. **92**, 749 (1953).
[4] Marshall, Marshall, Nedzel, and Warshaw, Phys. Rev. **88**, 632 (1952).
[5] Pontecorvo, Selivanov, and Zhukov, Report, p. 81, Inst. Nucl. Prob. Acad. Sci. (U.S.S.R.) (1952).
[6] Kozodaev, Tiapkin, Baiukov, Markov, and Prokoshkin, Izv. Akad. Nauk SSSR, ser. fiz. **19**, 589 (1955).
[7] L. Soroko, J. Exptl. Theoret. Phys. (U.S.S.R.) **30**, 296 (1956); Soviet Physics JETP **3**, 184 (1956).
[8] Tiapkin, Kozodaev, and Prokoshkin, Dokl. Akad. Nauk SSSR **100**, 689 (1955).
[9] R. Hildebrand, Phys. Rev. **89**, 1090 (1953).
[10] Iu. Prokoshkin and G. Tentiukova, Pribory i Tekhn. Eksper. (Instr. and Exptl. Engg.) (in press).
[11] Dzhelepov, Oganesian, and Fliagin, J. Exptl. Theoret. Phys. (U.S.S.R.) **29**, 886 (1955); Soviet Physics JETP **2**, 757 (1956).
[12] M. Kuliukin, Report, Inst. Nucl. Prob. Acad. Sci. (U.S.S.R.) (1955).
[13] W. Siri, *Isotopic Tracers and Nuclear Radiations*, New York, (1949).
[14] B. Rossi and K. Greisen, Rev. Mod. Phys. **13**, 240 (1941).
[15] Hollander, Perlman, and Seaborg, Rev. Mod. Phys. **25**, 469 (1953).
[16] Friedlander, Hudis, and Wolfgang, Phys. Rev. **99**, 263 (1955).
[17] Crandall, Millburn, Pyle, and Birnbaum, Phys. Rev. **101**, 329 (1956).
[18] L. Marquez, Phys. Rev. **86**, 405 (1952).
[19] A. Tiapkin, J. Exptl. Theoret. Phys. (U.S.S.R.) **30**, 1150 (1956); Soviet Physics JETP **3**, 979 (1957).
[20] Iu. Prokoshkin, J. Exptl. Theoret. Phys. (U.S.S.R.) **31**, 732 (1956); Soviet Physics JETP **4**, 618 (1957).
[21] Davis, Bethe, and Maximon, Phys. Rev. **93**, 788 (1954).
[22] Baiukov, Kozodaev and Tiapkin, J. Exptl. Theoret. Phys. (U.S.S.R.) **32**, 677 (1957); Soviet Physics JETP **5**, 552 (1957).
[23] Hughes, March, Muirhead, and Lock, CERN Symposium, 1956.
[24] Morris, Fowler, and Garrison, Phys. Rev. **103**, 472 (1956).
[25] A. Rosenfeld, Phys. Rev. **96**, 139 (1954).
[26] Iu. Prokoshkin and A. Tiapkin, Report, Inst. Nucl. Prob., Acad. Sci. (U.S.S.R.) (1955).

[27] M. Meshcheriakov and B. Neganov, Dokl. Akad. Nauk SSSR **100**, 677 (1955).
[28] Rosenfeld, Solmitz, and Hildebrand, Bull. Am. Phys. Soc. **1**, 72 (1956).
[29] L. Lapidus, Report, Inst. Nucl. Prob., Acad. Sci. U.S.S.R. (1955).
[30] D. Peaslee, Phys. Rev. **95**, 1580 (1954).
[31] B. Neganov and O. Savchenko, Report, Inst. Nucl. Prob., Acad. Sci. U.S.S.R. (1955).
[32] A. Rosenfeld, Phys. Rev. **96**, 146 (1954). (Citation to W. Cartwright.)
[33] Dzhelepov, Moskalev, and Medved', Dokl. Akad. Nauk SSSR **104**, 382 (1955).
[34] N. Bogachev, Dokl. Akad. Nauk SSSR **108**, 806 (1956).
[35] A. Rosenfeld, Phys. Rev., **96**, 146 (1954).
[36] S. Passman, M. M. Block and W. Havens, Phys. Rev. **88**, 1247 (1952).
[37] Clark, Roberts and Wilson, Phys. Rev. **83**, 649 (1951).
[38] Smith, McReynolds, and Snow, Phys. Rev. **97**, 1186 (1955); Lock, March, Muirhead, and Rosser, Proc. Roy. Soc. **A230**, 215 (1955); Duke, Lock, March, Gibson, McKeague, Hughes, and Muirhead, Phil. Mag. **46**, 877 (1955).
[39] Chen, Leavitt and Shapiro, Phys. Rev. **103**, 211 (1956).

Translated by M. Rosen
173

SOVIET PHYSICS JETP VOLUME 5, NUMBER 4 NOVEMBER, 1957

Asymptotic Meson-Meson Scattering Theory

I. T. DIATLOV, V. V. SUDAKOV, AND K. A. TER-MARTIROSIAN

(Submitted to JETP editor December 17, 1955)
J. Exptl. Theoret. Phys. (U.S.S.R.) **32**, 767-780 (February, 1957)

An asymptotic expression for the scattering amplitude for meson-meson interaction has been obtained from a theory of the Landau, Abrikosov, and Khalatnikov type by summation of an infinite number of graphs of a certain class. The problem reduces to an integral equation of a simple type, which can be solved exactly.

1. INTRODUCTION

NOT LONG AGO Landau, Abrikosov, Khalatnikov and Galanin[1,2] developed a new approach to the solution of field theory equations. While assuming that the coupling constant g_0 is small, i.e. $g_0^2 \ll 1$, and investigating the series expansion of all quantities for large momenta in powers of g_0^2 they do not however consider the quantity

$$\varkappa = g_0^2 \ln [\Lambda^2/(-p^2)] = g_0^2 (L - \xi)$$

to be small (in contrast with the assumption used in conventional perturbation theory), here

$$L = \ln (\Lambda^2/m^2) > 1, \quad \xi = \ln (-p^2/m^2) > 1,$$

where Λ is the limit for momentum cut-off and p the momentum pertinent to the problem.

The result is that the asymptotic expressions of different field theory quantities are represented by series of the type:

$$f_0(\varkappa) + g_0^2 f_1(\varkappa) + g_0^4 f_2(\varkappa) + \ldots, \qquad (1)$$

where the $f_n(\varkappa)$ are closed functions. In fact, the above authors[1,2] used the integral equations of field theory to construct the $f_0(\varkappa)$ term of the zero approximation for the case of a series expansion of the Eq. (1) type for propagation functions and functions for the vertex parts in quantum electrodynamics[1] and mesodynamics[2].

Essentially the condition that $g_0^2 < 1$ is not necessary for the existence of an expansion in a series of the Eq. (1) type. As has been shown by Pomeranchuk[3], when one introduces two cut-off limits[4]

$$L_p = \ln (\Lambda_p^2/m^2), \quad L_p > L_k \gg 1$$

then in all equations and in particular in Eq. (1), g_0^2 is replaced by the quantity

$$\tilde{g}_0^2 = g_0^2 [1 + (g_0^2/\pi)(L_p - L_k)]^{-1}, \qquad (2)$$

which can be as small as one likes for any g_0^2, provided that $(L_p - L_k)/\pi$ is large enough. Thus, when $(L_p - L_k)/\pi \to \infty$ the series in Eq. (1) converges as quickly as one may like, and its zero term is in fact an exact solution.*

From the standpoint of an expansion in a series like Eq. (1), the amplitude of meson-meson scattering is a quantity of the order of g_0^2 (or $\tilde{g}_0^2$ when there are two limits). Actually, the corresponding quantity for the simplest graphs in Fig. 1 has a value proportional to the product of g_0^4 and a logarithmically divergent integral of the type $\int d^4p/p^4 \sim L$ *i.e.*, a value on the order of g_0^2 [since $g_0^2 L = g_0^2(g_0^2 L)$].

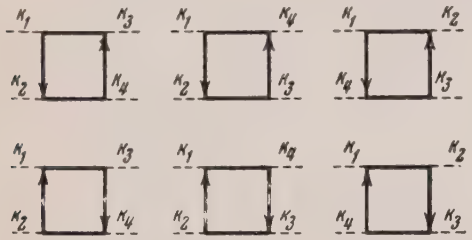

FIG. 1

Accurate computation, with inclusion of only the most important logarithmic part of the resultant integral**, shows that when the momenta are large, the sum of the contributions from the graphs in Fig. 1 depends only on the largest momentum, k, of the four momenta k_1, k_2, k_3, k_4 of the mesons, *i.e.*,

$$-k^2 = \max(-k_1^2, -k_2^2, -k_3^2, -k_4^2)$$

and can be written as

$$\times(k_1, k_2, k_3, k_4) \approx (g_0^2/4\pi i) R_0 [g_0^2 (L - \xi)], \qquad (3)$$

where for the neutral pseudoscalar theory

$$R_0 = 24(1 - Q^{-1/5}), \qquad (3a)$$

$$Q = 1 + (5g_0^2/4\pi)(L - \xi) \qquad (4)$$

and analogously* for the symmetrical pseudoscalar theory

$$R_0 = \rho_0 \delta_c, \quad \rho_0 = \frac{16}{30}[Q^{3/5} - 1], \qquad (3b)$$

with the quantity

$$\delta_c = \delta_{\xi_1\xi_2}\delta_{\xi_3\xi_4} + \delta_{\xi_1\xi_3}\delta_{\xi_2\xi_4} + \delta_{\xi_1\xi_4}\delta_{\xi_2\xi_3} \qquad (5)$$

being dependent of indices (or variables) ξ_i of the isotopic spin ($i = 1, 2, 3, 4$) of the four mesons ($\xi_i = 1, 2, 3$). It is noteworthy that electrodynamics differs from the pseudoscalar meson theory in that the logarithmically divergent part is eliminated when the contributions from the graphs in Fig. 1 are summed, so that they have a value of the order of e_0^4 (rather than of the order of e_0^2 as for the e_0^2 ($e_0^2 L$) type).

All of the more complicated graphs for meson-meson scattering can be categorized as "reducible" or "irreducible" to simplest forms (of the type in Fig. 1), if "reducible" is taken to mean those graphs

---

*This is due to the incompleteness of the present theory, according to which, as Pomeranchuk has observed[3], the renormalized charge $g^2 = g_0^2[1 + 5g_0^2 L/4\pi]^{-1}$ becomes zero when $L \to \infty$. Actually, if all the quantities in series (1) are renormalized, i.e. $fn(x) = Z_n(g^2 L) f_n(g^2 \xi)$, then we obtain $f_0(g^2\xi) + g^2 f_1(g^2\xi) + g^4 f_2(g^2\xi)$.

When $g^2 \to 0$ only the term f_0 is significant.

**If we include values for the propagation functions and vertex parts as given in Ref. 2 we have: $D(k) = d/k^2$, $G(k) = \beta/k$, $\Gamma_5 = \alpha\gamma_5$ where for the symmetrical theory $\alpha = Q^{1/5}$, $\beta = Q^{-3/10}$, $d = Q^{-4/5}$ and analogously for the neutral theory $\alpha = Q^{-1/5}$, $\beta = Q^{-1/10}$, $d = Q^{-2/5}$; Q is determined in Ref. 4.

*For example, the first graph in Fig. 1 has, to within a multiplicative factor $g_0^2/4\pi i$, the value

$$R_0 = (\rho_0/4)\,\mathrm{Sp}(\tau_{\xi_1}\tau_{\xi_2}\tau_{\xi_3}\tau_{\xi_4}),$$

$$\rho_0 = (g_0^2/\pi i)\int \mathrm{Sp}[\Gamma_5 G(p)\,\Gamma_5 G(p + k_1)$$

$$\times \Gamma_5 G(p + k_1 + k_2)\,\Gamma_5 G(p - k_3)]\,d^4p$$

$$(k_1 + k_2 + k_3 + k_4 = 0).$$

We have made use of Feynman's notation where $g_0\Gamma_5$ corresponds to the point, $G(P)$ to the nucleon line, $4\pi i D(k)$ to the meson line, and $\int d^4p/(2\pi)^4$ to the integration $\int dp_0\,dp_1\,dp_2\,dp_3/(2\pi)^4$.

$$\int d^4p/(2\pi)^2 = \int dp_0 dp_1 dp_2 dp_3/(2\pi)^4.$$

By including only the logarithmic region $-k^2 \ll -p^2 \ll \Lambda^2$ or $\xi < z < L$, $z = \log(-p^2/m^2)$ in the integral and changing variables to $q = 1 + (5g_0^2/4\pi)(L - z)$, we obtain

$$\rho_0 = (16/5)\int_1^Q \alpha^4(q)\,\beta^4(q)\,dq$$

$$= (16/5)\int_1^Q q^{-3/5}\,dq = (15/3)(Q^{3/5} - 1),$$

with the sum over the graphs in Fig. 1 of the quantity of the type $\frac{1}{4}\,\mathrm{Sp}(\tau_{\xi_1}\tau_{\xi_2}\tau_{\xi_3}\tau_{\xi_4})$ being equal to δ_c.

that consist only of nucleon squares joined by meson lines and subject to successive simplification to to one of the graphs in Fig. 1. Such simplification consists of substituting, in some sequence, one square for two joined by two meson lines in the complex graph (*e.g.*, the graphs in Fig. 2 are "reducible", while those in Fig. 3 are "irreducible").

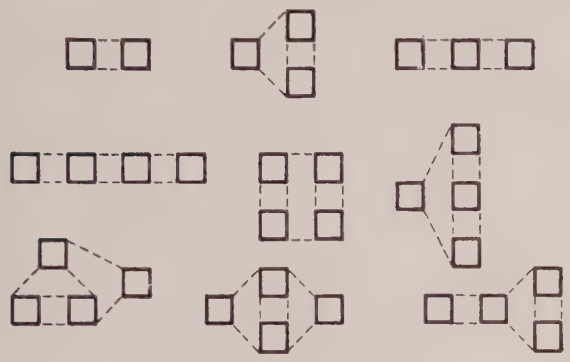

FIG. 2

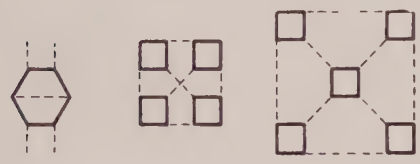

FIG. 3

It is easily seen that such substitutions do not entail any alteration in the order of magnitude of a graph (symbolically, in the sense of a location in an expansion of type (1)), because in this case the number of points on the graph is reduced by four, the number of divergent integrals by two, and the contribution from the graph changes by a factor of the form $g_0^4 (L-\xi)^2 = [g_0^2 (L-\xi)]^2$ which is of the order of unity. Therefore, any "reducible" graph makes a contribution of the same order

$$(g_0^2/4\pi i)\, R_n (k_1, k_2, k_3, k_4)$$
$$\approx (g_0^2/4\pi i)\, R_n [g_0^2 (L-\xi)]$$

(R_n is a dimensionless function and n is the number of the "reducible" graph) as contributions (3), (3a) and (3b) from the simplest graphs in Fig. 1. Analogously, simple calculation shows that "irreducible" graphs* have a value of a higher order in g_0^2. Therefore, if the scattering amplitude is written as

$$(g_0^2/4\pi i)\, P' (k_1, k_2, k_3, k_4),$$

then P' will be represented, when the momenta are large, by a series of type (1)

$$P' = P [g_0^2 (L-\xi)] + g_0^2 Q [g_0^2 (L-\xi)] + \ldots, \quad (6)$$

where the first term P of this expansion (which, as was mentioned above, gives in fact the exact value of the scattering amplitude in meson theory) is determined by the infinite sum of the contributions from all the "reducible" graphs

$$P (k_1, k_2, k_3, k_4) = \sum_{n=0}^{\infty} R_n (k_1, k_2, k_3, k_4). \quad (7)$$

Below we consider the problem of computing this sum (the so-called "parquet" problem) where it is shown that the total sum is determined from a quantity R_0 with the aid of an integral equation, which in the case of large momenta is simple in form and can be solved exactly.

When L is fixed, the magnitude of P proves to be of the same order as that of R_0 (despite the fact that the absolute value of the individual terms of the infinite alternating series, Eq. (7), increases rapidly as n increases), whereby P possesses the usual renormalization property and, in the limit as $L \to \infty$, can be renormalized without introducing interaction terms of the $\lambda \varphi^4$ type in the Hamiltonian.

The "parquet" problem is important for the evaluation of terms left out of the zeroth approximation[2] (in g_0^2), which proves, as Pomeranchuk has shown[4], a zero value for the renormalized charge g. In the theory advanced by Abrikosov, Galanin, and Khalatnikov[2], the equation for the vertex part operator (interaction operator) did not include (besides graphs with intersecting meson lines) graphs of the type shown in Fig. 4a and all the more complicated ones obtained from Fig. 4a by substituting

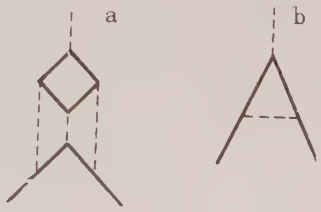

FIG. 4.

*This was noted by Landau and does not apply to electrodynamics, in which, for example (because of the elimination of the divergences in the graphs in Fig. 1), "reducible" graphs even with two squares (Fig. 5) have a value on the order of e_0^2 in comparison with the contribution from the graphs in Fig. 1.

any graph reducible to a square for a nucleon square. When $g_0^2 \ll 1$ or, $g_0^2 \ll 1$ in the theory with two limits, the contribution from the graph in Fig. 4a is small (it contains an extra factor $(g_0^2/4\pi i)\, R_0$, of the order of g_0^2 in comparison with the contribution by the graph in Fig. 4b which was calculated by Abrikosov, *et al.*[2]). However, the evaluation of the total contribution by all of the more complicated graphs of the type shown in Fig. 4a, but with the square replaced by a complex graph of meson-meson scattering, depends essentially on the value of the sum $P = \sum_{n=0}^{\infty} R_n$ (if this sum should turn out to be divergent, it is not permitted to neglect all the graphs of the type shown in Fig. 4a).

To avoid the difficulty of computing the sum $P = \sum_{n=0}^{\infty} R_n$ in order to evaluate the contribution by all graphs of the type shown in Fig. 4a, Pomeranchuk analyzed a special type of limit process for point interaction, in which $L_k/(L_p - L_k) \to 0$ as $L_k \to \infty$. In this case, all the complex graphs of meson-meson scattering (including the "reducible" ones) yield in the limit a contribution infinitely small in comparison with the simplest graphs shown in Fig. 1. For example, the contribution from graphs of the type a, b, c shown in Fig. 5 contains, in comparison with Eq. (3), twice the factor $g_0^2 = \pi/(L_p - L_k) \to 0$ and two divergent integrals over the nucleon and meson momenta that give the factor $L_p\, L_k$, so that the total is a factor of the order of

$$L_p L_k (\tilde{g}_0^2)^2 \sim L_p L_k / (L_p - L_k)^2 \sim L_k / L_p \to 0,$$

which goes to zero when $L_k \to \infty$. In the limit $P = R_0$, i.e. the sum of the contributions from all of the complex graphs of the type shown in Fig. 4a coincides with the contribution from a single simple graph of the type shown in Fig. 4a.

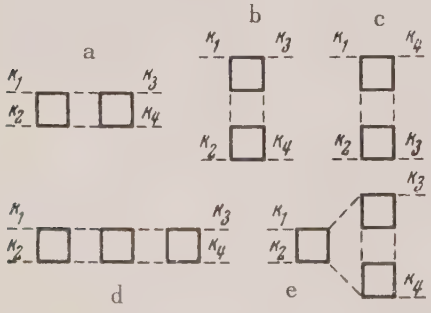

FIG. 5.

The conclusion obtained below concerning the finiteness of P is in agreement with Pomeranchuk's result which shows that the prediction that renormalized charge becomes zero in the pseudoscalar theory holds true not only for a special type of transition to the limit, *i.e.*, where $L_p/(L_p - L_k) \to 0$, but also for a more general case (if the sum P is a quantity of the same order as R_0, then the contribution from all graphs of the type shown in Fig. 4a is a quantity of the order of g_0^2 in comparison with the contribution from Fig. 4b and it may be disregarded if $g_0^2 \ll 1$, *i.e.*, if $[\pi/(L_p - L_k)]$ is sufficiently small as $L_k \to \infty$.

2. THE EXACT INTEGRAL EQUATION

We shall show that the sum (7) of the contribution by all of the "reducible" graphs* satisfies an exact integral equation whose form depends only on the value $R_0(k_1, k_2, k_3, k_4)$ of the contribution from the simplest graphs in Fig. 1.

First we shall introduce the concept of reducible and irreducible graphs and derive a simple general relation (analogous to the Dyson-Schwinger equations for propagation functions or to the Bethe-Salpeter equation), which is satisfied by the total contribution $P'(k_1, k_2, k_3, k_4)$, Eq. (6), of all general "reducible" and "irreducible" graphs.

Let us examine an arbitrary meson-meson scattering graph and call it reducible as regards the separation of meson lines ("ends") k_1 and k_2 from k_3 and k_4, if it can be divided, at least in one certain manner, into two parts connected with one another by only two meson lines, with the division made in such a way that lines k_1 and k_2 approach one part and k_3 and k_4 the other (*e.g.*, the graphs in Fig. 5a, d,e, are reducible). We shall call graphs that do not possess this property irreducible relative to "separation" of k_1, k_2 from k_3, k_4 (*e.g.*, the graphs in Fig. 1 and Fig. 5b, c).

One and the same graph, depending on how the meson lines approach it, can be reducible or irreducible relative to the separation of k_1, k_2 from k_3, k_4 (the graph in Fig. 5a is reducible, while 5b and 5c are irreducible).

Let us designate by $R'(k_1, k_2, k_3, k_4)$ the sum of

*Henceforth, to simplify the notation, we shall neglect the factor $(g_0^2/4\pi i)$, *i.e.*, we shall assume the contribution by the graph for meson-meson scattering to be a value determined in accordance with Feynman's rules and multiplied by $(4\pi i/g_0^2)$.

the contributions from all of the graphs generally irreducible in the indicated sense, and by $F'(k_1, k_2, k_3, k_4)$ the sum of the contributions from all of the reducible ones. Since any graph is either reducible or irreducible, it is obvious that

$$P'(k_1, k_2, k_3, k_4) = R'(k_1, k_2; k_3, k_4) + F'(k_1, k_2; k_3, k_4). \quad (8)$$

The quantity P' is symmetrical for any transposition of the meson lines, and the values of R' and F' in Eq. (8) are unchanged if k_1 and k_2 or k_3 and k_4 are transposed or if k_1 and k_2 are interchanged with k_3 and k_4 (because they include a contribution from all of the graphs). For example, R' includes a contribution from both the graph in Fig. 5b and that in 5c (the latter differs from 5b in the transposition of k_3 and k_4), so that one may write

$$R'(k_1, k_2; k_3, k_4) = R_1'(k_1, k_2; k_3, k_4) + R_1'(k_1, k_2; k_4, k_3), \quad (9)$$

where the quantity $R_1'(k_1, k_2; k_3, k_4)$ includes the irreducible graphs only for arrangement of lines k_3 and k_4 (thus, R' includes both graphs in Fig. 5b, 5c, while $R_1'(k_1, k_2; k_3, k_4)$ includes only one of them, *e.g.*, Fig. 5b).

In this case, it is not difficult to see that P' and R' are connected by the following integral equation

$$P'(k_1, k_2, k_3, k_4) = R'(k_1, k_2, k_3, k_4) - (g_0^2/2\pi i)\int R'(k_1, k_2; l, l') \times D(l) D(l') P'(-l, -l', k_3, k_4)\, d^4l, \quad (10)$$

where $-l' = l + k_1 + k_2$, D is the meson propagation function, and $d^4l = dl_0 dl_1 dl_2 dl_3/4\pi^2$.

In order to check the correctness of this relation, let us examine an arbitrary reducible graph (relative to the separation from k_1, k_2 and from k_3, k_4) and select the point of separation such that the part adjoining k_1, k_2 is already reducible as regards the separation of k_1, k_2 from meson lines l and l', which connect both parts of the graph. Let us use $\rho_n'(k_1, k_2; l, l')$ to designate the contribution from the part of the (irreducible) graph adjoining lines k_1, k_2 (we assume all graphs to be renumbered, with index n indicating the graph number in the part adjoining k_1, k_2) and $\sigma_m'(-l, -l', k_3, k_4)$ to designate the contribution from the part (of number m) adjacent to k_3 and k_4.* Then the form of the reducible graph under consideration will be determined by the two numbers n and m, and the corresponding contribution $fnm(k_1, k_2; k_3, k_4)$ can be written as

$$f_{nm}'(k_1, k_2; k_3, k_4) = -(g_0^2/\pi i)\int \rho_n'(k_1, k_2; l, l') D(l) D(l') \times \sigma_m'(-l, -l', k_3, k_4)\, d^4l. \quad (11)$$

The factor $-(g_0^2/\pi i)d^4l$ is the product of the quantities $g_0^2(4\pi i$ from the definition of the contribution from the graph (*cf.*, footnote, p. 634), $(4\pi i)^2$ from the two meson lines, and $d^4l/4\pi^2$ from the integration over the meson momentum.

Let us now sum both sides of Eq. (11) over all numbers n, m (*i.e.*, over all of the graphs); it is now obvious that

$$\sum_m \sigma_m'(-l, -l', k_3, k_4) = P'(-l, -l', k_3, k_4), \quad (12)$$

since any particular graph may be adjacent to k_3 and k_4. By the same token

$$\sum_n \rho_n'(k_1, k_2; l, l') = R'(k_1, k_2; l, l'), \quad (13)$$

since only irreducible graphs are, by definition, adjacent to k_1 and k_2. Furthermore, it is evident that

$$\sum_{n,m} f_{nm}'(k_1, k_2; k_3, k_4) = 2F'(k_1, k_2; k_3, k_4); \quad (14)$$

the factor 2 appears because half of all the graphs from the sum in Eq. (13) that enter into $R_1'(k_1, k_2; l, l')$ will, on account of the symmetry of P' in l and l', give exactly the same set of all reducible graphs as will the other half of the sum in Eq. (12), which enters into $R_1'(k_1, k_2; l', l)$.

By utilizing equalities (12) to (14) we obtain, after summing both halves members of (11) over n and m,

*Since k or l always represent the momentum *entering* into any graph, then $k_1 + k_2 + l + l' = -l - l' + k_3 + k_4 = 0$, while the momenta l and l', which enter into the part adjacent to k_1 and k_2, *come out* of the other part and are written in σ_m' with a minus sign.

$$F'(k_1, k_2; k_3, k_4) = -(g_2^0/2\pi i)\int R'(k_1, k_2; l, l') \times D(l)\, D(l')\, P'(-l, -l', k_3, k_4)\, d^4l. \quad (15)$$

It is obvious that Eq. (15) together with Eq. (8) gives Eq. (10).

Now let us consider only the "reducible" graphs and designate by P, R and F the corresponding sums determined by them only. With respect to these graphs, all of the considerations that led to Eq. (8), (15) and (10) can be repeated literally; in an analogous fashion we obtain

$$P(k_1, k_2, k_3, k_4) = R(k_1, k_2; k_3, k_4) + F(k_1, k_2; k_3, k_4), \quad (16)$$

$$F(k_1, k_2; k_3, k_4) = -(g_0^2/2\pi i)\int R(k_1, k_2; l, l')\, D(l) \times D(l')\, P(-l, -l', k_3, k_4)\, d^4l.$$

These relations permit one to solve the problem stated above, if one bears in mind that the "reducible" graph, if it is not the simplest one (Fig. 1), is necessarily reducible as regards the separation of any one pair of meson lines from another,

k_1, k_2 from k_3, k_4, or k_1, k_3 from k_2, k_4, or k_1, k_4 from k_2, k_3.

Actually, the "reduction" process makes it possible to bring any reducible graph to the form of Fig. 5a, 5b or 5c, where that which has been said becomes obvious.* In accordance with this, all reducible complex graphs fall into three classes, and their contribution is contained either in $F(k_1, k_2; k_3, k_4)$, in $F(k_1, k_3; k_2, k_4)$, or in $F(k_1, k_4; k_2, k_3)$ (the contribution from each reducible graph belongs in one and only one of these three functions, because if a graph is reducible as regards the separation of any one pair of lines from another, it is then irreducible to any other division of meson lines into pairs. This is made clear by any analysis of the graphs a, b, c in Fig. 5 to which any complex reducible graph may be "reduced"). Therefore, by including the independent contribution R_0 from the simplest graphs in Fig. 1 we obtain

$$P(k_1, k_2, k_3, k_4) = R_0(k_1, k_2, k_3, k_4) + F(k_1, k_2; k_3, k_4) + F(k_1, k_3; k_2, k_4) + F(k_1, k_4; k_2, k_3). \quad (17)$$

Taken with Eq. (16) this yields

$$R(k_1, k_2; k_3, k_4) = R_0(k_1, k_2, k_3, k_4) + F(k_1, k_3; k_2, k_4) + F(k_1, k_4; k_2, k_3), \quad (18)$$

$$F(k_1, k_2; k_3, k_4) = -(g_0^2/2\pi i)\int [R_0(k_1, k_2, l, l') + F(k_1, l; k_2, l') + F(k_1, l'; k_2, l)] \times D(l)\, D(l')\, [R_0(-l, -l', k_3, k_4) + F(-l, k_3; -l', k_4) + F(-l, k_4; -l', k_3) + F(-l, -l'; k_3, k_4)]\, d^4l. \quad (19)$$

Transposing k_2 and k_3 or k_2 and k_4 in both sides of Eq. (19), we obtain two more analogous equations and thus have a system of three integral equations, which identically determine the functions

$F(k_1, k_2; k_3, k_4)$, $F(k_1, k_3; k_2, k_4)$ and $F(k_1, k_4; k_2, k_3)$,

in terms of the known quantity $R_0(k_1, k_2,; k_3, k_4)$

3. THE INTEGRAL EQUATION FOR THE CASE OF LARGE MOMENTA

a) Consequences of Eq. (19).

If the meson momenta k_i are large, as in the case of the neutral theory, Eq. (19) can be reduced to the form

$$\varphi(\xi, \eta, \zeta) = \frac{-g_0^2}{8\pi}\int_\eta^\xi [R_0(\xi) + 2F(\xi)]\,[R_0(\zeta) + 2F(\zeta) + \varphi(\lambda, \eta, \zeta)]\, d^2(\lambda)\, d\lambda - \frac{g_0^2}{8\pi}\int_\zeta^\xi [R_0(\xi) + 2F(\xi)]\,[R_0(\lambda) + 2F(\lambda) + \varphi(\lambda, \eta, \zeta)]\, d^2(\lambda)\, d\lambda - \frac{g_0^2}{8\pi}\int_\xi^L [R_0(\lambda) + 2F(\lambda)][R_0(\lambda) + 2F(\lambda) + \varphi(\lambda, \eta, \zeta)]\, d^2(\lambda)\, d\lambda. \quad (20)$$

*By carrying out the "reduction" process in reverse we can restore to the original form both parts of the graph which were obtained from each square of the graph (e.g., Fig. 5a). However, these parts will be joined by only two meson lines.

here

$$\xi = \ln(-k_1^2/m^2),\ \zeta = \ln(-k_{11}^2, m^2),\quad \eta = \ln[-(k_1+k_2)^2/m^2],$$
$$\lambda = \ln(-l^2/m^2),\ -k_1^2 = \max(-k_1^2,\ -k_2^2,\ -(k_1+k_2)^2),$$
$$-k_{11}^2 = \max(-k_3^2,\ -k_4^2,\ -(k_3+k_4)^2),$$

for which the most general case $\xi > \zeta > \eta$ is treated, when $F(k_1, k_2; k_3, k_4)$ is dependent on all three quantities ξ, η, ζ, *i.e.*,

$$F(k_1, k_2; k_3, k_4) = \varphi(\xi, \eta, \zeta) \tag{21}$$

and when, according to Eq. (17) and Eq. (18),

$$P(k_1, k_2; k_3, k_4) = R_0(\xi) + 2F(\xi) + \varphi(\xi, \eta, \zeta),$$
$$R(k_1, k_2; k_3, k_4) = R_0(\xi) + 2F(\xi), \tag{22}$$

with*

$$F(\xi) = \varphi(\xi, \xi, \xi) \approx F(k_1, k_3; k_2, k_4)$$
$$\approx F(k_1, k_4; k_2, k_3).$$

If, however, all the momenta k_i and all of their sums $k_i + k_j$ are quantities of the same order, then $\xi = \eta = \zeta$ and

$$P(k_1, k_2; k_3, k_4) = R_0(\xi) + 3F(\xi). \tag{23}$$

It is assumed everywhere that the quantities P and F depend, like R_0, logarithmically on the momenta when the momenta are large [this is confirmed by the solution of Eq. (20)]. When Eq. (20) was obtained from Eq. (19), the only region included was $\eta < \lambda < L$, in which the integral over l is logarithmic and for which $D(l)D(l')d^4l \approx (i/4)d^2(\lambda)d\lambda$. In the integration over λ, it was taken into account that in region a (see Fig. 6) where $\gamma \leq \lambda \leq \zeta$, the quantities

$$R_0(k_1, k_2; l, l') + F(k_1, l; k_2, l')$$
$$+ F(k_1, l', k_2, l),\ R_0(-l, -l'; k_3, k_4)$$
$$+ F(-l, k_3; -l', k_4) + F(-l, k_4; -l', k_3)$$

which appear under the integral in Eq. (19) do not depend on λ; in region b, where $\zeta \leq \lambda \leq \xi$, the first of these quantities does not depend on λ, but in region c, where $\xi \leq \lambda \leq L$, both are functions of λ.

*It is easy to see that when k_2 and k_3 are transposed, i.e. when there is a transition from $F(k_1, k_2; k_3, k_4)$ to $F(k_1, k_3; k_2, k_4)$ the quantities ξ', η', ζ', which correspond to the new arrangement of momenta, are all of the same order equal to ξ. By the same token the quantities corresponding to $F(k_1, k_4; k_2, k_3)$ are $\xi'' = \eta'' = \zeta'' = \xi$.

If we put in Eq. (20) $\eta = \zeta$ and $\eta = \zeta = \xi$ we obtain two equations whose simultaneous solution determines the functions $F(\xi)$ and $\varphi(\xi, \eta, \eta) = P(\xi, \eta)$,

$$P(\xi, \eta) = -(g_0^2/8\pi)\int_\eta^\xi [R_0(\xi) + 2F(\xi)]\,[R_0(\lambda)$$
$$+ 2F(\lambda) + \Phi(\lambda, \eta)]\,d^2(\lambda)\,d\lambda - (g_0^2/8\pi)\int_\xi^L [R_0(\lambda)$$
$$+ 2F(\lambda)]\,[R_0(\lambda) + 2F(\lambda) + \Phi(\lambda, \eta)]\,d^2(\lambda)\,d\lambda,$$
$$F(\xi) = -(g_0^2/8\pi)\int_\xi^L [R_0(\lambda) + 2F(\lambda)]\,[R_0(\lambda) \tag{24}$$
$$+ 2F(\lambda) + \Phi(\lambda, \xi)]\,d^2(\lambda)\,d\lambda.$$

It is evident from these equations that the value $F(\xi)$ of the function $F(k_1, k_2; k_3, k_4)$ is, in the case where all the momenta are of the same order of magnitude, essentially dependent on the quantity $\Phi(\lambda, \xi)$ i.e. on the value of $F(-l, -l'; k_3, k_4)$ for the case when the two momenta l and l' are very large in comparison with their sum ($|l + l'| = |k_3 + k_4|$). This circumstance is a troublesome peculiarity of Eq. (19) and complicates considerably the subsequent computations.

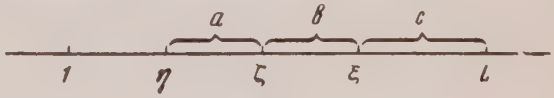

FIG. 6.

In the case of the symmetrical theory the equations look even more awkward. In this case the isotopic meson spin variables, a_i, can be left out of the calculations if one desires asymptotic solutions for Eq. (19) of the form,

$$F(k_1, k_2; k_3, k_4) \approx \Phi(\xi, \eta)\,\delta_c + \Phi_1(\xi, \eta)\,\delta_{\alpha_1\alpha_2}\delta_{\alpha_3\alpha_4},$$
$$(\eta = \zeta);$$
$$F(k_1, k_2; k_3, k_4) = F(\xi)\,\delta_c + F_1(\xi)\,\delta_{\alpha_1\alpha_2}\delta_{\alpha_3\alpha_4},$$
$$(\xi = \eta = \zeta),$$

where $F(\xi) = \Phi(\xi, \xi)$, $F_1(\xi) = \Phi_1(\xi, \xi)$. Then, according to eq. (17) and Eq. (18)

$$P(k_1, k_2, k_3, k_4) = \Pi(\xi, \eta_1)\,\delta_c + \Pi_1(\xi, \eta_1)\,\delta_{\alpha_1\alpha_2}\delta_{\alpha_3\alpha_4},$$
$$P(k_1, k_2, k_3, k_4) = P(\xi)\,\delta_c, \quad (\xi = \eta_1), \tag{25}$$

where $P(\xi) = \Pi(\xi, \xi)$, $\Pi_1(\xi, \xi) = 0$ (the latter is due to the fact that P, which is symmetrical over all coordinates of all the mesons, can only contain the factor δ_c for those cases where all the momenta are of the same order).

Substituting the above expression for F in Eq. (19) and equating the coefficients of δ_c and $\delta_{\alpha_1\alpha_2}\delta_{\alpha_3\alpha_4}$ which occur in both sides of the equation, we obtain, just as in the case of the neutral theory,

$$\Phi(x, y) = -\frac{1}{3}[\rho_0(x) + 2F(x)]\int_x^y [\rho_0(z) + 2F(z) + F_1(z) + \Phi(z, y)]\frac{dz}{z^2}$$
$$-\frac{1}{3}\int_1^x [\rho_0(z) + 2F(z) + F_1(z)][\rho_0(z) + 2F(z) + F_1(z) + \Phi(z, y)]\frac{dz}{z^2},$$
$$\Phi_1(x, y) = -\frac{1}{3}\int_x^y \left\{\frac{5}{2}[\rho_0(x) + 2F(x)][\rho_0(z) + 2F(z) + \Phi(z, y)\right.$$
$$\left. + \Phi_1(z, y)] + F_1(x)[\Phi_1(z, y) - F_1(z)]\right\}\frac{dz}{z^2} - \frac{1}{3}\int_1^x \left\{\frac{5}{2}[\rho_0(z) + 2F(z)]\right.$$
$$\left. \times [\rho_0(z) + 2F(z) + \Phi(z, y) + \Phi_1(z, y)] + F_1(z)[\Phi_1(z, y) - F_1(z)]\right\}\frac{dz}{z^2}. \tag{26}$$

Here instead of ξ, η and λ we have used more convenient variables, viz.

$$x = [1 + (5g_0^2/4\pi)(L - \xi)]^{1/5} \tag{27b}$$

and, accordingly, for y and z. If we assume $x = y$ in Eq. (26), we obtain two more equations (analogous to the second equation in Eq. (24); consequently we have a system of four equations for the four functions Φ, Φ_1, F, and F_1. It is not difficult to solve Eq. (26) provided that $x - 1 > 1$ (this provision corresponds to the conventional perturbation theory) and that $x > 1$. Omitting the computations, the results are

$$\Pi(x, y) = \begin{cases} \frac{16}{3}(x-1)\left\{1 - \frac{88}{27}(x-1)^2 - \frac{8}{3}[(y-1)^2 - (x-1)^2] + \cdots\right\}, \\ \qquad x - 1 < 1, \quad y - 1 < 1; \\ \frac{16}{11}x\left\{1 + \frac{5}{3}[x^{40/33}y^{-40/33} - x^{16/33}y^{-16/33}] + \cdots\right\}, \quad x > 1, \ y > 1, \end{cases}$$

$$\Pi_1(x, y) = \begin{cases} -\frac{5}{12}\left(\frac{16}{3}\right)^2(x-1)\{[(y-1)^2 - (x-1)^2] + \cdots\}, \\ \qquad x - 1 < 1, \ y - 1 < 1; \\ \frac{16}{11}\{x[x^{16/33}y^{-16/33} - 1] + \cdots\}, \quad x > 1, \ y > 1, \end{cases}$$

whence

$$P(x) = \Pi(x, x) = \begin{cases} \frac{16}{3}(x-1)\left\{1 - \frac{88}{27}(x-1)^2 + \cdots\right\}, & x - 1 < 1; \\ \frac{16}{11}x + \cdots, & x > 1 \end{cases} \tag{28}$$

b) Direct Integral Equation for $P(\xi)$.

We shall show that one can obtain an equation for $P(\xi)$ and $F(\xi)$ directly, and in this fashion avoid the case where two of the four momenta are very large and eliminate completely functions like $\Phi(\xi, \eta)$ and $\varphi(\xi, \nu, \zeta)$. For this purpose we shall

derive once more an equation which, like Eq. (19), determines the function $F(k_1, k_2; k_3, k_4)$, although we shall assume from the outset that all momenta and their sums are large quantities and of the same order of magnitude. We shall consider only the asymptotic value of all the functions and include only the most essential region—the region where all the integrals vary logarithmically.

Let us examine an arbitrary reducible (as regards the separation of k_1, k_2 from k_3, k_4) graph and write the function belonging to it in a form analogous to Eq. (11). Then in the part adjacent to lines k_3 and k_4 a graph may be reducible, as well as irreducible as regards the separation of lines l and l' from k_3, k_4. In the first case, *i.e.*, if the graph is reducible, we again present it in the form of an integral like Eq. (11) and so on until no irreducible graph remains in the part adjacent to k_3 and k_4. Consequently, the graph in question is broken down into a series of irreducible ones (Fig. 7) connected to each other by pairs of meson lines. We shall designate the momenta in these lines by $l_1, l_1', l_2, l_2'; \ldots; l_N, l_N'$ (with $l_i = l_i' + k_1 + k_2$, $i = 1, 2, \ldots, N$) and use $\rho_{n_0}, \rho_{n_1}, \ldots, \rho_{n_N}$ to designate the values of the contributions from the irreducible graphs in Fig. 7 (here n_i is the number of the corresponding graphs in the i-th irreducible part). Then, in analogy with Eq. (11), we can write

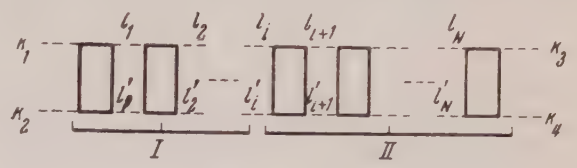

FIG. 7.

$$\sigma_{n_0, n_1, \ldots, n_N}(k_1, k_2; k_3, k_4) = \int\int \cdots \int \rho_{n_0}(k_1, k_2; l_1, l_1')\, A(l_1)\, d^4 l_1$$

$$\times \rho_{n_1}(-l_1', -l_1';\ l_2, l_2')\, A(l_2)\, d^4 l_2 \cdots A(l_N)\, d^4 l_N \rho_{n_N}(-l_N, -l_N'; k_3, k_4);$$

$$A(l_i) = -(g_0^2/\pi i)\, D(l_i)\, D(l_i'),$$

or, if we include only the region of logarithmic variation of l_i (for which $A(l_i)d^4 l_i = -(g_0^2/4\pi)d^2(\lambda_i)d\lambda_i$ [see footnote* following Eq. (7)], we obtain for the case where all momenta k_1, k_2, k_3, k_4 and all of their sums are of the same magnitude, *i.e.*, where $\sigma = \sigma(\xi)$,

$$\sigma_{n_0,\ n_1, \ldots, n_N}(\xi) = (-g_0^2/4\pi)^N \int_\xi^L d\lambda_1 \int_\xi^L d\lambda_2 \cdots \int_\xi^L d\lambda_N \rho_{n_0}(\xi, \lambda_1)\, d^2(\lambda_1)\, \rho_{n_1}(\lambda_1, \lambda_2)$$
$$\times d^2(\lambda_2) \cdots d^2(\lambda_N)\, \rho_{n_N}(\lambda_N, \xi). \tag{29}$$

Here $\rho_{n_i}(\lambda_i, \lambda_{i+1})$ stands for the value of $\rho_{n_i}(-l_i, -l_i', l_{i+1}, l_i' + 1)$ when l_i and l_{i+1} are large. It is essential that ρ_{n_i} be in fact dependent only on the largest of quantities λ_i, λ_{i+1}, because ρ_{n_i} is the contribution from the graph which is irreducible as regards the separation of $-l_i, -l_i'$ from l_{i+1}, l_{i+1} (the contribution from graphs of this type is contained in $F(-l_i, l_i' + 1; -l_i', l_{i+1})$ or in $F(-l_i, l_{i+1}; l_i', l_{i+1})$ and, in agreement with what has been said above, when l_i and l_i' are large these F functions depend only on the largest momentum.* This last assertion can be easily checked directly on simple graphs with two, three, and more squares. Thus, the integrand in Eq. (29) does not, in fact, depend on ξ, *i.e.*, when $\lambda_1 \geq \xi$ and $\lambda_N \geq \xi$, then

$$\rho_{n_0}(\xi, \lambda_1) = \rho_{n_0}(\lambda_1), \qquad \rho_{n_N}(\lambda_N, \xi) = \rho_{n_N}(\lambda_N).$$

The region of integration over $\lambda_1, \lambda_2, \ldots, \lambda_N$ in Eq. (29) can be broken down into N regions, in any one of which one of the variables, say λ_i, is smaller than the others; accordingly Eq. (29) is presented as a sum of N integrals

$$\sigma_{n_0, n_1, \ldots, n_N}(\xi) =$$
$$-\sum_{i=1}^{N} \frac{g_0^2}{4\pi} \int_\xi^L \sigma_{n_0, n_1, \ldots, n_{i-1}}(\lambda_i)\, \sigma_{n_i, n_{i+1}, \ldots, n_N}(\lambda_i)\, d\lambda_i. \tag{30}$$

*In contrast to $F(-l_i, -l_i'; l_{i+1}, l_i' + 1) = \varphi(\lambda_i, \eta, \lambda_{i+1})$ which depends on three quantities: λ_i, η, λ_{i+1}.

where the quantity

$$\sigma_{n_0, n_1, \ldots, n_{i-1}}(\lambda_i) = \left(-\frac{g_0^2}{4\pi}\right)^{i-1} \int_{\lambda_i}^{L} d\lambda_1 \ldots \int_{\lambda_i}^{L} d\lambda_{i-1} \rho_{n_0}(\lambda_1) d^2(\lambda_1) \rho_{n_1}(\lambda_1, \lambda_2) \ldots \quad (31)$$

$$\ldots d^2(\lambda_{i-1}) \rho_{n_{i-1}}(\lambda_{i-1})$$

is determined in a manner exactly analogous with Eq. (29), *i.e.*, it may be regarded as the contribution from the part of the reducible graph under consideration that adjoins lines k_1, k_2 and l_i l_i' (part I in Fig. 7), which would be made if the momenta k_1 and k_2 were of the same order as l_i, l_i'. Analogously $\sigma_{n_i, n_{i-1}, \ldots, n_N}(\lambda_i)$ may be regarded as the contribution that would come from part II in Fig. 7 if k_3 and k_4 were of the same order as l_i, l_i'.

It is not difficult to see that, in analogy with Eq. (12)

$$\sum_{i=1}^{\infty} \sum_{n_0, n_1, \ldots, n_{i-1}} 2^{-(i-1)} \sigma_{n_0, n_1, \ldots, n_{i-1}}(\lambda) = P(\lambda),$$

where $P(\lambda)$ is the desired value for the sum of all the reducible graphs provided that all the momenta are of the same order. In exactly the same way as in Eq. (14) we obtain

$$\sum_{N-i=1}^{\infty} \sum_{n_i, n_{i-1}, \ldots, n_N} 2^{-(N-i)} \sigma_{n_i, n_{i+1}, \ldots, n_N}(\lambda) = P(\lambda).$$

The negative powers of 2 in the left side of these equations are due to the fact that when we sum over all possible irreducible parts, *i.e.*, over n_i ($j = 0, \ldots, N$), we obtain (in the last case) 2^N identical resulting graphs.

Using these equalities, we obtain, by the summation of Eq. (29) over all types (or numbers) of n_i graphs in each irreducible part and over the number N of these parts,

$$F(\xi) = -(g_0^2/8\pi) \int_{\xi}^{L} P(\lambda) d^2(\lambda) P(\lambda) d\lambda. \quad (32)$$

For the neutral pseudoscalar theory we obtain according to Eq. (32) a simple integral equation,

$$P(\xi) = R_0(\xi) - \frac{3g_0^2}{8\pi} \int_{\xi}^{L} P^2(\lambda) d^2(\lambda) d\lambda, \quad (33a)$$

where R_0 is determined in Eq. (3a).

Introducing [as in Eq. (27b)] a more convenient variable

$$x = [1 + (5g_0^2/4\pi)(L - \xi)]^{-1/5} = Q^{-1/5}, \quad (27a)$$

we can write Eq. (33a) as

$$P(x) = 24(1 - x) - \frac{3}{2} \int_{x}^{1} P^2(z) \frac{dz}{z^2}. \quad (34a)$$

Differentiation with respect to x converts this equation into a simple differential one, which is easily solved. A simple computation gives us

$$P(x) = \frac{\sqrt{145} + 1}{3} \times x \frac{1 - x^{\sqrt{145}}}{1 + (\sqrt{145} + 1) x^{\sqrt{145}} / (\sqrt{145} - 1)}. \quad (35a)$$

In the case of the symmetrical theory Eq. (25) should be substituted in Eq. (32) and summed over the indices of the isotopic spin; this will give

$$F(k_1, k_2; k_3, k_4) \approx [2\delta_c + 5\delta_{\xi_1, \xi_2} \delta_{\xi_3, \xi_4}] \times \left(\frac{-g_0^2}{8\pi}\right) \int_{\xi}^{L} P^2(\lambda) d^2(\lambda) d\lambda,$$

where [see footnote* following Eq. (2)] $d(\lambda) = Q^{-3/5}$. In conformance with Eq. (17), we then obtain (upon dividing through δ_c)

$$P(\xi) = \rho_0(\xi) - \frac{11g_0^2}{8\pi} \int_{\xi}^{L} P^2(\lambda) d^2(\lambda) d\lambda, \quad (33b)$$

$$P(x) = \frac{16}{3}(x - 1) - \frac{11}{6} \int_{1}^{x} P^2(z) \frac{dz}{z^2}, \quad (34b)$$

or, if we introduce the variable x, make use of Eq. (3b), and integrate, we obtain

$$P(x) = \frac{16x}{11} \frac{1 - x^{-11/3}}{1 + (8/11) x^{-11/3}} \quad (35b)$$

Thus, the total sum $P(x)$ of the reducible graphs is a finite quantity of the same order as the contri-

bution R_0 from the simplest graphs in Fig. 1 (when $Q \to \infty$, Eq. (35b) for example, differs from Eq. (28) only in the factor 3/11).

Eq. (33a) and (33b) could, it would seem, also be derived mathematically directly from Eq. (24) to (26). However, we were unable to do this. The value of Eq. (35b) for $x - 1 < 1$ and $x > 1$ coincide with the value of Eq. (28) derived directly from Eq. (26).

4. THE RENORMALIZATION PROPERTIES OF THE AMPLITUDE P FOR MESON-MESON SCATTERING

In the conventional scheme for charge renormalization the amplitude for meson-meson scattering

$$(g_0^2/4\pi i)\, P\,(k_1, k_2, k_3, k_4),$$

which corresponds to graphs with four external meson lines, is multiplied by a factor Z_3^2 (where $D = Z_3 D_c$), $\sqrt{Z_3}$ for each external meson line. Thus every renormalized expression will contain the quantity

$$Z_3^2\, (g_0^2/4\pi i)\, P.$$

Since, according to Ref. 2, $g^2 = (g_0^2/Q_0)$ and $Z_3 = d\,(0) = Q_0^{-2/5}$ for the neutral theory and $Z_3 = Q^{-4/5}$ for the symmetrical theory, we obtain in both cases

$$Z_3^2\,(g_0^2/4\pi i)\, P\,(x) = (g^2/4\pi i)\,(P\,(x)/x_0),$$

$$Q_0 = 1 + (5g_0^2/4\pi)\, L$$

where, according to Eq. (27a), (27b) $x_0 = Q_0^{-1/5}$ for the neutral theory and $Q_0^{3/5}$ for the symmetrical one. Thus, after renormalization of the charge, instead of $P\,(x)$ all of the equations will contain

$$P_c\,(x) = P\,(x)/x_0.$$

If we set $x/x_0 = x_c$ where $x_c = Q^{-1/5}$ for the neutral theory and $x_c = Q_c^{3/5}$ for the symmetrical theory, and where

$$Q_c = 1 - (5g^2/4\pi)\,\xi$$

we see that $Q \to \infty$ when $L \to \infty$ and

$$P_c\,(x) = P\,(x_c),$$

where P is given by Eq. (35a) or (35b) with $Q \to \infty$ (*i.e.*, $P = (\sqrt{145} + 1/3)\, x_c$ for Eq. (35a) and $P = (16/11) x_c$ for Eq. (35b)).

Thus, when $L \to \infty$ the quantities (35a) and (35b) are automatically renormalized without introducing any counter terms proportional to φ^4 in the Hamiltonian.

In principle it is not difficult to think of a case where the Hamiltonian would, in additional to the usual interaction terms, have a term proportional to φ^4 [or $(\varphi_\alpha \varphi_\alpha)^2$ in the case of the symmetrical theory, with α as the index for the isotopic spin].

At the same it is obvious that there will be a change in the term R_0, which corresponds to the simplest graphs in Fig. 1. A constant λ, which is proportional to the coefficient of the φ^4 term is added to Eq. (3a) and (3b), *i.e.*,

$$R_0 = 24\,(1 - x) + \lambda, \quad \rho_0 = (16/3)\,(x - 1) + \lambda.$$

Consequently, instead of (34a) and 34b) we obtain

$$P\,(\lambda, x) = 24\,(1 - x) + \lambda - \frac{3}{2}\int_x^1 P^2\,(\lambda, z)\, z^{-2}\, dz, \tag{36a}$$

$$P\,(\lambda, x) = \frac{16}{3}\,(x - 1) + \lambda - \frac{11}{6}\int_1^x P^2\,(\lambda, z)\, z^{-2}\, dz \tag{36b}$$

($P\,(\lambda, x)$ is the scattering amplitude when a direct interaction is present characterized by the constant λ). These equations, as in the case of Eq. (35a) and (35b), are simple to solve. By way of example let us take the case of the symmetrical theory. The solution to Eq. (36b), as is easily seen, has the form

$$P\,(\lambda, x) = \frac{16x}{11}\,\frac{A - x^{-19/3}}{A + (8/11)\, x^{-19/3}}, \qquad A = \frac{1 + \lambda/2}{1 - 11\lambda/16} \tag{37}$$

[when $\lambda = 0$, $A = 1$ and Eq. (37) coincides with Eq. (36b)]. It should be noted that the quantity $P\,(\lambda, x)$ is renormalized for any λ (as are the functions d, β, a found in Abrikosov, *et al.*[2]) if the renormalization entails change in λ. Actually, according to Eq. (37), if we have that $x = x_0\, x_c$, we directly obtain

$$P\,(\lambda, x) = x_0\, P\,(\lambda_c, x_c), \tag{38}$$

where the right half is the same function as Eq. (37), and where λ_c and λ are connected by the equality

$$\frac{1 + \lambda_c/2}{1 - (11/16)\,\lambda_c} = x_0^{19/3}\,\frac{1 + \lambda/2}{1 - (11/16)\,\lambda}. \tag{39}$$

Note that according to Eq. (36) or Eq. (37), $P(\lambda, 1) = \lambda$ i.e. $\lambda_c = P(\lambda_c, 1)$ determines the magnitude of the interaction observed in experiments with mesons at low energies, when $\xi = 0$, $x_c = 1$. If this quantity is considered known and one considers Eq. (38) as specifying λ in terms of λ_c, g_0^2 and L, then Eq. (38) and Eq. (39) constitute the usual means for renormalizing the amplitude of meson-meson scattering, which, as is apparent, also occurs outside the framework of the perturbation theory.

The authors wish to express their gratitude to I. Ia. Pomeranchuk for his helpful advice and unfailing interest in this paper. An expression of thanks is also due D. Bulianitsa for assistance in computing the number of graphs and in the graphic check on the integral equations.

[1] Landau, Abrikosov, and Khalatnikov, Dokl. Akad. Nauk SSSR **95**, 497, 773, 1177 (1954).

[2] Abrikosov, Galanin, and Khalatnikov, Dokl. Akad. Nauk SSSR **97**, 793 (1954).

[3] I. Ia. Pomeranchuck, Dokl. Akad. Nauk SSSR **103**, 1005; **104**, 51; **105**, 461 (1955).

[4] A. A. Abrikosov and I. M. Khalatnikov, Dokl. Akad. Nauk SSSR **103**, 993 (1955).

Translated by A. Skumanich
174

SOVIET PHYSICS JETP VOLUME 5, NUMBER 4 NOVEMBER, 1957

Nonlinearity of the Field in Conformal Reciprocity Theory

A. POPOVICI
Bucharest, Rumania

(Submitted to JETP editor February 16, 1956)
J. Exptl. Theoret. Phys. (U.S.S.R.) **32**, 781-793 (April, 1957)

The first version of Born and Infeld's nonlinear electrodynamics and the variability of the gravitational constant are deduced from the conformally covariant gravitational equations derived from a certain generalized reciprocity law which is based on group theory and yields a nonlocal field theory. A correspondence principle is established between relativity theory and reciprocity theory.

I. FIELD EQUATIONS

1. LET k BE Einstein's gravitational constant, $ds^2 = g_{ik}dx^i dx^k$ be the element of interval with the metric $g_{ik} = g_{ki}$, $g = \|g_{ik}\|$ $(i, k = 1, \ldots, 4)$. Let Γ_{ik}, $\Gamma = \Gamma_r^r$ be the contracted curvature tensor and the curvature scalar constructed from Weyl's conformal connection[1] Γ_{kl}^i, Riemannian in the metric $u_{ik} = \Psi g_{ik}$, and of weight zero with respect to the g_{ik} ($\Psi = E^{-2}\psi$ is of weight -1 with respect to the g_{ik}). Let $p_{ik} = (\partial p_k/\partial x^i - \partial p_i/\partial x^k)$ be the electromagnetic field of absolute magnitude $P/\sqrt{2} = P'\sqrt{k/2}$. Let $P_{ki} = P_{ik} = p_{ir}p_k^r/P$, $P = P_r^r$,

$$L_{ik} = \Gamma\Gamma_{ik} + PP_{ik}, \quad L = L_r^r = \Gamma^2 + P^2, \tag{1}$$

$$Q_{ik} = \Gamma Q'_{ik} = \Gamma(\Gamma_{ik} - {}^1/_4\Gamma g_{ik}),$$
$$S_{ik} = PS'_{ik} = P(P_{ik} - {}^1/_4 P g_{ik}). \tag{2}$$

The Γ_{ik}, P_{ik} (as well as the p_{ik}) depend only on the ratios of the g_{ik} (and therefore on those of the of the u_{ik}). Variation of $L\sqrt{g}$ with respect to g_{ik} and p_i gives[2] the gravitational $Q_i^k\sqrt{g}$ and electromagnetic $S_i^k\sqrt{g}$ energy-momentum tensor densities of weight zero and current-charge vector densities $s^i\sqrt{g}$ and $s'^i\sqrt{g}$ of weight zero. This leads,[2,3] to the conformal covariant equations which satisfy the reciprocity principle[2-12]

$$Q_{ik} = -S_{ik} \text{ or } L_{ik} = {}^1/_4 Lg_{ik}, \tag{3}$$

$$\partial(p^{ik}\sqrt{g})/\partial x^k = s^i\sqrt{g}. \tag{4}$$

when $\partial(\Gamma^2\sqrt{g})/\partial p_i = 0$, Equations (4) become

$$\partial(p^{ik}\sqrt{g})/\partial x^k = 0; \tag{4'}$$

Eq. (3) and (4) describe the gravitational, and electromagnetic fields respectively.

2. Equations (3) and (4), which are conformal in V_4 with metric g_{ik}, are Riemannian in the manifold U_4 with metric u_{ik}. The general form of the gravitational equations (3) and their variational derivation are independent of the factor Ψ and therefore of the arbitrary vector $\psi_i = \partial\psi/\partial x^i$ (where $\psi = -\frac{1}{2}\ln\Psi$) which defines the corresponding conformal affinity of Weyl. Elsewhere[13], gravitational equations of the form $Q_{ik} = 0$ are derived from $\Gamma^2\sqrt{g}$ in the special case $\Psi = \Gamma$. We have $L\sqrt{g} = \sqrt{\overset{0}{g}}$, where the metric $\overset{0}{g}_{ik} = g_{ik} L^{\frac{1}{2}}$, $\overset{0}{g} = \| \overset{0}{g}_{ik} \|$. It would seem that Ψ is a function of the absolute magnitude of the conformal curvature tensor of Weyl for the congruences noted by Vranceanu[1]. Ψ is directly related to the conformal generalization of the scalar field χ of Rumer[14] or more generally with a scalar meson field, since the meson field is conformal[15-19]. In the conformal six-dimensional theory, the equation for Ψ is a generalization of the scalar Klein-Gordon equation[14,20-22]. Conformal reciprocity theory includes the theory of particles with spin 0, 1, and 2 (scalar mesons, photons, gravitons). Let R_{ik} and R be the contracted curvature tensor and the curvature scalar constructed from the Riemannian affinities $\left| \overset{i}{kl} \right|$ with respect to the metric $g_{ik} = U_{ik}/\Psi$. We shall have the symbol ( ); denote covarient differentiation with respect to the Riemannian affinity $\left| \overset{i}{kl} \right|$. We have[1]

$$\varphi_{ik} = (\psi)_{;\,i;\,k} + \psi_l \psi_k - \frac{1}{2}\psi^r \psi_r g_{ik},$$

$$\varphi = \varphi^r_r = g^{rs}\,(\psi)_{;\,r;\,s} - \psi^r \psi_r, \qquad (5)$$

$$\Gamma_{ik} = R_{ik} + 2\varphi_{ik} + \varphi g_{ik}, \quad \Gamma = R + 6\varphi.$$

The tensor Q'_{ik} breaks up into a pure gravitational tensor $R_{ik} - (\frac{1}{4}) R g_{ik}$ and a meson tensor $2(\varphi_{ik} - \frac{1}{4}\varphi g_{ik})$. If we introduce the vector $g_i = p_i/\Psi^{\frac{1}{2}}$, we obtain a similar decomposition of S'_{ik}. Since Q_{ik} and S_{ik} are symmetric and $Q^r_{r\cdot} = S^r_r = 0$, their conformal divergences reduce to the Riemannian ones. The conservation laws for the energy-momentum and charge-current which follow from Equations (3) and (4), respectively, are

$$(Q^k_i \sqrt{g})_{;\,k} = -\,(S^k_i \sqrt{g})_{;\,k}, \quad \partial(s^i\sqrt{g})/\partial x^i = 0. \qquad (6)$$

3. Let $U^k_i = L^k_i/2\Gamma$, $V^k_i = L^k_i/2P$,

$$U = U^r_r = L/2\Gamma, \quad V = V^r_r = L/2P. \qquad (7)$$

The gravitational equations (3) become

$$U_{ik} = \tfrac{1}{4} U g_{ik} \text{ or } V_{ik} = \tfrac{1}{4} V g_{ik}, \qquad (8)$$

$$L = \Gamma^2 + P^2 = 2\Gamma U = 2PV. \qquad (9)$$

With the aid of conformal transformation of the metric g_{ik} of the manifold V_4 into the metrics $g^*_{ik} = g_{ik}\,U$ and $g^{**}_{ik} = -ig_{ik}\,V$, we obtain ($i^2 = -1$)

$$L^* = 2\Gamma^*, \quad L^{**} = 2iP^{**}, \quad \Gamma^{**} = -iP^*,$$
$$U^* = -iV^{**} = 1. \qquad (9')$$

Setting $(1 - P^2/U^2)^{\frac{1}{2}} = (1 - \Gamma^2/V^2)^{-\frac{1}{2}} = \epsilon$, Eq. (9) leads to

$$(\alpha = \pm 1), \qquad (10)$$

and thus Eq. (9) has two pairs of solutions Γ, P and V, U

$$\underset{1}{\Gamma} = \underset{1}{U}(1+\varepsilon), \quad \underset{1}{P} = \underset{1}{V}(1-\varepsilon)$$
$$\text{and } \underset{2}{\Gamma} = \underset{1}{U}(1-\varepsilon), \quad \underset{1}{P} = \underset{2}{V}(1+\varepsilon). \qquad (11)$$

Now setting $U = -if$, $V = in$, and defining the scalars J, N, H, F, γ, j, h and the antisymmetric tensors h_{ik}, f_{ik} by the relations

$$\Gamma/J = J/N = P/H = H/F = \gamma/j = j/n$$
$$= p/h = h/f = p_{ik}/h_{ik} = h_{ik}/f_{ik} = \sqrt{\varepsilon}, \qquad (12)$$

we arrive at the following expression for L [see Eq. (9)]:

$$\underset{00}{L} = 2\underset{1}{U}^2(1+\varepsilon) = 2\underset{1}{V}^2(1-\varepsilon) = 4h_1 = 4\varepsilon l_1,$$
$$\underset{01}{L} = 2U^2(1-\varepsilon) = 2\underset{2}{V}^2(1+\varepsilon) = 4h_2 = -4\varepsilon l_2, \qquad (13)$$

where

$$\varepsilon = 1/\mu = (1 + P^2/f^2)^{1/2} = (1 - F^2/f^2)^{-1/2}, \qquad (14)$$

$$\varepsilon = 1/\mu = (1 + \Gamma^2/n^2)^{1/2} = (1 - N^2/n^2)^{-1/2}. \qquad (14')$$

Setting $s = 1/w = (\epsilon + 1)/(\epsilon - 1)$, we obtain $\epsilon = 1/\mu = (s+1)/(s-1)$; ϵ and s are of weight zero. Conversely, Eq. (7) follows from L [see Eq. (1)], (13), and (14) or (14′); to each general solution Γ, P of Eq. (3) and (4′) there corresponds one value of U and V. Eq. (9) follows from (13) and (17). The same results are obtained by the conformal generalization of the five-dimensional theory[14, 19-22]

4. The quantities ϵ and μ in Eq. (14) are just the dielectric constant and permeability of the field as defined in the first version of Born and Infeld's nonlinear electrodynamics[7, 8, 23-25]. The quantities $f_{ik} = \mu p_{ik}$ and $p_{ik} = \epsilon f_{ik}$ are Born and Infeld's electromagnetic field of zero weight with absolute magnitudes $F/\sqrt{2} = F'\sqrt{k/2}$, $P/\sqrt{2} = P'\sqrt{k/2}$, and $U/\sqrt{2} = -if/\sqrt{2} = -ip\mu/\sqrt{2}$ is the "maximum" electromagnetic field ($F^2 \leq 0$, $P^2 \leq 0$, $f^2 \leq 0$, $p^2 \leq 0$). Similarly, $-iV/\sqrt{2} = n/\sqrt{2} = \gamma\mu/\sqrt{2}$ is the "maximum" gravitational field. The electromagnetic equations of Born and Infield are a special case of the nonlinear electromagnetic equations (4'), valid for $p_{ik} = \epsilon f_{ik}$, $P = \epsilon F$, $f = \text{const}$, and Eq. (14). The Born-Infeld equations are derived from the Lagrangian $l_2 = -\frac{1}{2} f^2 (1-\mu) = -\mu h_2$, and therefore from the Hamiltonian $h_2 = -\frac{1}{2} f^2 (1-\epsilon) = -\epsilon l_2$. The quantities l_2, h_2, l_1, h_1 are equivalent to L from the conformal point of view. Thus the arbitrariness in the choice of the lagrangian l_2 and the Hamiltonian h_2 in classical nonlinear electrodynamics is removed, and the irrational form of Eq. (13) reduces to the quadratic form of Eq. (9). The gravitational equations (3) are a generalization of the gravitational equations previously derived by the author[2] from the Langragian density $(\Gamma^2 + F^2)\sqrt{g}$. These two set of equations become identical for $p_{ik} = f_{ik}$. As is known, the mutual transformation of particles into each other, the interaction of different fields, and the polarization of fields lead necessarily to a nonlinear theory; the nuclear mass defect[26] also follows from the nonlinear gravitational equations. Nonlinearity also makes it possible to avoid infinite self-masses and dipole difficulties in nuclear theory, as well as to derive the equations of motion from the field equations.

5. Let us consider the case of a static spherical distribution of a field and a particle. Let a be a constant proportional to the point charge $e_0 = ec/\sqrt{k}$, $C^2 = 2a^2/C'$ be a constant of integration, and $\rho = x$ be the radius vector with the origin at the center of the particle.[1] In polar coordinates we have

$$\begin{gathered} \underset{1}{P} = 2P_1^1 = 2P_4^4, \quad P_2^2 = P_3^3 = 0, \\ \underset{1}{U} = -if_1 = 2\Gamma_2^2 = 2\Gamma_3^3, \\ \varepsilon \underset{1}{U} = -ip = 2\ \Gamma_1^1 = 2\Gamma_4^4. \end{gathered} \tag{15}$$

We obtain two solutions $\rho_{1,2} = CE^{\pm\omega/2}$, which correspond, respectively to the internal and external regions of a sphere of radius $C \approx a(\rho_1\rho_2 = C^2)$. Let $\rho' = \cosh\omega$, $\rho'' = \sinh\omega$. We have $\epsilon = 1/\mu = \pm\cot h\omega$ (depending on whether $\rho \gtrless C$), $s = 1/\overline{w} = \rho^4/C^4 = E^{\pm 2\omega}$. The gravitational equations are identical with (9); we have $4(\Gamma_1^1)^2 - 4(\Gamma_2^2)^2 = -P_1^2$ [see Eq. (28') below]. In the zero-weight metric $u_{ik} = g_{ik}\ \Psi = \tilde{g}_{ik}$, we have

$$\begin{gathered} \underset{1}{\tilde{\Gamma}} = 2(\tilde{\Gamma}_1^1 + \tilde{\Gamma}_2^2) = \mp C', \quad \underset{2}{\tilde{\Gamma}} = -2(\tilde{\Gamma}_1^1 - \tilde{\Gamma}_2^2) = \pm 2\alpha^2 C^2/\rho^4, \\ \underset{1}{\tilde{P}^2} = \tilde{\Gamma}\,\tilde{\Gamma} = C'^2/s = -4\alpha^4/\rho^4, \quad -i\tilde{f}_1 = \mp 2\alpha^2\rho''^2/\rho^2, \\ -i\underset{1}{\tilde{p}} = \mp 2\alpha^2\rho'^2/\rho^2, \quad \underset{1}{\tilde{n}} = \mp 2\alpha^2\rho''^2/C^2, \quad \underset{2}{\tilde{n}} = \pm 2\alpha^2 C^2\rho''^2/\rho^4. \end{gathered} \tag{16}$$

The existence of a continuous solution $\underset{1}{\tilde{\Gamma}} = \mp C'$ and a divergent one $\underset{2}{\tilde{\Gamma}}$ is analogous to the theory of the double solution of a wave equation (de Broglie[27]). In the present (static and spherical case) we therefore have $\Psi = \Gamma/C'$. In terms of the metrics $g^*_{ik} = g_{ik}\ \underset{1}{U}$, $g^{**}_{ik} = -ig_{ik}\ \underset{2}{V}$, we obtain

$$\begin{gathered} -i\underset{1}{f^*} = \underset{2}{n^*} = 1, \quad -i\underset{1}{p^*} = \underset{2}{\gamma^{**}} = \varepsilon, \\ -i\underset{1}{F^*} = \underset{2}{N^{**}} = 1/\rho'^2, \quad -i\underset{1}{P^*} = \underset{2}{\Gamma^{**}} = 1/\rho''^2. \end{gathered} \tag{16'}$$

II. THE GROUP OF CONFORMAL QUANTITIES

1. Let us define the general scalar curvatures $A = A^r$, a, Lagrangians $L = L^r$, and tensors A^k_i, G^k_i, Q'^k_i, A'^k_i, L^k_i, l'^k_i, L'^k_i, by the relations

$$A/A = a/a = \sqrt{\varepsilon}, \quad A/A = a/a = i\sqrt{s}, \tag{17}$$

$$L = A^2 + A^2 = -2iA\,a = 2i\,A\,a, \quad L = \varepsilon\,L = -sL, \tag{18}$$

$$A^k_i + A^k_i = -(1-s)\,G^k_i/i\sqrt{s}, \quad A^k_i - A^k_i = -(1+s)\,A^k_i/i\sqrt{s}, \tag{19}$$

$$G^k_i = A^k_i - \tfrac{1}{2}A\delta^k_i, \quad Q'^k_i = A^k_i - \tfrac{1}{4}A\,\delta^k_i, \quad A'^k_i/A^k_i = A^k_i/A'^k_i = i\sqrt{s}, \tag{20}$$

$$L^k_i = A\,A^k_i + A\,A^k_i, \quad l'^k_i = G\,G^k_i + G\,G^k_i, \quad L'^k_i = A'A'^k_i + A'\,A'^k_i \tag{21}$$

(β and α are integers, positive or negative, including 0). For $\beta = 0, 1, 2$, we identify the quantities A with Γ, J, N, respectively; similarly the a are identified with γ, j, n, $= -iV$, the quantities A with P, H, F, the quantities a with p, h, f, $= iU$; then from Eq. (17) we have

$$P/H = H/F = \sqrt{\varepsilon}, \quad \Gamma/P = P/\Gamma = i\sqrt{s}. \tag{17'}$$

From Eq. (18), to each pair of values of A, a there correspond four values of $\pm A$, $\pm A$ and $\pm a$, $\pm a$. For instance, to each pair of P, U there correspond four values of $\pm\Gamma$, $\pm\Gamma$ and $\pm V$, V such that $\Gamma\,\Gamma = P^2$, $\Gamma + \Gamma = 2U$; conversely, to each pair of values of Γ, V there correspond four values of $\pm P$, $\pm P$ and $\pm U$, $\pm U$ such that $P\,P = \Gamma^2$, $P + P = 2V$.

2. We have

$$s = (1 - 4a^2/A^2)^{1/2} = (1 + 4a^2/A)^{-1/2},$$
$$\varepsilon = (1 + A^2/a)^{1/2} = (1 - A^2/a^2)^{-1/2}, \tag{22}$$

$$2ia/A = 1 - s, \quad -2ia/A = 1 + s, \tag{23}$$

$$L/a^2 = 2iA/a = -2(1-\varepsilon), \quad L/a^2 = -2iA/a = -2(1+\varepsilon), \tag{24}$$

$$Q'^k_i/Q'^k_i = Q'^k_i/Q'^k_i = 1/i\sqrt{s}, \quad L^k_i = -l'^k_i + \tfrac{1}{2}L\delta^k_i = L'^k_i, \tag{25}$$

$$A = -G = A', \quad L = l' = L', \tag{26}$$

$$a - a = a + a = -iA, \quad A - A = A + A = 2a, \tag{27}$$

$$A^2 - a^2 + a^2 = 0, \quad 4a^2 - A^2 + A^2 = 0, \quad L = a^2 - a^2 + a^2 - a^2. \tag{28}$$

The quantities in Eq. (23) and (24) and the normalized scalars and Lagrangians of (26) are obtained by contraction of the tensor of (19), (20), and (21), and Eq. (28) follow from (27). From (28) we have ($f\mu = q$, $n\mu = m$, $f\sqrt{\mu} = q'$, $n\sqrt{\mu} = m'$):

$$P^2 - p^2 + f^2 = 0\,(F^2 - f^2 + q^2 = 0),$$
$$\Gamma^2 - \gamma^2 + n^2 = 0\,(N^2 - n^2 + m^2 = 0); \qquad (28')$$

$$P^2 - P^2 - 4j^2 = 0\,(F^2 - F^2 - 4m'^2 = 0),$$
$$\Gamma^2 - \Gamma^2 - 4h^2 = 0\,(N^2 - N^2 - 4q'^2 = 0). \qquad (28'')$$

In (18) we have $L_{00} = 4h_1$, $L_{10} = 4l_1 = \mu L_{00}$, $L_{01} = 4h_2 = -wL_{00}$, $L_{11} = 4l_2 = \mu w L_{00}$,

$$h_1 + l_1 = {}^1/_2 J_1^2, \quad h_1 - l_1 = -{}^1/_2 H_1^2,$$
$$h_2 + l_2 = -{}^1/_2 J_2^2, \quad h_2 - l_2 = {}^1/_2 H_1^2. \qquad (18')$$

The conformal transformations

$$\overset{\beta\alpha}{\gamma}_{ik} = g_{ik}\,\varepsilon^{\beta/2}(-s)^{\alpha/2}\,(g_{ik} = \overset{00}{\gamma}_{ik}) \qquad (29)$$

permute separately the scalars $A_{\beta\alpha}$, $a_{\beta\alpha}$, the scalars of (26), the tensors $Q'^{k}_{i\,\beta\alpha}$ and the tensors of (21). For arbitrary β and α, the gravitational equations

$$L^k_{i\,\beta\alpha} = \frac{1}{4} L \delta^k_i, \quad \text{or} \quad l'^k_{i\,\beta\alpha} = \frac{1}{4} l' \delta^k_i \qquad (30)$$
$$\text{or} \quad L'^k_{i\,\beta\alpha} = \frac{1}{4} L' \delta^k_i$$

are therefore equivalent, from the conformal point of view, to Eq. (3). Owing to relations (25) and (26), they are all equivalent for fixed α and β. The components of any tensor density of arbitrary weight and order, for instance the scalars $A_{\beta\alpha}$ and $a_{\beta\alpha}$, those of (26), the tensors $Q'^{k}_{i\,\beta\alpha}$, and those of (21) satisfy the relation

$$T_{\beta-\beta',\,\alpha+\alpha'}\; T_{\beta-\beta',\,\alpha-\alpha'} = T^2_{\beta\alpha}. \qquad (31)$$

3. The normalized fundamental scalars of the nonlinear conformal reciprocity theory form a group which is isomorphic to the cubic dihedral (projective) group D_6; in quantum mechanics they are therefore replaced by operator groups. Expressing the relations between the scalars $A_{\beta\alpha}$, $a_{\beta\alpha}$, for instance in terms of the quantities Γ, P, U, and V with indices 1 and 2, we obtain the groups B_2, B_1, B_{12}, A_2, A_1, and A_{12}.

$$(B_2): \qquad \Gamma_2 / U_1 = P_1 / V_1 = 2/(1-s) = 1 - \varepsilon,$$
$$-N_2 / U_1 = -F_1 / V_1 = 2/(1+s) = 1 - \mu,$$

and their inverse quantities and scalars are $p_1/iU_1 = P/F_1 = \Gamma/N_1 = \Gamma/N_2 = (s+1)/(s-1) = \epsilon$, $(s-1)/(s+1) = \mu$.

$$(B_1): \qquad \Gamma_1 / U_1 = P_1 / V_2 = 2/(1-w) = 1 + \varepsilon,$$
$$N_1 / U_1 = F_1 / V_2 = 2/(1+w) = 1 + \mu,$$

and their inverse scalars are $-\epsilon$, $-\mu$.,

$$(B_{12}): \quad P_1^2 / U_1^2 = \Gamma_1^2 / V_1^2 = \Gamma_2^2 / V_2^2 = -4w/(1-w)^2 = 1 - \varepsilon^2,$$
$$-F_1^2 / U_1^2 = -N_1^2 / V_1^2 = -N_2^2 / V_2^2 = 4w/(1+w^2) = 1 - \mu^2,$$

and their inverse quantities are ϵ^2, μ^2.

$$(A_2): \qquad 2U_1 / \Gamma_2 = 2V_1 / P_1 = 2/(1-\varepsilon) = 1 - s,$$
$$2U_1 / \Gamma_1 = 2V_2 / P_1 = 2/(1+\varepsilon) = 1 - w,$$

and their inverse quantities and scalars are $-\Gamma_1/\Gamma_2 = -P_1/P_2 = -V_1/V_2 = -U_1/U_2 = (\epsilon+1)/(\epsilon-1) = s$, w.

$$(A_1): \qquad -2U_1/N_2 = -2V_1/F_1 = 2/(1-\mu) = 1 + s,$$
$$2U_1 / N_1 = 2V_2 / F_1 = 2/(1+\mu) = 1 + w,$$

and their inverse quantities and scalars are $-s$, $-w$.

$$(A_{12}): \quad -4U_1^2/J_2^2 = -4V_1^2/H_1^2 = -4\mu/(1-\mu)^2 = 1 - s^2,$$
$$4U_1^2/J_1^2 = 4V_2^2/H_1^2 = 4\mu/(1+\mu)^2 = 1 - w^2,$$

and their inverse quantities and scalars are s^2, w^2.

More generally, the groups A and B describe the normalized fields (curvatures) of (23) and the normalized Lagrangians of (24) for *arbitrary* indices β and α. Interchange of the conformal factors $\epsilon \leftrightarrow s$, $\mu \leftrightarrow w$ causes interchange of the groups according to $B_1 \leftrightarrow A_1$, $B_2 \leftrightarrow A_2$, $B_{12} \leftrightarrow A_{12}$. In the same way $\epsilon \leftrightarrow -\epsilon$, $s \leftrightarrow w$ leads to $B_2 \leftrightarrow B_1$. Similarly, $s \leftrightarrow -s$, $\epsilon \leftrightarrow \mu$ leads to $A_2 \leftrightarrow A_1$. The elements of the groups A_{12} and B_{12} are products of the elements of A_1, A_2 and B_1, B_2. In this way we again obtain, for arbitrary distributions and motion of matter, the cubic dihedral group D_6 as described in the author's dissertation[9] (as well as elsewhere[11, 28]), independent of linear electrodynamics, in the capacity of the basis for a certain group algebra (the subalgebra of a generalization of the Dirac algebra) and a certain isomorphic operator or field-function group which corresponds to a spherical distribution of particle and field. The group $D_6 = C_3C_2'$ is a direct product of the two cyclic subgroups C_3, C_2'. The group C_3 corresponds to a triplet: the kinematic variables (space-time), the 4-current variables (3-current–charge), and the dynamical variables (momentum–energy) (and therefore to a pair of C_2: 4-current–kinematic and dynamical variables). The subgroup C_2' corresponds to the pair: gravitation-electromagnetism (and therefore essentially to a triplet C_3': electricity–gravitation–magnetism).

III. CONSTANT AND VARIABLE QUANTITIES

1. Let us set $\delta = \sqrt{k}/c$. Let, in Kalantarov's[10] system of units, $\epsilon_0\epsilon'$ be the dielectric constant (of dimensionality $Q\Phi^{-1}L^{-1}T$), $\mu_0\mu'$ the magnetic permeability (of dimensionality $Q^{-1}\Phi L^{-1}T$), $q_0 = e'\sqrt{\epsilon_0}/\delta$, $\phi_0 = \phi_0'/C = e''/\sqrt{\epsilon_0}\delta c$ the electric and magnetic units of charge (of dimensionality Q and Φ)(canonical conjugates), and $e_0 = e/\delta$ the mechanical ("gravitational") unit of charge [of dimensionality $(Q\Phi LT^{-1})^{1/2}$]. In this system of units the dimensionalities of the fields P, H, F (as also the appropriate mixed components) are QL^{-2}, $(Q\Phi L^{-3}T^{-1})^{1/2}$, $\Phi L^{-1}T^{-1}$, respectively. Let a be the radius of a charged elementary particle, and $W = m/\delta^2$ be its energy in gravitational (mechanical) units. We have the following "conformal" relations with the constant coefficients $(\epsilon_0\epsilon')^{1/2} = (\mu_0\mu' c^2)^{-1/2}$, $\delta\lambda = 1/\delta'\lambda'$ (where ϵ', μ', λ, λ' are dimensionless)[10]

$$q_0/e_0 = e_0/\varphi_0' = (\varepsilon'\varepsilon_0)^{1/2}(e'/e = e/e'' = \sqrt{\varepsilon'}), \quad (32)$$

$$a/e_0 = e_0/W = \lambda\delta \; (a/e = e/m = \lambda)$$

and similar relations for the "quanta" of time $b_0 = b/c$ (Ambartsumian, Ivanenko[29]), momentum, and current, related by powers of the constant "conformal" factor $\delta c\lambda = \sqrt{k}\lambda$. Since h is the quantum of action, and $l^2 = hk/c \approx 10^{-64}$ cm^2, the canonically conjugate quantities are related by expressions of the type

$$b_0W = h \quad \text{or} \quad bm = l^2. \quad (32')$$

2. We have the associations $\underset{\alpha}{P}, \underset{\alpha}{H}, \underset{\alpha}{F} \leftrightarrow \underset{\alpha}{\Gamma}, \underset{\alpha}{J}, \underset{\alpha}{N}$ and $\underset{\alpha}{P}, \underset{\alpha+1}{\Gamma}$, $\underset{\alpha+1}{P} \leftrightarrow \underset{\alpha}{\Gamma}, \underset{\alpha}{P}, \underset{\alpha+1}{\Gamma}$, which are determined by by the conformal factors $\sqrt{\epsilon} = 1/\sqrt{\mu}$, $i\sqrt{s} = i/\sqrt{w}$ (and similarly for all $\underset{\beta\alpha}{A}$ and $\underset{\beta\alpha}{a}$). The close relation deduced above between the field f_{ik} and the curvature tensor Γ_{ik} is in some sense similar to the relation noted within the framework of Fock's[30] quantum theory. The conformal relations (17')[or the more general relations (17), (31)] correspond exactly to the "conformal" relations (32). The constants $\epsilon'\epsilon_0$ and λ^2k [or $(\epsilon'\epsilon_0)^{1/2}$ and $\lambda\delta$] become the variable quantities $\epsilon_1 = 1/\sqrt{\epsilon_2} = \epsilon\epsilon_0 c = (\mu\mu_0 c)^{-1}$ and $k_1 = 1/k_2 = sk = k/w$. The conform invariant quantity $\sqrt{\epsilon_1} = 1/\sqrt{\epsilon_2}$ relates the magnitudes of the triplet C_3' (and therefore those of the pair C_2'). The conform invariant quantity $\sqrt{k_1} = 1/\sqrt{k_2}$ relates the magnitudes of the triplet C_3 (and therefore of the pair C_2).

3. The quantities ϵ and s are associated with themselves as a result of reciprocity. The replacements $s \leftrightarrow w$ and $\epsilon \leftrightarrow -\epsilon$ are equivalent, as is similarly true for the replacements $\epsilon \leftrightarrow \mu$ and $s \leftrightarrow -s$. The variability of the dielectric constant (or the nonlinearity of electrodynamics) and the variability of the gravitational constant (postulated by Dirac and developed in the projective theory of relativity[31-34]) are equivalent, in a certain sense, and follow automatically from the gravitational equations of the conformal reciprocity theory developed above and therefore from the Lagrangian density $L\sqrt{g} = (\Gamma^2 + P^2)\sqrt{g}$. We shall differentiate between two types of nonlinearity. The first kind of nonlinearity of the gravitational field is due to the nonlinearity of the gravitational curvature tensor Γ_{ik} with respect to the electromagnetic potentials g_{ik} (or $u_{ik} = \Psi g_{ik}$) and their first derivatives and to the nonlinearity of the electromagnetic curvature tensor P_{ik} with respect to the electromagnetic potentials g_i (or $p_i = \Psi^{1/2}g_i$) and their first derivatives. Nonlinearities of the second kind arise from the fact that the Lagrangian L is quadratic (that is,

the density $L\sqrt{g}$ is conform invariant) and therefore the gravitational equations (3) and equations (9) are quadratic in Γ, P (and ϕ). The second kind of nonlinearity (and therefore the existence of "maximum" fields) reflects the fact that it is inconsistent to treat the separate fields, or the quantities C_3 and C_3' (as well as meson, spinor, etc. fields) alone, and thus reflects the reciprocity principle inherent in the structure of the field equations and in the many-dimensional conformal metric (see Section IV).

4. The "maximum" electromagnetic field $U = -if = L/2\Gamma$ (and all $\underset{\alpha}{U} = -if$) and the "maximum gravitational field" $-iV = n = -iL/2P$ (and all $-\underset{\alpha}{iV} = \underset{\alpha}{n}$), as opposed to those of the Born-Infeld theory, are variable and given by the conformal field equations. As a nonlinear theory, the conformal reciprocity theory bears the same relation to the Born-Infeld theory of relativity, based on a variable maximum velocity $v_4 = cv_4' = i(g_{44})^{1/2}$, bears to the special theory in which the maximum velocity c is a constant. With the aid, however, of the conformal transformations $g^*_{ik} = g_{ik}\underset{\alpha}{U}$, $g^{**}_{ik} = -ig_{ik}\underset{\alpha}{V}$, the fields $\underset{\alpha}{U}$ and $-\underset{\alpha}{iV}$ in terms of the metrics $\underset{\alpha}{g^*_{ik}}$ (and $\underset{\alpha}{g^{**}_{ik}}$, respectively) become quantum constants $\underset{\alpha}{U^*} = -\underset{\alpha}{iV^{**}}$, which we have taken above equal to we have taken above equal to unity. In the metrics $\underset{1}{g^*_{ik}}$ and $\underset{2}{g^{**}_{ik}}$, L becomes linear: $L^* = 2\Gamma^*$ (Einstein's Lagrangian), $L^{**} = 2iP^{**}$ [see Eq. (9′)]. The gravitational equations (4) become

$$L_i^{*k} - \frac{1}{2}\Gamma^*\delta_i^k = 0 \quad \text{or} \quad L_i^{**k} - \frac{1}{2}P^{**}\delta_i^k = 0. \tag{33}$$

Similar results hold for arbitrary β or α. In analogy with the (nonconformal covariant) theory of the Broglie's double solution, the continuous fields (F^*, N^{**}) and singular fields ($-i\underset{1}{P^*} \to \underset{1}{\Gamma^{**}} \to \infty$ as $\epsilon \to \infty$, $s \to 1$, and analogously $-\underset{0}{iP^*} \to \infty$ as $s \to \infty$, $\epsilon \to 1$ and $\underset{1}{\Gamma^{**}}$ is finite) are solutions of the same conformal equations.

The metric $\underset{1}{g^*_{ik}}$ corresponds to the Born-Infeld theory. A "point" particle (singularity of the matter field), described by the quantities p^*_{ik}, Γ^{**}_{ik} is only the first approximation to an actual "smeared out" particle, identified with the matter field described by the quantities F^*_{ik}, N^{**}_{ik}. In the case $P \neq 0$ and $F \neq 0$, the limiting value $\epsilon = \mu = 1 (s = 1/w = \infty)$, corresponding to $\underset{1}{U} \to -\underset{1}{iV} \to \infty$ and $\underset{2}{V} \to \underset{1}{F}/2$, implies that $\underset{1}{\Gamma} \to \underset{1}{N} \to \infty$, $\underset{00}{L} \to \infty$, $\underset{2}{\Gamma} \to \underset{2}{N} \to 0$, and $\underset{01}{L} \to \underset{1}{F^2}$. The scalar $l_2 = \underset{01}{L}/4$ therefore approaches the Maxwell Lagrangian $F^2/4$. In the case $\epsilon = \mu = 1 (s = 1/w = \infty)$ and $P = F = 0$, we have $\underset{1}{U} \to \underset{1}{\Gamma}/2$, $\underset{00}{L} \to 4\underset{1}{U^2} \to \underset{1}{N^2} \to \underset{1}{\Gamma^2}$, and $\underset{01}{L} \to \underset{2}{N} \to \underset{2}{\Gamma} \to 0$.

IV. THE METRIC OF RECIPROCITY THEORY

1. Let $ds = ds_1/f$, $d\bar{s} = id\bar{s}_1$, $d\bar{\bar{s}} = (ds\,d\bar{s})^{1/2} = (id\bar{s}_1\,ds_1/f)^{1/2}$ be, respectively, the kinematic (space-time), dynamic (momentum-energy) and 4-current (3-current–charge) "world" intervals. Let $dS = idS_1/f$, $d\bar{S} = d\bar{S}_1$, $d\bar{\bar{S}} = (dS\,d\bar{S})^{1/2} = (id\bar{S}_1\,dS_1/f)^{1/2}$ be the corresponding "proper intervals" ($\underset{1}{f} = f$, $\underset{1}{p} = p$, $\underset{1}{F} = F$, $\underset{1}{P} = P$). Let

$$d\tau^2 = d\bar{s}_1^2 + ds_1^2 + 2g_1\,d\bar{s}_1\,ds_1, \tag{34}$$

$$dT^2 = -(d\bar{S}_1^2 + dS_1^2 + 2G_1\,d\bar{S}_1 dS_1).$$

The total conformal interval (with the same dimensions as $d\bar{s}^2$, that is those of the energy-momentum tensor) will be

$$d\tau'^2 = d\tau^2 + dT^2 = 0; \tag{35}$$

$d\tau^2$ is a "kinematic" quantity (C), a "dynamic" quantity (D), or an "isobaric" quantity, depending on whether $d\tau^2$ is less than, greater than, or equal to zero. Let $g_1 = G_1 = 0$. If $d\tau^2 < 0 (d\bar{s}^2 < f^2\,ds^2)$ or, respectively, $d\tau^2 > 0 (d\bar{s}^2 > f^2\,ds^2)$, there exists a standard coordinate system in which

$$\begin{aligned} &(C)\quad d\bar{S}_1 = 0,\ ds_1 = p^*dS_1,\ ds_1 = iP^*dS_1, \\ &\quad (d\bar{S} = 0,\ ds = \varepsilon dS,\ d\bar{s} = Fds = PdS); \\ &(D)\quad ds_1 = 0,\ d\bar{S}_1 = p^*d\bar{s}_1,\ dS_1 = iP^*d\bar{s}_1, \\ &(ds = 0,\ d\bar{S} = \varepsilon d\bar{s},\ dS = Fd\bar{S}/f^2 = Pd\bar{s}/f^2) \end{aligned} \tag{36}$$

are the conformal relations between the "world" and "proper" kinematic and dynamic intervals. The interval (35) is therefore equivalent to (28′). When the "world" and "proper" kinematic and dynamic

quantities are interchanged, Eq. (36) and (36′) are interchanged.

By reciprocity with the space interval $d\sigma^2$ or the momentum interval dl^2, the dynamic interval $d\bar{s}^2$ probably corresponds to r rows of four variables $\overset{a}{x}{}^i$ (where $a = 1, 2, \ldots, r$) analogous to the variables x^i (space-time) of the intervals ds^2. Then $d\bar{s}_1^2$ is a quadratic form in the variables $\overset{a}{dx}{}^i$, the metric $\overset{a}{ds}$, or the Pfaffian $\overset{a}{d\varphi}$ (real or matrix); the product $2g_1 d\bar{s}_1 ds_1$ is accordingly replaced by $2\lambda_{aik}\overset{a}{dx}{}^i dx^k$, $2\lambda_a \overset{a}{ds} ds$, or $2\lambda'_a \overset{a}{d\varphi} d\varphi$; similar statements hold for the proper quantities dS_1^2 and $2G_1 d\bar{S}_1 dS_1$.

2. From the above we obtain a correspondence principle between relativity theory and reciprocity theory. The fact that the interval $d\tau^2$ breaks up into a dynamic $d\bar{s}^2$ and kinematic ds^2 interval and mixed terms $d\bar{s}ds$, corresponds exactly to the general relativistic case, that is, the splitting of the $d\bar{s}^2 = dl^2 - dW^2/v_4^2 + 2h'_\gamma dl^\gamma dW$ ($\gamma = 1, 2, 3$) into the intervals dl^2 (momentum), dW^2 (energy), and mixed terms, as well as the splitting of the interval $ds^2 = d\sigma^2 - v_4^2 dt^2 + 2l'_\gamma dx^\gamma dt$ into the space interval $d\sigma^2$, the time interval dt^2, and mixed terms. The case $G_1 = g_1 = 0$ corresponds to the general relativistic static case.

From the above we obtain relations between the zero weight quantities $F/f = P/p = iF^*$ and $v/v_4 = u/u_4 = iv$,

$$\varepsilon = 1/\mu,\ s = 1/w \text{ and } z = 1/z'$$

$$= (x+1)/(x-1) = (1 + u^2/v_4^2)^{1/2} \qquad (37)$$

$$= (1 - v^2/v_4^2)^{-1/2},\ x = 1/x' = (z+1)/(z-1).$$

We also obtain definite relations between the conformal many-dimensional components of the "proper" electromagnetic field ("dynamic" field $F = d\bar{s}/ds$ corresponding to the force $q_0 F = q_0 d\bar{s}/ds$; the "kinematic" field $f = fds/ds$ equal to the maximum field which corresponds to the maximum force $q_0 f$; the field $q = f\mu$) and between the conformal components of the velocity: the spatial velocity $v = d\sigma/dt$ ($= dW/dl$ for $v_4 = \text{const}$), the time-component of the velocity $v_4 = v_4 dt/dt = v_4 dl/dl$ (= maximum velocity = the general relativistic velocity of light $v_4 = cv_4' = -i(g_{44})^{1/2}$) and the velocity $w_0 = v_4 z'$. Similarly, the "world" electromagnetic field ("dynamical" field $P = \epsilon F = d\bar{s}/dS$, "kinematic" field $p = \epsilon f = fds/dS$, and the field $f = p\mu$) corresponds to the world velocity [spatial velocity $u = zv = d\sigma/ds'$ ($= dW/d\bar{s}$ for $v_4 = \text{const}$), the time-component of the velocity $u_4 = zv_4 = v_4 dt/ds'$ ($= v_4 dl/ds$ for $v_4 = \text{const}$), and the velocity $v_4 = u_4 z'$ ($ds = iv_4 ds'$)]. The absolute values of Equation (28′) of the "world" and "proper" electromagnetic fields correspond, therefore, to the absolute values of the world and proper velocities: $u^2 - u_4^2 + v_4^2 = 0$ ($v^2 - v_4^2 + w_0^2 = 0$). The relations

$$\underset{D}{d\bar{s}} = \mu \underset{D}{d\bar{S}},\quad \underset{C}{ds} = \varepsilon \underset{C}{dS} \qquad (38)$$

[see Eq. (36), (36′)] are analogous to the contraction of length and slowing down of time for a moving particle; the first relation indicates the mass defect of a particle interacting with the aggregate, and the second, the corresponding elongation of the interval; the invariant product $\underset{C\,D}{ds}\underset{C\,D}{d\bar{s}} = \underset{C\,D}{dS}\underset{C\,D}{d\bar{S}}$ is analogous to an invariant space-time hypervolume.

Under the conformal transformation (29), the electromagnetic quantities P, H, F and p, h, f, which are related by the many-dimensional relations (34)–(38), transform into a column of the matrices $\|A\|$ and $\|a\|$. Thus, Eq. (34)–(38) and the correspondence between the fields and velocities are valid for arbitrary indices β, α, or for gravitational and other fields, as well as the electromagnetic.

3. We can formulate our conclusions more generally. Let $\overset{\beta\alpha}{V}_4$ be the manifold with the interval $\overset{\beta\alpha}{ds}_1$ (where $\beta, \alpha = 0, 2, 4$); $\overset{\beta 4}{V}_4$, $\overset{\beta 2}{V}_4$, $\overset{\beta 0}{V}_4$ and $\overset{4\alpha}{V}_4$, $\overset{2\alpha}{V}_4$, $\overset{0\alpha}{V}_4$ are the kinematic, 4-current, and dynamic manifolds, and correspondingly the electric ("world"), gravitational ("mixed"), and magnetic ("proper") manifolds. For $G_1 = g_1 = 0$, let $\overset{\beta\alpha}{ds}_1 = \overset{\beta\alpha}{ds} f^{\alpha/4}$ in absolute value. For $\beta\alpha = 00$, 04, 40, and 44 the interval $\overset{\beta\alpha}{ds}_1$ coincides with $d\bar{S}_1$, dS_1, $d\bar{s}_1$ and ds_1 respectively, and $\overset{\beta\alpha}{ds}$ coincides with $d\bar{S}$, dS, $d\bar{s}$, and ds. In the special coordinate systems corresponding to Eq. (36) (case C) and (36′) (case D), respectively, we have

$$(C) \qquad \|\overset{\beta\alpha}{ds'}\| = ds \begin{pmatrix} 0 & 0 & q \\ 0 & 0 & q^{1/2} \\ F & F^{1/2} & 1 \end{pmatrix} \qquad (39)$$

$$\overset{\beta\alpha}{ds}_1 = \overset{\beta\alpha}{ds'} f^{(\alpha+\beta-4)/4}$$

$$(\overset{44}{ds}_1 / f = \overset{44}{ds} = \overset{44}{ds'} = ds_1 / f = ds)$$

$$\| \overset{\beta\alpha}{ds'} \| = d\bar{S} \begin{pmatrix} 1 & F^{1/2} & F \\ q^{1/2} & 0 & 0 \\ q & 0 & 0 \end{pmatrix}$$

(D) (39′)

$$\overset{\beta\alpha}{ds_1} = \overset{\beta\alpha}{ds'} f^{-(\alpha+\beta)/4}$$

$$(\overset{00}{ds_1} = \overset{00}{ds} = \overset{00}{ds'} = d\bar{S}_1 = d\bar{S})$$

In case C [see Eq. (39)] $\overset{44}{ds'}$, $\overset{42}{ds'}$, $\overset{40}{ds'}$ and $\overset{44}{ds'}$, $\overset{24}{ds'}$, $\overset{04}{ds'}$ are obtained from $ds = \overset{44}{ds'}$ by multiplication by the conformal factors 1, $F^{1/2} = (-F_0 w)^{1/2}$, $F = -F_0 w$ and 1, $q^{1/2} = (f\mu)^{1/2}$, $q = f\mu$. These conformal relations, based on the reciprocity of the conformal factors $w = 1/s$ and $\mu = 1/\epsilon$, F and q, can be combined with Eq. (17′) and (32). In case D [Eq. (39′)] the indices 0 and 4 commute, so that the world and proper, kinematic and dynamic nami-

folds commute (in particular $\overset{44}{ds} = ds$ and $\overset{00}{ds} = d\bar{S}$).

4. In case C we have the conformal relation

$$\overset{4\alpha}{ds'} / \overset{2\alpha}{ds'} = \overset{2\alpha}{ds'} / \overset{0\alpha}{ds'} = 1/q \; (= \varepsilon / f), \qquad (40)$$

$$\overset{\beta 4}{ds'} / \overset{\beta 2}{ds'} = \overset{\beta 2}{ds'} / \overset{\beta 0}{ds'} = 1/F \; (= -s/F_0)$$

and the more general conformal relations, which follow from (46) [or (48), (48′)] of the form

$$\underset{C\ D}{ds}\,\underset{C\ D}{ds} = \underset{C\ D}{dS}\,\underset{C\ D}{dS} \quad \text{or} \quad \underset{C\ D}{\overset{44\ 40}{ds\ ds}} = \underset{C\ D}{\overset{04\ 00}{ds\ ds}} \qquad (41)$$

In case D the indices 0 and 4 are interchanged in (40). More generally, the components T of any relative tensor of zero order and arbitrary weight (depending on $r' \gtrless 4$ variables) satisfy, in $\overset{\beta\alpha}{V_4}$, the conformal relations

$$\overset{4\alpha\,0\alpha}{TT} = \overset{2\alpha}{(T)^2}, \quad \overset{\beta 4\beta 0}{TT} = \overset{\beta 2}{(T)^2}, \quad \underset{C\ D}{\overset{44\ 40}{(TT}} = \underset{C\ D}{\overset{04\ 00}{T\ T)}}. \qquad (42)$$

In particular, for the components of F, q we have

$$\underset{C}{\overset{42}{F}} = \underset{C}{\overset{24}{q}} = \underset{D}{\overset{02}{F}} = \underset{D}{\overset{20}{q}} = i.$$

Eqs. (40) [as well as (41) and (42)] generalize Eqs. (32), (32′) with the constant conformal factors $\lambda\delta$, $(\epsilon' \epsilon_0)^{1/2}$, which are valid for an elementary particle as a whole; they also generalize the uncertainty relations, and in particular Eqs. (41) generalize Eqs. (32′) for canonically conjugate quantum quantities. Eqs. (40)–(42) reflect to some extent the uncertainty of field quantities, as noted by Bogoliubov and co-workers[35,36], Markov[37], Born, Raiskii[38], Yukawa and others.

5. The above conformal theory generalizes the reciprocity principle[2-12,28], which leads to covariance of physical laws [see Eqs. (3), (4), (6), and (35)] with respect to the variables of the manifold $\overset{\beta\alpha}{V_4}$, and therefore with respect to pairs of opposite variable forms of the existence (I) and attributes (fundamental properties) (II) of matter. In (I) we include the space-time variables, in I′ the space and proper variables (in the relativistic sense), in II the kinematic and dynamic variables, and in II′ the "world" (electric) and "proper" (magnetic) variables. Each pair corresponds to canonically conjugate quantities. Mixed products, that is elements of the type $dx\gamma\, dt$ [space-time (γ = 1, 2, 3], $dt\, ds$ (world-proper element), $d\bar{s}\, ds$ (4-current), $ds\, dS$ ("gravitational" element), correspond to "self-conjugate" quantities. With respect to I, the kinematic variables II break up into coordinates and time, the dynamical variables into momentum and energy, and the 4-current into the 3-current and charge. The elements of II break up in the same way with respect to II′, I′. The conformal factor $\sqrt{k_1} = 1/\sqrt{k_2}$ (or $\delta\sqrt{s} = \delta/\sqrt{w}$) thus relates the variables of II and the 4-current (that is the fields $\underset{\alpha}{\Gamma}$, $\underset{\alpha+1}{\Gamma}$, $\underset{\alpha}{P}$), and the conformal factor $\sqrt{\epsilon_1} = 1/\sqrt{\epsilon_2}$ [or $\sqrt{\epsilon\epsilon_0} = \mu\mu_0 c^2)^{-1/2}$] relates the variables of II′ and the mixed (gravitational) variables (in other words the fields $\underset{\alpha}{\Gamma}$, $\underset{\alpha}{N}$, $\underset{\alpha}{J}$, or $\underset{\alpha}{P}$, $\underset{\alpha}{F}$, $\underset{\alpha}{H}$). I, II, I′, and II′, correspond to the cyclic groups C_2' or C_3, or to the Pauli groups[9,10,11,28]. The complete abstract group[9,10,11,28] (their direct product) is represented by groups of operators or functions and the elements of a certain isomorphic group algebra which is a generalization of the Dirac algebra.

The above theory can be extended to the case of complex Langrangians[39,40], nonlinear Infeld action functions[25], nonsymmetric g_{ik}[7,8,23-25], as well as to the cases of meson and spinor fields[7,8,15,23,37,41-44].

---

[1] Gh. Vranceanu, *Lectii de geometrie diferentiala* I, II, Bucuresti (1951)

[2] A. Popovici, Rev. Univ. "C. I. Parhon", Bucuresti 3, 78 (1953); Bul. Sect. Acad. RPR 6, 65 (1954).

[3] A. Popovici, Dokl. Akad. Nauk SSSR 111, 1, 74 (1956)

[4] M. Born, Proc. Roy. Soc. (London) **165**, 291 (1937), **166**, 552 (1938); Proc. Roy. Soc (Edinbg.) **59**, 219 (1939).

[5] M. Born, Rev. Mod. Phys. **21**, 463 (1949).

[6] M. Born, K. Fuchs, Proc. Roy. Soc. (Edinbg.) **60**, 141, 147 (1940).

[7] D. Ivanenko, A. Sokolov, *Classical Field Theory*, M.-L. (1949).

[8] R. Ingraham, Proc. Nat. Ac. USA, **38**, 921 (1952); Nuovo cimento **9**, 886 (1952); **12**, 825 (1954).

[9] A. Popovici, Bul. Politehn. Jassy **3**, 543 (1948).

[10] A. Popovici, Rev. Univ. "C. I. Parhon", Bucuresti **1**, 77 (1952).

[11] A. Popovici, C. R. du Congrès des mathémat. hongrois 665 (1950).

[12] J. Rayski, Acta Phys. Pol. **5**, 1 (1950).

[13] E. Reichenbacher, Z. Phys. **45**, 663 (1921).

[14] Iu. B. Rumer, J. Exptl. Theoret. Phys. (U.S.S.R.) **19**, 86, 207 (1949).

[15] J. A. Schouten, Rev. Mod. Phys. **21**, 421 (1949).

[16] J. K. Lubanski, L. Rosenfeld, Physica **9**, 116 (1942).

[17] L. Hill, Phys. Rev. **72**, 237 (1947).

[18] A. Pais, Physica **9**, 267 (1942).

[19] B. Hoffman, Phys. Rev. **72**, 458 (1947); **73**, 30 (1948).

[20] V. Rodivech, J. Exptl. Theoret. Phys. (U.S.S.R.) **21**, 869 (1951).

[21] O. Veblen, B. Hoffman, Phys. Rev. **36**, 810 (1930).

[22] V. A. Fock, Z. Phys. **39**, 226 (1926).

[23] M. Born, Proc. Roy. Soc. (London) **143**, 410 (1934); Proc. Cambridge Phil. Soc. **32**, 102 (1936); Ann. inst. Henri Poincare **7** (1937).

[24] M. Born, L. Infeld, Proc. Roy. Soc. (London) **144**, 425 (1934); **147**, 522 (1934); **150**, 141 (1935).

[25] L. Infeld, Proc. Cambridge Phil. Soc. **32**, 127 (1936); **33**, 70 (1937).

[26] W. Thirring, Z. Naturforsch. **5**, 714 (1950).

[27] L. de Broglie, J. phys. **8**, 225 (1927), Compt. rend. **183**, 447 (1926); **184**, 273 (1927); **232**, 12 (1951); **233**, 18 (1951); **234**, 3 (1952).

[28] A. Popovici, Bul. Sec. I. Acad. RPR (Sesiunea generala stiintifica, June, 1950).

[29] V. Ambartsumian, D. Ivanenko, Z. Phys. **64**, 563 (1930).

[30] V. A. Fock, Z. Phys. **57**, 261 (1929).

[31] P. Jordan, Ann. d. Phys. **36**, 64 (1929).

[32] P. Jordan, Cl. Müller, Zs. f. Naturforsch 1 (1947).

[33] G. Ludwig, Arch. Math. **1**, 212 (1948); **124**, 450 (1948); **125**, 545 (1949).

[34] G. Ludwig, *Fortschritte der projektiven Relativitätstheorie*, Hannover, 1948.

[35] Bogoliubov, Bonch-Bruevich, and Medvedev, Dokl. Akad. Nauk SSSR **74**, 681 (1950).

[36] V. L. Bonch-Bruevich and V. V. Medvedev, J. Exptl. Theoret. Phys. (U.S.S.R.) **22**, 4 (1952).

[37] M. A. Markov, Dokl. Akad. Nauk SSSR **75**, 1 (1950).

[38] J. Rayski, J. Exptl. Theoret. Phys. (U.S.S.R.) **22**, 194 (1952).

[39] P. Weiss, Proc. Phil. Soc. Cambridge **33**, 79 (1937).

[40] Madhava Rao, Proc. Ind. Acad. Sc. **A4**, 377, 575 (1936); **A7**, 333 (1936).

[41] D. Blokhintsev, Usp. Fiz. Nauk **42**, 76 (1950); Dokl. Akad. Nauk SSSR **82**, 4 (1952).

[42] D. Ivanenko, V. Rodichev, J. Exptl. Theoret. Phys. (U.S.S.R.) **9**, 526 (1939).

[43] D. Ivanenko, M. Brodskii, Dokl. Akad. Nauk SSSR **84**, 4 (1951).

[44] D. Ivanenko, V. Kurdgelaidze, S. Larin, Dokl. Akad. Nauk SSSR **88**, 22 (1953).

Translated by E. J. Saletan
175

Diffraction Scattering of Fast Deuterons by Nuclei

A. I. AKHIEZER AND A. G. SITENKO
Physical-Technical Institute, Academy of Sciences, Ukrainian SSR

(Submitted to JETP editor May 20, 1956;
after revision, January 14, 1957)
J. Exptl. Theoret. Phys. (U.S.S.R.) **32**, 794-805 (April, 1957)

The cross section for elastic scattering and the cross section for diffraction splitting of fast deuterons by completely black nuclei are determined. The energy distribution of the disintegration products is found. The cross section for splitting of a fast deuteron by a completely black nucleus is calculated, taking the diffraction and Coulomb interactions into account. Expressions are obtained for the cross sections for elastic deuteron scattering and splitting, taking into account the semi-transparency of the nucleus.

1. IT IS WELL KNOWN that the absorption of particles scattered by a nucleus brings about a perturbation of the incident wave and leads to elastic scattering not connected with compound-nucleus formation. In the case of point particles (for example, neutrons) with a wavelength short compared with nuclear dimensions, this scattering is analogous to the scattering of light by a completely black sphere.

The diffraction scattering of deuterons should differ by specific characteristics. In addition to purely elastic scattering, analogous to the diffraction scattering of point particles, diffraction splitting should also take place in the case of deuterons. In fact, owing to the small binding energy of the deuteron, a comparatively small change in its momentum in diffraction scattering can lead to splitting that takes place far from the nucleus. Together with the stripping reaction, the diffraction splitting of the deuteron leads to liberation of a neutron and proton, *i.e.*, increases the yield of neutrons coming from the interaction of fast deuterons with nuclei*.

The diffraction scattering of point particles by absorbing nuclei can be studied by an optical method using Huygens' principle. In order to generalize this method to the case of deuterons, we consider first the simple problem of the diffraction scattering of point particles by absorbing nuclei.

The free motion of a particle in a plane perpendicular to the wave vector of the incident particle (Z-axis) is described by the wave function

$$\psi_\varkappa = L^{-1}\exp\{i\varkappa\rho\}, \quad \int \psi_\varkappa \psi_{\varkappa'}^* d\rho = \delta_{\varkappa\varkappa'},$$

where L is the normalization length, $\varkappa$ and ρ are the projections of the wave vector and radius vector of the particle on a plane perpendicular to the Z-axis. The wave function $\psi_0 = 1/L$ corresponds to the incident particles.

The presence of the absorbing nucleus leads to disappearance of particles of this function for $\rho \leq R$ (R is the radius of the nucleus). The diffraction pattern determined by this disappearance can be obtained by expansion of the modified wave function, equal to $\Psi = \Omega(\rho)\Psi_0$, where

$$\Omega(\rho) = \begin{cases} 0, & \rho \leqslant R, \\ 1, & \rho > R, \end{cases}$$

in terms of the functions $\Psi_\varkappa$

$$\Psi = \Omega(\rho)\psi_0 = \sum_\varkappa a_\varkappa \psi_\varkappa. \tag{1}$$

The probability of diffraction scattering in which the wave vector $\varkappa$ of the scattered particle lies in the interval $d\kappa$, is connected with $a_\varkappa$ by the relation $dw = |a_\varkappa|^2 L^2\, d\varkappa/(2\pi)^2$, and the corresponding differential scattering cross section is equal to

$$d\sigma = L^2 dw = |a_\varkappa|^2 L^4 d\varkappa/(2\pi)^2.$$

If K is the magnitude of the wave vector of the particle, then $\varkappa = K\sin\vartheta \approx K\vartheta$ and $d\varkappa = K^2 do$, where do is the element of solid angle. The scattering amplitude $f(\vartheta)$ is connected with the expansion coefficient $a_\varkappa$ by the relation

$$f(\vartheta) = -i\frac{L^2 K}{2\pi} a_\varkappa. \tag{2}$$

From (1) follows that

$$a_\varkappa = \int \psi_\varkappa^* \Omega(\rho)\psi_0 d\rho.$$

*The possibility of diffraction splitting of the deuteron was independently established by E. Feinberg, R. Glauber and the authors[1-4].

Carrying out the integration and employing Eq. (2), we obtain the well known formula

$$f(\vartheta) = iRJ_1(KR\vartheta)/\vartheta, \quad d\sigma = R^2\vartheta^{-2}J_1^2(KR\vartheta)\,d\sigma$$

(since the diffraction considerations are valid only for small angles, we replace $\sin\vartheta$ by ϑ).

2. The treatment given for the diffraction of point particles can be generalized to the case of the diffraction scattering of weakly bound complex particles (deuterons) by completely black nuclei, if the expansion of the modified wave function for this case is carried out as before, but instead of one, two multipliers, Ω_n and Ω_p, describing the disappearance of a neutron and proton are introduced. The idea of this generalization is due to L. D. Landau.

In order to investigate the diffraction of deuterons it is necessary to take into account both the motion of their center of gravity and the relative motion of the neutron and proton in the deuteron. The motion of the center of gravity of the deuteron in a plane perpendicular to the direction of the wave vector of the incident deuteron (Z-axis) is described by the wave function $\psi_\varkappa(\rho_d) = \exp(i\varkappa\rho_d)$, where $\varkappa$ and ρ_d are the projections of the wave vector of the scattered deuteron and the radius vector of the center of gravity of the deuteron on the plane perpendicular to the Z-axis. (The normalization length L is taken hereinafter to be unity.) The functions $\psi_\varkappa(\rho_d)$ form the complete orthonormal system

$$\int \psi_\varkappa^*(\rho_d)\,\psi_\varkappa(\rho_d')\,d\varkappa/(2\pi)^2 = \delta(\rho_d - \rho_d').$$

The relative motion of the particles in the deuteron is described by the wave function

$$\varphi_0(r) = \sqrt{\alpha/2\pi}\;\; e^{-\alpha r}/r, \; \alpha = 1/2R_d$$

(R_d is the radius of the deuteron). The relative motion of the neutron and proton freed as a result of the splitting of the deuteron is described by the wave function

$$\varphi_{\mathbf{f}}(\mathbf{r}) = e^{i\mathbf{fr}} + \frac{a}{r}e^{-ifr},$$

where $\hbar\mathbf{f}$ is the momentum of relative motion of the particles and $a = -1/(\alpha - if)$, the neutron-proton scattering length for the S-state. Here it is assumed that the interaction between neutron and proton exists only in S-states. The sum of the plane wave and incoming spherical waves corresponds to the production of particles. The functions $\varphi_{\mathbf{f}}(\mathbf{r})$ together with the functions $\varphi_0(r)$, describing the bound state of the system, form a complete set of orthonormal functions satisfying the relation

$$\varphi_0(r)\,\varphi_0(r') + \int \varphi_{\mathbf{f}}(\mathbf{r})\,\varphi_{\mathbf{f}}(\mathbf{r}')\,d\mathbf{f}/(2\pi)^3 = \delta(\mathbf{r} - \mathbf{r}').$$

Because the deuteron is a weakly bound system in which the neutron and proton spend most of their time outside the range of nuclear force, the pattern for the diffraction of deuterons by a completely black nucleus is determined by the expansion of the modified wave function $\Psi = \Omega_n\Omega_p\psi_0(\rho_d)\varphi_0(r)$ in terms of the complete set of functions $\psi_\varkappa(\rho_d)\varphi_0(r)$ $\psi_\varkappa(\rho_d)\varphi_{\mathbf{f}}(\mathbf{r})$:

$$\Psi = \sum_{\varkappa} A_\varkappa\psi_\varkappa(\boldsymbol{\rho}_d)\,\varphi_0(r) + \sum_{\varkappa,\,\mathbf{f}} A_{\varkappa\mathbf{f}}\psi_\varkappa(\rho_d)\,\psi_{\mathbf{f}}(\mathbf{r}), \quad (3)$$

where $A_\varkappa$ and $A_{\varkappa_{\mathbf{f}}}$ are the probability amplitudes for diffraction scattering and diffraction splitting of the deuteron. From (3) it follows that

$$\begin{aligned} A_\varkappa &= \int\int \varphi_0(r)\,\psi_\varkappa^*(\rho_d)\,\Omega_n\Omega_p\psi_0(\rho_d)\,\varphi_0(r)\,d\rho_d d\mathbf{r} \\ &= -\int\int \varphi_0(r)\,\psi_\varkappa^*(\rho_d)\,\{\omega_n + \omega_p - \omega_n\omega_p\} \\ &\quad \times \psi_0(\rho_d)\,\varphi_0(r)\,d\rho_d d\mathbf{r}, \end{aligned} \quad (4)$$

$$\begin{aligned} A_{\varkappa\mathbf{f}} &= \int\int \varphi_{\mathbf{f}}^*(\mathbf{r})\,\psi_\varkappa^*(\rho_d)\,\Omega_n\Omega_p\psi_0(\rho_d)\,\varphi_0(r)\,d\rho_d d\mathbf{r} \\ &= -\int\int \varphi_{\mathbf{f}}^*(\mathbf{r})\,\psi_\varkappa^*(\rho_d)\,\{\omega_n + \omega_p - \omega_n\omega_p\} \\ &\quad \times \psi_0(\rho_d)\cdot\varphi_0(r)\,d\rho_d d\mathbf{r}, \end{aligned} \quad (5)$$

where $\omega = 1 - \Omega$ (in writing the last equalities, we used the orthogonality of the functions φ_0 and $\varphi_{\mathbf{f}}$).

3. Employing the expansion

$$\omega(\rho) = \frac{1}{2\pi}\int \frac{RJ_1(gR)}{g}\exp\{i\mathbf{g}\boldsymbol{\rho}\}\,d\mathbf{g} \quad (6)$$

and the formula

$$\int \varphi_0^2(r)\exp(i\varkappa\rho/2)\,d\mathbf{r} = \frac{4\alpha}{\varkappa}\tan^{-1}\frac{\varkappa}{4\alpha}, \quad (7)$$

it is possible to express the amplitude for elastic scattering $f(\vartheta)$, connected with $A_\varkappa$ by the relation (2), in the form

$$f(\vartheta) = iK\left\{ 2\frac{4\alpha}{\varkappa}\tan^{-1}\frac{\varkappa}{4\alpha}\frac{RJ_1(\varkappa R)}{\varkappa} - \right.$$
$$\left. -\frac{1}{2\pi}\int \frac{4\alpha}{|2\mathbf{g}-\boldsymbol{\varkappa}|}\tan^{-1}\frac{|2\mathbf{g}-\boldsymbol{\varkappa}|}{4\alpha}\frac{RJ_1(gR)}{g}\frac{RI_1(|\boldsymbol{\varkappa}-\mathbf{g}|(R)}{|\boldsymbol{\varkappa}-\mathbf{g}|}d\mathbf{g}\right\} \quad (8)$$

The differential cross section for elastic scattering is equal to

$$d\sigma_e = R^2\left| 2\frac{2p}{\varkappa'}\tan^{-1}\frac{\varkappa'}{2p}\cdot\frac{J_1(\varkappa')}{\varkappa'} - \frac{1}{2\pi}\int\frac{2p}{|2\mathbf{g}'-\boldsymbol{\varkappa}'|}\tan^{-1}\frac{|2\mathbf{g}'-\boldsymbol{\varkappa}'|}{2p}\frac{J_1(g')}{g'}\right.$$
$$\left.\times\frac{J_1(|\boldsymbol{\varkappa}'-\mathbf{g}'|)}{|\boldsymbol{\varkappa}'-\mathbf{g}'|}d\mathbf{g}'\right|^2 d\varkappa', \quad (9)$$

where $\varkappa' = \varkappa R$, $\mathbf{g}' = \mathbf{g}R$, $p = R/R_d$.

In the limiting case of large p this formula greatly simplifies:

$$d\sigma_e = 2\pi R^2\left\{\left(\frac{2p}{\varkappa'}\tan^{-1}\frac{\varkappa'}{2p}\right)^2\frac{J_1^2(\varkappa')}{\varkappa'}\right.$$
$$\left.+\frac{1}{2p}J_1(\varkappa')J_0(\varkappa')\right\}d\varkappa',\ \varkappa' \ll p,\ p \gg 1. \quad (10)$$

To obtain the integral cross section for elastic scattering we use the completeness of the functions $\psi_{\boldsymbol{\varkappa}}$. From Eq. (4) it follows that

$$\sigma_e = \int I^2(\rho_d)\,d\rho_d,$$
$$I(\rho_d) = \int\{\omega_n + \omega_p - \omega_n\omega_p\}\varphi_0^2(r)\,dr.$$

If $p \gg 1$, the term in the cross section σ_e, coming from the region $\rho_d < R$, is equal to πR^2 to within an accuracy of terms of the order $1/p^2$.

In the region $\rho_d > R$, $\omega_n\omega_p = 0$ and therefore

$$I(\rho_d) = \frac{1}{\pi}\int d\mathbf{g}\exp\{i\mathbf{g}\boldsymbol{\rho}_d\}\frac{RJ_1(gR)}{g}$$
$$\times\int\varphi_0^2(r)\exp\{i\mathbf{g}\mathbf{r}/2\}/d\mathbf{r}$$
$$= 2\int_0^\infty\frac{2p}{g}\tan^{-1}\frac{g}{2p}J_1(g)J_0(g\rho_d/R)\,dg,\ \rho_d > R.$$

Because

$$\frac{\tan^{-1}a}{a} = \int_0^1\frac{dy}{1+a^2y^2},$$
$$\int_0^\infty\frac{J_1(bx)J_0(ax)}{k^2+x^2}dx = \frac{1}{k}I_1(bk)K_0(ak)$$

then

$$I(\rho_d) = 4p\int_0^1\frac{dy}{y}I_1\left(\frac{2p}{y}\right)K_0\left(\frac{\rho_d}{R}\frac{2p}{y}\right),\ \rho_d > R.$$

Employing asymptotic expressions for $I_1(x)$ and $K_0(x)$ for $x \gg 1$ we obtain

$$I(\rho_d) = \sqrt{\frac{R}{\rho_d}}\int_1^\infty\frac{d\xi}{\xi^2}e^{-4\alpha b\xi},\quad b = \rho_d - R,\ p \gg 1,$$

and, consequently, the term in σ_e coming from the region $\rho_d > R$ is equal to

$$2\pi R\int_0^\infty db\left|\int_1^\infty e^{-4\pi b\xi}\frac{d\xi}{\xi^2}\right|^2 = \frac{2\pi}{3}(1-\ln 2)RR_d.$$

Thus, the integral cross section for elastic scattering is equal to

$$\sigma_e = \pi R^2 + \frac{2\pi}{3}(1-\ln 2)RR_d,\ R_d \ll R. \quad (11)$$

We note that, integrating (10) with respect to $\varkappa'$, we would obtain as correction to the main term πR^2 a coefficient two times smaller than in (11)[2]. This is connected with the fact that large $\varkappa'$ have an appreciable role in the correction to πR^2.

4. The cross section for differential splitting is connected with the amplitude $A_{\varkappa_f}$ by the relation

$$d\sigma_d = |A_{\varkappa\mathbf{f}}|^2(2\pi)^{-2}d\varkappa\,(2\pi)^{-3}d\mathbf{f}. \quad (12)$$

Using Eq. (6) we put $A_{\varkappa_f}$ into the form

$$A_{\varkappa\mathbf{f}} = -\frac{(2\pi)^{7/2}R}{\alpha^{5/2}}a_{\mathbf{zu}} =$$
$$-\frac{(2\pi)^{7/2}R}{\alpha^{5/2}}\left\{\frac{J_1(pz)}{z}[\Phi(\mathbf{u},\mathbf{z}) + \Phi(\mathbf{u},-\mathbf{z})]\right.$$
$$\left.-\frac{1}{2\pi}\int d\mathbf{g}\frac{J_1(g)}{g}\cdot\frac{J_1(p)|\mathbf{z}-\mathbf{g}/p|)}{|\mathbf{z}-\mathbf{g}/p|}\Phi\left(\mathbf{u},\frac{2\mathbf{g}}{p}-\mathbf{z}\right)\right\}, \quad (13)$$

$$\Phi(\mathbf{u},\mathbf{z}) = \frac{1}{4\pi}\int\frac{e^{-x}}{x}\left(e^{-i\mathbf{u}\mathbf{x}} - \frac{1}{1+iu}\cdot\frac{e^{iux}}{x}\right)e^{i\mathbf{z}\mathbf{x}}d\mathbf{x}, \quad (14)$$

where $\mathbf{z} = \mathbf{x}/2\alpha$, $\mathbf{u} = \mathbf{f}/\alpha$ and $\mathbf{x} = \alpha\mathbf{r}$.

For the integral cross section for diffraction splitting we obtain the following expression:

$$\sigma_d = \frac{R^2}{\pi^2}\int\int d\mathbf{z}d\mathbf{u}\left|\frac{J_1(pz)}{z}\left[\Phi(\mathbf{u},\mathbf{z}) + \Phi(\mathbf{u},-\mathbf{z})\right] - \frac{1}{2\pi}\int d\mathbf{g}\frac{J_1(g)}{g}\frac{J_1(p|\mathbf{z}-\mathbf{g}/p|)}{|\mathbf{z}-\mathbf{g}/p|}\Phi\left(\mathbf{u},\frac{2\mathbf{g}}{p}-\mathbf{z}\right)\right|^2. \quad (15)$$

If $p \gg 1$, then

$$\sigma_d = \frac{2}{3}RR_d\int_0^\infty uI(u)\,du,$$

where $I(u)$ gives the energy distribution of the products of the splitting and has the form

$$I(u) = \frac{3}{(1+u^2)^2}\left[1 + \frac{2u}{1+u^2} - \arcsin\frac{u}{\sqrt{1+u^2}}\right] - 16(1-\ln 2)\frac{u}{(1-u^2)^3}. \quad (16)$$

The integral cross section for splitting is equal to

$$\sigma_d = \frac{\pi}{3}\left(2\ln 2 - \frac{1}{2}\right)RR_d,\ R_d \ll R,\ \lambda \ll R_d. \quad (17)$$

This formula agrees with the formula obtained by Glauber[4]. (We note that in the expression for σ_d obtained in Ref. 2 the region of large $\varkappa$ was not correctly taken into account. Therefore the numerical coefficient of RR_d in Ref. 2 is equal to 1.25, differing from the correct coefficient which is 0.96.)

5. In addition to diffraction scattering and diffraction splitting of the deuteron, the reaction of splitting of the neutron and proton and absorption of both by the nucleus is also possible. The cross sections for the first two processes are given, for $p \gg 1$ (Ref. 5) by

$$\sigma_n = \sigma_p = \pi RR_d/2,\ R_d \ll R. \quad (18)$$

Since the cross section of absorption of a single particle by the nucleus is equal to πR^2, and the cross section for the process in which one particle of the deuteron hits the nucleus and the other passes outside the nucleus is equal to $\pi RR_d/2$, the cross section for absorption of both particles is equal to

$$\sigma_a = \pi R^2 - \pi RR_d/2,\ R_d \ll R. \quad (19)$$

The total cross section of all processes σ_t can be determined knowing the elastic scattering amplitude at zero angle[6]

$$\sigma_t = 4\pi\lambda\,\mathrm{Im}\,f(0). \quad (20)$$

For point particles $f(0) = iKR^2/2$ and $\sigma_t = 2\pi R^2$. In the case of deuterons the scattering amplitude at zero angle is equal to

$$f(0) = i\frac{K}{2\pi}\int\int\varphi_0^2(r)\{\omega_n + \omega_p - \omega_n\omega_p\}\,d\rho_d d\mathbf{r},$$

and the total cross section σ_t is determined by the expression

$$\sigma_t = 2\int\int\varphi_0^2(r)\{\omega_n + \omega_p - \omega_n\omega_p\}\,d\rho_d d\mathbf{r}. \quad (21)$$

Using Eqs. (6) and (7), we obtain

$$\sigma_t = 4\pi R^2\left\{1 - \int_0^\infty \frac{p}{\xi}\tan^{-1}\frac{\xi}{p}\cdot\frac{J_1^2(\xi)}{\xi}d\xi\right\}, \quad (22)$$

$$p = \frac{R}{R_d}.$$

For $p \to \infty$

$$\sigma_t = 4\pi R^2\left\{1 - \int_0^\infty \frac{J_1^2(\xi)}{\xi}d\xi\right\} = 2\pi R^2.$$

In order to find the correction to this quantity for $R_d \ll R$, we calculate the difference of the integrals

$$\int_0^\infty \frac{p}{\xi}\tan^{-1}\frac{\xi}{p}\cdot\frac{J_1^2(\xi)}{\xi}\,d\xi - \int_0^\infty \frac{J_1^2(\xi)}{\xi}$$

$$d\xi = \int_0^\infty \frac{J_1^2(pz)}{z}\left\{\frac{\tan^{-1}z}{z} - 1\right\}dz \equiv \delta_p.$$

In the latter integral the region of small z is not important, large pz playing the main role; therefore, the well known asymptotic representation of the Bessel function can be employed. Setting here $\sin^2(pz - \pi/4) \cong 1/2$, we obtain

$$\delta_p = \frac{1}{\pi p}\int_0^\infty(\tan^{-1}z - z)\frac{dz}{z^3} = -\frac{1}{4p},\ p \gg 1.$$

Thus, for $p \gg 1$

$$\int_0^\infty \frac{p}{\xi}\tan^{-1}\frac{\xi}{p}\cdot\frac{J_1^2(\xi)}{\xi}\,d\xi = \frac{1}{2} - \frac{1}{4p},$$

and, consequently, the total cross section of all processes is equal to

$$\sigma_t = 2\pi R^2 + \pi RR_d,\ R_d \ll R. \quad (23)$$

For an arbitrary value of p, one has the following relations

$$\sigma_e + \sigma_d = {}^1/_2\sigma_t, \quad \sigma_n + \sigma_p + \sigma_a = {}^1/_2\sigma_t. \qquad (24)$$

In fact, substituting the expression (5) into Eq. (12) instead of $A_{\varkappa\mathbf{f}}$ and integrating over $\varkappa$ and $\mathbf{f}$, we find

$$\sigma_e + \sigma_d = \int\int \varphi_0^2(r)\{\omega_n + \omega_p - \omega_n\omega_p\}\, d\rho_d d\mathbf{r}.$$

Comparing this expression with Eq. (20) we obtain Eq. (24).

6. We show now how to take into account the Coulomb interaction in the treatment of diffraction. In the scattering by absorbing nuclei of fast charged particles, whose energies E are considerably above the Coulomb barrier ze^2/R, we should, obviously, take the factor $\Omega(\rho)$ equal to

$$\Omega^z(\rho) = \begin{cases} 0 & \rho \leqslant R, \\ e^{2i\eta(\rho)} & \rho > R, \end{cases}$$

where $\eta(\rho)$ is the scattering phase in the Coulomb field at infinity; for $KR \gg 1$ it is equal to

$$\eta(\rho) = n\ln(K\rho), \quad n = Ze^2/\hbar v$$

(v is the velocity of the particle at infinity).

The diffraction scattering and splitting of fast deuterons by completely black nuclei with account taken of the Coulomb interaction is determined by expansion of the modified deuteron wave function

$$\Psi^z \equiv \Omega(\rho_n)\,\Omega^z(\rho_p)\,\psi_0(\rho_d)\,\varphi_0(r) = \sum_{\varkappa} A^z_{\varkappa}\psi_{\varkappa}(\rho_d)\,\varphi_0(r) + \sum_{\varkappa,\,\mathbf{f}} A^z_{\varkappa\mathbf{f}}\psi_{\varkappa}(\rho_d)\,\varphi_{\mathbf{f}}(\mathbf{r}), \qquad (25)$$

where the expansion coefficients $A^z_{\varkappa}$ and $A^z_{\varkappa\mathbf{f}}$ are the probability amplitudes for elastic diffraction scattering and diffraction splitting of the deuteron.

The amplitude for elastic scattering, which is connected with $A^z_{\varkappa}$ by Eq. (2), is equal to

$$f(\vartheta) = -iK\left\{\frac{4\alpha}{\varkappa}\tan^{-1}\frac{\varkappa}{4\alpha}\int_R^\infty e^{2i\eta(\rho)}J_0(\varkappa\rho)\,\rho\,d\rho - \int\frac{4\alpha}{|2\mathbf{g}-\varkappa|}\tan^{-1}\frac{|2\mathbf{g}-\varkappa|}{4\alpha}\cdot\frac{RJ_1(|\varkappa-\mathbf{g}|R)}{|\varkappa-\mathbf{g}|}\theta(g)\,d\mathbf{g}\right\},$$

$$\theta(g) = \frac{1}{2\pi}\int_R^\infty e^{2i\eta(\rho)}J_0(g\rho)\,\rho\,d\rho. \qquad (26)$$

In the limiting case $R_d \ll R$, the scattering amplitude has the form

$$f(\vartheta) = -iK\left\{\frac{4\alpha}{\varkappa}\tan^{-1}\frac{\varkappa}{4\alpha}\int_R^\infty e^{2i\eta(\rho)}J_0(\varkappa\rho)\,\rho\,d\rho - \frac{RJ_0(\varkappa R)}{8\alpha}e^{2i\eta(R)}\right\} =$$

$$= i\lambda\left\{\frac{2p}{l_0\vartheta}\tan^{-1}\frac{l_0\vartheta}{2p}\left[l_0^{2in+1}\frac{J_1(l_0\vartheta)}{\vartheta} + 2in\vartheta^{-2in-2}\int_{l_0\vartheta}^\infty J_1(\zeta)\,\zeta^{2in}\,d\zeta\right] + \frac{l_0^{2in+2}}{4p}J_0(l_0\vartheta)\right\}, \qquad (27)$$

$$l_0 = KR, \quad E \gg Ze^2/R, \quad p \gg 1.$$

The differential cross section for elastic deuteron scattering is equal to

$$\sigma(\vartheta) = |f(\vartheta)|^2.$$

If $n \ll 1$ and $1 \ll p \ll l_0$ then

$$\sigma(\vartheta) = 4n^2\lambda^2/\vartheta^4, \quad \vartheta \ll \sqrt{2n}/l_0,$$
$$\sigma(\vartheta) = l_0^2\lambda^2 J_1^2(l_0\vartheta)/\vartheta^2, \quad \sqrt{2n}/l_0 \ll \vartheta \ll 2p/l_0,$$
$$\sigma(\vartheta) = (l_0^3\lambda^2/8\pi p^2)\cos^2\left(l_0\vartheta - \frac{\pi}{4}\right)\Big/\vartheta, \qquad (28)$$
$$2p/l_0 \ll \vartheta \ll 1.$$

Thus, in the case $n \ll 1$ and $1 \ll p \ll l_0$ purely Coulomb scattering occurs only in the angular region $\vartheta \ll \sqrt{2n}/l_0$. In the angular region $\sqrt{2n}/l_0 \ll \vartheta \ll 2p/l_0$ the scattering of deuterons has just the same character as the diffraction scattering of neutral particles. Finally, in diffraction scattering of deuterons in the angular region $2p/l_0 \ll \vartheta \ll 1$, their spatial structure shows up.

If $n \gg 1$ and $n \ll p \ll l_0$, then

$$\sigma(\vartheta) = 4n^2\lambda^2/\vartheta^4, \quad \vartheta \ll 2n/l_0,$$
$$\sigma(\vartheta) = (2l_0\lambda^2/\pi)\sin^2\left(l_0\vartheta - \frac{\pi}{4}\right)\Big/\vartheta^3,$$
$$2n/l_0 \ll \vartheta \ll 2p/l_0, \qquad (29)$$
$$\sigma(\vartheta) = (l_0^3\lambda^2/8\pi p^2)\cos^2\left(l_0\vartheta - \frac{\pi}{4}\right)\Big/\vartheta,$$
$$2p/l_0 \ll \vartheta \ll 1.$$

Thus, in this case the region of purely Coulomb scattering broadens in comparison with the preceding case, right up to angles of the order of $2n/l_0$. For $\vartheta \sim 2n/l_0$, a sharp decrease in the scattering, by a factor of the order of n takes place[7]. In the angular interval $2n/l_0 \ll \vartheta \ll 2p/l_0$ the deuteron scattering has the same character as diffraction scattering of point neutral particles. The spatial structure of the deuterons shows up in the angular interval $2p/l_0 \ll \vartheta \ll 1$.

If, finally, $1 \ll p \ll n \ll l_0$, then

$$\begin{gathered}\sigma(\vartheta) = 4n^2\lambda^2/\vartheta^4, \quad \vartheta \ll 2p/l_0, \\ \sigma(\vartheta) = 4\pi^2 p^2 n^2 \lambda^2 / l_0^2 \vartheta^6, \\ 2p/l_0 \ll \vartheta \ll 2(\pi^3 n^2 p^4)^{1/5}/l_0, \\ \sigma(\vartheta) = (l_0^3\lambda^2/8\pi p^2)\cos^2\left(l_0\vartheta - \frac{\pi}{4}\right)\Big/\vartheta, \\ 2(\pi^3 n^2 p^4)^{1/5}/l_0 \ll \vartheta \ll 1.\end{gathered} \tag{30}$$

We see that in this case the region of Coulomb scattering does not extend to angles $2n/l_0$, but to angles of the order of $2p/l_0$. The region of diffraction scattering of point particles vanishes, in general. The finite size of the deuteron begins to show up at angles of the order of $2p/l_0$. In the angular interval $2p/l_0 \ll \vartheta \ll 2(\pi^3 n^2 p^4)^{1/5}/l_0$ the cross section falls off as $1/\vartheta^6$, and then changes as $1/\vartheta$.

7. We turn now to consideration of the splitting of fast deuterons, taking into account the Coulomb interaction.

The amplitude $A^z_{\varkappa \mathbf{f}}$ in the expansion is determined by the relation

$$\begin{aligned}A^z_{\varkappa\mathbf{f}} &= \int\int \exp\{-i\varkappa\rho_d\}\ \varphi^*_{\mathbf{f}}(\mathbf{r})\,\Omega(\rho_n)\,\Omega^z(\rho_p)\,d\rho_d\,d\mathbf{r} \\ &= e^{2i\eta(R)}\Big\{A_{\varkappa\mathbf{f}} + 2\pi\int_R^\infty [e^{2i\{\eta(\rho)-\eta(R)\}} \\ &\quad - 1]\,J_0(\varkappa\rho)\,\rho d\rho \int e^{-i\varkappa\mathbf{r}/2}\,\varphi^*_{\mathbf{f}}(\mathbf{r})\,\varphi_0(r)\,d\mathbf{r} \\ &\quad - \int d\mathbf{g}\int_R^\infty [e^{2i\{\eta(\rho)-\eta(R)\}} - 1]\,J_0(g\rho)\,\rho\,d\rho \\ &\quad \times \frac{RJ_1(|\varkappa - g|R)}{|\varkappa - \mathbf{g}|}\cdot\int e^{-i(\mathbf{g}-\varkappa/2)r}\varphi^*_{\mathbf{f}}(\boldsymbol{r})\,\varphi_0(r)\,d\mathbf{r}\Big\}\end{aligned} \tag{31}$$

The differential cross section for splitting of a fast deuteron is equal to

$$d\sigma_{\mathbf{f}} = |A^z_{\varkappa\mathbf{f}}|^2 (2\pi)^{-2} d\varkappa \cdot (2\pi)^{-3} d\mathbf{f}. \tag{32}$$

For $p \gg 1$ we have

$$\begin{aligned}A^z_{\varkappa\mathbf{f}} \approx e^{2i\eta(R)}\Big\{A_{\varkappa\mathbf{f}} - 2\pi\frac{2in}{\varkappa}\int_R^\infty J_1(\varkappa\rho)\,e^{2i\{\eta(\rho)-\eta(R)\}}\,d\rho \\ \times\int e^{-i\varkappa\mathbf{r}/2}\varphi^*_{\mathbf{f}}(\mathbf{r})\,\varphi_0(r)\,d\mathbf{r}\Big\},\end{aligned} \tag{33}$$

and the integral cross section for deuteron splitting is equal to

$$\begin{aligned}\sigma_f = \frac{R^2}{\pi^2}\int\int dz\,d\mathbf{u}\Big|a_{z\mathbf{u}} \\ + \frac{2in}{p}\,\frac{(pz)^{-2in}}{z^2}\int_{pz}^\infty J_1(\zeta)\,\zeta^{2in}d\zeta\cdot\Phi(\mathbf{u},\mathbf{z})\Big|^2\end{aligned} \tag{34}$$

The expression for σ_f diverges logarithmically for $z \to 0$. This is connected with the Coulomb character of the interaction, which leads to divergence of the elastic scattering cross section at small angles, *i.e.*, at small z. In so far as the deuteron is assumed to be practically unbound, this sort of divergence obviously ought to take place also for the splitting cross section. In reality, for splitting of the deuteron to take place, z must exceed some minimum value z_m. This value can be determined, if we take into account the fact that the change of energy of the deuteron connected with the change of its momentum, which is approximately equal to $\hbar^2 K\varkappa/2M$, must exceed the binding energy of the deuteron $\epsilon = \hbar^2\alpha^2/M$. From this it follows that $z_m \approx \alpha/K = \lambda/2R_d$.

Just this value of the lower limit of the z integration can be obtained in the following way. The treatment of deuteron splitting is valid for sufficiently large z satisfying the inequality $z > z'$ $(1 \gg z' \gg \alpha/K)$, since in this region of z the deuteron can be considered approximately as an unbound system. On the other hand, small z corresponds to large values of the impact parameter, for which splitting of the deuteron can be considered using perturbation theory. Going to the system in which the center of gravity of the deuteron before collision is at rest, and employing the perturbation energy in the form

$$V(t) = Ze^2/[\rho_p^2 + (z_p - vt)^2]^{1/2},$$

it is easy to obtain the following expression for the part of the cross section for splitting in a Coulomb field which corresponds to large values of the impact parameter

$$d\sigma_c' = \frac{n^2}{2\pi^3}\left|\int e^{-i\mathbf{K}'\mathbf{r}/2}\varphi_{\mathbf{f}}(\mathbf{r})\,\varphi_0(\mathbf{r})\,d\mathbf{r}\right|^2 \delta\left\{\frac{\mathbf{K}'\mathbf{v}-\omega}{v}\right\}\frac{d\mathbf{K}'}{K'^4}\,d\mathbf{f},$$

where $\mathbf{K}'$ is the wave vector of the center of gravity of the deuteron after collision and $\hbar\omega = \epsilon + \hbar^2 f^2/M + \hbar^2 K^2/4M$. Getting rid of the δ-function by integration over the angle between the vectors $\mathbf{K}'$ and $\mathbf{v}$ and carrying out the integration over $\mathbf{f}$ we obtain

$$\sigma_c' = 8\pi n^2 R_d^2 \int_{z_m}^{z'} z^{-5}\left[z^2 - 4\left(\tan^{-1}\frac{z}{2}\right)^2\right]dz, \qquad (35)$$

$$z = \frac{K'}{2\varkappa},$$

where $z_m \approx \alpha/K$ and the upper limit z' is chosen such that perturbation theory can be employed.

In order to obtain the total cross section for splitting it is necessary to add Eq. (34), in which the integration over z is carried out from z' to infinity, to Eq. (35). Since both these expressions behave as $\ln z$ for small z, the sum will not contain z' and leads to the expression (34) in which $z_m = \alpha/K$ is taken as lower limit.

Carrying out the integration in Eq. (34) over u and the angle determining the direction of the vector $\mathbf{z}$ we obtain

$$\sigma_f = \sigma_d + \sigma_c + \sigma_{\text{int}},$$

$$\sigma_c = 8\pi n^2 R^2 p^2 \int_{pz_m}^{\infty}\left\{\frac{x^2}{p^2} - 4\left(\tan^{-1}\frac{x}{2p}\right)^2\right\}\left|\int_x^{\infty} J_1(\zeta)\,\zeta^{2in}d\zeta\right|^2\frac{dx}{x^5},$$

$$\sigma_{\text{int}} = 4\pi R^2 p^2\,\mathrm{Re}\int_0^{\infty}\left\{\frac{x^2}{p^2} - 4\left(\tan^{-1}\frac{x}{2p}\right)^2\right\}\frac{J_1(x)}{x}\,2inx^{-2in-2}\int_x^{\infty} J_1(\zeta)\,\zeta^{2in}d\zeta\,\frac{dx}{x}, \qquad (36)$$

where σ_d is the cross section found earlier for diffraction splitting of the deuteron with neglect of Coulomb interaction, and σ_c is the cross section for splitting of the deuteron due to the Coulomb field of the nucleus. The quantity σ_{int} determines the part of the splitting cross section coming from interference of diffraction and Coulomb scattering. In the expressions for σ_d and σ_{int} we set the lower limit of the z-integration equal to zero, since these expressions do not diverge as $z_m \to 0$.

It is easy to see that the interference term σ_{int} is equal to zero for $p \gg 1$. In fact,

$$\sigma_{\text{int}} = \frac{4\pi R_d^2}{3}\,\mathrm{Re}\left\{in\int_1^{\infty}dx\,x^{2in}\int_0^{\infty}dy\,yJ_1(y)\,J_1(xy)\right\} = \frac{4\pi R_d^2}{3}\,\mathrm{Re}\left\{in\int_1^{\infty}dx\,x^{2in}\,\delta(x-1)\right\} = 0.$$

Thus, for $p \gg 1$, the integral cross section for splitting is equal to the sum of the cross sections for diffraction splitting and splitting coming from the Coulomb field of a black nucleus. It can be shown that the interference term is the order of p times smaller than σ_c.

We consider in detail the cross section for splitting of the deuteron in a Coulomb field for $p \gg 1$, defined by the general formula Eq. (36). It can be evaluated in the two limiting cases of small and large n. If $n \ll 1$, then

$$\int_x^{\infty} J_1(\zeta)\,\zeta^{2in}\,d\zeta \approx \int_x^{\infty} J_1(\zeta)\,d\zeta = J_0(x),$$

$$\sigma_c = \frac{4\pi}{3}n^2R_d^2\int_{pz_m}^{\infty}\frac{J_0^2(x)}{x}\,dx, \quad n \ll 1, \quad p \gg 1.$$

Integrating by parts we find

$$\int_{pz_m}^{\infty}\frac{J_0^2(x)}{x}\,dx = J_0^2(pz_m)\ln\frac{1}{pz_m} + A,$$

where A is the order of unity. Thus, the cross section for splitting of fast deuterons coming from the Coulomb field is equal, for $n \ll 1$, to

$$\sigma_c = \frac{4\pi}{3}n^2R_d^2\left\{\ln\frac{1}{pz_m} + A\right\} \approx \frac{4\pi}{3}n^2R_d^2\ln\frac{R_d^2}{R\lambda}, \quad n \ll 1, \qquad (37)$$

(the last formula is valid if $pz_m \ll 1$). This expression coincides with the result obtained by Dancoff[8], and Mullin and Guth[9], using perturbation theory.

We look now at the case of large n. Noting that

$$\int_x^\infty J_1(\zeta)\,\zeta^{2in}\,d\zeta = 2^{2in}\frac{\Gamma(1+in)}{\Gamma(1-in)} - \int_0^x J_1(\zeta)\,\zeta^{2in}\,d\zeta,$$

and using the asymptotic expansion

$$\int_0^x J_1(\zeta)\,\zeta^{2in}\,d\zeta = \frac{1}{2in}J_1(x)\,x^{2in+1} + \frac{1}{4n^2}J_0(x)\,x^{2in+2} + O(n^{-3}),$$

we obtain, neglecting terms of order $0(n^{-3})$,

$$\begin{aligned}\sigma_c = {} & 8\pi n^2 R_d^2 \int_{z_m}^\infty \frac{z^2 - 4\left(\tan^{-1}\frac{z}{2}\right)^2}{z^5}\,dz \\ & - 2\pi R^2 \int_0^\infty \frac{z^2 - 4\left(\tan^{-1}\frac{z}{2}\right)^2}{z^3} J_1^2(pz)\,dz \\ = {} & \frac{4\pi}{3} n^2 R_d^2 \left\{\ln\frac{2}{z_m} + 1 - \frac{3}{4}\frac{\pi^2}{8}\right\} \\ & - \frac{\pi}{3}\left(\ln 2 + \frac{1}{2}\right) RR_d.\end{aligned} \tag{38}$$

The second term in this expression is of the same order of magnitude as the cross section for diffraction splitting. In order that the asymptotic expansion can be used this term must be small compared with the first; in other words, the inequality $n^2 \gg p$ should be fulfilled. We see that in this case the cross section for diffraction splitting is a small correction to the cross section coming from the Coulomb field. The total cross section for splitting is determined by the formula (accurate to within a constant factor in the logarithm):

$$\sigma_f = (4\pi/3)\,n^2 R_d^2 \ln(R_d/\lambda\!\!\!^{-}),\quad n \gg 1. \tag{39}$$

8. In the high-energy region when the mean free path of the particle in nuclear matter becomes comparable with nuclear dimensions, the nucleus cannot be considered completely black, and must be viewed as a semi-transparent body characterized by a complex absorption coefficient $b = b_1 - ib_2$, where b_1 is the absorption coefficient of nuclear matter and $b_2 = 2(\nu-1)K$, where ν is the index of refraction of nuclear matter[10]. In the investigation of diffraction problems in this case, the expansion of the modified wave function can be used as before, if we consider the factor $\Omega(\rho)$ equal, for uncharged particles, to

$$\Omega(\rho) = \begin{cases} \exp(-b\sqrt{R^2-\rho^2}), & \rho \leqslant R \\ 1 & \rho > R. \end{cases}$$

Application of these formulae to the scattering of fast neutral particles leads to the well known expression for the amplitude of elastic scattering[10]

$$\begin{aligned} f(\vartheta) &= -\frac{iK}{2\pi}\int \Omega(\rho)\,e^{-i\varkappa\rho}\,d\rho \\ &= iK\int_0^R (1 - \exp\{-b\sqrt{R^2-\rho^2}\})\,J_0(\varkappa\rho)\,\rho\,d\rho, \end{aligned}$$

which, in the limiting cases of large and small absorption has the form

$$\begin{aligned} f(\vartheta) &= iK\left\{\frac{RJ_1(\varkappa R)}{\varkappa} - \frac{J_0(\varkappa R)}{b^2}\right\}, \quad \varkappa \ll R\,|b|^2, \\ f(\vartheta) &= iR\frac{Kb}{\varkappa^2}\left\{\frac{\sin\varkappa R}{\varkappa R} - \cos\varkappa R\right\}, \quad \varkappa \gg R\,|b|^2. \end{aligned} \tag{40}$$

The following expression can be obtained for the amplitude of elastic diffraction scattering of fact deuterons by semi-transparent nuclei with no account of the Coulomb interaction

$$\begin{aligned} f(\vartheta) = 2\pi iKR^2 \Big\{ & \frac{2p}{\varkappa'}\tan^{-1}\frac{\varkappa'}{2p}\,[\chi_n(\varkappa') + \chi_p(\varkappa')] \\ & - \int \frac{2p}{|2\mathbf{g}' - \boldsymbol{\varkappa}'|}\tan^{-1}\frac{|2\mathbf{g}' - \boldsymbol{\varkappa}'|}{2p} \\ & \times \chi_n(g')\,\chi_p(|\boldsymbol{\varkappa}' - \mathbf{g}'|)\,d\mathbf{g}'\Big\}, \end{aligned} \tag{41}$$

$$\chi_{n,p}(\varkappa') = \frac{1}{2\pi}\int_0^1 (1 - \exp\{-b_{n,p}R\sqrt{1-y^2}\}) \times J_0(\varkappa' y)\,y\,dy$$

(b_n and b_p are the complex absorption coefficients of neutrons and protons). For $p \gg 1$

$$\begin{aligned} f(\vartheta) = iKR^2 \Big\{ & \frac{2p}{\varkappa'}\tan^{-1}\frac{\varkappa'}{2p} \\ & \times \int_0^1 (1 - \exp\{-BR\sqrt{1-y^2}\})\,J_0(\varkappa' y)\,y\,dy \\ & - 2\pi\int\left(\frac{\tan^{-1}\xi/p}{\xi/p} - 1\right)\chi_n(\xi)\,\chi_p(|\boldsymbol{\xi} - \boldsymbol{\varkappa}'|)\,d\boldsymbol{\xi}\Big\}, \end{aligned} \tag{42}$$

where B is the complex absorption coefficient for deuterons equal to $B = B_1 - iB_2 = b_n + b_p$.

The total cross section for all processes is given by the relation

$$\begin{aligned} \sigma_t = 4\pi R^2\,\mathrm{Re}\Big\{ & \int_0^1 (1 - \exp\{-BR\sqrt{1-y^2}\})\,y\,dy \\ & - 4\pi^2\int_0^\infty \left\{\frac{\tan^{-1}(\xi/p)}{\xi/p} - 1\right\}\chi_n(\xi)\,\chi_p(\xi)\,\xi\,d\xi\Big\}. \end{aligned} \tag{43}$$

In the case of large absorption of particles ($|b_n|^2R^2 \gg p$, $|b_p|^2R^2 \gg p$) the total cross section

and the cross sections of elastic scattering and diffraction splitting of the deuteron are given by the relations:

$$\sigma_t = 2\pi R^2 \left\{1 - 2\frac{B_1^2 - B_2^2}{(B_1^2+B_2^2)^2 R^2}\right\} + \pi R R_d,$$

$$\sigma_e = \pi R^2 \left\{1 + \frac{1}{2B_1^2R^2} - \frac{4(B_1^2 - B_2^2)}{(B_1^2 + B_2^2)^2R^2}\right\} + \frac{2\pi}{3}(1 - \ln 2) R R_d,$$

$$\sigma_d = \frac{\pi}{3}\left(2\ln 2 - \frac{1}{2}\right) R R_d.$$

In the case of small absorption of particles ($|b_n|^2R^2 \ll p$, $|b_p|^2R^2 \ll p$) the cross sections are given by the formulae:

$$\sigma_t = \sigma_t^0 + \frac{2\pi}{3} R_d^2 \operatorname{Re}(b_n b_p) R^2 \ln\frac{R}{R_d},$$

$$\sigma_t^0 = \frac{4\pi}{3} R^3 B_1$$

$$\sigma_e = \sigma_e^0 - \frac{\pi}{6} R_d^2 |B|^2 R^2 \ln\frac{R}{R_d},$$

$$\sigma_e^0 = \frac{\pi}{2} R^4 |B|^2$$

$$\sigma_d = \frac{\pi}{6} R^2 |B|^2 R_d^2 \ln\frac{R}{R_d},$$

where σ_t^0 is the total cross section for all processes and σ_e^0 is the cross section for the elastic scattering of point particles, the complex absorption coefficient of which is the sum of complex absorption coefficients of neutron and proton.

The authors express their deep gratitude for valuable advice to Academician L. Landau, whose idea of generalizing the optical method to the case of a completely black nucleus was employed in this work. They also thank L. Rozentsveig, E. Feinberg, G. Liubarskii and R. Glauber for valuable discussions.

[1] A. Akhiezer and A. Sitenko, Scient. Reports of Khar'kov Univ. **64**, 9 (1955).

[2] A. Akhiezer and A. Sitenko, Dokl. Akad. Nauk SSSR **107**, 385 (1956).

[3] E. Feinberg, J. Exptl. Theoret. Phys. (U.S.S.R.) **29**, 115 (1955). Soviet Physics JETP **2**, 58 (1956).

[4] R. Glauber, Phys. Rev. **99**, 1515 (1955).

[5] R. Serber, Phys. Rev. **72**, 1008 (1947).

[6] B. Lippmann, Phys. Rev. **79**, 481 (1950).

[7] A. Akhiezer and I. Pomeranchuk, J. Exptl. Theoret. Phys. (U.S.S.R.) **16**, 396 (1946).

[8] S. Dancoff, Phys. Rev. **72**, 1017 (1947).

[9] C. Mullin and E. Guth, Phys. Rev. **82**, 141 (1951).

[10] Fernbach, Serber and Taylor, Phys. Rev. **75**, 1352 (1949).

[11] G. Watson, *Theory of Bessel Functions* (Russian translation) IIL, 1949.

Translated by G. E. Brown
176

Disintegration of Light Nuclei in a Coulomb Field

V. I. MAMASAKHLISOV AND G. A. CHILASHVILI
Tbilissii State University

(Submitted to JETP editor February 24, 1956)
J. Exptl. Theoret. Phys. (U.S.S.R.) 32, 806-810 (April, 1956)

General formulae for the effective cross section for disintegration of light nuclei in a Coulomb field are derived. The formulae obtained are applied to the cases of the Li^7 and O^{17} nuclei, where it is assumed that the former splits into an α-particle and a triton, and the latter into O^{16} and a neutron.

1. IN CONNECTION WITH the development of techniques of acceleration it has proved possible to accelerate a beam of light nuclei to high energies. In going through the Coulomb field of other nuclei, these nuclei can split, analogously to what happens in the case of the deuteron nucleus moving in a Coulomb field. The analogy with deuterons is complete for those nuclei in which the odd neutron is weakly bound with the remaining nucleus. Such nuclei are, for example, Be^9 (the binding energy of the last neutron is $\epsilon = 1.67$ Mev), C^{13} ($\epsilon = 4.9$ Mev), O^{17}($\epsilon = 4.1$ Mev) and others. Sawicki[1] considered the splitting of Be^9 into the residual Be^8 and a neutron in a Coulomb field. He showed that for energies of the Be^9 nucleus of 170 Mev the effective disintegration cross section of this nucleus was equal to $4.10^{-29}\ Z^2\ cm^2$, where Z is the charge of the nucleus through whose Coulomb field the beryllium nucleus passes. It is clear that analogous calculations can be carried out for the nuclei C^{13}, O^{17} and others. The difference will consist in the fact that the odd neutron in these nuclei can be in states different from the states it is in for the deuteron or beryllium. For example, according to the shell model the unpaired neutron in the O^{17} nucleus is in a $d_{5/2}$ state. Formulae will be given below for the calculation of the disintegration of a nucleus in a Coulomb field for the general case where the odd neutron in these nuclei occurs in an arbitrary state of angular momentum l.

We consider more interesting, however, the consideration of those cases in which the light nucleus splits in the Coulomb field into two charged particles. In Ref. 2, as a result of the study of stars in photographic emulsions irradiated by 340 Mev protons, it is proposed that light nuclei have a clear cut structure. Such nuclei, according to these authors, can be considered as formed from groups of nucleons (for example, α-particles, tritons and deuterons).

A number of authors[3, 4] have obtained satisfactory results by considering the Li^6 nucleus as a system consisting of an α-particle and a deuteron. There are grounds to believe that the Li^7 nucleus can be viewed as a system consisting of an α-particle and a triton, in some approximation. We note, first of all, that the binding energy of the triton in the Li^7 nucleus is equal to only 2.52 Mev, whereas the internal binding energies of the α-particle and triton are 28.2 and 8.48 Mev, respectively.

The binding energy in the Li^7 nucleus is unequally distributed. The nucleons in the triton and α-particle are bound considerably more tightly than the triton and α-particle are bound with each other. In this context one can speak of the triton and α-particle as constituting the nucleus.

We indicate, further, that such a model of the Li^7 nucleus leads to satisfactory agreement with experiment in relation to the magnetic moment of this nucleus. If the g-factor of triton is defined by the formulae

$$\mu_l = (e\hbar / 2M_t c)\, g_l\, l, \quad \mu_s = (e\hbar / 2Mc)\, g_s\, s,$$

where M_t denotes the reduced mass of the triton, then the magnetic moment (in nuclear magnetons)

$$\mu = {}^7/_{12}\, g_l + g_s / 2 = 3{,}56,$$

is obtained, assuming that the Li^7 nucleus is in a $p_{3/2}$ state, and the experimental value of the magnetic moment of the triton is taken for μ_s. The value of the magnetic moment of Li^7 obtained agrees well with the experimental value of 3.25.

It is interesting to note that for several other light nuclei, also, values of the magnetic moments which are in satisfactory agreement with experimental data are obtained if it is assumed that in these nuclei of the type X^{4k+3}_{2k+1} the magnetic moment is

determined not by the odd proton, but by the triton moving in the field of the remaining part X_{2k}^{4k}. For example, the magnetic moment of the Al_{13}^{27} nucleus which, as is well known, is in a $d_{5/2}$ state, is equal to 3.72 under this assumption. This agrees well with the experimental value of 3.64. More or less acceptable values of the magnetic moments of B_5^{10} (2.11) and F_9^{19}(2.98) are obtained on the basis of this assumption.

It is natural to assume that those nuclei which, with relation to asymmetry in distribution of mass and charge, can be represented as consisting of two particles with relatively weak binding between them, split into two particles in going through the Coulomb field of a heavy nucleus if the frequency of variation of the field is such that the corresponding energy quanta are larger than the energy of binding of these particles with each other.

The present work is devoted to a study of the probability of splitting of light nuclei in a Coulomb field.

2. We denote the masses and charges of the constituents of the nucleus by M_1 and M_2 and Z_1' and Z_1'', respectively. In the case where, in addition to the residual X_{2k}^{4k}, there is a weakly bound neutron, $Z_1'' = 0$ and $M_2 = M$, where M is the mass of the neutron. We assume that a light nucleus of mass $M_0 = M_1 + M_2$ and charge $Z_1 = Z_1' + Z_1''$ goes through the Coulomb field of a heavy nucleus of charge Z. The Coulomb interaction, in the general case, will have the form

$$V = Z_1 Ze^2 / r_1 + Z_1'' Z^2 e / r_2, \tag{1}$$

where r_1 and r_2 are the distances from the center of mass of both particles of the light nucleus to the center of mass of the heavy nucleus. We can consider the radius of the light nucleus to be significantly less than the distance between centers of the nuclei considered. Therefore, in Eq. (1), we can set approximately $r_1 = r_2 \approx r$, where r is the distance between centers of the given nuclei. In the system of reference in which the light nucleus, as a whole, is at rest but the heavy nucleus is moving, the electrostatic energy of the light nucleus, viewed as a perturbation, is equal to

$$V = Z_1 Z e^2 / [b^2 + (z - vt)^2]^{1/2}, \tag{2}$$

where $Z_1 = Z_1' + Z_2''$, v is the velocity of the heavy nucleus moving along the z-axis, z and b are the projections of the center of mass of the light nucleus—where, in the present approximation its charge Ze is concentrated—on the z-axis and on the perpendicular to it.

The effective differential cross section of the process considered can, as is well known, be written in the form[5]

$$d\sigma = |A|^2 L^2 d\varepsilon_1 d\Omega_{\mathbf{k}} (L/2\pi)^3 d\mathbf{k}_1, \tag{3}$$

where ϵ_1 is the energy of relative motion of the constituents of the light nucleus after disintegration, $\mathbf{k}_1$ is the wave vector of the center of mass of the light nucleus after disintegration, $\mathbf{k}$ is the wave vector of relative motion of the products of the light nucleus after disintegration, L is the edge of the cube,

$$A = \frac{1}{\hbar} \int V_{if} e^{i\omega t} dt, \tag{4}$$

$$V_{if} = \int \psi_i V \psi_f^* d\mathbf{r}\, d\mathbf{r}_c. \tag{5}$$

Here $\mathbf{r}_c$ is the radius vector of the center of mass of the moving nucleus and $\mathbf{r}$ is the radius vector of the relative motion of the products of the light nucleus after splitting. The wave functions of the initial and final states, which enter into Eq. (5), have the form

$$\begin{aligned} \Psi_i &= L^{-3/2} e^{i\mathbf{k}_0\mathbf{r}} \psi_l(\mathbf{r})\, e^{iE_0 t/\hbar}, \\ \Psi_f &= L^{-3/2} e^{i\mathbf{k}_1\mathbf{r}} \psi(\mathbf{r})\, e^{iE_1 t/\hbar}, \end{aligned} \tag{6}$$

where $\mathbf{k}_0$ is the wave vector of the center of mass of the light nucleus before disintegration, $E_0 = -\epsilon$ is the binding energy of the constituents of the light nucleus before disintegration, $E_1 = \epsilon_1 + \hbar^2 k_1^2/2(M_1 + M_2)$ is the total energy of the light nucleus after splitting, $\psi_l(\mathbf{r})$ is the wave function of the ground state of the light nucleus before disintegration, normalized with respect to volume, $\psi(\mathbf{r})$ is the wave function of relative motion of the products of the light nucleus after disintegration. The wave function of the final state can be taken as a plane wave, normalized with respect to energy, *i.e.*,

$$\psi(\mathbf{r}) = (p\mu/(2\pi\hbar)^3)^{1/2} e^{i\mathbf{kr}}, \tag{7}$$

where p is the momentum of relative motion of the products of disintegration, and $\mu = M_1 M_2/(M_1 + M_2)$. According to the law of conservation of energy we have

$$\hbar\omega = E_1 - E_0 = \varepsilon_1 + \varepsilon + \hbar^2 k_1^2/(M_1 + M_2). \quad (8)$$

As Dancoff[5] has shown, the matrix element A can be represented in the form

$$A = 2L^{-3}(Z_1 Ze^2/\hbar v) J_k J_r, \quad (9)$$

$$J_k = \frac{4\pi}{q^2} \frac{\sin[(q_z - \omega/v)L/2]}{(q_z - \omega/v)},$$

$$J_r = \int d\mathbf{r} \exp\left[-i \frac{M_1}{M_1 + M_2}(\mathbf{k}_1\mathbf{r})\right] \psi_l(\mathbf{r}) \psi^*(\mathbf{r}), \quad (10)$$

where q_z is the projection of the vector $\mathbf{q} = \mathbf{p}_1/\hbar$ on the z-axis. It is possible to show that for sufficiently high energies of the light nucleus ~ 100 Mev the quantity $k_1 r \ll 1$. Therefore, it is possible to set

$$\exp\left\{-i \frac{M_1}{M_1 + M_2}(\mathbf{k}_1\mathbf{r})\right\} = 1 - i \frac{M_1}{M_1 + M_2}(\mathbf{k}_1\mathbf{r}). \quad (11)$$

Taking Eq. (11) and the orthogonality condition of the Ψ-functions, J_r can be written

$$J_r = -i \frac{M}{M_1 + M_2} \int (\mathbf{k}_1, \mathbf{r}) \psi^*(\mathbf{r}) \psi_l(\mathbf{r}) r^2 \sin\theta d\theta d\varphi. \quad (12)$$

Here M_1 denotes the mass of the lighter of the products, freed in the breaking up of the light nucleus, *i.e.*, the mass of the neutron, deuteron or triton.

Denoting the angle between $\mathbf{k}_1$ and $\mathbf{r}$ by ϑ we have

$$\cos\vartheta = \cos\gamma\cos\theta + \sin\gamma\sin\theta\cos(\varphi - \varphi'), \quad (13)$$

where γ is the angle between the vectors $\mathbf{k}_1$ and $\mathbf{k}$. The last term in Eq. (13) does not contribute to the integral in Eq. (12). Therefore, we can write J_r as

$$J_r = -i \frac{M_1}{M_1 + M_2} k_1 \cos\gamma \int \psi_l(\mathbf{r}) \psi^*(\mathbf{r}) r^3 dr. \quad (14)$$

The wave function $\Psi(\mathbf{r})$ is given by Eq. (7). In order to determine the wave function of the bound state $\Psi_l(\mathbf{r})$, the form of the interaction between the decay products must be chosen. We assume that this interaction can be represented as a potential well of depth V_0 and radius R. In this case we can take

$$\psi_l(\mathbf{r}) = R_l(r) Y_{lm}(\theta, \varphi),$$

$$R_l(r) = C_l f_l(\beta r) \quad \text{for} \quad r < R, \quad (15)$$

$$R_l(r) = C_l \frac{f_l(\beta R)}{k_l(\alpha R)} k_l(\alpha r) \quad \text{for} \quad r > R,$$

where

$$f_l(x) = \sqrt{\frac{\pi}{2x}} J_{l+1/2}(x),$$

$$k_l(x) = \sqrt{\frac{2}{\pi x}} K_{l+1/2}(x) = \sqrt{\frac{2}{\pi x}} \frac{i\pi}{2} e^{il\pi/2} H^{(1)}_{l+1/2}(ix),$$

$$\beta^2 = 2\mu(V_0 - \varepsilon)/\hbar^2, \quad \alpha^2 = 2\mu\varepsilon/\hbar^2. \quad (16)$$

Here $J_{l+1/2}$ and $H^{(1)}_{l+1/2}$ are the Bessel and Hankel functions.

The conditions of continuity at $r = R$ and normalization give

$$-\alpha k_{l-1}(\alpha R)/k_l(\alpha R) = \beta f_{l-1}(\beta R)/f_l(\beta R), \quad (17)$$

$$C_l^2 = -2\alpha^2/(\alpha^2 + \beta^2) R^3 f_{l-1}(\beta R) f_{l+1}(\beta R). \quad (18)$$

It is easy to show that, after averaging over initial states, we finally obtain for $|J_r|^2$

$$|J_r|^2 = \left(\frac{M_1}{M_1 + M_2}\right)^2 \frac{p_1 \cos^2\gamma}{\hbar^2} \frac{4\pi\mu p}{(2\pi\hbar)^3} \left\{\frac{(l+1)^2}{(2l+1)^2} D^2_{l,\,l+1} + \frac{l^2}{(2l+1)^2} D^2_{l,\,l-1}\right\},$$

$$D_{l,\,l\pm1} = C_l \int_0^R f_l(\beta r) f_{l\pm1}(kr) r^3 dr + C_l \frac{f_l(\beta R)}{k_l(\alpha R)} \int_R^\infty k_l(\alpha r) f_{l\pm1}(kr) r^3 dr. \quad (19)$$

3. We consider several special cases. We assume that $l = 1$ in the initial state. This is the case, for example, in the Li^7 nucleus. We will view the latter as consisting of an α-particle and triton. Here the orbital moment of relative motion of the triton is $l = 1$ ($p_{3/2}$ state).

As a result of calculation, we obtain for the differential cross section

$$d\sigma = \frac{1080}{2989}\left(\frac{Z_1 Ze^2}{\hbar v}\right)^2 \Phi_1(\varepsilon_1) \frac{d\varepsilon_1}{\varepsilon_1^{3/2}} \ln \frac{\hbar v}{(\varepsilon + \varepsilon_1) R}, \quad (20)$$

where

$$\Phi_1(\varepsilon_1) = \left\{\left(a_1 + \frac{a_2}{\sqrt{\varepsilon_1}}\right)\sin\sqrt{\rho\varepsilon_1} - \left(\frac{a_3}{\varepsilon_1} + a_4 - \frac{a_5}{\sqrt{\varepsilon_1}}\right)\cos\sqrt{\rho\varepsilon_1}\right\}^2;$$

$$a_1 = C_1/\beta^2, \quad a_2 = \hbar(2\mu)^{-1/2}[\beta R^2 f_0(\beta R) - 1/\beta] C_1,$$

$$a_3 = (\hbar^2/2\mu) 2\beta R f_0(\beta R) C_1,$$

$$a_4 = [(1 + \alpha R)/\alpha^2] \beta R f_0(\beta R) C_1,$$

$$a_5 = \hbar R C_1/\sqrt{2\mu}, \quad \rho = 2\mu R^2/\hbar^2.$$

The coefficient C_1 is defined by Eq. (18); the quantity ϵ, which enters into Eq. (20), denotes the binding energy of the triton in the Li^7 nucleus and is equal to 2.52 Mev.

4. We consider further the case in which the light nucleus has orbital momentum $l = 2$ in the initial state. This case is encountered, for example, in the O^{17} nucleus, where the odd neutron is in a $d_{5/2}$ state.

For the effective differential cross section of the process we obtain

$$d\sigma = \frac{1}{61}\left(\frac{Z_1 Ze^2}{\hbar v}\right)^2 \frac{\hbar}{\sqrt{8\mu}} \frac{\sin^2 \sqrt{\rho\varepsilon_1}}{\varepsilon_1^{3/2}} \Phi_1(\varepsilon_1)\, d\varepsilon_1 \ln \frac{\hbar v}{(\varepsilon + \varepsilon_1) R}, \tag{21}$$

where

$$\Phi_1(\varepsilon_1) = \left\{\frac{B}{\varepsilon_1} - \frac{D(1 + \cot^2 \sqrt{\rho\varepsilon_1})}{\sqrt{\varepsilon_1}} + A - D_1 \cot \sqrt{\rho\varepsilon_1}\right\}^2,$$

$$A = \frac{6\alpha^2}{(\alpha^2 + \beta^2) f_1(\beta R) f_3(\beta R) R^3}\left[\frac{1 - f_0(\beta R)}{\beta^2} + \frac{\beta^2(1 + \alpha R)}{\alpha^4} f_0(\beta R)\right],$$

$$B = 6\left(\frac{\hbar^2}{2\mu}\right) \frac{\beta^2 \alpha}{(\alpha^2 + \beta^2) R^2} \frac{f_0(\beta R)}{f_3(\beta R) f_1(\beta R)},$$

$$D = \frac{\hbar^2}{(2\mu)^{3/2}} \frac{2\beta^2}{(\alpha^2 + \beta^2) R^2} \frac{f_0(\beta R)}{f_3(\beta R) f_1(\beta R)}, \qquad D_1 = \frac{\hbar^2}{(2\mu)^{3/2}} D.$$

All formulae for the effective differential cross section which we introduced above contain the quantity (βR), which is the solution of the transcendental equation (17). By giving the nuclear radius R and requiring the depth of the well representing the interaction of particles of the light nucleus to lie in an acceptable interval of values between 5 and 30 Mev, β can be unambiguously determined by solving Eq. (17) for a given value of l. The formulae obtained by us hold for the system in which the light nucleus is at rest. In order to obtain expressions for the effective cross section in the laboratory system, in which the heavy nucleus is at rest, it is necessary to carry out a transformation analogous to that which is made in the theory of disintegration of the deuteron in a Coulomb field[5].

We note, in conclusion, that the order of magnitude of the effective cross section for the disintegration of light nuclei in a Coulomb field, at energies in the range ~ 100 Mev turns out to be equal to $10^{-29}(ZZ_1)^2$ cm^2.

[1] J. Sawicki, Acta Phys. Polon. **14**, 135 (1955).
[2] P. Cüer and G. Combe, Compt. rend. (Paris) **239**, 351 (1954).
[3] I. Sh. Vashakidze and G. A. Chilashvili, J. Exptl. Theoret. Phys. (U.S.S.R.) **26**, 254 (1954).
[4] J. Dabrowki and J. Sawicki, Phys. Rev. **97**, 1002 (1955).
[5] S. Dancoff, Phys. Rev. **72**, 1017 (1947).

Translated by G. E. Brown
177

Thermal Radiation from an Anisotropic Medium

F. V. BUNKIN
P. N. Lebedev Physical Institute, Academy of Sciences, USSR
(Submitted to JETP editor March 9, 1956)
J. Exptl. Theoret. Phys. (U.S.S.R.) 32, 811-821 (February, 1957)

The radiation emitted by an element of volume of an anisotropic medium is examined on the basis of the electrodynamic theory of thermal radiation. A generalization of Kirchhoff's law is given. The thermal radiation from continuously varying magnetoactive media is considered. The case of weak gyrotropy is considered in some detail.

1. INTRODUCTION

KIRCHHOFF'S LAWS, which constitute the basis of the classical theory of thermal radiation, were established for an *isotropic* medium. Attempts to apply these laws directly to an anisotropic medium* encounter certain difficulties due mainly to the birefringent properties of such a medium. However, thermal radiation from anisotropic media has lately acquired practical importance—principally in connection with the development of radioastronomy. By way of example one may cite problems such as the role of thermal radiation (at radio frequencies) from the sun's corona in the general magnetic field of the sun[1-3], or radiation from sunspots. Another example, which concerns apparatus by itself, is that of the thermal emission from the ferrite used in the wave guides of modern instruments.

This paper formulates the problem of the thermal radiation of an anisotropic medium and solves that problem from the point of view of the electrodynamic theory of electric field fluctuations and thermal radiation as evolved by Rytov[4]. According to the basic concept of this theory, thermal fluctuations of the electric field in a medium may be described as the result of action by several extraneous random fields (or currents). In the same way these fields are also used to describe the random (thermal) radiation from each volume element of the medium.

In order to compute statistical averages of the energy values (which are quadratic in the extraneous field) one need know only the statistical characteristic of the extraneous random field, *i.e.*, the *correlation matrix* of the field components. The form of this matrix has been determined by Rytov[4] for an isotropic medium. Recently L. D. Landau and E. M. Lifshitz, in reporting on the papers by Callen *et al.*[5-8], have generalized the form of this matrix to media with arbitrary anisotropy*. In this case, when the medium experiences only electrical losses, the correlation matrix of extraneous random currents $j_\alpha(\mathbf{r})$

$$\overline{j_\alpha(\mathbf{r})\, j^*_{\beta'}(\mathbf{r}')} = \frac{\hbar\omega^2}{8\pi^2}\coth\frac{\hbar\omega}{2\Theta}\,\frac{\varepsilon^*_{\beta\alpha}-\varepsilon_{\alpha\beta}}{2i}\,\delta(\mathbf{r}-\mathbf{r}') = C_{\alpha\beta}\,\delta(\mathbf{r}-\mathbf{r}'), \tag{1.1}$$

where $\hbar$ is Planck's constant divided by 2π; $\Theta = kT$ the temperature in energy units; and $\epsilon_{\alpha\beta}$ is the dielectric permittivity tensor for the medium**.

Thermal radiation from a plasma situated in a constant magnetic field (magnetoactive medium***) is of practical importance. It is a medium of this type that we shall have in mind henceforth in this paper. Absorption in such a medium is caused, as is known, by collisions, ordinarily with $\nu/\omega \ll 1$ where ν is the collision frequency and ω is the wave frequency. The smallness of ν/ω implies the smallness of the absorption coefficient for an *ordinary* wave throughout all space available to it (see, for example, Ref. 11). In this case the maximum absorption occurs in the region of reflection, *i.e.*, where the refractive index is nearly zero.

The nature of the absorption coefficient for an *extraordinary* wave is more complicated on account of resonance absorption. The resonance is the strongest when the wave travels along the maghetic field and when $\omega = \omega_H$, ω_H being the gyrofrequency ($= eH/2mc$) of the plasma. The width of

*Under the meaning of "anisotropic media" we include both optically inactive and active (gyrotropic) crystals.

*These results have not yet been published. I wish to thank the authors for making their manuscript available to me.

**We point out that Levin[9] and the author[10] have used Eq. (1.1) before but without thorough substantiation.

***From a phenomenological point of view, ferrites located in a magnetic field can be assigned to this same type of category.

the resonance frequency band, in which the absorption is large, is on the order of ν. Outside of this comparatively narrow band, *i.e.*, where $|\omega - \omega_H| \gg \nu$, the absorption coefficient for the extraordinary wave then becomes of the same order of magnitude as in the case of an ordinary wave, ν/ω. The spatial distribution of the absorption coefficient is the same as for an ordinary wave, *i.e.*, with its maximum in the reflection area.

Therefore, if one disregards the resonance region that exists for longitudinal propagation, absorption in true magnetoactive media may be considered small. This is the principal argument in favor of the assumption made below that the radiating medium* is a weak absorber.

The subjects analyzed below have been examined in more detail in the author's dissertation[10].

2. INTENSITY OF THERMAL RADIATION FROM A VOLUME ELEMENT OF A MAGNETOACTIVE MEDIUM

Let us examine how a volume element of a magnetoactive medium radiates, *i.e.*, how one must generalize Kirchhoff's law,

$$\eta_\omega = \alpha_\omega I_\omega, \tag{2.1}$$

where η_ω and α_ω are respectively the emission and absorption coefficients of an isotropic medium, and I_ω is the intensity of the equilibrium thermal radiation in the given absorbing medium. As has been noted before[4], the concepts of equilibrium intensity and emission coefficient in an absorbing medium have definite meanings only when the absorption is so small that it is possible to disregard terms of the second order so far as losses are concerned. In this case Clausius' law is fulfilled

$$I_\omega = I_{0\omega} n^2, \tag{2.2}$$

where $I_{0\omega}$ is the intensity of the equilibrium radiation in vacuum, and n is the index of refraction for a *transparent* medium.

In the case of an anisotropic medium the problem is complicated first because two types of waves are propagated and secondly because the radiation intensity must depend on the angle formed by the direction of propagation and the axis of symmetry of the medium. Therefore, the generalized law (2.1) must specify both the distribution of the radiated energy for the two possible types of waves (polarizations) and the mentioned angular dependence.

Let us first write the components of the tensor $C_{\alpha\beta}$, which enters into the correlation matrix (1.1) of the extraneous random currents, for the case of a magnetoactive medium. If the magnetic field is directed along the Z axis, the tensor ε_{ik} is written as (see, for example Ref. 11, p. 326):

$$\varepsilon_{ik} = \begin{Vmatrix} \varepsilon & -ig & 0 \\ ig & \varepsilon & 0 \\ 0 & 0 & \eta \end{Vmatrix}. \tag{2.3}$$

When there is absorption, the quantities ε, η and g are, in general, complex. The explicit dependence of the components ε_{ik} on the parameters of the plasma do not concern us here.

Substituting (2.3) in (1.1) we obtain

$$\begin{aligned} C_{11} &= C_{22} = \frac{\hbar\omega^2}{8\pi^2} \coth \frac{\hbar\omega}{2\Theta} \cdot \frac{\varepsilon^* - \varepsilon}{2i}, \\ C_{33} &= \frac{\hbar\omega^2}{8\pi^2} \coth \frac{\hbar\omega}{2\Theta} \cdot \frac{\eta^* - \eta}{2i}, \\ C_{12} &= -C_{21} = -\frac{\hbar\omega^2}{8\pi^2} \coth \frac{\hbar\omega}{2\Theta} \cdot \frac{g^* - g}{2}, \\ C_{13} &= C_{31} = C_{23} = C_{32} = 0. \end{aligned} \tag{2.4}$$

We shall assume a weakly absorbing medium and therefore disregard terms of second order (*i.e.*, terms $\sim C^2_{\alpha\beta}$). Then when the emission coefficient is computed, the medium external to the radiating volume element dV can generally be treated as transparent.

The emission coefficient characterizes that portion of the total flow of energy from an element dV which diminishes only according to the exponential law as it travels away from the element, *i.e.*, that portion which is due to the wave field. However, from our point of view, the volume element dV is a dipole with a random moment of $d\mathrm{p} = \mathrm{j}dV/i\omega$ where j represents the density of the random extraneous currents. The wave field of the dipole in a magneto-

*In actuality, nearly longitudinal wave propagation may be found, for instance, in sun spots. Here, however, no resonance region is in fact observed because of the special nature of the inhomogeneity of the solar atmosphere whereby an increase in the radius ρ causes a monotonic decrease in both the electron concentration $N(\rho)$ and magnetic field intensity $H_0(\rho)$. The result is that extraordinary waves, whether they are generated by an element in the medium at resonance frequencies ($|\omega - \omega_H| \lesssim \nu$), or pass during emergence from the medium through a region of resonance absorption (ω_H decreases with increasing layer height) are unable to emerge outside[12].

active medium was previously found to be [see Bunkin[13], Eq. (5.3)]:

$$E_j^{(i)}(\mathbf{r}) = 4\pi k^6 A^{(i)}(\theta)(kr)^{-1}\exp\{ikr\psi^{(i)}(\theta)\}\alpha_{jk}^{(i)}(\theta,\varphi)\,p_k, \tag{2.5}$$

where p_k represents the components of the dipole moment and where the $A^{(i)}$, $\psi^{(i)}$, $\alpha_{ik}^{(i)}$ are determined by the components ε_{ik} and thus depend on polar angle θ (measured from the axis of symmetry, *i.e.*, from the direction of the external magnetic field) and on the azimuth angle φ of the radius vector r, as well as being determined by the index of refraction n_i and its first and second derivatives [Bunkin[13], Eq. (5.4) and (5.5)]. The index i refers to one of the two possible types of waves ($i = 1$ for an ordinary wave, $i = 2$ for an extraordinary one).

From Eq. (2.5) for the dipole field and correlation matrix (1.1) and (2.4) for the current j, one can compute the emission coefficient η_ω for the medium under discussion. The following result is obtained

$$\eta_\omega = \eta_\omega^{(1)} + \eta_\omega^{(2)} + \eta_\omega^{(12)}, \tag{2.6}$$

where $\eta_\omega^{(i)}$ is the emission coefficient for i-type waves (the natural emission coefficient) and $\eta_\omega^{(12)}$ is the "interference" emission of thermal radiation. We are omitting the equations for the dependence of these coefficients on the values $A^{(i)}$, $\alpha_{jk}^{(i)}$ and $\psi^{(i)}$, since our main interest is not in these equations but rather in presenting η_ω in such a form as to generalize Kirchhoff's law, Eq. (2.1). In this connection there arises a difficulty due to the presence of the interference emission $\eta_\omega^{(12)}$. However, as detailed examination reveals, the interference term proves quite inconsequential in practical problems. In clarifying this further we shall limit ourselves to a few remarks only.

The interference term describes the "fine structure" of the thermal radiation field. The difference in the propagation velocities of the ordinary and extraordinary waves causes the three-dimensional oscillatory character of the interference emission (see F. V. Bunkin[10]) thus

$$\eta_\omega^{(12)} = g^2 B(\theta,\omega)\cos\{kr[\psi^{(1)}(\theta,\omega) - \psi^{(2)}(\theta,\omega)] + \varphi(\theta,\omega)\}, \tag{2.7}$$

We have indicated an explicit dependence on frequency ω, since we allow for the presence of dispersion, *i.e.*, the dependence of ε_{ik} on ω. As is evident the emission coefficient $\eta_\omega^{(12)}$ is of second order in the gyrotropy parameter g. When $\theta = 0$ and $\theta = \pi/2$, the "amplitude" $B(\theta,\omega)$ becomes zero, *i.e.*, there is no interference emission in directions along and across the external magnetic field.

Because of the oscillatory dependence of $\eta_\omega^{(12)}$ on r and θ, this interference between the ordinary and extraordinary waves is totally lost when the investigated radiation is only slightly nonmonochromatic (slightly, that is, relative to the bandwidth of the receiver).

We note that the presence of interference between ordinary and extraordinary waves in thermal emission is precisely characteristic of a magnetoactive (gyrotropic in the general case) medium. In inactive crystals, such as uniaxial crystals, for which $g = 0$, there is no interference.

As for the natural emission of thermal radiation, the problem, as has been stated, is to write $\eta_\omega^{(i)}(\theta)$, expressed in terms of $A^{(i)}(\theta)$, $\psi^{(i)}(\theta)$, and $\alpha_{jk}^{(i)}(\theta,\varphi)$, in such a form as to obtain a generalized Kirchhoff's law, *i.e.*, as

$$\eta_{|\omega}^{(i)}(\theta) = \alpha_\omega^{(i)} I_\omega^{(i)}, \qquad (i = 1,2). \tag{2.8}$$

It is natural to take $I_\omega^{(i)}$ as the intensities of *equilibrium* thermal radiation in a *transparent* magnetoactive medium, in which case $I_\omega^{(i)}$ depends on the parameters ε, η, g and angle θ, and is given by Rytov[4], page 150*.

The following expression is then obtained for the coefficients $\alpha_\omega^{(i)} = \alpha_\omega^{(i)}(\theta)$,

$$\alpha_\omega^{(i)}(\theta) = 2kn_i(\xi_{0i})\varkappa_i(\xi_{0i})\cos(\xi_{0i} - \theta). \tag{2.9}$$

Here $n_i(\xi)$ and $\varkappa_i(\xi)$ are related in the usual way to the real and imaginary parts of the complex index of refraction $n_i(\xi)[1 - i\varkappa_i(\xi)]$ for an i-type *plane* wave propagating at angle ξ to the z axis (terms

*Rytov derives equations for equilibrium intensities $I_\omega^{(i)}$ due to a beam of plane waves whose *normals* form an angle θ with the z-axis. The *energy* flow vector of this beam forms a different angle, which Rytov designates by ξ. It must be borne in mind that our notation is different, we use ξ to represent the angle between the normal and the z-axis and θ to represent the angle of the energy flow. We find it expedient to express the intensity $I_\omega^{(i)}$ in terms of the angle θ.

$\sim \kappa_i^2$ are neglected). The angle $\xi_{0i} = \xi_{0i}(\theta)$ is determined from the equation

$$n_i'(\xi_{0i})/n_i(\xi_{0i}) = \tan(\xi_{0i} - \theta) \qquad (2.10)$$

and is equal to the angle between the wave normal of a plane wave and the direction of the magnetic field, where the energy flow vector of this wave makes an angle θ with the magnetic field[11]. The components $C_{\alpha\beta}$ of the correlation tensor no longer enter in Eq. (2.9) because they are expressed in terms of $n_i(\xi_{0i})$ and $\kappa_i(\xi_{0i})$.

For an isotropic medium, $\xi_{0i} = \theta$, $n_1 = n_2$, $\kappa_1 = \kappa_2$ and are independent of direction, so that Eq. (2.9) now becomes the usual one for the absorption coefficient of an isotropic medium $a_\omega = 2kn\kappa$. Since in this case $I_\omega^{(2)} = I_\omega^{(1)} = \frac{1}{2}n^2 I_{0\omega}$ (see Rytov[4], p. 150), Eq. (2.8) reduces to Eq. (2.1). Thus, Eq. (2.8) and Eq. (2.9) are actually rational generalizations of Kirchhoff's law and the concept of absorption coefficient.

As has been mentioned, Eq. (2.8) is the solution to the problem of the division of the energy radiated by a point thermal source between the two possible types of waves, and this in turn makes it possible for one to determine the degree of polarization of this radiation (see next Section).

Let us pause briefly to examine the results of some numerical computations. In solving practical problems it is convenient to express the components of the tensor ε_{ik} in terms of the plasma parameters h, v, and q[11]. These are determined in the following manner,*

$$h = \omega_H/\omega, \quad v = (\omega_0/\omega)^2, \quad q = \nu/\omega, \qquad (2.11)$$

where ω_H and ω_0 are respectively the gyromagnetic and critical frequencies of the plasma and ν is the collision frequency. The requirement of small absorption means the one must eliminate that frequency region ω, which satisfies the condition $|1-h| \lesssim q$. The expression for the absorption coefficient $\alpha_\omega^{(i)}(\theta)$ is given by [with $n_i = n_i(\xi_{0i})$,

$$\alpha_\omega^{(i)}(\theta) = q\frac{k}{n_i}\cos(\xi_{0i} - \theta)\frac{(1-n_i^2)^2}{v(1-v)} \times \frac{2(1-v)^2(v-1+n_i^2) + h^2 v n_i^2 \sin^2\xi_{0i}}{2(1-v)(v-1+n_i^2) + h^2(1-n_i^2)\sin^2\xi_{0i}}. \qquad (2.12)$$

The curves in the figure illustrate the dependence of the dimensionless quantity $\eta_\omega^{(i)}(\theta)/qkI_{0\omega}$ on the angle θ when $v = 0.4$ and $h^2 = 0.3$. Numerals I and II refer to the ordinary and the extraordinary types of radiation respectively; the straight dotted line represents the emission coefficient of an isotropic medium ($v = 0.4$, $h = 0$).

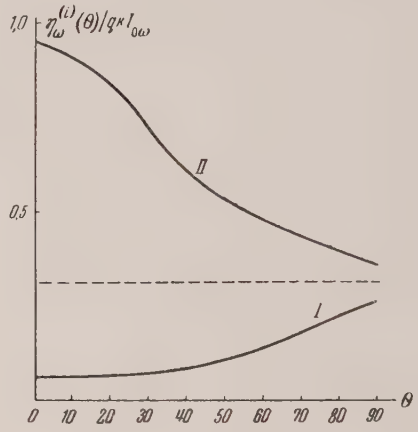

It is obvious from the figure that the introduction of a magnetic field with $\omega_H \approx 0.55\omega$ increases the emissive power of each volume element of the plasma for extraordinary waves and decreases it for ordinary waves for all directions of emission. The total emissive power (for both wave types) when the field is present exceeds the emissivity when the field is absent. For other values of h (*i.e.*, for other frequencies with the same magnetic field) the ratio between $(\eta_\omega^{(1)} + \eta_\omega^{(2)})$ and $\eta_\omega^{(0)}$ the emission coefficient of an isotropic medium ($h = 0$) will, of course, be different, but invariably*

$$\eta_\omega^{(1)}(\theta) + \eta_\omega^{(2)}(\theta) \geqslant \eta_\omega^{(0)}. \qquad (2.13)$$

Thus, when the magnetic field is applied, there is an increase in the output of thermal energy by each volume element of the plasma. Of course, this does not mean that there must of necessity be an increase also in the emissive power of the total volume of the plasma, for as the emission coefficient grows larger, reabsorption of the energy also increases (just as an increase in the resonance radiation of atoms is accompanied by an increase in their absorption). The general considerations indicating

*Al'pert, *et al*[11] use the parameter $u = h^2$ instead of h, and furthermore use s instead of q.

*Further on it will be shown that when h is small, $\eta_\omega^{(1)}(\theta) + \eta_\omega^{(2)}(\theta) = \eta_\omega^{(0)}$.

this circumstance were once set forth in connection with the discussion of the increase in the radiation of sun spots [14, 15].

3. POLARIZATION OF THE THERMAL RADIATION FROM A VOLUME ELEMENT

In the study of the thermal radiation of anisotropic media, questions concerned with polarization are of special interest in addition to the questions of radiation intensity. In general only partial polarization occurs, *i.e.*, the flow of radiation at any one point is the sum of the unpolarized (randomly polarized) and completely polarized (in general, elliptically polarized) components. The completely polarized portion of the flow is, of course, also random, but the field here fluctuates in such a way that the amplitude ratio and the difference in the phases of the two orthogonal projections remain constant.

In this Section we shall determine the degree of polarization of the thermal radiation emitted by a point source (volume element of the medium), *i.e.*, the ratio $p(\theta)$ of the intensity in a given direction of the totally polarized component to the total intensity. Moreover, we shall determine the degree of ellipticity (the ratio of semiaxes $a/b = \tan\beta(\theta)$ of the polarization ellipse of the electric field) and the position of the polarization plane, *i.e.*, the angle of inclination $\chi(\theta)$ of the major axis of the ellipse to a certain direction. These questions can be most simply solved by using Stokes' parameters Q, U, and V which must be expressed in terms of the components of the tensor $C_{\alpha\beta}$*. In this case we have for $\beta(\theta)$ and $\chi(\theta)$

$$\sin 2\beta = V/\sqrt{Q^2 + U^2 + V^2}, \quad \tan 2\chi = U/Q, \tag{3.1}$$

where χ is the angle formed by the major axis of the ellipse and the ξ_1 axis. The double valuedness of these equations is eliminated by the following auxiliary condition: if of the two values for β the smaller in absolute magnitude is selected, then the sign of $\cos 2\chi$ should coincide with the sign of Q. The sign of β is understood to be counter-clockwise (from axis ξ_1 toward axis ξ_2).

Let us introduce an auxiliary Hermitian tensor

$$P_{ik}(\mathbf{r}) = \overline{E_i(\mathbf{r})\, E_k^*(\mathbf{r})}, \tag{3.2}$$

where E(r) represents the electric field. The determination of Stokes' parameters [where one utilizes the definitions* and Eq. (3.2)] leads to a connection between Q, U, V and P_{ik}. If, for example, the polarization in plane (x, y) is of interest, we have

$$Q = P_{11} - P_{22}, \quad U = P_{12} + P_{21}, \quad V = -i(P_{12} - P_{21}). \tag{3.3}$$

Returning to the question of the polarization of thermal radiation in a homogeneous medium, which is of interest to us, we make use of the representation of the field E(r) by the extraneous current j(r) (see Bunkin [13]),

$$E_i(\mathbf{r}) = \frac{4\pi k}{ic}\int_V T_{ik}(\mathbf{r}, \mathbf{r}_1)\, j_k(\mathbf{r}_1)\, dV_1. \tag{3.4}$$

Substituting Eq. (3.4) into Eq. (3.2) and utilizing Eq. (1.1), we find

$$P_{ik} = \frac{16\pi^2 k^2}{c^2}\int T_{i\alpha}(\mathbf{r}, \mathbf{r}_1)\, T^*_{k\beta}(\mathbf{r}, \mathbf{r}_1)\, C_{\alpha\beta}\, dV_1 = \int p_{ik}(\mathbf{r}, \mathbf{r}_1)\, dV_1. \tag{3.5}$$

The additivity of components P_{ik} is obviously a consequence of the incoherence of the radiation from separate volume elements of the medium. The tensor $p_{ik}(\mathbf{r}, \mathbf{r}_1)dV_1$ characterizes the radiation polarization at point r due to the volume element dV_1, which is at point $\mathbf{r}_1$, and allows for both ordinary and extraordinary waves. Thus, in the general case we have

$$p_{ik} = p_{ik}^{(1)} + p_{ik}^{(2)} + p_{ik}^{(12)}, \tag{3.6}$$

where $p_{ik}^{(12)}$ is the interference term. For the same reasons as those given above in the discussion of the interference term in the energy flow, the term

---

*If

$$\xi_1 = \xi_1^0 \sin(\omega t - \varepsilon_1), \qquad \xi_2 = \xi_2^{(0)} \sin(\omega t - \varepsilon_2)$$

are two mutually perpendicular components of the electric field, then by definition the Stokes parameters are [16–18]

$$Q = \overline{(\xi_1^{(0)})^2} - \overline{(\xi_2^{(0)})^2}, \quad U = 2\overline{\xi_1^{(0)}\, \xi_2^{(0)} \cos\delta},$$

$$V = 2\overline{\xi_1^{(0)}\xi_2^{(0)} \sin\delta}, \quad \delta = \varepsilon_1 - \varepsilon_2.$$

Stokes introduced yet a fourth parameter $I = \overline{(\xi_1^{(0)})^2} + \overline{(\xi_2^{(0)})^2}$, to determine the intensity in isotropic media. In anisotropic media this parameter does not determine intensity and therefore is of no interest.

$p_{ik}^{(12)}$ may be disregarded. The components of the tensor $p_{jk}^{(i)}(i = 1, 2)$ are determined with the aid of Eq. (3.4).

In the wave region which is, of course, the only one of interest, we obtain

$$p_{jk}^{(i)} = B^{(i)} a_{j\alpha}^{(i)}(\theta, \varphi)\, a_{k\beta}^{(i)}(\theta, \varphi)\, C_{\alpha\beta}, \tag{3.7}$$

$$B^{(i)} = (16\pi^2 k^8/c^2\rho^2)\, |A^{(i)}(\theta)|^2, \rho = |\mathbf{r} - \mathbf{r}_1|, \tag{3.8}$$

where the functions $A^{(i)}$, $a_{jk}^{(i)}$ are the same as in Eq. (2.5).

By substituting Eq. (3.7) into Eq. (3.3) we establish the relationship of the Stokes parameters, which relate to the radiation from a volume element with the components of the tensor $C_{\alpha\beta}$. The expressions thus obtained for the parameters $Q^{(i)}(\theta)$, $U^{(i)}(\theta)$, and $V^{(i)}(\theta)$, which depict the polarization of the field in a plane orthogonal to an arbitrary direction of emission, are rather cumbersome and are not given here. These expressions show that thermal radiation from a volume element in waves of every type will be completely polarized, and in general elliptically. However, it is a matter of practical importance to determine the state of polarization of the total emission (*i.e.*, the flow of ordinary and extraordinary waves, assuming, of course, that there is emission of both types of waves, *i.e.*, that the refraction index at any given point be real for both waves). Since we disregard the interference term $p_{jk}^{(12)}$, then the Stokes parameters Q, U, V for the total beam are

$$Q = Q^{(1)} + Q^{(2)},\ U = U^{(1)} + U^{(2)},\ V = V^{(1)} + V^{(2)}. \tag{3.9}$$

In this case the flux is only partly polarized. The degree of polarization $p(\theta)$ can be evaluated by the equation

$$p(\theta) = \frac{|\eta_\omega^{(1)}(\theta) - \eta_\omega^{(2)}(\theta)|}{\eta_\omega^{(1)}(\theta) + \eta_\omega^{(2)}(\theta)} = \frac{|\alpha_\omega^{(1)}(\theta) I_\omega^{(1)}(\theta) - \alpha_\omega^{(2)}(\theta) I_\omega^{(2)}(\theta)|}{\alpha_\omega^{(1)}(\theta) I_\omega^{(1)}(\theta) + \alpha_\omega^{(2)}(\theta) I_\omega^{(2)}(\theta)}. \tag{3.10}$$

In the case of weak gyrotropy, *i.e.*, when $h \ll 1$, the approximate expression for $\eta_\omega^{(i)}(\theta)$, which was obtained in Section 5 of this article, yields a very simple equation for $p(\theta)$, correct to terms $\sim h$

$$p(\theta) = 2h\left(1 + \frac{v}{4(1-v)}\right)|\cos\theta|. \tag{3.11}$$

As an example, let us examine the case of longitudinal ($\theta = 0$) thermal emission from a volume element. For the Stokes parameters we obtain

$$V^{(i)} = \mp 4g^2\eta^2 (C_{11} \pm iC_{12})\, B^{(i)}, \quad Q^{(i)} = U^{(i)} = 0. \tag{3.12}$$

Thus [see Eq. (3.1)]

$$\sin 2\beta^{(i)} = \mp 1, \tag{3.13}$$

i.e., as might have been expected, longitudinal thermal emission from a point source is circularly polarized. The total flux is only partly polarized, naturally, though again circularly and with the same direction of rotation as for an extraordinary plane wave. The degree of polarization for this particular case is,

$$p(0) = \frac{|n_1(1-h)^2(n_2^2+1-v)^2 - n_2(1+h)^2(n_1^2+1-v)^2|}{n_1(1-h)^2(n_2^2+1-v)^2 + n_2(1+h)^2(n_1^2+1-v)^2}, \tag{3.14}$$

$$n_i^2 = 1 - v/(1 \pm h). \tag{3.15}$$

4. THE EQUATION FOR TRANSFER OF THERMAL RADIATION IN A MAGNETOACTIVE MEDIUM

The problem of thermal radiation in inhomogeneous media reduces, as is known, to solving the transfer equation; to write this equation one must know the emission and absorption coefficients of the medium. Since we have obtained these values for a magnetoactive medium, it is now easy for us to write the transfer equation. If $J_\omega^{(i)}$ is the intensity of the i-type thermal radiation ($i = 1, 2$) in the direction θ (θ is the angle between the direction of interest and the magnetic field at the given point), then

$$(dJ_\omega^{(i)}/d\sigma) + \alpha_\omega^{(i)}(\theta)\, J_\omega^{(i)} = \eta_\omega^{(i)}(\theta), \tag{4.1}$$

where $d\sigma$ is the element of ray length, and $\alpha_\omega^{(i)}(\theta)$ and $\eta_\omega^{(i)}(\theta)$ are respectively the absorption and emission coefficients of the medium.

The intensity of radiation emitted from the medium in a given direction is obtained from Eq. (4.1),

thus

$$J_\omega^{(i)} = \int_0^\infty \eta_\omega^{(i)}(\theta, \sigma)\, e^{-\tau_i(\sigma)}\, d\sigma, \qquad (4.2)$$

where $\tau_i(\sigma)$ is the optical thickness,

$$\tau_i(\sigma) = \int_0^\sigma \alpha_\omega^{(i)}(\theta, \sigma)\, d\sigma. \qquad (4.3)$$

The integration in Eq. (4.2) and Eq. (4.3) is to be performed along the ray under consideration.

Thus the problem reduces to (as in the case of an isotropic medium) a computation of the trajectory of the ray. However, in contrast to the case of an isotropic medium, where it is sufficient to use the refraction law (Snell's law) to determine the trajectory of the ray, the corresponding computations in the present case require consideration of both the refraction law (whose form is considerably more complicated) and the relationship between the directions of the wave normal and the energy flow. The result is that even for a comparatively simple case of anisotropy (*e.g.*, a plane inhomogeneous ionosphere stratum in a homogeneous magnetic field[19-20]) the computation of the trajectory of the ray necessitates cumbersome calculations and can be completed only by combining analytic and graphic methods. In the case of the sun, which is of practical interest, the ray trajectories have not, to our knowledge, been computed with allowance for the magnetic field (*i.e.*, for the "anisotropic" sun).

It is not out purpose here to compute the ray trajectories for any concrete problems, but to examine the particular, but practically important, case of weak gyrotropy, *i.e.*, effects due to anisotropy which can be treated more or less as *corrections* to the solution for a corresponding isotropic medium.

5. THE CASE OF WEAK GYROTROPY

The condition for weak gyrotropy $\omega_H/\omega \equiv h \ll 1$ is realized in the earth's ionosphere (where the magnetic field $H_0 \approx 0.5$ oersted) for wavelengths of a meter or less and on the sun—for the general magnetic field ($H_0 \approx 50$ oersted) and the field of small sun spots ($H_0 \approx 10^2$ oersted)—for wavelengths from a decimeter to a centimeter (here $h \lesssim 0.1$).

We shall find approximate expressions for the quantities that are of interest which are accurate to terms of the order of h. The general expression for the index of refraction for an ionized gas in a magnetic field[11,19] reduces in this approximation to a simple equation,

$$n_i^2 = 1 - v \pm hv\,|\cos\xi|, \qquad (5.1)$$

where ξ is the angle formed by the wave normal and the magnetic field. The quadratic term in h in the expansion of n_i^2 is one order of magnitude smaller than the preceeding term only when the angle satisfies the following condition,

$$\sin\xi \cdot \tan\xi \ll 2(1 - v). \qquad (5.2)$$

When this condition is not fulfilled the anisotropy of the medium proves to be of order h^2, *i.e.*, the medium is isotropic in the approximation discussed here ($\sim h$) and consequently an analysis of the phenomena that interest us becomes superfluous. Eq. (5.2) obviously means that the directions of propagation must not be too close to the transverse direction.* Thus, when $v = 0.4$, the angle ξ should not exceed about 56°. Henceforth we shall invariably assume Eq. (5.2) to be fulfilled.

When Eq. (5.1) holds, it is easy to produce the corresponding approximate expression for the angle $\chi_i(\xi_{0i}) = \xi_{0i} - \theta$, as well as for the absorption $[\alpha_\omega^{(i)}(\theta)]$ and emission $[\eta_\omega^{(i)}(\theta)]$ coefficients [the exact expressions for these quantities are given by Eq. (2.8), (2.9) and (2.10) respectively]. Thus,

$$\chi_i[\xi_{0i}(\theta)] = \mp \frac{v \sin\theta}{2(1-v)} h, \qquad (5.3)$$

$$\alpha_\omega^{(i)}(\theta) = \alpha_\omega^{(0)}\left[1 \mp 2\left(1 + \frac{1}{4}\frac{v}{1-v}\right) h\,|\cos\theta|\right], \qquad (5.4)$$

$$\eta_\omega^{(i)}(\theta) = \alpha_\omega^{(i)}(\theta)\, I_\omega^{(i)}(\theta)$$

$$= {}^1/_2\,\eta_\omega^{(0)}\left[1 \mp 2\left(1 + {}^1/_4\frac{v}{1-v}\right) h\,|\cos\theta|\right]. \qquad (5.5)$$

Here

$$\alpha_\omega^{(0)} = qkv / \sqrt{1-v},$$

$$\eta_\omega^{(0)} = \alpha_\omega^{(0)} I_\omega^{(0)} = \alpha_\omega^{(0)} I_{0\omega}(1 - v)$$

are the absorption and emission coefficients in the corresponding isotropic medium ($h = 0$). We note that the equilibrium intensities $I_\omega^{(i)}(\theta)$ in the dis-

*It should be noted that Eq. (5.2) is not a condition of "quasilongitudinality" (Ref. 11).

cussed approximation are equal to just half of the equilibrium intensity in the corresponding isotropic medium,

$$I_\omega^{(i)}(\theta) = {}^1/_2 I_\omega^{(0)} + O(h^2) = {}^1/_2(1-v) I_{0\omega} + O(h^2), \quad (5.6)$$

where $I_{0\omega}$ is the equilibrium intensity in a vacuum.

Let us now compute by Eq. (4.2) and (4.3), accurate to terms of the order of h, the radiation intensities $J_\omega^{(i)}$ from an inhomogeneous magnetoactive medium.

Let the ray equation be given in parametric form,

$$x = x(\sigma, h), \quad y = y(\sigma, h), \quad z = z(\sigma, h), \quad (5.7)$$

i.e., the arc length σ $(0 < \sigma < \infty)$ is treated as a parameter. Since the angle $\chi_i(\xi_{i0})$ between the wave normal and the energy flow vector is of order h, according to Eq. (5.3), the perturbation of the ray trajectory by the magnetic field is also of order h. This means that the expansion of x, y and z in powers of h is linear,

$$x(\sigma, h) = x_0(\sigma) + x_1(\sigma) h + \ldots, \quad (5.8)$$

where $x_1(\sigma)$, in general, differs from zero.

In our computations we shall allow for continuous changes in the properties of the medium by treating all the subsequent quantities as dependent on the coordinates only through

$$\xi = \mu x, \quad \eta = \mu y, \quad \zeta = \mu z, \quad (5.9)$$

where μ is a small parameter. The magnitude of μ is determined by consideration of the fact that the relative changes in all the quantities over a wave length must be on the order of μ.* We shall consider henceforth that

$$\nu \lesssim h. \quad (5.10)$$

Substituting Eq. (5.4) in Eq. (4.3) and utilizing Eq. (5.8) to (5.10) we obtain the following expression for the optical thickness

$$\tau_i(\sigma) = \tau^{(0)}(\sigma) \mp \Delta\tau(\sigma), \quad (5.11)$$

$$\tau^{(0)}(\sigma) = \int_0^\sigma \alpha_\omega^{(0)} d\sigma, \quad (5.12)$$

$$\Delta\tau(\sigma) = 2\int_0^\sigma \alpha_\omega^{(0)} \left(1 + {}^1/_4 \frac{v}{1-v}\right) h |\cos\theta| d\sigma, \quad (5.13)$$

where the integration is along the unperturbed ray $x = x_0(\sigma)$, $y = y_0(\sigma)$, $z = z_0(\sigma)$.

An approximate expression for intensity is obtained by substituting Eq. (5.5) and (5.11) in Eq. (4.2) and employing Eq. (5.8) – (5.10). This gives

$$J_\omega^{(i)} = {}^1/_2 (J_\omega^{(0)} \mp \Delta J_\omega), \quad (5.14)$$

$$J_\omega^{(0)} = \int_0^\infty \eta_\omega^{(0)} e^{-\tau^{(0)}(\sigma)} d\sigma, \quad (5.15)$$

$$\Delta J_\omega = \int_0^\infty \eta_\omega^{(0)} \left\{2\left(1 + {}^1/_4 \frac{v}{1-v}\right) \times h |\cos\theta| - \Delta\tau(\sigma)\right\} e^{-\tau^{(0)}(\sigma)} d\sigma, \quad (5.16)$$

again, as in Eq. (5.12) and (5.13), the integrals are taken along the unperturbed ray.

On the basis of Eq. (5.14), the degree of polarization of thermal radiation from a magnetoactive medium in this approximation is,

$$p = |J_\omega^{(1)} - J_\omega^{(2)}| / (J_\omega^{(1)} + J_\omega^{(2)}) = |\Delta J_\omega| / J_\omega^{(0)}. \quad (5.17)$$

The question of thermal radiation from the "anisotropic" sun was analyzed by Smerd[3] who calculated its total magnetic field assuming $h \ll 1$. He made use of earlier unpublished theoretical equations that in some respects do not coincide with the results obtained here. Thus, our expression for the correction to the optical depth $\Delta\tau(\sigma)$ [Eq. (5.13)] differs from the corresponding expression in Smerd's paper by having the factor $\left(1 + {}^1/_4 \frac{v}{1-v}\right)$. Coincidence is obtained only if terms of the order of v^2 $(\alpha_\omega^{(0)} \sim v)$ are neglected, a procedure that is far from being always justified.

The advantage of the approximate method outlined here for solving the transfer equation is that it permits one to deal with only the unperturbed form of the ray. This is due to the assumption that $\mu \lesssim h$. It can be shown that this advantage remains valid also for calculation up to terms on the order of h^k, if it is assumed that $\mu \lesssim h^k$.

In conclusion the author wishes to avail himself of the opportunity to express his deep gratitude to Prof. S. M. Rytov for suggesting this subject and for his constant help in the preparation of this paper.

*The region in which the transfer equation is valid coincides, as is known, with the region to which geometric optics apply.

[1] D. F. Martyn, Proc. Roy. Soc. 193, 44 (1948).
[2] V. L. Ginzburg, Astr. Zhurnal 26, 84 (1949).
[3] S. F. Smerd, Austr. J. Sci. Res. 3, 34, 265 (1950).
[4] S. M. Rytov, *Theory of Electrical Fluctuations and Thermal Emission*, Moscow-Leningrad 1953.
[5] H. B. Callen and T. A. Welton, Phys. Rev. 83, 34 (1951).
[6] H. B. Callen and R. F. Greene, Phys. Rev. 86, 702 (1952).
[7] Callen, Barasch and Jackson, Phys. Rev. 88, 1382 (1952).
[8] R. F. Greene and H. B. Callen, Phys. Rev. 88, 1387 (1952).
[9] M. L. Levin, Dokl. Akad. Nauk SSSR 102, 53 (1955).
[10] F. V. Bunkin, Dissertation, Moscow, Physical Inst., Acad. of Sci. (1955).
[11] Al'pert, Ginzburg and Feiberg, *Radiowave Propagation*, Moscow-Leningrad (1953).
[12] M. Ryle, Proc. Roy. Soc. 195, 82 (1948).
[13] F. V. Bunkin, J. Exptl. Theoret. Phys. (U.S.S.R.) 32, 338 (1957); Soviet Physics JETP 5, 277 (1957).
[14] V. L. Ginzburg, Usp. Fiz. Nauk. 32, 26 (1947).
[15] G. G. Getmantsev, Usp. Fiz. Nauk 44, 527 (1951).
[16] G. G. Stokes, Trans. Cambr. Phil. Soc. 9, 339 (1852).
[17] S. Chandrasekar, *Radiative Transfer*, (Russ. Transl.). III (1953).
[18] G. V. Rosenberg, Usp. Fiz. Nauk 56, 77 (1955).
[19] Ia. L. Al'pert, Izv. Akad. Nauk SSSR, Fiz 12, 241 (1948).
[20] J. Scott, Proc. Inst. Radio Engrs. 38, 1057 (1950).

Translated by A. Skumanich
178

SOVIET PHYSICS JETP VOLUME 5, NUMBER 4 NOVEMBER, 1957

On the Mechanism of Fission of Heavy Nuclei

V. V. VLADIMIRSKII

(Submitted to JETP editor March 16, 1956)
J. Exptl. Theoret. Phys. (U.S.S.R.) 32, 822-825 (April 1957)

The effect of the state of individual nucleons on the shape of the nucleus prior to fission is studied. It is shown that the presence of excess nucleons with large values of the angular momentum projection on the symmetry axis of the nucleus may lead to loss of stability of the nucleus with respect to asymmetric deformations in the saddle point. This facilitates the explanation of some of the experimental facts.

OUR PRESENT IDEAS about the fission of heavy nuclei at low excitation, based on the liquid drop model[1], are connected with the fact that, for a sufficient elongation of an incompressible drop, the sum of the Coulomb and of the surface energies attains a maximum equal to the fission threshold, further elongation of the drop being energetically favorable. It was shown by various authors[2] that, at the critical elongation, the nucleus retains its stability with respect to asymmetric deformations. The energy of the nucleus expressed in terms of the deformation parameters possesses therefore a saddle point at the critical elongation, the loss of stability depending only on the one deformation parameters that characterizes the elongation. The shape of the nucleus in the saddle point remains symmetric.

The quantitative comparison of calculations based on the liquid drop model with experimental data encounters a number of difficulties. The theoretically predicted strong dependence of the fission threshold $U \sim (1-x)^3$ on the parameter $x \sim Z^2/A$ has not been confirmed experimentally[3,4]. In fact, the threshold was found to be almost identical for a number of elements. Difficulties are also encountered in attempts to explain the observed asymmetry in the mass distribution of fission fragments. It has been shown in recent works[5,6] that it possible to explain this asymmetry on the basis of the liquid drop model. The authors indicate that upon further elongation of the nucleus, after the saddle point has been passed, the stability with respect to asymmetric deformations is lost and there may be a fast increase in the asymmetry of the nucleus. It seems very probable that their estimate of the mean ratio of the masses of the fission fragments is correct. The calculations pertaining to the dynamics of

such systems, however, have not been done as yet and the correctness of the above explanations cannot, therefore, be regarded as sufficiently established.

It is easier to explain many of the singularities of the fission process by assuming that the loss of stability with respect to asymmetric deformations during elongation of the nucleus occurs before the energy maximum of the symmetric shape has been passed. In fact, instead of a single saddle point we have in this case two saddle points with an asymmetric configuration of the nucleus. The inequality of masses of the fission fragments is therefore basically explained. If the saddle points of the different nuclei correspond to elongations of the same order, the value of the fission threshold should be proportional to $(1-x)$ and, therefore, the dependence on A and Z should be much weaker than the one predicted by the Bohr-Wheeler theory. Still another experimental fact can be explained more easily by assuming that the shape of the nucleus is asymmetric at the saddle point. Fraser and Milton[7] measured the ratio of secondary neutrons emitted in the direction of motion of the light and of the heavy fission fragments respectively. It was found that this ratio differs considerably from unity and, which is of special interest, does not approach unity (remains of the order of 3) even when the fragments have almost equal masses, namely $m_H/m_L = 1.1$. This fact indicates that the fission of the nucleus into fragments of similar mass is not really a symmetric event and the excitation energies of the two fragments differ considerably. Were the symmetric shape of nucleus to correspond to the saddle point, the fission into two equal fragments would correspond to the not very probable case of the nuclear shape changing by a sequence of completely symmetric deformations and there would not be any serious reason for the occurrence of such a case. On the other hand, for an asymmetric saddle point the inequality of the light and heavy fragments is inherent from the very beginning and there is no reason to expect all the parameters characterizing the fragments (charge, excitation energy) to be equal in case of a change equality of masses.

The above considerations add interest to the study of possible conditions for the occurrence of asymmetric saddle points, despite the fact that such a notion does not lie within the classical framework of the liquid drop model. The explanation of this effect, given below, is based upon the study of the states of individual nucleons in the deformed nucleus in the spirit of the collective model, and is of a qualitative character.

We shall consider only such states of deformation of the nucleus for which the nucleus possesses rotational symmetry with respect to the OZ axis. Such states are most favorable energetically for a given elongation of the nucleus and there are all reasons to suppose that they lead more easily to fission. For such a symmetry of the nucleus the wave functions of free nucleons can be classified in terms of the quantum number $\Omega = l_z + s_z$, equal to the projection of the total angular momentum of the nucleon on the nuclear axis of symmetry[8]. The quantum numbers Ω represent the approximate integrals of motion and are adiabatically invariant with respect to slow changes in the shape of the nucleus. Out of the variables r, z, φ and s_z which determine the position and spin of a nucleon in the cylindrical system of coordinates, the latter two can be separated by introducing the functions $\exp\{i(\Omega \pm \tfrac{1}{2})\varphi\}$. The order variables, as a rule, cannot be separated. For a symmetric deformation of the nucleus we have to account also for the classification of the wave functions of individual nucleons with respect to their parity, which is not conserved for asymmetric deformations. Evidently, for excitation energies of the order of 5–6 Mev, corresponding to fission resulting from slow neutron capture, the quantum number will not represent the integrals of motion so accurately as in the case when the nucleus is in the ground state. Strongly elongated states that are prone to fission should, however, approach the unexcited state since the greater part of the energy surplus has been already used up for the elongation. The nucleus in this state has so to speak cooled down, which renders transitions between various states of individual nucleons more difficult in view of the Pauli principle. Besides, departures from rotational symmetry which would facilitate the mixing of states with different Ω, are reduced, owing to the lack of a sufficient amount of energy for the excitation of the corresponding degrees of freedom of the nucleus.

With the progress of the elongation of the nucleus the states with high Ω become energetically unfavorable because of the centrifugal energy $\hbar^2 l_z^2/2mr^2$, the mean value of which rises sharply with diminishing radial dimensions of the nucleus. At the same time, the number of energetically favorable states with small values of Ω increases with increasing length of the nucleus. Consequently, a reorganization of the filling of nucleonic levels occurs during the elongation of the nucleus. As men-

tioned above, for the largest energetically permissible elongations such reorganization is difficult and there is every reason to believe that the nucleus in such a state will posses an excess of nucleons with large values of the angular momentum projection Ω, while there will be a deficiency in the filling of levels with low Ω.

In the asymptotic approximation of a large number of particles, the energy of the degenerated Fermi gas depends only on the volume and not on the shape of the container. This, however, is true first for the case of the nucleus only for a very large number of nucleons, and secondly for the equilibrium distribution of levels with different values of angular momentum. As it is well known[9], it is indeed the deviations of the state distribution of nuclei from the asymptotic laws that lead to a marked elongation of nuclei with unfilled shells in the ground state. An analogous influence of the nucleon distribution on the shape of the nucleus should take place in fission as well.

It is easy to show that the presence of excess nucleons with high values of Ω in a strongly elongated nucleus should sharply diminish its stability with respect to asymmetric deformations and should slightly increase the stability with respect to symmetric deformations. This effect can be approximately estimated in the following way: let the elongated nucleus be of the shape of an axially symmetric body with a symmetric generator $r_1(z) = r_1(-z)$, the maximum $r_1(z)_{max} = b$ being attained for $z = 0$. We shall consider a small asymmetric deformation of the nucleus $\Delta r = \beta\eta(z) = -\beta\eta(-z)$. The maximum of the cross-section of the nucleus will be shifted in the direction of positive Δr and will be equal

$$r_{1\,max} = b + {}^1/_2\,\beta^2\,(d\eta/dz)^2_{z=0}\,|\,d^2r_1/dz^2\,|^{-1}_{z=0}.$$

The energy of a nucleon with the largest value of angular momentum Ω can be estimated from the maximum cross-section of the nucleus r_m:

$$W \sim \hbar^2\, l_z^2/2mr_m^2.$$

For an asymmetric deformation the energy increases by the amount

$$\Delta W \sim -\beta^2\,(\hbar^2\, l_z^2/2mb^3)\,(d\eta/dz)^2_{z=0}\,|\,d^2r_1/dz^2\,|^{-1}_{z=0},$$

the sign of which indicates the decrease in stability with respect to the deformation $\beta\eta(z)$. We shall note that, even for $d^2\,r_1/dz^2 > 0$ the sign of the effect is invariant, although the change of the maximum radius cannot be estimated in such a simple way. For the shape of the nucleus approximating an ellipsoid of revolution with semiaxes a_0 and $b_0 = \sqrt{a_0^2 - e^2}$:

$$r = \sqrt{a^2 - e^2}\,\sqrt{1-\mu^2},$$

$$z = a\mu, \quad a = a_0\,[1 + \beta P_3(\mu)],$$

we obtain

$$d^2r/dz^2 = b/a^2; \quad \Delta r \approx 3az\beta/2b,$$

$$\Delta W \sim -9\hbar^2 l_z^2\, a^4\beta^2/8mb^6.$$

The sum of these values for the excess nucleons with the largest Ω has to be equated to the deformation parameter distribution of the Coulomb and of the surface energies, separating the terms proportional to β^2 which determine the shape stability with respect to asymmetric deformations. For a spherical nucleus this term equals

$$\Delta E = -\frac{2}{7}\left(\frac{5}{2} - \frac{10}{7}\,x\right)E_s\beta^2,$$

where β is the coefficient of the third-order Legendre polynomial, E_s is the surface energy of the nucleus and x is the fission parameter. For the case of elongated nuclei with the axis ratio equal to $1.5-2$ this value, according to the estimates of Ref. 5 and 6, is reduced by a factor of ½ at least. Assuming for our estimate $x = 0.7$ and $E_s = 500$ Mev, we obtain, for the case of elongated nuclei

$$\Delta E \approx \beta^2 \cdot 100 \text{ Mev}.$$

Assuming for the case of the uranium nucleus $ab^3 = (1.3\times10^{-13})^3\,A$ and $b = 0.5\,a$, we shall estimate the effect of one excess nucleon with orbital angular momentum $l_z = 5$:

$$\Delta W \approx -\beta^2 \cdot 350 \text{ Mev}.$$

For the case of a strongly elongated nucleus, therefore, the effect of a single additional nucleon with a large value of angular momentum is very large and the shape stability with respect to asymmetric deformations is, evidently, lost much sooner. It is possible that this occurs at elongations only slightly larger than the initial elongation of the nucleus in the ground state.

It should be noted that the loss of stability with respect to small asymmetric deformations, due to such a mechanism, should not cause an unlimited increase of asymmetry. When a pear-like shape is attained by the nucleus, any further dilatation of the wider end should stop as soon as the maximum

radius attains such a value that the energy of nucleons with the largest value of angular momentum equals the Fermi limit. This makes it possible to explain qualitatively the experimentally observed fact that the mass of the larger fission fragment is is equal for different elements. As it is well known, the mass of the lighter fragment varies within much wider limits. Evidently, for all studied fissile nuclei, the maximum values of the nucleonic angular momentum coincide prior to fission. Most probably, all of them then posses a pair of neutrons with an angular momentum of the order of 5–6. The angular momentum of these nucleons determines the cross-section of the wider end of the nucleus which subsequently forms the heavier fission fragment. It follows from this approximate quantization of the size of the heavy fragment that the variations in its mass are smaller than is the case for the lighter fragment.

[1] N. Bohr and J. A. Wheeler, Phys. Rev. **56**, 426 (1939); Ia. I. Frenkel', J. Exptl. Theoret. Phys. (U.S.S.R.) **9**, 641 (1939).

[2] R. D. Present and J. K. Knipp, Phys. Rev. **57**, 751, 1188 (1940); S. Frankel and N. Metropolis, Phys. Rev. **72**, 914 (1947).

[3] Koch, McElhinney and Gasteiger, Phys. Rev. **77**, 329 (1950).

[4] D. L. Hill and J. A. Wheeler, Phys. Rev. **89**, 1102 (1953).

[5] V. G. Nosov, Geneva Conference for the Peaceful Applications of Atomic Energy (1955), Report 653.

[6] U. L. Businaro and S. Gallone, Nuovo Cimento **1**, 629 (1955).

[7] J. S. Fraser and J. C. D. Milton, Phys. Rev. **93**, 818 (1954).

[8] S. G. Nilsson, Dan. Mat Fis. Medd. **29**, 16 (1955).

[9] A. Bohr, Dan. Mat Fis. Medd **26**, 14 (1952); A. Bohr and B. Mottelson, Dan. Mat. Fis. Medd. **27**, 16 (1953); A. Bohr, *Rotational States of Atomic Nuclei*, Copenhagen (1954).

Translated by H. Kasha
179

SOVIET PHYSICS JETP VOLUME 5, NUMBER, 4 NOVEMBER, 1957

Moment of Inertia of a System of Interacting Particles

A. S. DAVYDOV AND G. F. FILIPPOV
Moscow State University

(Submitted to JETP editor March 20, 1957)
J. Exptl. Theoret. Phys. (U.S.S.R.) **32**, 826-836 (April, 1957)

The problem of singling out the collective degrees of freedom of a system consisting of N interacting particles is considered. It is shown that for some special states of internal motion, the energy of the system in the center of mass system can be represented as the sum of the energy of internal motion and the rotational energy. The concept of the moment of inertia of a system of N interacting particles is introduced.

INTRODUCTION

AT PRESENT it has been established that the lowest excited states of nuclei in the mass number range $150 < A < 190$ and $A > 225$ are rotational states. Such states arise in Coulombic excitation of the nuclei, in processes of radioactive decay, and also in inelastic collisions of particles with the nucleus.

An explanation of rotational states of the nucleus in the quasi-molecular model of the nucleus proposed by A. Bohr[1] is related to the motion of a wave around the nucleus. The nuclear matter is regarded as an incompressible, irrotational fluid (the hydrodynamical model). The part of the nuclear matter which participates in the rotation, according to the hydrodynamical model, is proportional to the square of the deviation of the form of the nucleus from a sphere. If we assume that the nucleus has the form of an ellipsoid of rotation with semiaxes c and a, then the moment of inertia of the nucleus is given by

$$J = {}^1/_5 mA\,(c^2 - a^2)^2 / (c^2 + a^2),$$

where m is the mass of the nucleon, and A is the mass number of the nucleus. For small deviations from spherical form $J = {}^2/_5 mAR_0^2(\Delta R / R_0)^2$, where R_0 is the radius of the sphere with volume equal to that of the nucleus, and ΔR is the difference between the larger and the smaller semiaxis. If it is assumed that the nuclear charge is uniformly distributed, then the quantity $\Delta R/R_0$ will correspond to the quadrupole moment $Q_0 = {}^4/_5 ZR_0^2 \Delta R / R_0$. in a coordinate system fixed with respect to the nucleus. Determining $\Delta R/R_0$ from experimental values of the quadrupole moments, we find values of the moments of inertia (for $R = 1.2\, A^{1/3}\, 10^{-13}$ cm.) which are 3–5 times less than the experimental valvalues[2]. In addition, it is found that the experimentally determined moments of inertia of nuclei with odd A are (up to 40 percent) larger than the moments of inertia of even-even nuclei with approximately the same deviation from spherical form[3]. Both of these facts indicate the inadequacy of the hydrodynamical model of the nucleus[2, 3]. In this connection, a number of papers have appeared recently concerning the separation of collective and one-particle degrees of freedom in nuclei. In the paper by Inglis[4] the kinetic energy of rotation was obtained by studying the motion of the nucleons in the rotating self-consistent field of a three-dimensional harmonic oscillator, which deviates slightly from spherical symmetry. Similar calculations are carried out by A. Bohr and Mottelson[3] who take into account deviation from the self-consistent field due to the sum of pair interactions. In both of these papers over-determined coordinate systems are used, *i.e.*, coordinates describing the orientation of the self-consistent field and coordinates of the center of mass are introduced as additional superfluous variables. As is well known, a similar difficulty concerning the center of mass coordinates occurs in the shell models. It is usually assumed that for a large number of nucleons the superfluous coordinates change only slightly the results of investigations of internal nuclear motions. However, in investigations of the collective motions of the nucleons in the nucleus, it is necessary to study the change of just these superfluous variables, so that a special investigation of the possibility of such investigations is needed. In the papers of Tolhoek[5] and Coester[6], which are devoted to a study of collective motions in nuclei on the basis of the N-body problem, the possibility of separating collective and internal motion is assumed; however, the choice of the coordinates describing the internal degrees of freedom remains unspecified.

In the present paper we examine the question of distinguishing collective motions in a system consisting of N interacting particles. In the first section, using the example of a system consisting of three interacting spinless particles, we carry out an explicit separation of the collective degrees of freedom associated with the translational motion of the center of mass of the system and the rotation of the system. We give an expression for the square of the angular momentum of the whole system in terms of collective angular variables, and conditions are indicated under which the energy of the system can be represented as a sum of an internal energy and a rotational energy, determined by a moment of inertia which depends on the internal motion. The results obtained in the second section are applied to the case of a system consisting of one light and two heavy particles (hydrogen molecule ion). A system consisting of N particles is studied in the third section.

1. SYSTEM CONSISTING OF THREE PARTICLES OF EQUAL MASS

We consider three spinless particles of equal mass m, interacting with central forces of an arbitrary type. Let $\mathbf{r}_1$, $\mathbf{r}_2$, $\mathbf{r}_3$ be the radius vectors locating the position of these particles in space. We go into the center of mass system (c.m.s.) xyz by introducing new coordinates according to:

$$ {}^1/_3(\mathbf{r}_1 + \mathbf{r}_2 + \mathbf{r}_3) = \mathbf{R}, \quad -\mathbf{r}_1 + {}^1/_2(\mathbf{r}_2 + \mathbf{r}_3) = \mathbf{r}, $$
$$ -\mathbf{r}_2 + \mathbf{r}_3 = \boldsymbol{\rho} = 2\mathbf{q}/\sqrt{3}. \tag{1.1} $$

In the c.m.s. the kinetic energy operator

$$ T = T_q + T_r, \quad T_q = -(\hbar^2/2\mu)\,\Delta_q, \quad T_r = -(\hbar^2/2\mu)\,\Delta_r \tag{1.2} $$

is the sum of the kinetic energy operators of two equivalent particles of mass $\mu = 2m/3$, which completely describe the behavior of the system of three particles in the xyz coordinate system. Instead of the vectors $\mathbf{q}$, $\mathbf{r}$ we introduce polar coordinates. Then

$$T_q = -\frac{\hbar^2}{2\mu q^2}\left\{\frac{\partial}{\partial q}\left(q^2\frac{\partial}{\partial q}\right) - L_q^2\right\},$$

$$T_r = -\frac{\hbar^2}{2\mu r^2}\left\{\frac{\partial}{\partial r}\left(r^2\frac{\partial}{\partial r}\right) - L_r^2\right\},$$

$$L_q = -i\,[\mathbf{q}\nabla_q], \quad L_r = -i\,[\mathbf{r}\nabla_r],$$

$$L_j^2 = -\left\{\frac{1}{\sin\vartheta_j}\frac{\partial}{\partial\vartheta_j}\left(\sin\vartheta_j\frac{\partial}{\partial\vartheta_j}\right) + \frac{1}{\sin^2\vartheta_j}\frac{\partial^2}{\partial\varphi_j^2}\right\},$$

$$\{L_j\}_z = -i\frac{\partial}{\partial\varphi_j}, \quad j = r, q.$$

We introduce a new, moving coordinate system (ξ, η, ζ) related to our particles in such a way that the ζ-axis coincides with the direction of the vector $\mathbf{q}$, and the ξ, ζ-plane coincides with the plane of the vectors $\mathbf{r}$, $\mathbf{q}$. In Fig. 1

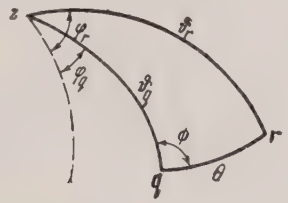

FIG. 1.

the direction of the z axis and the vectors $\mathbf{q}$ and $\mathbf{r}$ are indicated by the points z, q, r on the surface of a unit sphere. The broken line represents the intersection of this surface with the xz plane. The polar angles φ_q and δ_q of the vector $\mathbf{q}$, and the angle ϕ between the planes going through the axes z, ζ and ζ, ξ, completely determine the position of the system. In addition, let θ be the angle between the vectors $\mathbf{q}$ and $\mathbf{r}$. The angles φ, ϑ, ϕ, θ are determined by the angles φ_q, $\vartheta_q\phi_r$, ϑ_r with the help of the relations

$$\varphi = \varphi_q, \quad \vartheta = \vartheta_q, \quad \cos\theta = \sin\vartheta_q\sin\vartheta_r\cos(\varphi_q - \varphi_r)$$

$$+ \cos\vartheta_r\cos\vartheta_q, \quad \sin\theta\sin\phi = \sin\vartheta_r\sin(\varphi_q - \varphi_r),$$

$$\sin\theta\cos\phi$$

$$= \cos\vartheta_q\sin\vartheta_r\cos(\varphi_q - \varphi_r) - \cos\vartheta_r\sin\vartheta_q.$$

The potential energy of the system as a function of the distances between the particles will depend only on the coordinates q, r, θ., which we shall call the internal coordinates

$$V = V\left(\sqrt{r^2 + q^2/3 + 2qr\cos\theta/\sqrt{3}}, \quad 2q/\sqrt{3}, \right.$$

$$\left.\sqrt{r^2 + q^2/3 - 2qr\cos\theta/\sqrt{3}}\right). \tag{1.3}$$

We shall call the angles $\varphi\vartheta\phi$ determining the orientation of the system $\xi\eta\zeta$ the external or collective coordinates.

The operator corresponding to the total angular momentum of the entire system has the form

$$\hbar\mathbf{L} = -i\hbar\{\mathbf{q}\times\nabla_r + \mathbf{r}\times\nabla_r\}. \tag{1.4}$$

In the new variables we have for the operator corresponding to the square of the angular momentum (1.4).

$$\hbar^2L^2 = -\hbar^2\left\{\frac{1}{\sin\vartheta}\frac{\partial}{\partial\vartheta}\left(\sin\vartheta\frac{\partial}{\partial\vartheta}\right)\right.$$

$$\left. + \frac{1}{\sin^2\vartheta}\left(\frac{\partial^2}{\partial\varphi^2} + 2\cos\vartheta\frac{\partial^2}{\partial\varphi\partial\phi} + \frac{\partial^2}{\partial\phi^2}\right)\right\}, \tag{1.5}$$

$$\hbar L_z = -ih\partial/\partial\varphi. \tag{1.6}$$

In going over to the variables r, q, θ, ϑ, φ, ϕ, the $H = T + V$ of the entire system is expressed by the equation

$$H = \mathscr{K} + V + \hbar^2L^2/2\mu q^2 - \pi, \tag{1.7}$$

$$\mathscr{K} = -\frac{\hbar^2}{2\mu}\left\{\frac{1}{r^2}\frac{\partial}{\partial r}\left(r^2\frac{\partial}{\partial r}\right)\right.$$

$$\left. + \frac{1}{q^2}\frac{\partial}{\partial q}\left(q^2\frac{\partial}{\partial q}\right) - \frac{2}{q^2}\frac{\partial^2}{\partial\phi^2}\right.$$

$$\left. + \left(\frac{1}{q^2} + \frac{1}{r^2}\right)\left[\frac{1}{\sin\theta}\frac{\partial}{\partial\theta}\left(\sin\theta\frac{\partial}{\partial\theta}\right) + \frac{1}{\sin^2\theta}\frac{\partial^2}{\partial\phi^2}\right]\right., \tag{1.8}$$

$$\pi = \frac{\hbar^2}{\mu q^2}\left\{\left[\frac{\sin\phi}{\sin\vartheta}\frac{\partial}{\partial\varphi} - \cos\phi\frac{\partial}{\partial\vartheta} + \cot\vartheta\sin\phi\frac{\partial}{\partial\phi}\right]\frac{\partial}{\partial\theta}\right.$$

$$\left. + \cot\theta\left[\cot\vartheta\cos\phi\frac{\partial}{\partial\phi} + \sin\phi\frac{\partial}{\partial\vartheta} + \frac{\cos\phi}{\sin\vartheta}\frac{\partial}{\partial\varphi}\right]\frac{\partial}{\partial\phi}\right\}, \tag{1.9}$$

the other operators involved in (1.7) were defined earlier.

It is easy to see that the operator corresponding to the square of the angular momentum (1.5) and its projection (1.6) commute with the complete Hamiltonian of the system (1.7). Consequently, the quantities corresponding to them will be integrals of motion. The square of the total angular momentum operator and its projection have eigenvalues and eigenfunctions given by the equations

$$\hat{L}^2 D^L_{MK} = L(L+1)D^L_{MK}, \tag{1.10}$$

$$\hat{L}_z D^L_{MK} = M D^L_{MK}, \quad M, K = 0, \pm 1 \pm \ldots \pm L,$$
$$D^L_{MK} = e^{iM\varphi} d^L_{MK}(\vartheta)\, e^{iK\varphi},$$
$$d^L_{MK}(\vartheta) = \sum_{\varkappa} (-1)^{\varkappa} \frac{\sqrt{(L+M)!\,(L-M)!\,(L+K)!\,(L-K)!}}{(L-K-\varkappa)!\,(L+M-\varkappa)!\,\varkappa!\,(\varkappa+M-K)!} \times \cos^{2L+M-K-2\varkappa}\left(\frac{\vartheta}{2}\right) \sin^{2\varkappa+M-K}\left(\frac{\vartheta}{2}\right). \tag{1.11}$$

The functions D^L_{MK} are the irreducible representations of the three-dimensional rotation group, first introduced by Wigner[7]. They form a unitary matrix and satisfy the orthogonality relations

$$\int_0^{\pi} \sin\vartheta d\vartheta \int_0^{2\pi} d\varphi \int_0^{2\pi} d\phi D^L_{MK} D^{*l}_{mK'} = \frac{8\pi^2}{2L+1} \delta_{Ll}\, \delta_{Mm}\, \delta_{KK'}.$$

For $M = 0$ or $K = 0$, the functions D^L_{MK} reduce to the spherical functions

$$D^L_{M0} = \sqrt{\frac{4\pi}{2L+1}}\, Y_{LM}(\varphi, \vartheta),$$
$$D^L_{0K} = \sqrt{\frac{4\pi}{2L+1}}\, Y_{LK}(\phi, \vartheta). \tag{1.12}$$

The stationary states of the system of three particles are determined by the Schroedinger equation

$$(H - E)\,\psi = 0. \tag{1.13}$$

Let us consider the states with definite values of the integrals of motion L and M. The wave functions of such a state can be represented in the form

$$\psi^L_M = \sqrt{\frac{2L+1}{8\pi^2}} \sum_K D^L_{MK}(\varphi,\ \vartheta,\ \phi)\, \varphi_K(r,\ q,\ \theta). \tag{1.14}$$

In particular $\psi^0_0 = \varphi_0(r, q, \theta)$ for $L = 0$, *i.e.*, the properties of the system in the s-state do not depend on its spatial orientation and are determined only by the internal coordinates r, q, θ. The wave function $\varphi_0(r, q, \theta)$ satisfies the equation

$$\left\{-\frac{\hbar^2}{2\mu}\left[\frac{1}{r^2}\frac{\partial}{\partial r}\left(r^2\frac{\partial}{\partial r}\right) + \frac{1}{q^2}\frac{\partial}{\partial q}\left(q^2\frac{\partial}{\partial q}\right) + \left(\frac{1}{q^2} + \frac{1}{r^2}\right)\frac{1}{\sin\theta}\frac{\partial}{\partial\theta}\left(\sin\theta\frac{\partial}{\partial\theta}\right)\right] + V - E\right\}\varphi_0(r,\ q,\ \theta) = 0. \tag{1.15}$$

We substitute (1.14) into (1.13), multiply the result by $\sqrt{(2L+1)/8\sigma^2}\, D^{*L}_{MK'}$ and integrate over the external variables. Then we obtain the system of equations

$$\left\{\frac{\hbar^2}{2\mu q^2}[L(L+1) - K(K+1)] + \mathscr{L}(K) - E\right\} \times \varphi_K = \sum_{K'} (K \mid \pi \mid K')\, \varphi_{K'}, \tag{1.16}$$

$$(K \mid \pi \mid K') = \frac{2L+1}{8\pi^2} \int D^L_{MK'}\, \pi D^{*L}_{MK}\, d\Omega, \tag{1.17}$$

$$\mathscr{L}(K) = -\frac{\hbar^2}{2\mu}\left\{\frac{1}{r^2}\frac{\partial}{\partial r}\left(r^2\frac{\partial}{\partial r}\right) + \frac{1}{q^2}\frac{\partial}{\partial q}\left(q^2\frac{\partial}{\partial q}\right) + \left(\frac{1}{q^2} + \frac{1}{r^2}\right) \times \left[\frac{1}{\sin\theta}\frac{\partial}{\partial\theta}\left(\sin\theta\frac{\partial}{\partial\theta}\right) - \frac{K^2}{\sin^2\theta}\right] - \frac{K(1-K)}{q^2}\right\} + V. \tag{1.18}$$

The operator of internal motion (1.18) depends only on the absolute value of K. The diagonal elements of the matrix (1.17) are equal to zero.

If we omit the right side of (1.16), we get the system of independent equations

$$\{(\hbar^2/2\mu q^2)[L(L+1) - K(K+1)] + \mathscr{L}(K) - E\}\,\varphi_K(r, q, \theta) = 0. \tag{1.19}$$

The system of equations (1.19) will be a good approximation to (1.16) if two conditions are met: a) the system of three particles has axial symmetry in the coordinate system fixed with respect to these particles, and b) the ζ axis of this coordinate system coincides with the axis of symmetry*.

We shall assume that both these conditions are fulfilled. In this approximation the number K is a good quantum number; its value determines the projection of the angular momentum on the ζ axis. For $K = L$, equation (1.19) goes over into the equation

* The multiple-valued nature of the choice of the system ξ, η, ζ is important for the symmetry properties of the wave function, and will be considered in a subsequent paper, where systems of particles with spin will be studied.

$$[\mathcal{L}(K) - \varepsilon_K]\,\varphi(r, q, \vartheta) = 0. \tag{1.20}$$

Solving equation (1.20) we obtain a series of energy levels. We number these levels in order of increasing index α, which takes on the values 0, 1, 2, ..., and designate the corresponding wave functions by $\varphi_{\alpha K}$. In particular, the wave function φ_{0K} corresponds to the lowest energy.

We introduce the concept of the moment of inertia of the system in the state φ_{0K} with the help of the relation

$$J_{0K} = \left[\frac{1}{\mu}\int \varphi^*_{0K}\,\frac{1}{q^2}\,\varphi_{0K}\,d\tau\right]^{-1}. \tag{1.21}$$

If the inequality

$$\hbar^2 / 2J_{0K} < \varepsilon_{1K} - \varepsilon_{0K}, \tag{1.22}$$

is fulfilled, then, according to (1.19), for a given value of K, the energy of the system corresponding to the state of lowest energy of internal motion can be represented approximately in the form of a sum of the internal energy ε_{0K} and the rotational energy with $L > K$.

$$E_{0KL} = \varepsilon_{0K} + (\hbar^2 / 2J_{0K})\{L(L+1) - K(K+1)\}. \tag{1.23}$$

If inequality (1.22) is not satisfied, a division of the energy into internal and rotational energy is impossible. The representation of the energy in the form (1.23) is approximate. If we take further approximations into consideration, we can find a relation between the internal motion of the system of particles and the rotation of the system as a whole.

Thus, in states of a system of particles which exhibit an axis of symmetry coinciding with the ζ axis, the problem of determining the energy levels of the system of particles can be divided into two parts: first the energy levels of the system of particles are determined by solving Eq. (1.20) for a given value of K, and then the motions of the entire system (rotation) are studied for a given state $\varphi_{\alpha K}$ and different values of the total angular momentum $L > K$ of the system. The rotational angular momentum is $\mathbf{R} = \mathbf{L} - \mathbf{K}$. Since only values of $L \geq K$ are possible in (1.23), the projection of the angular momentum on the axis of symmetry ζ must always be zero. In other words, a system of particles with axial symmetry in a state of internal motion described by the function $\varphi_{\alpha K}$ can rotate as a whole only about an axis perpendicular to the axis of symmetry of the system.

2. SYSTEM CONSISTING OF THREE PARTICLES OF DIFFERENT MASS

The example just considered of a system of three particles of equal mass has only methodological interest, since in this case the states with the lowest internal energy do not have a sharply distinguished axial symmetry. In order to deal with a system of three particles which satisfy the above-mentioned conditions for the possibility of distinguishing rotational energy, we study a system consisting of two particles of identical mass ($m_2 = m_3 = m$) and a third particle of considerably smaller mass $m_1 = \alpha m$, where $\alpha \sim 10^{-3}$.

If the position of the particles is described by vectors $\mathbf{r}_1$, $\mathbf{r}_2$, $\mathbf{r}_3$, then the transition to the center of mass system is effected by the coordinate transformation

$$\mathbf{r}_3 - \mathbf{r}_2 = \boldsymbol{\rho} = 2\sqrt{\frac{\alpha}{2+\alpha}}\,\mathbf{q}, \quad -\mathbf{r}_1 + \frac{\mathbf{r}_2 + \mathbf{r}_3}{2} = \mathbf{r},$$
$$\frac{\mathbf{r}_3 + \mathbf{r}_2 + \alpha\mathbf{r}_1}{2+\alpha} = \mathbf{R}. \tag{2.1}$$

In the c.m.s. the kinetic energy has the form

$$T = -(\hbar^2 / 2\mu)(\Delta_q + \Delta_r), \tag{2.2}$$
$$\mu = 2\alpha m / (2+\alpha). \tag{2.3}$$

Thus, all the results of the preceding section can be retained, if by q and μ we understand the quantities defined by (2.1) and (2.3). Since we are considering the case $\alpha \ll 1$, we have approximately

$$\mu = \alpha m, \quad \rho = q\sqrt{2\alpha}. \tag{2.4}$$

Since both particles lie in the direction of the vector $\mathbf{q}$, this direction will coincide with the direction of the axis of symmetry of the system (for $\alpha \ll 1$).

For the case $K = 0$, Eq. (1.20) has the form

$$\left\{-\frac{\hbar^2}{2\alpha m}\left[\frac{1}{r^2}\frac{\partial}{\partial r}\left(r^2\frac{\partial}{\partial r}\right) + \frac{2\alpha}{\rho^2}\frac{\partial}{\partial \rho}\left(\rho^2\frac{\partial}{\partial \rho}\right) + \left(\frac{2\alpha}{\rho^2} + \frac{1}{r^2}\right)\frac{1}{\sin\vartheta}\frac{\partial}{\partial\vartheta}\left(\sin\vartheta\frac{\partial}{\partial\vartheta}\right)\right] + V - \varepsilon_0\right\}\varphi_0(r, \rho, \vartheta) = 0, \tag{2.5}$$

$$V = V(\rho) + V\left(\sqrt{r^2 + (\rho^2/4) + r\rho\cos\vartheta}\right) + V\left(\sqrt{r^2 + (\rho^2/4) - r\rho\cos\vartheta}\right). \tag{2.6}$$

in terms of the variables r, ρ, θ.

Since the small coefficient α appears in the derivatives with respect to ρ, the solution of (2.6) can be accomplished in two steps. First we define the lowest energy of the system for fixed values of ρ (the adiabatic approximation), *i.e.*, we solve the equation

$$\left\{-\frac{\hbar^2}{2\mu}\left[\frac{1}{r^2}\frac{\partial}{\partial r}\left(r^2\frac{\partial}{\partial r}\right)+\left(\frac{2\alpha}{\rho^2}+\frac{1}{r^2}\right)\frac{1}{\sin\theta}\frac{\partial}{\partial\theta}\left(\sin\theta\frac{\partial}{\partial\theta}\right)\right]-V-E_0(\rho)\right\}f_0(r,\theta)=0. \tag{2.7}$$

Solving (2.7) we obtain the energy as a function of the parameter ρ. Then setting

$$\varphi_0(r,\rho,\theta)=f_0(r,\theta)\,u(\rho)/\rho, \tag{2.8}$$

and using (2.7), we obtain from (2.5) an equation which determines the function $u(\rho)$.

$$[-(\hbar^2/m)\,d^2u/d\rho^2+E_0(\rho)-\varepsilon]\,u(\rho)=0. \tag{2.9}$$

If we designate by ρ_0 the value of ρ for which $E_0(\rho)$ has a minimum, then, expanding $E_0(\rho)$ in powers of the difference $(\rho-\rho_0)$ we obtain

$$E_0(\rho)=E_0+\frac{m\omega^2}{4}(\rho-\rho_0)^2,\qquad \frac{m\omega^2}{4}=\frac{1}{2}\left(\frac{\partial^2E}{\partial\rho^2}\right)_{\rho=\rho_0}. \tag{2.10}$$

to within an accuracy of terms of the second order. Equation (2.9) reduces to the equation of a one-dimensional harmonic oscillator. Therefore we can immediately write for the energy and eigenfunctions

$$\varepsilon_\alpha=E_0+\hbar\omega(\alpha+1/2),$$
$$u_\alpha(\rho)=(m\omega/2\hbar)^{1/4}e^{-x^2/2}H_\alpha(x),$$
$$x=(\rho-\rho_0)(m\omega/2\hbar)^{1/2}.$$

We are interested in the case $\alpha=0$, where

$$u_0(\rho)=(m\omega/2\hbar)^{1/4}e^{-x^2/2}. \tag{2.11}$$

Setting (2.8) in (1.20), and taking into consideration (2.4), we obtain

$$J_{00}=\left[\frac{2}{m}\int u_0^2(\rho)\,\rho^{-2}\,d\rho\right]^{-1}\approx\frac{m\rho_0^2}{2},$$

i.e., we obtain the usual expression for the moment of inertia of two bodies of mass m, a distance ρ_0 apart, with respect to the axis which is the perpendicular bisector of the line joining them.

3. SYSTEM OF N INTERACTING PARTICLES

We consider a system of N identical particles of equal mass, interacting with central forces. Let $\mathbf{r}_1, \mathbf{r}_2, \ldots, \mathbf{r}_N$ be the radius vectors of these particles. We go into the c.m.s. by introducing Jacobi coordinates

$$\begin{aligned}&\frac{1}{N}(\mathbf{r}_1+\mathbf{r}_2+\ldots+\mathbf{r}_N)=\mathbf{R},\\ &-\mathbf{r}_1+\frac{1}{N-1}(\mathbf{r}_2+\mathbf{r}_3+\ldots\mathbf{r}_N)=\boldsymbol{\rho}_1,\\ &-\mathbf{r}_2+\frac{1}{N-2}(\mathbf{r}_3+\mathbf{r}_4+\ldots+\mathbf{r}_N)=\boldsymbol{\rho}_2,\ldots,\\ &-\mathbf{r}_{N-1}+\mathbf{r}_N=\boldsymbol{\rho}_{N-1}.\end{aligned} \tag{3.1}$$

The kinetic energy operator in the c.m.s. is

$$T=-\frac{\hbar^2}{2\mu}\sum_{i=1}^{N-1}\frac{(N+1-i)(N-1)}{N(N-i)}\Delta_{\rho_i}, \tag{3.2}$$

$$\mu=(N-1)\,m/N. \tag{3.3}$$

For convenience we modify the length of the radius vectors in accordance with the following relations

$$\mathbf{q}_i=\boldsymbol{\rho}_i\,[N(N-i)/(N+1-i)(N-1)]^{1/2}, \tag{3.4}$$

Then the kinetic energy operator is

$$T=-\frac{\hbar^2}{2\mu}\sum_{i=1}^{N-1}\Delta_i,\qquad \Delta_i=\Delta_{q_i}. \tag{3.5}$$

We go over from the vectors $\mathbf{q}_1, \mathbf{q}_2, \ldots, \mathbf{q}_{N-1}$ to polar coordinates $q_1, \vartheta_1, \varphi_1, \ldots, q_{N-1}, \vartheta_{N-1}, \varphi_{N-1}$ with respect to a center of mass coordinate system with a fixed direction of the polar axis. In these coordinates (3.5) has the form

$$T=-\frac{\hbar^2}{2\mu}\sum_{i=1}^{N-1}q_i^{-2}\left\{\frac{\partial}{\partial q_i}\left(q_i^2\frac{\partial}{\partial q_i}\right)+L_i^2\right\}, \tag{3.6}$$

where the operator corresponding to the square of the angular momentum of the i'th particle is defined by the equation

$$\hbar^2L_i^2\equiv\{-i\hbar\,[q_i\nabla_i]\}^2$$
$$=-\hbar^2\left\{\frac{1}{\sin\vartheta_i}\frac{\partial}{\partial\vartheta_i}\left(\sin\vartheta_i\frac{\partial}{\partial\vartheta_i}\right)+\frac{1}{\sin^2\vartheta_i}\frac{\partial^2}{\partial\varphi_i^2}\right\}. \tag{3.7}$$

We introduce a new coordinate system ξ, η, ζ, associated with the system of particles in such a way that the plane $\xi\eta$ coincides with the plane of the vectors $\mathbf{q}_1$, $\mathbf{q}_2$, and the ζ axis lies along the vector $\mathbf{q}_1$. The position of this coordinate system is determined by the polar angles φ_1, ϑ_1 of the vector $\mathbf{q}_1$ and the angle ϕ_2 between the planes $Z\zeta$ and $\zeta\xi$. If φ_1, ϑ_1, ϕ_2 are given, then the position of the vector $\mathbf{q}_2$ is completely specified by the angle θ_2 between the vectors $\mathbf{q}_1$ and $\mathbf{q}_2$. The position of the remaining vectors $\mathbf{q}_1$, $\mathbf{q}_2$, $\cdots$ $\mathbf{q}_{N-1}$ in the $\xi\eta\zeta$ system is determined by the angles $\alpha_i = \phi_i - \phi_2$ for $i \geqslant 3$. In Fig. 2 the intersection of this plane with the plane xz is represented on the surface of a unit sphere by the dotted line. The points z, q_1, q_2, q_3 characterize the position of the z axis and of the radius vectors $\mathbf{q}_1$, $\mathbf{q}_2$, $\mathbf{q}_3$ drawn from the center of the sphere. The arcs ϑ_1, ϑ_2, ϑ_3 correspond to the polar angles of these vectors with respect to the z axis.

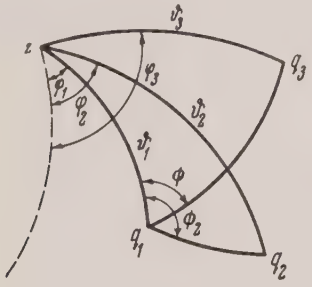

FIG. 2

We go from the angles φ_1, ϑ_1, φ_2, $\cdots$ $_{N-1}$ to the angles φ, ϑ, ϕ_2, θ_2, $\cdots$ θ_{N-1} with the help of the relations

$$\begin{aligned}
&\vartheta = \vartheta_1,\ \varphi = \varphi_1,\ \cos\theta_j = \sin\vartheta_1 \sin\vartheta_j \cos(\varphi_1 - \varphi_j) \\
&\qquad + \cos\vartheta_1 \cos\vartheta_j, \\
&\sin\theta_j \sin\phi_j = \sin\vartheta_j \sin(\varphi_1 - \varphi), \\
&\sin\theta_j \cos\phi_j = \cos\vartheta_1 \sin\vartheta_j \cos(\varphi_1 - \varphi_j) \\
&\qquad - \sin\vartheta_1 \cos\vartheta_j.\ j = 2,3,\ldots N-1.
\end{aligned} \tag{3.8}$$

The operator corresponding to the total angular momentum of the entire system has the form

$$\hbar\mathbf{L} = -i\hbar \sum_{i=1}^{N-1} [q_i\ \nabla_i]. \tag{3.9}$$

In the new variables (3.8) the projections of the total angular momentum (3.9) on the axes x, y, z have the form

$$\begin{aligned}
L_x &= -i\Big\{\sin\varphi \frac{\partial}{\partial\vartheta} + \cot\vartheta\cos\vartheta \frac{\partial}{\partial\varphi} \\
&\qquad + \frac{\cos\varphi}{\sin\vartheta} \sum_{j=2}^{N-1} \frac{\partial}{\partial\phi_j}\Big\}, \\
L_y &= -i\Big\{\cos\varphi \frac{\partial}{\partial\vartheta} - \cot\vartheta\sin\varphi \frac{\partial}{\partial\varphi} \\
&\qquad - \frac{\sin\varphi}{\sin\vartheta} \sum_{j=2}^{N-1} \frac{\partial}{\partial\phi_j}\Big\},\ L_z = -i\frac{\partial}{\partial\varphi}.
\end{aligned} \tag{3.10}$$

We introduce the new notation $\phi = \phi_2$ and $\alpha_j = \phi_j - \phi_2$, if $j \geqslant 3$, then

$$\frac{\partial}{\partial\phi_2} = \frac{\partial}{\partial\phi} - \sum_{j\geqslant 3}^{N-1} \frac{\partial}{\partial\alpha_j},\quad \frac{\partial}{\partial\phi_j} = \frac{\partial}{\partial\alpha_j},\quad i \geqslant 3,$$

and the components L_x, L_y of the total angular momentum simplify to

$$\begin{aligned}
L_x &= -i\Big\{\sin\varphi \frac{\partial}{\partial\vartheta} + \cot\vartheta\cos\varphi \frac{\partial}{\partial\varphi} + \frac{\cos\varphi}{\sin\vartheta} \frac{\partial}{\partial\phi}\Big\}, \\
L_y &= -i\Big\{\cos\varphi \frac{\partial}{\partial\vartheta} - \cot\vartheta\sin\varphi \frac{\partial}{\partial\varphi} - \frac{\sin\varphi}{\sin\vartheta} \frac{\partial}{\partial\phi}\Big\}.
\end{aligned} \tag{3.11}$$

The operator corresponding to the square of the total angular momentum depends only on the external (collective) angles φ, ϑ, ϕ

$$\begin{aligned}
\hbar^2 L^2 = -\hbar^2 \Big\{&\frac{1}{\sin\varphi} \frac{\partial}{\partial\vartheta}\Big(\sin\vartheta \frac{\partial}{\partial\vartheta}\Big) \\
&+ \frac{1}{\sin^2\vartheta}\Big[\frac{\partial}{\partial\varphi^2} + 2\cos\vartheta \frac{\partial^2}{\partial\varphi\partial\phi} + \frac{\partial}{\partial\phi^2}\Big]\Big\}
\end{aligned} \tag{3.12}$$

and, of course, has the same form as the total angular momentum operator (1.5) of the system of three particles.

The potential energy of a system of N particles interacting with central forces depends only on the absolute values of the vectors $\mathbf{q}_i$ and the cosines of the angles between them. The cosines of the angles between $\mathbf{q}_1$ and all the other vectors $\mathbf{q}_2$, $\cdots$ $\mathbf{q}_{N-1}$ are $\cos(\mathbf{q}_1\mathbf{q}_j) = \cos\theta_j$, $j \geqslant 2$, respectively. The cosines of the angles between the other pairs of vectors are

$$\begin{aligned}
\cos\overset{\wedge}{(\mathbf{q}_i\mathbf{q}_j)} &= \sin\theta_j\sin\theta_j\cos(\phi_j - \phi_i) \\
&\quad + \cos\theta_i\cos\theta_j,\ i,j \geqslant 2.
\end{aligned}$$

Consequently, the potential energy depends on the $3N-6$ internal variables $\{r_j\} \equiv q_1, q_2, \dots q_{N-1}, \theta_2 \dots \theta_{N-1}, \alpha_3 \dots \alpha_{N-1}$, and does not depend on the collective variables φ, ϑ, ϕ. Therefore the operator corresponding to the square of the total angular momentum of the system (3.12) and its projections on the Z axis commute with the total Hamiltonian of the system.

In the new variables the kinetic energy operator of the system has the form

$$T = -\frac{\hbar^2}{2\mu}\left\{\sum_{i=1}^{N-1}\frac{1}{q_i^2}\left[\frac{\partial}{\partial q_i}\left(q_i^2\frac{\partial}{\partial q_i}\right)\right] + \sum_{i=2}^{N-1}\left[\left(\frac{1}{q_i^2}+\frac{1}{q_1^2}\right)R_i + \frac{1}{q_1^2}P_i\right]\right\} + \frac{\hbar^2}{2\mu q_1^2}L^2 - \tau,$$

$$R_2 = -\left\{\frac{1}{\sin\theta^2}\frac{\partial}{\partial\theta^2}\left(\sin\theta_2\frac{\partial}{\partial\theta_2}\right) + \frac{1}{\sin^2\theta_2}\left(\frac{\partial}{\partial\phi} - \sum_{i=3}^{N-1}\frac{\partial}{\partial\alpha_i}\right)^2\right\},$$

$$R_i = -\left\{\frac{1}{\sin\theta_i}\frac{\partial}{\partial\theta_i}\left(\sin\theta_i\frac{\partial}{\partial\theta_i}\right) + \frac{1}{\sin^2\theta_i}\frac{\partial}{\partial\alpha_1^2}\right\},\ i \geqslant 3,$$

$$P_i = -2\frac{\partial^2}{\partial\phi^2} + \sum_{\substack{i\\ i\neq j\geq 2}}\sum_{j}\left\{\cos(\alpha_i-\alpha_j)\frac{\partial}{\partial\theta_i\partial\theta_j} + [\cot\theta_i\cot\theta_j\cos(\alpha_i-\alpha_j)-1]\right.$$

$$\times\frac{\partial^2}{\partial\alpha_i\partial\alpha_j} + 2\cot\theta_i\sin(\alpha_i-\alpha_j)\left.\frac{\partial^2}{\partial\theta_j\partial\alpha_i}\right\} + 2\sum_{i=3}^{N-1}\cos\alpha_i\frac{\partial^2}{\partial\theta_i\partial\theta_2} \qquad (3.13)$$

$$+\cot\theta_i\cot\theta_2\cos\alpha_i\frac{\partial}{\partial\phi}\left(\frac{\partial}{\partial\phi} - \sum_{j=3}^{N-1}\frac{\partial}{\partial\alpha_j}\right)$$

$$+\cot\theta_2\sin\alpha_i\frac{\partial}{\partial\theta_i}\left(\frac{\partial}{\partial\phi} - \sum_{j=3}^{N-1}\frac{\partial}{\partial\alpha_j}\right)\Big].$$

$$\tau = \frac{\hbar^2}{\mu q_1^2}\sum_{i=3}^{N-1}\left\{\cot\vartheta\left[\cot\theta_i\cos(\alpha_i+\phi)\frac{\partial}{\partial\alpha_i} + \sin(\alpha_i+\phi)\frac{\partial}{\partial\theta_i}\right]\frac{\partial}{\partial\phi}\right.$$

$$+\frac{1}{\sin\vartheta}\left[\sin(\alpha_i+\phi)\frac{\partial}{\partial\theta_i} + \cot\theta_i\cos(\alpha_i+\phi)\frac{\partial}{\partial\alpha_i}\right]\frac{\partial}{\partial\varphi} + \left[\cot\theta_i\sin(\alpha_i+\phi)\frac{\partial}{\partial\alpha_i}\right.$$

$$\left.\left.-\cos(\alpha_i+\phi)\frac{\partial}{\partial\theta_i}\right]\frac{\partial}{\partial\vartheta}\right\} + \frac{\hbar^2}{2\mu q_1^2}\left\{\cot\theta_2\left[\frac{\cos\phi}{\sin\vartheta}\frac{\partial}{\partial\varphi}\left(\frac{\partial}{\partial\phi} - \sum_{j=3}^{N-1}\frac{\partial}{\partial\alpha_j}\right)\right.\right.$$

$$\left.\left.+\cot\vartheta\cos\phi\frac{\partial^2}{\partial\phi^2} + \sin\phi\frac{\partial^2}{\partial\phi\,\partial\vartheta}\right] + \left[\frac{\sin\phi}{\sin\vartheta}\frac{\partial}{\partial\varphi} - \cos\phi\frac{\partial}{\partial\vartheta} + \cot\vartheta\sin\phi\frac{\partial}{\partial\phi}\right]\frac{\partial}{\partial\theta_2}\right.$$

The stationary states of the system of N particles are determined by the Schroedinger equation (1.13). The wave function of the state with definite values of the integrals of motion L and M can now be written in the form

$$\psi_M^L = \sqrt{\frac{2L+1}{8\pi^2}}\sum_K D_{MK}^L(\vartheta\,\varphi\,\phi)\,\varphi_K(\{r_i\}). \qquad (3.14)$$

Substituting (3.14) in (1.13), we obtain the system of equations

$$\left\{\frac{\hbar^2}{2\mu q_1^2}[L(L+1) - K(K+1)]\right.$$

$$\left.+\mathcal{L}_N(K) - E\right\}\varphi_K = \sum_{K'}(K|\tau|K')\,\varphi_{K'}, \qquad (3.15)$$

where

$$(K|\tau|K') = \frac{2L+1}{8\pi^2}\int D_{MK}^{*L}\,\tau\,D_{MK'}^L\,d\Omega$$

is a matrix with vanishing non-diagonal elements;

$$\mathscr{L}_N(K) = -\hbar^2(2L+1)(16\mu\pi^2)^{-1}\int D^{*L}_{MK}\left\{\sum_{i=1}^{N-1}\frac{1}{q_i^2}\left[\frac{\partial}{\partial q_i}\left(q_i^2\frac{\partial}{\partial q_i}\right)\right]\right.$$
$$\left.+\sum_{i=2}^{N-1}\left[\left(\frac{1}{q_i^2}+\frac{1}{q_1^2}\right)R_i+\frac{1}{q_1^2}P_i\right]\right\}D^{L}_{MK}\,d\Omega+\frac{\hbar^2K(K+1)}{2\mu q_i^2}$$

is the Hamiltonian operator of the "internal" motion. For systems such that K is a good quantum number, the right side of (3.15) can also be omitted here, and we obtain a system of independent equations for each value of K. For $L = K$ equation (3.15) reduces to

$$\{\mathscr{L}_N(K) - \varepsilon_{\alpha K}\}\,\varphi_{\alpha K} = 0, \qquad (3.16)$$

which determines the "internal" state of the system N interacting particles. Furthermore, we can carry out the same considerations as in Sec. 1, and obtain the moment of inertia of the system of N interacting particles, corresponding to the internal state of motion φ_{0K}:

$$J_{0K} = \left[\frac{1}{\mu}\int \varphi^*_{\alpha K}\, q_1^{-2}\,\varphi_{\alpha K}\,d\tau\right]^{-1}. \qquad (3.17)$$

The index α characterizes the quantum numbers which, together with K, determine the internal state of the system of N particles. If inequality (1.22) is satisfied, we can represent the energy approximately in the form of a sum of the internal energy and the energy of rotation

$$E_{0KL} = \varepsilon_{0K} + \hbar^2[L(L+1) - K(K+1)]/2J_{0K}. \qquad (3.18)$$

The normalized wave function describing the rotation of the system has the form

$$\Phi^L_{MK}(\varphi\vartheta\phi) = \sqrt{\frac{2L+1}{8\pi^2}}D^L_{MK}(\varphi\vartheta\phi). \qquad (3.19)$$

For $K = 0$, according to (1.12), this function reduces to the usual spherical function

$$\Phi^L_{M0}(\varphi\vartheta\phi) = Y_{LM}(\varphi\vartheta).$$

The complete wave function of a system with energy (3.18) is the product of the function (3.19) of the collective degrees of freedom and the wave function (3.19) of the collective degrees of freedom and the wave function $\varphi_{\alpha K}(\{r_i\})$ describing the internal motion in the system

$$\Psi^L_{MK\alpha} = \Phi^L_{MK}(\varphi\vartheta\phi)\,\varphi_{\alpha K}(\{r_i\}). \qquad (3.20)$$

The separation of the total energy of the system into rotational energy and internal energy, and the representation of the wave function in the form of a product of functions of internal and collective coordinates is possible only in systems with marked axial symmetry and where the inequality (1.22) is satisfied, *i.e.*, in the case where the rotation takes place slowly enough so that it does not substantially change the internal structure of the system of N particles. As the frequency of rotation $\omega = \hbar J_{0K}^{-2}\sqrt{L(L+1) - K(K+1)}$ increases, the particles will not be able to follow adiabatically the change of orientation of the mean field. Centrifugal and Coriolis forces will arise in the system, leading to an interaction between the rotational motion and the internal motion of the particles. If the frequencies of rotation are small with respect to the frequency $|\varepsilon_{\alpha K} - \varepsilon_{\alpha+1,K}|/\hbar$, corresponding to transitions to excited states near $K\alpha$, then according to (3.17) each state of internal motion has its own moment of inertia. This conclusion does not agree with the remark by Coester[6] that the moment of inertia does not depend on the internal wave function. In systems which deviate slightly from spherical symmetry, which were studied in the papers of Inglis[4] and Coester[6], the projection of the total angular momentum on the axis of symmetry is not conserved, and the representation of the wave function in the form of the simple product (3.21) is not justified.

[1] A. Bohr, Kong. Dan. Vid. Selsk. Mat.-fys. Medd. **26**, 14 (1952).

[2] K. Ford, Phys. Rev. **95**, 1250 (1954).

[3] A. Bohr, B. Mottelson, Kong. Dan. Vid. Selsk., Mat.-fys. Medd. **30**, 1 (1955).

[4] D. Inglis, Phys. Rev. **96**, 1059 (1954).

[5] H. Tolhoek, Physica **21**, 1 (1955).

[6] F. Coester, Phys. Rev. **99**, 170 (1955).

[7] E. Wigner, *Gruppentheorie und ihre Anwendungen auf die Quantenmechanik der Atomspektren* (1931).

Translated by R. S. Silverman
180

Ultrasonic Absorption in Metals

A. I. AKHIEZER, M. I. KAGANOV AND G. IA. LIUBARSKII
Physico-technical Institute, Academy of Sciences, Ukrainian SSR

(Submitted to JETP editor April 3, 1956)
J. Exptl. Theoret. Phys. (U.S.S.R.) 32, 837-841 (April, 1957)

The absorption coefficient for metals has been computed. It is shown that if $\omega\tau \ll s/v$ (ω = frequency, τ = relaxation time, s = sound velocity, v = boundary electron velocity), the absorption coefficient is proportional to $\omega^2\tau$. For $\omega\tau \gg s/v$, the absorption is proportional to the first power of the frequency and does not depend on τ, *i.e.*, it is independent of the temperature.

1. IN THE INVESTIGATION of the absorption of sound waves in solids, we must distinguish two cases, as is well known [1-3]: when the frequency of the sound waves ω is much greater than the reciprocal of the relaxation time τ, and when the frequency of the sound waves is much smaller than τ^{-1}. In the first case ($\omega\tau \gg 1$), we can treat the sound absorption as the absorption of sound quanta of energy $\hbar\omega$ and momentum $\hbar\mathbf{k}$ ($\mathbf{k}$ = wave vector of the sound wave), which takes place as the result of collisions of the sound quanta with the quasi-particles which characterize the energy spectrum of the solid, *i.e.*, with phonons in ordinary dielectrics [1] and with electrons and phonons in metals.

In the second case, when $\omega\tau \ll 1$, the sound vibrations can be considered as a certain external field in which the gas of quasi-particles is located, and which modulates the energy of these particles.[2,3] This modulation leads to the result that the frequency of the phonon ω_f and the energy of the electron acquire additions proportional to the deformation tensor produced by the sound wave:

$$\omega_{\mathbf{f}} = \omega_f^0(1 + \mu_{ik}u_{ik}),\quad \varepsilon = \varepsilon_0 + \lambda_{ik}u_{ik}, \qquad (1)$$

where ω_f^0 and ϵ_0 are the phonon frequency and electron energy in the absence of sound, u_{ik} is the deformation tensor, μ_{ik} and λ_{ik} are tensors of second rank which characterize the solid; the tensor μ_{ik} depends only on the direction of the wave vector of the phonon $\mathbf{f}$, while λ_{ik} depends both on the direction and on the magnitude of the quasi-momentum $\mathbf{p}$ of the electron.

We note that in reality the change of the energy of the electron brought about by the sound field must contain, in addition to the term $\lambda_{ik}\mu_{ik}$, an additional term connected with the Stewart-Tolman effect. This term is equal to $m(\partial\epsilon/\partial p_i)(\partial u_i/\partial t)$, where m = mass of the free electron, u_i = vector displacement. However, this term is significantly smaller than $\lambda_{ik}\mu_{ik}$ and is disregarded. Actually, in order of magnitude, λ_{ik} is equal to the limiting Fermi energy μ_0, whence

$$\lambda_{ik}u_{ik} \sim \mu_0 ku \sim mv_0^2\omega u/s,$$

$$m(\partial\varepsilon/\partial p_i)\,\partial u_i/\partial t \sim mv_0\omega u,$$

where v_0 = velocity of an electron on the Fermi surface ($\sim 10^8$ cm/sec), s = sound velocity ($\sim 10^5$ cm/sec) and, consequently,

$$\left| m\frac{\partial\varepsilon}{\partial p_i}\frac{\partial u_i}{\partial t}\right| \Big/ |\lambda_{ik}u_{ik}| \sim \frac{s}{v_0} \ll 1.$$

2. In the present paper, we shall consider the sound absorption in metals at low temperatures. In this case, the role of the phonons is important,[3] since their number tends to zero with decrease in temperature (proportional to T^3) and the sound absorption is determined by the interaction of the sound waves with the conduction electrons. We note that this is possibly connected with the experimentally observed difference in the absorption coefficients of ultrasound in metals in the normal and superconducting states.

We first consider the case in which $\omega\tau \ll 1$. Here the sound wavelength $\lambda\!\!\!^{-} = s/\omega$ can be larger or smaller than the mean free path of the electron $l = v_0\tau$. Therefore, both the time and space changes in the electron distribution function brought about by the sound field are important.

We denote the electron distribution function by $n(\mathbf{p}, \mathbf{r}, t)$. For simplicity, we shall assume that the collision integral has the form

$$(\partial n/\partial t)_c = -(n - \bar{n})/\tau, \qquad (2)$$

where $\bar{n} = \bar{n}(\epsilon, \mathbf{r}, t)$ is the mean value of the distri-

bution function over a surface of equal energy

$$\bar{n} = \oint n \frac{ds}{v} \Big/ \oint \frac{ds}{v}, \tag{3}$$

ds is the element of area in momentum space of the isoenergetic surface and $v = |\partial t/\partial \mathbf{p}|$. The kinetic (Boltzmann) equation in this case can be written in the following manner:

$$\frac{\partial n}{\partial t} + \mathbf{v}\frac{\partial n}{\partial \mathbf{r}} + \dot{\mathbf{p}}\frac{\partial n}{\partial \mathbf{p}} + \frac{n - \bar{n}}{\tau} = 0. \tag{4}$$

Setting

$$n = n_0 - \chi \frac{\partial n_0}{\partial \varepsilon}, \qquad n_0 = \left(\exp\frac{\varepsilon - \mu}{T} + 1\right)^{-1}, \tag{5}$$

where μ is the limiting energy, and noting that at low temperatures

$$-\partial n_0/\partial \varepsilon = \delta(\varepsilon - \mu),$$

it is easy to show that the energy dissipation per unit volume is equal to the product of the temperature and the time derivative of the entropy, and has the form

$$T\dot{S} = (2\pi\hbar)^{-3}\left\{\frac{1}{\tau}\overline{(|\chi|^2 - |\bar{\chi}|^2)}\oint\frac{ds}{v}\right\}_{\varepsilon=\mu}, \tag{6}$$

where the values of all the quantities entering into the formula are taken on the Fermi surface.

The sound absorption coefficient is connected with the dissipation function by the relation[4]

$$\gamma = T\dot{S}/E_s \tag{7}$$

where E_s is the energy of the sound wave per unit volume.

Thus the computation of the sound absorption coefficient reduces to the determination of the function $\chi(\mathbf{p}, \mathbf{r}, t)$.

3. As has been shown, the sound field leads to a change in the energy of the electrons given by Eq. (1). In turn, this brings about a change in the chemical potential μ and temperature T:

$$\mu = \mu_0 + \mu', \quad T = T_0 + T',$$

where μ_0 and T_0 are the values of μ and T at $u_{ik} = 0$, while μ' and T' are the additions to μ and T, and are proportional to u_{ik}. They can be found from the conservation laws of the number of the electrons and the energy. Taking it into consideration that the sound vibrations represent a plane monochromatic wave

$$u_{ij} = {}^1/_2[\partial u_i/\partial x_j + \partial u_j/\partial x_i], \quad u_i = u_i^0 e^{i(\omega t - \mathbf{kr})}, \tag{8}$$

we can show that

$$\mu' = \bar{\lambda}_{ik}u_{ik}, \quad T' = T\rho_{ik}u_{ik}, \tag{9}$$

where the bar over the λ_{ik} denotes an averaging over the Fermi surface, and ρ_{ik} is a certain tensor of second rank whose explicit form was derived in Ref. 3. Since a temperature change enters the kinetic equation in the form

$$-\frac{\partial n_0}{\partial \varepsilon}\frac{\varepsilon - \mu}{T}\dot{T}',$$

then the contribution brought about by this change in the dissipation function is proportional to the $(T/\mu_0)^2$, which is significantly less than unity. This means that at low temperatures in metals the thermal conductivity does not play an important role in the dissipation of energy, which is determined chiefly by the "friction" of the electron gas. Therefore we do not have to take the temperature change into consideration.

The force $\dot{\mathbf{p}}$ (which acts on the electron) entering the kinetic equation (4) is obviously equal to

$$\dot{\mathbf{p}} = e\mathbf{E} - \nabla\varepsilon = e\mathbf{E} - \lambda_{ik}\nabla u_{ik}, \tag{10}$$

where $\mathbf{E}$ is the electric field which arises as the result of the redistribution of charges in the metal under the action of the sound wave. This field can be found from the simultaneous solution of the kinetic equation and the Maxwell equation. Since the velocity of the electrons and the sound velocity are significantly smaller than the velocity of light, one does not have to take the resulting magnetic field into account, and we regard the electric field as longitudinal. On the other hand, thanks to the high conductivity of the metal, the volume density of the charge ρ is practically equal to zero.

Inasmuch as

$$\rho = \frac{2e}{(2\pi\hbar)^3}\oint\frac{ds}{v}\cdot\bar{\chi},$$

then, to find the field, we must start from the condition

$$\bar{\chi} = 0. \tag{11}$$

Substituting the expression for n in the form (5) in the kinetic equation (4), and making use of the second relation of (1), and also (8)-(10), we obtain the following equation for the function χ (in the linear approximation in u_{ik}):

$$\frac{\partial \chi}{\partial t} + (\mathbf{v}\nabla)\chi + \frac{\chi}{\tau} = e\mathbf{v}\mathbf{E} + (\lambda_{ik} - \bar{\lambda}_{ik})\dot{u}_{ik} - \mathbf{v}(\nabla)\lambda_{ik}\dot{u}_{ik}, \quad (12)$$

whence

$$\chi = \frac{\tau'(\lambda_{ik} - \bar{\lambda}_{ik})\dot{u}_{ik} + l'\varkappa\nu(eE + \bar{\lambda}_{ik}\dot{u}_{ik}/s)}{1 - ikl'\varkappa\nu}, \quad (13)$$

$$\varkappa = \mathbf{k}/k, \ \nu = \mathbf{v}/v, \ \tau' = \tau/(1 + i\omega\tau), \ l' = v\tau'.$$

It follows from (13) and (11) that

$$eE = -\frac{1}{s}\bar{\lambda}_{ik}\dot{u}_{ik} + i\frac{\omega\tau'}{s(1-J)}\Lambda_{ik}\dot{u}_{ik}. \quad (14)$$

Here

$$J = \overline{\frac{1}{1 + z\varkappa\nu}}, \ \Lambda_{ik} = \overline{\frac{\lambda_{ik} - \bar{\lambda}_{ik}}{1 + z\varkappa\nu}}, \ z = -ikl'. \quad (15)$$

Substituting (14) in (13), we get

$$\chi = \tau'\left\{\frac{(\lambda_{ik} - \bar{\lambda}_{ik}) + \Lambda_{ik}/(1-J)}{1 + z\varkappa\nu} - \frac{1}{1-J}\Lambda_{ik}\right\}\dot{u}_{ik}.$$

Then, by Eq. (6) we can find the energy dissipation. The quantity $|\chi|^2$ ($|\overline{\chi}|^2 = 0$) entering into Eq. (6) has a complicated form in the general case of arbitrary z. We therefore consider only the main term in the equation for $|\overline{\chi}|^2$, which gives the principal contribution in the limiting cases of large and small $|z|$:

$$|\overline{\chi}|^2 = |\tau'|^2\dot{u}_{ik}\dot{u}_{lm} \times \oint \frac{ds}{v}\frac{(\lambda_{ik} - \bar{\lambda}_{ik})(\lambda_{lm} - \bar{\lambda}_{lm})}{|1 + z\varkappa\nu|^2} \Big/ \oint \frac{ds}{v}. \quad (16)$$

Noting that the tensor λ_{ik} is of the order of magnitude of μ_0, we obtain, in the limiting case of small $|z|$ (*i.e.*, for $\omega\tau \ll s/v$), the following formula for the sound absorption coefficient:

$$\gamma \sim \tau\omega^2 N\mu_0/\rho s^2, \ \omega\tau \ll s/v, \quad (17)$$

where ρ is the density of the metal and N is the number of electrons per unit volume. This formula coincides with the result obtained in Ref. 3. In this case, Eq. (17) is applicable if $\omega\tau \ll s/v$ (the inexact criterion $\omega\tau \ll 1$ is given in Ref. 3). We note that we can represent the quantity τ in terms of the electronic conductivity.

In the case of large $|z|$, we can represent (16) in the following form:

$$\overline{|\chi|^2} = -\pi|\tau'|^2\dot{u}_{ik}\dot{u}^*_{lm} \int_0^{2\pi} \frac{(\lambda_{ik} - \bar{\lambda}_{ik})(\lambda_{lm} - \bar{\lambda}_{lm})}{vK(\varphi)\,\mathrm{Im}z}\,d\varphi \Big/ \oint \frac{ds}{v},$$

where $K(\varphi)$ is the Gaussian curve of the Fermi surface and the integration is carried out along the line where $\nu \perp \kappa$. (This circumstance is connected with the fact that the electrons moving in the planes of equal phase of the sound wave play the principal role in the energy dissipation.)

The absorption coefficient for $|z| \gg 1$, *i.e.*, for $\omega\tau \gg s/v$, is equal in magnitude to

$$\gamma \sim \omega N\mu_0/v\rho s, \quad \omega\tau \gg s/v. \quad (18)$$

We see that in this case the absorption coefficient is proportional not to the second, but to the first power of the frequency, and does not depend on τ, *i.e.*, on the temperature. This expression can be obtained formally from (17), by substituting for the path l the wavelength $\lambda = s/\omega$.

We note that all considerations are valid if $\gamma \ll \omega$. As it is easy to see, this condition reduces, in the case $\omega\tau \gg s/v$, to the inequality $m/M \ll s/v$, where M is the atomic mass.

4. Up to the present we have used the classical description of the sound wave, regarding it as a certain field in which the electrons are located. Such a consideration is known to be valid if $\omega\tau \ll 1$. On the other hand, for $\omega\tau \gg s/v$, the relaxation time τ does not enter into the absorption coefficient, for the computation of which we have not used the inequality $\omega\tau \ll 1$. This shows that Eq. (18) ought to be valid for $\omega\tau \gg 1$.

We can establish this by considering the damping of the sound as the absorption of a sound quantum which takes place as the result of its collision with the conduction electrons. The probability of the absorption of a sound quantum is given by

$$\gamma = \frac{2\pi}{\hbar}\int |U_{12}|^2[n_1(1-n_2) - n_2(1-n_1)] \times \delta(\varepsilon_1 + \hbar\omega - \varepsilon_2)\frac{2d\mathbf{p}}{(2\pi\hbar)^3}, \quad (19)$$

where $n_{1,2}$ are Fermi functions corresponding to the energy values $\epsilon_1 \equiv \epsilon(\mathbf{p}_1)$ and $\epsilon_2 \equiv \epsilon(\mathbf{p}_1 + \hbar\mathbf{k})$, and U_{12} is the matrix element of the transition, equal to

$$u_i = e_i \sqrt{\hbar/2\rho\omega}\; e^{i\mathbf{kr}}$$

(**e** is the unit vector of the polarization of the sound wave). We note that the change in the chemical potential is taken into account by having $\lambda_{ij} - \bar{\lambda}_{ij}$, and not $\bar{\lambda}_{ij}$, enter into U_{12}.

Since $\hbar\omega \ll \mu_0$, $\hbar k \ll p_0$, then

$$n_1(1-n_2) - n_2(1-n_1) \approx -(\partial n/\partial \varepsilon)\,\hbar\omega,$$
$$\delta(\varepsilon_1 + \hbar\omega - \varepsilon_2) \approx \frac{s}{\hbar\omega v}\,\delta\left(\cos\theta - \frac{s}{v}\right),$$

where θ is the angle between the vectors **k** and $\mathbf{v} = \partial\epsilon/\partial\mathbf{p}$. Substituting this expression in Eq. (19), we get the value of γ given by Eq. (18). We note that the coincidence of the results of classical and quantum theory in the case $\omega\tau \gg s/v$ is essentially connected with the small value of s/v in comparison with unity.

In conclusion the authors express their gratitude for valuable discussions to L. D. Landau, I. M. Lifshitz and I. Ia. Pomeranchuk.

[1] L. Landau and Iu. Rumer, Z. Phys. Sowjetunion 11, 18 (1937).

[2] A. Akhiezer, J. Exptl. Theoret. Phys. (U.S.S.R.) 8, 1318 (1938).

[3] A. Akhiezer, J. Exptl. Theoret. Phys. (U.S.S.R.) 8, 1330 (1938).

[4] L. Landau and E. Lifshitz, *Mechanics of continuous media*, Gostekhizdat, Moscow, 1953.

Translated by R. T. Beyer
181

SOVIET PHYSICS JETP VOLUME 5, NUMBER 4 NOVEMBER, 1957

Excitation of Rotational States in the Interaction Between Neutrons and Nuclei

V. N. GRIBOV

(Submitted to JETP editor April 4, 1956)
J. Exptl. Theoret. Phys. (U.S.S.R.) 32, 842-851 (April, 1957)

The excitation of rotational states in nuclei by neutrons is studied in the energy range from the threshold up to 1.5–2 Mev.

1. STATEMENT OF THE PROBLEM

WE SHALL INVESTIGATE interactions between neutrons and nonspherical nuclei and the excitation of rotational states, using an optical model which has been modified to take into account the nuclear deformation caused by the existence of rotational states.

On the usual optical model [1] the total scattering cross section is divided into two parts:

$$\sigma = \sigma_{se} + \sigma_c, \qquad (1)$$

where σ_{se} is the elastic scattering cross section for a spherically symmetrical complex potential, and σ_c includes both the cross section σ_{ce} for the formation of a compound nucleus with subsequent emission of particles of the same energy and the reaction cross section (Feshbach, Porter and Weisskopf call σ_c the cross section of compound nucleus formation, which is not quite correct because it includes the cross sections of direct expulsion processes and the excitation of collective motions which will be considered below). All these processes are described by the imaginary part of the complex potential.

For nonspherical nuclei this model must be modified as follows: 1) the complex potential must be nonspherical; 2) since the deformed nucleus is capable of rotational motion, the nonspherical potential of the optical model must be capable of a change of orientation.

In the interaction between a neutron and a nucleus different rotational levels can be excited, *i.e.*, the rotational velocity in the potential can change. We thus have a problem in which the variables which characterize the orientation of the nonspherical potential must be regarded as dynamical

variables. The Hamiltonian can then be put into the form

$$\hat{H} = -(\hbar^2/2m)\nabla^2 + \tilde{V}(\mathbf{r}, \theta_i) + \hat{T}_{\text{rot}}, \qquad (2)$$

where $\tilde{V}(\mathbf{r}, \theta_i)$ is the nonspherical complex potential, $\mathbf{r}$ is the neutron radius vector, θ_i are the Euler angles which define the directions of the nuclear deformation axes, and $\hat{T}_{\text{rot}}$ is the nuclear rotational energy operator which acts on the θ_i. Bohr[2] showed that for an axially symmetrical deformation the operator can be written in the form

$$\hat{T}_{\text{rot}} \equiv (\hbar^2/2J)[\hat{Q}^2 - Q_0(Q_0+1)], \qquad (3)$$

where $\hat{Q}^2$ is the operator of the square of the total nuclear angular momentum and $Q_0(Q_0+1)$ is its value in the unexcited state. By solving the Schroedinger equation

$$\hat{H}\psi(\mathbf{r}, \theta_i) = E\psi(\mathbf{r}, \theta_i), \qquad (4)$$

we can calculate the elastic scattering cross section σ_{se} for a nonspherical potential, the cross section σ_{rot} for the excitation of different rotational states, and the combined cross section $\tilde{\sigma}_c$ of the other processes which are associated with the imaginary part of the potential. On this model the total cross section is thus divided into three parts, *viz:*

$$\sigma = \sigma_{se} + \sigma_{\text{rot}} + \tilde{\sigma}_c. \qquad (5)$$

Just as σ_{se} is only the portion of the elastic scattering cross section that is not associated with the formation of a compound nucleus, σ_{rot} is only that portion of the excitation cross section which is not associated with the same process. However, the small value of the imaginary part of the potential, obtained by comparing the calculated and measured total neutron cross sections up to about 3 Mev, shows that for such energies the average probability of compound nucleus formation is small. It therefore seems that the excitation of rotational states in the interaction between a neutron and a nucleus does not proceed principally through the formation of a compound nucleus but rather through the direct transfer of energy to the collective motion. This means that in the indicated energy range σ_{rot} is the main portion of the excitation cross section for rotational states. We shall hereinafter limit ourselves to these energies.

The exact solution of (4) would evidently be very complicated. No solution has yet been obtained even for the simpler problem of scattering by a nonspherical potential without rotation. We shall therefore consider slightly deformed nuclei. More precisely, if

$$\tilde{V}(\mathbf{r}, \theta_i) = \tilde{V}_0(r) + \tilde{V}_1(\mathbf{r}, \theta_i);$$
$$V_0(r) = 0 \quad \text{for} \quad r > R_1; \qquad (6)$$
$$V_1(\mathbf{r}, \theta_i) = 0 \quad \text{for} \quad r < R_1, \; r > R_2,$$

we shall regard as small and shall neglect the quantities $(k\Delta R)^2$ and $(\Delta R/R_1)^2$, where $\Delta R = R_2 - R_1$, $k^2 = 2mE/\hbar^2$. If we do not claim high precision in calculating the cross section, these conditions are valid for the majority of nuclei in the given energy range. Whenever the conditions are not satisfied, our treatment will be of the nature of a limiting case.

We shall also assume that the nuclear deformations are axially symmetrical and thus $\tilde{V}_1(\mathbf{r}, \theta_i) = \tilde{V}(r, \vartheta)$, where ϑ is the angle between the radius vector and the deformation axis. This is well fulfilled for almost all deformed nuclei. Introducing for convenience

$$U(\mathbf{r}, \theta_i,) = r\psi(\mathbf{r}, \theta_i); \; V_0(r) = (2m/\hbar^2)\tilde{V}_0(r);$$
$$V_1(r, \vartheta) = (2m/\hbar^2)\tilde{V}_1(r, \vartheta),$$

we obtain

$$[(d^2/dr^2) + k^2 - V_0(r) - V_1(r, \vartheta)$$
$$- (\hat{l}^2/r^2) - (2m/\hbar^2)\hat{T}_{\text{rot}}]U(\mathbf{r}, \theta_i) = 0, \qquad (7)$$

where $\hat{l}^2$ is the operator of the square of the neutron angular momentum. Eq. (7) must be solved subject to the conditions

$$(k\Delta R)^2 \ll 1, \; (\Delta R/R_1)^2 \ll 1. \qquad (8)$$

We note that $k'\Delta R$ (where k' is the average wave vector of the neutron inside the nucleus) will not be regarded as small. Therefore the phase difference of the neutron waves traversing the nucleus parallel to the major and minor semi-axes can be large and the pattern of scattering by a nonspherical nucleus can thus differ essentially from that for a spherical nucleus. For real nuclei, for which we can expect to obtain a rotational spectrum, $k'\Delta R \gg 1$; therefore for such nuclei the scattering is strongly influenced by the deformation and cannot be treated by perturbation theory.

We shall show that a solution can be obtained be-

cause when (8) is satisfied we can neglect in (7) the terms k^2, $2m\hat{T}_{\text{rot}}/\hbar^2$ and $\hat{l}^2/r^2$ in the region $R_1 < r < R_2$. The equation can then easily be solved in this region. The problem is then solved by smoothly joining this solution with the solutions for $r < R_1$ and $r > R_2$.

2. THE WAVE FUNCTION FOR $R_1 < r < R_2$

For the purpose of proving our last statement we write (7) in the form

$$U(\mathbf{r}, \vartheta_i) = U^0(\mathbf{r}, \vartheta_i) + \int G(\mathbf{r}, \vartheta_i; \mathbf{r}', \vartheta_i') V_1(\mathbf{r}', \vartheta') U(\mathbf{r}', \vartheta_i') \, dr' \, d\Omega' \, d\vartheta_i'; \quad (9)$$

$$U^0(\mathbf{r}, \vartheta_i) = \psi_{\mathbf{k}}(\mathbf{r}) \tilde{D}^{Q_0}_{M_0 \varkappa}(\vartheta_i), \quad (10)$$

where $\tilde{D}^{Q_0}_{M_0 \varkappa}$ is the eigenfunction of the operator $\hat{T}_{\text{rot}}$ for the ground state.

From the symmetry properties of the nuclear wave function it follows[2] that each state can be described by a superposition of the functions $\tilde{D}^{Q_0}_{M_0 \varkappa}$ and $\tilde{D}^{Q_0}_{M_0 -\varkappa}$. But it can be shown that this does not change the result.

Let $G(\mathbf{r}, \vartheta_i; \mathbf{r}', \vartheta_i)$ be the Green's function of (7) without the term $V_1(r, \vartheta)$. It is given by ($r, r' > R_1$):

$$G(\mathbf{r}, \vartheta_i; \mathbf{r}', \vartheta_i') = \sum_{Q, M} G_{k_Q}(\mathbf{r}, \mathbf{r}') \tilde{D}^{Q}_{M\varkappa}(\vartheta_i) \tilde{D}^{*Q}_{M\varkappa}(\vartheta_i'); \quad (11)$$

$$G_{k_Q}(\mathbf{r}, \mathbf{r}') = -\frac{1}{k_Q} \begin{cases} \sum_{l,m} j_l(k_Q r) h_l(k_Q r') Y_{lm}(\Omega) Y^*_{lm}(\Omega') & \text{for } r' > r; \\ \sum_{l,m} j_l(k_Q r') h_l(k_Q r) Y_{lm}(\Omega) Y^*_{lm}(\Omega') & \text{for } r' < r; \end{cases}$$

$$j_l(x) = \frac{1}{2i}[h_l(x) \exp(2i\delta_l^Q) - h_l^*(x)]; \quad h_l(x) = \sqrt{\frac{\pi x}{2}} H^{(1)}_{l+1/2}(x);$$

$$k_Q^2 = k^2 - (m/J)[Q(Q+1) - Q_0(Q_0+1)];$$

$$\psi_{\mathbf{k}}(\mathbf{r}) = \frac{4\pi}{k} \sum_{l,m} i^l j_l(kr) Y_{lm}(\Omega) Y^*_{lm}(\Omega_{\mathbf{k}}), \quad (10a)$$

where δ_l^Q is the complex scattering phase of a neutron with a wave vector k_Q by the complex potential $V_0(r)$.

For (9) in the region $R_1 < r < R_2$ and with (8) satisfied for all essential k_Q of the problem we can expand the functions $j_l(x)$ and $h_l(x)$ in (10) and (11) in powers of $k_Q(r - R_1)$, of which only the first two terms of the series are retained. In complete analogy to the calculations given in Ref. 3 we obtain for this similar problem

$$U(\mathbf{r}, \vartheta_i) = F^{(1)}(\Omega, \vartheta_i) + (r - R_1) F^{(2)}(\Omega, \vartheta_i) + \int_0^r (r - r') V_1(r', \vartheta) U(r', \Omega, \vartheta_i) \, dr';$$

$$F^{(1)}(\Omega, \vartheta_i) = U^0(R_1, \vartheta_i) + \int \Big[G(\mathbf{R}_1, \vartheta_i; \mathbf{R}_1', \vartheta_i') \xi(\Omega', \vartheta_i') + \frac{\partial G(\mathbf{R}_1, \vartheta_i; \mathbf{R}_1', \vartheta_i')}{\partial R_1'} \eta_i(\Omega', \vartheta_i') \Big] d\Omega' \, d\vartheta_i'; \quad (12)$$

$$F^{(2)}(\Omega, \vartheta_i) = \frac{\partial U^0(\mathbf{R}_1, \vartheta_i)}{\partial R_1} + \int \Big[\frac{\partial G(\mathbf{R}_1, \vartheta_i; \mathbf{R}_1', \vartheta_i')}{\partial R_1} \xi(\Omega', \vartheta_i') + \frac{\partial^2 G(\mathbf{R}_1, \vartheta_i; \mathbf{R}_1', \vartheta_i')}{\partial R_1 \partial R_1'} \eta(\Omega', \vartheta_1') \Big] d\Omega' \, d\vartheta_i'. \quad (13)$$

$$G(\mathbf{R}_1, \vartheta_i; \mathbf{R}_1', \vartheta_i') = -\sum_{QMlm} \frac{1}{k_Q} \tilde{D}^{Q}_{M\varkappa}(\vartheta_i) \tilde{D}^{Q*}_{M\varkappa}(\vartheta_i') \times Y_{lm}(\Omega) Y^*_{ln}(\Omega') j_l(k_Q R_1) h_l(k_Q R_1');$$

$$\xi(\Omega, \vartheta_i) = \int_0^\infty V_1(r, \vartheta) U(\mathbf{r}, \vartheta_i) \, dr;$$

$$\eta_i(\Omega, \vartheta_i) = \int_0^\infty V_1(r, \vartheta) U(\mathbf{r}, \vartheta_i)(r - R_1) \, dr. \quad (14)$$

In the expansion it was considered that the joining conditions make $j_l(kR_1) \sim k/k'$ extremely small while $j_l' \sim 1$; therefore in the expansion of the

products $j_l h_l$ we consider terms of the order $j_l' h_l' (k\Delta R)^2$. Differentiating (12) twice with respect to r we obtain

$$d^2U(\mathbf{r}, \theta_i)/dr^2 = V_1(r, \vartheta)\, U(\mathbf{r}, \theta_i), \tag{15}$$

which is the desired proof.

In accordance with (15) we have

$$U(\mathbf{r}, \theta_i) = A(\Omega, \theta_i)\, \varphi_1(r, \vartheta) + B(\Omega, \theta_i)\, \varphi_2(r, \vartheta), \tag{16}$$

where φ_1 and φ_2 satisfy (15) and the conditions

$$\begin{aligned} &\varphi_1(R_1, \vartheta) = 1;\ \partial\varphi_1(R_1, \vartheta)/\partial R_1 = 0; \\ &\varphi_2(R_1, \vartheta) = 0;\ \partial\varphi_2(R_1, \vartheta)/\partial R_1 = 1. \end{aligned} \tag{17}$$

By joining (16) with the solutions for $r < R_1$ and $r > R_2$ we can obtain A and B and thus complete the solution. The usual method of joining requires that we obtain the derivative $\partial U/\partial r$, which is not desirable because when $U(\mathbf{r}, \theta_i)$ is calculated to terms of the order $k\Delta R$ inclusive, differentiation can reduce the accuracy by one degree. We therefore proceed as follows. According to (12)

$$A = F^{(1)},\quad B = F^{(2)}; \tag{18}$$

$U(\mathbf{r}, \theta_i)$ in the region $R_1 < r < R_2$ is therefore expressed in terms of $\xi(\Omega, \theta_i)$ and $\eta(\Omega, \theta_i)$, which in turn according to (14) depend on the behavior of $U(\mathbf{r}, \theta_i)$ for $R_1 < r < R_2$. Therefore by inserting (16) and (13) in (14) we obtain an equation for ξ and η.

In the next section it will be shown that the excitation amplitude can be expressed simply in terms of ξ and η. The equations for the latter are

$$\xi(\Omega, \theta_i) = F^{(1)}(\Omega, \theta_i)\, \alpha_1(\vartheta) + F^{(2)}(\Omega, \theta_i)\, \alpha_2(\vartheta), \tag{19}$$

$$\begin{aligned} \eta(\Omega, \theta_i) &= F^{(1)}(\Omega, \theta_i)\, \beta_1(\vartheta) + F^{(2)}(\Omega, \theta_i)\, \beta_2(\vartheta), \\ \alpha_{1,2}(\vartheta) &= \int V_1(r, \vartheta)\, \varphi_{1,2}(r, \vartheta)\, dr, \\ \beta_{1,2}(\vartheta) &= \int V_1(r, \vartheta)\, \varphi_{1,2}(r, \vartheta)\, (r - R_1)\, dr. \end{aligned} \tag{20}$$

For simple potentials $V_1(r, \vartheta)$ Eq. (15) can easily be solved; therefore we can assume that $\varphi_1(r, \vartheta)$, $\varphi_2(r, \vartheta)$ and thus $\alpha_{1,2}(\vartheta)$, $\beta_{1,2}(\vartheta)$ are known. The coefficients in (19) are thus determined and our problem is now the solution of the latter.

The pair of integral equations (19) can conveniently be converted into a pair of equations for the coefficients of the expansions of $\xi(\Omega, \theta_i)$ and $\eta(\Omega, \theta_i)$ in terms of the functions $Y_{lm}(\Omega)$ and $\widetilde{D}^{Q}_{M\varkappa}(\theta_i)$, or more precisely for the quantities $\xi^{I}_{Ql;Q_0l_0}$ and $\eta^{I}_{Ql;Q_0l_0}$ defined by

$$\begin{aligned} \xi(\Omega, \theta_i) &= \frac{2\pi^{1/2}}{k} \sum_{\substack{l_0IQ \\ lm}} i^{l_0} \sqrt{2l_0 + 1}\, j_{l_0}(kR_1)\, C^{IM_0}_{QM;\, lm} \\ &\times C^{IM_0}_{Q_0M_0;\, l_00} Y_{lm}(\Omega) \widetilde{D}^{Q}_{M\varkappa}(\theta_i) \xi^{I}_{Ql;Q_0l_0}; \\ \eta(\Omega, \theta_i) &= \frac{2\pi^{1/2}}{k} \sum_{\substack{l_0IQ \\ lm}} i^{l_0} \sqrt{2l_0 + 1}\, j_{l_0}(kR_1)\, C^{IM_0}_{QM;\, lm} \\ &\times C^{IM_0}_{Q_0M_0;\, l_00} Y_{lm}(\Omega)\, \widetilde{D}^{Q}_{M\varkappa}(\theta_i)\, \eta^{I}_{Ql;\, Q_0l_0} \end{aligned} \tag{21}$$

$C^{IM}_{QM;lm}$ are the Clebsch–Gordan coefficients.

Inserting (21) into (19) we obtain

$$\begin{aligned} \xi^{I}_{Ql;\, Q_0l_0} &= K^{I}_{Ql;\, Q_0l_0} - \sum_{Q'l'} K^{I}_{Ql;\, Q'l'} \frac{j_{l'}h_{l'}}{k_{Q'}} [\xi^{I}_{Q'l';\, Q_0l_0} \\ &+ k_{Q'} \Phi_{l'} \eta^{I}_{Q'l';\, Q_0l_0}]; \end{aligned} \tag{22}$$

$$\begin{aligned} \xi^{I}_{Ql;\, Q_0l_0} &= \overline{K}^{I}_{Ql;\, Q_0l_0} - \sum_{Q'l'} \overline{K}^{I}_{Ql;\, Q'l'} \frac{j_{l'}h_{l'}}{k_{Q'}} [\xi^{I}_{Q'l';\, Q_0l_0} \\ &+ k_{Q'} \Phi_{l'} \eta_{Q'l';\, Q_0l_0}], \end{aligned}$$

$$\begin{aligned} &K^{I}_{Ql;\, Q'l'} \\ &= \sum_{\lambda} [(2l + 1)(2l' + 1)(2Q + 1)(2Q' + 1)]^{1/2} \\ &\times C^{\lambda 0}_{l0;\, l'0} C^{\lambda\theta}_{Q\varkappa;\, Q'-\varkappa} W(ll'QQ'; \lambda I)\, (-1)^{I-\varkappa} \tfrac{1}{2} [\alpha_1^{(\lambda)} \\ &+ k_{Q'} \chi_{l'} \alpha_2^{(\lambda)}]; \\ &j_l = j_l(k_Q R_1);\ h_l = h_l(k_Q R_1); \\ &\Phi_l = h_l'/h_l,\ \chi_l = j_l'/j_l; \end{aligned} \tag{23}$$

$W(abcd; ef)$ is the Racah coefficient;

$$\alpha^{(\lambda)}_{1,2} = \int_0^{\pi} \alpha_{1,2}(\vartheta)\, P_\lambda(\cos\vartheta) \sin\vartheta d\vartheta, \tag{24}$$

and $\overline{K}^{I}_{Ql;Q_0l_0}$ differs from $K^{I}_{Ql;Q_0l_0}$ through the replacement of $\alpha_{1,2}(\vartheta)$ by $\beta_{1,2}(\vartheta)$.

If instead of (22) we introduce $\zeta^{I}_{Ql;Q_0l_0}$ as defined by

$$\xi^I_{Ql;\,Q_0l_0} + k_Q\Phi_l\eta^I_{Ql,\,Q_0l_0} = \frac{k}{j_{l_0}h_{l_0}}\left[\delta_{ll_0}\delta_{QQ_0} + \frac{k_Q}{i_lh_l}\zeta^I_{Ql;\,Q_0l_0}\right], \qquad (25)$$

then considering that $1/j_l h_l = \chi_l - \Phi_l$ we obtain

$$-k_Q(\chi_l - \Phi_l)\zeta^I_{Ql;\,Q_0l_0} = \delta_{QQ_0}\delta_{ll_0} + \sum_{Q'l'}(K^I_{Ql;\,Q'l'} + k_Q\Phi_l\bar{K}^I_{Ql;\,Q'l'})\zeta^I_{Q'l';\,Q_0l_0}; \qquad (26)$$

$$\xi^I_{Ql;\,Q_0l_0} = -(k/j_{l_0}h_{l_0})\sum_{Q'l'}K^I_{Ql;\,Q'l'}\zeta^I_{Q'l';\,Q_0l_0},$$

$$\eta^I_{Ql;\,Q_0l_0} = -(k/j_{l_0}h_{l_0})\sum_{Q'l'}\bar{K}^I_{Ql;\,Q'l'}\zeta^I_{Q'l';\,Q_0l_0}. \qquad (27)$$

In the next section the excitation amplitude will be expressed directly in terms of ζ; therefore we shall consider only (26). From the latter it follows that the ζ's are slightly dependent on the energy. Indeed since by virtue of the joining conditions $k\chi_l \sim k'$ is slightly energy dependent the same true for $k(\chi_l - \Phi_l) \sim k'$. Similarly

$$K^I_{Ql;\,Q_0l_0} + k_Q\Phi_l\bar{K}^I_{Ql;\,Q_0l_0} \approx K^I_{Ql;\,Q_0l_0} \approx \text{const.}$$

The complexity of the equations depends on how many of the $K^I_{Ql;Q'l'}$ are non-vanishing for given Q and l (on the number of interconnections). According to (23) this depends on how many coefficients $\alpha^{(\lambda)}_{1,2}$ must be taken into account when the $\alpha_{1,2}(\vartheta)$ are expanded in Legendre polynomials.

In the majority of cases which are of practical interest this number is small and a numerical solution can be obtained. In many practical cases (see Sec. 4) the nondiagonal elements in (26) are small compared with the diagonal elements. This equation can then easily be solved by perturbation theory with the result

$$\zeta^I_{Q_0l_0;Q_0l_0} = -[k(\chi_{l_0} - \Phi_{l_0}) + K^I_{Q_0l_0;\,Q_0l_0} + k_{Q_0}\Phi_{l_0}\bar{K}^I_{Q_0l_0;\,Q_0l_0}]^{-1};$$

$$\zeta^I_{Ql;\,Q_0l_0} = \frac{K_{Ql;\,Q_0l_0} + k_Q\Phi_l\bar{K}^I_{Ql;\,Q_0l_0}}{[k_Q(\chi_l - \Phi_l) + K^I_{Ql;\,Ql} + k_Q\Phi_l\bar{K}^I_{Ql;\,Ql}]}\zeta^I_{Q_0l_0;\,Q_0l_0}; \qquad (28)$$

$$Q \neq Q_0 \quad \text{or} \quad l \neq l_0.$$

This solution is unacceptable if any of the diagonal elements

$$C^I_{Ql} = k_Q(\chi_l - \Phi_l) + K^I_{Ql;\,Ql} + k_Q\Phi_l\bar{K}^I_{Ql;\,Ql}$$

is smaller than any of the nondiagonal elements, in spite of the fact that in general the nondiagonal elements are considerably smaller than the diagonal elements. But the equations can easily be corrected in this case. For this purpose we must in the equation containing this diagonal element retain the nondiagonal terms in the first approximation and append equations for the quantities $\zeta^I_{Q'l';Q_0l_0}$ which appear in these terms. In the nondiagonal elements it is only necessary to retain terms containing $\zeta^I_{Ql;Q_0l_0}$ and $\zeta^I_{Q_0l_0;Q_0l_0}$. By solving these equations we obtain the corrected value of $\zeta^I_{Ql;Q_0l_0}$. We then obtain instead of (28) expressions in which C^I_{Ql} is replaced by

$$C^I_{Ql} - \sum_{Q'l'}(1/C^I_{Q'l'})(K^I_{Ql;\,Q'l'} + k_Q\Phi_l\bar{K}^I_{Ql;\,Q'l'})(K^I_{Q'l';\,Ql} + k_{Q'}\Phi_{l'}\bar{K}^I_{Q'l';\,Ql}).$$

A general solution of (26) can also be obtained in the form of continuous fractions, incorporating the corrections in convenient form.

3. CALCULATION OF THE EXCITATION CROSS SECTION OF ROTATIONAL STATES

The amplitude of a nuclear transition to a state with angular momentum Q and projection M, with simultaneous scattering of the neutron into the solid angle $\Omega_{\mathbf{k}_Q}$ can be written as

$$f_{QM}(\Omega_{\mathbf{k}_Q}) = -\frac{1}{4\pi}\int\psi^{(-)*}_{\mathbf{k}_Q}(\mathbf{r})\,\widetilde{D}^Q_{M\varkappa}(\theta_i)\,V_1(r,\vartheta) \times U(\mathbf{r},\theta_i)\,dr\,d\Omega\,d\theta; \qquad (29)$$

$$\psi^{(-)}_{\mathbf{k}_Q}(\mathbf{r}) = \frac{4\pi}{k_Q}\sum_{lm}i^lY_{lm}(\Omega)\,Y^*_{lm}(\Omega_{\mathbf{k}_Q})\,j^*(k_Qr).$$

Expanding $\psi^{(-)}_{\mathbf{k}_Q}(\mathbf{r})$ in powers of $k_Q(r - R_1)$ and retaining the first two terms, inserting (21) and (27) into (30) and using the equality

$$\sum_{Q'l'} (K^I_{Ql;\,Q'l'} + k_Q \Phi_l \overline{K}^I_{Ql;\,Q'l'})\,\zeta^I_{Q'l';\,Q_0l_0} + k_Q(\chi_l - \Phi_l) \sum_{Q'l'} \overline{K}^I_{Ql;\,Q'l'}\zeta^I_{Q'l';\,Q_0l_0}$$
$$= -\delta_{QQ_0}\delta_{ll_0} - (k_Q/j_l h_l)\left[\zeta^I_{Ql;\,Q_0l_0} - \sum_{Q'l'} \overline{K}^I_{Ql;\,Q'l'}\zeta^I_{Q'l';\,Q_0l_0}\right],$$

we obtain

$$f_{QM}(\Omega) = 2\pi^{1/2} \sum_{ll_0I} \frac{i^{l_0-l}\sqrt{2l_0+1}}{h_{l_0}(kR_1)\,h_l(k_QR_1)} C^{IM_0}_{QM;\,lm} C^{IM_0}_{Q_0M_0;\,l_00} Y_{lm}(\Omega)\, f^I_{Ql;\,Q_0l_0}; \tag{30}$$

$$f^I_{Ql;\,Q_0l_0} = \zeta^I_{Ql;\,Q_0l_0} - \sum_{Q'l'} \overline{K}^I_{Ql;\,Q'l'}\zeta^I_{Q'l';\,Q_0l_0}. \tag{31}$$

With the use of (30) we easily calculate the excitation cross section

$$d\sigma_Q(\Omega)/d\Omega = [k_Q/(2Q_0+1)\,k] \sum_{M,M_0} |f_{QM}(\Omega)|^2$$
$$= \frac{k_Q}{k} \sum_{\substack{ll_0l'l'_0 \\ II'n}} \frac{f^I_{Ql;\,Q_0l_0} f^I_{Ql';\,Q_0l'_0}}{h_l(k_QR_1)\,h_{l_0}(kR_1)\,h^*_{l'}(k_QR_1)h^{*\prime}_{l_0}(kR_1)} N(QQ_0ll_0l'l'_0II'n)\,P_n(\cos\vartheta); \tag{32}$$

$$N(QQ_0ll_0l'l'_0II'n) = \frac{(2I+1)(2I'+1)}{2Q_0+1}[(2l+1)(2l'+1)(2l_0+1)(2l'_0+1)]^{1/2}$$
$$\times (-1)^{l_0+l'_0-Q-Q_0} C^{n0}_{l0;\,l'0} C^{n0}_{l_00;\,l'_00} W(ll'II';nQ)\,W(l_0l'_0II';nQ).$$

Following integration over the angles the result is considerably simplified and the total excitation cross section becomes

$$\sigma_Q = 4\pi \frac{k_Q}{k} \sum_{ll_0I} \frac{2I+1}{2Q_0+1} |f^I_{Ql;\,Q_0l_0}|^2\, |h_l(k_QR_1)\,h_{l_0}(kR_1)|^{-2}. \tag{33}$$

The $f^I_{Ql;Q_0l_0}$ like the $\zeta^I_{Ql;Q_0l_0}$ are only slightly dependent on energy, so that the energy dependence of the cross section is determined mainly by the $|h_l h_{l_0}|^{-2}$ factors, each of which is the product of the penetrabilities of the centrifugal barrier for an incident neutron with angular momentum l_0 and a scattered neutron with angular momentum l.

Since these factors decrease rapidly as l_0 and l increase, only a few terms of the summation in (27) are actually important. For example, when the first rotational level of an even-even nucleus ($Q_0 = 0$, $Q = 2$) is excited by 1–2 Mev neutrons the three important terms of the summation in (33) are those for $l = 0$, $l_0 = 2$; $l = 1$, $l_0 = 1$; $l = 2$, $l_0 = 0$. Eq. (33) is considerably simplified when we consider excitation near the threshold ($k_Q \to 0$). In this case $|h_l|^{-2} \to \delta_l$ and

$$\sigma_Q = 4\pi \frac{k_Q}{k} \frac{2Q+1}{2Q_0+1} \sum_{l_0} \frac{|f^Q_{Q0;\,Q_0l_0}|^2}{|h_{l_0}(kR_1)|^2}. \tag{34}$$

When we consider excitation of the first rotational level, in most cases $kR \ll 1$ and the sum in (34) is reduced to a single term:

$$\sigma_Q = 4\pi \frac{k_Q}{k} \frac{2Q+1}{2Q_0+1} \frac{(kR_1)^{2(Q-Q_0)}}{[(2Q-2Q_0-1)!!]^2} |f^Q_{Q0;\,Q_0Q-Q_0}|^2. \tag{35}$$

The formulae derived enable us to make a rough estimate of the magnitude of the excitation cross section without detailed calculation. The $f^I_{Ql;Q_0l_0}$ like the $\zeta^I_{Ql;Q_0l_0}$ have an average magnitude $\sim 1/k'$. Assuming

$$f^I_{Ql;\,Q_0l_0} \sim f/k', \quad k' = 1{,}4\cdot 10^{13}\ \text{cm}^{-1},$$

we obtain for the excitation cross section of the first rotational level of an even-even nucleus near the threshold

$$\sigma_2 \sim 3\,(k_2/k)\,|f|^2 \cdot 10^{-28}\ \text{cm}^2$$

and for energies near 1 Mev $\sigma_2 \sim 2\times 10^{-25}\,|f|^2$ cm^2.

4. AN ELLIPSOIDAL SQUARE WELL MODEL

We shall consider in this section a square well of ellipsoidal shape; we shall assume

$$V_0(r) = \begin{cases} -k'^2(1+i\xi) & r < R_1 \\ 0 & r > R_1 \end{cases}$$

$$V_1(r,\vartheta) = \begin{cases} -k'^2(1+i\xi) & R_1 < r < R_1 + \Delta R\cos^2\vartheta \\ 0 & r < R_1;\ r > R_1 + \Delta R\cos^2\vartheta. \end{cases} \tag{36}$$

Let us consider a prolate nucleus. It was shown in Ref. 1 that ξ can assumed to be 0.03. Absorption in a layer of thickness ΔR is determined by the magnitude of $k'\Delta R\,\xi$, which is small when $k'\Delta R \sim 1$. The assumptions already made give $k'\Delta R \sim 1$ so that we shall neglect $k'\Delta R\xi$ compared with 1.

Subject to this condition, it follows (15) and (17) that

$$\varphi_1(r,\vartheta) = \cos k'(r - R_1),$$
$$\varphi_2(r,\vartheta) = \sin k'(r - R_1)/k, \tag{37}$$
$$R_1 < r < R_1 + \Delta R\cos^2\vartheta.$$

Furthermore, in accordance with (20)

$$\alpha_1(\vartheta) = -k'\sin(x\cos^2\vartheta);$$
$$\alpha_2(\vartheta) = -1 + \cos(x\cos^2\vartheta); \tag{38}$$
$$\beta_1(\vartheta) = -x\cos^2\vartheta\sin(x\cos^2\vartheta) - \alpha_2(\vartheta);$$

Inserting these expressions in (24) we obtain $\alpha^{(\lambda)}_{1,2}$ and $\beta^{(\lambda)}_{1,2}$ as integrals which are expressed simply in terms of Fresnel integrals. After calculating these integrals we obtain, for example

for $x = 1$:

$$\begin{aligned} &\alpha_1^{(0)} = -0{,}62\,k'; \quad \alpha_2^{(0)} = -0{,}2; \quad \beta_1^{(0)} = -0{,}16; \quad \beta_2^{(0)} = -0{,}09\ 1/k';\\ &\alpha_1^{(2)} = -0{,}23\,k'; \quad \alpha_2^{(2)} = -0{,}1; \quad \beta_1^{(2)} = -0{,}1; \quad \beta_2^{(2)} = -0{,}02\ 1/k';\\ &\alpha_1^{(4)} = -0{,}002\,k'; \quad \alpha_2^{(4)} = -0{,}006; \quad \beta_1^{(4)} = -0{,}1; \quad \beta_2^{(4)} = 0{,}048\ 1/k'; \end{aligned} \tag{39}$$

for $x = 2$:

$$\begin{aligned} &\alpha_1^{(0)} = -1\,k'; \quad \alpha_2^{(0)} = -0{,}34; \quad \beta_1^{(0)} = -0{,}2; \quad \beta_2^{(0)} = -0{,}23\ 1/k';\\ &\alpha_1^{(2)} = -0{,}31\,k'; \quad \alpha_2^{(2)} = -0{,}18; \quad \beta_1^{(2)} = -0{,}09; \quad \beta_2^{(2)} = 0{,}06\ 1/k';\\ &\alpha_1^{(4)} = -0{,}16\,k'; \quad \alpha_2^{(4)} = -0{,}03; \quad \beta_1^{(4)} = -0{,}11; \quad \beta_2^{(4)} = 0{,}045\ 1/k'. \end{aligned} \tag{40}$$

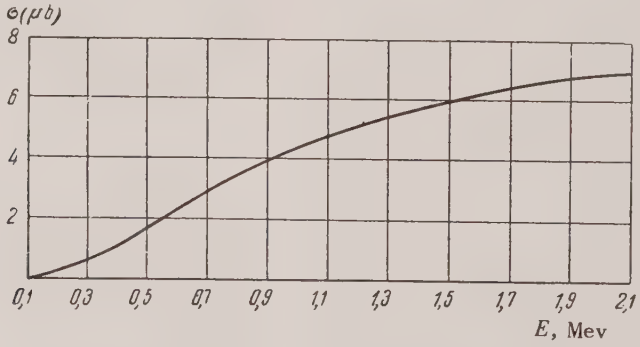

Energy dependence of the excitation cross section of the first rotational level of an even-even nucleus

Inserting (39) or (40) in (23) and (26) we see readily that for these values of $\alpha^{(\lambda)}_{1,2}$ and $\beta^{(\lambda)}_{1,2}$ the non-diagonal elements in (26) are considerably smaller than the diagonal elements, so that the formulas (28) can be used for the $\zeta^{I}_{Ql;Q_0l_0}$. Exceptions are certain values of R_1, *i.e.*, of the mass number A, for which some diagonal element is unusually small. For such values of A the equations must be

solved more exactly. For the values $k'R_1 = 11.2$; $k'\Delta R = 2$ ($\Delta R/R \sim 0.2$; $A \sim 190$) and using the values of $\alpha_{1,2}^{(\lambda)}$ and $\beta_{1,2}^{(\lambda)}$ from (40) we calculated first $\zeta_{2l;0l_0}^{l_0}$ (with (28) applying in this case) and then $f_{2l,0l_0}^{l_0}$ for the excitation of the first rotational level of an even-even nucleus with 0.1 Mev excitation energy.

As has already been indicated, for this case the three important terms in (33) are those with: $f_{22;00}^{0}$, $f_{21;21}^{1}$ and $f_{20;02}^{2}$. The figure shows the result of substituting the values of these quantities in (27).

5. EFFECT OF NUCLEAR DEFORMATION ON THE TOTAL NEUTRON SCATTERING CROSS SECTION

The existence of deformation and rotational levels in nuclei will affect both the elastic cross section and the total scattering cross section. Formulae for these quantities are easily obtained by using the results of the preceding sections.

For the elastic scattering amplitude we easily obtain instead of (30)

$$f_{Q_0M}(\Omega) = 2\pi^{1/2} \sum_{ll_0I} C_{Q_0M;lm}^{IM_0} C_{Q_0M_0;l_00}^{IM_0} Y_{lm}(\Omega) \left[\frac{1}{2ik} \delta_{ll_0} \left(\frac{h_l^*}{h_l} - 1 \right) + \frac{i^{l_0-l}}{h_l^* h_{l_0}} f_{Q_0l;Q_0l_0}^{I} \right] \sqrt{2l_0+1}. \tag{41}$$

The differential and the total elastic scattering cross section σ_{se} differ from (32) and (33) respectively through the replacement of $f_{Ql;Q_0l_0}^{I}$ by the expression in the square brackets in (41). The total cross section can be calculated by using (41) and the optical theorem:

$$(4\pi/k) \operatorname{Im} f_{Q_0M_0}(0) = \sigma = \sigma_{se} + \sigma_c, \tag{42}$$

where $f_{Q_0M_0}(0)$ is the forward scattering amplitude. Averaging $f_{Q_0M_0}(0)$ over the values of M_0 we obtain

$$\sigma = \frac{4\pi}{k} \sum_{I,l_0} \frac{2I+1}{2Q_0+1} \operatorname{Im} \left[\frac{1}{2ik} \left(\frac{h_{l_0}^*}{h_{l_0}} - 1 \right) + h_{l_0}^{-2} f_{Q_0l_0;Q_0l_0}^{I} \right] \tag{43}$$

At low energies ($kR \ll 1$) this expression becomes

$$\sigma = 4\pi (R_1^2 - 2R_1 \operatorname{Re} f_{Q_00;Q_00}^{Q_0}) + \frac{4\pi}{k} \operatorname{Im} f_{Q_00;Q_00}^{Q_0}. \tag{44}$$

It was shown in Ref. 1 that at low energies there exists a simple relation between the total scattering cross section and the ratio of the average level width of a compound nucleus to the average level spacing:

$$\sigma = 4\pi R'^2 + 2\pi^2 k^{-2} \Gamma / D. \tag{45}$$

Hence

$$\frac{\Gamma}{D} = \frac{2}{\pi} k \operatorname{Im} f_{Q_00;Q_00}^{Q_0}. \tag{46}$$

Feshbach, Porter and Weisskopf compared the value of Γ/D which was obtained experimentally with the value that was calculated on an optical model with a spherically symmetrical square potential. A marked deviation was found in the region $A \sim 150 - 160$. The theoretical curve shows a sharp peak in this region, whereas the experimental data do not reveal this peak. Following Bohr and Mottelson these authors state that the discrepancy results from the fact that nuclei of such mass numbers are highly deformed. The matter can investigated by using (46). We are interested in the position of the maximum of $f_{00;00}^{0}$. When $f_{00;00}^{0}$ is calculated by using (28), (31) and (40) we find that the maximum is only slightly shifted by comparison with a spherically symmetrical potential. But (28) cannot be used near the maximum because at the maximum the diagonal element of (26)

$$k(\chi_0 - \Phi_0) + K_{00;00}^{0} + k\Phi_0 K_{00;00}^{0}$$

is extremely small. When the solution of (28) is corrected as shown in Sec. 2 the maximum shows a greater shift. Thus for $k'\Delta R \sim 2$, it is shifted forward $A \sim 175$. This in itself is insufficient to explain the discrepancy. It must be noted, however, that the magnitude of the deformation varies strongly but not monotonically with A. The existence of a deformation in the region $A \sim 150 - 160$ transfers the maximum to another region where the deformation is either much greater or much smaller. Consequently, the maximum may either be nonexistent or much less steep.

In conclusion I wish to express my deep appre-

ciation to K. A. Ter-Martirosian for suggesting the problem and for his assistance.

[1] H. Feshbach, C. E. Porter and V. F. Weisskopf, Phys. Rev. 96, 448 (1954).
[2] A. Bohr, Kgl. Danske Videnskab. Selskab, Mat.-fys. Medd. 26, 4 (1952).
[3] V. N. Gribov, J. Exptl. Theoret. Phys. (U.S.S.R.) this issue, p. 647, Soviet Physics JETP 5, 537 (1957).

Translated by I. Emin
182

SOVIET PHYSICS JETP VOLUME 5, NUMBER 4 NOVEMBER, 1957

Covariant Equation for Two Annihilating Particles

A. I. ALEKSEEV
Moscow Institute of Engineering and Physics

(Submitted to JETP editor April 10, 1956)
J. Exptl. Theoret. Phys. (U.S.S.R.) 32, 852-862 (April, 1957)

The functional-derivative technique is used to investigate the annihilation (or production) of two interacting particles which may also exist in a bound state. Covariant equations have been found for the Green function (probability amplitude) which describes the annihilation of an electron and a positron into two quanta as well as for the Green function of the reverse process. The equations thus obtained have been used to solve the problem of interaction between the electron and positron during pair production (or annihilation) with account of radiative corrections.

RELATIVISTICALLY invariant equations for bound states were obtained by various authors[1-5]. Not enough attention, however, was paid to equations that take into account a possible annihilation of particles. In the present work the functional-derivative technique is applied to the solution of the problem concerning the annihilation (or production) of two interacting particles which may also exist in a bound state. While up to now functional equations were derived for the probability amplitudes (Green functions) describing transitions not accompanied by any change in the number of particles, in the present case functional equations have been set up for the probability amplitudes (Green functions) describing the annihilation or production of particles. The resulting equations are, therefore, of a different form. Starting with these equations, it is easy to obtain the wave equation of positronium, the possible annihilation of the electron and positron being taken into the account[6]. Such generalization of the method of functional derivatives to problems involving a change in the number of particles during the studied process enables us to calculate with any desired accuracy the probability of a two-photon (and in general, n-photon) annihilation of particles existing in a bound state. The results of previous works[7-9] dealing with the annihilation of two interacting particles in the S and P states are essentially reproduced if we limit ourselves to the first non-vanishing approximation. The contribution of Coulomb interaction in pair production is also accounted[10]. The proposed method, however, makes it also possible to find the radiative corrections for the above processes (*cf.*, Ref. 11 and 12). The investigation of radiative corrections for the probability of photoproduction and annihilation of positronium confirms the results of Ref. 13 with respect to the infra-red divergence in bound states of the particles.

1. DERIVATION OF THE EQUATION FOR THE GREEN FUNCTION OF TWO PARTICLES ANNIHILATING INTO TWO QUANTA

The Green function $G_2(x_1 x_2, \xi\xi')$ describing the transmutation of two photons into an electron-positron pair (and the two-photon annihilation of the particles as well) is defined, according to Ref. 14, in the following way:

$$G_2(x_1x_2, \xi\xi') \equiv \frac{\delta^2 G(x_1x_2)}{\delta J(\xi)\,\delta J(\xi')}\Big|_{J=0} = i\langle\psi(x_1)\bar{\psi}(x_2)A(\xi)A(\xi')\rangle - i\langle\psi(x_1)\bar{\psi}(x_2)\rangle\langle A(\xi)A(\xi')\rangle, \quad (1)$$

where $G(x_1x_2)$ is the Green function of one particle[1], $J(x)$ is the external current, and $\delta/\delta J(x)$ denotes the functional derivative with respect to the current[1]. $\psi(x)$ and $A(\xi)$ are the operators of the free fields of electrons and photons respectively, and the brackets $\langle\ldots\rangle$ should be understood to mean, for example,

$$\langle\psi(x_1)\bar{\psi}(x_2)\rangle = [T(\psi(x_1)\bar{\psi}(x_2)S)]_{\text{vac}}S^{-1}_{\text{vac}} = [ST(\psi(x_1)\bar{\psi}(x_2))]_{\text{vac}}S^{-1}_{\text{vac}}, \quad (1')$$

where the subscript "vac" indicates that the corresponding expression is averaged over the state of the vacuum. The index T denotes the T-product of operators standing within the parentheses and, operators in the Heisenberg representation are everywhere in boldface. Furthermore,

$$S = T\left(\exp\left\{-i\int H_{\text{int}}(x)\,d^4x\right\}\right),$$

$$H_{\text{int}}(x) = (-J(x) + j(x))A(x), \quad (1'')$$

$$j_\mu(x) = \frac{e}{2}\gamma^\mu_{\alpha\beta}(\bar{\psi}_\alpha(x)\psi_\beta(x) - \psi_\beta(x)\bar{\psi}_\alpha(x)), \quad (1''')$$

while $\bar{\psi} = \psi^*\gamma^0$, $\gamma^0 = \beta$ and $\gamma^{1,2,3} = \beta a^{1,2,3}$. Besides, the system of units in which $\hbar = c = 1$ is always used and the following summation rule is adopted: $ab = a_0b_0 - a_1b_1 - a_2b_2 - a_3b_3$.

In order that the electron and positron (with coordinates x_1 and x_2 respectively) enter the theory symmetrically, we shall go over in Eq. (1) to the charge-conjugate field with respect to variable x_2, *i.e.*, we shall exchange $\bar{\psi}(x_2)$ by $\psi'(x_2)$, so that the Green function G_{ep} describing the transmutation of two photons into an electron and a positron will be now of the following form:

$$G_{\text{ep}}(x_1x_2, \xi\xi') = i\langle\psi(x_1)\psi'(x_2)A(\xi)A(\xi')\rangle - i\langle\psi(x_1)\psi'(x_2)\rangle\langle A(\xi)A(\xi')\rangle, \quad (2)$$

where $\psi'(x_2)$ is the field operator, charge conjugate with $\psi(x_2)$:

$$\psi'_\sigma(x) = C_{\sigma\rho}\bar{\psi}_\rho(x), \quad \psi_\sigma(x) = C_{\sigma\rho}\bar{\psi}'_\rho(x),$$

$$C^{*T} = C^{-1}, \quad C^T = -C, \quad C\gamma^T = -\gamma C.$$

We shall define the Green function $\bar{G}_{\text{ep}}$ describing the reverse process, *i.e.*, the annihilation of an electron and a positron with the emission of two quanta, in the following way:

$$\bar{G}_{\text{ep}}(\xi\xi', x_2x_1) = i\langle A(\xi)A(\xi')\bar{\psi}'(x_2)\bar{\psi}(x_1)\rangle - i\langle A(\xi)A(\xi')\rangle\langle\bar{\psi}'(x_2)\bar{\psi}(x_1)\rangle. \quad (3)$$

It can be easily seen that all the relations obtained for $G_{\text{ep}}(x_1x_2, \xi\xi')$ will be fulfilled for the function $\bar{G}_{\text{ep}}(\xi\xi', x_2x_1)$ if we make the following substitutions:

$$\gamma \to \gamma^T, \quad C \to C^{-1}, \quad p \to -p \quad (4)$$

(the last one for the momentum of both the electron and the positron). We shall limit ourselves therefore to the derivation of the equation for G_{ep} only, since from this will follow automatically, taking into account relation (4), the equation for $\bar{G}_{\text{ep}}$.

In the following it is convenient to make use of the matrix notation of Karplus and Klein, which consists in the following: the set of all coordinates and the spinor indices of a particle will be denoted by one number, while ξ (or ξ', $\xi''\ldots$) will be denote the set of all coordinates and projections of the photon polarization vector. The matrix index will be represented as the argument of a function, being a number in the case of a particle and ξ (or ξ', $\xi''\ldots$) in the case of a photon. Summation is understood in case of repeating arguments (for the spin indices and the projections of the polarization vectors) and integration in the case of coordinate variables. In this notation, the functions $\gamma(\xi, 12)$ and $C(12)$ have the following meanings:

$$\gamma(\xi, 12) \equiv \gamma^\nu_{\alpha_1\alpha_2}\delta(\xi - x_1)\delta(x_1 - x_2),$$

$$C(12) \equiv C_{\alpha_1\alpha_2}\delta(x_1 - x_2).$$

To find the equation satisfied by the function $G_{\text{ep}}(12, \xi\xi')$ we shall introduce, following Schwinger[1], the auxiliary function $J(\xi)$ of the external sources of the photon field [$J(\xi)$ does not contain field operators], *i.e.*, we shall assume again that the interaction operator H_{int} is of the form $H_{\text{int}} = (-J + j)A$. All the Green functions determined above will then represent functionals of the

sources J, depending on them through the operator $S(1'')$. It should be assumed henceforth that $J = 0$ when the Green function is applied to the calculation of real physical processes.

If we make use now of the fact that in the Heisenberg representation the electron and positron operators fulfill the Dirac equation, respectively,*

$$(p(11') - e\gamma(\bar{\xi}, 11')\mathbf{A}(\bar{\xi}) - m\delta(11'))\psi(1') = 0, \tag{5}$$

$$(p(22') + e\gamma(\bar{\xi}, 22')\mathbf{A}(\bar{\xi}) - m\delta(22'))\psi'(2') = 0, \tag{5'}$$

we can write the functional derivative equation for $G_{ep}(12, \xi\xi')$. In fact, applying the operator $p(11') - m\delta(11')$ to the function G_{ep} and taking into account relations (5) and (5') we obtain

$$\begin{aligned}&(p(11') - m\delta(11'))G_{ep}(1'2, \xi\xi')\\ &= ie\gamma(\bar{\xi}, 11')\langle A(\bar{\xi})\psi(1')\psi'(2)A(\xi)A(\xi')\rangle\\ &- ie\gamma(\bar{\xi}, 11')\langle A(\bar{\xi})\psi(1')\psi'(2)\rangle\langle A(\xi)A(\xi')\rangle.\end{aligned} \tag{6}$$

Making use of the self-evident equalities

$$\begin{aligned}\frac{\delta}{\delta J(\bar{\xi})}\langle\psi(1)\psi'(2)\rangle &= i\langle A(\bar{\xi})\psi(1)\psi'(2)\rangle\\ &- i\langle\psi(1)\psi'(2)\rangle\langle A(\bar{\xi})\rangle,\\ \frac{\delta}{\delta J(\bar{\xi})}\langle\psi(1)\psi'(2)A(\xi)A(\xi')\rangle &= i\langle A(\bar{\xi})\psi(1)\psi'(2)A(\xi)A(\xi')\rangle\\ &- i\langle\psi(1)\psi'(2)A(\xi)A(\xi')\rangle\langle A(\bar{\xi})\rangle\end{aligned} \tag{7}$$

we can write Eq. (6) in the following form:

$$\begin{aligned}&\mathscr{F}^e(11')G_{ep}(1'2, \xi\xi')\\ &= e\gamma(\bar{\xi}, 11')\langle\psi(1')\psi'(2)\rangle\frac{\delta}{\delta J(\bar{\xi})}\langle A(\xi)A(\xi')\rangle,\end{aligned} \tag{8}$$

where the following notation has been introduced:

$$\begin{aligned}\mathscr{F}^e(11') \equiv p(11') &- e\gamma(\bar{\xi}, 11')\langle A(\bar{\xi})\rangle - m\delta(11')\\ &+ ie\gamma(\bar{\xi}, 11')\delta/\delta J(\bar{\xi}).\end{aligned} \tag{9}$$

If we apply from the left the operator $F^p(22')$, which differs from

$$\begin{aligned}\mathscr{F}^p(22') \equiv p(22') &+ e\gamma(\bar{\xi}, 22')\langle A(\bar{\xi})\rangle\\ &- m\delta(22') - ie\gamma(\bar{\xi}, 22')\delta/\delta J(\bar{\xi})\end{aligned}$$

by replacing $m\delta(22') + ie\gamma(\bar{\xi}, 22')\delta/\delta J(\bar{\xi})$ by the mass operator (*cf.*, Ref. 1) $M^p(22')$ and from $F^e(11')$ by the sign of the charge, to both sides of equation (8), we shall obtain the following functional equation for G_{ep}:

$$\begin{aligned}&F^p(22')\mathscr{F}^e(11')G_{ep}(1'2', \xi\xi')\\ &= -e\gamma(\bar{\xi}, 11')C(1'2)\frac{\delta}{\delta J(\bar{\xi})}D(\xi\xi')\\ &- ie\gamma(\bar{\xi}, 11')C(1'2)\frac{\delta}{\delta J(\bar{\xi})}\langle A(\xi)\rangle\langle A(\xi')\rangle,\\ &D(\xi\xi') \equiv \frac{\delta}{\delta J(\xi')}\langle A(\xi)\rangle;\end{aligned} \tag{10}$$

where $D(\xi, \xi')$ is the photon Green function[1].

It is convenient to write the first term of the right-hand side of Eq. (10) in another form, making use of the relation

$$\begin{aligned}&-e^2\gamma(\bar{\xi}, 11')C(1'2)\frac{\delta}{\delta eJ(\bar{\xi})}D(\xi\xi')\\ &= ie^2\gamma(\bar{\xi}, 13)C(32)D^0(\bar{\xi}\xi')\\ &\times C^{-1}(2'3')\gamma(\bar{\xi}', 3'1')G_{ep}(1'2', \xi\xi'),\end{aligned} \tag{11}$$

the correctness of which can be easily ascertained expanding both sides of Eq. (11) in a series in e^2. D^0 denotes the zero approximation of the Green function of the photon.

$$\begin{aligned}&\{F^p(22')F^e(11') - I(12,1'2')\}G_{ep}(1'2', \xi\xi')\\ &= -ie\gamma(\bar{\xi}, 11')C(1'2)\frac{\delta}{\delta J(\bar{\xi})}\langle A(\xi)\rangle\langle A(\xi')\rangle,\end{aligned} \tag{12}$$

where the interaction operator is defined, according to (10) and (11), in the following way:

$$\begin{aligned}&I(12, 1'2')G_{ep}(1'2', \xi\xi')\\ &= ie^2\gamma(\bar{\xi}, 13)C(32)D^0(\bar{\xi}\bar{\xi}')\\ &\times C^{-1}(2'3')\gamma(\bar{\xi}', 3'1')G_{ep}(1'2', \xi\xi')\\ &+ F^p(22')\left[m\delta(11') - ie\gamma(\bar{\xi}, 11')\frac{\delta}{\delta J(\bar{\xi})}\right.\\ &\left. - M^e(11')\right]G_{ep}(1'2', \xi\xi').\end{aligned} \tag{13}$$

Eq. (13) may be transformed by means of Eq. (12) into a functional equation for the operator I:

* $p(12) \equiv i\delta(x_1 - x_2)\gamma^\nu_{\alpha_1\alpha_2}\partial/\partial x_2^\nu$.

$$I(12,1'2')\,G_{ep}(1'2',\xi\bar{\xi}') = ie^2\gamma(\bar{\xi},11')\,D(\xi\bar{\xi}')\,\Gamma^p(\bar{\xi}',22')\,G_{ep}(1'2',\xi\bar{\xi}')$$
$$+ ie^2\gamma(\bar{\xi},13)\,C(32)\,D^0(\xi\bar{\xi}')\,C^{-1}(2'3')\,\gamma(\bar{\xi}',3'1')\,G_{ep}(1'2',\xi\bar{\xi}') -$$
$$- e^2\gamma(\bar{\xi},11')\,G^e(1'3)\,\gamma(\bar{\xi}',33')\,C(3'2)\,\frac{\delta^2}{\delta J(\bar{\xi})\,\delta J(\bar{\xi}')}\langle A(\xi)\rangle\langle A(\xi')\rangle \qquad (14)$$
$$- ie^2\gamma(\bar{\xi},11')\,G^e(1'3)\,\frac{\delta}{\delta eJ(\bar{\xi})}(I(32,3'2')\,G_{ep}(3'2',\xi\bar{\xi}')),$$

where

$$\Gamma^p(\xi,22') \equiv \delta F^p(22')/\delta e\langle A(\xi)\rangle,$$

$$\Gamma^e(\xi,11') \equiv -\delta F^e(11')/\delta e\langle A(\xi)\rangle$$

denote vertex operators.

Since the term in Eq. (14) containing the functional derivative of (IG_{ep}) is of secondary importance compared with other terms (this term includes the radiative corrections), Eq. (14) can be solved for the operator I by the method of successive approximations. This makes it possible to find the interaction operator in any approximation of e^2. If the iteration process of solution of Eq. (14) is continued ad infinitum, the operator I will be represented as the sum of an infinite number of terms corresponding to all the irreducible diagrams[2] describing both the electron-positron interaction and their two-photon annihilation. The interaction operator found in this way yields, upon substitution in Eq. (12), when $J = 0$, the covariant equation for the determination of the Green function G_{ep}.

It should be noted that, although the interaction operator I is found in the form of a series in e^2, the fact that we obtain the corresponding approximations of the Green function G_{ep} does not mean that this function has been expanded in powers of the charge. The situation we encounter here is similar to the case of the Bethe-Salpeter equation[2]. In fact, if we retain in the operator only the terms proportional to e^2, then it is equivalent in the S-matrix scheme to accounting, in the infinite sum determining G_{ep}, of an infinite number of reducible diagrams of the ladder type* (Fig. 2) beside the irreducible diagram of Fig. (1).

FIG. 1.

In order to obtain finite results (for $J = 0$) it is necessary to carry out a renormalization of the operators $F(11')$, $F(22')$ and $I(12, 1'2')$ in Eq. (12) at all degrees of approximation in e^2. As it can be seen from Eq. (14) and the relation $F = G^{-1}$, the renormalization of $F(11')$, $F(22')$ and $I(12, 1'2')$ is carried out in the usual way (*cf.*, for example, Ref. 14)

Eq. (12) will take the following form for $J = 0$ and for the operator I corresponding to the first non-vanishing approximation in e^2

$$\{F^0(22')\,F^0(11') - ie^2\gamma(\bar{\xi},11')\,D^0(\xi\bar{\xi}')\,\gamma(\bar{\xi}',22')$$
$$- ie^2\gamma(\bar{\xi},13)\,C(32)\,D^0(\xi\bar{\xi}')\,C^{-1}(2'3')\,\gamma(\bar{\xi}',3'1')\}\,G_{ep}(1'2',\xi\bar{\xi}') \qquad (15)$$
$$= -e^2\gamma(\bar{\xi},11')\,G^0(1'3)\,\gamma(\bar{\xi}',33')\,C(3'2)\,(D^0(\xi\bar{\xi})\,D^0(\bar{\xi}'\xi') + D^0(\xi\bar{\xi}')\,D^0(\bar{\xi}'\xi)),$$

where the index 0 denotes that the functions are taken in the lowest order in e^2. The indices p and e in G and F may be dropped for $J = 0$.

The first term of the operator I in (15) represents the interaction of particles by means of exchange of one virtual quantum, while the second one refers to the interaction of particles due to a single-photon virtual annihilation.

Hereinafter we shall be interested in the interaction operator I, taken with an accuracy of e^4. For this purpose, it is necessary to calculate in Eq. (14) the variational derivative of $(I^{(1)}G_{ep})$ with respect to the current, where $I^{(1)}$ is the first non-

*For brevity we omitted diagrams corresponding to the single-photon virtual annihilation of particles.

FIG. 2.

vanishing approximation of the operator I. Besides, in all other terms of the right-hand side of Eq. (14) the functions G, D and Γ should be taken in such approximation that the terms up to e^4 inclusively should be taken into account.

For the calculation of the variational derivative it is convenient to represent $(I^{(1)}G_{ep})$, by means of relations (14) and (12), in the following way:

$$\begin{aligned}
&\{(F^p(22')F^e(11') - ie^2\gamma(\bar{\xi}, 11')D^0(\bar{\xi}\bar{\xi}')\gamma(\bar{\xi}', 22')\\
&- ie^2\gamma(\bar{\xi}, 13)C(32)D^0(\bar{\xi}\bar{\xi}')C^{-1}(2'3')\gamma(\bar{\xi}', 3'1'))G^e(1'5)G^p(2'4)\}\\
&\times I^{(1)}(54, 5'4')G_{ep}(5'4', \xi\xi') =\\
&= -e^2\gamma(\bar{\xi}, 11')G^e(1'3)\gamma(\bar{\xi}', 33')C(3'2)\frac{\delta^2}{\delta J(\bar{\xi})\delta J(\bar{\xi}')}\langle A(\xi)\rangle\langle A(\xi')\rangle\\
&+ e^3\gamma(\bar{\xi}, 11')D^0(\bar{\xi}\bar{\xi}')\gamma(\bar{\xi}', 22')G^e(1'3)G^p(2'4)\gamma(\bar{\bar{\xi}}33')C(3'4)\\
&\times\frac{\delta}{\delta J(\bar{\bar{\xi}})}\langle A(\xi)\rangle\langle A(\xi')\rangle + e^3\gamma(\bar{\xi}, 13)C(32)D^0(\bar{\bar{\xi}}\bar{\xi}')C^{-1}(2'3')\\
&\times\gamma(\bar{\xi}', 3'1')G^e(1'5)G^p(2'4)\gamma(\bar{\bar{\xi}}, 55')C(5'4)\frac{\delta}{\delta J(\bar{\bar{\xi}})}\langle A(\xi)\rangle\langle A(\xi')\rangle.
\end{aligned} \tag{16}$$

Denoting for the time being the left-hand side of Eq. (16) by $\Lambda(12, 54)I^{(1)}(54, 5'4')G_{ep}(5'4', \xi\xi')$ and the right hand side by $B(12, \xi\xi')$, we shall rewrite Eq. (16) in the form

$$\Lambda(I^{(1)}G_{ep}) = B. \tag{17}$$

From this we obtain the expression for the required derivative

$$\partial(I^{(1)}G_{ep})/\partial J = -\Lambda^{-1}\frac{\delta\Lambda}{\delta J}(I^{(1)}G_{ep}) + \Lambda^{-1}\frac{\delta B}{\delta J}. \tag{18}$$

After a calculation we obtain (for $J = 0$) the following expression for the interaction operator I with accuracy up to e^4:

$$\begin{aligned}
&I(12, 1'2')G_{ep}(1'2', \xi\xi') = I_i(12, 1'2')G_{ep}(1'2', \xi\xi')\\
&- e^2\Gamma(\bar{\xi}, 11')G(1'3)\Gamma(\bar{\xi}', 33')C(3'2)(D(\bar{\xi}\bar{\xi})D(\bar{\xi}'\xi') + D(\bar{\xi}\bar{\xi}')D(\bar{\xi}'\xi)),
\end{aligned} \tag{19}$$

where

$$\begin{aligned}
&I_i(12, 1'2') = ie^2\Gamma(\bar{\xi}, 11')D(\bar{\xi}\bar{\xi}')\Gamma(\bar{\xi}', 22')\\
&+ ie^2\gamma(\bar{\xi}, 13)C(32)D^0(\bar{\xi}\bar{\xi}')C^{-1}(2'3')\gamma(\bar{\xi}', 3'1')\\
&+ (ie^2)^2\gamma(\bar{\bar{\xi}}, 13)G^0(33')\gamma(\bar{\xi}, 3'1')D^0(\bar{\xi}\bar{\xi}')D^0(\bar{\bar{\xi}}\bar{\bar{\xi}}')\gamma(\bar{\xi}', 24)G^0(44')\gamma(\bar{\bar{\xi}}', 4'2')\\
&+ (ie^2)^2\gamma(\bar{\bar{\xi}}, 13)G^0(33')\gamma(\bar{\xi}, 3'5)C(52)D^0(\bar{\xi}\bar{\xi}')D^0(\bar{\bar{\xi}}\bar{\bar{\xi}}')\\
&\times[C^{-1}(1'4)\gamma(\bar{\xi}', 44')G^0(4'6)\gamma(\bar{\bar{\xi}}', 62')\\
&- C^{-1}(2'7')\gamma(\bar{\xi}', 7'7)G^0(75')\gamma(\bar{\bar{\xi}}', 5'1')].
\end{aligned} \tag{19'}$$

As it can be easily seen, the interaction operator I (19) contains two groups of terms. The first group, denoted by I_i, is determined by the effects of exchange of one and of two virtual quanta and the one-and two-photon virtual pair annihilation. This group coincides exactly with the electron-positron interaction operator, found in Ref. 6. The second group of terms in expression (19) is determined by

the possibility of the real annihilation of particles.

The required equation for the Green function G_{ep} with the interaction operator I calculated up to e^4 inclusively is of the form:

$$\{F(22')F(11') - I_i(12, 1'2')\}G_{ep}(1'2', \bar{\xi}\bar{\xi}') = -e^2\Gamma(\bar{\xi}, 11')G(1'3)\Gamma(\bar{\xi}', 33')C(3'2)(D(\bar{\xi}\bar{\xi}') D(\bar{\xi}'\bar{\xi}') + D(\bar{\xi}\bar{\xi}')D(\bar{\xi}'\bar{\xi}).) \quad (20)$$

where the operators $F(11')$ and $F(22')$ contain also the radiative corrections up to terms proportional to e^4. The latter can be easily found if we note that $F = G^{-1}$ and make use of the corresponding corrections [15] to the single-particle Green function G.

Eq. (20) describes the production (or the annhilation, if transformation (4) is carried out) of free and bound particles. It can be applied as well to the calculation of radiative corrections to the photoproduction and the single-photon annihilation of positronium in an external field. The application of Eq. (20) leads to the following wave equation of the electron and positron with possible annihilation of the particles:

$$\{F(22')F(11') - I_i(12, 1'2')\}\Psi(1'2') = 0, \quad (21)$$

where $\Psi(1'2')$ is the wave function of the electron and positron and the operators F and I_i were defined above. This wave equation for the system electron-positron was obtained by another method in the work of Karplus and Klein[6].

The generalization of the results for the case of the n-photon annihilation of particles is straightforward.

2. ACCOUNT OF THE INTERACTION BETWEEN THE ELECTRON AND POSITRON DURING PAIR PRODUCTION

As an application of equations derived in the preceding paragraph we shall consider the problem of accounting for the electron-positron interaction during pair production (or annihilation), paying attention to radiative corrections.

The interaction between the electron and positron is usually not taken into account in all calculations of pair production. The final state of each particle is considered as free. This is caused by a considerable simplification of calculations involved, since accounting for the interaction between the components of a pair correspond to taking into the account the higher approximations of the scattering matrix.

It was established by Sakharov[10] that for the case of a small relative velocity of produced particles, the account of the Coulomb interaction reduces to the multiplication of the differential cross-section $d\sigma_f$ of the free-particle production by the factor $|\psi(0)|^2 / |\psi_f(0)|^2$, where $\psi(x)$ is the non-relativistic wave function of interacting particles in the relative system of coordinates and $\psi_f(x)$ is the wave function of free particles,

$$d\sigma = (|\psi(0)|^2 / |\psi_f(0)|^2)\, d\sigma_f \quad (22)$$

where $d\sigma$ is the differential cross-section with the interaction between the produced particles taken into account.

We shall show in which way relation (22) should be generalized for the case of arbitrary relative velocity of produced particles and an arbitrality high degree of approximation.* For the sake of generality we shall deal first with interacting particles which are not necessarily in a bound state, while for simplicity we shall study in detail the case of pair production by two quanta. For the case of photoproduction in an external field it is necessary to add to the matrix element considered below a certain number of matrix elements corresponding to the single, triple, *etc.*, scattering of the produced particle by the external field (higher Born approximations). These matrix elements can be found by means of the Green functions $G_{ep}(12, \xi\xi'\xi'')$, $G_{ep}(12, \xi\xi'\xi''\xi''')$, *etc.*, describing pair production by two quanta with the complementary emission of one, two, *etc.*, quanta. The given proof is afterwards extended for the case of pair production in an external field.

a) *First non-vanishing approximation*

The relation (22) can be easily obtained if we make use of the expression (15) for the Green function describing the photoproduction of interacting particles. In fact, the solution of Eq. (15) is of the form

*The problem whether Eq. (22) remains correct for higher approximations was considered by Sakharov[10]. In that work, however, the meaning of higher approximations remains unclear, since non-covariant perturbation theory is used.

$$G_{ep}(12,\bar{\xi}\bar{\xi}') = -e^2 K(12,1'2')\,\gamma(\bar{\xi},1'3)\,G^0(33')\,\gamma(\bar{\xi}',3'5)\,C(52')\,(D^0(\bar{\bar{\xi}}\bar{\xi})\,D^0(\bar{\bar{\xi}}'\bar{\xi}') + D^0(\bar{\bar{\xi}}\bar{\xi}')\,D^0(\bar{\bar{\xi}}'\bar{\xi})), \tag{23}$$

where $K(12, 1'2')$ is the Green function of the interacting electron and positron. Making use of Eq. (23) we can write the amplitude $\mathcal{A}$ of photoproduction of particles as

$$\begin{aligned}\mathcal{A} &= -e^2\bar{\Psi}(12)\,\gamma(\bar{\xi},11')\\ &\times G^0(1'3)\,\gamma(\bar{\xi}',33')\,C(3'2)\,\Phi_{kk'}(\bar{\xi}\bar{\xi}')\\ &= -2\frac{-e^2}{V\sqrt{k_0 k_0'}}\int\bar{\Psi}(x_1x_2)(\hat{l}^r G^0(x_1x_2)\hat{l}^{r'}Ce^{i(kx_1+k_2)}\\ &+\hat{l}^{r'}G^0(x_1x_2)\hat{l}^r Ce^{i(kx_2+k'x_1)})d^4x_1\,d^4x_2,\end{aligned} \tag{24}$$

where the wave function of produced particles $\Psi(12)$ fulfills Eq. (21), with the operator I_1 containing only terms proportional to e^2.

$$\Phi_{kk'}(\bar{\xi}\bar{\xi}') = \frac{1}{2}(k_0k_0')^{-1/2}[l^r_{\nu_{\bar{\xi}}}\,l^{r'}_{\nu_{\bar{\xi}'}}\exp i(k\bar{\xi}+k'\bar{\xi}') + l^r_{\nu_{\bar{\xi}'}}\,l^{r'}_{\nu_{\bar{\xi}}}\exp i(k\bar{\xi}'+k'\bar{\xi})]$$

is the symmetrized function of photons with momenta k and k' and polarization l^r and $l^{r'}$, while $\hat{l} = \gamma^\nu l_\nu$.

The calculation of the matrix element (24) with the exact function $\Psi(12)$ of interacting particles is difficult. We shall, therefore, as in the non-relativistic case (22), find the relation between the photoproduction amplitude of interacting particles and the amplitude of photoproduction of particles which are free in the final state, this task being much more simple.

The wave function $\Psi^{E\sigma}(x_1x_2)$ of interacting particles, entering into Eq. (24), is an eigenfunction of the total energy E and also of all other constants of motion σ, forming the given full set of physical values. We shall denote by $\Psi_f^{E\sigma}(x_1x_2)$ the wave function of free particles which is an eigenfunction of the full set E and σ. Since, however, the equations of motion (determining the eigenvalues of E) of the wave functions $\Psi^{E\sigma}$ and $\Psi_f^{E\sigma}$ are different, the following expansion is true:

$$\Psi^{E\sigma}(x_1x_2) = \int C(E,E')\,\Psi_f^{E'\sigma}(x_1x_2)\,dE'. \tag{25}$$

The coefficient $C(E, E')$ is a δ-like function with a sharp maximum at the point $E' = E$, while interaction disappears, $e^2 \to 0$, the coefficient $C(E, E')$ tends to $\delta(E - E')$. This means that the essential domain of integration over E' is, for the coefficient $C(E, E')$, the region close to E. We shall, therefore, bring the smooth (with respect to E') function $\Psi_f^{E'\delta}$ outside the integral sign at the maximum point of the coefficient ($E = E'$), and obtain as an approximation

$$\Psi^{E\sigma}(x_1x_2) = \left(\int C(E,E')\,dE'\right)\Psi_f^{E\sigma}(x_1x_2) \equiv N\,\Psi_f^{E\sigma}(x_1x_2), \tag{26}$$

where the coefficient N is defined by the relation

$$\psi_f^{E\sigma}(0) = N\,\psi_f^{E\sigma}(0). \tag{27}$$

where $\psi^{E\sigma}(0)$ and $\psi_f^{E\sigma}(0)$ are the same wave functions as in Eq. (26) in relative coordinates, taken at the point $x = 0$. For the square of the absolute value of N we have

$$|N|^2 = \bar{\psi}_{\alpha_2\alpha_1}(0)\,\psi_{\alpha_1\alpha_2}(0)\,/\,\bar{\psi}_{f\,\beta_2\beta_1}(0)\,\psi_{f\,\beta_1\beta_2}(0), \tag{28}$$

(identical indices denote summation and the indices E and σ are omitted).

The amplitude (24) of the photoproduction of interacting particles can be now written, making use of (26), as follows:

$$\begin{aligned}\mathcal{A} = N^*[&-e^2\bar{\Psi}_f(12)\,\gamma(\bar{\xi},11')\\ &G^0(1'3)\,\gamma(\bar{\xi}',33')\,C(3'2)\,\Phi_{kk'}(\bar{\xi}\bar{\xi}')].\end{aligned} \tag{29}$$

The coefficient of N^* in (29) represents the amplitude of photoproduction of free particles.

Consequently, if we denote the differential cross-section for the photoproduction of free particles by $d\sigma_f$, the differential cross-section $d\sigma$ for the photoproduction of a pair of interacting particles can be written in the form

$$d\sigma = [(\bar{\psi}(0)\,\psi(0))\,/\,(\bar{\psi}_f(0)\,\psi_f(0))]\,d\sigma_f, \tag{30}$$

where $(\bar{\psi}(0)\,\psi(0)) = \mathrm{Sp}[\bar{\psi}(0)\,\psi(0)]$, and the wave functions (in relative coordinates) ψ and ψ_f of interacting and free particles respectively are eigenfunction of the same set of values.

In contrast to Eq. (22), Eq. (30) is true for arbitrary relative velocities of produced particles, in-

cluding relativistic values. For small relative velocities of the produced particles the coefficient $(\bar{\psi}(0)\psi(0))$ is equal to its non-relativistic value and relation (30) coincides with formula (22) given by Sakharov [10].

If pair production takes place in the external field of a nucleus of charge Ze, then, in order that Eq. (30) be applicable, it is necessary that the produced particles move with relativistic velocities (namely $Ze^2/\hbar v_1 \ll 1$, $Ze^2/\hbar v_2 \ll 1$), since in derivation of Eq. (30) the external field is regarded as a perturbation, while the relative velocity of these particles can be arbitrarily small.

We shall prove that Eq. (30) remains in force when we take into the account radiative corrections of any order. $(\bar{\psi}(0)\psi(0))$ should then be calculated in Eq. (30) with the same accuracy that is chosen for $d\sigma_f$.

b) *Radiative corrections*

The amplitude of the photoproduction of the interacting electron and positron can be written using Eq. (20) as an approximation with first order radiative corrections:

$$\begin{aligned}\mathcal{A} = &-e^2\overline{\Psi}(12)\gamma(\xi,11')G^0(1',3)\gamma(\xi',33')C(3'2)\Phi_{kk'}(\xi\xi') + \\ &+ie^4\overline{\Psi}(12)\gamma(\xi,11')G^0(1'3)\gamma(\bar{\xi},33')G^0(3'5)D^0(\bar{\xi}\,\bar{\xi}')\gamma(\bar{\xi}',55')G^0(5'7)\gamma(\xi',77') \\ &\times C(7'2)\Phi_{kk'}(\xi\xi') + ie^4\overline{\Psi}(12)\gamma(\bar{\xi},11')G^0(1'3)\gamma(\xi,33')G^0(3'5)D^0(\bar{\xi}\,\bar{\xi}')\gamma(\bar{\xi}',55') \\ &\times G^0(5'7)\gamma(\xi',77')C(7'2)\Phi_{kk'}(\xi\xi') + ie^4\overline{\Psi}(12)\gamma(\xi,11')G^0(1'3)\gamma(\bar{\xi},33') \\ &\times G^0(3'5)D^0(\bar{\xi}\,\bar{\xi}')\gamma(\xi',55')G^0(5'7)\gamma(\bar{\xi}',77')C(7'2)\Phi_{kk'}(\xi\xi').\end{aligned} \tag{31}$$

Calculating in (31) the matrix coefficients proportional to the highest (fourth) power of e we can make use of relation (26), remaining within the limits of the given accuracy. Such an approximation for the wave function $\Psi(12)$ of interacting particles is, however, not satisfactory for the calculation of those matrix elements in Eq. (31) which are proportional to e^2. It is necessary to introduce a correction of the order e^2 into the approximation (26) of the wave function $\Psi(12)$. Owing to the weakness of the electromagnetic binding, this can be done by successive approximations, using for this purpose the wave equation of interacting particles (21) in the integral form

$$\begin{aligned}\Psi(12) &= \Psi^{(0)}(12) \\ &+ G(13')G(24')I_i(3'4',1'2')\Psi(1'2'),\end{aligned} \tag{32}$$

where $\Psi^{(0)}$ fulfills the equation for free particles $F(11')F(22')\Psi^{(0)}(1'2') = 0$, and the particle interaction operator I_i is assumed to be given [*cf.*, (14) and (19)] in the form of a series in e^2. In fact, the exchange of the wave function of the interacting particles for the wave function of free particles multiplied by N means that we neglect in some way the interaction between the particles.* The proposed method of successive approximations make a correction for this interaction.

We shall obtain the first correction to the zero-order approximation (26) if we exchange the wave function $\Psi(1'2')$ on the right-hand side of Eq. (32) by its zero-order approximation and in the operator I_i we shall leave only the terms proportional to e^2 (denoted below by $I_i^{(1)}$. We have then

$$\Psi^{(1)}(12) = (N\Psi_f(12)) + G^0(13')G^0(24')I_i^{(1)}(3'4',1'2')(N\Psi_f(1'2')). \tag{33}$$

For the amplitude (31) we obtain now, using Eq. (26) and (33)

$$\begin{aligned}\mathcal{A} = N^*[&-e^2\overline{\Psi}_f(12)\gamma(\xi,11')G^0(1'3')\gamma(\xi',3'5')C(5'2)\Phi_{kk'}(\xi\xi') \\ &+ie^4\overline{\Psi}_f(12)\gamma(\bar{\xi},22')D^0(\bar{\xi}\,\bar{\xi}')\gamma(\bar{\xi}',11')G^0(1'3)G^0(2'4)\gamma(\xi,33')G^0(3'5) \\ &\times\gamma(\xi',55')C(5'4)\Phi_{kk'}(\xi\xi') + ie^4\overline{\Psi}_f(12)\gamma(\xi,11')G^0(1'3)\gamma(\bar{\xi},33')G^0(3'5) \\ &\times D^0(\bar{\xi}\,\bar{\xi}')\gamma(\bar{\xi}',55')G^0(5',7)\gamma(\xi',77')C(7'2)\Phi_{kk'}(\xi\xi') + ie^4\overline{\Psi}_f(12)\gamma(\bar{\xi},11') \\ &\times G^0(1'3)\gamma(\xi,33')G^0(3'5)D^0(\bar{\xi}\,\bar{\xi}')\gamma(\bar{\xi}',55')G^0(5'7)\gamma(\xi',77')C(7'2)\Phi_{kk'}(\xi\xi') \\ &+ ie^4\overline{\Psi}_f(12)\gamma(\xi,11')G^0(1'3)\gamma(\bar{\xi},33')G^0(3'5)D^0(\bar{\xi}\,\bar{\xi}')\gamma(\xi',55')G^0(5'7)\gamma(\bar{\xi}',77')C(7'2)\Phi_{kk'}(\xi\xi')].\end{aligned} \tag{34}$$

*It should be noted that the interaction between the particles is already accounted for to a large extent in the coefficient N of the wave function of free particles (26) since the coefficient is proportional to $\psi(0)$ – the exact wave function of interacting particles for $x=0$.

The photoproduction amplitude of interacting particles with the account of the first two radiative corrections differs therefore from the photoproduction amplitude of free particles also by the factor N^* and, consequently, Eq. (30) remains in force and is even more exact since $(\overline{\psi}(0)\psi(0))$ is now calculated with the same degree of acurracy as $d\sigma_f$. Correctness of Eq. (30) with radiative corrections of the n-th order in e^2 is proved in an analogous way. It is only necessary to bear in mind that using the method of successive approximations for finding the $(e^2)^n$-th order correction to the corresponding approximation of the wave function, Eq. (32) should be used with the operator I_i written with corresponding accuracy, *i.e.*, with terms up to the order $(e^2)^n$ inclusive only.

It can be easily seen [*cf.*, Eq. (4)] that in the case of annihilation of an electron-positron pair we again obtain Eq. (30).

c) *A Note about the Bound State*

If the produced (or annihilated) particles are in a bound state, the total energy of these particles can be written

$$E = \mathcal{E} - \varepsilon, \tag{35}$$

where $\varepsilon > 0$ is the binding energy ($\varepsilon/m \sim e^4$). Eq. (26) can then be written

$$\Psi^{E\sigma}(x_1x_2) = \left(\int c(E, E')\, dE'\right) \tag{36}$$

$$\Psi_f^{E\sigma}(x_1x_2) \equiv N\Psi_f^{\mathcal{E}\sigma}(x_1x_2)$$

where $\Psi_f^{\mathcal{E}\sigma}(x_1x_2)$ is the wave function of free particles with the total energy $\mathcal{E}$ and zero relative velocity. This function enters Eq. (30) in the case of production of particles in a bound state.

In conclusion, the author wishes to express his gratitude to A. D. Galanin for advice and discussion of the results.

[1] J. Schwinger, Proc. Nat. Acad. Sc. US **37**, 452 (1951).
[2] H. A. Bethe and E. E. Salpeter, Phys. Rev. **84**, 1232 (1951).
[3] M. Gell-Mann and F. Low, Phys. Rev. **84**, 350, (1951).
[4] A. D. Galanin, J. Exptl. Theoret. Phys. (U.S.S.R.) **23**, 488 (1952).
[5] S. Deser and P. Martin, Phys. Rev. **90**, 1075 (1953).
[6] R. Karplus and A. Klein, Phys. Rev. **87**, 848 (1952).
[7] I. Ia. Pomeranchuk, Dokl. Akad. Nauk SSSR **60**, 213 (1948).
[8] D. D. Ivanenko and A. A. Sokolov, Dokl. Akad. Nauk SSSR **61**, 51 (1948); A. Ore and J. Powell, Phys. Rev **75**, 1696 (1949).
[9] K. A. Tumanov, J. Exptl. Theoret. Phys. (U.S.S.R.) **25**, 385 (1953).
[10] A. D. Sakharov, J. Exptl. Theoret. Phys. (U.S.S.R.) **18**, 631 (1948).
[11] A. I. Alekseev, J. Exptl. Theoret. Phys. (U.S.S.R.) **31**, 164 (1956), Soviet Physics JETP **4**, 261 (1957).
[12] A. I. Alekseev, J. Exptl. Theoret. Phys. (U.S.S.R.) **31**, 909 (1956), Soviet Physics JETP **4**, 771 (1957).
[13] F. Rohrlich, Phys. Rev. **98**, 181 (1955).
[14] Utiyama and al., Progr. Theor. Phys. **8**, 77 (1952).
[15] R. Karplus and N. Kroll, Phys. Rev. **77**, 536 (1950).

Translated by H. Kasha
183

On a Possible Mechanism for the Increase in the Conductivity of Atomic Semiconductors in a Strong Electric Field

F. G. BASS

(Submitted to JETP editor March 30, 1956)
J. Exptl. Theoret. Phys. (U.S.S.R.) 32, 863-865 (April, 1957)

We investigate the effect of a decrease of the electron recombination rate in a strong electric field on the conductivity of atomic semiconductors.

AS IS WELL KNOWN, the conductivity of a semiconductor increases in a strong electric field. Various investigators explain this phenomenon by the increase in the conduction electron concentration due to collision ionization[1], the Stark effect, the tunnel effect[2], *etc.* Davydov and Shmushkevich[3] have indicated the possibility that the conduction electron concentration may be caused by a decrease in the coefficient of recombination which, in turn, is due to a decrease in the probability of electron trapping in impurity centers. In the same work, however, it was noted that this situation can cause effects only in external fields comparable with the internal atomic fields.

In addition, however, the recombination coefficient depends not only on the probability of electron capture by an impurity center, but also on the concentration of electrons about the impurity center and on the diffusion of electrons to the impurity center[4]. The last two factors may be altered by electric fields which are much weaker than the internal atomic ones.

In strong electric fields, when accounting for Coulomb interactions, the electron energy distribution is Maxwellian with a temperature depending on the electric field and differing from the phonon temperature.

The energy distribution function of the electrons, and the temperature Θ of the electron gas are given by the following formulas[5]:

$$f = 2\pi^{-1/2}(k\Theta)^{-3/2}e^{-\varepsilon/k\Theta}\sqrt{\varepsilon},$$

$$\Theta = {}^1/_2 T\left(1+\sqrt{1+(M/3m)(eEl/kT)^2}\right) \qquad (1)$$

Here ε is the electron energy, $M = kT/c^2$ is the effective mass of the phonon, k is Boltzmann's constant, T is the temperature of the phonon gas, m is the electron effective mass, e is the electron charge, l is the mean free path, and c is the velocity of sound. It is seen from Eq. (1) that

$$\Theta = T\left\{1+\frac{1}{12}\left(\frac{eEl}{kT}\right)^2\frac{M}{m}\right\} \quad \text{when } \frac{M}{3m}\left(\frac{eEl}{kT}\right)^2 \ll 1,$$
$$\Theta = \frac{1}{2\sqrt{3}}\sqrt{\frac{M}{m}}\,\frac{eEl}{kT} \quad \text{when } \frac{M}{3m}\left(\frac{eEl}{kT}\right)^2 \gg 1. \qquad (2)$$

In order to calculate the recombination coefficient, we make use of a formula derived by Pekar[4], namely

$$\beta = \beta_1 e^{-eV(r_0)/k\Theta}\left[1+\frac{\beta_1}{4\pi D}e^{-eV(r_0)/k\Theta}\int_0^{1/r_0} e^{eV(x)/k\Theta}\,dx\right], \qquad (3)$$

where β_1 is the capture probability, V is the potential of the impurity center, r_0 is a certain effective cutoff radius, and D is the diffusion constant. In this formula, the common temperature T of the electrons and lattice is replaced by the temperature of the electron gas in the presence of an electric field. In order for this replacement to be possible, a stationary state corresponding to the temperature Θ must be established. For this to happen, the electron must have to go over to a stationary state before recombination, which means that the mean free path must be several times less than the distance between impurity centers. This condition is not a new restriction on the calculation we are here making, since it lies at the basis of the derivation of Eq. (3).

In addition, in order that the formula be applicable, it is necessary that drift motion due to the external field E be negligible close to the impurity center compared with diffusion toward the center. This condition is satisfied if the external field E is much less than the field of the impurity center at $r = r_0$. Let $V(r) \approx e/\kappa r$ (where κ is the dielectric constant). In this case the condition that Eq. (3) be applicable reduces to the inequality $E \ll e/\kappa r_0^2$; setting $r_0 \sim 10^{-6}$ cm and $\kappa \sim 5$, we obtain $E \ll 10^6$ cgs electrostatic units. Effects due to the electric

field will be observable at $\sqrt{M/m}\,eEl/kT \sim 1$, and with $T \sim 300°$ and $l \sim 10^{-6}$ cm, we have

$$E \sim \sqrt{m/M}\,kT/el \sim 0{,}2 \text{ cgs esu}$$

Thus the present considerations are meaningful in the field interval $0.2 \leq E \ll 10^6$ cgs esu.

If the impurity levels are nowhere near depleted, the electron concentration in the conduction band is given by the equation[1]

$$N = (\bar{\alpha}/2\beta) + \sqrt{(\bar{\alpha}/2\beta)^2 + N'/\beta}. \tag{4}$$

Here N is the electron concentration in the conduction band, $\bar{\alpha}$ is the mean coefficient of collision ionization, and N' is the number of electrons per unit time which enter the conduction band due to thermal excitation; $\bar{\alpha}$ can be calculated by averaging the cross section for collision ionization with the distribution function of Eq. (1)[1]. Simple calculation leads to the expression

$$\bar{\alpha} = \frac{2\alpha_0\sqrt{\varepsilon_0/k\Theta}}{\sqrt{\pi}} \int_{\varepsilon_0/k\Theta}^{\infty} \frac{e^{-u}}{u}\,du, \tag{5}$$

where α_0 is a constant in the formula for the collision ionization cross section, and ε_0 is the separation between the impurity level and the conduction band. If, as is the case for usual fields, $\varepsilon_0/k\Theta \gg 1$, then

$$\bar{\alpha} = 2\alpha_0\sqrt{k\Theta/\pi\varepsilon_0}\,e^{-\varepsilon_0/k\Theta}. \tag{5'}$$

Let us now assume that electrons enter the conduction band primarily due to collision ionization. In this case N'/β can be ignored in the radical of radical of Eq. (4). Combining Eqs. (3)-(5) we obtain the following expression for the conduction electron concentration:

$$N = \frac{\alpha_0}{\beta_1}\sqrt{\frac{2k\Theta}{\pi\varepsilon_0}}\,e^{-\varepsilon'/k\Theta}(1+F),$$
$$F = \frac{\beta_1}{4\pi D}\,e^{-eV(r_0)/k\Theta}\int_0^{1/r_0} e^{eV(x)/k\Theta}\,dx. \tag{6}$$

Here $\varepsilon' = \varepsilon_0 + |eV(r_0)|$. If $F \ll 1$, then

$$N = (\alpha_0/\beta_1)\sqrt{2k\Theta/\pi\varepsilon_0}\,e^{-\varepsilon'/k\Theta}. \tag{6'}$$

As the electric field is increased, N first increases as e^{aE^2}, and then as $\sqrt{E}$.

The conductivity σ is defined by the expression

$$\sigma = (4\sqrt{2}\,\alpha_0 e^2 l/3\pi\beta_1\sqrt{m\varepsilon_0})\,e^{-\varepsilon'/k\Theta}. \tag{7}$$

For small fields $\sigma \sim e^{aE^2}$, and for large fields it approaches saturation.

In order to investigate the dependence of N on Θ for $F \gg 1$, the form of V must be given. If V is a Coulomb potential, then N and σ become

$$N = (3\alpha_0 k\Theta\varkappa\sqrt{m}/4\sqrt{2}\,\pi e^3 l\sqrt{\varepsilon_0})\,e^{-\varepsilon_0/k\Theta}, \tag{8}$$
$$\sigma = (\varkappa\alpha_0/2\pi^{3/2})\sqrt{k\Theta/\varepsilon_0}\,e^{-\varepsilon_0/k\Theta}. \tag{9}$$

In this case, the change of recombination in an electric field plays practically no role.

If $N' \gg \bar{\alpha}^2/4\beta$, then for $F \ll 1$ we obtain

$$N = \sqrt{N'/\beta_1}\exp\{-|eV(r_0)|/k\Theta\}, \tag{10}$$
$$\sigma = (2/3e^2 l\sqrt{2N'/\pi\beta_1 mk\Theta})\exp\{-|eV(r_0)|/k\Theta\}. \tag{11}$$

Here the variation of N and σ with the field is the same as in Eqs. (7)–(9), and the effect is due entirely to the decrease in the recombination rate caused by the electric field.

If $F \gg 1$, on the other hand, $N \sim \Theta^{1/4}$, and $\sigma \sim \Theta^{-1/4}$ and hardly depend on the field.

In conclusion I should like to express my gratitude to M. I. Kaganov for a discussion of the results of the present work.

[1] N. L. Pisarenko, Izv. Akad. Nauk SSSR, Ser. Fiz. 3, 631 (1938).

[2] F. F. Vol'kenshtein, *Electric Conductivity of Semiconductors*, Gostekhizdat, 1947.

[3] B. I. Davydov, I. M. Shmushkevich, J. Exptl. Theoret. Phys. (U.S.S.R.) 10, 1042 (1940).

[4] S. I. Pekar, *Investigations in the Electron Theory of Crystals*, GTTI, 1951.

[5] B. I. Davydov, J. Exptl. Theoret. Phys. (U.S.S.R.) 7, 1069 (1937).

Translated by
E. J. Saletan
184

Electrical, Optical, and Elastic Properties of Diamond-Type Crystals

II. Lattice Vibrations with Calculation of Atomic Dipole Moments

V. S. MASHKEVICH
Kiev Polytechnic Institute

(Submitted to JETP editor November 13, 1955)
J. Exptl. Theoret. Phys. (U.S.S.R.) 32, 866-873 (April, 1957)

The equations of motion corresponding to the crystal energy, deduced previously in Ref. 1, are considered. The vibration spectrum for long waves is investigated. A qualitative study is being made of the possibility of infrared absorption by the lattice vibrations and of birefringence and interaction between the conductivity electrons and lattice vibrations.

THE SPECTRUM OF ELASTIC VIBRATIONS of the diamond lattice has been investigated by many workers[2,3]. However, a general shortcoming of these investigations is that they do not take into consideration the extent of the internal degrees of freedom of the atoms. In addition, the results are unsatisfactory in their consideration of the propagation and absorption of light, and in many other problems, since they do not use the polarization vector (because of atomic neutrality). On the other hand, it was shown in Ref. 1 that the components of the atomic dipole moments $\mathbf{P}_s^l$ (l is the cell number, s is the atom number in the cell) may be selected as variables describing the internal degrees of freedom of the atoms. An expression for the potential energy U of the crystal as a function of $\mathbf{u}_s^l$ (the displacement of the atoms) and $\mathbf{P}_s^l$ may not be considered negligibly small in comparison with the terms which depend only on $\mathbf{u}_s^l$. In this work we consider the equations of motion derived from U. This allows one to study from one point of view a series of elastic, optical, and electrical properties of the above-mentioned crystals.

1. EQUATIONS OF MOTION

The equations of motion are:

$$m\ddot{\mathbf{u}}_s^l = -\partial U/\partial \mathbf{u}_s^l, \quad 0 = -\partial U/\partial \mathbf{P}_s^l, \tag{1}$$

where m is the atomic mass; we neglect the inertia of the dipole moments.

As usual, the solution of these equations is sought in the form of plane monochromatic waves:

$$\mathbf{u}_s^l = \mathbf{u}_s \exp(-i\omega t + i\mathbf{K}\mathbf{r}_s^l),$$
$$\mathbf{P}_s^l = \mathbf{P}_s \exp(-i\omega t + i\mathbf{K}\mathbf{r}_s^l). \tag{2}$$

For dipole moments of this form the internal field $\mathbf{E}_s^l$ contained in the equations of motion[1], may be calculated by means of a direct summation – the Ewald method[4]. As the result of these calculations, we obtained the following

$$\mathbf{E}_s^l = \mathbf{E}_s \exp(-i\omega t + i\mathbf{K}\mathbf{r}_s^l),$$
$$\mathbf{E}_1 = \frac{1}{d^3}\left[\frac{16\pi}{3}\mathbf{P} - 16\pi\frac{(\mathbf{P}\cdot\mathbf{k})\,\mathbf{k} - \mathbf{P}k_0^2}{k^2 - k_0^2} + \right. \tag{3}$$
$$\left. + Si\,(\mathbf{k} \overset{+}{\times} \mathbf{P}_2) + \mathbf{F}_1(\mathbf{k}; \mathbf{P}_1) + \mathbf{F}_2(\mathbf{k}; \mathbf{P}_2)\right],$$

$\mathbf{E}_s^l$ is the intensity at the point $\mathbf{r}_s^l$ of the electric field generated by all of the dipoles, including the one located at that point; d is a lattice constant; $\mathbf{k} = \mathbf{K}d/2$ is a dimensionless wave vector; $k_0 = \omega d/2c$ is a dimensionless frequency; c is the velocity of light in a vacuum;

$$\mathbf{P} = \mathbf{P}_1 + \mathbf{P}_2;$$
$$(\mathbf{k} \overset{+}{\times} \mathbf{P}) = \mathbf{i}(k_y P_z + k_z P_y) + \mathbf{j}(k_z P_x + k_x P_z) + \mathbf{k}(k_x P_y + k_y P_x),$$

where, as everywhere hereinafter, the positions of the coordinate axes, i, j, and k are directed along the edges of the cubic crystal; $S = 20.11$;

$$\mathbf{F}_s(\mathbf{k}; \mathbf{P}) = e_s^{(1)}\mathbf{P}k^2 + e_s^{(2)}\mathbf{k}(\mathbf{P}, \mathbf{k}) + e_s^{(3)}(\mathbf{P}; \mathbf{kk}),$$
$$(\mathbf{P}; \mathbf{kk}) = \mathbf{i}P_x k_x^2 + \mathbf{j}P_y k_y^2 + \mathbf{k}P_z k_z^2,$$
$$e_1^{(1)} = -1.845, \quad e_1^{(2)} = 2.348, \quad e_1^{(3)} = 3.708,$$
$$e_2^{(1)} = -2.135, \quad e_2^{(2)} = -3.335,$$
$$e_2^{(3)} = 9.772;$$

E_2 results from E_1 by interchanging P_1 and P_2 and substituting i for $-i$. Eq. (3) gives the series expansion of E_1 in powers of k up to the second inclusive. This is sufficient for long waves ($k \ll 1$), which we shall investigate.

The equations of motion can be solved by the usual Born method, expanding the frequency k_0 and the amplitudes $\mathbf{u}_s$ and $\mathbf{P}_s$ in powers of k. We, however, shall use a somewhat different method. We introduce the dimensionless variables:

$$\mathbf{v}_s = \mathbf{u}_s / d, \quad \mathbf{w}_s = \mathbf{P}_s / ed, \quad M = 4mc^2 d / e^2,$$
$$Mk_0^2 = \Omega^2, \quad n = \frac{k}{k_0} = \frac{2\pi c}{\lambda\omega}, \quad n\Omega = \varkappa, \quad M^{-1/2} = \mu,$$

$$A = d^3 / \alpha, \quad B = 4b_p d^3 / e, \quad C = c_p d^5 / 4e,$$
$$D = d_p d^5 / 2e^2, \quad G = g_p d^3 / e^2,$$
$$F = B + C, \quad L = D + 8G$$

(α, b_p, c_p, d_p, g_p are parameters from the expression for U in Ref. 1, e is the charge on an electron, λ is the wave length.) Then from (1) to (3) we obtain equations for the amplitudes in the following form:

$$\begin{aligned} &-\Omega^2\mathbf{v}_1 + L(\mathbf{v}_1 - \mathbf{v}_2) + F(\mathbf{w}_1 - \mathbf{w}_2) \\ &= i\mu\varkappa\left[\frac{D}{2}(\mathbf{s} \overset{+}{\times} \mathbf{v}_2) + \frac{C}{2}(\mathbf{s} \overset{+}{\times} \mathbf{w}_2)\right] - \mu^2\varkappa^2\varphi(\mathbf{v}_2; \mathbf{w}_2), \\ &A\mathbf{w}_1 + F(\mathbf{v}_1 - \mathbf{v}_2) - \frac{16\pi}{3}\mathbf{w} + 16\pi\frac{\varkappa^2(\mathbf{w}, \mathbf{s})\mathbf{s} - \Omega^2\mathbf{w}}{\varkappa^2 - \Omega^2} \\ &= i\mu\varkappa\left[\frac{C}{2}(\mathbf{s} \overset{+}{\times} \mathbf{v}_2) + S(\mathbf{s} \overset{+}{\times} \mathbf{w}_2)\right] + \mu^2\varkappa^2\mathbf{f}(\mathbf{v}_2; \mathbf{w}_1; \mathbf{w}_2), \end{aligned} \tag{4}$$

the two remaining equations here and in what follows are obtained by exchanging the subscripts 1 and 2 of the amplitudes and substituting i for $-i$; $\mathbf{w} = \mathbf{w}_1 + \mathbf{w}_2$; $\mathbf{s}$ is the position of the wave vector;

$$\begin{aligned} \varphi(\mathbf{v}, \mathbf{w}) &= \frac{L}{8}\mathbf{v} + \frac{D}{4}\mathbf{s}(\mathbf{s}, \mathbf{v}) - \frac{D}{4}(\mathbf{v}; \mathbf{ss}) + \frac{F}{8}\mathbf{w} \\ &+ \frac{C}{4}\mathbf{s}(\mathbf{w}, \mathbf{s}) - \frac{C}{4}(\mathbf{w}; \mathbf{ss}), \end{aligned} \tag{4a}$$
$$\begin{aligned} \mathbf{f}(\mathbf{v}; \mathbf{w}_1; \mathbf{w}_2) &= -\frac{F}{8}\mathbf{v} - \frac{C}{4}\mathbf{s}(\mathbf{s}, \mathbf{v}) + \frac{C}{4}(\mathbf{v}; \mathbf{ss}) \\ &+ \mathbf{F}_1(\mathbf{s}; \mathbf{w}_1) + \mathbf{F}_2(\mathbf{s}; \mathbf{w}_2). \end{aligned}$$

Equation (4) contains κ and Ω. It is clear that these equations can be presented in such a form that they would include any two of the three variables κ, Ω, or n. For a solution of the equations by the method of successive approximations, we shall compute one of these two variables by means of an independent parameter, but the other, together with the amplitudes $\mathbf{v}_s$ and $\mathbf{w}_s$ will be sought in the form of an expansion in powers of μ. The inclusion of a small parameter of fixed value μ in place of the variables k allows one to carry out the solution more rigorously; in particular, this makes it possible to take into account the large numerical value of $M(\sim 10^{40})$. In those cases where it does not result in inconsistencies, the independent parameter κ, Ω, or n, should be considered to be of order of magnitude $\mu^0 = 1$.

2. ACOUSTICAL VIBRATIONS

Let us consider κ as an independent parameter and Ω^2 as a dependent one which is taken to be

$$\Omega^2 = \Omega_0^2 + \mu\Omega_1^2 + \mu^2\Omega_2^2 + \ldots, \tag{5}$$

$$\begin{aligned} \mathbf{v}_s &= \mathbf{v}_s^0 + \mu\mathbf{v}_s' + \mu^2\mathbf{v}_s'' + \ldots, \\ \mathbf{w}_s &= \mathbf{w}_s^0 + \mu\mathbf{w}_s' + \mu^2\mathbf{w}_s'' + \ldots. \end{aligned} \tag{6}$$

Substituting (5) and (6) in (4) and retaining only the terms $\sim\mu^0$, we have zero-approximation equations:

$$\begin{aligned} &-\Omega_0^2\mathbf{v}_1^0 + L(\mathbf{v}_1^0 - \mathbf{v}_2^0) + F(\mathbf{w}_1^0 - \mathbf{w}_2^0) = 0, \\ &A\mathbf{w}_1^0 + F(\mathbf{v}_1^0 - \mathbf{v}_2^0) - \frac{16\pi}{3}\mathbf{w}^0 \\ &+ 16\pi\frac{\varkappa^2(\mathbf{w}^0 \cdot \mathbf{s})\mathbf{s} - \Omega_0^2\mathbf{w}^0}{\varkappa^2 - \Omega_0^2} = 0. \end{aligned} \tag{7}$$

The system (7) has the following obvious solution:

$$\Omega_0^2 = 0, \quad \mathbf{v}_2^0 = \mathbf{v}_1^0, \quad \mathbf{w}_2^0 = \mathbf{w}_1^0 = 0. \tag{8}$$

It obviously has the nature of acoustic vibrations: in the zero approximation the frequency is zero, the dipole moment is absent, and the displacements of the two atoms of the cell are identical.

After investigating the terms of order μ in (4) we find the first approximation equations, from which we obtain

$$\Omega_1^2 = 0, \tag{9}$$

$$\begin{aligned} \mathbf{v}_1' - \mathbf{v}_2' &= \frac{AD - 2FC}{2(AL - 2F^2)} i\varkappa(\mathbf{s} \overset{+}{\times} \mathbf{v}_1^0), \\ -\mathbf{w}_2' = \mathbf{w}_1' &= \frac{LC - FD}{2(AL - 2F^2)} i\varkappa(\mathbf{s} \overset{+}{\times} \mathbf{v}_1^0). \end{aligned} \tag{10}$$

The second-approximation equations result in

$$\begin{aligned} &2\Omega_2^2\mathbf{v}_1^0 - i\varkappa\frac{D}{2}(\mathbf{s} \overset{+}{\times} \mathbf{v}_1' - \mathbf{v}_2') - i\varkappa\frac{C}{2}(\mathbf{s} \overset{+}{\times} \mathbf{w}_1' - \mathbf{w}_2') \\ &- 2\varkappa^2\varphi(\mathbf{v}_1^0; 0) = 0, \end{aligned} \tag{11}$$

which after inserting (1) gives an equation for the firection of $\mathbf{v}_1^0$:

$$\Omega_2^2\mathbf{v}_1^0 + \frac{AD^2 + 2LC^2 - 4FCD}{8(AL - 2F^2)}\varkappa^2(\mathbf{s} \overset{+}{\times} (\mathbf{s} \overset{+}{\times} \mathbf{v}_1^0)) - \varkappa^2\boldsymbol{\varphi}(\mathbf{v}_1^0; 0) = 0. \quad (12)$$

Having set the determinant of this system equal to zero, we have a cubic equation for Ω_2^2 and, accordingly, three branches of acoustic vibrations. If we introduce the symbols

$$b_1 = \frac{(AD^2 + 2LC^2 - 4FCD)e^2}{4(AL - 2F^2)d^4}, \quad b_2 = \frac{Le^2}{4d^4}, \quad b_3 = \frac{De^2}{2d^4} \quad (13)$$

and make some simple transformations, the first of the three scalar equations (12) takes the form

$$v_{1x}^0[-\rho v^2 + b_2 s_x^2 + (b_2 - b_1)(s_y^2 + s_z^2)] + v_{1y}^0(b_3 - b_1)s_x s_y + v_{1z}^0(b_3 - b_1)s_x s_z = 0, \quad (14)$$

in which ρ is the density and v is the velocity of sound in the crystal. Comparing (14) with the analogous equation of the theory of elasticity

$$u_x[-\rho v^2 + c_{11}s_x^2 + c_{44}(s_y^2 + s_z^2)] + u_y(c_{12} + c_{44})s_x s_y + u_z(c_{12} + c_{44})s_x s_z = 0 \quad (15)$$

(c_{ik} is the modulus of elasticity), we have

$$b_1 = c_{11} - c_{44}, \quad b_2 = c_{11}, \quad b_3 = c_{11} + c_{12}. \quad (16)$$

These three relations can be used for determining the parameters of the theory.

According to (8) and (10) the dipole moment of the cell is equal to zero in the first approximation (it is possible to show that $\mathbf{w}' \neq 0$). However, a calculation of the dipole moments is essential for investigation of the acoustic vibrations. According to (13), the parameters F, C, and A, which appear on account of the dipole moments, enter into (14).

3. OPTICAL VIBRATIONS

We now take n as the independent parameter, and Ω as the dependent one:

$$\Omega = \Omega_0 + \mu\Omega_1 + \mu^2\Omega_2 + \dots. \quad (17)$$

Substituting (6) and (17) in (4), we obtain for the zero approximation:

$$-\Omega_0^2\mathbf{v}_1^0 + L(\mathbf{v}_1^0 - \mathbf{v}_2^0) + F(\mathbf{w}_1^0 - \mathbf{w}_2^0) = 0,$$
$$A\mathbf{w}_1^0 + F(\mathbf{v}_1^0 - \mathbf{v}_2^0) - \frac{16\pi}{3}\mathbf{w}^0 + 16\pi\frac{n^2\mathbf{s}(\mathbf{w}^0, \mathbf{s}) - \mathbf{w}^0}{n^2 - 1} = 0. \quad (18)$$

[It is apparent that (18) is the same as (7)]. Let us examine the solution for the case when

$$\Omega_0 \neq 0, \quad n^2 \neq 1,$$
$$n^2 \neq n_0^2 = (A + 64\pi/3)/(A - 32\pi/3).$$

The solution takes the following form:

$$\Omega_0^2 = (2LA - 4F^2)/A = \Omega_{\lim}^2, \quad \mathbf{v}_2^0 = -\mathbf{v}_1^0,$$
$$-\mathbf{w}_2^0 = \mathbf{w}_1^0 = -(2F/A)\mathbf{v}_1^0, \quad (19)$$

i.e., it has the nature of optical vibrations: the limiting frequency differs from zero and the displacements of the two atoms of the cell are opposite in the zero approximation.

From the condition for solvability of the first-approximation equations, it is possible to ascertain that $\Omega_1 = 0$. Using this, from the first-approximation equations we obtain

$$\mathbf{v}_1' + \mathbf{v}_2' = \Omega_{\lim}^{-1}(D - 2FC/A)\,i(\mathbf{s} \overset{+}{\times} \mathbf{v}_1^0),$$
$$\mathbf{w}' = \frac{\Omega_{\lim} n(n_0^2 - 1)(C - 4FS/A)}{32\pi(n^2 - n_0^2)} i\left[\frac{n^2}{n_0^2}(n_0^2 - 1)((\mathbf{s} \overset{+}{\times} \mathbf{v}_1^0), \mathbf{s})\mathbf{s} - (n^2 - 1)(\mathbf{s} \overset{+}{\times} \mathbf{v}_1^0)\right]. \quad (20)$$

Examining the condition of solvability of the second-approximation equations and using (20), it is easy to obtain an equation for the direction of $\mathbf{v}_1^0$:

$$2\Omega_{\lim}\Omega_2\mathbf{v}_1^0 - (D/2 - FC/A)^2 n(\mathbf{s} \overset{+}{\times} (\mathbf{s} \overset{+}{\times} \mathbf{v}_1^0)) + {}^1/_4 n\Omega_{\lim}(C - 4FS/A)i\mathbf{w}' + n^2\Omega_{\lim}^2[\boldsymbol{\varphi}(\mathbf{v}_1^0; \mathbf{w}_1^0) - \mathbf{f}(\mathbf{v}_1^0; \mathbf{w}_2^0; \mathbf{w}_1^0)] = 0, \quad (21)$$

in which $\mathbf{w}'$, $\mathbf{w}_1^0$, and $\mathbf{w}_2^0$ are substituted from (20) and (19). This equation gives, as is apparent, three modes of optical vibrations with one and the same limiting frequency $\Omega_{\lim}$. Therefore, there is only one line in the first-order Raman spectrum. Optical vibrations with limiting frequency $\Omega_{\lim}$ are active in the Raman effect since the polarizability of the crystal in opposite senses is dissimilar.[5] This theoretical result was reported long ago and confirmed experimentally.[6]

From (20) it follows that our solution cannot be used to find the values of n close to n_0. For $|n - n_0| \sim \mu$, the terms of first order become comparable with the terms of zero order and the series for solutions do not converge. Thus $n = n_0$ is a singular point of this solution.

4. RADIATION VIBRATIONS

We now make Ω as the independent parameter and n dependent:

$$n = n_0 + \mu n_1 + \mu^2 n_2 + \dots \tag{22}$$

When $\Omega \neq \Omega_{\lim}$ and $n_0 \neq 1$, the zero-approximation equations yield the following solution:

$$\mathbf{v}_2^0 = \mathbf{v}_1^0 = 0, \quad \dot{\mathbf{w}}_2^0 = \mathbf{w}_1^0,$$
$$n_0^2 = (A + 64\pi/3)/(A - 32\pi/3), \tag{23}$$

$$(\mathbf{w}_1^0 \cdot \mathbf{s}) = 0. \tag{23a}$$

It describes the propagation of electromagnetic waves in the crystal, while the index of refraction n_0 corresponds with the longest wavelength. Let us call these vibrations radiation vibrations. They differ from the usual optical vibrations for which, according to (19), $\mathbf{w}^0 = 0$, $\mathbf{v}_s^0 \neq 0$.

The conditions of solvability of the first-approximation equations give $n_{11} = 0$. Taking this into account, we obtain from the first-approximation equation

$$-\mathbf{v}_2' = \mathbf{v}_1' = \frac{n_0\Omega(AC - 4FS)}{2A(\Omega_{\lim}^2 - \Omega^2)} i(\mathbf{s} \overset{+}{\times} \mathbf{w}_1^0), \quad (\mathbf{w}' \cdot \mathbf{s}) = 0,$$
$$\mathbf{w}_1' - \mathbf{w}_2' = \frac{n_0\Omega[(2L - \Omega^2)2S - 2FC]}{A(\Omega_{\lim}^2 - \Omega^2)} i(\mathbf{s} \overset{+}{\times} \mathbf{w}_1^0). \tag{24}$$

Eq. (24) indicates that the solution under consideration is not applicable for $|\Omega - \Omega_{\lim}| \sim \mu$.

The condition of solvability of the second-approximation equations, taking (24) into account, gives

$$\left\{-n_2\mathbf{w}_1^0 + q\Omega^2\left[\mathbf{f}(0; \mathbf{w}_1^0; \mathbf{w}_1^0) + \frac{S^2}{A}(\mathbf{s} \overset{+}{\times} (\mathbf{s} \overset{+}{\times} \mathbf{w}_1^0))\right] + Q\frac{\Omega^2}{\Omega_{\lim}^2 - \Omega^2}(\mathbf{s} \overset{+}{\times} (\mathbf{s} \overset{+}{\times} \mathbf{w}_1^0))\right\} \times \mathbf{s} = 0, \tag{25}$$
$$q = n_0(n_0^2 - 1)^2/64\pi, \quad Q = q(C/2 - 2FS/A)^2.$$

(25) and (23a) represent a system of equations for n_2 and the direction of $\mathbf{w}_1^0$. It is clear that only three of these equations are linearly independent. The corresponding characteristic equation is:

$$n_2^2 - n_2\Omega^2\{2N + H[1 - (s_x^4 + s_y^4 + s_z^4)]\} + \Omega^4\{N^2 + NH[1 - (s_x^4 + s_y^4 + s_z^4)] + 3H^2 s_x^2 s_y^2 s_z^2\} = 0, \tag{26}$$
$$N = q(e_1^{(1)} + e_2^{(1)} + S^2/A) + Q/(\Omega_{\lim}^2 - \Omega^2),$$
$$H = q(e_1^{(3)} + e_2^{(3)} - 2S^2/A) - 2Q/(\Omega_{\lim}^2 - \Omega^2).$$

It gives two modes of the radiation vibrations. Thus double refraction must take place, reaching a maximum in the vicinity of $\Omega_{\lim}$.

At the point $\Omega = \Omega_{\lim}$ we have $n_2 = \pm\infty$, and the $\mathbf{v}_s$ are similarly infinitely large. This indicates absorption of light in the vicinity of this point. The latter absorption represents an effect of first-order in $\mu \sim d/\lambda$ (and not zero order as occurs in ionic crystals), since $\mathbf{v}_s^0 = 0$ and only the $\mathbf{v}_s'$ increase without limit. Therefore, the absorption must be considerably weaker than in ionic crystals; this is confirmed experimentally[6].

5. μ-REGION OF SINGULAR POINT

The remarks made in connection with (20) and (24) indicate that the μ-region of the point $\Omega = \Omega_{\lim}$, $n = n_0$, (which we shall call the singular point) requires special investigation since the solutions obtained (the optical as well as the radiation vibrations) do not hold in this region. In order to investigate this region, we assume

$$\varkappa = \varkappa_0 + \mu\varkappa_1, \quad \varkappa_0 = n_0\Omega_{\lim},$$
$$\Omega^2 = \Omega_{\lim}^2 + \mu\Omega_1^2 + \mu^2\Omega_2^2 + \dots \tag{27}$$

and we consider $\varkappa_1$ as an independent parameter of order unity. Substituting (27) and (6) in (4), we obtain to a zero approximation

$$-\Omega_{\lim}^2\mathbf{v}_1^0 + L(\mathbf{v}_1^0 - \mathbf{v}_2^0) + F(\mathbf{w}_1^0 - \mathbf{w}_2^0) = 0,$$
$$A\mathbf{w}_1^0 + F(\mathbf{v}_1^0 - \mathbf{v}_2^0) - 16\pi\mathbf{w}^0/3 \tag{28}$$
$$+ 16\pi[\varkappa_0^2\mathbf{s}(\mathbf{w}^0, \mathbf{s}) - \Omega_{\lim}^2\mathbf{w}^0]/(\varkappa_0^2 - \Omega_{\lim}^2) = 0.$$

The most general solution of this system is

$$-\mathbf{v}_2^0 = \mathbf{v}_1^0, \quad \mathbf{w}_1^0 = \mathbf{w}^0/2 - (2F/A)\,\mathbf{v}_1^0, \quad \mathbf{w}_2^0 = \mathbf{w}^0/2 + (2F/A)\,\mathbf{v}_1^0, \tag{29}$$

$$(\mathbf{w}^0 \cdot \mathbf{s}) = 0. \tag{29a}$$

It represents a superposition of optical and radiation vibrations, which is not surprising, for in the zero approximation the singular point is a point of intersection of the optical and radiation modes.

The conditions of solvability of the first approximation equation lead to the following results:

$$\Omega_1^2 \mathbf{v}_1^0 + Q_1 i\,(\mathbf{s} \overset{+}{\times} \mathbf{w}^0) = 0, \tag{30}$$

$$[{}^1\!/_2\,(n_0^2\Omega_1^2 - 2\varkappa_0\varkappa_1)\,\mathbf{w}^0 + iR_1\,(\mathbf{s} \overset{+}{\times} \mathbf{v}_1^0)] \times \mathbf{s} = 0,$$

$$Q_1 = {}^1\!/_4\varkappa_0\,(C - 4FS/A), \tag{30a}$$

$$R_1 = \varkappa_0\,(4FS/A - C)\,(\varkappa_0^2 - \Omega_{\lim}^2)\,/\,(A - 32\pi/3).$$

The system of equations (30), (30a), and (29a) determines the directions of the vectors $\mathbf{v}_1^0$ and $\mathbf{w}^0$, giving a solution in the vicinity of the singular point. In this system there are six linearly independent equations, since in (30a) one of the three scalar equations is a consequence of the other two. Setting the determinant equal to zero, we obtain an equation of fifth degree in Ω_1^2. Thus in the vicinity of the singular point we get five modes, which correspond to three optical and two radiation modes far from the singular point.

We give the name "singular" to the direction of s, parallel to the diagonals of the faces of a lattice cube. It can be shown that for non-singular directions of s, there are one optical and four mixed modes (Fig. 1), but the singular directions of s correspond to two optical, one radiation, and two modes (Fig. 2); the vector $\mathbf{w}^0$ of the radiation mode lies in the plane of the same face of the cube as does s.

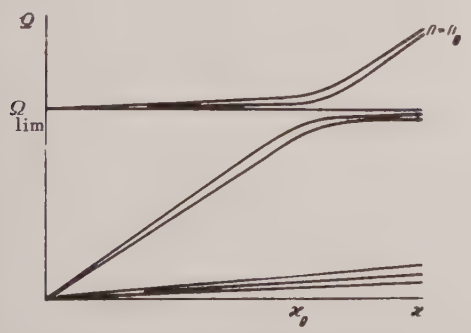

FIG. 1. Vibration spectra for non-singular directions of s. $\varkappa_0$ and $\Omega_{\lim}$ are the coordinates of the singular point.

Let us note that system (4) allows one more solution, for which $\Omega^2 = \kappa^2$, $(n = 1)$, $\mathbf{w}^0 \,||\, \mathbf{s}$. We shall not examine this solution. Although this method was already pointed out by Born for ionic crystals, doubt arises concerning the applicability in this case of the Ewald method[4] for finding $\mathbf{E}_s^1$ (the Fourier expansion will contain an infinitely large zero term). This problem requires a separate investigation.

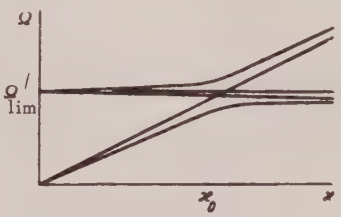

FIG. 2. Optical and radiation modes for singular directions of s.

6. INVESTIGATION OF THE GENERAL EQUATIONS OF MOTION

We shall show here that the limitations used in Ref. 1 in the derivation of the expression for U do not disturb the generality of the qualitative results already derived. With this goal, we investigate the most general equations for long-wave harmonic oscillations. Substituting (2) in (1), assuming U to be an arbitrary quadratic form in $\mathbf{u}_s^1$ and $\mathbf{P}_s^1$, separating explicitly the amplitude of the internal field $\mathbf{E}_s$, and expanding in powers of $\mathbf{k}$, we obtain

$$m\omega^2 T_{x'}^{is}\delta_{i1} + \sum_{s'i'x''}\left(A_{x'x''}^{(0)ii'ss'}\,T_{x''}^{i's'} + \sum_{y'} A_{x'x''y'}^{(1)ii'ss'}\,T_{x''}^{i's'}\,k_{y'} + \sum_{y'z'} A_{x'x''y'z'}^{(2)ii'ss'}\,T_{x''}^{i's'}\,k_{y'}k_{z'}\right) + E_{sx'}\delta_{i2} = 0, \tag{31}$$

$$T_{x'}^{is} = \begin{cases} u_{sx'}, & i = 1 \\ P_{sx'}, & i = 2 \end{cases} \qquad x' = x, y, z. \tag{32}$$

We require that the following obvious conditions be fulfilled: I) The system of equations (31) must be self-conjugate. II) The forces contained in (31) must vanish upon translation of the lattice as a whole. III) The coefficients $A^{(0)}$ and $A^{(2)}$ must be real, and $A^{(1)}$ pure imaginary, which follows from the expansion in powers of k. IV) The system (31) must be invariant relative to symmetry transformations of the crystal. The symmetry elements of a

crystal of the diamond type are determined from the conditions that (a) the center of the segment between two neighboring atoms is the center of symmetry and (b) the diamond lattice belongs to the point group T_d[8].

The above conditions lead to a series of relationships between the coefficients $A^{(l)}$, from which it is possible to determine the independent $A^{(l)}$s; these turn out to number twenty-six, namely four $A^{(0)}$s:

$$A_{xx}^{(0)1111} = a_1', \quad A_{xx}^{(0)1211} = a_2', \qquad A_{xx}^{(0)2211} = a_3', \quad A_{xx}^{(0)2212} = a_4', \tag{33}$$

four $A^{(1)}$s:

$$A_{xyz}^{(1)1112} = ib_1', \quad A_{xyz}^{(1)2212} = ib_2', \qquad A_{xyz}^{(1)1212} = ib_3', \quad A_{xyz}^{(1)1211} = ib_4' \tag{34}$$

and eighteen $A^{(2)}$s:

$$x'y'x''y'' = xxxx,\ xxyy,\ xyxy; \qquad ii' = 11, 22, 12;\ ss' = 11, 12. \tag{35}$$

Introducing, as in Sec. 1, dimensionless quantities and calculating by means of the independent parameter κ, we obtain in the zero approximation relative to μ

$$\begin{gathered} -\Omega_0^2 \mathbf{v}_1^0 + a_1(\mathbf{v}_2^0 - \mathbf{v}_1^0) + a_2(\mathbf{w}_2^0 - \mathbf{w}_1^0) = 0, \\ a_2(\mathbf{v}_2^0 - \mathbf{v}_1^0) - a_3\mathbf{w}_1^0 - a_4\mathbf{w}_2^0 - \frac{16\pi}{3}\mathbf{w}^0 \\ + 16\pi \frac{\varkappa^2(\mathbf{w}^0, \mathbf{s}) - \Omega_0^2 \mathbf{w}^0}{\varkappa^2 - \Omega_0^2} = 0. \end{gathered} \tag{36}$$

Equations (7) result from (36) if we assume

$$a_1 = -L, \quad a_2 = -F, \quad a_3 = -A, \quad a_4 = 0. \tag{37}$$

Thus the generality of (7) would be invalidated only if a_4 were to vanish. However, examining the solution of the zero-approximation equations, it is easy to establish that the coefficient of $\mathbf{w}^0$, which equals $-16\pi/3$, does not affect the qualitative character of the solutions, and bears only on their quantitative character. Hence follows the qualitative similarity of (7) and (36), *i.e.*, the generality of all the qualitative results of the zero-order approximation considered above.

The first-approximation equations give significant results only in the vicinity of the singular point. Therefore, we examine only that region. Everything concerning these conclusions results from the conditions of solvability of the first-approximation equations, which after some calculations yield

$$\begin{gathered} 2\Omega_1^2 \mathbf{v}_1^0 + i\varkappa_0 \left(b_3 + b_4 - \frac{2a_2 b_2}{a_2 - a_4}\right)(\mathbf{s}_\times^+ \mathbf{w}^0) = 0, \\ \left\{ i\varkappa_0 \left[\frac{4a_2}{a_2 - a_4} - 2(b_3 + b_4) \right] (\mathbf{s}_\times^+ \mathbf{v}_1^0) \right. \\ \left. + \frac{a_3 + a_4 + 32\pi/3}{\varkappa_0^2 - \Omega_{\lim}^2} (2\varkappa_0 \varkappa_1 - n_0^2 \Omega_1^2) \mathbf{w}^0 \right\} \times \mathbf{s} = 0. \end{gathered} \tag{38}$$

Comparing (38) with (30) and (30a), we see that these systems of equations differ only in their constants. Therefore, all the qualitative results of Sec. 5 should be correct in the general case.

Second-approximation equations are essential only for obtaining quantitative results: calculation of the corrections to the frequencies and determination of the directions of $\mathbf{v}_s^0$ and $\mathbf{w}_s^0$. Therefore, examination of their general form is not of interest.

CONCLUSIONS

1. The spectrum of vibrations consists of eight modes (far from the singular point — three acoustic, three optical, and two radiation modes). In the vicinity of the singular point, the transistions occur from the optical modes to the radiation modes and vice versa. For the non-singular directions of s, both of the radiation and two (of the three) optical modes experience discontinuity and mutual transition (Fig. 1). For the singular directions of s only one radiation and one optical mode experience discontinuity and transition (Fig.2).

2. The theory explains qualitatively the absorption of light at a frequency close to $\Omega_{\lim}$. Polychromism (the dependence of absorption on the direction of s and the polarization of the light waves) should be observed. A separate work will be devoted to a more detailed and quantitative investigation of the absorption.

3. Double refraction must take place, reaching a maximum in the vicinity of the singular point. A more detailed investigation, to which a separate work will be devoted, shows that the crystal possesses seven optical axes with directions of type (111) and (100).

4. The conduction electrons must interact with both acoustic and optical vibrations, owing to the polarization w which is associated with them. This question will be investigated in a separate work.

5. All the results enumerated above are independent in their qualitative aspects of any special choice of the potential energy U.

I take this opportunity to express my deep appreciation to K. B. Tolpygo who suggested and guided this work.

[1] V. S. Mashkevich and K. B. Tolpygo, J. Exptl. Theoret. Phys. (U.S.S.R.) 32, 520 (1957), Soviet Physics JETP 5, 435 (1957).

[2] N. S. Nagendra Nath, Proc. Indian Acad. Sci. 1, 333 (1934).

[3] H. M. J. Smith, Trans. Roy. Soc. (London) A241, 105 (1948).

[4] P. P. Ewald, Ann. Physik 64, 253 (1921).

[5] E. Fermi, *Molecules and Crystals* (IIL, 1947).

[6] M. Lax and E. Burstein, Phys. Rev. 97, 39 (1955).

[7] M. Born and M. Goeppert-Mayer, *Theory of the Solid State* (ONTI, 1938).

[8] F. Seitz, Phys. Rev. 73, 549 (1948).

Translated by L. A. D'Assaro
185

SOVIET PHYSICS JETP VOLUME 5, NUMBER 4 NOVEMBER, 1957

Band Structure of the Polaron Energy Spectrum

M. SH. GITERMAN AND K. B. TOLPYGO
Kiev State University

(Submitted to JETP editor April 21, 1956)
J. Exptl. Theoret. Phys. (U.S.S.R.) 32, 874-882 (April 1957)

Using the macroscopic treatment of the polaron as the zeroth approximation, the periodic potential of a crystal and the periodic variation of its polarizability with variations in the position of the polaron center of gravity are calculated in the first approximation. We determine the dependence of the energy of a crystal with a polaron on the position of the polaron's center of gravity, and it is found possible to treat polaron motion as the motion of a particle with the polaron mass M in a field with a periodic potential. We determine the widths and spacings of the lowest forbidden and allowed energy bands. A numerical calculation is performed for NaCl, KCl, KBr, and KI.

1. STATUS OF THE PROBLEM

GREAT SUCCESSES in the theory of the electric conductivity of ionic crystals were attained as a result of Pekar's polaron theory[1, 2] in which the interaction between electrons and polar vibrations of the crystal are introduced into the fundamental Hamiltonian of the problem. The periodic potential of the crystal is eliminated with the aid of the effective-mass method[3] (EMM). It is found that electron motion is composed of vibration within a polarization well and wave-like translation of the electron together with the polarization well through the crystal[4]. For a fixed crystal polarization the electron energy spectrum is found to be discrete. At the same time, the problem of electron and ion motion possesses translational degeneracy[2], so that the energy spectrum of the whole crystal is found to be continuous:

$$E = J[\psi] + (\hbar^2 K^2 / 2M) - {}^3/_2 \hbar\omega + E_{\text{ion}}, \quad (1)$$

where K and M are the wave vector and effective mass of the polaron[5], $J[\psi]$ is the energy of the crystal with a stationary polaron, and ω is the limiting longitudinal optical crystal vibrations.

The translational degeneracy of the problem of polaron motion led several authors[6, 7] to assert that the electron energy spectrum should have a band-like structure, and that therefore polaron theory is essentially band theory in which the interaction between the electron and the crystal polarizations has been accounted for. This leads only to a formal change of the specific parameters of the current carriers, and according to Tiablikov[7] is of no great consequence, since these parameters are usually obtained experimentally anyway. As was asserted by Tiablikov[8], Eq. (1) gives the energy only in the neighborhood of the lower edge of the first polaron band.

In other works[9-11], Tiablikov suggested a method for calculating the electron energy spectrum by accounting for interactions with the phonon field sim-

ilarly as is done in quantum electrodynamics. According to his calculations, this spectrum consists of relatively narrow (10^2 ev) bands separated by relatively wide forbidden gaps.

These calculations, however, cannot be considered reliable, since the formulae of the last article [11] are not carried to final form, and the first two articles[9,10] contain several defects: 1) in spite of the fact that he is treating a polaron of small radius the author makes use of the macroscopic formula for the interaction only with longitudinal optical vibrations of the lattice, and neglects frequency dispersion; 2) Tiablikov's[8] Eq. (13′), which describes electron vibrations and involves the potential $V_0(\mathbf{r})$ of a single ion rather than the periodic potential, gives an electron-state radius less than the dimensions of the ion, and a level lying at a depth of the order of the ionization potential of the hydrogen atom; in this one may not ignore the orthogonality of this wave function to the internal electron functions of the ion; 3) according to Tiablikov[8], electron motion reduces to skipping from atom to atom, and the crystal polarization occurs each time after the electron "jumps." Thus the polarization potential is actually periodic and the total polarization is non-inertial, so that the author is in fact simply considering a band electron with a different effective mass. Thus the conclusion on the existence of polaron bands is contained in the original assumptions of Tiablikov's work, and according to the above, the numerical calculations may give results which differ significantly from actual values.

Furthermore, it is impossible to agree with Vol'kenshtein and Tiablikov when they state that Pekar obtained a continuous polaron spectrum as a result of an inconsistent treatment of translational degeneracy [the wave function of the polaron is not of the form $e^{i\mathbf{K}\mathbf{r}}u_{\mathbf{K}}(\mathbf{r})$] and the application of the EMM.

As has been shown by Pekar[2], the Hamiltonian of an electron in an inertially polarizable crystal is invariant with respect to simultaneous translation of the electron and polarization of the crystal along an arbitrary vector ξ. The wave function of the polaron is not an eigenfunction of the translation operator, but is a linear combination of such eigenfunctions belonging to the same energy level. It is therefore an eigenfunction of the energy operator. By a special choice of variables one may easily obtain an eigenfunction of the translation operator which has the same characteristics as Pekar's function. In this case, however, the mass and mobility of the polaron will be exactly the same as that given by Pekar. Elsewhere[12] Pekar has shown by several examples that the fact of translational symmetry alone does not lead to a band spectrum.

As for the use of the EMM, it is well known that its accuracy increases when $r_p \gg a$, where r_p is the polarization radius of the polaron, and a is the separation between closest ions. As has been shown by one of the present authors[13], when r_p is of the order of several times a, the error in the EMM is insignificant, so that in dealing with a polaron of energy spectrum is by no means only of academic interest, and it is far from sufficient to answer it affirmatively "in principle" and leave the determination of the specific current carrier parameters to the experimentalists. For certain definite relations between the forbidden and allowed bandwidths and the magnitude of kT, qualitatively new effects may take place. If a suitable quantitative theory were to predict such relations, it could provide direction also for experimental work.

The present work, to our knowledge, is the first attempt to perform a quantitative calculation of the lowest polaron bands.

2. METHOD OF APPROXIMATION

In view of the great complexity of the general problem, we consider relatively slow motion of the polaron, when we can neglect energy transfer to the crystal[14]. In addition, we assume that the polaron radius is large enough ($r_p \gg a$) for the results of Pekar's macroscopic theory[2] to be treated as the zeroth approximation. The consideration of even a stationary polaron of small radius is an independent and quite difficult problem.

The reason that the polaron spectrum is continuous in Pekar's theory lies in the fact that the energy $J[\psi]$ of the crystal with an electron is independent of the coordinate ξ of the polaron center of gravity. As a result, the equation for the translational motion of the polaron[2]

$$-(\hbar^2/2M)\nabla_\xi^2\Psi + J[\psi]\Psi = E\Psi \qquad (2)$$

has plane-wave solutions $\psi = e^{i\mathbf{K}\xi}$ with energy given by Eq. (1).

Strictly speaking, the functional $J[\psi]$ which determines the electron energy in the first stage of the

adiabatic approximation for the equilibrium positions of the ions should depend on the coordinate ξ of the polaron center of gravity: $J[\psi] = J(\xi)$.

The quantity $J(\xi)$ has the periodicity of the lattice, and therefore Eq. (2) has solutions in the form of the Bloch function

$$\psi = e^{i\mathbf{K}\xi} u_{\mathbf{K}}(\xi); \quad E = E(\mathbf{K}). \tag{3}$$

Our problem reduces to finding an explicit expression for $J(\xi)$ and integration of Eq. (2). This expression depends on the discrete crystal structure, which must therefore be borne in mind. In calculating the energy in the first approximation, we may use the wave function of the zeroth approximation which is obtained with the aid of the EEM, in which the crystal is treated as a continuum.

Let the Schroedinger equation for the polaron

$$[-(\hbar^2/2m)\Delta + V_p(\mathbf{r}) + W(\mathbf{r})]\psi(\mathbf{r}) = E\psi(\mathbf{r}) \tag{4}$$

have the zeroth approximation solution

$$\psi = \sum_{\mathbf{K}} a_{\mathbf{K}} \psi_{\mathbf{K}}(\mathbf{r}) = \sum_{\mathbf{K}} a_{\mathbf{K}} e^{i\mathbf{K}\mathbf{r}} u_{\mathbf{K}}(\mathbf{r}), \tag{5}$$

where $\psi_{\mathbf{K}}(\mathbf{r})$ are Bloch functions, $a_{\mathbf{K}}$ are the Fourier coefficients of the function $\phi(\mathbf{r})$ which satisfies the equation

$$[-(\hbar^2/2\mu)\Delta + W]\varphi = E\varphi, \tag{6}$$

$$\varphi = V^{-1/2} \sum_{\mathbf{K}} a_{\mathbf{K}} e^{i\mathbf{K}\mathbf{r}}, \tag{7}$$

μ is the effective mass of the electron in the conduction band[3], V is the volume of the fundamental region of the crystal, and $W(\mathbf{r})$ is the polarization potential calculated in the macroscopic theory[1] using the "smoothed out" functions $\phi(\mathbf{r})$ of Eq. (7):

$$W \to \widetilde{W}(\mathbf{r}) = -e^2 \int \frac{\operatorname{div} \boldsymbol{P}(\mathbf{r}')\, d\tau'}{|\mathbf{r} - \mathbf{r}'|} = -e^2 C \int \frac{|\varphi(\mathbf{r}')|^2\, d\tau'}{|\mathbf{r} - \mathbf{r}'|}. \tag{8}$$

In the first approximation we obtain the energy by multiplying Eq. (4) by $\psi^*(\mathbf{r})$ and integrating over V,

$$E = \sum_{\mathbf{K}',\mathbf{K}} a^*_{\mathbf{K}'} a_{\mathbf{K}} \int \psi^*_{\mathbf{K}'} \Big(-\frac{\hbar^2}{2m}\Delta + V_p + W\Big)\psi_{\mathbf{K}} d\tau = \sum_{\mathbf{K}} |a_{\mathbf{K}}|^2 E(\mathbf{K}) + \sum_{\mathbf{K},\mathbf{K}'} a^*_{\mathbf{K}'} a_{\mathbf{K}} \int \psi^*_{\mathbf{K}'} W \psi_{\mathbf{K}} d\tau, \tag{9}$$

where $E(\mathbf{K})$ is the energy of a band electron in the state $\psi_{\mathbf{K}}$.

Let $\phi^0(\mathbf{r})$ be the smoothed out function for a polaron at rest at the origin, and $a^0_{\mathbf{K}}$ be its expansion coefficients. Then the solution of Eq. (6) for a polaron whose center is at ξ will be, taking account of Eq. (8),

$$\varphi(\mathbf{r}) = \varphi^0(\mathbf{r} - \xi) : a_{\mathbf{K}} = a^0_{\mathbf{K}} e^{-i\mathbf{K}\xi}. \tag{10}$$

The first term of Eq. (9) is independent of ξ, and the ξ-dependence of the second term is lost in the macroscopic theory (without any significant error in the absolute magnitude of the energy[13, 15], since when calculating the integral

$$\int \psi^*_{\mathbf{K}'} W \psi_{\mathbf{K}}\, d\tau = \int e^{i(\mathbf{K}-\mathbf{K}')\mathbf{r}} W u^*_{\mathbf{K}'} u_{\mathbf{K}}\, d\tau$$

the rapidly oscillating factor $u^*_{\mathbf{K}'} u_{\mathbf{K}}$ was taken outside the integral sign and its average value, about equal to unity, was used, and W was replaced by $\widetilde{W}$ of Eq. (8).

We shall calculate E from Eq. (9) using the detailed polaron function $\psi_{\mathbf{K}}(\mathbf{r})$ given by Eq. (5) instead of the smoothed out function, and shall account for the discrete structure of the crystal in finding the mean polarization energy W. To do this one must specify the form of the Bloch functions $\psi_{\mathbf{K}}(\mathbf{r})$. For reasons given elsewhere[13], we shall make use of the approximation of strongly bound electrons and assume that for energies that are not very large the electron moves only on positive ions of the lattice:

$$\psi_{\mathbf{K}}(\mathbf{r}) = N^{-1/2} \sum_{l} \psi_a(\mathbf{r} - \mathbf{r}^l_1) \exp(i\mathbf{K}\mathbf{r}^l_1), \tag{11}$$

where ψ_a is the atomic function of a valence electron on the positive site $\mathbf{r}^l_1$, l is the number of the cell, and N is the number of cells in the fundamental region.

We shall write $\pi^l_s = \mathbf{p}^l_s + \widetilde{\mathbf{P}}^l_s$ for the inertial dipole arising at site $\mathbf{r}^l_s$ under the action of the polaron field, and due both to the displacement $\mathbf{p}^l_s$ of the ions, and to the deformation $\mathbf{P}^l_s$ of these ions;[16, 17];

$$\mathbf{D}(\mathbf{r}^l_s) = \int \frac{(\mathbf{r}^l_s - \mathbf{r}')}{|\mathbf{r}^l_s - \mathbf{r}'|^3} |\psi(\mathbf{r}')|^2\, d\tau'$$

shall be used to denote the induction at the site $\mathbf{r}^l_s$ due to the polaron. Then the mean potential energy of the electron is

$$\overline{W} = -\sum_{sl} \pi_s^l \mathbf{D}(\mathbf{r}_s^l) = -N \sum_{s,\varkappa} \pi_{s\varkappa} \mathbf{D}_{s-\varkappa}, \qquad (12)$$

where $\pi_{s\varkappa}$ and $\mathbf{D}_{s\varkappa}$ are the Fourier expansion coefficients of π_s^l and $\mathbf{D}(\mathbf{r}_s^l)$,

$$\pi_s^l = \sum_{\varkappa} \pi_{s\varkappa} \exp(i\varkappa \mathbf{r}_s^l), \quad \mathbf{D}(\mathbf{r}_s^l) = \sum_{\varkappa} \mathbf{D}_{s\varkappa} \exp(i\varkappa \mathbf{r}_s^l). \qquad (13)$$

Detailed analysis of the natural vibration spectra of binary crystals[16, 17] shows that all natural vibrations have some dipole moment, but that for a large-radius polaron, interacting primarily with the longitudinal optical mode, the fundamental contributions to $\pi_{s\varkappa}$ come from this mode. As has been shown elsewhere[17], in the zeroth approximation (long waves) each normal vibration of this mode has a dipole moment given by

$$\pi_{s\varkappa}^{(1)} = (\varkappa / |\varkappa|)(1/\mu_s + c_s/a_0)$$

(see Tolpygo's[17] Equation (21) and Table II, where the values of the parameters $\mu_s c_s$ and a_0 are given). The magnitude of the dipole moment $\pi_{s\varkappa}$ due to the field $\mathbf{D}_{s\varkappa}$ can be found by considering the equations for the normal coordinate $q_{1\varkappa}$ introduced by the equation $\pi_{s\varkappa} = \pi_{s\varkappa}^{(1)} q_{1\varkappa}$:

$$\ddot{q}_{1\varkappa} + \omega_{1\varkappa}^2 q_{1\varkappa} = (e_s^2/\mu) Q_{1\varkappa}, \qquad (14)$$

where e_s is the charge of the s-th ion, and μ is the reduced mass of a pair of ions.

The generalized force[14, 18] $Q_{1\varkappa}$ is $\sum_s \mathbf{D}_{s\varkappa} \pi_{s-\varkappa}^{(1)}$. Thus, in a quasi-stationary external field

$$\pi_{s\varkappa} = (\pi_{s\varkappa}^{(1)}/\omega_{1\varkappa}^2) \sum_{s'} \pi_{s'-\varkappa}^{(1)} \mathbf{D}_{s'\varkappa}. \qquad (15)$$

According to Eq. (12) the mean potential energy of the electron will be

$$\overline{W} = -N \sum_{s\varkappa} \frac{e_s^2}{\mu\omega_{1\varkappa}^2} \mathbf{D}_{s-\varkappa} \pi_{s\varkappa}^{(1)} \sum_{s'} \pi_{s'-\varkappa}^{(1)} \mathbf{D}_{s'\varkappa}, \qquad (16)$$

and the potential energy of the deformed crystal[18] will be

$$U^0 = \frac{N}{2} \sum_{\varkappa} \frac{\mu}{e_s^2} q_{1\varkappa} q_{1-\varkappa} \omega_{1\varkappa}^2 = \frac{N}{2} \sum_{\varkappa} \frac{e_s^2}{\mu} \frac{Q_{1\varkappa}}{\omega_{1\varkappa}^2} \frac{Q_{1-\varkappa}}{\omega_{1\varkappa}^2} \omega_{1\varkappa}^2 = -\frac{1}{2} \overline{W}. \qquad (17)$$

In agreement with the long-wave approximation, we shall neglect dispersion and set[2] $\omega_{1\varkappa} = \omega$. Then from Eq. (9), (16), and (17) the energy of a crystal with a polaron is

$$J[\psi] = \sum_{\mathbf{K}} |a_{\mathbf{K}}|^2 E(\mathbf{K}) + \overline{W} + U^0 = \sum_{\mathbf{K}} |a_{\mathbf{K}}|^2 E(\mathbf{K}) - \frac{N}{2\omega^2} \sum_{\varkappa s s'} \frac{e_s^2}{\mu} \pi_{s\varkappa}^{(1)} \pi_{s'-\varkappa}^{(1)} \mathbf{D}_{s-\varkappa} \mathbf{D}_{s'\varkappa}. \qquad (18)$$

3. THE DEPENDENCE OF THE ENERGY OF A CRYSTAL WITH A POLARON ON THE POSITION OF THE CENTER OF GRAVITY OF THE POLARON

In order to find the components $\mathbf{D}_{s\varkappa}$ of the induction, let us find the mean potential $v(\mathbf{r})$ of the ψ-shell from the equation

$$\Delta v = -4\pi e |\psi|^2 \qquad (19)$$

with the ψ given by Eq. (5) and (11). Expanding the atomic functions ψ_a in a Fourier series

$$\psi_a(\mathbf{r}) = \sum_{\mathbf{K}''} \psi_{\mathbf{K}''} e^{i\mathbf{K}''\mathbf{r}},$$

we solve Eq. (19), after which we calculate $\mathbf{D}(\mathbf{r}) = -\nabla v(\mathbf{r})$ and find its Fourier coefficients. When these calculations are performed, we obtain the following expression for $J[\psi]$ of Eq. (18).

$$J[\psi] = J(\xi) = \sum_{\mathbf{K}} |a_{\mathbf{K}}|^2 E(\mathbf{K}) - \frac{8\pi^2 e^2 N^3 e_s^2}{\omega^2 \mu} \sum_{ss'} \pi_{s-\varkappa}^{(1)} \pi_{s'\varkappa}^{(1)} \times \sum a_{\mathbf{K}}^0 a_{\mathbf{K}}^{0} a_{\mathbf{K}-\varkappa-\mathrm{p}+\mathrm{p}'-\mathrm{p}''+\mathrm{m}}^{0*} a_{\mathbf{K}'+\varkappa+\mathrm{p}-\mathrm{p}'+\mathrm{p}''}^{0*} \psi_{\mathbf{K}+\mathrm{q}} \psi_{\mathbf{K}'+\mathrm{p}}^{*} \psi_{\mathbf{K}'+\varkappa+\mathrm{p}+\mathrm{p}''}^{*} \times \psi_{\mathbf{K}-\varkappa-\mathrm{p}+\mathrm{p}'-\mathrm{p}''+\mathrm{q}'+\mathrm{m}} \times \frac{(\mathrm{p}''+\varkappa)(\mathrm{p}''+\mathrm{p}+\mathrm{q}-\mathrm{p}'-\mathrm{q}'-\mathrm{m}+\varkappa)}{|\mathrm{p}''+\varkappa|^2 |\mathrm{p}''+\mathrm{p}+\mathrm{q}-\mathrm{p}'-\mathrm{q}'-\mathrm{m}+\varkappa|^2} \exp\{i(\mathrm{q}'-\mathrm{q}+\mathrm{p}-\mathrm{p}')\mathbf{r}_1 - i\mathrm{p}''\mathbf{r}_{s'} + i(\mathrm{p}''+\mathrm{q}+\mathrm{p}-\mathrm{p}'-\mathrm{q}'-\mathrm{m})\mathbf{r}_s + i\mathrm{m}\xi\}, \qquad (20)$$

where q, q′, p, p′, p″, and m are reciprocal lattice vectors, and the summation is taken over all indices.

Eq. (20) can be simplified: a) the EMM assumes that the $a_{\mathbf{K}}$ decrease rapidly with increasing K and only terms with $|\mathbf{K}| \ll 1/a$ are significant in Eq. (5), and b) the coefficients $\psi_{\mathbf{K}+\mathbf{q}}$ decrease rapidly

with increasing q (in the examples below the decreases are as $1/q^4$ and $1/q^6$ and terms with $q = 0$ are the important ones. Therefore the main contribution to the sum in Eq. (20) is given by terms in which the indices of a_K and ψ_{K+q} are simultaneously small, that is those terms for which $q = p = p' = q' = 0$. Of these, the largest will be those in which the product of the a coefficients is not too small. Since the main contribution comes from terms with small K, K′ and the vector $\varkappa$ is restricted by the limits of the first cell of the reciprocal lattice so that $|\varkappa| < 1/2|p''|$, this product will be largest when $p'' = 0$ or $p'' = m$. If K is replaced by K′ and $\varkappa$ by $-\varkappa$ these two terms transform into each other. The next largest terms will be those in which one of the indices of the ψ_K differs from the index of a_K by the smallest vector of the reciprocal lattice (ψ_K decreases with K less rapidly than does a_K). This gives eight types of terms, and these can be transformed to four types by replacing K by K′, $\varkappa$ by $-\varkappa$, p by q, and p′ by q′:

1) $q \neq 0$, $p'' = 0$; 2) $q \neq 0$, $p'' = m$;

3) $q' \neq 0$, $p'' = 0$; 4) $q' \neq 0$, $p'' = m$

(other q and p vectors are equal to 0.)

Further calculations have been performed for a lattice of the NaCl type, where

$$r_1 = 0,\ r_2 = a(i + j + k);$$

$$q_{min} = (\pi/a)(\pm i \pm j \pm k);$$

the sum over s, s' gives the factor $\pi_{1\varkappa}^{(1)2} - \pi_{2\varkappa}^{(1)2}$, in the principal term, the factor $(\pi_{1\varkappa}^{(1)} + \pi_{2\varkappa}^{(1)})^2$ in terms 1) and 3), and the factor $(\pi_{1\varkappa}^{(1)} - \pi_{2\varkappa}^{(1)})^2$ in terms 2) and 4).

4. POLARON BAND WIDTHS FOR SPECIFIC CRYSTALS

Let us take the smoothed out function $\phi(r)$ to be of the form

$$\varphi(r) = \left(\frac{\alpha}{\sqrt{\pi}}\right)^{3/2} e^{-\alpha^2 r^2/2};$$

$$a_K^0 = 2\sqrt{\frac{2}{V}}\left(\frac{V\pi}{\alpha}\right)^{3/2} e^{-K^2/2\alpha^2} \qquad (21)$$

and consider NaCl, KCl, KBr, KI crystals, for which the parameters of polaron theory are known. The 3s atomic functions of Na and the 4s functions of K have been approximated from the data of Fock and Petrashen'[19] and Hartree[20] by one of the authors[15] and by Dykman[21]:

$$\text{Na}: \psi_a = \frac{0{,}727}{\sqrt{4\pi a_b^3}}(1 - r/a_b)\exp(-0{,}712\, r/a_b);$$

$$\psi_K = \frac{0{,}727\sqrt{4\pi a_b^3}}{V}\,\frac{2{,}31 - 3{,}42\,K^2 a_b^2}{[0{,}504 + K^2 a_b^2]^3};$$

$$\text{K}: \psi_a = \frac{0{,}472}{\sqrt{4\pi a_b^3}}(1{,}62 - r/a_b)\exp(-0{,}569\, r/a_b); \qquad (22)$$

$$\psi_K = \frac{0{,}944\sqrt{4\pi a_b^3}}{V}\,\frac{1{,}922\,K^2 a_b^2 - 0{,}674}{[0{,}324 + K^2 a_b^2]^3}.$$

We may go over, in Eq. (20), from the sum over K, K′, $\varkappa$ to an integral which can be calculated approximately by finding the maximum of the product of the four α_K coefficients and setting the indices K in the more smoothly varying factors ψ_K equal to their values at the maximum (for large-radius polarons this maximum is sufficiently sharp): $K = -(m/4) + K_1$; $K = -(m/4) + K_2$; $\varkappa = \pm[(m/2) - K_0]$, and $\cos(\hat{mK}) > 0$, since $|\varkappa| \leq |m/2|$. In the principal term and in 2) and 4) we must take the minus sign, and in 1) and 3), the plus sign for $\varkappa$. Replacing q′ by $-q$ and accounting for the dependence of ψ_K only on $|K|$ [see Eq. (22)], terms 1) and 3) are joined into a single term, as are terms 2) and 4). As a result, we get the ξ-dependence of $J[\psi]$ in Eq. (20) in the form

$$J[\psi] = J_0 + \sum_m J_m \exp(im\xi) = J_0 - \frac{2e^2 N^3 V a^3}{\Omega_\parallel^2 \pi^4 \alpha^6}\sum_m |\psi_{m/4}|^4 \exp(im\xi)$$

$$\times \iiint \exp -\frac{1}{2\alpha^2}\left\{\frac{m^2}{4} + K_1^2 + K_2^2 + |K_2 + K_0|^2 + |K_1 - K_0|^2\right\}\left\{\left(\pi_{1\varkappa}^{(1)2} - \pi_{2\varkappa}^{(1)2}\right)\right. \qquad (23)$$

$$\times \frac{K_0^2 - m^2/4}{(K_0^2 + m^2/4)^2 - (K_0 m)^2} + 2\sum_q{}' \frac{\psi_{q-m/4}}{\psi_{m/4}}\left[(\pi_{1\varkappa}^{(1)} + \pi_{2\varkappa}^{(1)})^2 \frac{[q - (m/2) - K_0][(m/2) - K_0]}{[q - (m/2) - K_0]^2 [(m/2) - K_0]^2}\right.$$

$$\left.\left. + (\pi_{1\varkappa}^{(1)} - \pi_{2\varkappa}^{(1)})^2 \frac{[q - (m/2) + K_0][(m/2) + K_0]}{[q - (m/2) + K_0]^2 [(m/2) + K_0]^2}\right]\right\} dK_1\, dK_2\, dK_0;\ \ \Omega_\parallel^2 = \frac{4\pi a^3}{\varepsilon^2}\omega^2.$$

The integration over dK_1 and dK_2, as well as that over the angles of the vector K_0 is now performed directly. The terms with $\pi_{1\varkappa}^{(1)2} + \pi_{2\varkappa}^{(1)2}$ in the sum over q may be joined by pairs and the integration over K_0 can be taken over all space. The integral over $|K_0|$ in the principal term and in the next largest ones with $q = m$ has been calculated by Simpson's method. Finally, in the terms with $q \neq m$ the quantity K_0 is neglected compared with $m/2$ and $q - m/2$, as a result of which the results obtained by calculation are somewhat too large for these terms.

The magnitudes of α, a, $\pi_{1\varkappa}^{(1)}$, $\pi_{2\varkappa}^{(1)}$, and $\Omega_{\parallel}^2$ are taken from previous works[2, 16, 17]. The results of the calculation are shown in Table I. As can be

TABLE I

Crystal	$\alpha \cdot 10^{-8}$	$a \cdot 10^{8}$	$\Omega_{\parallel}^2$	$J'_m \cdot 10^4$, eV $p'' = 0$, m	$J''_m \cdot 10^4$, eV $q = m$	$J'''_m \cdot 10^4$, eV $q \neq m$	$J_m \cdot 10^4$, eV Total
NaCl	0.359	2.82	5.320	—132.0	23.4	45.9	—62.7
KCl	0.233	2.14	6.487	— 1.086	—0.370	0.444	— 1.012
KBr	0.205	3.30	6.335	— 0.5108	—0.0859	0.2102	— 0.3865
KJ	0.196	3.53	6.186	— 0.7876	—0.0529	0.4139	— 0.4266

TABLE II.

Crystal	$\pi_{1\varkappa}^{(1)}$	$\pi_{2\varkappa}^{(1)}$	$J'_m \cdot 10^4$, eV $p'' = 0$, m	$J''_m \cdot 10^4$, eV $q = m$	$J'''_m \cdot 10^4$, eV $q \neq m$	$J_m \cdot 10^4$, eV Total
NaCl	0.592	—0.124	—185.7	—13.3	39.7	—159.3
KCl	0.420	0.092	— 0.9612	— 0.3782	0.0676	— 1.272
KBr	0.628	—0.161	— 0.5741	— 0.1618	0.0468	— 0.6891
KJ	0.732	—0.305	— 1.186	— 0.395	0.152	— 1.429

seen by comparison of the last three columns, the convergence of the series in q, q′ is found to be quite slow, so that the results are quite rough. This is related to the rapid oscillation of the Na and K atomic functions near zero, and the insufficiently rapid decrease of the ψ_K. At the same time the number of terms increases rapidly as $q \neq 0$ and $q' \neq 0$.

For a more reliable calculation of J_m, we calculated it according to Eq. (23) with the aid of smoother cation functions, as proposed by Slater[22], namely $\psi_a(r) \sim r^n e^{-\alpha_n r}$, where $n = 2$ and 2.7, $a_n = 0.733/a_B$ and $0.55/a_B$ for Na and K, respectively. (For convenience, the number 2.7 was rounded out to 3.) Then

$$\text{Na: } \psi_K = \sqrt{\frac{8\pi a}{5}} \frac{16\, a^4 a_b^6}{V} \frac{a^2 a_b^2 - K^2 a_b^2}{[a^2 a_b^2 + K^2 a_b^2]^4}; \tag{24}$$

$$\text{K: } \psi_K = \sqrt{\frac{4\pi a}{35}} \frac{16 a^4 a_b^6}{V} \frac{5 a_b^4 a^4 - 10\, a^2 K^2 a_b^4 + K^4 a_b^4}{[a^2 a_b^2 + K^2 a_b^2]^5}.$$

The calculation was performed using the same Eq. (23), except with different values of $\psi_{m/4}$ and $\psi_{q-m/4}$.

As can be seen from the result shown in Table 2, the correction terms here decrease somewhat more rapidly and therefore the value obtained for J_m is more reliable.

For KCl, KBr, and KI crystals, in which the polaron radius is relatively large, the Fourier coefficients J_m are small compared with the kinetic energy $\hbar^2 K^2/2M$ of the "free" polaron, and the solution of Eq. (2) may be obtained with the approximation of almost free electrons. Then the forbidden band width is $2|J_m|$, which is much less than both the minimum and maximum widths of the first allowed band, namely $3\hbar^2\pi^2/2Ma^2$ and $5\pi^2\hbar^2/2Ma^2$. Therefore the first allowed band should overlap the second. All higher bands overlap even more. One may thus conclude that for polarons whose quantum state radius $1/\alpha \geq 1.5a$, the band structure of the energy spectrum is of no significance. The spectrum consists of close-lying and overlapping allowed bands with narrow (10^{-3} ev) gaps. On the average the energy is described approximately by Eq. (1).

In the NaCl crystal $1/\alpha \approx a$, and the oscillations of $J(\xi)$ are comparable with the mean kinetic energy. The approximation of "almost free electrons" is not applicable to a solution of Eq. (2). One may expect measurable energy gaps between the lowest allowed bands. The energy gaps are even wider for small-radius polarons (LiF, BaO crystals, etc.). For them, however, as for NaCl, the present calculation gives results which are too approximate, since the EMM is not a sufficiently good zeroth approximation. Here the question of the energy spectrum structure goes over into the problem of constructing a small-radius polaron theory.

The authors express their gratitude to Professor S. I. Pekar for several valuable remarks.

[1] S. I. Pekar, J. Exptl. Theoret. Phys. (U.S.S.R.) **16**, 335 (1946).

[2] S. I. Pekar, *Investigations in the Electron Theory of Crystals*, Gostekhizdat, 1957.

[3] S. I. Pekar, J. Exptl. Theoret. Phys. (U.S.S.R.) **16**, 933 (1946).

[4] S. I. Pekar, J. Exptl. Theoret. Phys. (U.S.S.R.) **19**, 796 (1949).

[5] L. D. Landau, S. I. Pekar, J. Exptl. Theoret. Phys. (U.S.S.R.) **18**, 419 (1948).

[6] F. F. Vol'kenshtein, Usp. Fiz. Nauk **43**, 11 (1951).

[7] S. V. Tiablikov, Usp. Fiz. Nauk **48**, 447 (1952).

[8] S. V. Tiablikov, J. Exptl. Theoret. Phys. (U.S.S.R.) **23**, 381 (1952).

[9] S. V. Tiablikov, J. Exptl. Theoret. Phys. (U.S.S.R.) **21**, 377 (1951).

[10] S. V. Tiablikov, J. Exptl. Theoret. Phys. (U.S.S.R.) **22**, 325 (1952).

[11] S. V. Tiablikov, J. Exptl. Theoret. Phys. (U.S.S.R.) **26**, 545 (1954).

[12] S. I. Pekar, Tr. Phys. Fac., Kiev State Un. **8**, 29 (1955).

[13] K. B. Tolpygo, J. Exptl. Theoret. Phys. (U.S.S.R.) **21**, 443 (1951).

[14] K. B. Tolpygo and Z. I. Uritskii, J. Exptl. Theoret. Phys. (U.S.S.R.) **30**, 929 (1956). Soviet Physics JETP **3**, 725 (1956).

[15] M. Sh. Giterman, J. Exptl. Theoret. Phys. (U.S.S.R.) **30**, 991 (1956), Soviet Physics JETP **3**, 785 (1956).

[16] K. B. Tolpygo, Dissertation, Kiev Inst. of Phys., USSR **6**, 102 (1955).

[17] K. B. Tolpygo, Trans. Inst. Phys. Acad. Sci. USSR **6**, 102 (1955).

[18] K. B. Tolpygo, Matem. Sb. KGU (Math. Coll. Kiev State Un.) **5**, 99 (1951).

[19] V. A. Fock and M. Petrashen', Phys. ZS. Sowj. Un. **6**, 368 (1934).

[20] D. R. Hartree and W. Hartree, Proc. Cambridge Phil. Soc. **34**, 550 (1938).

[21] I. M. Dykman, Tr. IFAN USSR **5**, 48 (1954).

[22] J. C. Slater, Phys. Rev. **36**, 56 (1930).

Translated by E. J. Saletan
186

Energy Loss of a Charged Particle Passing Through a Laminar Dielectric, I

IA. B. FAINBERG AND N. A. KHIZHNIAK
Physico-Technical Institute, Academy of Sciences of Ukrainian S.S.R.

(Submitted to JETP editor April 29, 1956)
J. Exptl. Theoret. Phys. (U.S.S.R.) 32, 883-895 (April, 1957)

The energy losses of a uniformly moving charged particle in a laminar dielectric are considered. A general expression is obtained for the losses in the case in which the particle moves in an unbounded laminar medium or in a wave guide filled with a laminar dielectric. The polarization losses are studied in detail. An expression is derived for the spectral distribution of the parametric Cerenkov radiation. The Cerenkov radiation in the case of thin layers is studied. It is shown that division of the dielectric into layers leads to an increase of the intensity of the Cerenkov radiation. The Cerenkov radiation in a thin-layered plasma is considered.

AS IS WELL KNOWN, the Cerenkov and Doppler effects can be reduced to the ordinary resonance between the driving force caused by the uniform motion of a charged particle or dipole through a homogeneous medium and the characteristic vibrations of the electromagnetic field in the medium[1,2]. The condition for appearance of the Cerenkov effect is that the speed v of the motion of the particle must exceed the phase velocity of the propagation of waves in the given medium.

In the case of uniform motion of a particle through a laminar (spatially periodic) medium one can obtain conditions in which forced parametric resonance can occur. Unlike the cases of ordinary Cerenkov or Doppler effects, the condition for resonance is here not the equality of the frequency of the driving force and the characteristic frequency of the field, but the equality of the frequency of the driving force and the frequency of vibration of the free electromagnetic oscillations in the laminar medium. It can therefore be expected that the conditions for Cerenkov radiation in the presence of forced parametric resonance will be different from the conditions for the ordinary Cerenkov effect, and the parametric Cerenkov effect will have a number of special features.

As is well known, the use of parametric resonance for the generation of electromagnetic oscillations has been the subject of a great many papers. First to be considered in this connection are the papers of Mandel'shtam and Papaleksi and their collaborators[3]. It must be pointed out, however, that in these papers the wavelengths generated were large, on account of the large inertia of the variable parameters determing the parametric resonance. In the present case the system is almost without inertia. This makes it possible to use the phenomenon of parametric resonance for the generation and amplification of very short electromagnetic waves.

It can be expected that the parametric Cerenkov effect will occur also if the speed of the particle is less than the phase velocity of the wave in the medium. Indeed, as was pointed out by Vavilov[4], it follows from the interference treatment of the Cerenkov effect that on passage of a uniformly moving particle through a layer of dielectric radiation occurs even when the speed of the particle is less than the phase velocity of the wave in the dielectric. Here, however, it is necessary that the optical thickness of the layer of dielectric be less than π. The multiple repetition of this effect in parametric resonance must lead to its amplification. It can also be expected that the parametric Cerenkov effect will occur in media with dielectric constant less than unity, and even in media in which the dielectric constant can take negative values. A special study will therefore be made of the case of the parametric Cerenkov effect in a laminar electron plasma.

When a uniformly moving particle passes through a medium a considerable part of the energy is expended in polarization losses. It is important therefore to study the peculiarities of polarization losses in laminar media.

In considering the energy losses of a particle in a laminar medium we shall start with the system of Maxwell equations describing the interaction of a uniformly moving charged particle with electromagnetic waves propagated in the medium:

$$-\frac{\partial H_\varphi}{\partial z}=\frac{\hat{\varepsilon}(z)}{c}\frac{\partial E_r}{\partial t},\quad \frac{\partial E_r}{\partial z}-\frac{\partial E_z}{\partial r}=-\frac{\hat{\mu}(z)}{c}\frac{\partial H_\varphi}{\partial t},$$

$$\frac{1}{r}\frac{\partial}{\partial r}rH_\varphi=\frac{\hat{\varepsilon}(z)}{c}\frac{\partial E_z}{\partial t}+\frac{4\pi}{c}ev\,\delta(vt-z)\frac{\delta(r)}{2\pi r},\quad (1)$$

where the operators $\hat{\varepsilon}$ and $\hat{\mu}$ are defined by the relations

$$\hat{\varepsilon}(z)\,e^{i\omega t}=\varepsilon(\omega,z)\,e^{i\omega t},\ \hat{\mu}(z)\,e^{i\omega t}=\mu(\omega,z)\,e^{i\omega t},\quad (2)$$

and e is the charge and v the speed of the particle.

We shall seek solutions for the components of the electromagnetic field in the form of Fourier integrals

$$u(r,z,t)=\int_{-\infty}^{\infty}e^{i\omega t}u_\omega(r,z)\,d\omega.\quad (3)$$

Then from Eq. (1), using Eq. (2), we get the following equation for the longitudinal component of the electric induction $D_{z,\omega}=\varepsilon(\omega,z)E_{z,\omega}$:

$$\frac{1}{r}\frac{\partial}{\partial r}\left(r\frac{\partial D_{z,\omega}}{\partial r}\right)+\varepsilon\frac{\partial}{\partial z}\left(\frac{1}{\varepsilon}\frac{\partial D_{z,\omega}}{\partial z}\right)+k^2\varepsilon\mu D_{z,\omega}$$
$$=\frac{ik e\varepsilon\mu}{\pi c}e^{-i\omega z/v}\frac{\delta(r)}{r}+\frac{e\varepsilon}{\pi v}\frac{\delta(r)}{r}\frac{\partial}{\partial z}\left(\frac{1}{\varepsilon}e^{-i\omega z/v}\right),\quad (4)$$
$$k=\frac{\omega}{c}.$$

In the case in which one has to consider the energy losses of a charged particle moving along the axis of a wave guide filled with dielectric, the dependence of D_z on r can be written in the form

$$D_{z,\omega}(r,z)=\sum_{n=1}^{\infty}\frac{2}{R^2J_1^2(\alpha_n)}J_0\left(\alpha_n\frac{r}{R}\right)D_{z,\omega n}(z),\quad (5)$$

where R is the radius of the waveguide and α_n is the nth zero of the Bessel function of order zero. Sub- Eq. (5) into Eq. (4) and using the orthgonality con- tion of the Bessel functions, we obtain the following equation for $D_{z,\omega n}=X(z)$:

$$\varepsilon\frac{d}{dz}\left(\frac{1}{\varepsilon}\frac{dX}{dz}\right)+\left(k^2\varepsilon\mu-\frac{\alpha_n^2}{R^2}\right)X$$
$$=\frac{ik e\varepsilon\mu}{\pi c}e^{-i\omega z/v}+\frac{\varepsilon e}{\pi v}\frac{\partial}{\partial z}\left(\frac{1}{\varepsilon}e^{-i\omega z/v}\right).\quad (6)$$

If the charged particle is moving in an unbounded laminar dielectric, perpendicular to the layers, it is natural to look for the dependence of D_z on r in the form

$$D_{z,\omega}=\int_0^{\infty}X(z)\,J_0(k_\perp r)\,k_\perp\,dk_\perp,\quad (7)$$

where $X=D_{z,\omega k_\perp}$ is also determined by Eq. (6), with α_n/R replaced by $k_\perp$. This equation is valid for an arbitrary variation of $\varepsilon(z)$ and $\mu(z)$, and is the basic equation of our problem.

In the case in which $\varepsilon(z)$and $\mu(z)$ are periodic functions of the variable z, Eq. (6) is an equation with periodic coefficients, the right half of which is a known function of z. The general solution of the inhomogeneous equation (6) is

$$X(z)=U_1(z)[A-V_2(z)]+U_2(z)[B+V_1(z)],\quad (8)$$

where A and B are constants of integration and

$$V_1(z)=\frac{1}{W}\int_0^z\left[\frac{ik e\mu}{\pi c}U_1(z)-\frac{e}{\pi v}\frac{1}{\varepsilon}\frac{dU_1(z)}{dz}\right]e^{-i\omega z/v}\,dz,$$

$$V_2(z)=\frac{1}{W}\int_0^z\left[\frac{ik e\mu}{\pi c}U_2(z)-\frac{e}{\pi v}\frac{1}{\varepsilon}\frac{dU_2(z)}{dz}\right]e^{-i\omega z/v}\,dz,$$

$$W=U_1(z)\frac{1}{\varepsilon}\frac{dU_2(z)}{dz}-U_2(z)\frac{1}{\varepsilon}\frac{dU_1(z)}{dz},$$

$U_1(z)$ and $U_2(z)$ being linearly independent solutions of the corresponding homogeneous equations which satisfy the conditions

$$U_1(z+L)=\rho_1U_1(z),\ U_2(z+L)=\rho_2U_2(z),\quad (9)$$

L is the period of the structure of the laminar medi- um, and ρ_1 and ρ_2 are constants of absolute value unity. Using Eq. (9), one readily shows that

$$V_1(z+L)=V_1(L)+\rho_1V_1(z)\,e^{-i\omega L/v},$$
$$V_2(z+L)=V_2(L)+\rho_2V_2(z)\,e^{-i\omega L/v}.\quad (10)$$

Since the energy losses of a uniformly moving charged particle in a laminar medium must be a periodic function of z with the same period as the structure, we find from Eq. (3) ($\omega t=\omega z/v$):

$$e^{i\omega z/v}D_{z,\omega}(r,z)=e^{i\omega(z+L)/v}D_{z,\omega}(r,z+L).\quad (11)$$

This condition means that if the field at a certain point z where the charge is present at a given instant is E_z, then this value of the field will occur at the point $z+L$ only when the charge arrives at this point. In particular, condition (11) is satisfied if we assume that a similar relation holds for the field component X

$$X(z)=e^{i\omega L/v}X(z+L).\quad (12)$$

Condition (12) enables us to determine the arbi- trary constants A and B, and thus to find the field

produced by a uniformly moving charge in a laminar medium.

The total energy loss of the charged particle is found by the well known formula[6]

$$-d\mathcal{E}/dz = e\int E_{z,\,\omega k_\perp}|_{z=vt}\, k_\perp\, dk_\perp\, d\omega, \qquad (13)$$

where $E = X/\varepsilon(\omega)$ and X is the field of the charge in the medium, determined above. We calculate the loss in the case in which the medium is composed of alternate layers of two dielectrics.

We assume that the dielectric constant and permeability of the layer of dielectric of thickness $a(0 \leq z \leq a)$ are ε_1 and μ_1, and those of the layer of thickness $b\,(a \leq z \leq L$, where $L = a + b)$ are ε_2 and μ_2. Then the solutions of the homogeneous equation corresponding to the inhomogeneous equation (6), which satisfy the conditions (9), have the form

$$U_1(z) = U_1(0)\left[u_1(z) - \frac{u_1(L) - \rho_1}{u_2(L)}\,u_2(z)\right],$$
$$U_2(z) = U_2(0)\left[u_1(z) - \frac{u_1(L) - \rho_2}{u_2(L)}\,u_2(z)\right], \qquad (14)$$

where

$$u_1(z) = \cos p_1 z,\ u_2(z) = (\varepsilon_1/p_1)\sin p_1 z,\ p_1^2 = \varepsilon_1\mu_1 k^2 - k_1^2 \ \text{ for } \ 0 \leqslant z \leqslant a;$$
$$u_1(z) = \cos p_1 a \cos p_2 (z-a) - (\varepsilon_2 p_1/\varepsilon_1 p_2)\sin p_1 a \sin p_2 (z-a),$$
$$u_2(z) = (\varepsilon_1/p_1)\sin p_1 a \cos p_2 (z-a) + (\varepsilon_2/p_2)\cos p_1 a \sin p_2 (z-a), \qquad (15)$$
$$p_2^2 = \varepsilon_2\mu_2 k^2 - k_1^2 \quad \text{for} \quad a \leqslant z \leqslant L,$$

$k_1 = \alpha_n/R$ for a laminar dielectric bounded by a waveguide, and $k_1 = k_\perp$ for an unbounded laminar dielectric. The quantities ρ_1 and ρ_2 are found as the roots of the quadratic equation:

$$\rho^2 - 2A\rho + 1 = 0, \quad A = \cos p_1 a \cos p_2 b - \frac{1}{2}\left(\frac{p_1\varepsilon_2}{p_2\varepsilon_1} + \frac{p_2\varepsilon_1}{p_1\varepsilon_2}\right)\sin p_1 a \sin p_2 b. \qquad (16)$$

The relations (8) and (15) make it possible to determine the field E_z produced by a uniformly moving particle in the laminar medium under consideration and, according to Eq. (13), to determine the total energy loss of the particle.

We note, however, that the greatest practical interest attaches to the energy loss averaged over the period of the structure, *i. e.*,

$$\overline{d\mathcal{E}}/dz = e\int \overline{E}_{z,\,\omega k_\perp}|_{z=vt}\, k_\perp\, dk_\perp\, d\omega,$$
$$\overline{E}_{z,\,\omega k_\perp}|_{z=vt} = \frac{1}{L}\int_0^L \left(\frac{1}{\varepsilon(\omega, z)}\,X(z)\,e^{i\omega t}\right)_{z=vt} dz. \qquad (17)$$

Using Eqs. (8) and (14), and also Eqs. (15) and (16), we find:

$$\overline{E}_{z,\,\omega k_\perp}|_{z=vt} = \frac{ike}{\pi c}\left\{\frac{a}{L}\,\frac{(\mu_1 - 1/\varepsilon_1\beta^2)}{p_1^2 - \omega^2/v^2} + \frac{b}{L}\,\frac{(\mu_2 - 1/\varepsilon_2\beta^2)}{p_2^2 - \omega^2/v^2}\right\}$$
$$+ \frac{iek_\perp^2}{\pi L v(\cos(\omega L/v) - \cos\psi)}\left\{Z_1^2\left[\frac{p_1 v}{\varepsilon_1\omega}\sin p_1 a\left(\cos p_2 b - \cos\frac{\omega}{v}\,b\right)\right.\right.$$
$$\left. + \frac{p_2 v}{\varepsilon_2\omega}\sin p_2 b\left(\cos p_1 a - \cos\frac{\omega}{v}\,a\right)\right] - 2Z_1 Z_2\left[\sin\frac{\omega}{v}\,a\left(\cos p_2 b\right.\right.$$
$$\left.\left. - \cos\frac{\omega}{v}\,b\right) + \sin\frac{\omega}{v}\,b\left(\cos p_1 a - \cos\frac{\omega}{v}\,a\right)\right] + \qquad (18)$$
$$\left. + Z_2^2\left[\frac{\varepsilon_1\omega}{p_1 v}\sin p_1 a\left(\cos p_2 b - \cos\frac{\omega}{v}\,b\right) + \frac{\varepsilon_2\omega}{p_2 v}\sin p_2 b\left(\cos p_1 a - \cos\frac{\omega}{v}\,a\right)\right]\right\},$$
$$Z_1 = \left(\frac{1}{p_1^2 - \omega^2/v^2} - \frac{1}{p_2^2 - \omega^2/v^2}\right), \quad Z_2 = \left(\frac{1}{\varepsilon_1(p_1^2 - \omega^2/v^2)} - \frac{1}{\varepsilon_2(p_2^2 - \omega^2/v^2)}\right),$$
$$\cos\psi = \cos p_1 a \cos p_2 b - \frac{1}{2}\left(\frac{p_1\varepsilon_2}{p_2\varepsilon_1} + \frac{p_2\varepsilon_1}{p_1/\varepsilon_2}\right)\sin p_1 a \sin p_2 b.$$

The first two terms in (18) represent the fields produced by the uniformly moving charge in the first and second media respectively. The remaining terms describe interference effects that arise in the passage of the charged particle through the laminar medium. As can be seen from Eq. (18), these terms go to zero if a or b goes to zero.

Before proceeding to the study of the expression (18), we note that these formulas can also be obtained in another way.

The laminar medium under consideration consists of alternate layers of two homogeneous and isotropic dielectrics. Therefore in each of these layers Eq. (6) is an equation with constant coefficients. To obtain the solutions in the entire medium, it is necessary to satisfy the proper boundary conditions at the surfaces separating the layers.

We suppose that the parameters of the layer $-a \leq z \leq 0$ are ε_1 and μ_1 and those of the layer $0 \leq z \leq b$, are ε_2 and μ_2. These layers are repeated, forming an unbounded laminar dielectric with a period $L = a + b$. Then in the first region, according to Eq. (6), we have:

$$E'_{z,\,\omega k_\perp} = Ae^{ip_1 z} + Be^{-ip_1 z} + \frac{ike}{\pi c}\,\frac{(\mu_1 - 1/\varepsilon_1\beta^2)}{p_1^2 - \omega^2/v^2}\,e^{-i\omega z/v}, \tag{19}$$

and in the second region:

$$E''_{z,\,\omega k_\perp} = Ce^{ip_2 z} + De^{-ip_2 z} + \frac{ike}{\pi c}\,\frac{(\mu_2 - 1/\varepsilon_2\beta^2)}{p_2^2 - \omega^2/v^2}\,e^{-i\omega z/v}. \tag{20}$$

From Eq. (1) we find the corresponding expressions for the radial components of the field.

The arbitrary constants A, B, C, and D are determined from the boundary conditions at the surfaces of the dielectrics and the conditions of periodicity for the fields. We present here only the expressions for the coefficients C and D, which are needed in what follows:

$$\begin{aligned}
C = {} & \frac{2ie}{\pi\Delta} Z_1 \{[ip_1^2 \varepsilon_2 \sin p_1 a - \varepsilon_1 p_1 p_2 (\cos p_1 a - e^{i\omega a/v})]\,(e^{-ip_2 b} - e^{-i\omega b/v})\,e^{-i\omega L/v} \\
& + \varepsilon_1 p_1 p_2 e^{-2i\omega L v}\,(1 - 2\cos p_1 a \cdot e^{i\omega a/v} + e^{2i\omega a/v})\} \\
& - \frac{2ie}{\pi\Delta} Z_2 \{[ip_2 \varepsilon_1^2 \sin p_1 a - \varepsilon_1 \varepsilon_2 p_1 (\cos p_1 a - e^{i\omega a/v})]\,(e^{-ip_2 b} - e^{-i\omega b/v})\,e^{-i\omega L/v} \\
& + \varepsilon_1 \varepsilon_2 p_1 e^{-2i\omega L/v}\,(1 - 2\cos p_1 a \cdot e^{i\omega a/v} + e^{2i\omega a/v})\}, \\
D = {} & \frac{2ie}{\pi\Delta} Z_1 \{\varepsilon_1 p_1 p_2 e^{-2i\omega L/v}\,(1 - 2\cos p_1 a \cdot e^{i\omega a/v} + e^{2i\omega a/v}) \\
& - [ip_1^2 \varepsilon_2 \sin p_1 a + \varepsilon_1 p_1 p_2 (\cos p_1 a - e^{i\omega a/v})]\,(e^{ip_2 b} - e^{-i\omega b/v})\,e^{-i\omega L/v}\} \\
& + \frac{2ie}{\pi\Delta} Z_2 \{\varepsilon_1 \varepsilon_2 p_1 e^{-2i\omega L/v}\,(1 - 2\cos p_1 a \cdot e^{-i\omega a/v} + e^{2i\omega a/v}) \\
& - [i\varepsilon_1^2 p_2 \sin p_1 a + \varepsilon_1 \varepsilon_2 p_1 (\cos p_1 a - e^{i\omega a/v})]\,(e^{ip_2 b} - e^{-i\omega b/v})\,e^{-i\omega L/v}\}, \\
\Delta = {} & -4\varepsilon_1 \varepsilon_2 p_1 p_2\,(e^{-2i\omega L/v} - 2\cos\psi \cdot e^{-i\omega L/v} + 1);
\end{aligned} \tag{21}$$

Z_1, Z_2 and $\cos\psi$ were determined previously.

Carrying out the averaging of the field (19), (20) and making a number of simplifications, one can again obtain Eq. (18).

In calculating the total losses according to Eq. (17), one must integrate Eq. (18) over all frequencies in the range $(-\infty, \infty)$. Since (18) is an odd function of ω, the value of the integral is determined only by the residues of the integrand at the singularities located on the real axis. The path of integration consists therefore of the real axis and suitable detours around the singularities located on it.

By direct calculations one can convince oneself that all the singularities of (18) are simple poles. They are given by the equations

$$\text{a)}\ \varepsilon_1(\omega) = 0, \quad \text{b)}\ \varepsilon_2(\omega) = 0, \quad \text{c)}\ \cos(\omega L/v) - \cos\psi = 0, \quad \text{d)}\ p_1^2 - \omega^2/v^2 = 0, \quad \text{e)}\ p_2^2 - \omega^2/v^2 = 0. \tag{22}$$

The energy losses of the charged particle that are associated with the zeroes of the dielectric constants ε_1 or ε_2 are polarization losses.

The roots of Eq. (22, c) give the radiation of the particle in the medium. In fact, the frequencies determined by these poles satisfy the relation

$$\cos\omega L/v = \cos p_1 a \cos p_2 b - \frac{1}{2}\left(\frac{p_1\varepsilon_2}{p_2\varepsilon_1} + \frac{p_2\varepsilon_1}{p_1\varepsilon_2}\right)\sin p_1 a \sin p_2 b \tag{23}$$

and correspond to waves propagated in the medium in question, since Eq. (23) is the dispersion equation of the laminar dielectric.

Radiation at a frequency satisfying Eq. (22, c) but not satisfying Eqs. (22, d or e), does not occur in a homogeneous dielectric with dielectric constants ε_1 or ε_2, and is a special Cerenkov effect due to parametric resonance. It can therefore be called Cerenkov radiation.

The connection between this radiation and the Cerenkov effect appears particularly clearly in the case of thin and closely spaced dielectric layers, when the laminar dielectric is electrodynamically equivalent to a homogeneous and anisotropic dielectric. In this case the parametric Cerenkov radiation reduces to the ordinary Cerenkov radiation in the anisotropic dielectric.

The energy losses associated with the roots of Eqs. (22, d or e) give the proper Cerenkov radiation in the first and second dielectrics, respectively. This radiation is propagated in the laminar medium if the corresponding frequencies satisfy also condition (23). The energy lost by the particle in proper Cerenkov radiation in the unbounded laminar medium is propagated also in directions perpendicular to the motion of the particle. The frequencies so radiated do not satisfy Eq. (23).

Consider now the polarization losses. Assume that if $\varepsilon_2(\omega) = 0$, then $\varepsilon_1(\omega) \neq 0$. In this case, in the integration of the (18) over the frequency it is necessary to keep only those terms for which $\varepsilon_2 = 0$ is a pole.

By several transformations of Eq. (18) we obtain:

$$\overline{E}_{z,\,\omega k_\perp\; z=vt} = -\frac{b}{L}\frac{ike}{\pi c}\frac{1}{\beta^2\varepsilon_2}\frac{1}{p_2^2 - \omega^2/v^2} + \frac{2ie k_\perp^2\,\omega\,(\cos p_2 b - \cos(\omega b/v))}{\pi L \varepsilon_2 v^2 p_2 \sin p_2 b\,(p_2^2 - \omega^2/v^2)^2} + O(\varepsilon_2),$$

and consequently:

$$-(d\overline{\mathscr{E}}/dz)_{\text{polar}} = \frac{2e^2}{v^2}\frac{b}{L}\frac{\omega_0}{(d\varepsilon_2/d\omega)_0}\int_0^{\varkappa_m}\frac{k_\perp\,dk_\perp}{k_\perp^2 + \omega_0^2/v^2} - \frac{4e^2\omega_0}{Lv^2(d\varepsilon_2/d\omega)_0}\int_0^{\infty}\frac{k_\perp^2\,dk_\perp}{(k_\perp^2 + \omega_0^2/v^2)^2}\frac{\left(\cosh k_\perp b - \cos\frac{\omega_0}{v}b\right)}{\sinh k_\perp b}, \quad (24)$$

where ω_0 is a root of the equation $\varepsilon_2(\omega) = 0$.

The first term in Eq. (24) is the ordinary polarization loss in a layer of dielectric of thickness b with dielectric constant ε_2. The second term is due to the presence of the boundaries.

From Eq. (24) it follows that the presence of boundaries always leads to a reduction of the polarization losses. In fact, in the second term the integral is taken with an essentially positive integrand, and thus always reduces the total polarization loss.

Since the interference effects caused by the boundaries of the dielectrics are important only for wavelengths that are not very small in comparison with the structure period, and the thicknesses of the discs are at least such that a macroscopic treatment is valid, it is clear that for very high $k_\perp$ the boundary effects already do not play any important part. Therefore the second integral in Eq. (24) does not diverge at the upper limit, and the integration over $k_\perp$ is taken to infinity.

In the evaluation of this integral it is expedient to divide the region of integration into two parts: $(0, 1/b)$ and $(1/b, \infty)$. Then in the integration over the first region the integrand can be simplified by supposing that $k_\perp b \ll 1$. This is justified, since the integrand reaches its maximum for $k_\perp b \ll 1$. In the second integral the main contribution comes from the region $k_\perp b \gg 1$. Therefore:

$$-(d\overline{\mathscr{E}}/dz)_{\text{polar}} = \frac{e^2}{v^2}\frac{\omega_0}{(d\varepsilon_2/d\omega)_0}\frac{b}{L}\ln\frac{\varkappa_m^2 b^2 + (\omega_0 b/v)^2}{1 + (\omega_0 b/v)^2} - \frac{2e^2}{v^2}\frac{\omega_0}{(d\varepsilon_2/d\omega)_0}\frac{b}{L}\left[\frac{(1 + \omega_0^2 b^2/2v^2) - \cos(\omega_0 b/v)}{(\omega_0 b/v)^2(1 + (\omega_0 b/v)^2)} + \frac{v}{b\omega_0}\arctan\frac{b\omega_0}{v}\right]. \quad (25)$$

For sufficiently small values of b we have $\omega_0 b/v \ll 1$, so that the polarization losses are given by:

$$-(d\overline{\mathscr{E}}/dz)_{\text{polar}} = \frac{2e^2}{v^2}\frac{\omega_0}{(d\varepsilon_2/d\omega)_0}\frac{b}{L}\ln\frac{\varkappa_m b}{7{,}4}. \quad (26)$$

When the thickness of the dielectric discs is increased, the role of the boundary effects is diminished, and thus the second term in Eq. (25) is also decreased. For sufficiently large b we have $\omega_0 b/v \gg 1$, and Eq. (25) goes over into the well known expression for the polarization losses in an unbounded dielectric with dielectric constant ε_2:

$$-(d\overline{\mathscr{E}}/dz)_{\text{polar}} = \frac{e^2}{v^2}\frac{\omega_0}{(d\varepsilon_2/d\omega)_0}\ln\left(1 + \frac{\varkappa_m^2 v^2}{\omega_0^2}\right). \quad (27)$$

From Eqs. (26) and (27) it follows that a particle loses less energy through the polarization of the

medium in a laminar dielectric than in a solid dielectric, if it travels the same distance in the dielectric in the two cases. If zeroes of the dielectric constant ε_2 occur at not just one but at several values of the frequency, the polarization losses in the medium are given by the sum of expressions (25) calculated for each of the frequencies ω_i for which $\epsilon_2 = 0$.

In order to study in more detail the role played by transition processes in polarization losses, we consider these losses within a single dielectric layer, before averaging over the period of the structure. In doing this we shall start from the expression (20) for the fields. The zeroes of the dielectric constant ε_2 will be poles only for the coefficients C and D which determine the field in the dielectric layers with the constant ε_2. Since for $0 \leq z \leq b$ we have Eq. (20), where C and D are given by (21), we get the following expression for the polarization losses:

$$-(d\mathcal{E}/dz)_{\text{polar}} = \frac{e^2\omega_0}{v^2(d\varepsilon_2/d\omega)_0}\ln\left(1+\frac{\varkappa_m^2 v^2}{\omega_0^2}\right)$$

$$-\frac{2e^2}{v(d\varepsilon_2/d\omega)_0 b}[\sin\varkappa(1-\gamma_1)J(\gamma_1)+\sin\varkappa\gamma_1\cdot J(1-\gamma_1)],$$

$$J(\gamma_1)=\int_0^\infty \frac{x^2dx\cosh\gamma x}{x^2+\varkappa^2\sinh x}, \quad \gamma_1=\frac{z}{b}, \quad \varkappa=\frac{\omega_0 b}{v} \tag{28}$$

From the relation (28) it follows that in a single dielectric layer the loss of energy by the particle in polarization of the medium is not uniform. The integrals J cannot be expressed in terms of known functions, so that the dependence of the energy loss on the depth can be found only by numerical calculations.

The integral $J(\gamma)$ is a monotonically increasing function of the parameter $\gamma = z/b$. Since the main contribution to the value of the integral comes from large values of x, and for large x the integrand is proportional to $e^{-x(1-\gamma)}$, $J(\gamma)$ increases exponentially with increasing γ. The integral $J(1-\gamma)$ decreases with increase of γ. Consequently, these integrals take their greatest values at the corresponding boundaries of the dielectric. Each of the integrals is multiplied by a periodic function, so that as a whole the second term in Eq. (28) is an oscillating function with amplitude decreasing toward the center of the dielectric layer. The amplitude of the maximum variation is proportional to $1/b$, so that the part played by the second term decreases with increasing thickness of the layers.

The decrease of the polarization losses near the boundaries of the dielectric also explains the previously noted reduction of the average polarization losses in laminar dielectrics.

We now consider the parametric Cerenkov radiation. In the general expression (17) for the total losses, the parametric Cerenkov effect corresponds to the poles of the integrand (18) which give radiation and do not lead to the ordinary Cerenkov effect. *i.e.*, the roots of the equation (22, c) when $p_1^2 \neq \omega^2/v^2$ and $p_2^2 \neq \omega^2/v^2$.

For the parametric Cerenkov radiation we can find the spectral distribution of the radiation and write down in general form the expression for the energy lost by the particle to the radiation. Integrating Eq. (18) with respect to frequency [taking into account only the poles given by Eq. (22, c)], we have

$$-(d\mathcal{E}/dz)_{\text{par.}} = \frac{e^2}{L^2}\int \frac{k_\perp^3\,dk_\perp\,(p_1^2-p_2^2)^2}{\sin\frac{\omega}{v}L(1-v/v_{bd})\,[(p_1^2-\omega^2/v^2)(p_2^2-\omega^2/v^2)]^2}F,$$

$$F=\left\{\frac{p_1 v}{\varepsilon_1\omega}\sin p_1 a\left(\cos p_2 b-\cos\frac{\omega}{v}b\right)+\frac{p_2 v}{\varepsilon_2\omega}\sin p_2 b\left(\cos p_1 a-\cos\frac{\omega}{v}a\right)\right\} \tag{29}$$

$$\times\left\{1-\frac{\left[\varepsilon_2\left(p_2^2-\frac{\omega^2}{v^2}\right)-\varepsilon_1\left(p_1^2-\frac{\omega^2}{v^2}\right)\right]\left[\sin\frac{\omega}{v}a\left(\cos p_2 b-\cos\frac{\omega}{v}b\right)+\sin\frac{\omega}{v}b\left(\cos p_1 a-\cos\frac{\omega}{v}a\right)\right]}{\varepsilon_1\varepsilon_2(p_1^2-p_2^2)\left[\frac{p_1 v}{\varepsilon_1\omega}\sin p_1 a\left(\cos p_2 b-\cos\frac{\omega}{v}b\right)+\frac{p_2 v}{\varepsilon_2\omega}\sin p_2 b\left(\cos p_1 a-\cos\frac{\omega}{v}a\right)\right]}\right\}^2.$$

Here $v_{bd} = L\partial\omega/\partial\psi$, while ω and $k_\perp$ are related by Eq. (23). The region of integration over $k_\perp$ is the segment of the real axis on which Eq. (23) is satisfied for real ω.

Eq. (23) can be used to change variables in the integral (29). In fact, from this equation we find:

$$dk_\perp = [L(1-v/v_{bd})/(\partial\psi/\partial k_\perp)]\,d\omega/v,$$

and the integral takes the form:

$$-(\overline{d\mathcal{E}/dz})_{\text{par.}}=\int f_\omega\, d\omega,$$

$$f_\omega=\frac{e^2}{L\overline{v}}\frac{k_\perp^3(\omega)\,(p_1^2-p_2^2)^2}{\sin\frac{\omega}{v}L\cdot\frac{\partial\psi}{\partial k_\perp}\left|\left(p_1^2-\frac{\omega^2}{v^2}\right)\left(p_2^2-\frac{\omega^2}{v^2}\right)\right|^2}F, \quad (30)$$

f_ω is the spectral distribution of the parametric Cerenkov radiation. The limits of the integration in Eq. (30) are determined by means of Eq. (23), and the direction of integration is chosen in such a way that it corresponds to increasing $k_\perp$.

The conditions for the parametric radiation, like those for the ordinary Cerenkov effect, restrict the frequencies emitted by the particle. Therefore in the integration of the expression (18) over ω the integral is in reality different from zero only over a certain range of frequencies. It can turn out that over this whole region or over a certain part of it the wavelengths radiated exceed considerably the period of the dielectric structure, *i.e.*,

$$\beta_\phi\lambda\gg 1, \quad (31)$$

where $\beta_\phi=v_\phi/c$, v_ϕ being the phase velocity of the wave.

When the condition (31) holds, the study of the expression for the energy loss is decidedly simplified. As is well known[7,8], a laminar medium in which electromagnetic waves satisfying the condition (31) are propagated is equivalent in its electrodynamic properties to an anisotropic dielectric with effective values of the dielectric constants ε_r and ε_z given by

$$\varepsilon_r=(a\varepsilon_1+b\varepsilon_2)/(a+b),$$
$$\varepsilon_z=(a+b)\,\varepsilon_1\varepsilon_2/(a\varepsilon_2+b\varepsilon_1). \quad (32)$$

It is natural to expect that in this case Eq. (18) will reduce to the well known expression for the field of a charge moving uniformly in an anisotropic dielectric[9-11]. In fact, using Eq. (31), we get from Eq. (18) for $\mu_1=\mu_2=1$:

$$\bar{E}_{z,\,\omega k_\perp}\big|_{z=vt}=\frac{ie\omega}{\pi c^2}\frac{1-1/\varepsilon_r\beta^2}{k^2\varepsilon_z-k_\perp^2-\omega^2\varepsilon_z/v^2\varepsilon_r}. \quad (33)$$

According to Eq. (17) the total energy loss in this case is given by

$$-(\overline{d\mathcal{E}/dz})=\frac{ie^2}{\pi c^2}\int_0^{\varkappa_m}k_\perp dk_\perp\int_{-\infty}^{\infty}\frac{\omega d\omega\,(1-1/\varepsilon_r\beta^2)}{(\omega^2\varepsilon_z/v^2\varepsilon_r)(\varepsilon_r\beta^2-1)-k_\perp^2}. \quad (34)$$

In integrating Eq. (34) over frequency we shall assume that owing to a slight attenuation in the dielectric the poles of the integrand are displaced from the real axis. These poles are given by the roots of the equation

$$k_\perp^2=(\omega^2\varepsilon_z/v^2\varepsilon_r)(\varepsilon_r\beta^2-1). \quad (35)$$

After integration with respect to frequency the attenuation is let go to zero. Since in Eq. (34) the integral with respect to ω is equal to the sum of the residues at the points given by Eq. (35), the integration is taken only over the range of frequencies that satisfy this equation as $k_\perp$ is varied from 0 to $\varkappa_m$:

$$\varkappa_m^2>(\omega^2\varepsilon_z/v^2\varepsilon_r)(\varepsilon_r\beta^2-1)>0. \quad (36)$$

Consequently:

$$-\overline{(d\mathcal{E}/dz)}=\frac{e^2}{c^2}\int\left(1-\frac{1}{\varepsilon_r\beta^2}\right)\omega d\omega. \quad (37)$$

The direction of integration over this range is chosen in such a way that the quantity $k_\perp$ given by the relation (35) is increasing. Then the integrand will change sign with change of direction of integration, and the necessity of taking the absolute value is avoided.

The result obtained agrees with that of Sitenko and Kaganov[12]*; *i.e.*, when the condition (31) holds one can in fact calculate the energy loss of a charged particle moving in a laminar medium from the formulas for the Cerenkov radiation in an anisotropic dielectric. The dielectric constants of the equivalent anisotropic dielectric are given by formulas (32).

Let us consider some concrete cases. Take

$$\varepsilon_1=1,\quad \varepsilon_2=1+A/(\omega_0^2-\omega^2),$$

Then

$$\varepsilon_r=1+\frac{bA}{L(\omega_0^2-\omega^2)},\quad \varepsilon_z=\frac{\omega_0^2-\omega^2+A}{\omega_0^2-\omega^2+aA/L}. \quad (38)$$

In the case under consideration the range of integration over frequency specified by Eq. (36) falls into two parts. This means that the spectrum of the radiation of the particle

$$\omega_0^2+A\geqslant\omega^2\geqslant\omega_0^2-R'\quad\text{for}\quad R'<\omega_0^2,$$

* For a homogeneous anisotropic medium.

or

$$\omega_0^2 + A \geqslant \omega^2 \geqslant \omega_0^2 \quad \text{for} \quad R' > \omega_0^2$$

[where $R' = bA\beta^2/L(1-\beta^2)$], does not contain the frequencies specified by the inequalities

$$\omega_0^2 + \frac{a}{L} A > \omega^2 > \omega_0^2 + bA/L \quad \text{for} \quad a > b,$$

$$\omega_0^2 + \frac{b}{L} A > \omega^2 > \omega_0^2 + aA/L \quad \text{for} \quad a < b.$$

when $a = b$ the two regions coincide.

It is convenient to represent the Cerenkov radiation loss (37) as the sum of two terms, obtained by integration over the first and second regions, respectively,

$$-\overline{d\mathcal{E}/dz} = J_1 + J_2.$$

For $a > b$:

$$J_1 = \frac{e^2 b}{2v^2 L} A \left\{(1-\beta^2) - \ln\frac{a-b}{a}\right\},$$

$$J_2 = \frac{e^2 b}{2v^2 L} A \left\{\ln\left[\frac{a-b}{a(1-\beta^2)} \frac{\varkappa_m^2 v^2}{\omega_0^2 + bA/L}\right] - 1\right\}, \quad \text{if} \quad R' < \omega_0^2, \tag{39}$$

$$J_2 = \frac{e^2}{2v^2}\left\{\frac{b}{L} A \ln\left[\frac{\varkappa_m^2 v^2}{A}\left(\frac{a}{b} - \frac{b}{a}\right)\right] - (1-\beta^2)\left(\omega_0^2 + \frac{b}{L} A\right)\right\}, \quad \text{if} \quad R' > \omega_0^2$$

For $a = b$:

$$J_1 = \frac{e^2}{4v^2} A \left\{(1-\beta^2) + \frac{1}{2} \ln\frac{\varkappa_m^2 v^2}{\omega_0^2 + A/2}\right\},$$

$$J_2 = \frac{e^2}{4v^2} A \left\{\frac{1}{2} \ln\left[\frac{\varkappa_m^2 v^2}{(1-\beta^2)^2(\omega_0^2 + A/2)}\right] - 1\right\}, \quad \text{if} \quad R' < \omega_0^2, \tag{40}$$

$$J_2 = \frac{e^2}{4v^2}\left\{\frac{A}{2} \ln\left[\frac{4\varkappa_m^2 v^2(\omega_0^2 + A/2)}{A^2}\right] - 2(1-\beta^2)\left(\omega_0^2 + \frac{1}{2} A\right)\right\}, \quad \text{if} \quad R' > \omega_0^2.$$

Finally, for $b > a$:

$$J_1 = \frac{e^2}{2v^2} A \left\{\frac{a}{L}(1-\beta^2) + \frac{b}{L} \ln\left[\frac{b-a}{b} \frac{\varkappa_m^2 v^2}{\omega_0^2 + bA/L}\right]\right\}, \tag{41}$$

$$J_2 = \frac{e^2}{2v^2} A \left\{\frac{b}{L} \ln\frac{b}{(b-a)(1-\beta^2)} - \frac{b}{L}\beta^2 - \frac{a}{L}(1-\beta^2)\right\}, \quad \text{if} \quad R' < \omega_0^2,$$

$$J_2 = \frac{e^2}{2v^2}\left\{A \frac{b}{L} \ln\left[\frac{L}{b-a} \frac{\omega_0^2 + bA/L}{A}\right] - (1-\beta^2)(\omega_0^2 + bA/L)\right\}, \quad \text{if} \quad R' > \omega_0^2.$$

From the formulas given it follows that on relative thickening of the dielectric discs the main part of the Cerenkov radiation loss is shifted from the first frequency region to the second.

Let us consider the case $b > a$, which allows the passage to the limit $a \to 0$ of the homogeneous and isotropic dielectric with dielectric constant $\varepsilon_2 = 1 + A/(\omega_0^2 - \omega^2)$. For $a \to 0$ the width of the first region goes to zero, and the integral J_1 over this region goes to the value

$$J_{1\,|a\to 0} = \frac{e^2 A}{2v^2} \ln\frac{\varkappa_m^2 v^2}{\omega_0^2 + A}. \tag{42}$$

The radiation given by (42) corresponds to the frequency $\omega^2 = \omega_0^2 + A$ at which the dielectric constant of the medium goes to zero, and, according to Eq. (36), it cannot be propagated in the medium. Therefore Eq. (42) gives the polarization losses

The integral over the second region is

$$J_2 = \frac{e^2 A}{2v^2}\left\{\ln\frac{1}{1-\beta^2} - \beta^2\right\} \quad \text{for} \quad R' < \omega_0^2,$$

$$J_2 = \frac{e^2 A}{2v^2}\left\{\ln\frac{\omega_0^2 + A}{A} - \frac{\omega_0^2}{A}(1-\beta^2)\right\} \quad \text{for} \quad R' > \omega_0^2, \tag{43}$$

and gives the ordinary Cerenkov radiation in the dielectric in question. From Eqs. (42) and (43) it follows that in an isotropic and homogeneous dielectric the polarization losses considerably exceed the Cerenkov radiation loss.

The effective constants ε_z and ε_r given by (38) no common zeroes. Therefore, according to Ref. 12, it could be expected that polarization losses are absent in the laminar dielectric. But the foregoing analysis shows that in this case the polarization losses may indeed be considerably reduced, but remain finite. This seeming inconsistency is explained by the fact that in a laminated dielectric the phase velocity of electromagnetic waves is zero in the neighborhood of the frequency given by $\omega^2 = \omega_0^2 + A$, and consequently the condition for the applicability of the approximation (31) is not satisfied. Therefore, Eqs. (39)–(41) for the Cerenkov radiation do not describe the total energy loss of a charged particle in a dielectric divided into thin layers. The radiation loss is accompanied by the polarization losses given by (26).

Comparison of Eqs. (41) and (43), which give the radiation energy losses in the laminar and solid dielectrics, shows readily that in the laminar dielectric the energy losses in the second region of frequencies is smaller by about a factor b/L than in the solid dielectric, *i.e.*, these are quantities of the same order. Together with these, in the laminar dielectric there are radiation losses, concentrated in the first region of frequencies. They are of the same order as the polarization losses in the solid dielectric, *i.e.*, are much greater than the radiation losses in the solid dielectric.

Thus when an isotropic dielectric is divided into layers, the frequency that previously determined the polarization losses broadens out into a band of frequencies, and an intense Cerenkov radiation arises in this band. The radiation loss increases and becomes comparable with the polarization loss. Furthermore, as b/L is decreased the frequency region in which the intense Cerenkov radiation is concentrated is displaced toward longer wavelengths.

For ordinary dielectrics the effect of reduction of the polarization loss can be observed only in very thin layers of the dielectric (films), since the polarization losses in such dielectrics are determined by frequencies lying in the optical region.

It must be remarked that conditions (31) and (36) can also be simultaneously satisfied in the microwave region, if the laminar medium is formed by an electron plasma. In particular, these conditions can be satisfied in the motion of charged particles through bunches of electrons.

As is well known, Cerenkov radiation is in general absent from an unbounded plasma. The radiation energy losses arise upon the application of an external magnetic field, when the plasma becomes an optically active medium[13]. On division of the plasma into layers, according to the results presented above, the intensity of the Cerenkov radiation becomes large, since the radiation losses become comparable with the polarization losses. Moreover, the radiated frequencies are in the microwave region. Therefore the occurrence of an intense Cerenkov radiation in laminar dielectrics (plasmas) can find wide application in radio physics for the generation and amplification of ultrahigh frequencies.

In the passage of a particle through a laminar plasma (bunched electrons)

$$\varepsilon_1 = 1, \quad \varepsilon_2 = 1 - \Omega^2/\omega^2, \quad \Omega^2 = 4\pi e^2 n/m.$$

Here n is the density of electrons in the bunches and b is the width of a bunch. Then the condition that the wavelengths radiated in the first frequency region be large in comparison with the structure period takes the form

$$\pi m v^2/ne^2 \gg Lb.$$

Putting $A = \Omega^2$ and $\omega_0^2 = 0$ in Eqs. (39)–(41), we get the following expression for the total Cerenkov radiation loss

$$-(\overline{d\mathscr{E}}/dz)_{\text{Cer.}} = \frac{2\pi ne^4}{mv^2}\frac{b}{L}\ln\left(\frac{L}{b}\frac{\varkappa_m^2 v^2 m}{4\pi ne^2}\right), \qquad (44)$$

and according to Eq. (26) the polarization loss is given by

$$-(\overline{d\mathscr{E}}/dz)_{\text{polar.}} = \frac{4\pi ne^4}{mv^2}\frac{b}{L}\ln\left(\frac{\varkappa_m b}{7{,}4}\right). \qquad (45)$$

Under the actual conditions the boundaries of the plasma layers are somewhat diffuse. Therefore it is of interest to take into account diffuseness of the boundaries. This problem can be solved when the condition (31) is satisfied. Indeed, it is shown in Ref. 7 that if the properties of the medium vary continuously and the period of these variations is sufficiently small, such a medium is equivalent in its electrodynamic properties to an anisotropic dielectric with effective values of its dielectric constants given by:

$$\varepsilon_r = \frac{1}{L}\int_0^L \varepsilon(z)\,dz, \qquad \frac{1}{\varepsilon_z} = \frac{1}{L}\int_0^L \frac{dz}{\varepsilon(z)}. \tag{46}$$

It is natural to expect that the energy loss of a charged particle in such a medium will also be determined by Eq. (37), with ε_r and ε_z given by (46).

Assuming a concrete form of the diffuse boundaries, one can solve the stated problem.

For example, if over the range of a single plasma layer the particle density increases linearly from zero to its maximum value n_0 in edge regions of thickness η, the effective values of the dielectric constants are given by:

$$\varepsilon_r = 1 - \frac{b}{L}\frac{(b-\eta)}{b}\frac{\Omega_0^2}{\omega^2},$$

$$\varepsilon_z = \left(1-\frac{\Omega_0^2}{\omega^2}\right)\left[1 - \frac{a}{Z}\frac{\Omega_0^2}{\omega^2} - \frac{2\eta}{L} - \frac{\omega^2\eta}{\Omega_0^2 L}\left(1-\frac{\Omega_0^2}{\omega^2}\right)\ln\left(1-\frac{\Omega_0^2}{\omega^2}\right)\right]^{-1}. \tag{47}$$

On the other hand, if over the range of a single plasma layer the particle density varies continuously according to the sinusodial law

$$n(z) = n_0 \sin\frac{\pi}{b}(b-z), \tag{48}$$

then

$$\varepsilon_r = 1 - 2b\Omega_0^2/\pi L\omega^2,$$

$$\varepsilon_z = \frac{L}{a}\left(1 - \frac{b}{\pi a}\frac{\omega^2}{\sqrt{\Omega_0^4-\omega^4}}\ln\frac{\Omega_0^2+\sqrt{\Omega_0^4-\omega^4}}{\Omega_0^2-\sqrt{\Omega_0^4-\omega^4}}\right)^{-1} \quad \text{for} \quad \Omega_0^2 > \omega^2,$$

$$\varepsilon_z = \frac{L}{a}\left(1 - \frac{4b}{\pi a}\frac{\omega^2}{\sqrt{\omega^4-\Omega_0^4}}\arctan\sqrt{\frac{\omega^2-\Omega_0^2}{\omega^2}}\right)^{-1} \quad \text{for} \quad \Omega_0^2 < \omega^2.$$

From these formulas it follows that the quantity ε_r depends only slightly on the degree of diffuseness of the plasma layers, while ε_z is mainly determined by the nature of the boundaries. Therefore the range of frequencies of the Cerenkov radiation arising in a laminar plasma depends essentially on the character of the boundaries [this frequency range is given by the inequalities (36)], while the spectral distribution of the radiation inside this range does not depend much on the diffuseness.

In conclusion the writers express their gratitude to K. D. Sinel'nikov, A. I. Akhiezer, and G. Ia. Liubarskii for valuable discussions.

[1] V. L. Ginzburg, J. Exptl. Theoret. Phys. (U.S.S.R.) 10, 601 (1940).

[2] Akhiezer, Liubarskii, and Fainberg, J. Tech. Phys. (U.S.S.R.) 25, 2526 (1955).

[3] L. I. Mandel'shtam and N. D. Papaleksi, J. Tech. Phys. (U.S.S.R.) 4, 5 (1934); L. I. Mandel'shtam, *Complete Collected Works*, vols. II and III, Acad. Sci. USSR Press, 1950.

[4] S. I. Vavilov, *Collected Works*, vol. II, Acad. Sci. USSR Press, 1952.

[5] V. L. Ginzburg and I. M. Frank, J. Exptl. Theoret. Phys. (U.S.S.R.) 16, 15 (1946).

[6] L. D. Landau, Editor's remarks on book by N. Bohr, "Passage of Atomic Particles through Matter", IIL, 1950.

[7] Ia. B. Fainberg and N. A. Khizhniak, J. Tech. Phys. (U.S.S.R.) 25, 711 (1955).

[8] S. M. Rytov, J. Exptl. Theoret. Phys. (U.S.S.R.) 29, 605 (1955).

[9] V. L. Ginzburg, J. Exptl. Theoret. Phys. (U.S.S.R.) 10, 608 (1940).

[10] A. A. Kolomenskii, Dokl. Akad. Nauk SSSR 86, 1097 (1952).

[11] M. I. Kaganov, J. Tech. Phys. (U.S.S.R.) 23, 507 (1953).

[12] A. G. Sitenko and M. I. Kaganov, Dokl. Akad. Nauk SSSR 100, 681 (1955).

[13] A. A. Kolomenskii, Dokl. Akad. Nauk SSSR 106, 982 (1956).

Translated by W. H. Furry
187

Theory of Cyclotron Resonance in Metals*

M. IA. AZBEL', AND E. A. KANER
Physical and Technological Institute Academy of Sciences of Ukrainian SSR
(Submitted to JETP editor May 3, 1956)
J. Exptl. Theoret. Phys. (U.S.S.R.) 32, 896-914 (1956)

Investigation of a new type of resonance, which takes place in metals located in a high frequency electromagnetic field and a stationary magnetic field parallel to the surface of the metal, the frequency ω of the alternating field being a multiple of the cyclotron frequency $\Omega = eH/mc$.

The shape of the resonance curve depends considerably on the electron dispersion law and permits one to determine from the experimental data the topology of the Fermi surface and find some of its concrete characteristics.

The surface impedance of the metal has been computed for an arbitrary direction of the stationary magnetic field relative to the surface. The analysis has been performed on basis of the most general assumptions of the electron theory of metals (arbitrary law of dispersion and collision integral). It has been proved that it is possible to introduce the mean free path time of the electrons under the conditions of an anomalous skin effect at arbitrary temperatures.

1. DIAMAGNETIC AND CYCLOTRON RESONANCES

IT IS WELL KNOWN that a free electron travelling through a uniform magnetic field moves in a spiral whose axis is in the direction of the magnetic field. The frequency of rotation of the electron in a plane perpendicular to the magnetic field, $\Omega = eH/mc$, is the same for all electrons and is independent of the magnitude or the direction of their velocity. As a consequence, an external high frequency field of frequency $\omega = \Omega$, impressed on a free electron gas, produces resonance.

In metals and semiconductors this resonance is "smeared out" because of electron collisions with phonons, with lattice imperfections and with the surface. For a substantial resonance to occur, it is necessary in every case, that the electron succeed in making a large number of revolutions over the mean free path $l = vt_0$, *i.e.*

$$t_0 \gg 2\pi/\Omega, \; H \gg 2\pi mc/et_0 \qquad (1.1)$$

(note that this condition requires that $r \ll l$). In these equations, v is the velocity, t_0 is the mean free path time and e is the electronic charge; $r = mvc/eH$ is the radius of the orbit of the electron in a magnetic field H. Since near resonance, ω is approximately equal to Ω, it follows that

$$\omega \gg 2\pi/t_0 \qquad (1.2)$$

(the case of an arbitrary value of ωt_0 and $\Omega \gg 2\pi(\omega + 1/t_0)$ has been previously examined[2]).

The mean free path time of electrons, t_0, is between 10^{-13} and 10^{-14} sec at room temperature and between 10^{-10} and 10^{-11} sec at liquid helium temperatures. Therefore, as the approximations in Eqs. (1.1) and (1.2) show, the resonance should become observable at helium temperatures in centimeter and millimeter wavelength ranges in magnetic fields with H between 10^3 and 10^4 oersteds.

Consider in particular the motion of electrons in the resonant condition with $\omega \approx \Omega \gg 2\pi/t_0$. The skin depth in this case does not depend on t_0 and is equal* to

$$\delta = (c^2 t_0/2\pi\sigma)^{1/2} = (mc^2/2\pi ne^2)^{1/2},$$

where $\sigma = ne^2 t_0/m$ is the dc conductivity and n is the density of electrons.

The ratio of δ to r, the radius of the orbit of the electron in a magnetic field, is:

$$\delta/r = H/(4\pi n\varepsilon)^{1/2}$$

(ε is the energy of the electron). In semiconductors, ε is approximately equal to kT, and since $H \gg 2\pi mc/et_0$ (Eq. 1.1), it follows that

*A preliminary report on this resonance is contained in Ref. 1.

*It should be recalled that the skin depth for the normal skin effect is given by $\delta = (c^2 \mid 1 + \omega t_0 \mid /2\pi\omega\sigma)^{1/2}$. For rough estimates this formula is always applicable.

$$\delta/r \gg mc/et_0 \sqrt{nkT} \gtrsim 1$$

Thus, if one assumes $m \sim 10^{-30}$ g, $t_0 \sim 10^{-10}$ sec, $T \sim 4°$K and $n \sim 10^{14}$ cm^{-3}, one finds that $\delta/r \gg 300$. Consequently, the electron in its orbit in semiconductors finds itself in a practically uniform electric field.

In metals*

$$\delta/r \sim Hm^{1/2}h^{-1}n^{-1/6} \sim 10^{-6}H \text{ Oe} \qquad (1.3)$$

($n \sim 10^{22}$ cm^{-3}) so that in all actually attainable magnetic fields, $\delta \ll r$. This means that only those electrons which move in a very thin layer ($z \sim \delta_{\text{eff}} \ll r \ll l/2\pi$) near the surface of the metal find themselves in a non-ignorable electric field.** For this reason it is exceedingly important whether the fixed magnetic field is parallel to the surface or not. In the latter case the electron passes through the layer δ_{eff} only once, the time of passage through if being δ_{eff}/v, which is small compared to the period of the field, and the resonance obviously does not occur*** (in the zero approximation for δ_{eff}/r).

If the magnetic field is parallel to the surface of the metal ($z = 0$) (or more exactly, if the angle between the surface and the field is given by $\Phi \lesssim \delta_{\text{eff}}/l$, then the principal contribution to the current density is made by those electrons moving near the surface (Fig. 1), but not colliding with it, which enter and re-enter the layer $z \sim \delta_{\text{eff}}$ many times ($l/2\pi r \gg 1$). They do not move into the interior of the metal, since the value of the projection of their velocity on the axis, averaged over the period, is

$$\overline{v}_z = -(c/eH)\,\overline{dp_y/dt} = 0.$$

The motion of these electrons is exactly analogous to the motion of charged particles in a cyclotron

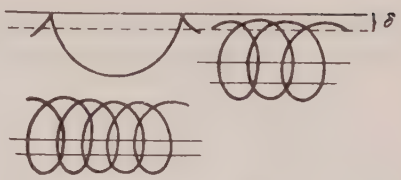

FIG. 1. Schematic form of some possible electron trajectories in a metal.

with only one gap, and at frequencies ω, which are multiples of Ω, resonance can occur.

This resonance in metals differ essentially from resonance in semiconductors. In the latter materials $\delta \gg r$, l, and Ohm's law is obeyed [$\mathbf{j} = \sigma(\mathbf{H})\mathbf{E}$] so that the ordinary skin effect takes place. Resonance evidently appears at a frequency $\omega = \Omega$ and it should of course be called diamagnetic resonance[3].

In metals which are in the resonance condition ($\delta_{\text{eff}} \ll r \ll l/2\pi$), Ohm's law $\mathbf{j} = \sigma\,\mathbf{E}$ is not satisfied, since the electric fields are essentially changed over the mean free path. The resonance arises under conditions of the anomalous skin effect for multiple frequencies with $\omega \approx q\Omega$ ($q = \pm 1, \pm 2, \pm 3, \ldots$). Furthermore in the zero approximation for $\delta_{\text{eff}}/r \ll 1$, resonance will occur only if the magnetic field is parallel to the surface of the metal. Such a resonance, which can be truly called "cyclotron" resonance, has not been previously described in the literature. (In the literature[3], diamagnetic resonance is also called "cyclotron" resonance. Since we have shown that diamagnetic and cyclotron resonances are based on phenomena which are physically distinguishable, the terminology change proposed here would take this distinction into account.)

The purpose of the present work is a calculation of the principal values Z_α of the complete surface impedance tensor of the metal $Z_{\mu\nu} = R_{\mu\nu} + iX_{\mu\nu}$:

$$-\frac{4\pi i\omega}{c^2} E_\mu(0) = \sum_{\nu=1}^{2} Z_{\mu\nu} E'_\nu(0) \qquad (\mu, \nu = x, y),$$

where $E_\mu(0)$ is the value of the component of the electric field at the surface of the metal ($z = 0$).

At resonance R and X pass through their minima (see below). The minima of R correspond to the maximum Q in the resonator and the minima of X occur at the smallest displacement of the resonant frequency.

2. THE ROLE OF THE DISPERSION LAW

Thus far, it was surmised that the "cyclotron" frequency Ω is the same for all electrons. This is true only in those cases, when the dispersion law

*Bismuth may be an exception since in bismuth $n \sim 10^{18}$ cm^{-3}, and the effective masses in certain directions are very small. Under such conditions diamagnetic resonance is possible[3].

**Note that δ is different from δ_{eff}, which is the effective skin depth in the general case

$$\delta_{\text{eff}} = \int_0^\infty j(z)\,dz/j(0).$$

***In this case δ_{eff} is approximately $\sigma\delta_{\text{eff}}/l$, *i.e.*, it assumes its value in the absence of a magnetic field[4]. Consequently, the impedance [$Z = 2\pi\omega\delta_{\text{eff}}(1+i)/c^2$] is independent of the magnetic field.

(*i.e.*, the relation between the energy ε of the quasi-particles, and their quasi-momentum $\mathbf{p}$) is quadratic:

$$\varepsilon(\mathbf{p}) = \sum_{i,k} \mu_{ik} p_i p_k / 2.$$

For the general case of an arbitrary dispersion law it is necessary to consider two possibilities. The trajectory of the quasi-particle in a fixed magnetic field $\mathbf{H}$ is given by the equations:

$$\varepsilon(\mathbf{p}) = \varepsilon, \; p_H = \text{const.} \tag{2.1}$$

(*i.e.*, the energy ε and the projection of the quasi-momentum p_H are integrals of the motion!) If the trajectory is not closed, the motion of the quasi particle in momentum space is infinite, non-periodic and, obviously, resonance is impossible.

If, on the other hand, the curve of Eq. (2.1) is closed, the motion in momentum space will be periodic with a frequency Ω, given by[5]

$$\Omega = (2\pi eH/c)\, \partial S/\partial \varepsilon, \tag{2.2}$$

where $S(\varepsilon, p_H)$ is the area of the cross section, bounded by the curves (2.1) (only this case will be considered in what follows). The quantity $(1/2\pi)\, \partial S/\partial \varepsilon$ plays the role of an effective mass. In the case of a non-quadratic dispersion law, Ω depends on ε and p_H, so that the resonance frequency can coincide exactly with one of the frequencies $\Omega = \Omega(\varepsilon; p_0)$. For electrons with p_H nearly equal to p_0 the frequency $\Omega(p_H)$ is equal to:

$$\Omega(p_H) = \Omega(p_0) + \Omega'(p_0)(p_H - p_0) + {}^1/_2 \Omega''(p_0)(p_H - p_0)^2 + \ldots$$

It is obvious that the number of electrons finding themselves close to resonance [*i.e.*, having a frequency $\Omega \approx \Omega(p_0)$], will be greatest when $\Omega'(p_0) = 0$, *i.e.*, when p_0 corresponds to an extremum of Ω, and consequently an extremum of $\partial S/\partial \varepsilon$. Therefore one naturally anticipates a resonance at a frequency ω, equal to

$$\Omega_{\text{ext}} = (2\pi eH/c)\, (\partial S/\partial \varepsilon)_{\text{ext}}.$$

Thus, cyclotron resonance is very sensitive to the shape of the boundary Fermi surface $\varepsilon(\mathbf{p}) = \varepsilon_0$. The resonance is absent if the direction of the magnetic field corresponds to an open section of Eq. (2.1). Furthermore, the shape of the resonance is different depending on how closely the Fermi surface resembles an ellipsoid. Therefore in the remainder of this paper we shall not introduce any assumptions concerning the form of the dispersion law.

3. THE COMPLETE SYSTEM OF EQUATIONS

The complete set of equations consists of Maxwell's equations:

$$\text{curl } \mathbf{H} = \frac{4\pi}{c}\mathbf{j}; \quad \text{curl } \mathbf{E} = -\frac{i\omega}{c}\mathbf{H}$$

and the kinetic equations for the perturbation $f_1 \exp(i\omega t)$ to the equilibrium Fermi distribution function

$$f_0(\varepsilon) = \left[\exp\left(\frac{\varepsilon - \varepsilon_0}{kT}\right) + 1\right]^{-1}$$

Eliminating $\mathbf{H}$ from Maxwell's equation, we get

$$E''_{x,y}(z) + (4\pi i\omega/c^2)\, j_{x,y}(z); \; j_z = 0,$$
$$j_i = -\frac{2e}{h^3}\int v_i f_1 \, d\tau_{\mathbf{p}}, \; \mathbf{v} = \nabla_{\mathbf{p}}\varepsilon(\mathbf{p}) \; (i = x, y, z); \tag{3.1}$$

where $d\tau_{\mathbf{p}} = dp_x\, dp_y\, dp_z$, and the integration is to be performed over all momentum space. The Oz axis is the direction of the inward normal to the surface of the metal, and the Ox axis is in the direction of the projection of the stationary magnetic field onto the metal surface. The kinetic equations for f_1 will be written with variables ε, p_H and $\tau = \Omega_0 t$. Here $\Omega_0 = eH/m_0 c$ (m_0 is the characteristic mass of the electron) and t is the time expended by the electron during one revolution in its orbit[5,6], which for closed orbits is given by $t = (c/eH)\, \partial S_t/\partial \varepsilon$ (where S_t is the area of the region of intersection between $\varepsilon(\mathbf{p}) = \varepsilon$, and $p_H = \text{const.}$) For simplicity, it will be assumed that $\partial S/\partial \varepsilon > 0$, *i.e.*, that the quasi particles under consideration are electrons.

The linearized kinetic equations have the form[5]:

$$v_z \frac{\partial f_1}{\partial z} + \Omega_0 \frac{\partial f_1}{\partial \tau} + i\omega f_1 + \left(\frac{\partial f_1}{\partial t}\right)_{\text{cr}} = e\,\mathbf{vE}\,\frac{\partial f_0}{\partial \varepsilon}, \tag{3.2}$$

where $(\partial f_1/\partial t)_{\text{col}}$ is the integral for collisions of electrons with photons, impurities and lattice imperfections. Here it is taken into account that $\dot{\varepsilon} = e(\mathbf{v}\cdot\mathbf{E})$ and $\dot{p}_k = -eE_k$. The boundary conditions for the z coordinate are determined from the nature of the reflection of the electrons at the surface. We shall assume that the electrons are scattered diffusely (this is almost always so[6,7]), *i.e.*,

that the reflected electrons have an equilibrium distribution function*

$$f_1|_{z=0,\, v_z>0} = 0. \tag{3.3}$$

At infinity f_1 is necessarily zero. A boundary condition of f_1 arises from the periodicity of f_1 with respect to τ with a period $\theta = m_0^{-1}\,\partial S/\partial\varepsilon$:

$$f_1(\tau+\theta) = f_1(\tau). \tag{3.4}$$

To solve the problem it is convenient to introduce

$$\Psi(z;\,\mathbf{v}) = f_1(z;\,\mathbf{v}) - f_1(z;\,-\mathbf{v}).$$

In order to obtain an equation for Ψ, we write Eq. (3.2) separately for $f_1(z;\,\mathbf{v})$ and for $f_1(z;\,-\mathbf{v})$. When the symmetry of the collision integral relative substitution of $\mathbf{v}$ by $-\mathbf{v}$ is taken into account, one finds the following:

$$\frac{\partial f_1(z;\,\mathbf{v})}{\partial z} + \hat{L} f_1(z;\,\mathbf{v}) = e\,\mathbf{E}\,\frac{\mathbf{v}}{v_z}\,\frac{\partial f_0}{\partial\varepsilon}; \tag{3.5}$$

$$\frac{\partial f_1(z;\,-\mathbf{v})}{\partial z} - \hat{L} f_1(z;\,-\mathbf{v}) = e\,\mathbf{E}\,\frac{\mathbf{v}}{v_z}\,\frac{\partial f_0}{\partial\varepsilon}; \tag{3.5a}$$

where

$$\hat{L} = \frac{1}{v_z}\left\{\Omega_0\frac{\partial}{\partial\tau} + i\omega + \left(\frac{\partial}{\partial t}\right)_{\text{CT}}\right\}.$$

If one now performs the operation $(\partial/\partial z - \hat{L})$ on (3.5) and the operation $(\partial/\partial z + \hat{L})$ on (3.5a) and substracts the resulting equations, one obtains:

$$\left(\frac{\partial^2}{\partial z^2} - \hat{L}^2\right)\Psi(z;\,\mathbf{v}) = -2e\,\mathbf{E}\,\hat{L}\left(\frac{\mathbf{v}}{v_z}\,\frac{\partial f_0}{\partial\varepsilon}\right). \tag{3.6}$$

Equation (3.1) is now written in the form:

$$E''_{x,y}(z) = -\frac{4\pi i\omega}{c^2}\,\frac{em_0}{h^3}\int v_{x,y}\,\Psi(z;\,\mathbf{v})\,d\tau\,d\varepsilon\,dp_H,$$
$$\int v_z\Psi(z;\,\mathbf{v})\,d\tau\,d\varepsilon\,dp_H = 0 \tag{3.7}$$

Here the relation $\varepsilon(-\mathbf{p}) = \varepsilon(\mathbf{p})$ has been used. Now it is possible to expand the functions $\mathbf{E}(z)$ and $\Psi(z;\,\mathbf{v})$ over the region $z<0$ [$\mathbf{E}(-z) = \mathbf{E}(z)$; $\Psi(-z;\,\mathbf{v}) = \Psi(z;\,\mathbf{v})$] and to introduce Fourier transformations:

$$k^2\mathcal{E}_\mu(k) + 2E'_\mu(0) = \frac{4\pi i\omega}{c^2}\,\frac{em_0}{h^3}\int v_\mu\psi(k;\,\mathbf{v})\,d\tau\,d\varepsilon\,dp_H; \tag{3.8}$$

$$\int v_z\psi(k;\,\mathbf{v})\,d\tau\,d\varepsilon\,dp_H = 0; \tag{3.8a}$$

$$k^2\psi(k;\,\mathbf{v}) + 2\Psi'(0;\,\mathbf{v}) + \hat{L}^2\psi(k;\,\mathbf{v}) = 2e\vec{\mathcal{E}}(k)\,\hat{L}\left(\frac{\mathbf{v}}{v_z}\,\frac{\partial f_0}{\partial\varepsilon}\right). \tag{3.9}$$

It is still necessary to determine the boundary conditions for $\Psi(z;\,\mathbf{v})$ based on Eq. (3.3). Subtracting (3.5) from (3.5a) and substituting $z=0$, we find:

$$\Psi'(0;\,\mathbf{v}) = -\hat{L}\{f_1(0;\,\mathbf{v}) + f_1(0;\,-\mathbf{v})\}. \tag{3.10}$$

But from Eq. (3.3):

$f_1(0;\,\mathbf{v}) = -f_1(0;\,\mathbf{v}) = 0$ for $v_z > 0$;

$f_1(0;\,-\mathbf{v}) = -f_1(0;\,-\mathbf{v}) = 0$ for $v_z < 0$.

Therefore Eq. (3.10) must written as

$$\Psi'(0;\,\mathbf{v}) = \hat{L}\{\operatorname{sgn} v_z\cdot\Psi(0;\,\mathbf{v})\};\ \operatorname{sgn} x = \begin{cases}+1\,(x>0)\\ -1\,(x<0)\end{cases}. \tag{3.11}$$

Substituting Eq. (3.11) into Eq. (3.9), we get

$$\{k^2 + \hat{L}^2\}\,\psi(k;\,\mathbf{v}) = 2\hat{L}\left\{\frac{g(k;\,\mathbf{v})}{v_z}\right\}, \tag{3.12}$$

where

$$g(k;\,\mathbf{v}) = e\vec{\mathcal{E}}(k)\,\mathbf{v}\,\partial f_0/\partial\varepsilon - |v_z|\,\Psi(0;\,\mathbf{v}).$$

Hence

$$\psi(k;\,\mathbf{v}) = (\hat{L}+ik)^{-1}\,g/v_z + (\hat{L}-ik)^{-1}\,g/v_z. \tag{3.13}$$

The condition that ψ is periodic with respect to τ has obviously been conserved. Thus the problem reduces to finding $(\hat{L}\pm ik)^{-1}\,g/v_z = \zeta$, *i.e.*, to finding a periodic solution to the equation

$$(\Omega_0\partial\zeta/\partial\tau) + i\omega\zeta + (\partial\zeta/\partial t)_{\text{col}} \pm ikv_z\zeta = g \tag{3.14}$$

and solving Eqs. (3.8) and (3.8a).

*Incidentally, the nature of the reflection from the surface does not materially affect the results.

4. THE FEASIBILITY OF INTRODUCING THE RELAXATION TIME INTO THE ANOMALOUS SKIN EFFECT

The formulae of the previous section are true with the same general conditions for the case of the normal, as well as for the anomalous skin effect, in both metals and semiconductors. Let us now examine the highly anomalous skin effect ($\delta_{\text{eff}} \ll r, l$). In this case the principal contribution to the current density is made by those electrons which are moving nearly parallel to the surface of the metal ($|v_z| \ll v$), *i.e.*, the electrons near to the zone $v_z = 0$ on the Fermi surface (Fig. 2, *a*). This is evident from the fact that, from Eq. (3.14), $kv_z \sim \Omega_0$, $|v_z|/v \sim \Omega_0/kv$, and, from Eq. (3.8), $k \sim 1/\delta_{\text{eff}}$, so that

$$|v_z|/v \sim \Omega_0 \delta_{\text{eff}}/v \sim \delta_{\text{eff}}/r \ll 1.$$

Accurate calculations lead to the same conclusion.

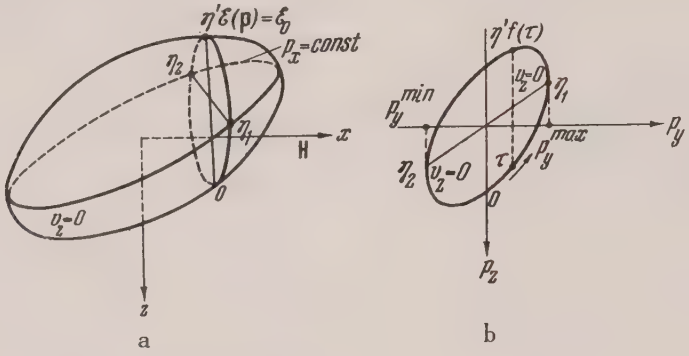

FIG. 2. a – Fermi surface $\varepsilon(\mathbf{p}) = \varepsilon_0$ b – intersection between the Fermi surface and $p_x = \text{const}$.

Therefore, the term $v_z \mathcal{E}_z$ in Eq. (3.12) can be neglected compared with $v_x \mathcal{E}_x + v_y \mathcal{E}_y$ and Eq. (3.8a), which determines $\mathcal{E}_z$, need not be considered further. For this reason the function ζ is large only when $|v_z| \ll v$.

Now let us return to the collision integral which is composed of two terms:

$$(\partial\zeta/\partial t)_{\text{col}} = \zeta(\mathbf{p}) \int A(\mathbf{p}; \mathbf{p}')\, d\tau_{\mathbf{p}'} - \int B(\mathbf{p}; \mathbf{p}')\, \zeta(\mathbf{p}')\, d\tau_{\mathbf{p}'},$$

where the magnitudes of A and B are related to the transition probabilities (their actual form depends on temperature[8]).

Because of the fact that $\zeta(\mathbf{p})$ has a sharp maximum for $v_z \sim 0$, in this region the first term will be significantly larger than the second (where $\zeta(\mathbf{p})$ is averaged), and the second term can be ignored in the approximation to the zeroth order of δ_{eff}/r. Consequently near the limit of the anomalous skin effect (when $\delta_{\text{eff}} \ll r, l$) we have at any temperature (consistent with this condition):

$$(\partial\zeta/\partial t)_{\text{col}} \approx \zeta(\mathbf{p})/t_0(\mathbf{p}); \quad 1/t_0(\mathbf{p}) = \int A(\mathbf{p}; \mathbf{p}')\, d\tau_{\mathbf{p}'}, \tag{4.1}$$

i.e., it is always possible to introduce the mean free path time of the electrons, $t_0(\mathbf{p})$.* The physical reason for this is that the populations of the non-equilibrium states with $|v_z| \ll v$ in the anomalous skin effect are significantly greater than the populations of states with $|v_z| \sim v$. Therefore, through collision, transitions from states with $|v_z| \ll v$ are more probable. Thus, Eq. (3.14) may finally be written in the form:

$$\frac{\partial\zeta}{\partial\tau} + \gamma_0\zeta \pm i\frac{kv_z}{\Omega_0}\zeta = \frac{1}{\Omega_0} g;$$

$$g = e\frac{\partial f_0}{\partial\varepsilon}\sum_{\mu=1}^{2} \mathcal{E}_\mu(k)\, v_\mu - |v_z|\,\Psi(0; \mathbf{v}). \tag{4.2}$$

$$\gamma_0(\mathbf{p}) = i\frac{\omega}{\Omega_0} + \frac{1}{\Omega_0 t_0(\mathbf{p})}.$$

5. SOLUTION OF THE EQUATIONS

Equation (4.2) is readily solved. Its periodic solutions have the form:

$$\zeta(k; \tau) = \frac{1}{\Omega_0}\int_{-\infty}^{\tau} g(\tau_1) \exp\left\{\int_{\tau}^{\tau_1}\left(\gamma_0 \pm i\frac{kv_z}{\Omega_0}\right)d\tau_2\right\} d\tau_1.$$

*This conclusion permits a considerably simpler representation of the results of Ref. 9.

llence according to Eq. (3.13)

$$\psi(k;\tau) = \frac{2}{\Omega_0}\int_{-\infty}^{\tau} g(\tau_1)\exp\left(\int_{\tau}^{\tau_1}\gamma_0 d\tau_2\right)\cos\left(\frac{k}{\Omega_0}\int_{\tau}^{\tau_1} v_z d\tau_2\right)d\tau_1. \tag{5.1}$$

First let us consider the case of a magnetic field $\mathbf{H}(H, 0, 0)$, parallel to the surface of the metal. In the zeroth approximation relative to the electric field*

$$\frac{d\mathbf{p}}{dt} = -\frac{e}{c}[\mathbf{vH}],\quad v_z = -\frac{1}{m_0}\frac{dp_y}{d\tau}.$$

Consequently,

$$\int_0^{\theta} v_z d\tau = 0$$

Using this relation and the periodicity of $g(\tau)$ with respect to τ, we get from (5.1):

$$\psi(k;\tau) = \frac{2}{\Omega_0\{e^{2\pi\gamma}-1\}}\int_{\tau}^{\tau+\theta}\left\{e\frac{\partial f_0}{\partial\varepsilon}\sum_{\mu=1}^{2}\mathcal{E}_\mu(k)\,v_\mu - |v_z|\,\Psi(0;\mathbf{v})\right\} \times \exp\left(\int_{\tau}^{\tau_1}\gamma_0 d\tau_2\right)\cos\left(\frac{k}{\Omega_0}\int_{\tau}^{\tau_1} v_z d\tau_2\right)d\tau_1, \tag{5.2}$$

where

$$\gamma = i\frac{\omega}{\Omega} + \overline{\left(\frac{1}{\Omega t_0}\right)};\quad \Omega = \frac{2\pi eH}{c\partial S/\partial\varepsilon};\quad \overline{\frac{1}{t_0}} = \frac{1}{\theta}\int_0^{\theta}\frac{d\tau}{t_0};\quad \theta = \frac{1}{m_0}\frac{\partial S}{\partial\varepsilon}.$$

Now let us determine

$$\Psi(0;\mathbf{v}) = \frac{1}{\pi}\int_0^{\infty}\psi(k;\mathbf{v})\,dk = \frac{1}{\pi}\lim_{N\to\infty}\int_0^{N}\psi(k;\mathbf{v})\,dk.$$

For this purpose, note that

$$\lim_{M\to\infty}\int_{\tau}^{\tau+\theta}\varphi(\tau_1)\frac{\sin M[p_y(\tau_1)-p_y(\tau)]}{p_y(\tau_1)-p_y(\tau)}d\tau_1 = \pi\left\{\frac{\varphi(\tau)+\varphi(\tau+\theta)}{2\,|\,p_y'(\tau)\,|} + \frac{\varphi(f(\tau))}{|\,p_y'(f(\tau))\,|}\right\}, \tag{5.3}$$

where $f(\tau)$ is a point symmetrical about τ (see Fig. 2, b). This point is determined from the relations

$$p_y(\tau) = p_y(f(\tau));\quad \tau < f(\tau) < \tau+\theta. \tag{5.4}$$

Here for simplicity it has been assumed that curve $\varepsilon(\mathbf{p}) = \varepsilon_0$, p_x = const. is convex and that the point $f(\tau)$ is unique. However, these last formulae are are also satisfied in the general case of non-convex curves, since only the value of $f(\tau)$ in the vicinity of $v_z = 0$ needs to be evaluated. If at the same time on the surface $\varepsilon(\mathbf{p}) = \varepsilon_0$ there are several curves with $v_z = 0$, then the resonance for given values of p_x will occur at the point $v_z = 0$, p_x = const, and $p_y = p_{y\max}$. This is connected with the fact that

$$z = \Omega_0\int v_z d\tau = -(\Omega_0/m_0)\,p_y(\tau),$$

and the recurring entrances of the electron into the layer $z \sim \delta_{\text{eff}}$ can occur only when the highest point of the trajectory with $z = z_{\min}$ occurs within this layer.

With the help of Eq. (5.3), it is easy to show from from Eq. (5.2), that

$$\Psi(0;\tau) + \Psi(0;f(\tau))\exp\left(\int_{\tau}^{f(\tau)}\gamma_0 d\tau_2 - 2\pi\gamma\right) = \frac{1}{\Omega_0}e^{-2\pi\gamma}F(\tau),$$

$$F(\tau) = \frac{e}{\pi}\frac{\partial f_0}{\partial\varepsilon}\sum_{\mu=1}^{2}\int_{\tau}^{\tau+\theta} v_\mu(\tau_1)\exp\left(\int_{\tau}^{\tau_1}\gamma_0 d\tau_2\right)d\tau_1 \times\int_0^{\infty}\mathcal{E}_\mu(k')\cos\left(\frac{k'}{\Omega_0}\int_{\tau}^{\tau_1} v_z d\tau_2\right)dk'. \tag{5.5}$$

*Remember that this equation defines the variable t.

In Eq. (5.5), let us substitute $f(\tau)$ for τ. Using the definition of $f(\tau)$, it is readily shown that $f(f(\tau)) = \tau + \theta$. Therefore, after the substitution, one has:

$$\Psi(0; f(\tau)) + \Psi(0, \tau) \exp\Big(\int_{f(\tau)}^{\tau+\theta} \gamma_0 d\tau_2 - 2\pi\gamma\Big) = \frac{1}{\Omega_0} e^{-2\pi\gamma} F(f(\tau)). \tag{5.6}$$

From Eq. (5.5) and (5.6)

$$\Psi(0; \tau) = \frac{e}{\pi\Omega_0} \frac{\partial f_0/\partial\varepsilon}{e^{2\pi\gamma} - 1} \sum_{\mu=1}^{2} \int_0^\infty \mathcal{E}_\mu(k')\, dk' \Big\{ \int_\tau^{\tau+\theta} v_\mu(\tau_1) \exp\Big(\int_\tau^{\tau_1} \gamma_0 d\tau_2\Big) \times \cos\Big(\frac{k'}{\Omega_0} \int_\tau^{\tau_1} v_z d\tau_2\Big) d\tau_1 - \int_{f(\tau)-\theta}^{f(\tau)} \cdots \Big\} = \tag{5.7}$$

$$= \frac{e}{\pi\Omega_0} \frac{\partial f_0}{\partial\varepsilon} \sum_{\mu=1}^{2} \int_0^\infty \mathcal{E}_\mu(k')\, dk' \int_{f(\tau)-\theta}^{\tau} v_\mu(\tau_1) \exp\Big(\int_\tau^{\tau_1} \gamma_0 d\tau_2\Big) \cos\Big(\frac{k'}{\Omega_0} \int_\tau^{\tau_1} v_z d\tau_2\Big) d\tau_1.$$

We have also made use of the fact that

$$\int_{f(\tau)}^{\tau_1} v_z d\tau_2 = \int_\tau^{\tau_1} v_z d\tau_2$$

and that in the case of a periodic function $\Phi(\tau)$

$$\{e^{2\pi\gamma} - 1\}^{-1} \int_\alpha^{\alpha+\theta} \Phi(\tau_1) \exp\Big(\int_\tau^{\tau_1} \gamma_0 d\tau_2\Big) d\tau_1 = \int_{-\infty}^{\alpha} \Phi(\tau_1) \exp\Big(\int_\tau^{\tau_1} \gamma_0 d\tau_2\Big) d\tau_1.$$

Substituting the simple expression of Eq. (5.7) for $\Psi(0, \tau)$ into Eq. (5.2) and calculating the current density as

$$j_\mu(k) = -\frac{em_0}{h^3} \int v_\mu \psi d\varepsilon\, dp_x\, d\tau,$$

we find

$$j_\mu(k) = \sum_{\nu=1}^{2} \Big\{ K_{\mu\nu}(k)\, \mathcal{E}_\nu(k) - \int_0^\infty Q_{\mu\nu}(k; k')\, \mathcal{E}_\nu(k')\, dk' \Big\}, \tag{5.8}$$

where

$$K_{\mu\nu}(k) = \frac{2e^2 m_0}{h^3 \Omega_0} \int_{\varepsilon=\varepsilon_0} [e^{2\pi\gamma} - 1]^{-1} dp_x \int_0^\theta v_\mu(\tau)\, d\tau \int_\tau^{\tau+\theta} v_\nu(\tau_1) \exp\Big(\int_\tau^{\tau_1} \gamma_0 d\tau_2\Big) \cos\Big(\frac{k}{\Omega_0} \int_\tau^{\tau_1} v_z d\tau_2\Big) d\tau_1; \tag{5.9}$$

$$Q_{\mu\nu}(k; k') = \frac{2e^2 m_0}{\pi h^3 \Omega_0^2} \int_{\varepsilon=\varepsilon_0} [e^{2\pi\gamma} - 1]^{-1} dp_x \int_0^\theta v_\mu(\tau)\, d\tau \int_\tau^{\tau+\theta} |v_z(\tau_1)| \cos\Big(\frac{k}{\Omega_0} \int_\tau^{\tau_1} v_z d\tau_2\Big) d\tau_1 \cdot \int_{f(\tau_1)-\theta}^{\tau_1} v_\nu(\xi) \times \exp\Big(\int_\tau^{\xi} \gamma_0 d\tau_2\Big) \cos\Big(\frac{k'}{\Omega_0} \int_{\tau_1}^{\xi} v_z d\tau_2\Big) d\xi. \tag{5.10}$$

Now we take into account that $kv/\Omega_0 \gg 1$. Using the method of steepest descent and noting that $df/d\tau = -1$*, in the vicinity of points of steepest descent $\eta_1(p_x)$ and $\eta_2(p_x)$, where $v_z(\varepsilon_0; p_x; \eta_\alpha) = 0$,

*In the vicinity of η_α we have $f(\tau) = \begin{cases} 2\eta_\alpha - \tau + \theta & (\text{for } 0\eta,\ \eta'\eta_2), \\ 2\eta_\alpha - \tau & (\text{for } \eta_1\eta',\ \eta_2 0). \end{cases}$

($\alpha = 1, 2$) (see Fig. (2, b).) after lengthy calculation we arrive at the expression:

$$j_\mu(k) = \frac{2\pi e^2 m_0}{h^3} \sum_{\nu,\alpha=1}^{2} \left\{ \frac{\mathcal{E}_\nu(k)}{k} \int \frac{v_\mu(\eta_\alpha) v_\nu(\eta_\alpha)}{|v_z'(\eta_\alpha)|} \frac{dp_x}{1 - e^{-2\pi\gamma}} - \right.$$
$$- \frac{1}{4\pi} \int_0^\infty \frac{\mathcal{E}_\nu(k')\, dk'}{(k+k')\sqrt{kk'}} \int \frac{v_\mu(\eta_\alpha) v_\nu(\eta_\alpha)}{|v_z'(\eta_\alpha)|} \frac{(1+e^{-2\pi\gamma})^2}{1-e^{-2\pi\gamma}} dp_x - \tag{5.11}$$
$$\left. - \frac{1}{2\pi^2} \int_0^\infty \frac{\ln(k/k')}{k^2 - k'^2} \mathcal{E}_\nu(k')\, dk' \int \frac{v_\mu(\eta_\alpha) v_\nu(\eta_\alpha)}{|v_z'(\eta_\alpha)|} (3 + e^{-2\pi\gamma})\, dp_x \right\}.$$

(Thus, we have verified the assumptions made in Section 4, and cited repeatedly, namely that only values $v_z \approx 0$ plays an important role.) Noting, that

$$J = m_0 \sum_{\alpha=1}^{2} \int \left[\frac{v_\mu v_\nu}{|v_z'(\tau)|} \right]_{\tau=\eta_\alpha} \Phi(p_x)\, dp_x$$
$$= \int v_\mu v_\nu \Phi \delta(v_z)\, \delta(\varepsilon - \varepsilon_0)\, d\tau_{\mathbf{p}},$$

and introducing spherical coordinates $\mathbf{v} = v\mathbf{n}$ $= (v \sin\vartheta \cos\varphi,\ v \sin\vartheta \sin\varphi,\ v \cos\vartheta)$ we find

$$J = \int_0^{2\pi} n_\mu(\varphi)\, n_\nu(\varphi)\, \Phi(\varphi)\, d\varphi / K(\varphi). \tag{5.11a}$$

where K is the Gaussian curvature of the Fermi surface. All the quantities are determined at $\vartheta = \pi/2$. Using Eqs. (5.11) and (5.11a), we can write Eq. (3.8) in the form

$$-k^2 \mathcal{E}_\mu(k) - 2E_\mu'(0) = i \frac{3\pi^2 \omega}{c^2} \sum_{\nu=1}^{2} \left\{ \frac{A_{\mu\nu}}{k} \mathcal{E}_\nu(k) \right.$$
$$- \frac{2}{\pi^2} C_{\mu\nu} \int_0^\infty \frac{\ln(k/k')}{k^2 - k'^2} \mathcal{E}_\nu(k')\, dk'$$
$$\left. - \frac{1}{\pi} \left(A_{\mu\nu} - C_{\mu\nu} \right) \int_0^\infty \frac{\mathcal{E}_\nu(k')\, dk'}{(k+k')\sqrt{kk'}} \right., \tag{5.12}$$

where*

$$A_{\mu\nu} = \frac{8e^2}{3h^3} \int_0^{2\pi} \frac{n_\mu n_\nu}{K} \frac{d\varphi}{1 - \exp\{-2\pi i(\omega/\Omega) - (\overline{2\pi/\Omega t_0})\}};$$

$$B_{\mu\nu} = \frac{8e^2}{3h^3} \int_0^{2\pi} \frac{n_\mu n_\nu}{K} d\varphi;$$

$$C_{\mu\nu} = B_{\mu\nu} - \frac{2e^2}{3h^3} \int_0^{2\pi} \frac{n_\mu n_\nu}{K} \left[1 \right. \tag{5.13}$$
$$\left. - \exp\left\{ -2\pi i \frac{\omega}{\Omega} - \left(\overline{\frac{2\pi}{\Omega t_0}} \right) \right\} \right].$$

Eqs. (5.12) and (5.13) allow $\mathcal{E}_\mu(k)$ to be determined in principle:

$$\mathcal{E}_\mu(k) = \sum_{\nu=1}^{2} W_{\mu\nu}(k)\, E_\nu'(0), \tag{5.14}$$

where $W_{\mu\nu}(k)$ are certain known functions.

Hence

$$E_\mu(0) = \sum_{\nu=1}^{2} E_\nu'(0) \frac{1}{\pi} \int_0^\infty W_{\mu\nu}(k)\, dk.$$

But, by definition, the surface impedance tensor, $Z_{\mu\nu}$, is given by:

$$-(4\pi i\omega/c^2)\, E_\mu(0) = \sum_{\nu=1}^{2} Z_{\mu\nu} E_\nu'(0)$$

Therefore,

$$Z_{\mu\nu} = R_{\mu\nu} + iX_{\mu\nu} = -(4i\omega/c^2) \int_0^\infty W_{\mu\nu}(k)\, dk. \tag{5.15}$$

The following section will be devoted to a calculation of $W_{\mu\nu}(k)$.

Note, that in the general case it is not possible to reduce the complex tensor $Z_{\mu\nu}$ to its principal

*Only the mean value of $t_0^{-1}(\varepsilon_0; p_x(\varphi))$ appears in the answer. This is not unexpected since the integrals of the motion (ε_0 and p_x) determine the system of quantum-mechanical states, and a degeneracy occurs with respect to τ and leads to an averaging of the collision frequency $\nu(p_x) = 1/t_0$.

axes. This means, that there are no directions, along which an electromagnetic wave is reflected without a rotation of the plane of polarization.

6. CALCULATION OF THE SURFACE IMPEDANCE. ANALYSIS OF THE RESULTING EQUATIONS.

First we will show that the surface impedance has a resonant character. $Z_{\mu\nu}$ can be calculated, along with $A_{\mu\nu}$ and $B_{\mu\nu}$ from Eqs. (5.12) through (5.15). For $\omega = q\Omega$ ($q = \pm 1, \pm 2, \ldots$), the denominator of the expression under the integral sign in the case of $A_{\mu\nu}$ is equal to $\overline{2\pi/\Omega t_0}$, *i.e.*, it is very small. Thus, there can exist two essentially different cases according to their dependence on the dispersion law.

For a quadratic dispersion law, or with

$$\left| \varepsilon(\mathbf{p}) - \frac{1}{2}\sum_{i,k} \mu_{ik} p_i p_k \right| / \varepsilon_0 \ll \overline{(2\pi/\Omega t_0)},$$

the cyclotron frequency Ω is independent of φ;

$$\Omega = (eH/c)(\mu_{yy}\mu_{zz} - \mu_{yz}^2)^{1/2}$$

and resonance occurs for all electrons at the Fermi surface for $\omega \approx q\Omega$.

For an arbitrary dispersion law $\varepsilon(\mathbf{p}) = \varepsilon$ the magnitude of Ω is a function of φ and resonance occurs only at a frequency $\omega \approx q\Omega_{ext}$, which corresponds to the extreme value of $\partial S/\partial\varepsilon$ with respect to φ.

Outside the resonance region* one can equate $\overline{2\pi/\Omega t_0}$ to zero in Eq. (5.13) for either dispersion law. (In the case of a non-quadratic dispersion law and $\omega/q = \Omega \neq \Omega_{ext}$, the integral $A_{\mu\nu}$ should be understood to be a principal value.)

Let us present the results of calculations in the vicinity of resonance in the case of a non-quadratic and of a quadratic dispersion law.

1. In the case of a non-quadratic dispersion law, in the vicinity of resonance ($\omega \approx q\Omega_{ext}$) the main contribution to $A_{\mu\nu}$ is given by the points $\varphi = \varphi_i$ ($i = 1, 2, \ldots, \beta$) where Ω has an extremum. Therefore,

$$A_{\mu\nu} \approx \frac{16e^2}{3h^3}\left\{\sum_{i=1}^{\beta}\left(\frac{n_\mu n_\nu}{\beta K}\right)_{\varphi=\varphi_i}\int_0^{\pi}\frac{d\varphi}{1-\exp(-2\pi i\omega/\Omega - 2\pi/\Omega t_0)} + d_{\mu\nu}\right\};$$
$$d_{\mu\nu} = \text{const}, \quad |d_{\mu\nu}| \sim K^{-1}; \quad \Omega^{-1}(\varphi) = \Omega^{-1}(\varphi_i) + \frac{1}{2}\frac{\partial^2\Omega^{-1}(\varphi_i)}{\partial\varphi^2}(\varphi - \varphi_i)^2. \tag{6.2}$$

It is easy to see that in this case, reducing these sums to principle axes and assuming, for simplicity, that $\overline{t_0^{-1}(\varphi_i)} = \overline{t_0^{-1}(\varphi_1)}$ we find that:

$$Z_{\alpha\alpha} = \frac{32}{9\sqrt{3}}\left(\frac{\sqrt{3}\pi\omega^2}{c^4 A_\alpha^0}\right)^{2/3}(q^2\varkappa)^{1/6}\exp\left\{\frac{i}{3}\left(\pi + s\tan^{-1}\frac{\sqrt{\varkappa + s\varkappa_1}}{\sqrt{\varkappa - s\varkappa_1} + a_\alpha q\varkappa}\right)\right\};$$
$$0 < a_\alpha \sim 1;$$
$$|Z_{xy}| \ll |Z_{\alpha\alpha}|; \tag{6.3}$$
$$\varkappa_1 = (\omega - q\Omega_{ext})/q\Omega_{ext}; \quad \varkappa = [\varkappa_1^2 + (\omega t_0^*)^{-2}]^{1/2},$$
$$s = \operatorname{sgn}\frac{\partial^3 S(\varphi_1)}{\partial\varepsilon\partial\varphi^2}; \quad \frac{1}{t_0^*} = \overline{t_0^{-1}}(\varphi_1);$$

A_α^0 are the principal values of the tensor

$$A_{\mu\nu}^0 = \frac{16e^2}{3h^3}\left\{\sum_{i=1}^{\beta}\frac{n_\mu(\varphi_i)\, n_\nu(\varphi_i)}{K(\varphi_i)}\left[\frac{1}{2}\frac{\partial S(\varphi_1)}{\partial\varepsilon}\Big/\left|\frac{\partial^3 S(\varphi_1)}{\partial\varepsilon\partial\varphi^2}\right|\right]^{1/2}\right\}$$
$$\varepsilon = \varepsilon_0, \quad v_z = 0, \quad p_y > 0.$$

(We have not written out the actual form of $d_{\mu\nu}$ and a_α in view of their unwieldiness).

Clearly (in consequence of the fact that $\varepsilon(-\mathbf{p}) = \varepsilon(\mathbf{p})$), $\beta \geqslant 2$ for all non-central sections and for $p_x = \text{const}$. In the case of the "topmost section" and of central sections which do not coincide

*In the case of strong magnetic fields with either dis-

with the base plane, $\beta = 1$, one of the principal values of A_y^0 is zero, and resonance takes place [and Eq. (6.3) holds] only if the incident wave is polarized along the x-axis. The direction of the electric field also gives the direction of the velocity at the point $\varphi = \varphi_1$; $v_z = 0$, and $\varepsilon = \varepsilon_0$.

The relative depth of the resonance for $R_{\alpha\alpha}$ and $X_{\alpha\alpha}$ are basically different for the cases of minimum and maximum values of $\partial S/\partial\varepsilon$ (*i.e.*, for $s > 0$ and $s < 0$).

The final forms of these equations are as follows:

a) $s > 0$, $\partial S/\partial\varepsilon$ has a minimum at $\varphi = \varphi_1$:

$$R_{xx}^{\text{res}} = \frac{4}{3\sqrt{3}}\left(\frac{\sqrt{3}\pi\omega^2}{c^4 A_x^0}\right)^{1/3}\left(\frac{q^2}{\omega t_0^*}\right)^{4/3}\left(\frac{25}{32a_x^2}\right)^{-5/18};\quad \Omega_{\text{res}} = \frac{\omega}{q}\left[1-\left(\frac{25}{32a_\alpha^2}\right)^{1/3}\left(\frac{1}{q\omega t_0^*}\right)^{2/3}\right];$$

$$X_{xx}^{\text{res}} = \frac{32}{9\sqrt{3}}\left(\frac{\sqrt{3}\pi\omega^2}{c^4 A_\alpha^0}\right)^{1/3}\left(\frac{q^2}{\omega t_0^*}\right)^{1/6}\sin^{5/6}\frac{2\pi}{5};\quad \Omega_{\text{res}} = \frac{\omega}{q}\left[1+\frac{1}{\omega t_0^*}\tan\frac{\pi}{10}\right]; \tag{6.4}$$

$$\left(\frac{X_{xx}}{R_{xx}}\right)^{\text{res}} = \left(\frac{16\omega t_0^*}{q^2 a_x^2}\right)^{1/3};\quad \Omega_{\text{res}} = \frac{\omega}{q}\left[1-\left(\frac{\sqrt{2}}{a_x q\omega t_0^*}\right)^{2/3}\right];$$

b) $s < 0$, $\partial S/\partial\varepsilon$ has a maximum at $\varphi = \varphi_1$:

$$R_{xx}^{\text{res}} = X_{xx}^{\text{res}} = \frac{32}{9\sqrt{3}}\left(\frac{\sqrt{3}\pi\omega^2}{c^4 A_x^0}\right)^{1/3}\left(\frac{q^2}{\omega t_0^*}\right)^{1/6}\sin^{1/6}\frac{\pi}{5};$$

$$\Omega_{\text{res}}^{R,X} = \frac{\omega}{q}\left[1\mp\frac{1}{\omega t_0^*}\cot\frac{\pi}{5}\right]; \tag{6.5}$$

(the minus sign is associated with R, the plus sign with X). Thus, in all cases R and X have minimum values at resonance. In all equations

$$\Omega_{\text{res}} = 2\pi e H_{\text{res}}/c\,(\partial S/\partial\varepsilon)_{\text{ext}};$$

The relative breadth of the resonance curve is

$$\Delta H/H \sim |\omega - q\Omega_{\text{res}}|/\omega. \tag{6.6}$$

At the same time* $|q| = 1, 2, 3, \ldots \ll (r/\delta)^{2/3}$, $(\omega t_0^*/2\pi)$. Eqs. (6.4) and (6.5) show that resonance occurs at frequencies Ω_{res} which are slightly shifted from the ratio ω/q. The amount of this shift is different for X_α and for R_α and its origin is different in the two cases. The frequency shift of X_α occurs because a small increase in the magnetic field, while it does not change the resonant condition, leads to an "advantageous" increase in the revolutions of the electron between collisions. The frequency shift of R_α is associated with the changing phase of the electric field as a function of distance from the surface. For a maximum acceleration of the electrons in the skin-layer, it is necessary that the thickness δ_1 at which the phase of the field is significantly changed should be large compared to the effective attenuation depth, δ_{eff}. For this reason it is necessary that $X \gg R$. But X/R depends on the frequency and on the magnetic field. Therefore when relatively small changes of the magnetic field can lead to $X \gg R$, such changes are found to be "advantageous", even if at the same time after $|\omega - q\Omega_{\text{res}}|\,t_0^*$ revolutions the electron finds itself near the surface with its phase changes by π from that of the electric field. This is possible when $\partial S/\partial\varepsilon$ has a minimum and impossible when $\partial S/\partial\varepsilon$ has a maximum. Precisely for this reason the essentially different depth of the resonance of R_α is explained by its dependence on the sign of $\partial^3 S(\varphi_1)/\partial\varepsilon\,\partial\varphi^2$.

2. Let us turn to the quadratic dispersion law. For simplicity consider the case where $\overline{1/t_0}$ is independent of φ. The surface impedance tensor can then be diagonalized, and the resultant formula holds for all frequencies and magnetic fields. In this case we get from (5.12)

$$-k^2\mathcal{E}_\alpha(k) - 2E'_\alpha(0) = i\frac{3\pi^2\omega}{c^2}\frac{B_\alpha}{1-e^{-2\pi\gamma}}\left\{\frac{\mathcal{E}_\alpha(k)}{k}\right.$$
$$-\frac{(1-e^{-2\pi\gamma})(3+e^{-2\pi\gamma})}{2\pi^2}\int_0^\infty\frac{\ln(k/k')}{k^2-k'^2}\mathcal{E}_\alpha(k')\,dk'$$
$$\left.-\frac{(1+e^{-2\pi\gamma})^2}{4\pi}\int_0^\infty\frac{\mathcal{E}_\alpha(k')\,dk'}{(k+k')\sqrt{kk'}}\right\}, \tag{6.7}$$

---

persion law, when $2\pi|\omega + (\overline{1/t_0})| \ll \Omega$, with $(\Omega/\pi\omega^2)$ $\overline{1/t_0} \ll 1$ $[(\overline{1/\omega t_0}) \ll 1]$

$$R_\alpha(H) \sim H^{-4/3},\quad X_\alpha(H) \sim H^{-1/3},$$

and for $(\Omega/\pi\omega^2)\,(\overline{1/t_0}) \gg 1$ $[(\overline{1/\omega t_0}) \lesssim 1]$, we have $Z_\alpha(H) \sim H^{-1/3}$.

* $q \ll (r/\delta)^{2/3}$ at $\Omega \gg \overline{1/t_0}$ corresponds to the condition of the anomalous skin-effect $\delta_{\text{eff}} \ll v/\omega$ whenever cyclotron resonance occurs $[(\delta = mc^2/2\pi e^2)^{1/3}]$.

where B_α are the principal values of the two dimensional tensor $B_{\mu\nu}$. Taking it into account that the only singularities of the solution of (6.7) in the region of the complex variable k, except for $k = 0$, are simple poles which are the roots of the equation

$$k^3 + i3\pi^2\omega B_\alpha/c^2\,(1 - e^{-2\pi\gamma}) = 0,$$

it is easy to show that

$$Z_\alpha(H) = R_\alpha + iX_\alpha = -\frac{4i\omega}{c^2}\int_0^\infty \mathcal{E}_\alpha(R)\,dk/E'_\alpha(0)$$
$$= \frac{8}{9} IZ_\alpha(0)\left[1 - \exp\left(-2\pi i\,\frac{\omega}{\Omega} - \frac{2\pi}{\Omega t_0^*}\right)\right]^{1/3};$$
$$Z_\alpha(0) = (\sqrt{3}\,\pi\omega^2/c^4B_\alpha)^{1/3}(1 + i\sqrt{3}); \quad (6.8)$$

Here $Z_\alpha(0)$ is the value of the impedance when $H = 0$ (Ref. 10);

$$I = \int_0^\infty G(x)\,dx \sim 1;$$

and $G(x)$ is a solution of the integral equation

$$G(x) = \frac{x}{2\pi(x^3+1)}\left\{3\sqrt{3}\right.$$
$$+ \frac{[1+e^{-2\pi\gamma}]^2}{2}\int_0^\infty \frac{G(x')\,dx'}{(x+x')\sqrt{xx'}} \quad (6.9)$$
$$\left. + \frac{(3+e^{-2\pi\gamma})(1-e^{-2\pi\gamma})}{\pi}\int_0^\infty \frac{\ln(x/x')}{x^2-x'^2}\,G(x')\,dx'\right\}.$$

The integral I, which enters into (6.8), changes slowly with the magnetic field and it can be easily evaluated by the method of successive approximations:

$$G(x) = \sum_{n=0}^{\infty} G_n(x),$$
$$G_0(x) = 3\sqrt{3}x/2\pi(x^3+1).$$

At resonance, the values of R_α, X_α, X_α/R_α and corresponding resonance frequencies are given by:

$$R_\alpha^{\text{res}} = \frac{16}{9\sqrt{3}}\left(\frac{2\pi q}{\omega t_0^*}\right)^{2/3} R_\alpha(0) = \frac{16}{9\sqrt{3}}\left(\frac{\sqrt{3}\,\pi}{c^4B_\alpha t_0^{*2}}\right)^{1/3}(2\pi q)^{2/3};$$
$$\Omega_{\text{res}} = \frac{\omega}{q}[1 - (2\pi q\omega t_0^*)^{-1/2}];$$
$$X_\alpha^{\text{res}} = \frac{32}{27}\left(\frac{\pi q}{\omega t_0^*}\right)^{2/3} X_\alpha(0) = \frac{32}{9\sqrt{3}}\left(\frac{\sqrt{3}\,\pi\omega^2}{c^4B_\alpha}\right)^{1/3}\left(\frac{\pi q}{\omega t_0^*}\right)^{2/3}; \quad (6.10)$$
$$\Omega_{\text{res}} = \frac{\omega}{q}\left[1 + \frac{1}{\omega t^*{}_0}\right];$$
$$\left(\frac{X_\alpha}{R_\alpha}\right)^{\text{res}} = \frac{3}{2}\left(\frac{\omega t_0^*}{\pi q}\right)^{1/2}; \quad \Omega_{\text{res}} = \frac{\omega}{q}[1 - (\pi q\omega t_0^*)^{-1/2}]$$
$$1/t_0^* = \overline{1/t}_0.$$

By way of an example, Fig. 3 shows the functions $R(H)/R(0)$, $X(H)/X(0)$, $X(H)/R(H)\sqrt{3}$ plotted for the case of an isotropic quadratic dispersion law ($\varepsilon(p) = p^2/2m$) for ωt_0^* equal to 1, 10 and 50. The graphs were constructed with the help of (6.8).

The small maxima of R and X at $\omega = (q + \frac{1}{2})\Omega$ are not due to resonance, since for $\Omega t_0^* \to \infty$ the magnitude of the impedance at these points approaches a constant value. Deviations from a quadratic dispersion law will reduce the height if the maxima in R and X to an even greater degree.

It can be shown by direct calculation that the equations derived hold not only for electrons ($\partial S/\partial\varepsilon > 0$) but also for "holes". To use the formulae for holes, it is only necessary to change $\partial S/\partial\varepsilon$ in all formulae into $|\partial S/\partial\varepsilon|$.

Similar formulae are found also in the case of several bands. It must be noted, that even if the number of holes is equal to the number of electrons and if the corresponding resonances coincide, the formulae retain their form. (This is because one can neglect the influence of the Hall field which would accompany the distortion of the trajectory of the electrons in the region $z \sim \delta_{\text{eff}} \ll r$).

It is interesting to note that the character of the dispersion law changes the form of the resonance curves in a qualitative way. In particular,

$$R_\alpha^{res}/R_\alpha(0) \sim (\Omega t_0^*/2\pi)^{-2/3}$$

for a quadratic dispersion law;

$$R_\alpha^{res}/R_\alpha(0) \sim (\Omega t_0^*/2\pi)^{-4/5}$$

for a non-quadratic dispersion law when $\partial S/\partial\varepsilon$ has a minimum, and

$$R_\alpha^{res}/R_\alpha(0) \sim (\Omega t_0^*/2\pi)^{-1/5}$$

for a non-quadratic dispersion law when $\partial S/\partial\varepsilon$ has a maximum.

7. DETERMINATION OF SOME OF THE MICROSCOPIC CHARACTERISTICS OF THE ELECTRON GAS IN METALS

By measuring the surface impedance in a magnetic field under the condition of the anomalous skin-effect, one can in principle determine the shape of the boundary Fermi surface $\varepsilon(\mathbf{p}) = \varepsilon_0$, the velocity of the electrons $\mathbf{v} = \mathbf{v}(\mathbf{p})$ on this surface and the mean free path time $t_0(\mathbf{p})$.

It has been shown previously[10] that the principal values of the surface impedance Z_α in the presence of the anomalous skin-effect, but in the absence of a magnetic field, are given by

$$Z_\alpha = R_\alpha + iX_\alpha = (\sqrt{3}\pi\omega^2/c^4 B_\alpha)^{1/3}(1 + i\sqrt{3}), \tag{7.1}$$

where B_α are the principal values of the tensor $B_{\mu\nu}$

$$B_{\mu\nu} = \frac{8e^2}{3h^3}\int_0^{2\pi}\frac{n_\mu n_\nu}{K}\,d\varphi. \tag{7.1a}$$

(notation the same as in preceding sections).

Consequently, a measurement of R_α makes it possible to find the mean value of $1/K$ on the equator $v_z = 0$:

$$\int_0^{2\pi}\frac{d\varphi}{K(\varphi)} = (B_x + B_y)\frac{3h^3}{8e^2}. \tag{7.2}$$

In Ref. 11 there was derived an equation by means of which it is possible to determine a function by evaluating its mean value along all equators. Therefore, by measuring the dependence of R_α on the angle between crystallographic axes and the normal to the metal surface, it is possible to compute the Gaussian curvature K for any point on the surface $\varepsilon(\mathbf{p}) = \varepsilon$.* If this surface turns out to be convex,

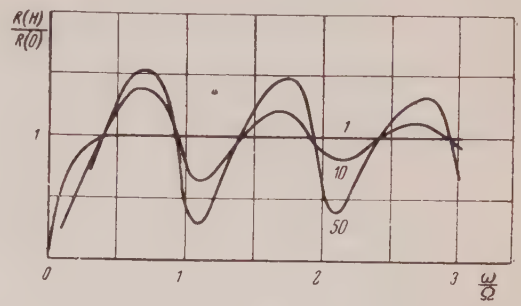

a

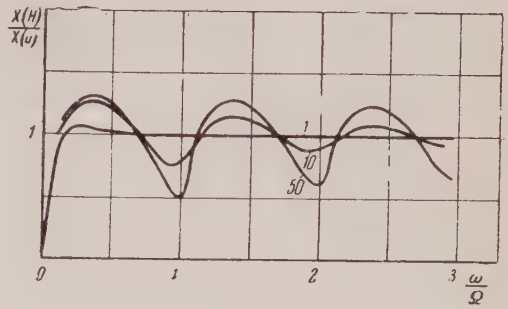

b

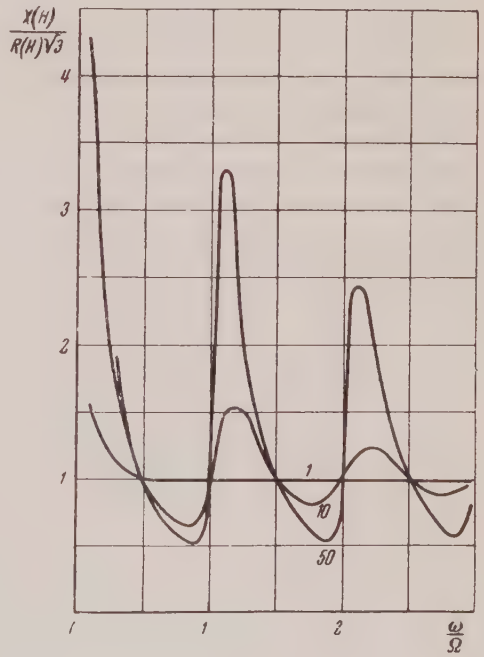

c

FIG. 3. The numbers alongside the curves are the values of ωt_0; $\omega/\Omega = (m\omega c/e)/H$.

*For this reason, it is necessary to perform experiments, similar to those of Pippard[12].

the computed Gaussian curvature will have its shape determined uniquely. When the equation $\varepsilon(\mathbf{p}) = \varepsilon_0$ defines several surfaces, the problem becomes substantially more complicated.

From Eqs. (6.4), (6.5) and (6.10) it can be seen that, if one knows the resonant frequency for R_α and X_α

$$\Omega_{res} = 2\pi e H_{res} / c\,(\partial S / \partial \varepsilon)_{ext} = (\omega / q)(1 + \Delta);\ |\Delta| \ll 1, \tag{7.3}$$

(where H_{res} and Δ are different for R_α and X_α in addition to which Δ depends only on t_0^*), then one can determine t_0^* and the extreme value $(\partial S/\partial\varepsilon)_{ext}$

If one knows $(\partial S/\partial\varepsilon)_{ext}$ and the shape of the surface $\varepsilon(\mathbf{p}) = \varepsilon_0$ it becomes possible, in accordance with Ref. 11, to evaluate the velocity $\mathbf{v} = \mathbf{v}(\mathbf{p})$ on the boundary Fermi surface.

From the quantity,

$$1 / t_0^* = \frac{1}{\theta}\int_0^\theta \frac{d\tau}{t_0(\mathbf{p})}$$

one can find[11]

$$\frac{1}{t_0(\mathbf{p})} = \int A(\mathbf{p};\ \mathbf{p}')\, d\tau_{\mathbf{p}'}$$

[see Eq. (4.1)]. When this integral equation has been solved, one can find in principle $A(\mathbf{p};\ \mathbf{p}')$ and consequently the transition probabilities, $w(\mathbf{p};\ \mathbf{p}')$.

Let us recall that values of $1/t_0(\mathbf{p})$ and $w(\mathbf{p};\ \mathbf{p}')$, determined from similar experiments, are applicable only to the narrow layer $z = \delta_{eff} \ll r$, l in the vicinity of the surface of the metal. They can, therefore, speaking generally, be distingushed from the values of $1/t_0(\mathbf{p})$ and $w(\mathbf{p};\ \mathbf{p}')$ in a large sample where they can be altered by surface treatment.

8. MAGNETIC FIELDS, INTERSECTING THE METAL SURFACE AT AN ANGLE; INTRODUCTION OF EFFECTIVE VALUES

In a manner similar to that which was followed for a magnetic field parallel to the surface of a metal, calculations can be made for an arbitrary orientation of the magnetic field, when $\sin\Phi \gg (r/l)(\delta/r)^{2/3}$ (here Φ is the angle between the direction of the magnetic field and the surface). In this case the impedance becomes equal to

$$Z_\alpha = (\sqrt{3}\,\pi\omega^2 / c^4 B_\alpha)^{1/3}(1 + i\sqrt{3}). \tag{8.1}$$

The equations which were derived above with the help of the kinetic equation can be understood from elementary considerations of the motion of electrons in stationary magnetic field with a variable electromagnetic field, parallel to the surface of the metal.

Following Pippard[4] and Ginsburg[13] let us assume that for electrons which are moving nearly parallel to the surface (and which comprise the main contribution to the electric field).

$$\mathbf{j} = \sigma_{eff}\mathbf{E}. \tag{8.2}$$

We shall assume that the field $E(z;\ t)$ inside the metal is parallel to the stationary magnetic field and directed along the x-axis. Then

$$E(z;\ t) = E_0 \exp(-z/\delta_{eff})\cos(\omega t + \chi);$$

$$\delta_{eff} = (c^2/2\pi\omega\sigma_{eff})^{1/2}. \tag{8.3}$$

Now we calculate the mean energy Δw, which the n electrons acquire along their path length, $l = vt_0$, under the action of the high frequency field;

$$\overline{\Delta w} = \frac{ne^2}{2m}E_0^2\left[\overline{\int_0^{t_0}\exp(-z(t)/\delta_{eff})\cos(\omega t + \chi)\,dt}\right]^2,$$
$$z(t) = z_0 + (v/\Omega)(1 - \cos\Omega t);\qquad \Omega = eH/mc, \tag{8.4}$$

where v is the mean velocity of the electron.

The average must be taken over all χ (χ is the phase of the field, which is encountered by the electron at the surface) and over all initial coordinates of the electron, z_0. From $v/\Omega\,\delta_{eff} = r/\delta_{eff} \gg 1$ we find:

$$\overline{\Delta w} = \frac{\pi\sigma}{2\Omega}\frac{\delta_{eff}^2}{l}E_0^2\,\frac{\sin^2(N\pi\omega/\Omega)}{\sin^2(\pi\omega/\Omega)}\cos^2(\pi\omega/\Omega). \tag{8.5}$$

Here $N(= l/2\pi r \gg 1)$ is the number of revolutions made by the electron between collisions and $\sigma = ne^2t_0/m$ is the dc conductivity.

From Eq. (8.5), it is seen that with $\omega = q\Omega$, $\overline{\Delta w}$ attains a maximum, *i.e.*, resonance takes place. During resonance,

$$\overline{\Delta w} = (\pi\sigma/2\Omega)(\delta_{eff}^2/l)E_0^2N^2.$$

On the other hand, the quantity of heat, Q, which is released in the metal during the time $t_0 \gg 1/\omega$ is equal to

$$Q = \int_0^{t_0} dt \int_0^{\infty} \sigma_{\text{eff}} E^2 dz = \frac{\pi \sigma_{\text{eff}}}{2\Omega} N \delta_{\text{eff}} E_0^2, \quad (8.6)$$

where σ_{eff} is the effective conductivity of the metal.

Equating Q and $\overline{\Delta w}$ we find that

$$\sigma_{\text{eff}} = \sigma \delta_{\text{eff}} / 2\pi r. \quad (8.7)$$

But, from Maxwell's equations $\delta_{\text{eff}} = (c^2/2\pi\omega\sigma_{\text{eff}})^{1/3}$, so that

$$\sigma_{\text{eff}} = \frac{1}{2\pi}\left(\frac{c^2\sigma^2}{r^2\omega}\right)^{1/3}, \qquad \delta_{\text{eff}} = \left(\frac{rc^2}{\omega\sigma}\right)^{1/3}. \quad (8.8)$$

Hence, during resonance

$$R(H) = \left(\frac{2\pi\omega}{c^2\sigma_{\text{eff}}}\right)^{1/2} = \left(\frac{4\pi}{\sqrt{3}}\right)^{1/3}\left(\frac{\sqrt{3}\pi\omega^2 l}{c^4\sigma}\right)^{1/3}\left(\frac{2\pi q}{\omega t_0}\right)^{1/3}, \quad (8.9)$$

where only the numerical factor differs from Eq. (6.8) for $\omega = q\Omega$. Such a difference should have been anticipated, because the complex character of δ_{eff} had not been taken into account. A similar method cannot be determined with Eq. (6.10), since it does not permit one to take into account the variation of the phase of the field with depth of penetration. Besides this, it can be applied only to the case of a quadratic dispersion law. A precise calculation shows that in reality the effective depth for the attenuation of the field, which is given by

$$\delta_{\text{eff}}^{(E)} = \int_0^{\infty} E(z)\, dz / E(0) \sim \delta (\delta / r)^{1/3} \ll \delta_{\text{eff}}$$

is considerably smaller than the effective depth for attenuation of the current, given by

$$\delta_{\text{eff}}^{(j)} = \int_0^{\infty} j(z)\, dz / j(0) \sim \delta (r/\delta)^{1/3} \sim \delta_{\text{eff}}.$$

(similar relations are valid even in the absence of the magnetic field; it is only necessary to replace r by l).

9. CONCLUSIONS

We have shown that in metals, at high frequencies and low temperatures, a new kind of resonance, namely cyclotron resonance, should take place. This resonance has not as yet been observed experimentally. It is readily distinguishable from other resonances, since 1) it occurs at a number of frequencies, rather than at a single frequency as is the case for diamagnetic or paramagnetic resonance (see Fig. 3); 2) it is possible only in stationary magnetic fields, which must be very nearly parallel to the surface of the metal, and 3) it persists through a reversal of the magnetic field.

An experimental investigation of cyclotron resonance is beset with a series of difficulties, such as the following:

(1) The frequency ω, is given by

$$2\pi / t_0 \ll \omega \ll (v/c)\,(2\pi n e^2/m)^{1/2} \quad (9.1)$$

(where t_0 is the characteristic relaxation time of the electrons), corresponds to centimeter and millimeter waves* for pure metals at very low temperatures;

(2) The stationary magnetic field must be

$$H \sim mc\omega/e \gg 2\pi mc/et_0, \quad (9.2)$$

i.e., fields of thousands of oersteds** are needed. (For the case of almost empty bands with small electron effective masses, the required value of H drops to tens or hundreds of oersteds).

(3) The stationary magnetic field must be very nearly parallel to the surface. The angle Φ between the field and the surface has to be such that

$$\Phi \lesssim \delta_{\text{eff}} / l \sim (r/l)\,(\delta/r)^{2/3}, \quad \delta = (mc^2/2\pi e^2 n)^{1/2} \quad (9.3)$$

(here δ_{eff} is the effective depth of the skin layer), *i.e.*, if $l \sim 10^{-2}$ cm, $\delta \sim 10^{-5}$ cm, the angle Φ may not exceed several tens of minutes. This also applies to the angular dimensions of surface inhomogeneities. Otherwise, the free-path-length of the electrons, which contribute to the resonance, is determined by collisions with surface irregularities. Therefore, the finish of the surface becomes especially significant.

By using the anisotropy of the surface impedance in a magnetic field, one can in principle determine the shape of the boundary Fermi surface, the ve-

*The inequality on the right occurs because at very high frequencies (in the infrared region) and at corresponding magnetic fields the normal skin effect is encountered again, since r turns out to be much smaller than δ_{eff}. In this case cyclotron resonance does not occur.

**It would be very interesting to investigate cyclotron resonance at very intense, pulsed magnetic fields with a pulse duration considerably greater than $t_0 \sim 10^{-11}$ sec. Of course in this case, the inequality on the right side of (9.1) should be satisfied.

locity of the electrons on it and the transition probability for passing from one state to the other. (It must be understood that this is valid only for closed cross sections of the Fermi surface. For open cross sections, an investigation of the anisotropy permits one to establish only that such cross sections are present and how they are oriented, which one learns from the absence of resonance in corresponding directions.)

An interpretation of the experimental curves in the case of partially filled bands is simpler than in the de-Haas, van-Alphen effect, because of the resonant nature of the curves.

By examining the dependence of the resonance minimum in R on the magnetic field, one can determine how much the dispersion law for the electrons differs from a quadratic law; *i.e.*, to what extent the electron bands are filled.

It should be emphasized that electrons in the fundamental band (and not just those in very slightly filled bands) participate in cyclotron resonance and that these electrons are the ones which make the main contribution to the electrical conductivity of the metal.

Quantum effects will lead to small oscillations superimposed on the fundamental periodic curves. These oscillations are completely non-essential to the phenomenon discussed here.

In conclusion the authors consider it their pleasant duty to thank L. D. Landau, I. M. Lifshiftz, M. I. Kaganov and A. Ia. Povzner for profitable discussions.

Note added in proof: Recently E. Fawcett[17] reported the experimental observation of cyclotron resonance in tin and of a decrease in the surface resistivity of tin and copper in a high intensity magnetic field, parallel to the surface of the metal. As was shown theoretically (see footnote in Sec. 6), the minuteness of the decrease in the surface resistance in the high intensity magnetic field is associated with the fact, that it is clearly not enough for the magnetic field be parallel to the surface within 1°, as was the case in Fawcett's experiments. As we have shown Φ should satisfy the conditions $\Phi < (r/l)\,(\delta/r)^{1/3} \ll 1°$. The smoother variation of $R(H)$ may also be attributed to an insufficiently smooth surface. A detailed consideration of the experimental results will be presented in a separate article.

[1] M. Ia. Azbel' and E. A. Kaner, J. Exptl. Theor. Phys. (U.S.S.R.) **30**, 811 (1956), Soviet Physics JETP **3**, 772 (1956).

[2] M. Ia. Azbel', Dokl. Akad. Nauk SSSR **100**, 437 (1955).

[3] Ia. G. Dorfman, Dokl. Akad. Nauk SSSR **81**, 765 (1951); R. B. Dingle, Proc. Roy. Soc. A**212**, 38 (1952); Dresselhaus, Kip and Kittel, Phys. Rev. **92**, 827 (1953); also **98**, 368 (1955) and **100**, 618 (1955); Lax, Zeiger, Dexter and Rosenblum, Phys. Rev. **93**, 1418 (1954); Dexter, Zeiger and Lax, Phys. Rev. **95**, 557 (1954).

[4] A. B. Pippard, Proc. Roy. Soc. A**191**, 385 (1947).

[5] Lifshitz, Azbel' and Kaganov, J. Exptl. Theor. Phys. (U.S.S.R.) **30**, 220 (1956), Soviet Physics JETP **3**, 143 (1956) and **31**, 63 (1956), Soviet Physics JETP **4**, 41 (1957).

[6] R. Chambers, Proc. Roy. Soc. A**215**, 481 (1952).

[7] K. Fuchs, Proc. Cambr. Phil. Soc. **34**, 100 (1938).

[8] A. H. Wilson, *Theory of Metals* London (1954).

[9] M. Ia. Azbel' and E. A. Kaner, J. Expt. Theor. Phys. (U.S.S.R.) **29**, 876 (1955), Soviet Physics JETP **2**, 749 (1956).

[10] M. I. Kaganov and M. Ia. Azbel', Dokl. Akad. Nauk SSSR **102**, 49 (1955).

[11] I. M. Lifshitz and A. V. Pogorelov, Dokl. Akad. Nauk SSSR **96**, 1143 (1954).

[12] A. B. Pippard, Proc. Roy. Soc. A**203**, 98 (1950) and A**203**, 195 (1950).

[13] V. L. Ginzburg and G. P. Motulevich, Usp. Fiz. Nauk **55**, 469 (1955).

[14] P. L. Kapitza, Proc. Roy. Soc. **123A**, 292, 342 (1929).

[15] B. I. Verkin and I. Mikhailov, J. Exptl. Theor. Phys. (U.S.S.R.) **24**, 342 and **25**, 471 (1953).

[16] I. M. Lifshitz and A. M. Kosevich, Dokl. Akad. Nauk SSSR **96**, 963 (1954). also J. Exptl. Theor. Phys. (U.S.S.R.) **29**, 730 (1955), Soviet Physics JETP **2**, 636 (1956).

[17] E. Fawcett, Phys. Rev. **103**, 1582 (1956).

Translated by J. J. Loferski
188

The Thermodynamics of Liquid He^3

I. M. KHALATNIKOV AND A. A. ABRIKOSOV

J. Exptl. Theoret. Phys. (U.S.S.R.) 32, 915-919
(April, 1957)

The thermodynamics of liquid He^3 is considered on the basis of the Fermi liquid model proposed by L. Landau. The entropy, the specific heat, and the magnetic susceptibility of liquid He^3 are computed for the possible types of the energy spectrum of the liquid. Comparison with experiment is carried out.

LET US CONSIDER the thermodynamics of liquid helium on the basis of the Fermi liquid model proposed by Landau[1]. According to Ref. 1, for small deviations of the distribution function from its equilibrium value at $T = 0$, the excitation energy may be presented in the form

$$\varepsilon = \varepsilon(p) + \int f(p, p')\,\nu(p')\,d\tau' \quad d\tau = g dp_x dp_y dp_z / (2\pi\hbar)^3, \tag{1}$$

where $\nu = n - n_0$, and g is the statistical weight (here ε does not depend on the spin). In the usually-employed perfect-gas model, the excitation energy $\varepsilon(p)$ is written in the form $p^2/2m$, where m is a certain effective mass. We will see later, however, that such a form of the spectrum leads to results which, although not in contradiction with the experimental data, do not agree with them too well. It is why we will consider for $\varepsilon(p)$ another function proposed by L. D. Landau, namely:

$$\varepsilon(p) = (p - p_0)^2/2m, \tag{2}$$

where m is the effective mass. In this case, for $T = 0$, the distribution function in momentum space will be not a sphere but a spherical shell. We will assume the thickness Δ of this shell as small with respect to its radius p_0 ("bubble"); rigorously speaking, in the opposite case Eq. (2) would be erroneous and $\varepsilon(p)$ could not be considered as a symmetric function with respect to the minimum point $p = p_0$. In the case of a spectrum of type (2), we are faced with a unique situation where the Fermi-liquid theory is only valid for such temperatures, for which the deviations from the zeroth distribution function are small. For the perfect-gas model this obviously corresponds to temperatures $T \ll T_D$, where T_D is the temperature of degeneracy. In the case of a spectrum of type (2), however, even for temperatures considerably higher than the temperature of degeneracy and which correspond to a Boltzmann distribution, the distribution function continues to decrease as one gets away from $p = p_0$, so that effectively all the excitations will be localized in the neighborhood of that point. One sees therefore that there exists a temperature region $T > T_D$ for which the deviation from the zeroth function is negligible. This makes possible in this case evaluation of the thermodynamical functions in the Fermi as well as in the Boltzmann regions.

As we will see, a spectrum of type (2) agrees with the experimental data better than the perfect gas model, but not so much as to exclude the possibility of this model for He^3, more so because it appears to be more natural.

1. *Specific Heat and Entropy.* For a non-zero temperature, the distribution function is the usual Fermi function

$$n = [e^{(\varepsilon-\mu)/kT} + 1]^{-1}$$

(μ — chemical potential). Let us compute the specific heat in the case of a spectrum of the type (2). We start from the expression for the energy of the system

$$E = \int \varepsilon n d\tau = \frac{4\pi p_0^2 g \sqrt{2m}}{(2\pi\hbar)^3} (kT)^{3/2} I_{1/2}, \tag{3}$$

where*

$$I_\alpha = \int_0^\infty \frac{x^\alpha dx}{(e^x / A) + 1}, \quad A = e^{\mu/kT}.$$

Further, differentiating this expression with respect to temperature, and using the condition $N = \text{const.}$, we find the specific heat per particle:

$$c = \frac{1}{N}\left(\frac{dE}{dT}\right)_N = k\left[\frac{3}{2}\frac{I_{1/2}}{I_{-1/2}} - \frac{1}{4}\frac{I_{-1/2}}{(\partial I_{1/2}/\partial A)}\right]. \tag{4}$$

In this fashion, the specific heat is expressed in

* Detailed tables of the integrals I_α are available (Ref. 2).

terms of the parameter A which, in turn, is expressed in terms of the temperature, making use of the relationship

$$N = \int n d\tau = \frac{4\pi p_0^2 g \sqrt{2m}}{(2\pi\hbar)^3} (kT)^{1/2} I_{-1/2}. \quad (5)$$

Let us also find the formula for the entropy. We start from the definition of the entropy

$$S = -k \int \{n \ln n + (1-n) \ln (1-n)\} d\tau. \quad (6)$$

Substituting here the expression for the distribution function, we get after simple integration by parts

$$s = S/N = k\{(3I_{1/2}/2I_{-1/2}) - \ln A\}. \quad (7)$$

Let us use the known expansion of the Fermi-type integrals I_α and find the asymptotic expressions for c and s at low temperatures:

$$c = s = \gamma T;$$

$$\gamma = g^2 p_0^4 mk^2 / 3\pi^2\hbar^6 N^2 = 4\pi^2 mk^2 / 3\Delta^2. \quad (8)$$

Analogous formulas correspond to the perfect gas model, for which

$$\gamma = (m/2\hbar^2)(\sqrt{2}\pi g/3N)^{2/3} k^2 = \pi^2 m p_{gr}^{-2} k^2. \quad (9)$$

Comparing formulae (8) and (9) with the experimental data on the entropy of He^3 at low temperatures[3], we can find the parameter γ and therefrom the parameters of the spectrum which occur in it. Unfortunately, at the present time, the experimental curve is extended only to the beginning of the linear region. On the basis of these data, it is possible to obtain an approximate value for the parameter γ. It turns out to be equal to $\gamma = 3$ cal/mol.deg.

In the perfect gas model the effective mass m turns out to be equal to $m = 1.43\ m_3$ (m_3 is the mass of the He^3 atom). The limiting momentum p_{lim} can be found from the total number of particles $(\rho = 0.078\ g/cm^3)(p_{lim}/\hbar) = (3\pi^2 N)^{1/3} = 0.76 \cdot 10^8\ cm^{-1}$. The limiting Fermi energy is equal to $\mu/k = \varepsilon_{lim}/k = p_{lim}^2/2mk = 3.3°K$. As to the parameters characterizing a spectrum of type (2), the situation is somewhat more complicated, since all the expressions for the thermodynamical observables depend on the sole combination of parameters $p_0^2\sqrt{2m}$. This is why we find from the experimental data on the specific heat only this combination $(p_0/\hbar)^2\sqrt{m/m_3} = 2 \times 10^{15}\ cm^{-2}$. In this case, as the momentum p_0 has to be larger than the momentum of the Fermi sphere, one can determine for the effective mass of this spectrum the inequality $m < 0.12 m_3$. No one should be surprised by the smallness of this effective mass. The effective mass for a spectrum of such a type does not have to be close to the mass of the particles of the liquid (let us recall, for instance, that the mass of a roton in liquid He^4 is close to the proton mass ($0.26 m_4$, m_4 – mass of He^4)). Let us express the number of particles through the limiting energy of such a spectrum, $N = \sqrt{\varepsilon_{lim}}\, 8\pi p_0^2 g\sqrt{2m}/(2\pi\hbar)^3$. This yields the value of the limiting energy $\varepsilon_{lim} = 1.05°$ K.

The linear law for the specific heat is observed experimentally only for temperatures of the order of 0.2°K. It seems to us that a spectrum of type (2) corresponds better to this situation because—for this spectrum—the temperature of degeneracy is equal to 1°K. It also seems that a spectrum of type (1) gives a temperature of degeneracy which is too high (3.3°K). If the temperature exceeds the temperature of degeneracy, the formulae of the Boltzmann statistics may be applied (in this case, the parameter A tends to zero). For the perfect-gas model, one obviously gets $c = 3k/2$. This law does not correspond to experiment; this shows, however, only the inapplicability of such a model above T_D

For a type (2) spectrum, $c \to k/2$ as A tends to zero. In this region, therefore, the specific heat of He^3 tends to $k/2$, or, calculated per mole, to 1 calorie. This result is absolutely natural because the law of equipartition applies at these temperatures, and for this type of spectrum there is only one degree of freedom $(p - p_0)$.

A characteristic property of such a spectrum is, therefore, that, above the temperature of degeneracy, the specific heat tends to $k/2$ and not to $3k/2$, as it does in the case of the perfect-gas model.

We obtain therefore the following qualitative picture for the temperature dependence of the specific heat in the case of a type (2) spectrum. At low temperature (below T_D), there is a linear low; above T_D, c tends to the constant magnitude 1 cal/mol. deg. (there is a very weak maximum in the neighborhood of T_D). The result of the calculations for the value

$$(p_0^2/\hbar^2)\sqrt{m/m_3} = 2 \cdot 10^{15}\ cm^{-2}.$$

are shown on Fig. 1. The qualitative and quantitative agreement of the theory and of the experimental

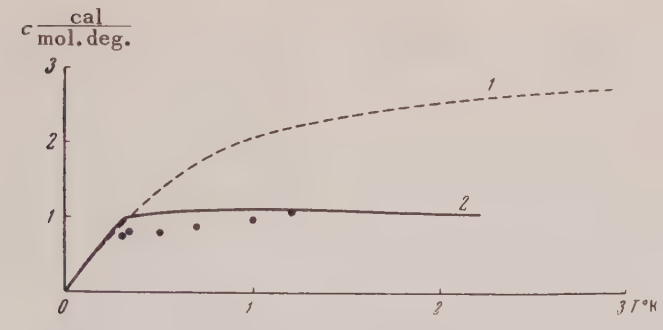

FIG. 1. Specific heat of liquid He^3: 1—perfect gas model, 2—spectrum of type (2), points—experimental data.[3]

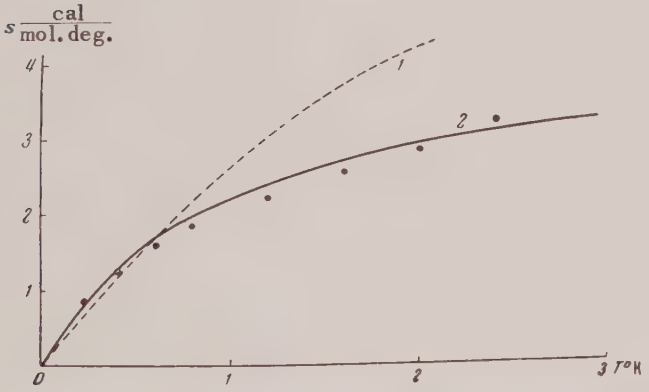

FIG. 2. Entropy of liquid He^3: 1—perfect gas model, 2—spectrum of type (2), points—experimental data[3].

data constitutes some evidence in favor of a type (2) spectrum for He^3.

We want to emphasize the existence of a large region of the experimental curve (about from 0.5 to 1.5°K), where the specific heat is approximately equal to 1 cal/mol. deg. The perfect-gas model cannot, of course, give a picture of such a kind. In this model the specific heat tends to 3 cal/mol.deg fairly rapidly, as the temperature increases. But one has to remark that the comparison of the experimental data with the results obtained from this model become, as already mentioned, forbidden as the temperature approaches the temperature of degeneracy. However, even away from the temperature of degeneracy, in the region of 1°K, the experimental data are twice as small as the theoretical results for the perfect-gas model with the parameters we chose.

The curves for the entropy are shown on Fig. 2.

2. *Magnetic Susceptibility.* Let us recall the equations of the magnetic susceptibility[1]. Let us assume that the spin interaction is of pure exchange type. With this assumption, let us separate from the function which characterizes the dependence of the excitation energy on the distribution function that part which depends on the spin interaction: $f = \varphi + \psi(s,s')$. According to Ref. 1, the magnetic susceptibility is

$$\chi = -\frac{\mu^2}{4}\int\frac{\partial n}{\partial\varepsilon}d\tau \Big/ \left[1 - \frac{\overline{\psi}}{4}\int\frac{\partial n}{\partial\varepsilon}d\tau\right], \qquad (10)$$

where μ is the magnetic moment of the He^3 atom and $\overline{\psi}$ is the ψ function averaged over angles for momenta corresponding to the Fermi limit.

Using the notation defined above, let us rewrite this formula in the form

$$\frac{\mu^2}{\chi} = \overline{\psi} - 4\Big/\int\frac{\partial n}{\partial\varepsilon}d\tau = \overline{\psi} + 4\Big/a\,(kT)^{\alpha}(\partial I_{\alpha}/\partial A)$$

$$a = 4\pi g m\sqrt{m}/(2\pi\hbar)^3,$$

$$\alpha = {}^1/_2 \quad \text{(perfect gas model)} \qquad (11)$$

$$a = 4\pi p_0^2\, g\sqrt{2m}/(2\pi\hbar)^3,$$

$$\alpha = -{}^1/_2 \quad \text{[spectrum (2)]}$$

In the low-temperature limit, the latter formula takes the form

$$\frac{\mu^2}{\chi} = \bar{\psi} + \frac{4}{a}\left(N\frac{1+\alpha}{a}\right)^{-\alpha/(\alpha+1)}.$$

Therefore, in the low temperature region (below T_D) the magnetic susceptibility of the Fermi liquid tends to a constant limit.

In the high temperature region, the asymptotic law for χ has the form $\mu^2/\chi_\infty T = 4k/N$. Usually the quantity $1/(\chi/\chi_\infty T)$ is used. In the low temperature region, this quantity is equal to

$$\frac{1}{(\chi/\chi_\infty T)} = \bar{\psi}\frac{N}{4k} + \frac{\pi^2 k}{3\gamma}, \qquad (12)$$

where γ is determined by Eq. (8) or (9).

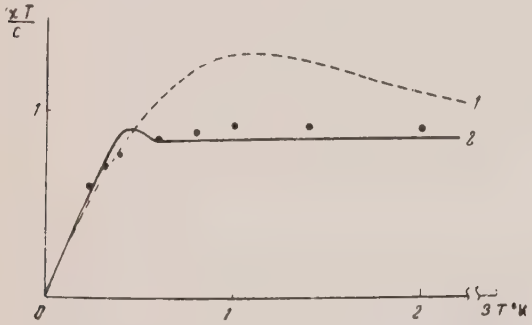

FIG. 3. Magnetic susceptibility of liquid He^3: 1 – perfect gas model, 2 – spectrum of type (2), points – experimental data[4].

From the comparison of Eq. (12) with experimental data[4], one gets for $\psi N/4k$ the value −1.05. This magnitude constitutes about 2/3 of the second term in (12). In this fashion, the exchange interaction plays a considerable role in the magnitude of the magnetic susceptibility of liquid He^3. The sign of the effect is such that the exchange interaction favors, in this case, a parallel orientation of the spins. However, this interaction does not yield ferro-magnetism, because the Fermi tendency for an anti-parallel orientation of the spin prevails. It is possible that with increasing pressure the parameters will change in such a way that ferromagnetism will be possible; however, so far, there are no experimental indications for such a possibility.

The curves for the susceptibility are shown on Fig. 3. (On this figure, c is the normalized Curie constant.) One sees from the curves that, here too, a type (2) spectrum agrees better with experimental data.

In conclusion, we wish to thank Academician L. D. Landau for useful advice and discussion of our results.

[1] L. Landau, J. Exptl. Theoret. Phys. (U.S.S.R.) **30**, 1058 (1956), Soviet Physics JETP **3**, 920 (1957).

[2] J. McDougall and E. Stoner, Trans. Royl Soc. (London) A, No. 773, **237**, 67 (1938).

[3] Abraham, Osborne and Weinstock, Phys. Rev. **98**, 551 (1955).

[4] Fairbank, Ard and Walters, Phys. Rev. **95**, 566 (1954).

Translated by E. S. Troubetzkoy
189

Ionization Losses of High-Energy Heavy Particles

P. V. VAVILOV

(Submitted to JETP editor Feb. 17, 1956)
J. Exptl. Theoret. Phys. (U.S.S.R) 32, 920-923 (April, 1957)

Analysis and rigorous solution of the problem of ionization losses of heavy particles in "thin absorbers," *i.e.*, absorbers in which the ionization losses are much smaller than the initial energy of the particles

IN PASSING THROUGH MATTER a charged particle loses its energy by collision with atomic electrons. Individual collisions are independent events, so that the energy losses may vary. The kinetic equation for the distribution function is of the form [1]

$$\frac{\partial f(x,\Delta)}{\partial x} = \int_0^b w(\varepsilon) f(x, \Delta-\varepsilon)\, d\varepsilon - f(x,\Delta) \int_0^{\varepsilon_{max}} w(\varepsilon)\, d\varepsilon, \tag{1}$$

and it is assumed that the total loss $\Delta = E_0 - E$ in a path x is small compared with the initial energy E_0, so that the probability $w(E, \varepsilon)$ of energy loss per unit length may be considered independent of the final energy E. Further, it is assumed that $w(\varepsilon) = 0$ for $\varepsilon > \varepsilon_{max}$, where ε_{max} is the maximum energy transferred during a single collision, $b = \Delta$ for $\Delta < \varepsilon_{max}$, and $b = \varepsilon_{max}$ for $\Delta > \varepsilon_{max}$. (We are using Landau's notation. [1])

We shall solve Eq. (1) by Laplace transforms:

$$\begin{aligned} f(x,\Delta) &= \frac{1}{2\pi i}\int_{c-i\infty}^{c+i\infty} e^{p\Delta}\frac{\varphi(x,p)}{p}\,dp,\\ \varphi(x,p) &= p\int_0^\infty e^{-p\Delta} f(x,\Delta)\,d\Delta,\\ w(\varepsilon) &= \frac{1}{2\pi i}\int_{c-i\infty}^{c+i\infty} e^{p\varepsilon}\frac{w(p)}{p}\,dp,\\ w(p) &= p\int_0^\infty e^{-p\varepsilon} w(\varepsilon)\,d\varepsilon. \end{aligned} \tag{2}$$

When $b = \Delta$, we use the well known multiplication theorem for Laplace transforms; inserting (2) into (1), we obtain

$$\frac{\partial\varphi(x,p)}{\partial x} = \varphi(x,p)\left(\frac{w(p)}{p} - \int_0^{\varepsilon_{max}} w(\varepsilon)\,d\varepsilon\right),$$

whence

$$\varphi(x,p) = \varphi(0,p)\exp\left[-x\left(\int_0^{\varepsilon_{max}} w(\varepsilon)\,d\varepsilon - \frac{w(p)}{p}\right)\right], \tag{3}$$

But

$$\frac{w(p)}{p} = \int_0^\infty e^{-\varepsilon p} w(\varepsilon)\,d\varepsilon = \int_0^{\varepsilon_{max}} e^{-\varepsilon p} w(\varepsilon)\,d\varepsilon,$$

further, when $x = 0$ we have $f(0, \Delta) = \delta(\Delta)$, so that

$$\varphi(0,p) = p\int_0^\infty e^{-p\Delta}\delta(\Delta)\,d\Delta = p.$$

Inserting this expression into (3), we arrive at

$$f(x,\Delta) = \frac{1}{2\pi i}\int_{c-i\infty}^{c+i\infty} \exp\left\{p\Delta - x\int_0^{\varepsilon_{max}} w(\varepsilon)\,(1-e^{-\varepsilon p})d\varepsilon\right\}dp. \tag{4}$$

The case $b = \varepsilon_{max}$ leads again to the same equation, so that Eq. (4) is the exact solution for arbitrary Δ. The solution obtained differs from Landau's [1] only in that Landau has $\varepsilon_{max} = \infty$.

Let us write the exponent in Eq. (4) in the form

$$I = p(\Delta - \alpha x) - x\int_0^{\varepsilon_{max}} w(\varepsilon)\,(1 - e^{-\varepsilon p} - \varepsilon p)\,d\varepsilon. \tag{4'}$$

Now distant collisions do not play as important a role in the integral with respect to $d\varepsilon$ as they do in α, and therefore for heavy particles (which are all we are considering in this article) we may use the expression

$$\begin{aligned} xw(\varepsilon) &= \xi\varepsilon^{-2}(1-\beta^2\varepsilon/\varepsilon_{max}),\\ \varepsilon_{max} &= 2m_e c^2\beta^2/(1-\beta^2),\\ \xi &= 0{,}300\, x\,(m_e c^2/\beta^2)\,Z/A, \end{aligned} \tag{5}$$

where x is given in gm/cm², Z is the atomic number of the substance, A is the atomic weight, m_e is the electron mass, βc is the particle velocity, and the initial energy of the particle $E_0 \ll Mc^2(M/m_e)$, where M is the mass of the particle. Inserting (5) into (4′), simple operations lead to

$$I = p(\Delta - \alpha x) - p\xi(1+\beta^2) + \varkappa(1 - e^{-\varepsilon_{\max} p}) + (\varkappa\beta^2 + \xi p)\int_0^{\varepsilon_{\max}} \frac{1-e^{-\varepsilon p}}{\varepsilon}\, d\varepsilon, \quad \varkappa = \frac{\xi}{\varepsilon_{\max}}.$$

It is easily shown[2] that

$$\int_0^{\varepsilon_{\max}} \frac{1-e^{-\varepsilon p}}{\varepsilon}\, d\varepsilon = C + \ln(\varepsilon_{\max} p) - \mathrm{Ei}(-\varepsilon_{\max} p), \tag{6}$$

where $C = 0.577\ldots$ is Euler's constant, and Ei is the exponential integral function. If we use the expression

$$x\alpha = \xi\left[\ln\frac{2m_e c^2 \beta^2 \varepsilon_{\max}}{(1-\beta^2) I^2(Z)} - 2\beta^2\right] \tag{7}$$

for the mean energy loss, we obtain (with the replacement $p\varepsilon_{\max} = z$)

$$f(x, \Delta) = \frac{1}{2\pi i \varepsilon_{\max}} e^{\varkappa(1+\beta^2 C)} \int_{c-i\infty}^{c+i\infty} \exp\{z\lambda_1 + \varkappa[(z+\beta^2)(\ln z - \mathrm{Ei}(-z)) - e^{-z}]\}\, dz, \tag{8}$$

$$\lambda_1 = (\Delta - \alpha x)/\varepsilon_{\max} - \varkappa(1 + \beta^2 - C).$$

If we set $z\varkappa = p$, then $\lambda_1 \to \lambda$, where λ is Landau's parameter. It is easily seen that when $\varkappa = 0$ we obtain Landau's solution (with the replacement $z\varkappa = p$)

$$f(x, \Delta) = \frac{1}{2\pi i \xi} \int_{c-i\infty}^{c+i\infty} e^{p\lambda + p\ln p}\, dp. \tag{9}$$

Let us consider the case $\varkappa \gtrsim 1$. Expanding the exponent in Eq. (4) into a series and introducing the notation

$$\gamma = \int_0^{\varepsilon_{\max}} \varepsilon^2 w(\varepsilon)\, d\varepsilon, \quad \delta = \int_0^{\varepsilon_{\max}} \varepsilon^3 w(\varepsilon)\, d\varepsilon, \tag{10}$$

we obtain

$$\exp\left\{p(\Delta - \alpha x) + \frac{\gamma x}{2!} p^2 - \frac{\delta x}{3!} p^3\right\}.$$

If we restrict ourselves to the term containing γ, we obtain a Gaussian curve, so that the third term gives the asymmetry of the curve. Let us write

$$z = (\delta x/2)^{1/3}(p - \gamma/\delta). \tag{11}$$

After some simple operations we obtain

$$f(x, \Delta) = e^{at - a^3/3} \frac{1}{2\pi i \eta} \int_{c-i\infty}^{c+i\infty} e^{zt - z^3/3}\, dz,$$

$$\frac{1}{\eta} = \left(\frac{2}{x\delta}\right)^{1/3} = \frac{1}{\xi}\left[(2\varkappa)^2 \Big/ \left(1 - \frac{2}{3}\beta^2\right)\right]^{1/3}, \tag{12}$$

$$a = \gamma_1 \frac{\gamma}{\delta} = \left(1 - \frac{3\beta^2}{2}\right)\left[(2\varkappa)\Big/\left(1 - \frac{2}{3}\beta^2\right)^2\right]^{1/3},$$

$$t = (\Delta - \alpha x)/\eta + a^2.$$

Integrating along the imaginary axis, we obtain

$$f(x, \Delta) = \frac{1}{\eta\sqrt{\pi}} e^{at - a^3/3} v(t),$$

$$v(t) = \frac{1}{\sqrt{\pi}} \int_0^{\infty} \cos\left(yt + \frac{y^3}{3}\right) dy, \tag{13}$$

where $v(t)$ is Airey's function, which has been tabulated by Fock[3]. Hines[4] has used a similar expansion, but was unable, using Mellin transforms, to obtain an exact solution.

The position of the maximum of the distribution function is found by differentiating Eq. (13) with respect to t,

$$a = -v'(t)/v(t). \tag{14}$$

From Eq. (14) and the tables we find $t_{\max} = (\Delta_{\max} - \alpha x)/\eta + a^2$.

We shall now show that for $\kappa \gg 1$ Eq. (13) becomes a Gaussian curve. Indeed, $a \approx (2\kappa)^{1/3}$ and as $\kappa \to \infty$ we have $a \to \infty$, so that the maximum of the curve moves towards large t. Using the asymptotic expression for Airey's function[3], we obtain

$$f(x, \Delta) \approx \frac{1}{2\eta\sqrt{\pi} t^{1/4}} \exp\left\{-\frac{a^3}{3} + at - \frac{2}{3} t^{3/2}\right\}.$$

Further

$$t^{1/4} \approx \sqrt{a},\ at - {}^2/_3\, t^{3/2} \approx (a^3/3) - z^2/4a$$

($z = (\Delta - \alpha x)/\eta \ll a$) and by expressing a, η, and z in terms of γ and δ, we obtain

$$f(x, \Delta) \approx (2\pi\gamma x)^{-1/2} \exp\{-(\Delta - \alpha x)^2/2\gamma x\}, \quad \varkappa \gg 1. \tag{15}$$

Performing the integration in Eq. (8) along the imaginary axis, we obtain the following expression for the distribution function:

$$f(x, \Delta) = \frac{1}{\pi\xi} \varkappa e^{\varkappa(1+\beta^2 C)} \int_0^\infty e^{\varkappa f_1} \cos(y\lambda_1 + \varkappa f_2)\, dy,$$
$$f_1 = \beta^2(\ln y - \mathrm{Ci}(y)) - \cos y - y\,\mathrm{Si}(y), \quad (16)$$
$$f_2 = y(\ln y - \mathrm{Ci}(y)) + \sin y + \beta^2\,\mathrm{Si}(y),$$

where Si and Ci are the sine and cosine integral functions, respectively. All the numerical calculations were performed in the Digital Control Systems Laboratory of the Academy of Sciences, USSR. Fig. 1 gives graphs of the functions

$$\varphi(\lambda_1) = \xi f(x, \Delta)$$

and $$(\lambda_1) = \int_\Delta^\infty f(x, \Delta)\, d\Delta = \frac{1}{\varkappa} \int_{\lambda_1}^\infty \varphi(x)\, dx$$

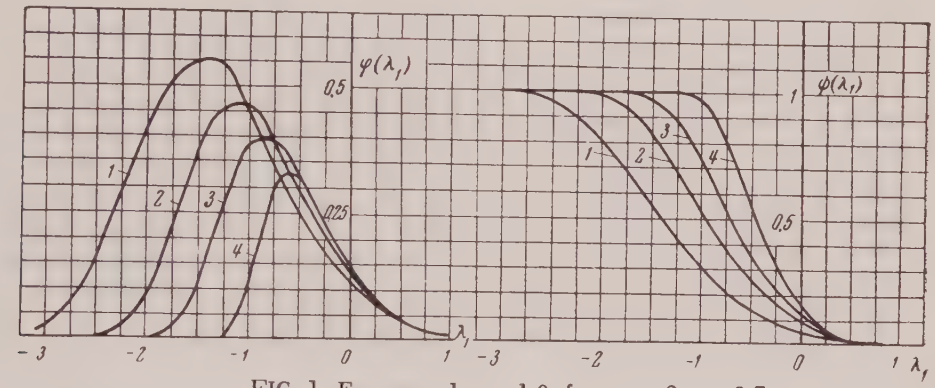

FIG. 1. For curve 1, $\varkappa = 1.0$; for curve 2, $\varkappa = 0.7$; for curve 3, $\varkappa = 0.5$; for curve 4, $\varkappa = 0.3$.

for various values of the parameter κ and for $\beta^2 = 0.9$.

Fig. 2 gives the curves for $\kappa = 0.1$ (curve 1) and $\kappa = 0.01$ (curve 2). For comparison, we also give Landau's function (curve L). The abscissa gives Landau's parameter:

$$\lambda = (\lambda_1/\varkappa) - \ln\varkappa = (\Delta - \alpha x)/\xi - 1 - \beta^2 + C - \ln\varkappa.$$

It is seen from Fig. 2 that when $\kappa = 0.01$ the exact function is practically the same as Landau's.

Thus Landau's approximation is valid for $\kappa \leq 0.01$, the exact solution (16) must be used in the interval $0.01 \leq \kappa \leq 1$, and the approximation of Eq. (13) may be used in the region $\kappa \gtrsim 1$.

In conclusion, I consider it my duty to express my gratitude to Iu. F. Orlov for valuable discussions and remarks. The author also expresses his gratitude to the staff of the Calculating Division, who performed the numerical calculations.

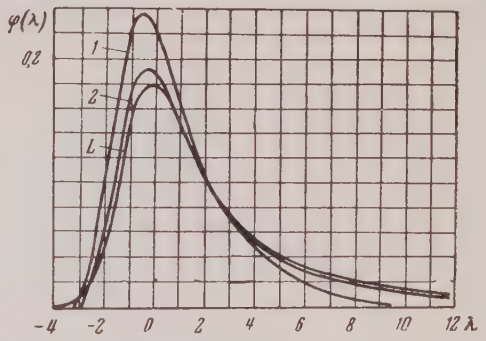

FIG. 2

[1] L. D. Landau, J. Phys. (U.S.S.R.) 8, 204 (1944).

[2] N. N. Lebedev, *Special Functions and Their Applications*, M., Gostekhizdat, 1953.

[3] V. A. Fock, *Table of Airey Functions*, M., 1946.

[4] K. C. Hines, Phys. Rev. 97, 1725 (1955).

Letters to the Editor

Account of Primary α-Particles in the Development of a Nucleon Shower in the Stratosphere

ZH. S. TAKIBAEV AND P. A. USIK
Physico-Technical Institute,
Academy of Sciences Kazakh SSR
(Submitted to JETP editor February 24, 1956)
J. Exptl. Theoret. Phys. (U.S.S.R.) 32, 924-925
(April, 1957)

HEAVY NUCLEI ($Z>2$) constitute a considerable part of the primary cosmic radiation. It follows from the data by Bradt and Peters[1], obtained by means of photo-emulsions, that 45% of the nucleons incident upon the top of the atmosphere are protons, 45.3% are α-particles, and 9.7% are heavier nuclei.

Measurements carried out at different geomagnetic latitudes[2] demonstrate that primary protons, α-particles and heavier nuclei possess similar energy-per-nucleon spectra up to 4000 Mc^2. In the account of α-particles we can therefore use the same spectrum exponent as used in the expression for the primary protons.

Haber-Shaim and Yekutiely[3], using the model of a mean nucleus for the atoms of air[4], estimated that in the mean 2.5 nucleons originating in the disintegration of an air nucleus by a high-energy α-particle are star-producing. In our calculations the mean number ν of star-producing nucleons which take their origin in the disintegration of an air nucleus by a primary α-particle is assumed to be equal to 2.5.

In the study of the interaction mean free path of heavy particles, Eisenberg[5] used the value $\lambda = 5\times 10^{-13}$ cm for the mean free path of a nucleon from the primary nucleus in the target nucleus. This value was obtained from experiments on the scattering of nucleons on nuclei at energies attained in accelerators. The resulting satisfactory agreement between theory and experiment makes it plausible to consider the behavior of the nucleons of the primary α-particle in the target nucleus as independent even at the energies involved. We shall therefore regard as fully grounded the use of the model of independent interaction of the incident nucleons with the target nucleus nucleons[6] for the calculation of cascade curves for nucleons in the stratosphere, caused by primary protons.

In our calculations we did not account for mesons, secondary α-particles, and ionization energy losses of charged particles. Assuming that the intensity of primary protons is normalized to unity, we shall use the following expression for the differential spectrum of primary α-particles:

$$S(E_0)\,dE_0 = \begin{cases} 0{,}3\gamma E_c^{\gamma} E_0^{-\gamma-1}\,dE_0 & \text{for } E_0 \geqslant E_c = 740\ \text{MeV}, \\ 0 & \text{for } E_0 < E_c, \end{cases}$$

where E_0 and E_c are energies per nucleon and $\lambda = 1.1$ (Ref. 6).

The value of the intensity of α-particles at the top of the atmosphere was obtained (using the above expression for the spectrum) recalculating the data of Bradt and Peters[1] obtained at the geomagnetic latitude of 30° N to the geomagnetic latitude of Moscow, 51° N, for which the proton cut-off energy was assumed to be equal to 2000 Mev. Correspondingly, the cut-off energy for α-particles equals 740 Mev per nucleon.

At an atmospheric depth x (measured in the units of the nucleon interaction mean free path, $\lambda = 75\,\text{g/cm}^2$), the flux intensity of primary α-particles will be equal to $I = I_0 e^{-x/l}$, where l is the interaction mean free path of α-particles in the air, measured in the units of λ. According to Fermi[7] we used the value of 44.5 g/cm^2 for the mean free path l.

The flux of nucleons with energy greater than E at a depth θ (in units of λ), produced by primary α-particles in a layer of thickness θ, can be represented as follows:

$$S_\alpha(E_c \geqslant E,\ \theta) = -\frac{\nu\gamma}{2\pi i}\int_{s_0-i\infty}^{s_0+i\infty}\int_{I_\theta}^{I_0}\left(\frac{E_c}{E}\right)^s \frac{e^{-f(D\alpha_s)z}}{s(\gamma-s)}\,dI\,ds,$$

where z is the atmospheric depth from the layer dx, in which the number of α-particles which interacted with air nuclei equals $-dI = (I_0/l)e^{-x/l}dx$, where $\theta = x+z$, $z = \theta - x$;

$$\alpha_s = 1 - 240/(s+2)(s+3)(s+4)(s+5).$$

We have then

$$S_x(E_c, \geqslant E, \theta) = -\frac{\gamma\nu I_0}{2\pi i l}\int_{s_0-i\infty}^{s_0+i\infty}\left(\frac{E_c}{E}\right)^s \int_0^\theta \frac{\exp\{-f(D\alpha_s)(\theta-x)\}\, e^{-x/l}}{s(\gamma-s)}\, dx\, ds$$

$$= \frac{\gamma\nu I_0}{2\pi i l}\int_{s_0-i\infty}^{s_0+i\infty}\int_0^\theta \left(\frac{E_c}{E}\right)^s \frac{\exp\{-f(D\alpha_s)\theta + f(D\alpha_s)x - x/l\}}{s(\gamma-s)\,[f(D\alpha_s) - 1/l]}\, d[-f(D\alpha_s)\theta$$

$$+ f(D\alpha_s)x - x/l]\, ds = \frac{\gamma\nu I_0}{2\pi i l}\int_{s_0-i\infty}^{s_0+i\infty}\left(\frac{E_c}{E}\right)^s \frac{e^{-f(D\alpha_s)\theta} - e^{-\theta/l}}{s(\gamma-s)\,[1/l - f(D\alpha_s)]}\, ds.$$

Therefore

$$S_\gamma(E_c, \geqslant E, \theta) = \frac{\gamma\nu I_0}{2\pi i l}\int_{s_0-i\infty}^{s_0+i\infty}\left(\frac{E_c}{E}\right)^s \frac{e^{-f(D\alpha_s)\theta} - e^{-\theta/l}}{s(\gamma-s)\,[1/l - f(D\alpha_s)]}\, ds.$$

The value $S_\alpha = (E_c, >E, \theta)$ was estimated by the saddle point method.

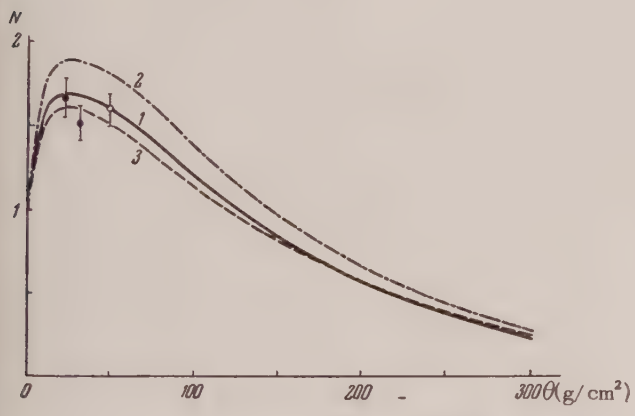

Altitude dependence of the number of stars and the flux of star-producing particles: 1- stars with account of primary α-particles, 2- flux of star-producing particles with account of primary α-particles, 3- stars without account of α-particles, ●- experimental data obtained in laboratory, ○- point of normalization of the experimental data. All curves are normalized to unity.

We calculated the curves for the star-producing particles with energy larger than E = 100 Mev for for various atmospheric depths. The calculations were carried out with and without account of the primary α-particles. Results are given in the figure.

[1] H. L. Bradt and B. Peters, Phys. Rev. 77, 54 (1950).

[2] B. Peters, Progress in Cosmic Ray Physics 1, 4 (Amsterdam, 1952).

[3] U. Haber-Shaim and G. Yekutieli, Nuovo cimento 11, 2, 172 (1954).

[4] U. Haber-Shaim, Phys. Rev. 84, 1199 (1951).

[5] Y. Eisenberg, Phys. Rev. 96, 1378 (1954).

[6] H. Messel, Progress in Cosmic Ray Physics 2, 4 (Amsterdam, 1954).

[7] E. Fermi, Progr. Theor. Phys. 5, 570 (1950).

Ponderomotive Forces in a Localized Plasma in the Electromagnetic Field of a Plane Wave

V. V. IANKOV

P. N. Lebedev Physical Institute, Academy of Sciences, USSR

(Submitted to JETP editor December 6, 1956)

J. Exptl. Theoret. Phys. (U.S.S.R.) 32, 926-927 (April, 1957)

WHEN THE FIELD of a plane wave is impressed on a localized plasma, there arise both a radiation pressure in the direction of the wave motion and ponderomotive forces tending to produce a deformation of the plasma. The present article is devoted to the explanation of the nature of these forces in the special case where the wavelength is much larger than the linear dimensions of the region of localization A quasi-neutral plasma may be described phenomenologically as a medium having dielectric constant ε, conductivity σ and magnetic permeability $\mu = 1$.

A sphere of ionized gas with a uniform density of ionization may be considered as a rough model of a localized plasma. The electromagnetic field inside and outside such a plasma sphere is in accordance with the theory of the diffraction of a plane wave by a homogeneous dielectric sphere

electromagnetic wave on a dielectric sphere as a whole has been investigated by Debye.[2]

We shall find the distribution of ponderomotive forces throughout the volume of the sphere by starting from the known expressions for the stress tensor of the electromagnetic field, according to which the time-averaged force per unit volume of the sphere is

$$\mathbf{f}^v = \frac{1}{c}[\mathbf{j}\times\mathbf{H}] - \frac{1}{8\pi} E_1^2 \operatorname{grad}\varepsilon + \frac{1}{8\pi}\operatorname{grad}\left(E_1^2 \frac{\partial\varepsilon}{\partial\tau}\tau\right),$$

and the force per unit surface area is

$$\mathbf{f}^s = \frac{1}{4\pi}\varepsilon E_{1n}(\mathbf{E}_2 - \mathbf{E}_1) - \frac{1}{8\pi}\left[E_2^2 - \left(\varepsilon - \frac{\partial\varepsilon}{\partial\tau}\tau\right)E_1^2\right]\mathbf{n},$$

where $\mathbf{E}_1$ and $\mathbf{E}_2$ are the electric fields inside and outside the sphere, $\mathbf{n}$ is the outward normal to the surface, and τ is the density of the medium.

Taking for the plasma $\varepsilon = 1-\omega_0^2/\omega^2$ (ω_0 is the plasma frequency) and, for simplicity, neglecting losses ($\sigma = 0$), we obtain

$$\mathbf{f}^v = \frac{\varepsilon - 1}{8\pi}\operatorname{grad} E_1^2,$$

$$\mathbf{f}^s = \frac{1}{4\pi}\varepsilon E_{1n}(\mathbf{E}_2 - \mathbf{E}_1) - \frac{1}{8\pi}(E_2^2 - E_1^2)\mathbf{n}.$$

If the radius a of the sphere is much smaller than the wavelength in space and in the plasma, then the time averaged volume density of the force within the sphere turns out, after rather tedious calculations[3], to be approximately equal to

$$f_x^v = \frac{E_0^2}{8\pi} k^2 \frac{(\varepsilon-1)^2(35\varepsilon^4 - 87\varepsilon^3 - 1032\varepsilon^2 - 2075\varepsilon - 1266)}{5(\varepsilon+2)^2(2\varepsilon+3)^2(7\varepsilon+12)} x,$$

$$f_y^v = -\frac{E_0^2}{8\pi} k^2 \frac{(\varepsilon-1)^2(91\varepsilon+158)}{5(\varepsilon+2)^2(7\varepsilon+12)} y,$$

$$f_z^v = \frac{E_0^2}{8\pi} k^2 \frac{(\varepsilon-1)^2(35\varepsilon^4 - 129\varepsilon^3 - 1209\varepsilon^2 - 2330\varepsilon - 1392)}{5(\varepsilon+2)^2(2\varepsilon+3)^2(7\varepsilon+12)} z.$$

Here the x axis of a right-handed system of coordinates with origin in the center of the sphere coincides with the direction of polarization of the electric field of the plane wave (with wave vector k) which is being propagated along the z axis. The time-averaged force density on the surface has here the following form

$$\mathbf{f}^s = \frac{E_0^2}{8\pi}\frac{9}{2}\frac{(\varepsilon-1)^2}{(\varepsilon+2)^2}\frac{x^2}{a^2}\mathbf{n}.$$

It follows from the preceding formulae that for certain values of ε the forces inside the sphere are directed inward. The forces on the surface of the sphere are always directed outward. A comparison of the volume and surface forces shows (in view of of the fact that $ka \ll 1$) the predominant role of the surface forces on the periphery of the sphere.

Hence the ponderomotive forces lead to an unstable surface layer in a plasma sphere in the field of a plane wave for $ka \ll 1$ and thus make possible a dislocalization of the plasma in all directions, which in the present case is connected with the presence of a density gradient at the bounded plasma, as at every localized medium. Hence we may consider that a tendency to spread in the field of a plane electromagnetic wave is characteristic of a plasma concentrated in a localized region of dimensions considerably smaller than a wavelength.

We have limited our consideration to continuous oscillations of the plasma under the influence of a plane wave and have not been concerned with transient processes.

Analogous problems may be of interest in connection with the recently proposed new methods of accelerating clusters of charged particles[4].

[1] J. A. Stratton, *Electromagnetic Theory* (Russian translation).

[2] P. Debye, Ann. phys. 30, 57 (1909).

[3] M. S. Rabinovich and V. V. Iankov, Forces Acting on a Dielectric Sphere in the Field of a Plane Electromagnetic Wave, Report of the Physics Institute, Academy of Sciences, USSR, 1955.

[4] V. I. Veksler, Report at the Geneva Conference on Meson Physics and Accelerators, June, 1956.

Translated by M. G. Gibbons
192

Motion of a Rarefied Plasma in a Variable Magnetic Field

IA. P. TERLETSKII
Moscow State University

(Submitted to JETP editor December 20, 1956)
J. Exptl. Theoret. Phys. (U.S.S.R.) 32, 927-928
(April, 1957)

CONSIDER A RAREFIED PLASMA in a quasistationary magnetic field which varies in time. Let us limit ourselves to the case where the free path length of the electrons and ions may be considered as great as we like and the magnetic field H is intense enough to fulfill always the condition

$$\rho\,|\,\nabla H\,|\,/\,H \ll 1, \tag{1}$$

where $\rho = p_\perp c/eH$ is the radius of curvature of the trajectory of a free charged particle in the magnetic field, $p_\perp$ is the component of momentum of the particle perpendicular to the direction of the magnetic field, e is the charge of an electron, and c is the velocity of light. It is assumed that condition (1) is true for all electrons and all ions.

In the case under consideration, in accordance with Ref. 1–3, the motion of the electrons and ions of the plasma may be represented as circular motion of radius ρ around the direction of the magnetic field with cyclical frequency $\Omega = e\mathbf{H}/mc$, while the center of rotation (we will call the point representing this center of rotation the drifting center) drifts in a direction perpendicular to the magnetic field with velocity

$$\mathbf{v}_\perp = c[\mathbf{E}\times\mathbf{H}]\,/H^2 - (c\mu/eH^2)[\nabla_\perp H\times\mathbf{H}] \tag{2}$$

and in a direction parallel to the magnetic field with a velocity determined by the equation

$$d\,(m\mathbf{v}_\parallel)\,/\,dt = e\,\mathbf{E}_\parallel = (c\mu\,/\,|\,e\,|\,)\,\nabla_\parallel H, \tag{3}$$

where $\mu = |\,e\,|\,\Omega\rho^2/2c$ is the magnetic moment produced by the particle rotation with frequency Ω, $\nabla_\perp$ and $\nabla_\parallel$ are the components of the gradient perpendicular and parallel to the magnetic field, and m is the mass of the particle. As a consequence of the conservation of the adiabatic invariant $\oint(m\mathbf{v} + e\mathbf{A}/c)d\mathbf{l}$, the magnitude of $\Omega\rho^2$ remains unchanged[2] in the case of a sufficiently slowly changing magnetic field ($H^{-1}\,|\,dH/dt\,|\ll\Omega/2\pi$). Hence

$$\mu = e\Omega\rho^2\,/\,2c = e^2H\rho^2\,/\,2mc^2 = \text{const}, \tag{4}$$

whence the energy of the rotational motion of the particle* is

$$W = p_\perp^2\,/\,2\,m = m\Omega^2\rho^2\,/\,2 = \mu H. \tag{5}$$

The drift in a direction perpendicular to H with velocity

$$\mathbf{u} = c[\mathbf{E}\times\mathbf{H}]/H^2, \tag{6}$$

may be considered as a motion "together with the lines of force," just as in the case of magnetic hydrodynamics[4]. Actually, if we determine the "velocity of motion of the lines of force," starting from the equation

$$\frac{d}{dt}\int \mathbf{H}\,d\sigma = \oint[\mathbf{u}\times\mathbf{H}]\cdot d\mathbf{l}, \tag{7}$$

then, in virtue of the law of electromagnetic induction, the velocity (6) coincides with the value of $\mathbf{u}$ occuring in Eq. (7) in the case where $\mathbf{E}\perp\mathbf{H}$. Thus even in the case of an extremely rarefied gas the picture of a substance "fastened" to the lines of force, or "frozen" into the lines of force, may be used as a descriptive representation of the motion of the plasma.

Let us consider the motion of the plasma in two simple cases with axial symmetry.

1) Let H be directed along the axis of symmetry z and be generated by sources situated on the outside of a cylinder of radius R. In virtue of the stipulation of a quasistationary state within this cylinder, we may consider $H_z = H(t)$. If r, z and θ are the cylindrical coordinates of the drifting center of the particle, then in virtue of Eq. (6) and the law of electromagnetic induction [or in view of Eq. (7)], we have

$$u = dr\,/\,dt = -\,(r\,/\,2\,H)\,dH\,/\,dt, \tag{8}$$

whence, as a result of integration, we obtain $r^2H = \text{const}$. By virtue of Eq. (4) $\rho^2H = \text{const}$. also, and thus we have

$$\rho\,/\,\rho_0 = r\,/\,r_0 = \sqrt{H_0\,/\,H}. \tag{9}$$

*In the relativistic case, obviously,

$$W = mc^2\sqrt{1 + 2\mu H\,/\,mc^2}.$$

An increasing magnetic field of the type considered may be created by the rapid compression of a conducting cylinder by means of a convergent explosive wave[5]. In this case, by virtue of the conservation of the current of the vector **H**, $H(t)R^2(t) = H(0)R^2(0)$, where $R(t)$ is the inside radius of a compressed cylinder. Thus, analogously to Eq. (9), $R/R_0 = \sqrt{H_0/H}$, that is, all the dimensions and distances are decreased in proportion to R. At the same time the energy of the rotational motion of the particle according to Eq. (5) increases as*:

$$W / W_0 = H / H_0 = [R_0 / R]^2. \tag{10}$$

If the magnetic field is not strictly parallel to the z axis, but decreases with distance from the axis, that is, has a barrel-shaped form, then as a result of Eq. (3), forces appear which draw the particles of the plasma together to the surface $H_z(r, z, t) = 0$ and guarantee the stability of the motion of the particles in the z direction.

2) Let the magnetic field be generated by an axially symmetrical current directed parallel to the z axis. In order to simplify the calculations we shall assume that the current density

$$j(r, t) = \begin{cases} j(t) & \text{for } r \leqslant R(t), \\ 0 & \text{for } r > R(t). \end{cases} \tag{11}$$

In this case, in accordance with Eq. (2) and Maxwell's equations, with cylindrical coordinates r and z for the drifting center, we have for $r > R$:

$$u_r = \frac{dr}{dt} = -\left\{\frac{1}{J}\frac{dJ}{dt}\left[\frac{1}{2} + \ln\left(\frac{r}{R}\right)\right] - \frac{1}{R}\frac{dR}{dt} + \frac{c^2}{2J}E_1\right\} r, \tag{12}$$

$$u_z = dz / dt\,(c\mu / e) / r, \tag{13}$$

where $J(t) = \pi R^2(t) j(t)$ is the total current strength and $E_1 = E_z$ for $r = 0$. On integrating Eq. (12) we obtain

$$\frac{rR_0}{r_0 R} = \left[\frac{r_0}{R_0}\, e^{1/2}\right]^{(J_0/J)-1} \exp\left\{-\frac{c^2}{J}\int_0^t E_1\, dt\right\}, \tag{14}$$

whence, in accordance with Eq. (5)

$$\frac{W}{W_0} = \frac{H}{H_0} = \frac{JR_0}{J_0 R}\left[\frac{r_0}{R_0}\, e^{1/2}\right]^{1-J_0/J} \exp\left\{\frac{c^2}{J}\int_0^t E_1\, dt\right\}. \tag{15}$$

The velocity in the z direction is obtained by substituting Eq. (14) into Eq. (13).

Formula (15) shows that even in the constant-current case the energy of rotational motion of the particles of a rarefied plasma may be increased many fold as a result of a decrease in R. In the light of this result, the manifold increase in the kinetic energy of electrons and ions which was discovered by Artsimovich and his coworkers[6,7] during the passage of powerful discharges through rarefied gases is not unexpected. (One can assume, for example, that the electrons and ions formed after the first compression in the region where $E_1 > H$ are first accelerated by the field E_1 to energies comparable to the potential difference between the discharge electrodes and then, as a result of the increase in density of the discharge current, the particles far from the axis enter the region $H > E$, where a supplementary manifold increase in the energy occurs as a result of the induction mechanism considered above.) The fields obtained in this case guarantee the fulfillment of condition (1) and, consequently, the applicability of formula (15).

*In the ultrarelativistic case, obviously,

$$W / W_0 = \sqrt{H / H_0} = R_0 / R.$$

[1] H. Alfven, *Cosmic Electrodynamics*, (Russian Translation), 1952.

[2] Ia. P. Terletskii, J. Exptl. Theoret. Phys. (U.S.S.R.) 19, 1059 (1949).

[3] Ia. P. Terletskii, J. Exptl. Theoret. Phys. (U.S.S.R.) 16, 403 (1946).

[4] P. E. Kolpakov and Ia. P. Terletskii, Dok. Akad. Nauk SSSR 76, 185 (1951).

[5] Ia. P. Terletskii, J. Exptl. Theoret. Phys. (U.S.S.R.) 32, 387 (1957), Soviet Physics 5, 301 (1957).

[6] Artsimovich, Andrianov, Bazilevskaia, Prokhorov and Filippov, Atomnaia Energiia 3, 76 (1956).

[7] I. V. Kruchatov, Atomnaia Energiia 3, 65 (1956).

Translated by
M. G. Gibbons
193

On the Energy Spectrum of μ-Mesons from $K_{\mu 3}$ Decay

S. G. MATINIAN
Institute of Physics
Academy of Sciences of the Georgian SSR
Submitted to JETP editor Dec. 24, 1956)
J. Exptl. Theoret. Phys. (U.S.S.R.) 32, 929-930
(April, 1957)

IN A PREVIOUS COMMUNICATION[1] concerning the problem of $K_{\mu 3}$ decay ($K^{\pm}_{\mu 3} \to \mu^{\pm} + \nu + \pi^0$) the energy spectrum of the μ-mesons from $K_{\mu 3}$ decay was calculated for the case of a scalar (pseudoscalar) particle with directly coupled fields. In the present note we consider decay of the same particle, but with derivative coupling between the fermion (μ, ν) and spin-0 boson ($K_{\mu 3}$, π) fields.

The interaction Hamiltonian is of the form

$$H' = f m_\pi^{-2} (\bar{\psi}_\mu \gamma \gamma_i \psi_\nu) (\partial/\partial x_i) (\varphi_\pi^* \varphi_K) \quad (\hbar = c = 1). \quad (1)$$

Here f is a dimensionless coupling constant, m_π is the mass of the π-meson, ψ is a spinor, and φ is a scalar wave function; γ is equal to unity or γ_5, depending on the parity of the $K_{\mu 3}$-meson.

Carrying through the calculation similarly as previously[1] we obtain the following expression for the differential decay probability of the $K_{\mu 3}$-meson at rest:

$$w dE_\mu = \frac{f^2}{32\pi^3 m_\pi^2} \frac{(A - 2ME_\mu)\sqrt{E_\mu^2 - m_\mu^2}}{M(B - 2ME_\mu)^2} \times$$
$$\times \{m_\pi^{-2}(A - 2ME_\mu)(H - 2ME_\mu)(ME_\mu - m_\mu^2) \quad (2)$$
$$- C - DE_\mu + 2M^2 E_\mu^2\}\, dE_\mu.$$

Here $H = M^2 + m_\mu^2 + m_\pi^2$, with the remaining notation being the same as that used previously[1].

We note that, as before, we have obtained a result which is independent of the $K_{\mu 3}$ parity: the decay probability of the scalar meson with scalar (vector) coupling is equal to the decay probability of the pseudoscalar meson with pseudoscalar (pseudovector) coupling[2]. This is clearly related to the zero mass of the neutrino.

Lee and Yang[3] and Morpurgo[4] have given experimental data on the μ-meson spectrum from $K_{\mu 3}$ decay. A characteristic of the results is the large number of low-energy μ-mesons. The maximum energy of the μ-meson spectrum given by Lee and Yang[3] is in the region of $T_\mu \approx 40$ Mev (where T_μ is the kinetic energy of the μ-mesons), whereas the spectrum corresponding to their phase volume has a maximum in the region of $T_\mu \approx 75$ Mev. According to our calculations the maximum in the spectrum lies in the region of 85 Mev for direct coupling, which is in disagreement with the experimental data. For derivative coupling, the μ-meson spectrum has a maximum at 60 Mev, which is in better agreement with experiment. The Figure shows the μ-meson spectra for (a) direct coupling and (b) derivative coupling of the fields. Also shown is the spectrum corresponding to the μ-meson phase volume (c). The spectra are given in arbitrary units and the curves are normalized to unit area.

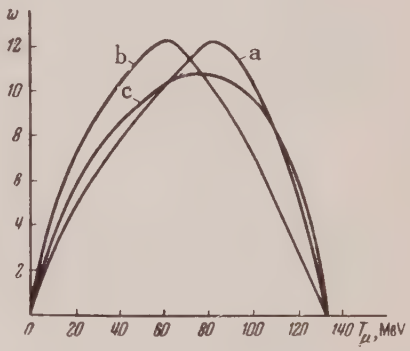

Energy spectra of μ-mesons from $K_{\mu 3}$ to K.

It should be noted that the μ-meson energy spectrum from $K_{\mu 3}$ decay has not yet been accurately measured. It is difficult to differentiate between fast μ-mesons ($T_\mu \approx 100$ Mev) from $K_{\mu 3}$ decay and π-mesons from $K_{\pi 2}$ decay and μ-mesons from $K_{\mu 2}$ decay.

The fact that vector (pseudovector) coupling is in better agreement with experiment may also be due to the following situation. As is well known, only vector (pseudovector) coupling gives the correct relation between the probabilities for $\pi \to \mu$ and $\pi \to e$ decays[5,6]. If we use the universal meson-lepton interaction[2], the same coupling must be used for $K_{\mu 2}$ decay (as is well known, the decay $K_{e2} \to e + \nu$ is not observed in experiment). Then the Hamiltonian of Eq. (1) for $K_{\mu 3}$ decay would seem to be reasonable if we consider the $K_{\mu 3}$-meson and the $K_{\mu 2}$-meson to be coupled through the π-field[1].

We note that at present there is no reason to assume the spin of the K-mesons to be nonzero. If, nevertheless, the spin of the $K_{\mu 3}$ is found to be different from zero, there may be a correlation between the spins of the $K_{\mu 3}$ and the μ in the decay of polarized $K_{\mu 3}$ particles.

The following Hamiltonians may be responsible for the decay of a vector $K_{\mu 3}$-meson at rest:

$$H_1' = g_1(\bar{\psi}_\mu \psi_\nu) A_i \partial\varphi_\pi/\partial x_i,\ H_2' = g_2(\bar{\psi}_\mu \gamma_i \psi_\nu) A_i \varphi_\pi,$$

$$H_3' = g_3(\bar{\psi}_\mu \gamma_i \gamma_k \psi_\nu) A_i \partial\varphi_\pi/\partial x_k,$$

where A_i is the vector wave function of the $K_{\mu 3}$-meson. If we calculate the probability for emission of polarized μ-mesons in the decay of spin-1 polarized $K_{\mu 3}$-mesons as was done by Okun',[7] we obtain the following results. The interactions H_i' separately do not lead to polarized μ-mesons. Neither does the "mixture" $H_i' + H_3'$. The "mixtures" $H_1' + H_2'$ and $H_2' + H_3'$, on the other hand, lead in general to polarized μ-mesons.

I take this opportunity to express my gratitude to Professor G. R. Khutsishvili for aid and discussions of the results of the present work.

[1] S. G. Matinian, J. Exptl. Theoret. Phys. (U.S.S.R.) 31, 529 (1956), Soviet Physics JETP 4, 434 (1957).

[2] S. A. Bludman, M. A. Ruderman, Phys. Rev. 101, 109 (1956).

[3] Crussard, Fouche, Hennesy, Kayas, Leprince-Ringuet, Morellet, and Renard, Nuovo cimento 3, 731 (1956).

[4] Ritson, Pevsner, Fung, Widgoff, Goldhaber, and Goldhaber, Phys. Rev. 101, 1085 (1956).

[5] B. d'Espagnat, Compt. rend. 228, 744 (1949).

[6] M. A. Ruderman and R. Finkelstein, Phys. Rev. 76, 1458 (1949).

[7] L. B. Okun', *Dissertation*, Akad. Sci. U.S.S.R., Moscow, 1956.

Translated by E. J. Saletan
194

On Strong Interaction between the K-Particle and the π-Particle

S. G. MATINIAN
Institute of Physics
Academy of Sciences of the Georgian SSR

J. Exptl. Theoret. Phys. (U.S.S.R.) 32, 930-931
(April, 1957)

EXPERIMENTAL DATA concerning K-mesons lead to two different conclusions which are difficult to reconcile. On the one hand, experiment gives the same (within the limits of experimental error) masses and lifetimes for different K-particles. In experiments performed under varying conditions, different K decay schemes are observed with equal frequency[1]. In addition, experiments with a beam of K^+-mesons before and after scattering[2] lead to the conclusion that the θ and τ-particles have the same interaction cross sections with matter. All this would seem to imply that the different K-meson decay schemes correspond to alternate modes of decay for the same particle. On the other hand, analysis of τ-decays and the existence of the $\theta^0 \to 2\pi^0$ decay implies that the θ and τ are different particles.

In order to eliminate this contradiction, Lee and Yang introduced the concept of parity doublets[3] and parity nonconservation in weak interactions[4]. Schwinger postulated a strong interaction between pions and K-mesons. In the present note the hypothesis of a strong π-K interaction is applied to obtaining certain relations between the probabilities of K decays according to various schemes.

We thus start from the following isotopic invariant interaction scheme between the π- and K-mesons.

$$K' \rightleftarrows K'' + \pi. \tag{1}$$

On the basis of Eq. (1) we may relate, for instance, the decay of the τ-meson with the decay of the θ-meson, and determine, in particular, the ratio of the probabilities for the two decays

$$\tau^{\pm\prime}(\to 2\pi^0 + \pi^\pm) \text{ and } \tau^\pm(\to \pi^+ + \pi^- + \pi^\pm).$$

According to (1) we may write the τ^+ decay

$$\tau^+ \xrightarrow{g_{K\pi}} \pi^+ + \theta^0 \xrightarrow{f} \pi^+ + \pi^+ + \pi^-, \tag{2}$$

where $g_{K\pi}$ is the coupling constant of the strong π-K interaction, and f is the coupling constant of the weak interaction between the θ-field and the π-field. For the $\tau^{+\prime}$ decay we have two possibilities:

$$\tau^{+\prime} \xrightarrow{g_{K\pi}} \begin{cases} \pi^+ + \theta^0 \xrightarrow{f} \pi^+ + \pi^0 + \pi^0, \\ \pi^0 + \theta^+ \xrightarrow{f} \pi^0 + \pi^0 + \pi^+. \end{cases} \tag{2'}$$

The probability of one or another τ decay is given by the product of the probability for formation of one or another $\pi + \theta$ configurations (this

probability is found from the hypothesis of isotopic invariance) and the probability w for the decay of the θ-meson according to one or another scheme. The ratio of the θ-meson decay probabilities can be found by assuming that in this decay the isotopic spin selection rule $|\Delta T| = 1/2$ is operative[5]. There exist two possibilities depending on the spin of the θ-meson.

1. The spin of the θ-meson is odd. Then the $\theta^0 \to 2\pi^0$ decay is impossible. According to the above, the ratio R of the τ' decay to that of the τ decay is

$$R = w(\theta^+ \mid 0+)/2w(\theta^0 \mid +-), \tag{3}$$

where, for instance, $w(\theta^+|0+)$ is the probability that the θ^+-meson decays into a π^0 and a π^+. According to Gatto[5], if the spin of the θ-particle is odd

$$w(\theta^+ \mid 0+) = 2w(\theta^0 \mid +-)$$

and $R = 1$.

2. The spin of the θ-meson is even. Then according to Gatto[5], $w(\theta^+ \mid +0) = 0$ (if the selection rule $|\Delta T| = \frac{1}{2}$ is operative), and

$$w(\theta^0 \mid +-) = 2w(\theta^0 \mid 00).$$

We then obtain $R = 0.5$.

As is well known, the ratio R can be found from the selection rule $|\Delta T| = \frac{1}{2}$ alone[5,6] and lies in the interval $\frac{1}{4} \leqslant R \leqslant 1$. The case $R = \frac{1}{4}$ occurs when the total isotopic spin of the system of three π-mesons is equal to unity in our case of a strong π-K interaction, R is subjected to another restriction. We note that the experimental values of R as found by various observers differ among themselves to a great extent. Recently Birge, Perkins, *et al.*,[1] have obtained $R = 0.39 \pm 0.096$.

Using the concept of a strong π-K interaction, we can also determine the ratio R_0 of the decays

$$\tau^{0\prime}(\to 3\pi^0) \text{ and } \tau^0(\to \pi^+ + \pi^- + \pi^0).$$

We obtain $R_0 = 0$ if the spin of the θ-particle is odd, and $R_0 = 0.5$ if the spin of the θ-particle is even.

Several experiments have indicated the existence of the so-called anomalous θ^0-decay[7], among which there are cases which have been interpreted according to the scheme

$$K^0_{\mu 3} \to \mu^\pm + \pi^\mp + \nu. \tag{4}$$

For $K^+_{\mu 3}$ and $K^0_{\mu 3}$ decays we may write (see also an earlier work by the present author[8])

$$\begin{aligned} K^+_{\mu 3} &\to K^+_{\mu 2} + \pi^0 \to \mu^+ + \nu + \pi^0, \\ K^0_{\mu 3} &\to K^+_{\ 2} + \pi^- \to \mu^+ + \nu + \pi^-. \end{aligned} \tag{5}$$

The ratio R_μ of the $K^+_{\mu 3}$ and $K^0_{\mu 3}$ decay probabilities is then $R_\mu = 0.5$ independent of the spin of the $K_{\mu 2}$ (in this case the absence of a neutral μ-meson is relevant).

I take this opportunity to express my gratitude to Professor G. R. Khutsishvili for discussions of the results.

[1] Birge, Perkins, Peterson, Stork, and Whitehead, Nuovo cimento 4, 834 (1956).
[2] M. Shapire *et al.*, Bull. Am. Phys. Soc. s. II 1, 185 (1956).
[3] T. D. Lee and C. N. Yang, Phys. Rev. **102**, 290 (1956). (1956).
[4] G. Morpurgo, Nuovo cimento 4, 1222 (1956).
[5] R. Gatto, Nuovo cimento 2, 318 (1956).
[6] G. Wentzel, Phys. Rev. **101**, 1215 (1956).
[7] Ballam, Grisaru, and Treiman, Phys. Rev. **101**, 1438 (1956).
[8] S. G. Matinian, J. Exper. Theoret. Phys. (U.S.S.R.) **31**, 529 (1956), Soviet Physics JETP 4, 434 (1957).

Translated by E. J. Saletan
195

Application of a Renormalized Group to Different Scattering Problems in Quantum Electrodynamics

V. Z. BLANK
Moscow State University

(Submitted to JETP editor December 28, 1956)
J. Exptl. Theoret. Phys. (U.S.S.R.) 32, 932-933
(April, 1956)

THE METHOD of renormalized group was applied[1,2] to obtain the assymptotic expressions for the quantum electrodynamic Green function and for the vertex part. The use of the renormalized group presents also a considerable interest in the case of concrete scattering processes.

For this purpose, let us first formulate the renormalized group for the transition probabilities. This is conveniently done by using the generalization of the Feynman diagrams proposed by Abriko-

sov[3]. Let us consider the transition probability for the process represented by the totality of the generalized diagrams. It can be written in the form $e^n W((p_i p_j), e^2)$, where p_i and p_j are 4-vectors corresponding to the i'th and j'th external lines and n is the number of vertices with external photon lines. The transition probability represented by the totality of the generalized diagrams is equal to the matrix element of some operator between the initial and final states of this generalized diagram. Let us denote this operator by the letter M. The operator M has an arbitrary multiplicative constant which is determined by the number of free ends of the generalized diagram. Let the number of external fermion lines be $2f$. The multiplicative transformation of the operator M has then the form $e^n M \to e'^n Z M$, where $Z = Z_2^f Z_3^{n/2}$. The charge transformation law is known and, in electrodynamics, because of the Ward identity, has the form $e^n \to e'^n = Z^{n/2} e^n$. The multiplicative transformation of the operator M is therefore determined by only the number of external fermion lines: $M \to Z_2^f M$.

Let the lowest order perturbation approximation of the operator M be M_0. In cases of practical interest, it is sufficient to limit oneself to the consideration of only those terms of M which are proportional to M_0, *i.e.*, $M = M_0 \mathfrak{M}$, where $\mathfrak{M}$ contains all the radiative corrections proportional to M_0. Including as usual the multiplicative constant of $\mathfrak{M}$ in its argument

$$\mathfrak{M}\,((p_i p_j)/\lambda^2,\ m^2/\lambda^2,\ e^2),$$

one obtains a functional, and then a differential equation for $\mathfrak{M}$. These equations are analogous to the equations for the vertex part in Ref. 2. They are cumbersome and we will not cite them here. One of the possible equations has the form (with the same notation):

$$\frac{\partial}{\partial x} \ln \mathfrak{M}(x, y, \ldots, z, u, e^2) = \frac{1}{x}\left[\frac{\partial}{\partial \xi} \ln \mathfrak{M}\left(\xi, \frac{y}{x}, \ldots, \frac{z}{x}, \frac{u}{x}, e^2 d\,(x, u, e^2)\right)\right]_{\xi=1}. \tag{1}$$

Integrating this equation, we obtain

$$\ln\left[\mathfrak{M}(x, y, \ldots, z, u, e^2)/\mathfrak{M}(x_0, y, \ldots, z, u, e^2)\right] = \int_{x_0}^{x} \frac{dt}{t}\left[\frac{\partial}{\partial \xi} \ln \mathfrak{M}\left(\xi, \frac{y}{t}, \ldots, \frac{z, u}{t, t}, e^2 d\,(t, u, e^2)\right)\right]_{\xi=1}$$

We will be interested in those solutions of equations of the type (1) which, for smaller e^2, coincide with the results of perturbation theory.

The obtained equations of renormalized group can be used effectively to avoid the infrared catastrophe in scattering problems. As known[4], in the usual perturbation theory, in addition to the main process, one considers also—in order to avoid the infrared catastrophe—scattering with emission of an additional long-wave quantum, the energy of which does not exceed $\Delta\varepsilon$. But then the dependence of the total cross section on $\Delta\varepsilon$ is no more true. The probability of pure elastic scattering is infinite. To obtain a physically admissible result, one has to make the summation of an infinite series of diagrams corresponding to the emission of different numbers of long wavelength photons. A direct summation of such a kind was carried out by Abrikosov[3]. The use of the renormalized group drastically simplifies the problem of such a summation, The physically admissible results then arise as the result of a decomposition that is invariant with respect to the renormalized group.

Let us consider, for instance, the scattering of an electron in an external field. Using the results of perturbation theory[4], we obtain—by solving equations of type (1)—an exponential dependence of the effective cross section on $\ln \Delta\varepsilon$. The probability of pure elastic scattering turns out to be zero, which is physically correct. An analogous situation arises when one considers the Compton effect.

The equations of type (1) for the renormalized group are also useful when one considers different high energy effects: scattering of an electron in an external field, Compton effect, and electron-electron scattering. The investigation of these phenomena by the method of summation of a series of diagrams was carried out by Abrikosov[5]. The renormalized group method permits to extend this investigation to much higher energies, because there is a simple possibility of taking vacuum polarization into account.

In conclusion, I express my deep gratitude to N. N. Bogoliubov who supervised this work, as well as to D. V. Shirkov for discussion of the results.

---

[1] N. N. Bogoliubov and D. V. Shirkov, Dokl. Akad. Nauk SSSR **103**, 203, 391 (1955), J. Exptl. Theoret. Phys. (U.S.S.R.) **30**, 77 (1956), Soviet Physics JETP **3**, 57 (1956): Nuovo cimento **3**, 845 (1956).

[2] V. Z. Blank and D. V. Shirkov, Dokl. Akad. Nauk SSSR 111, 1201 (1956): Nuclear Physics 2, 356 (1956/1957).

[3] A. A. Abrikosov, J. Exptl. Theoret. Phys. (U.S.S.R.) 30, 96 (1956); Soviet Physics JETP 3, 71 (1956).

[4] A. I. Akhiezer and V. B. Berestetskii, *Quantum Electrodynamics* (Moscow)(1953).

[5] A. A. Abrikosov, J. Exptl. Theoret. Phys. (U.S.S.R.) 30, 386, 544 (1956); Soviet Physics JETP 3, 474, 379 (1956).

Translated by E. S. Troubetzkoy
196

Simultaneous Creation of Λ and θ-Particles

I. Iu. KOBZAREV AND L. B. OKUN'

(Submitted to JETP editor January 10, 1956)
J. Exptl. Theoret. Phys. (U.S.S.R.) 32, 933-934
(April, 1957)

THE ANALYSIS OF ANGULAR and energy distributions of π-mesons from the decay $\tau^+ \to 2\pi^+ + \pi^-$ leads to the conclusion that the spin and parity of the τ-meson are 0^-. Such a meson cannot decay into two π-mesons, therefore there must be two kinds of K-mesons: τ^+ and θ^+. The experimental masses and lifetimes of the K^+-mesons coincide. The equality of the masses can be explained by the hypothesis of Lee and Yang[1] according to which the Hamiltonian of strong interactions is invariant with respect to the operation C_p which changes the parity. The equality of the lifetimes of the τ and θ-mesons remains, however, unexplained.

Another possible assumption is the hypothesis that the K-meson decay interaction does not conserve parity and that there exists only one K-meson.

We want to point out that the experiments on the pair production of Λ^0, K^0 can be used to answer the question on the number of K-mesons. Steinberger *et al.*,[2-4] observed the decays of Λ^0 and θ^0 particles, $\Lambda^0 \to p + \pi^-$, $\theta^0 \to \pi^+ + \pi^-$ produced in the process

$$\pi^- + p \to \Lambda^0 + \theta^0.$$

The lifetimes of these decays are $\tau \sim 10^{-10}$ sec. They determined the probabilities R_θ and R_Λ that the observed decay $\Lambda \to p + \pi^-$ will be followed by the fast decay $\theta \to \pi^+ + \pi^-$, and vice versa. The experiment gives $R_\theta \sim R_\Lambda \sim 0.3 - 0.4$.

Let us assume that there exists only the K-meson and that parity is not conserved. In order to explain the existence of the long-lived K^0-meson observed in the experiments of Lande *et al.*,[5] one has to assume that the Hamiltonian of the decay interaction is invariant with respect to C or CI, where C is the charge conjugation and I is the inversion[6]. The K-meson is the mixture

$$K^0 = (K_s^0 + K_a^0)/\sqrt{2},$$

where the wave function of K_s^0 is symmetric and the wave function of K_a^0 is antisymettric with respect to C or CI respectively K_s^0 decaying into two π-mesons with a lifetime of 10^{-10} sec and K_a^0 being long-lived. We then get for R_θ and R_Λ: $R_\theta = 0.5\, p_\theta$, $R_\Lambda = p_\Lambda$, where p_θ, p_Λ are the probability ratio

$$p_\theta = w(\theta^0 \to \pi^+ + \pi^-)/[w(\theta^0 \to \pi^+ + \pi^-) + w(\theta^0 \to \pi^0 + \pi^0)] < 1,$$

$$p_\Lambda = w(\Lambda \to p + \pi^-)/[w(\Lambda \to p + \pi^-) + w(\Lambda \to n + \pi^0)] < 1.$$

Comparing with experiment: $p_\theta = 0.6 - 0.8$, $p_\Lambda = 0.3 - 0.4$.

Experimentally, only the order of magnitude of these quantities is known at the present time. Osher and Mojer give p_Λ and $p_\theta \sim 0.5$ which, in view of the inaccuracy of these values, should be considered as not being in contradiction with the hypothesis of a single K-meson.

In the Lee and Yang scheme the τ and θ-mesons are produced in equal numbers and, taking into account that θ^0 is a mixture of symmetric and assymmetric components, we get

$$R_\theta = 0{,}25\, p_\theta < 0{,}25;\ R_\Lambda = p_\Lambda.$$

We come to a contradiction, as the experiment gives $R_\theta \sim 0.3 - 0.4$.

The contradiction can be avoided by taking into account the fact that, in the Lee and Yang scheme, even and odd Λ-particles should exist simultaneously with even and odd K-mesons, and by assuming that one of the Λ-particles is long-lived with a lifetime of $10^{-8} - 10^{-9}$ and that the θ-meson is produced only (or most of the time) with a short-lived Λ-particle. Such an assumption means that the θ and τ do not transform one into the other in strong interactions.

We then get, as in the case of a single K-meson:

$$R_\theta \sim 0{,}5\, p_\theta,\ R_\Lambda \sim p_\Lambda.$$

The assumption on the existence of a long-lived Λ-particle can be verified directly. In particular, such a long-lived particle should have been observed in experiments[5]. The fact that it has not actually been observed is in contradiction with such an assumption.

Therefore, the values R_Λ and R_θ agree most easily with the single K-meson hypothesis, the values of p_θ and p_Λ being $p_\theta = 0.3 - 0.4$, $p_\Lambda = 0.6 - 0.8$.

Let us now investigate the theoretical values of p_θ and p_Λ. In the Gell-Mann scheme, it is assumed that the decay interaction satisfies the selection rule $\Delta T_3 = \frac{1}{2}$ (T is the isotopic spin). One can assume that the decay interaction satisfies a more restricted selection rule $\Delta T = \frac{1}{2}$, which explains by a natural way the longer lifetime of θ^+ with respect to that of θ^0, because, for an interaction with $\Delta T = \frac{1}{2}$, the decay $\theta^+ \to \pi^+ + \pi^0$ is forbidden. For $\Delta T = \frac{1}{2}$, $p_\theta = p_\Lambda = \frac{2}{3} = 0.67$. These values are actually quite indeterminate because a small admixture of interaction with $\Delta T = \frac{3}{2}$ strongly influences p_Λ and p_θ.

In order to explain the decay $\theta^+ \to \pi^+ + \pi^0$, one has to introduce an impurity with $\Delta T = \frac{3}{2}$, the amplitude a_3 of which being $a_3 = 0.07\, a_1$, where a_1 is the amplitude of the transitions with $\Delta T = \frac{1}{2}$. The ratios

$$w(\theta^0 \to \pi^0 + \pi^0)/w(\theta^0 \to \pi^+ + \pi^-)$$

and $$w(\Lambda \to n + \pi^0)/w(\Lambda \to p + \pi^-)$$

vary between the limits

$$\frac{1}{2}\left|\frac{1 \pm \sqrt{2}\, a_3/a_1}{1 \mp a_3/a_1\sqrt{2}}\right|^2,$$

which, for $a_3/a_1 = 0.07$, give $0.62 < p_\Lambda < 0.72$; $0.62 < p_\theta < 0.72$.

In order to obtain $p_\Lambda \sim 0.3 - 0.4$, it is necessary that $a_3/a_1 \approx 0.3$ for the decay interaction of Λ-particles.

Finally, let us emphasize the existing experimental values of p_θ, p_Λ and of R_θ, R_Λ contain large errors which do not allow to draw a unique conclusion. We think therefore that an accurate measurement of these quantities would be very desirable.

[1] T. D. Lee and C. N. Yang, Phys. Rev. **102**, 290 (1956).

[2] Budde, Chretien, Leitner, Samios, Schwarts and Steinberger, Phys. Rev. 103, 1827 (1956).

[3] Blumenfeld, Booth, Lederman and Chinowsky, Phys. Rev. **102**, 1184 (1956).

[4] R. B. Leighton and G. H. Trilling, Proc. Rochester Conference (1956).

[5] Lande, Booth, Impeduglia and Lederman, Phys. Rev. **103**, 1901 (1956).

[6] Ioffe, Okun, and Rudik, J. Exptl. Theoret. Phys. (U.S.S.R.) 32, 396 (1957), Soviet Physics JETP 5, 328 (1957).

Translated by E. S. Troubetzkoy
197

Absorption of Sound in a Phase Change in Rochelle Salt

I. A. IAKOVLEV, T. S. VELICHKINA AND K. N. BARANSKII
Moscow State University

(Submitted to JETP editor January 7, 1957)
J. Exptl. Theoret. Phys. (U.S.S.R.) 32, 935-936 (April, 1957)

SOME TIME AGO Landau and Khalatnikov[1] looked into the problem of the relaxation time necessary for establishing thermodynamical equilibrium in the asymmetric phase of a body undergoing a second-order phase transition. From their calculations it turned out that the relaxation time increases as the temperature of the ordered phase approaches the λ-point. Applying M. A. Leontovich's and L. I. Mandel'shtam's relaxation theory of sound absorption to this problem, Landau and Khalatnikov predicted an increase in the absorption of sound in the absorption of sound in the low-temperature phase near the λ-point.

With the object of observing this phenomenon, we set up an experiment for investigating the absorption of sound in Rochelle salt near its upper Curie point. We used a pulse method for measuring the attenuation of sound in a single crystal of Rochelle salt. Transverse pulses at a frequency of 5 Mcs, 1 to 5 microseconds in length, occurring every 0.002 seconds were introduced into a lamina of Rochelle salt placed in a thermostat. The waves were propagated along the crystallographic z-axis. The oscillations received at the opposite side of the lamina were amplified and fed into cathode-ray oscillograph with a delayed sweep. The attenuation of the sound could be determined from oscillograms of pulses which had passed through different thicknesses of Rochelle salt.

The measured temperature dependence of the amplitude coefficient of absorption of sound α is shown in the Figure. The dotted part of the curve corresponds to a temperature region in which the measurements were only approximate. These results show that the anomalous absorption of sound in a second-order phase transition predicted in a general way by Landau and Khalatnikov does indeed occur in solids,* although the case which we investigated was not specifically taken into account in their work.

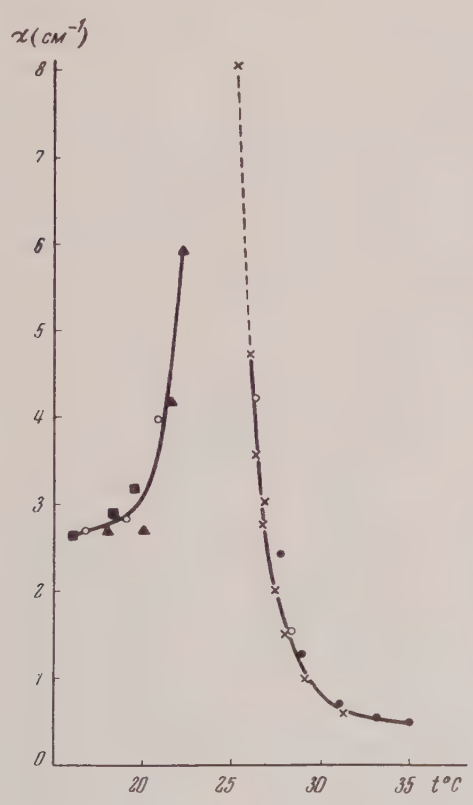

It turns out from our experiments that in a ferroelectric substance this phenomenon has its own characteristic features: a transverse sound wave of given polarization undergoes an anomalous absorption; this absorption increases in both phases as their temperatures approach the λ-point. These circumstances have already been explained theoretically by Landau, whose results will, with the permission of the author, be set forth in another more detailed report.

In conclusion it is interesting to note that in a paper (of which Landau and Khalatnikov were unaware) by Huntington[3] devoted to measurements of the elastic constants of various substances by an ultrasonic method, the author describes an observation which now becomes completely understandable. While not citing systematic data for the absorption of sound at different temperatures, Huntington reported, however, that with the apparatus at his disposal it was not possible for him to work with Rochelle salt at temperatures below 26.5°C because of the strong absorption of sound in this crystal. It is now clear that Huntington's observation was related to experimental conditions corresponding to the steep rise of the upper part of the right-hand branch of our curve showing the temperature dependence of α.

Finally, it is perhaps necessary to include within this same set of phenomena the jump in the coefficient of absorption of sound in tin at temperatures near 160°C, observed by Bordoni and Nuovo[4]. Unfortunately the brevity of their report and the absence of quantitative data in it make it difficult to interpret their results, so much more so since the nature of this phase transition in tin is apparently still not completely clear.

The authors are extremely grateful to Academician L. D. Landau for valuable discussions of the results of their experiments.

[1] L. D. Landau and I. M. Khalatnikov, Dokl. Akad. Nauk SSSR 96, 469 (1954).

[2] J. R. Pellam and O. F. Squire, Phys. Rev. 72, 1245 (1947).

[3] H. B. Huntington, Phys. Rev. 72, 321 (1947)

[4] P. G. Bordoni and M. Nuovo cimento 7, Supp. 2, 161 (1950).

Translated by W. M. Whitney
198

*This was shown for the phase transition in liquid helium by Pellam and Squire[2].

Nuclear Interaction in a Photoemulsion at an Energy of 8×10^{13} ev

I. M. GRAMENITSKII, G. B. ZHDANOV, E. A. ZAMCHALOVA AND M. N. SCHERBAKOVA
P. N. Lebedev Physical Institute of the Academy of Sciences of the USSR

(Received by JETP editor January 12, 1957)
J. Exptl. Theoret. Phys. (U.S.S.R.) 32, 936-938 (April 1957)

IN A STACK of unmounted pellicles, Ilford type G-5, 600μ thick (P stack), irradiated in 1955 in

the Po valley at a height of 25.5 km for 6 hours, a nuclear interaction of the type $1 + 37\alpha$ was found, in which the secondary particles of the shower traverse 6 cm of path before leaving the stack.

1. The angular distribution of secondary charged particles was measured, the small angles θ being measured from the center of axial symmetry of the narrow cone of particles. To get the angular distribution of the penetrating particles directly in the center-of-mass system of the colliding nucleons, the angular variable was taken as $\ln \tan \theta$. The differential angular distribution, obtained by averaging three independent measurements, is shown in the figure.

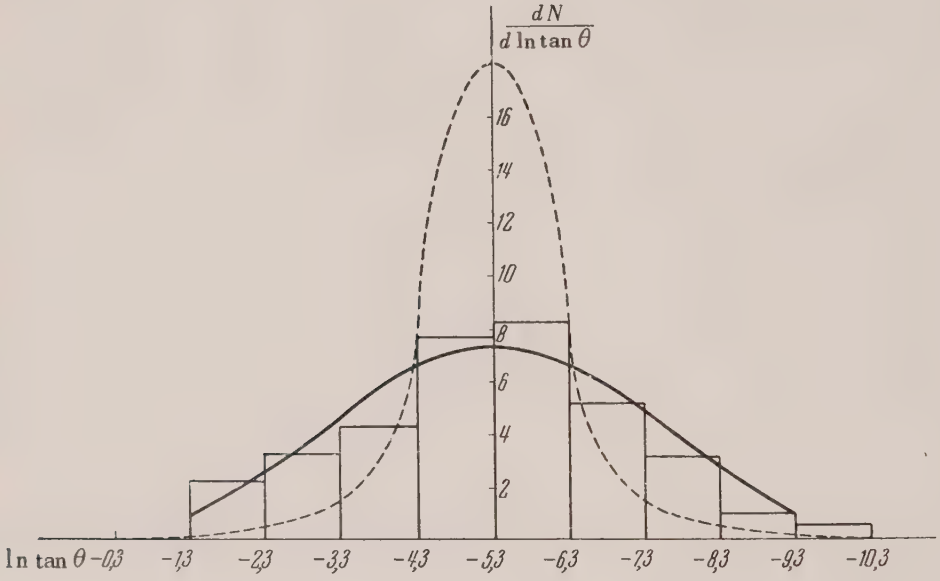

A necessary condition for the determination of the original energy from the angular distribution is the symmetry of this distribution in the center-of-mass system relative to the angle $\theta_0 = \pi/2$. To test the symmetry the so-called χ^2-test [1] was used. It turned out that the experimentally observed angular distribution was symmetric with a probability of 90%.

Similarly, the probability of agreement of the experimental data with the assumption of an isotropic angular distribution (dotted curve in the figure) is about 0.1%, and the distribution predicted by Landau's [2] theory (solid line in the figure) is correct to a probability of about 90%.

Starting with the symmetry of the angular distribution we got several partially independent determinations of the energy E_c from the values of $\ln \tan \theta$ for each pair of particles symmetric about the angle $\theta_{1/2}$. As a result, for the energy of the original particle in the center-of-mass system (E_c) and in the laboratory system (E_0) we got:

$$E_c = \left(200^{+50}_{-40}\right) Mc^2, \quad E_0 = \left(8^{+4}_{-3}\right) \cdot 10^{13} \text{ ev per nucleon.}$$

The relatively small number of generations of fast particles, and likewise the presence of only one slow particle, lead to the assumption that only one out of four incident nucleons took part in the interaction, as has been observed frequently in the work of Rao and others [3].

2. In the summed path lengths of the secondary particles in the emulsion, about 110 cm, three cases of secondary interaction were found, the characteristics of which are given in Table 1, where, along with the energy, we also determined the transverse momenta of the particles (in the Table

$$\gamma_c = \exp\{\overline{\ln \tan \theta}\}, \quad \varepsilon_0 = 2\gamma_c^2 f(2)$$

where $f(l)$ is a correction taking account of the possibility of collision with several nucleons of the nucleus). In determining the energy of the secondary particles from the angular distribution of the showers formed by them, account was taken of the possibility of the simultaneous interaction of the incident particle with several (l) nucleons of a nucleus of the photoemulsion (see for example Ref. 4). A third interaction occurred near the axis of a

shower and was caused, probably, by a fragment of a primary α-particle (p, d or t).

TABLE 1.

Angle θ between secondary particle and shower axis	Type of secondary interaction	γ_0	ε_0 Bev	$\frac{p_\perp}{\mu c} = \frac{\varepsilon_0 \theta}{\mu c}$
$3 \cdot 10^{-3}$	$9 + 13$ p	5.5 ± 1.5	180^{+120}_{-90}	$3.9^{+2.7}_{-1.8}$
$6 \cdot 10^{-4}$	$3 + 10$ p	13 ± 4	700^{+500}_{-400}	$3^{+2.3}_{-1.8}$
$\sim 3 \cdot 10^{-4}$	$1 + (10 \div 15)$ p	~ 200	$10^4 \div 10^5$	< 200

3. Another indirect method for the approximation measurement of the transverse momenta ($p_\perp^0$) of the shower particles is the determination of the energy and direction of flight of the photons arising from the decay of π^0-mesons. Table 2 gives the characteristics of all the pairs, which, as far as we can tell, are not connected with electron brehmstrahlung. The table gives all the information needed for

TABLE 2.

α	s, мм	$h\nu$, Bev	$\theta_{\gamma x}$	$p^0_{\perp x}/\mu c$	t
$1 \cdot 10^{-4}$	4.5	130	$1 \cdot 10^{-3}$	1.8	0.35
$1 \cdot 10^{-4}$	4.5	130	$1 \cdot 10^{-3}$	1.8	0.35
$3.5 \cdot 10^{-4}$	2.7	30	$2 \cdot 10^{-3}$	0.8	0.35
$2.5 \cdot 10^{-4}$	2.1	40	$2 \cdot 10^{-3}$	1.2	0.43
$1 \cdot 10^{-4}$	4.6	130	$0.6 \cdot 10^{-3}$	1.2	0.55
$2 \cdot 10^{-4}$	2.2	90	$1.4 \cdot 10^{-3}$	1.8	0.55
$4 \cdot 10^{-4}$	1.2	25	$0.7 \cdot 10^{-3}$	0.25	0.67
$1.2 \cdot 10^{-4}$	6.0	110	$0.3 \cdot 10^{-3}$	0.6	0.8
$0.9 \cdot 10^{-4}$	5.8	160	$0.2 \cdot 10^{-3}$	0.5	0.8

Note: $\theta_{\gamma x}$ is the direction of the photon relative to the axis. $p^0_\perp$ is the x-component of the momentum; t is the distance from the point of formation of the shower in radiation lengths.

calculating $p^0_\perp$. The energy $h\nu$ of the photon was obtained from the relation:

$$h\nu = (4 m_e c^2 / \alpha) \sqrt{\log^2 \left(\frac{h\nu}{m_e c^2} \right) + 5s} \qquad (1)$$

where $m_e c^2$ is the rest energy of the electron and α is the angle of divergence of the components of the pair, measured by the value of their mutual separation in a path s (in mm). Since Eq. (1) gives the energy $h\nu$ under the assumption that the energies of the electron and positron are equal, it gives low values of $h\nu$ in the mean.

As can be seen from Tables 1 and 2, the values of the transverse momenta, measured by the two independent methods, agree satisfactorily with one another, and give a mean value $\bar{p}_\perp \sim 2\mu c$ with a scattering $\overline{\Delta p}_\perp \sim \bar{p}_\perp$ about the mean. This result agrees well with the corresponding data[5] obtained from direct measurement of the angles and energies of the secondary particles.

As is shown in Ref. 6, the distribution of the particles relative to the value of $p_\perp$ is such that it can be considered the result of purely thermal motion of the nascent particles.

The authors thank Prof. C. F. Powell for his cooperation in getting the emulsion stack, Prof. N. A. Dobrotin, I. L. Rozental' and D. S. Chernavskii for a discussion of the results, and laboratory Iu. F. Sharapov, R. M. Gryzumov and M. F. Solov'ev for their assistance in working up the materials.

[1] I. V. Dunin-Barkovskii and N. V. Smirnov. *Theory of Probability and Mathematical Statistics in Engineering*, GITTL, 1955.

[2] L. D. Landau, Izv. Akad. Nauk. U.S.S.R., Ser. Fis. 17, 51 (1953).

[3] Appa Rao, Daniel, and Neelakantan, Proc. Ind. Acad. 43, 181 (1956).

[4] I. A. Ivanovskaia and D. S. Chernavskii. Nucl. Phys. (in press).

[5] Debenedetti, Garelli, Tallone, and Vigone, Nuovo cimento 4, 1142 (1956).

[6] G. A. Milekhin and I. L. Rosental, J. Exptl. Theoret. Phys. (U.S.S.R.) (in press).

Translated by C. V. Larrick
199

Paramagnetic Absorption in Some Manganese Salts in Parallel Fields at Super-High Frequencies

A. I. KURUSHIN

(Submitted to JETP editor Jan. 14, 1957)
J. Exptl. Theoret. Phys. (U.S.S.R.) 32, 938-939
(April, 1957)

EARLIER,[1,2] WE MEASURED the paramagnetic absorption in some powdered salts of gadolinium and of manganese in parallel fields, at room temperature, at frequencies of the order of 9×10^9 cps. It was found that, as in the case of frequencies of the order of 6×10^8 cps,[3,4] the absorption decreases monotonically with increase of the constant magnetic field. The experimental absorption curves obtained in Ref. 1 to 4 are in good agreement with Shaposhnikov's[5] phenomenological theory of paramagnetic absorption in parallel fields, if it is assumed that the spin relaxation time τ_s of that theory is independent of the value of the constant field.

Recently, Smits *et al.*[6] experimentally established a more complicated type of dependence of paramagnetic absorption on the value of the constant field and on the frequency of the alternating field at temperature 20.4° K, for frequencies of order 10^6 to 10^8 cps. It was found, in particular, that the curves of absorption *vs* value of the constant field, at a given frequency of the alternating field, have a maximum.

The present note communicates the results of measurements of paramagnetic absorption in parallel fields in the powdered salts $Mn(NO_3)_2 \cdot 6H_2O$ and $Mn(NH_4)_2(SO_4)_2 \cdot 6H_2O$ at room temperature ($T = 291°$ K), at frequency $\nu = 9.377 \times 10^9$ cps. The method used in the measurements is that described in Ref. 1. The results of the measurements are presented in the Figure, where curves I and II relate respectively to the first and the second of the substances indicated above. Plotted along the ordinate axis is the imaginary part of the magnetic susceptibility in arbitrary units, and along the abscissa axis the value of the constant field, which is parallel to the high-frequency field. It is evident that the absorption curves for the salts under study differ essentially from those obtained earlier for other substances;[1,2] there is an absorption maximum in a range of constant fields of order 1500 oersted. Thus our results, which relate to room temperature, are similar to the results obtained by Smits *et al.*[6] at temperature 20.4° K. In the range of fields of order 3400 oersted, the absorption curves are somewhat irregular; apparently the reason for these irregularities lies in a paramagnetic resonance absorption, caused by a slight deviation from paral-

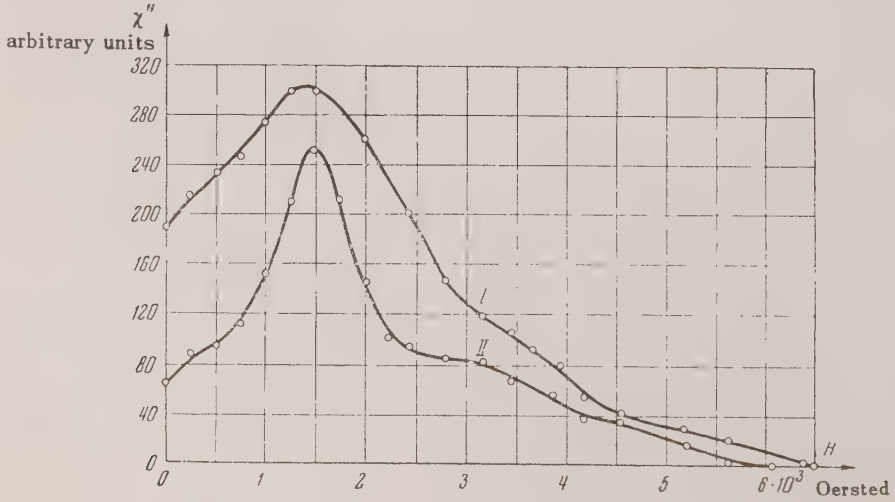

lelism of the fields (in favor of such an explanation are the locations of the irregularities on the curves, and the fact that the irregularities increase with increase of the angle between the fields).

The results presented in Ref. 6 and in the present note can not be explained within the framework of Shaposhnikov's theory if the spin relaxation time is considered to be independent of the value of the constant field. The problem of a theoretical explanation of these results requires further study.

[1] A. I. Kurushin, Izv. Akad. Nauk SSSR, Ser. Fiz. **20**, 1232 (1956).

[2] A. I. Kurushin, J. Exptl. Theoret. Phys. (U.S.S.R.) this issue, p. 727, Soviet Physics JETP **5**, 601 (1957) .

[3] N. S. Garif'ianov, J. Exptl. Theoret. Phys. (U.S.S.R.) **25**, 359 (1953).

[4] K. P. Sitnikov, Dissertation, Kazan' Univ., 1954.

[5] I. G. Shaposhnikov, J. Exptl. Theoret. Phys. (U.S.S.R.) **18**, 533 (1948).

[6] Smits, Derksen, Verstelle, and Gorter, Physica **22**, 773 (1956).

Translated by W. F. Brown, Jr.
200

On the Theory of "Strange" Particles

V. I. KARPMAN
Minsk Pedagogical Institute

(Submitted to JETP editor Jan. 15, 1957)
J. Exptl. Theoret. Phys. (U.S.S.R.) **32**, 939-940
(April, 1957)

IN GELL-MANN'S THEORY,[1] which successfully describes the formation and decay of many heavy unstable particles recently discovered, the quantum number S (the strangeness) is introduced by its relation to the electric charge Q, namely

$$Q = I_3 + (n/2) + S/2, \tag{1}$$

where I_3 is the projection of the isotopic spin, and n is the total baryon number of the system (we shall henceforth call n the nucleon charge of the system). Gell-Mann's scheme is in good agreement with experiment, though it should be complemented with a theory which gives an interpretation to the "strangeness" S.

Among the various attempts to interpret the strangeness, of particular interest is the mathematical formulation of Gell-Mann's scheme which has been suggested by d'Espagnat and Prentki[2]. These authors postulate that the particles with semi-integral isotopic spin can be described by spinors of the first and second kind[3] in isotopic spin space. These spinors differ from each other under inversion in isotopic spin space: the first are multiplied by $+i$ (or $-i$), and the second by $-i$ (or $+i$). The existing particles are called isofermions (nucleons, θ-particles, anti-Ξ-particles) and anti-isofermions (antinucleons, anti-θ-particles, Ξ). Further, it is postulated that the Lagrangian which describes strong and electromagnetic interactions (using Gell-Mann's terminology) is invariant with respect to inversion in isotopic spin space.

It is not difficult to see that the Lagrangian obtained on the basis of these assumptions is invariant under simultaneous changes of the wave functions of all iso- and anti-isofermions according to

$$\varphi \to \varphi e^{i\alpha}, \quad \varphi' \to \varphi' e^{-i\alpha}, \tag{2}$$

where φ and φ' are the wave functions of all the iso- and anti-isofermions, respectively. From this follows a conservation law for the "isofermionic charge" u, which is equal to the number of isofermions minus the number of anti-isofermions. The isofermionic charge u differs from the nucleonic charge n in that n is conserved in all interactions, but u is conserved only in strong and electromagnetic interactions. It is then found that Eq. (1) can be written[2]

$$Q = I_3 + u/2. \tag{3}$$

It thus follows from (1) and (3) that

$$S = u - n, \tag{4}$$

so that the strangeness is interpreted as the difference between the isofermionic and nucleonic charges of the system.

We should like to make some remarks with reference to the theory of d'Espagnat and Prentki. Similarly as with the nucleonic charge, the isofermionic charge u of a single particle can take on only the values +1 (for an isofermion), −1 (for an anti-isofermion), or 0 (for an isoboson).* From this and

*When $|u| > 1$ there arise difficulties which can be eliminated only by dropping some terms in the interaction Lagrangian[7]. In this case, however, the ambiguity that arises essentially eliminates the value of the d'Espagnat-Prentki-theory.

from Eq. (4) it follows that for a single particle

$$|S| \leqslant 2, \tag{5}$$

so that according to the d'Espagnat-Prentki theory the strangeness cannot have an absolute value greater than 2.

Relation (2) is of interest in connection with the slow secondary particles recently observed in K^--meson decay[4-6]. The analysis of these events shows quite definitely that they are the decays of some kind of negative "superheavy" mesons or hyperons, whose mass is greater than $M(K) \approx 965\, m_e$ and $M(\Xi) \approx 2586\, m_e$.

If we do not consider isotopic multiplets containing particles with charges greater than unity, then by using Eq. (1) it is not difficult to show that the only negative metastable particle heavier than the mesons and hyperons known at present can be the following isotopic singlets: the meson ω^- (with $S = -2$) and the hyperon Ω with $S = -3$). Expression (5) excludes the latter possibility.

Thus according to the d'Espagnat-Prentki theory, the observed[4-6] K^--meson decays may be considered the decays of "superheavy" ω^--mesons with strangeness $S = -2$. Applying the selection rule $\Delta S = \pm 1$, suggested by Gell-Mann for slow processes[1], one may suppose that in the decay of the ω^--meson, there appears in addition to the K^--meson a particle with strangeness $S = -1$. If the existence of negative metastable hyperons heavier than Ξ is nevertheless proved, this will mean either that the d'Espagnat-Prentki[2] interpretation of Gell-Mann's model is invalid, or that this hyperon belongs to an isotopic multiplet containing particles with charge greater than 1.

[1] M. Gell-Mann, Proc. Pisa Conference, 1955.

[2] B. d'Espagnat, J. Prentki, Phys. Rev. 99, 328 (1955).

[3] E. Cartan, *Theory of Spinors*, 1948 [A translation of *Leçons sur la théorie des spineurs* (Hermann et Cie., Paris, 1938)].

[4] Y. Eisenberg, Phys. Rev. 96, 541 (1954).

[5] W. Fry, J. Schneps, M. Swami, Phys. Rev. 97, 1189 (1955).

[6] A. A. Varfolomeev, R. I. Gerasimova, L. A. Karpova, Dokl. Akad. Nauk SSSR 110, 969 (1956).

[7] B. d'Espagnat, J. Prentki, Nucl. Phys. 1, 33 (1956).

Translated by E. J. Saletan
201

The Interaction Cross Section of π-Mesons and Nucleons at High Energies

P. V. VAVILOV

(Submitted to JETP editor Jan. 17, 1957)
J. Exptl. Theoret. Phys. (U.S.S.R.) 32, 940-941
(April, 1957)

IT IS WELL KNOWN that at high energies the interaction cross section of π-mesons with nucleons approaches a constant limit, which is a result of the finite dimensions of the nucleon (neglecting the Coulomb interaction). In order to calculate this limit let us make use of dispersion relations which connect the imaginary and real parts of the scattered amplitude for zero scattering angle. For instance, for scattering of negative mesons by protons we have[1]

$$\operatorname{Im} f_-(\omega) = \frac{1}{2} \operatorname{Im} f_-(\mu)\left(1 + \frac{\omega}{\mu}\right) + \frac{1}{2} \operatorname{Im} f_+(\mu)\left(\frac{\omega}{\mu} - 1\right) + \frac{\omega^2 - \mu^2}{\pi} \mathrm{P} \int_0^\infty \frac{d\omega'}{\omega'^2 - \mu^2} \left[\frac{\operatorname{Re} f_+(\omega')}{\omega' + \omega} - \frac{\operatorname{Re} f_-(\omega')}{\omega' - \omega}\right] - \pi \sum_k \delta(\omega_k - \omega) \operatorname{Res} f_-(\omega_k); \tag{1}$$

here we have accounted for the fact that the amplitude may have poles at the points ω_k (we have made use of the fact that the residues Res f_- are real). The symbol P indicates that we take the principal part of the integral not only at those points where the denominator vanishes but at all poles of the functions $f_\pm$. Letting ω approach infinity in Eq. (1), we obtain

$$\sigma_\infty = 4\mathrm{P} \int_0^\infty \frac{d\omega}{\omega^2 - \mu^2} \operatorname{Re}[f_+(\omega) + f_-(\omega) - f_+(\mu) - f_-(\mu)]. \tag{2}$$

Eq. (2) is symmetric with respect to f_+ and f_-, so that in the limit the cross sections for positive and negative mesons are equal[2]. In deriving Eq. (2), we have used the well known relation $\sigma = (4\pi/\omega)\operatorname{Im} f(\omega)$, as well as the condition $\operatorname{Im} f_\pm(\mu) = 0$. The term $\operatorname{Re}[f_+(\mu) + f_-(\mu)]$ is added for convenience (this clearly does not destroy the equality since $\mathrm{P} \int_0^\infty d\omega/(\omega^2 - \mu^2) = 0$).

Let us break up the integral in Eq. (2) into two integrals over the regions $0 \leq \omega \leq \mu$ and $\mu \leq \omega \leq \infty$. In the first region we make use of the relation[1]

$$\mathrm{Re}\,[f_+(\omega)+f_-(\omega)-f_+(\mu)-f_-(\mu)]$$
$$=\frac{\omega^2-\mu^2}{2\pi^2}\int_0^\infty \frac{dk'}{k'^2-k^2}\,[\sigma_+(k')+\sigma_-(k')] \qquad (3)$$
$$+\frac{2f^2}{M}\,\frac{\omega^2-\mu^2}{\omega^2-(\mu^2/2M)^2}\,.$$

Using the experimental values of the phase shifts[3], we obtain

$$\mathrm{Re}\,[f_+(\mu)+f_-(\mu)]=-0{,}04\lambda\!\!\!^{-}\,(1+\mu/M),$$

where $\lambda\!\!\!^{-}$ is the Compton wavelength of the meson, and μ and M are the meson and nucleon masses, respectively. Inserting (3) into (2), after some simple operations we obtain

$$\sigma_\infty=-1{,}5+I_0+I_1; \qquad (4)$$

$$I_0=\frac{1}{\pi^2}\int_0^\infty \frac{dE}{\sqrt{E\,(E+2\mu)}}\ln\frac{E+2\mu}{E}\,[\sigma_+(E)+\sigma_-(E)], \qquad (5)$$

$$I_1=4\lambda\!\!\!^{-2}\int_0^\infty \frac{dx}{x\,(x+2)}\left[\frac{1}{\lambda\!\!\!^{-}}\,\mathrm{Re}\,(f_+(x)+f_-(x))+0{,}04\,(1+\mu/M)\right],\quad x=\frac{E}{\mu} \qquad (6)$$

In order to calculate the integrals we make use of the experimental[4] values for $\sigma_\pm(E)$ and $\mathrm{Re}\,f_\pm(x)$. We obtain the following values: $I_0 = 20$ mb, $I_1 = 11.5$ mb. Inserting these values into (4), we obtain $\sigma_\infty = 30$ mb, which is in agreement with the experimental data[4],. The accuracy of σ_∞ is limited by the accuracy of the experimental data for $\sigma_\pm$ and $\mathrm{Re}\,f_\pm$.

[1] Goldberger, Miyazawa, and Oehme, Phys. Rev. 99, 986 (1955).

[2] L. B. Okun', I. Ia. Pomeranchuk, J. Exper. Theoret. Phys. 30, 424 (1956), Soviet Physics JETP 3, 307 (1956).

[3] J. Orear, Phys. Rev. 96, 176 (1954).

[4] Cool, Piccioni, and Clark, Phys. Rev. 103, 1082 (1956).

Translated by E. J. Saletan
202

On the Second Approximation in the Problem of Slow Neutron Scattering by Bound Protons

A. S. DAVYDOV AND D. M. MEL'NICHENKO
Moscow State University

(Submitted to JETP editor January 21, 1957)
J. Exper. Theoret. Phys. (U.S.S.R.) 32, 941-943
(April, 1957)

THE PROBLEM of scattering slow neutrons by protons bound in a molecule has been treated in the first approximation by Fermi[1]. In several other works[2-4] evaluations of the further approximations have been made. Of particular interest is the variational method developed by Schwinger and Lippmann[3], with the aid of which Lippmann calculated neutron scattering by a hydrogen molecule in the second approximation, and verified the results of Breit and Zilsel[2] who used a different model for the molecule. Soon, however, Ekstein's work[4] appeared, where it was proved that the second approximation of the Schwinger-Lippmann method for neutron scattering by bound protons always diverges, except if the proton is bound to an infinitely heavy nucleus. Ekstein commented, "whether the finite result found by Lippmann is due to the special choice of wave functions . . . or the limiting process used in the evaluation of the integral, remains undecided."

In this note we investigate the question of convergence of the second approximation in the problem of slow neutron ($E \approx 0$) scattering by a proton bound in a molecule of mass M.

In the Schwinger-Lippman method the scattering matrix T_{ba} for zero-energy neutrons from state a to state b is given in the second approximation by the equation

$$T_{ba}=-(4\pi\hbar^2 a/m)\left\{\int \chi_b^*(\mathbf{r})\,\chi_a(\mathbf{r})\,d\mathbf{r}+aI\right\},$$
$$I\equiv\int \chi_b^*(\mathbf{r})\left[\sum_\gamma \chi_\gamma^*(\mathbf{r}')\,\chi_\gamma(\mathbf{r})\,\frac{(2\mu/m)\exp(ik_\gamma a\,|\,\mathbf{r}-\mathbf{r}'\,|)-1}{a\,|\,\mathbf{r}-\mathbf{r}'\,|}\right]\chi_a(\mathbf{r}')\,d\mathbf{r}d\mathbf{r}', \qquad (1)$$

where m is the proton mass,

$$\mu = mM/(M+m);$$

$$\alpha = (M-m)/M,\ k_\gamma = [2\mu\hbar^{-2}(E - W_\gamma)]^{1/2},\quad E \approx 0,$$

$\mathbf{r}$ is the coordinate of the proton relative to the center of mass of the remainder of the molecule, $\chi_\gamma(\mathbf{r})$ is the eigenfunction of the proton in the molecule (for simplicity we shall not consider other degrees of freedom in the molecule), a is the scattering amplitude of a neutron by a free proton, and W_γ is the energy of the proton in the molecule. The summation over γ is taken over all proton states in the molecule.

Breit and Zilsel[2] replaced the molecule by an idealized system consisting of a three-dimensional oscillator. In this case

$$W_\gamma \equiv W_{n_1 n_2 n_3} = (\hbar^2/\mu_p)\sum_{i=1}^{3}(n_i + 1/2)\,\beta_i^{-2},\ \mu_p = m(M-m)/M,\ ik_\gamma\alpha = -b\,(2\sum_i n_i/\beta_i^2)^{1/2},$$
$$\chi_\gamma \equiv \chi_{n_1 n_2 n_3} = \prod_i \frac{\exp\{-r_i^2/2\beta_i^2\}}{(\beta_i 2^{n_i} n_i!\sqrt{\pi})^{1/2}} H_{n_i}\left(\frac{r_i}{\beta_i}\right),\quad b = \left(\frac{M-m}{M+m}\right)^{1/2}, \tag{2}$$

where the β_i are constants which determine the potential energy of the proton for elastic scattering on the ground state. Using Eq. (2), it can be shown that in Eq. (1)

$$[\cdots] = \frac{1}{2\sqrt{\pi}}\int_0^\infty \frac{d\tau}{\tau^{3/2}}\left\{\frac{2\mu}{m}\prod_i \frac{\exp\left(-\frac{1+q_i^2}{2(1-q_i^2)\beta_i^2}[r_i'^2 + r_i^2 + 4q_i r_i r_i']\right)}{\beta_i\sqrt{\pi}\sqrt{1-q_i^2}} - \delta(\mathbf{r}-\mathbf{r}')\right\} e^{-|\mathbf{r}-\mathbf{r}'|/4\tau},$$

$$q_i = \exp\{-2b^2\tau/\beta_i^2\}.$$

Inserting $[\cdots]$ into (1), we obtain

$$I = \frac{8}{V\pi}\int_0^\infty d\tau\left\{\frac{\mu}{m}\prod_i [4\tau + 2\beta_i^2(1-q_i)]^{-1/2} - (16\tau^{3/2})^{-1}\right\}. \tag{3}$$

From the form of the integral of Eq. (3) it follows that it diverges only in the region of small τ. In order to investigate the integrand as $\tau \to 0$, let us expand q_i in a series, so that

$$\{\cdots\} = \frac{\mu}{m}[4\tau(1+b^2)]^{-3/2} - 1/2(4\tau)^{-3/2}.$$

In order for the integral of Eq. (3) to converge, it is necessary that

$$2\mu/m = (1+b^2)^{-3/2}. \tag{4}$$

Noting Eq. (2), we see that condition (4) is not satisfied, so that the integral diverges in the region $\tau \approx 0$.

Thus the second approximation in the Schwinger-Lippmann theory diverges for neutron scattering on a harmonically bound proton. Breit and Zilsel[2] obtained a finite value in solving a similar problem as a result of eliminating the divergent part of the integral by the replacement $\tau \to 2\tau$ on going over from the second integral in their expression (3.1) to their expression (3.2). This method is mathematically invalid.

It is easily shown that, however, the second approximation of Eq. (1) always converges if we use the wave functions of real molecules rather than of idealized systems. In a real molecule a highly excited state corresponds to a decaying system, when the wave functions of the proton motion relative to the rest of the molecule can be given in terms of plane waves $\chi_\gamma = \exp(i\mathbf{pr})$ with energies $W_\gamma = \hbar^2 p^2/2\mu_p$. In this case $ik_\gamma a = -bp$, and after replacing summation over γ by integration with respect to p, the integral over that part of the sum over γ in Eq. (1) which corresponds to high excitations (which are all that can cause the integral to diverge) can be written

$$I_{p_0} = \frac{2\mu}{m\alpha}\int d\mathbf{r}\,\chi_b^*(\mathbf{r})\left\{\int_{p_0}^\infty d\mathbf{p} e^{i\mathbf{pr}}\int d\mathbf{r}'\,\frac{\exp(-bp|\mathbf{r}-\mathbf{r}'|) - m/2\mu}{|\mathbf{r}-\mathbf{r}'|}e^{-i\mathbf{pr}'}\chi_a(\mathbf{r}')\right\}. \tag{5}$$

For sufficiently large p_0, Eq. (5) can be calculated in the same way as was done by Ekstein[4], obtaining

$$\{\cdots\} = (4\pi)^2 \chi_a(\mathbf{r}) \left[\frac{1}{1+b^2} - \frac{m}{2\mu}\right] \int_{p_0}^{\infty} dp. \qquad (6)$$

From the definition of b and μ it follows that the expression in square brackets in Eq. (6) vanishes. It is not difficult to show that nonzero neutron energies also give a finite result.

Thus when using wave functions for real molecules in the calculation according to Eq. (1), we obtain a finite result. This conclusion contradicts that of Ekstein, since he mistakenly omitted the factor α in the exponent of Eq. (1) and stated that $k_\gamma = ip$, rather than the correct expression $k_\gamma = ip\sqrt{\mu/\mu_p}$.

The results of Breit and Zilsel are correct because an artificial (mathematically nonrigorous) method was used to eliminate the divergent part of the integral, which in turn, is due to the idealization of the problem being considered.

[1] E. Fermi, Ricerca sci. 7, 2, 13 (1936).
[2] G. Breit, P. Zilsel, Phys. Rev. 71, 232 (1947).
[3] B. Lippmann, J. Schwinger, Phys. Rev. 79, 481 (1950).
[4] H. Ekstein, Phys. Rev. 87, 31 (1952).

Translated by E. J. Saletan
203

Fluctuations in Gases

B. B. KADOMTSEV

(Submitted to JETP editor January 24, 1957)
J. Exptl. Theoret. Phys. (U.S.S.R.) 32, 943-944
(April, 1957)

THE STATE OF A GAS is completely described by the particle-distribution function in the phase space $f(\mathbf{r}, \mathbf{v}, t)$; therefore the problem of fluctuations in gases leads to the study of the correlation characteristics of the distribution function. Ordinarily one understands by f the statistically-average density of the particles in the phase space which, naturally, cannot fluctuate. Speaking of the fluctuations of the distribution function we must, however, bear in mind the "true" density

$$F(\mathbf{r}, \mathbf{v}, t) = \sum_i \delta(\mathbf{r} - \mathbf{r}_i)\, \delta(\mathbf{v} - \mathbf{v}_i),$$

where the summation is carried out with respect to all particles. We shall consider the density F to be a random quantity which only on the average coincides with f.

The function F satisfies the equation

$$\frac{\partial F}{\partial t} + (\mathbf{v}\nabla) F = \frac{1}{m} \frac{\partial F(\mathbf{r}, \mathbf{v}, t)}{\partial \mathbf{v}} \int \frac{\partial U(|\mathbf{r} - \mathbf{r}'|)}{\partial \mathbf{r}} F(\mathbf{r}', \mathbf{v}', t)\, d\mathbf{r}'\, d\mathbf{v}', \qquad (1)$$

where m is the mass of a molecule, and U is the potential energy of the interaction of the molecules among themselves. In an ideal gas we may neglect the interaction of the particles and obtain then from (1) $F(\mathbf{r}, \mathbf{v}, t) = F(\mathbf{r} - \mathbf{v}(t - t_0), \mathbf{v}, t_0)$ whence

$$\langle \varphi(\mathbf{r}, \mathbf{v}, t)\, \varphi(\mathbf{r}_0, \mathbf{v}_0, t_0) \rangle = f(\mathbf{r}, \mathbf{v}, t)\, \delta(\mathbf{r} - \mathbf{v}(t - t_0) - \mathbf{r}_0)\, \delta(\mathbf{v} - \mathbf{v}_0), \qquad (2)$$

where $\varphi = F - f$ and the angular brackets denote the averaging.

Our problem consists in finding the correlation of (2) with allowance for the collisions. If the gas is not very dense, we may confine ourselves only to the accounting of paired collisions, and then the right half of Eq. (1) may be approximately represented in the form of the collision term $S(F, F)$:

$$S(F, F) = \int \{F(\mathbf{r}, \mathbf{v}', t)\, F(\mathbf{r}_1, \mathbf{v}_1', t) - F(\mathbf{r}, \mathbf{v}, t)\, F(\mathbf{r}_1, \mathbf{v}_1, t)\} |\mathbf{v} - \mathbf{v}_1| \rho d\rho\, d\chi\, d\mathbf{v}_1, \qquad (3)$$

where ρ is the collision parameter, $\rho\, d\rho\, d\chi$ is an element of the surface which is perpendicular to the relative velocity $\mathbf{v} - \mathbf{v}_1$ and passes through the point $\mathbf{r}$, $\mathbf{r}_1$ is the coordinate of this element, $\mathbf{v}'$ and $\mathbf{v}_1'$ are the velocities of the particles before the impact which are transformed after the collision into $\mathbf{v}$, $\mathbf{v}_1$. It is approximately assumed here that the collision occurs at that instant when both particles intersect the surface which is perpendicular to their relative velocity.

If we average (1) using the collision term in the form of (3) and neglect the correlation of the particles before the collision and the difference between $\mathbf{r}$ and $\mathbf{r}_1$, we shall obtain the ordinary Boltzmann equation

$$\frac{\partial f}{\partial t} + (\mathbf{v}\nabla) f = \int \{f(\mathbf{r}, \mathbf{v}', t)\, f(\mathbf{r}, \mathbf{v}_1', t) - f(\mathbf{r}, \mathbf{v}, t)\, f(\mathbf{r}, \mathbf{v}_1, t)\} |\mathbf{v} - \mathbf{v}_1| \rho d\rho\, d\chi\, d\mathbf{v}_1. \qquad (4)$$

Taking (4) into consideration, we transform (1) into the form

$$(\partial\varphi/\partial t) + (\mathbf{v}\nabla)\varphi + A\varphi = q, \quad (5)$$

where A is an operator determined by the expression $A\varphi = -S(f, \varphi) - S(\varphi, f)$ and $q = S(\varphi, \varphi)$. Since use of a distribution function makes sense only where one deals with sufficiently large volumes containing many particles, we must assume the function φ to be a small quantity. Therefore, we may approximately use in q, which is a quantity of the second order of smallness with respect to φ, the correlation (2) whence we obtain

$$\langle q(\mathbf{r}, \mathbf{v}, t)\, q(\mathbf{r}_0, \mathbf{v}_0, t_0)\rangle = (A + A^*) f(\mathbf{r}, \mathbf{v}, t)\, \delta(\mathbf{r} - \mathbf{r}_0)\, \delta(\mathbf{v} - \mathbf{v}_0)\, \delta(t - t_0), \quad (6)$$

where A* is the operator acting upon the velocity $\mathbf{v}_0$.

Let us denote by G the Green function for Eq. (5), *i.e.*, the operator by whose action on the source we can obtain the solution of this equation. Then we obtain from (5) and (6):

$$\langle \varphi(\mathbf{r}, \mathbf{v}, t)\, \varphi(\mathbf{r}_0, \mathbf{v}_0, t_0)\rangle = GG^*(A + A^*) f(\mathbf{r}, \mathbf{v}, t)\, \delta(\mathbf{r} - \mathbf{r}_0)\, \delta(\mathbf{v} - \mathbf{v}_0)\, \delta(t - t_0), \quad (7)$$

where G* is the operator acting upon $\mathbf{r}_0$, $\mathbf{v}_0$, t_0.

Eq. (7) also furnishes a solution for our problem. If we put, approximately, $A = 1/\tau$, where τ is the average time between collisions and assume that f is not a function of $\mathbf{r}$ and t, then (7) takes the form

$$\langle \varphi(\mathbf{r}, \mathbf{v}, t)\, \varphi(\mathbf{r}_0, \mathbf{v}_0, t_0)\rangle = e^{-|t-t_0|/\tau} f(\mathbf{v})\, \delta(\mathbf{r} - \mathbf{r}_0 - \mathbf{v}(t - t_0))\, \delta(\mathbf{v} - \mathbf{v}_0). \quad (8)$$

However, for a more exact consideration of the problem and also in the non-stationary case, we must solve Eq. (5), that is, a linearized kinetic equation with a random source.

The physical sense of this equation is evident. Actually, every act of collision leads to two particles being withdrawn from the initial density and to two particles with different velocities appearing in their place at that same point in the space. Eq. (5) also describes the further development of such a random disturbance of the distribution function.

Eq. (5) is, with respect to form, entirely analogous to the Maxwell equations with random sources[1] used in the theory of electric fluctuations. This is not surprising, since in the case of thermodynamic equilibrium, equations of this type can be obtained by starting from the general theory of fluctuations[2,3]. The kinetic derivation of the formulae (5) and (6) considered here possesses, in addition to greater clarity, the advantage that it is correct also in the non-stationary case.

It must be noted that according to (7) the particles are found to be only slightly correlated before collision. The correlation arises from such chains of collisions where two impinging particles collide with two others and these latter collide with one another. Since four particles participate in this chain and we have even neglected triple collisions, we may neglect the correlation of the particles before the collision resulting from (7).

I should like to express my deep gratitude to Academician M. A. Leontovich fordiscussing this report with me.

[1] S. M. Rytov, *Theory of Electric Fluctuations*, AN SSSR, 1953.

[2] Callen, Barasch, and Jackson, Phys. Rev. 88, 1382 (1952).

[3] S. M. Rytov, Dokl. Akad. Nauk SSSR 110, 371 (1956).

Translated by L. Mahler
204

The Effect of Neutron Irradiation on the Compressibility of Metals

A. I. LIKHTER AND A. I. KIKOIN
Institute of the Physics of Metals of the Ural Branch of the Academy of Sciences of the USSR
Ultra-High-Pressure Physics Laboratory of the Academy of Sciences of the USSR

(Received by JETP editor January 25, 1957)
J. Exptl. Theoret. Phys. (U.S.S.R.) 32, 945
(April, 1957)

THE FEW STUDIES that have been made so far on the effect of fast neutron irradiation on the elastic properties of metals and alloys show either that the effect is entirely absent or that it is exceedingly small. The modulus of elasticity, as far as we know, has been studied only in austenite steel and in copper. Neither case showed any change in the modulus of elasticity for a total flux of 10^{19} neutrons/cm^2 [1]. The shear modulus was studied in neutron-irradiated copper, and the residual change at room temperature was not greater than 1%[1].

The latest measurements on copper[2] show that the change in the modulus of elasticity on irradiation does not amount to more than 1 – 2%.

We studied the effect of fast neutron irradiation in a nuclear reactor on the compressibility of aluminum and magnesium. Since this quality is directly connected with the elasticity and shear moduli, and since no change in these moduli was found in the materials investigated so far, it was to be expected that the compressibility, too, would not change appreciably, under the influence of neutron irradiation. Samples in the form of cylinders 6 mm in diameter and 6 mm high, were prepared from electrolytic materials of engineering purity. The compressibility measurement was made with apparatus developed in the ultra-high-pressure physics laboratory for measuring volume compressibility by the piston displacement method, which apparatus will be described in another communication. The effect of friction was allowed for by taking the piston displacement *vs.* pressure curves on both rising and falling pressure and plotting the mean curve. The measurements were carried out after first subjecting the sample to a maximum pressure of about 15,000 kg/cm^2.

The samples were irradiated in a nuclear reactor. The total neutron irradiation was 1.07×10^{19} neutrons/cm^2. After irradiation, the compressibility was measured under the same conditions as before irradiation, although, on account of the residual activity of the samples, the measurements could not be carried out until 72 hours after the irradiation.

The measurements showed that for magnesium and aluminium the piston displacement *vs.* pressure curves coincide completely before and after irradiation, *i.e.*, irradiation has no effect on the compressibility, to the accuracy of our measurements, about 5%. Since the experiments were carried out at ordinary temperature, the distortions produced by the irradiation may have been partly wiped out. Possibly at lower temperatures, with a preliminary annealing of the samples, the effect of irradiation would be considerably greater.

[1] J. V. Glen, Uspekhi Fiz. Nauk 60, 445,(1956).

[2] D. O. Thompson, and K. Holmes, J. Appl. Phys. 27, 713 (1956).

Translated by C. V. Larrick
205

Quadrupole Moments and Zero-Point Surface Vibrations of Axially Symmetrical Nuclei

A. S. DAVYDOV AND G. F. FILIPPOV
Moscow State University

(Submitted to JETP editor January 26, 1957)
J. Exptl. Theoret. Phys. (U.S.S.R.) 32, 945-947
(April, 1957)

FOR SIMPLICITY WE SHALL consider even-even nuclei. In the collective model of the nucleus it is assumed that nucleons outside of filled shells can be described by a single-particle approximation and that the nucleons in the nuclear core of completely filled shells have only collective properties. As collective coordinates we shall use the three Euler angles which describe the orientation of the nucleus in space and β and γ[1], which define the deviation of the nucleus from a perfectly spherical shape.

In an adiabatic approximation we can regard the outer nucleons as moving in the field of a nuclear core of fixed shape. The interaction energy of the outer nucleons with the core, averaged over their states of motion is $\langle H_{\text{int}} \rangle = A\beta \cos\gamma$, which will depend on the coordinates β and γ and will act as additional energy to determine the equilibrium shape of the nucleus. A depends on the number of outer nucleons and their quantum numbers and can be either positive or negative.

In the collective model[1] this energy is defined by

$$E = \frac{B}{2}(\dot{\beta}^2 + \beta^2\dot{\gamma}^2) + \frac{C}{2}\beta^2 + \sum_{\lambda=1}^{3} \frac{M_\lambda^2}{8B\beta^2 \sin^2(\gamma - 2\pi\lambda/3)} + A\beta\cos\gamma + E_p. \quad (1)$$

For a given value of β the potential energy in (1) possesses a minimum at $\gamma = 0$ and π and becomes infinite for $\gamma = \pm\pi/3, \pm 2\pi/3$.

Nuclei are evidently very stable with respect to variation of γ around the two possible equilibrium values 0 and π, which correspond to axial symmetry. Therefore we shall hereinafter consider only the vibrations which are associated with a variation of of β for the fixed values $\gamma = 0, \pi$.

For $\gamma = 0$ Eq. (1) becomes

$$E - E_p + \frac{C}{2}\beta_0^2 = \frac{B}{2}\dot{\beta}^2 + \frac{C}{2}(\beta - \beta_0)^2 + \frac{M^2}{6B\beta^2}, \quad (2)$$

where $\beta_0 = -A/C$. The corresponding Schroedinger equation for states with definite total angular momentum is for the S state ($j = 0$)

$$\left\{-\frac{\hbar^2}{2B\beta^2}\frac{\partial}{\partial\beta}\left(\beta^2\frac{\partial}{\partial\beta}\right)+\frac{C}{2}\left(\beta-\beta_0\right)^2-\varepsilon\right\}\Phi(\beta)=0. \tag{3}$$

We put

$$\Phi(\beta)=\frac{1}{\beta}v(\zeta)\exp\left\{-\frac{\zeta^2}{2}\right\},\ \zeta=\delta\frac{\beta-\beta_0}{\beta_0},$$

$$\delta=\beta_0\left(\frac{BC}{\hbar^2}\right)^{1/4},\ \omega=\sqrt{\frac{B}{C}}.$$

Then $v(\zeta)$ will satisfy the equation

$$v''(\zeta)-2\zeta v'(\zeta)+2\nu v(\zeta)=0,\quad -\delta\leqslant\zeta<\infty,$$

$$\nu=\frac{\varepsilon}{\hbar\omega}-{}^1/_2. \tag{4}$$

The function $v(\zeta)$ must satisfy the boundary conditions

$$e^{-\zeta^2/2}v(\zeta)\to 0,\quad \text{if}\quad \zeta\to\infty, \tag{5}$$

$$v(-\delta)=0. \tag{6}$$

For nonintegral ν the general solution of (4) can be expressed in terms of Hermite functions[2]

$$H_\nu(\zeta)\equiv\{2\Gamma(-\nu)\}^{-1}\sum_{k=0}^{\infty}(-1)^k\Gamma\left(\frac{k-\nu}{2}\right)(k!)^{-1}(2\zeta)^k$$

by the relation

$$v_\nu(\zeta)=aH_\nu(\zeta)+bH_\nu(-\zeta).$$

The asymptotic behavior of the Hermite functions for large ζ gives $b = 0$ according to the boundary condition (5). Then boundary condition (6) leads to the transcendental equation $H_\nu(-\delta) = 0$, which determines the eigenvalues of ν and thus the energy levels ε_i of the nuclear S state for $\gamma = 0$. The energy ε_i corresponds to the wave function

$$u_i(\beta)=a\,H_{\nu_i}(\zeta)\,e^{\zeta^2/2}. \tag{7}$$

When $\gamma = \pi$ Eq. (1) becomes

$$E-E_p+\frac{C}{2}\beta_0^2=\frac{B}{2}\dot{\beta}^2+\frac{C}{2}(\beta-\beta_0)^2+\frac{M}{6B\beta^2},$$

for $0\leqslant\beta<\infty$. It is easily seen that the transformation $\beta\to-\beta$ can result in (4) without changing any of the preceding specifications only in the interval $-\infty<\zeta\leqslant-\delta$. From the requirement that the boundary conditions be satisfied at the ends of this interval it results that

$$v_\nu(\zeta)=bH_\nu(-\zeta)$$

and the transcendental equation which determines the eigenvalue of γ when $\gamma = \pi$ becomes $H_\nu(+\delta) = 0$.

The table contains the energy values of the zero-point surface vibrations of a nucleus in an S state when the states of the outer nucleons correspond to positive β_0 and consequently $\delta > 0$ for $\gamma = 0$ and π.

δ	0	0.1	0.2	0.3	0.5	0.8	1.0	2.0
$\frac{\varepsilon}{\hbar\omega}$ ($\gamma=0$)	1.5	1.39	1.29	1.21	1.03	0.81	0.72	0.50
$\frac{\varepsilon}{\hbar\omega}$ ($\gamma=\pi$)	1.5	1.61	1.73	1.84	2.16	2.66	3.02	6.5

A higher energy level is represented by $\gamma = \pi$. As δ increases the energy of the zero-point vibrations which corresponds to $\gamma = 0$ is reduced and the energy of the vibrations for $\gamma = \pi$ is increased.

The operator of the intrinsic electric quadrupole moment of the nucleus, which results from the collective degrees of freedom, is

$$\hat{Q}_0=\frac{3ZR}{\sqrt{5\pi}}\beta\cos\gamma.$$

In the ground state of an even-even nucleus $\gamma = 0$, the wave function is given by (7) and $\langle\beta\rangle > \beta_0$. The difference between $\langle\beta\rangle$ and β_0 is reduced as δ increases, but for small δ it can be of considerable magnitude*.

$\gamma = \pi$ corresponds to a special kind of excited states for which $\langle\beta\cos\pi\rangle < 0$. $\langle\beta\cos\pi\rangle$ is considerably smaller than β_0 in absolute value and tends to vanish as δ increases. Thus when the nucleus

*Our adiabatic approximation will be valid only when β_0 exceeds a certain critical value.

makes a transition from the ground state with $\gamma = 0$ to the S state which corresponds to $\gamma = \pi$ the quadrupole moment is changed in sign and magnitude.

In nuclei where the states of the outer nucleons correspond to negative values of β_0 the lowest energy levels occur for $\gamma = \pi$. However it appears from experiment that there are no nuclei with large negative values of β_0.

The author is deeply indebted to Academician I. E. Tamm for his interest and for valuable comments.

[1] A. Bohr, Kgl. Danske Videnskab. Selskab, Mat.-fys. Medd. **26**, 14 (1952).

[2] N. N. Lebedev, *Special Functions and their Applications*, GITTL, 1953.

Translated by I. Emin
206

Reactions Produced by μ-Mesons in Hydrogen

IA. B. ZEL'DOVICH AND A. D. SAKHAROV
P. G. Lebedev Physics Institute, USSR Academy of Sciences

J. Exper. Theoret. Phys. (U.S.S.R.) **32**, 947-949 (April, 1957)

AT PRESENT THERE IS EVIDENCE that at Berkeley[1] in a bubble chamber, filled with liquid hydrogen having a varying deuterium content, there could be observed a nuclear reaction catalyzed by μ-mesons. The possibility of such a type of reaction was first pointed out by Frank[2] in connection with the analysis of π-μ disintegrations in emulsions. This process was investigated in liquid deuterium by both of the authors of this article, independently of one another[3,4].

The presence of a μ-meson changes the form of the potential barrier which previously prevented nuclear reactions among slow proton and deuteron nuclei, increasing sharply the penetrability of the barrier and making possible the reactions

$$p + D = He^3, \quad D + D = He^3 + n, \quad D + D = T + p.$$

In the presence of tritium there are also possible the reactions

$$D + T = He^4 + n, \quad T + T = He^4 + 2n, \quad p + T = He^4.$$

The reaction $p + p = D + e^+ + \nu$, catalyzed by mesons, is practically impossible, since in addition to the barrier there is also the factor of a low probability for the beta process.

It has been predicted[4] that the probability of the reaction in flight is low, the production of mesomolecules practically always leads to nuclear reactions, the rate of the process is determined by the production of mesomolecules, and the probability of mesomolecule formation during the lifetime of a meson may amount to several hundredths or even tenths, depending on the arrangement of the mesomolecule levels.

The experimental data of Alvarez[1] shows that in natural hydrogen (deuterium content ratio 1 : 7000), the reaction $p + d = He^3$ occurs on the average once for each 150 mesons. If the deuterium ratio is 1 : 300, the reaction occurs once per 40 mesons, and if the ratio is 1 : 20, the reaction occurs once per 33 mesons. Furthermore, the energy of the resulting He^3 (5.4 Mev) is carried away by the μ-meson, so that monochromatic μ-mesons are observed while the reaction is taking place. The relatively high probability found for the reaction in the natural mixture is explained[1] by the transfer of the meson from the proton to the deuteron (charge exchange): $p\mu + d = p + d\mu$. Due to the difference in reduced mass, the energy of the $D\mu$ bond (2655 ev) is greater by $\Delta E = 135$ ev than the energy of the $p\mu$ bond. Therefore the charge-exchange process appears to be irreversible under the experimental conditions.

We shall give a rough estimate of the probability of the transition. If ΔE is equal to zero, the cross section should be of the order of πa^2, where a is the radius of the Bohr orbit of the mesoatom, 2.5×10^{-11} cm.

Indeed, if the masses of the two nuclei are equal, with $\Delta E = 0$, the states of the systems $\sum_+^g$ and $\sum_-^u$ appear to be proper, and the cross section for charge exchange can be expressed by the scattering lengths a_g and a_u of these states in a continuous spectrum: $\sigma = \pi(a_g - a_u)^2$. When $\Delta E \neq 0$, but is still small with respect to the molecular dissociation energy, then

$$\sigma = \pi(a_g - a_u)^2 v_f / v_i,$$

where v_i is the velocity before collision and v_f is the velocity after collision.

In actual fact, ΔE is of the same order as the dissociation energy, so that the formula is corrected at least in order of magnitude. If v_i is small $\sigma \sim 1/v$ $\sigma \sim 1/v_i$. It follows that in order of magnitude,

$$\sigma \approx \pi a^2 v_* / v_i,$$

where v_* is the characteristic velocity corresponding to 135 ev. Using the masses of the proton and deuteron, $v_* = 2 \times 10^7$ cm/sec. Such an estimate yields qualitative agreement with the observed facts. Calculation shows that saturation should be reached at deuterium concentrations of 1 in 300 to 1 in 20. In the natural mixture of hydrogen, the probability of $D\mu$ production and consequently the probability of the reaction should be three-fold less than in enriched mixtures; experimentally it is found to be 4 to 5 times less.

Let us examine the reaction in the $pD\mu$ molecule. The observed high probability a of the giving up of the meson energy does not agree with the hypothesis that the reaction proceeds like an electric dipole transition ($E1$), since a becomes 2×10^{-3} for the meson under this hypothesis. Therefore, to estimate the probability we cannot use the experimental cross section for $p + D = He^3 + \gamma$ (as was done before[4]), since under the conditions of the measurement, it is precisely the cross section of the $E1$ process which is observed.

In the case of zero orbital momentum, the system $p + D$ can be found in either of the states $+\frac{3}{2}$ or $+\frac{1}{2}$. The transition to He^3 ($+\frac{1}{2}$ state) is possible in the first case as $M1$ and $E2$, and in the second case as $M1$ and $E0$*.

The conversion coefficients have the following values: for $M1$, $a = 10^{-4}$; for $E2$, $a = 0.1$; for $E0$, only the giving up of meson energy is possible (the probability of pair production e^+ and e^- at the expense of $E0$ is 10^{-3} of the probability of the giving up of meson energy in the case of $p + D$, but is of the order of unity in the case of $p + H^3 = He^4$).

Calculations concerning barrier penetration for the $pD\mu$ molecule under adiabatic investigation of the motion of the proton and deuteron yield $\psi^2(0) = 6 \times 10^{-27}$ cm^{-3}.

For the mirror reaction $n + D$, it is assumed that for the purposes of computation[8] the process proceeds from the state $\frac{3}{2}$ as the result of $M1$. Experimentally for thermal neutrons[9], $\sigma = 5.7 \times 10^{-28}$ with $v = 2200$ m/sec and $\sigma v = 1.3 \times 10^{-22}$ cm^3/sec.

Hence for mesomolecules the probability of the reaction ($\tau = 2.15 \times 10^{-6}$ being the meson lifetime) is

$$w = \frac{\sigma v \psi^2(0)}{(1/\tau) + \sigma v \psi^2(0)} = 0{,}6.$$

*Church and Wenezer[7] have recently drawn attention to the role of $E0$ in the case of internal conversion in the transition $J \to J \neq 0$.

During the approach of the proton and deuteron in the spin state $\frac{1}{2}$, the approximate determination of the magnitude of the monopole moment was carried out by examining one charged particle with the wave function $\psi = \frac{1}{\sqrt{2\pi\lambda}} \frac{1}{r} e^{-r/\lambda}$ in the final (combined) state and $\psi = \psi(0)(1 - \lambda/r)$ in the initial state (continuous spectrum, $\psi(0)$ being the previously calculated wave function under the barrier, $\psi^2(0) = 6 \times 10^{-27}$).

The probability of a process with a release of energy, to a meson in a $p + D$, in spin state $\frac{1}{2}$, and with $\lambda = 2.4 \times 10^{-13}$ cm turned out to be equal to 0.5*.

Thus from the rough estimates made above, it follows that the probability observed by Alvarez for the process which involves release of energy to the meson and the probability of the process which involves emission of a gamma quantum can both be close to unity during the meson lifetime.

In a more accurate investigation, not only will it be necessary to take into account the fact that the processes is not adiabatic (thus involving terms of the order of the meson-nucleon mass ratio), but it will also be necessary to make a separate investigation of the nuclear reaction with different values of total molecular spin.

Note added in proof (February 9, 1957). The probabilities for mesomolecule production in the collisions $D\mu + p = Dp\mu$ and $D\mu + D = D_2\mu$ differ not only due to the different positions of the excited vibrational levels of the molecules[4], but also because in $pD\mu$ the center of mass does not coincide with the charge center, and thus possesses a dipole moment ($\frac{1}{3}$ ea). Therefore in the collision of slow $D\mu + p$ there is possible the dipole transition ($E1$) in the molecule into the momentum state 1, with the giving up of energy to the electron. In the case of $D\mu + D$, only the $E2$ transition into momentum state 2 competes with the $E0$ transition investigated[4].

[1] L. W. Alvarez *et al.*, Lithographed document, December 1956.

[2] F. C. Frank, Nature **160**, 525 (1947).

[3] A. D. Sakharov, Report, Phys. Inst. Acad. Sci. U.S.S.R. (1948).

[4] Ia. B. Zel'dovich. Dokl. Akad. Nauk SSSR **95**, 454 (1954).

*Choosing $\lambda = \hbar/\sqrt{2ME}$, where M is the reduced mass of p and D, and E is the binding energy, 5.4 Mev.

[5] G. M. Griffiths and I. B. Warren, Proc. Phys. Soc 68, 781 (1955).
[6] D. H. Wilkinson, Phil. Mag. 43, 659 (1952).
[7] E. L. Church and Wenezer, Phys. Rev. 103, 1035 (1956).
[8] N. Austern, Phys. Rev. 83, 672 (1951); 85, 147 (1952).
[9] Kaplan, Ringo and Wilzbach, Phys. Rev. 87, 785 (1952).
[10] E. E. Salpeter, Phys. Rev. 88, 547 (1952).

Translated by D. A. Kellog
207

Corrections to the Articles "Dispersion Formulas of the Quantum Optics of Metals in the Many-Electron Theory"

A. V. SOKOLOV, V. I. CHEREPANOV
Institute of Metal Physics, Ural Branch of the Academy of Sciences, Ural State University
(submitted to JETP editor December 30, 1956)
J. Exptl. Theoret. Phys. (U.S.S.R.) 32, 949-950
(April, 1957)

IN PREVIOUS WORKS[1-3] the dispersion formulas of the quantum optics of metals were obtained both without taking account of electron damping and with taking it into account for the infrared, visible, and ultra-violet regions of the spectra. The present note is intended to indicate errors in the above works, as well as finally to give the correct dispersion formulas for ε and σ.

The many-electron wave function of the crystal used in the cited works was taken from Seitz[4] and is of the form

$$\psi(\mathbf{r}_1 \ldots \mathbf{r}_N, s) = \chi_{\mathbf{k}_1 \ldots \mathbf{k}_N}(\mathbf{r} \ldots \mathbf{r}_N, s) \exp\left(i \sum_{j=1}^{N} \mathbf{k}_j \mathbf{r}_j\right), \tag{1}$$

where χ is a periodic function with period a. It should be noted that the use of the wave function of Eq. (1) for a set of interacting electrons in a crystal is inconsistent, since it gives the total quasimomentum of the system (a conserved quantity) as the sum of the quasimomenta of the separate electrons; this is true, strictly speaking, only for a system of noninteracting electrons.

As was pointed out by Volz and Haken[5,6], if the independent variables are chosen as the coordinates of the center of gravity of the system $\mathbf{R}(X, Y, Z)$ and the appropriate number of relative coordinates, the wave function of a system of interacting electrons in the crystal may be written in the form

$$\psi_{\mathbf{K}, I, s}(\mathbf{R}, \mathbf{r}_{jk}) = \chi_{\mathbf{K}, I, s}(\mathbf{R}, \mathbf{r}_{jk}) \exp(i \mathbf{K}\mathbf{R}), \tag{2}$$

where the three quantum numbers K_x, K_y, and K_z give total quasimomentum of the system and characterize the motion of the center of mass $\mathbf{R}$ of the total electron system, and I is a continuous quantum number related to the relative motion of the electrons, that is, to the relative coordinates $\mathbf{r}_{jk} = \mathbf{r}_j - \mathbf{r}_k$, and characterizes changes in the configuration of the electron systems; s denotes the number of the band together with the other discrete quantum numbers of the system. The function χ is periodic with respect to translation of the center of mass of the system along the lattice vector a.

The use of wave functions such as those of Eq. (2) is more correct, since in this case the total quasimomentum $\mathbf{K}$ of the system of interacting electrons uniquely characterizes the system as a whole.

If we calculate the matrix element for the probability of optical transition, using the wave function of Eq. (3), in the same way as previously[1], we obtain the energy conservation law and interference condition for the whole system of interacting electrons, namely

$$\begin{gathered} E(\mathbf{K}', I', s') = E(\mathbf{K}, I, s) \pm \hbar\omega, \\ \mathbf{K}' = \mathbf{K} + \mathbf{K}_0 + 2\pi\mathbf{g}, \end{gathered} \tag{3}$$

where $\mathbf{K}_0$ is the wave vector of the electromagnetic wave, and g is the reciprocal lattice vector. For selection rules, see also Haken[7].

In connection with this, we note that in the previous works[1-3], essentially single-electron selection rules $\xi_i' = \xi_i$ were used. In actuality, however, the set[8] of quantum numbers $(\mathbf{K}', I')$ need not necessarily be the same as the set $(\mathbf{K}, I)$, but must merely satisfy Eq. (3). The use of the correct wave functions of Eq. (2) in the derivation of the dispersion formulas leads to the following expressions for ε and σ:

$$\varepsilon(\omega) = 1 - \frac{4\pi e^2}{m^2\omega^2 G^3 a^3} \sum_s \int d\xi \rho_0(\xi, s) \left\{ e^{-\Gamma t} + \frac{1}{m\hbar} \sum_{s'} \int d\xi' \left[\frac{\omega' - \omega}{(\omega' - \omega)^2 + \Gamma^2} + \right. \right.$$

$$\left. \left. + \frac{\omega' + \omega}{(\omega' + \omega)^2 + \Gamma^2} \right] \tilde{D}(\xi s;\ \xi' s') \right\}, \tag{4}$$

$$\sigma(\omega) = -\frac{e^2}{m^2 \hbar\, \omega\, G^3 a^3} \sum_{s,s'} \left\{ \iint d\xi d\xi' \rho_0(\xi, s) \left[\frac{\Gamma}{(\omega' - \omega)^2 + \Gamma^2} - \frac{\Gamma}{(\omega + \omega)^2 + \Gamma^2} \right] \tilde{D}(\xi s;\ \xi' s') \right.$$

$$\left. + \pi \int du_1 \ldots du_{6+2p-1} \frac{\rho_0(\xi', s') - \rho_0(\xi, s)}{|\operatorname{grad}_{\xi\xi'} \omega'|} \tilde{D}(\xi s; \xi' s') \right\}, \tag{5}$$

where we have introduced the notation

$$\xi = (K, I),\ \hbar\omega' = \hbar\omega'(\xi' s';\ \xi s) = E(\xi', s') - E(\xi, s),$$

p is the number of continuous quantum numbers I, and $\tilde{D}$ is a tensor with components

$$\{\tilde{D}(\xi s;\ \xi' s')\}_{\alpha,\beta} = (\xi' s' | \sum_j \mathbf{P}_{j\alpha} | \xi s)(\xi s | \sum_j \mathbf{P}_{j\beta} | \xi' s'),$$

$$(\alpha, \beta = x, y, z).$$

[1] A. V. Sokolov, J. Exper. Theoret. Phys. (U.S.S.R.) 25, 341 (1953).

[2] Soklov, Cherepanov, and Shteinberg, J. Exper. Theoret. Phys. (U.S.S.R.) 28, 330 (1955), Soviet Phys. JETP 1, 231 (1955).

[3] V. I. Cherepanov, J. Exper. Theoret. Phys. (U.S.S.R.) 30, 598 (1956), Soviet Physics JETP 3, 623 (1956).

[4] F. Seitz, *Modern Theory of Solids*, (Russian Transl.) (1948).

[5] H. Volz, H. Haken, Z. physik. Chem. 198, 61 (1951).

[6] H. Haken, Z. Naturforsch. 9A, 228 (1954).

[7] H. Haken, Z. Physik. 144, 91 (1956).

[8] V. I. Cherepanov, Fiz. Metal i Metaloved. 4, 2 (1957).

Translated by E. J. Saletan
208

CONTENTS – *continued*

CONTENTS

(Contents continued on inside back cover)